OCS Study
BOEMRE 2011-019

A Comparison of Marine Productivity Among Outer Continental Shelf Planning Areas

Final Report

April 2011

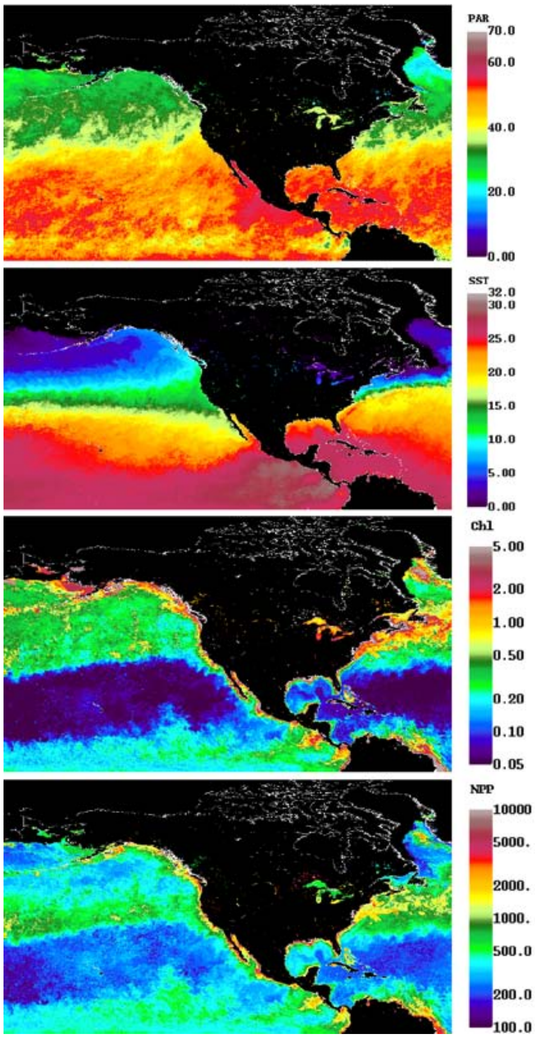

OCS Study
BOEMRE 2011-019

A Comparison of Marine Productivity Among Outer Continental Shelf Planning Areas

Final Report

Authors

Brian J. Balcom
Douglas C. Biggs
Chuanmin Hu
Paul Montagna
Dean A. Stockwell

Editor

Neal W. Phillips

April 2011

Prepared under BOEMRE Contract
GS10F0443M
by
CSA International, Inc.
8502 SW Kansas Avenue
Stuart, Florida 34997

Published by

U.S. Department of the Interior
Bureau of Ocean Energy Management,
Regulation and Enforcement

Herndon, VA
April 2011

DISCLAIMER

This report was prepared under contract between the Bureau of Ocean Energy Management, Regulation and Enforcement (BOEMRE) and CSA International, Inc. This report has been technically reviewed by the BOEMRE and has been approved for publication. Approval does not signify that the contents necessarily reflect the view and policies of the BOEMRE, nor does mention of trade names or commercial products constitute endorsement or recommendation for use. It is, however, exempt from review and in compliance with BOEMRE editorial standards.

REPORT AVAILABILITY

Copies of this report may be obtained from the Public Information Office at the following address:

U.S. Department of the Interior
Bureau of Ocean Energy Management,
Regulation and Enforcement
Public Information Office
381 Elden Street
Herndon, VA 20170-4917

Telephone: (703) 787-1755

CITATION

Suggested citation:

Balcom, B.J., D.C. Biggs, C. Hu, P. Montagna, and D.A. Stockwell. 2011. A comparison of marine productivity among Outer Continental Shelf planning areas. Prepared by CSA International, Inc. for the U.S. Dept. of the Interior, Bureau of Ocean Energy Management, Regulation and Enforcement, Herndon, VA. OCS Study BOEMRE 2011-019. 195 pp. + apps.

ABOUT THE COVER

Cover images: Examples of inputs and outputs of the Vertically Generalized Production Model (VGPM), or net primary production (NPP) model, for April 2000. From top to bottom: Sea-viewing Wide Field-of-view Sensor (SeaWiFS) photosynthetically available radiation (PAR) (Mol photons m^{-2} d^{-1}); Advanced Very High Resolution Radiometer (AVHRR) sea surface temperature (SST) (°C); SeaWiFS chlorophyll (mg m^{-3}); and modeled NPP (mg C m^{-2} d^{-1}).

Executive Summary

ES.1 Background

Section 18(a)(2) of the Outer Continental Shelf (OCS) Lands Act (OCSLA) Amendments of 1978 specifies eight factors that the U.S. Department of the Interior (USDOI) must consider in the timing and location of OCS oil and gas activities, including “the relative environmental sensitivity and marine productivity of different areas of the OCS.” Thus, by law, marine productivity is one of the factors that USDOI’s Bureau of Ocean Energy Management, Regulation and Enforcement (BOEMRE; formerly Minerals Management Service [MMS]) must consider in its OCS Oil and Gas Leasing Program. Given that the most recent synthesis of marine productivity estimates were prepared in 1990, BOEMRE recognized the need to update productivity estimates in support of ongoing decision-making and future program documents.

During the 1990 analysis, water column primary productivity data were analyzed and each of the 26 OCS planning areas established by USDOI under its oil and gas leasing program (**Figure ES-1**) were characterized; in addition, benthic primary productivity and the feasibility of available secondary productivity measures were also evaluated as part of the 1990 analysis. The USDOI employed the 1990 water column primary productivity estimates as one of the factors for comparisons among planning areas, the most recent of which occurred with development of the Proposed Revised Program for 2007–2012 and the Draft Proposed Program for 2010–2015. USDOI has also considered productivity estimates in conjunction with its utilization of shoreline Environmental Sensitivity Index (ESI) characteristics within previous 5-y programmatic documents. Meaningful comparisons based on other productivity measures were found to be problematic. Benthic primary productivity comparisons are complicated by geographic differences in types and areal extent of producers as well as by methodological problems and inconsistencies. No suitable method was identified for consistently estimating total secondary or tertiary productivity.

What is Marine Productivity?

Marine productivity is a broad term that can include water column and/or benthic sources. In this report, ***production*** is defined as the generation of biomass within the environment of interest – that is, biomass elaboration.

Productivity is the rate of production (biomass elaborated per unit time). For primary producers such as phytoplankton, this is done by photosynthesis (primary production). Secondary production is the conversion of energy from primary producers by consumers to produce new biomass. Tertiary production is the conversion of energy from prey by higher-trophic level predators. In some studies, all production higher than primary is referred to as secondary production.

Figure ES-1. Planning areas for the Outer Continental Shelf Oil and Gas Leasing Program.

ES.2 Objectives

The goal of this study was to provide the BOEMRE with current estimates of marine productivity for the 26 OCS planning areas. Specific objectives were to evaluate current methods of estimating marine productivity, to select the preferred method or methods, and, using the preferred method, to develop updated estimates for all OCS planning areas. This included updating the 1990 report to the present state of knowledge on water column primary productivity and secondary/tertiary productivity.

ES.3 Study Methods

Results of the 1990 productivity assessment indicated that water column primary productivity was an excellent metric for estimating marine productivity. BOEMRE determined that a review of existing methodology for estimating water column primary productivity, including evaluation of the latest methods and available technology for data acquisition and interpretation, should be the main focus for updating productivity estimates. This methodology is sufficiently developed to offer the best chance of consistent, comprehensive estimates across planning areas. For secondary and tertiary productivity, the focus was on evaluating methods that hold the best promise for developing comprehensive estimates, and searching for published results applicable to the planning areas.

Evaluation of Primary Productivity Methods

Current methods for estimating marine primary productivity were evaluated, including a discussion of data sources (e.g., remote sensing and other methods) and data analysis or calculation methods. The evaluation of available modeling approaches included characterizing the various types of models currently used to estimate depth-integrated primary productivity from satellite measurements of the ocean.

Important considerations included 1) scientific acceptance (whether the method has published in peer-reviewed literature and generally accepted and used in other studies); 2) data requirements; 3) spatial and temporal resolution (including whether the method can provide details of "hot spots" and seasonal productivity peaks within a planning area); 4) potential uncertainties and biases in the predictions; and 5) the degree to which the method lends itself to readily updating productivity estimates in the future.

Development of Primary Productivity Estimates for OCS Planning Areas

The earlier primary productivity review completed in 1990 developed estimates by tabulating individual studies conducted in each planning area. The major problem noted in the 1990 report was "the lack of a consistent and uniform database," as evidenced by studies conducted in different areas employing different methodologies, sampling at different spatial scales, and/or sampling at different frequencies. Because of advances in modeling, satellite imagery, and online databases during the past 20 y, the approach in the current study was fundamentally different. Several models are now available to estimate photosynthetic rates from satellite-based measurements of chlorophyll concentrations. This study used the Vertically Generalized Production Model (VGPM) to estimate net primary productivity (NPP) in each planning area as a function of chlorophyll, available light, and photosynthetic efficiency.

Primary Productivity Literature Updates

The water column primary productivity database last compiled in 1990 was updated, with an emphasis on the published literature and reports for each planning area. A search of electronic databases was completed, and the data were reviewed and evaluated. Data sources of interest included 1) results from studies that measured rates of marine primary and secondary production; 2) results from studies that measured marine biomass or standing stocks; 3) relationships between marine biomass and productivity; and 4) relationships between size (length or marine biomass), respiration (or metabolism), and growth (or productivity).

Eleven electronic databases were queried, using search criteria largely similar to those employed in 1990. The literature search included potential data sources dating back to 1988. The search found 614 titles, and, from those, 319 full citations/abstracts were requested.

Secondary and Tertiary Productivity Methods and Literature Updates

Secondary and tertiary productivity measurement and calculation methods were reviewed and evaluated. There are few well developed modeling approaches or software tools available to estimate secondary or tertiary productivity. Instead, there are many independent studies, each using unique approaches or simply relying on empirical biomass or harvest estimates that are used as estimates of productivity. This task included a consideration of tools and approaches that could provide generality, such as allometric relationships (to calculate productivity based on biomass) and recent developments in ecological modeling software tools (e.g., the Ecopath model, the Atlantis model, the nutrient-phytoplankton-zooplankton [NPZ] model). Important considerations in this review and evaluation were similar to those noted for primary productivity, namely: scientific acceptance, data requirements, spatial and temporal resolution, potential uncertainties, and ease of use for future updating.

Based on the literature review and evaluation, the Ecopath modeling approach was chosen for further detailed investigation. This choice was based primarily on scientific acceptance and the existence of well developed software tools that are promoting a large user community. A total of 18 Ecopath modeling studies were found that were applicable to one or more planning areas, and these modeling results were tabulated for comparison. In addition, potential empirical methods available to establish secondary and tertiary productivity were evaluated, including summarization of zooplankton sampling data and fisheries landings.

ES.4 Sources of Primary Productivity Data

The 1990 report noted that “Oceanic primary production can also be estimated from remote sensing of ocean color, bio-optical modeling, other biological models, and combinations of these techniques.” Since issuance of the 1990 report, various new tools have become available, including satellite sensors of upper ocean color (as a proxy for phytoplankton distributions), fluorescence and flow cytometry, molecular biological probes, sophisticated moored and shipboard instrumentation, and increased numerical modeling capabilities.

The discussion of measurement of ocean color from space encompassed four different satellite-based instruments, several of which provided source data for this study, including:

- Coastal Zone Color Scanner (CZCS) – launched to collect a global set of observations of visible radiation reflected by the ocean. The CZCS acquired radiance data in five visible bands and one infrared band, each with a pixel size of about 1 km x 1 km. However, only the first four of these bands proved useful for estimating phytoplankton concentration.

- Sea-viewing Wide Field-of-view Sensor (SeaWiFS) – launched in 1997; SeaWiFS raw data are 10-bit digitization and have spatial resolution of 1.1 km (local area coverage, LAC) or 4.5 km (global area coverage, GAC). Revisit time is approximately 1 d. At one or more locations on the U.S. east coast, west coast, Gulf of Mexico coast, Alaska, and Hawaii, SeaWiFS data are captured in real-time using ground-based tracking antennae and are immediately processed, distributed, and archived.

- Moderate Resolution Imaging Spectrometers (MODIS) – launched in 1999 and 2002; MODIS radiometers have five radiance bands in the 400-600-nm range. However, there are several important differences between MODIS and SeaWiFS. MODIS data are 12-bit (not 10-bit) digitization, and MODIS radiometers can measure chlorophyll fluorescence, as well as water-leaving radiance in the spectral range 400-600 nm, with 1-km resolution.

- Medium Resolution Imaging Spectrometer (MERIS) – launched in 2002; a polar-orbiting programmable imaging spectrometer with 15 spectral bands in the range 412-900 nm; MERIS has a spatial resolution of about 1 km x 1 km over ocean, with higher spatial resolution (260 m x 300 m) over land and coasts. MERIS can achieve global coverage every 3 d.

Based on the review of available primary productivity data sources, SeaWiFS and the MODIS ocean color algorithm validation provided the necessary characteristics and scientific justification for their selection in the VGPM modeling effort. The SeaWiFS and MODIS data sets, along with Advanced Very High Resolution Radiometer (AVHRR) data, provided the basic input parameters needed for the modeling effort. **Table ES-1** summarizes the data source characteristics used to estimate NPP in this study; all data were obtained from the National Aeronautics and Atmospheric Administration.

Table ES-1. Data source characteristics used to estimate net primary production.

Variable	Units	Sensor(s)	Resolution	Period	Frequency
Sea surface temperature (SST)	°C	AVHRR	9 km	1998-Present	Monthly
Chlorophyll (C_{sat})	mg m^{-3}	SeaWiFS MODIS/A	9 km	1998-2007 2003-Present	Monthly Monthly
Photosynthetically available radiation (PAR)	Mol photons m^{-2} d^{-1}	SeaWiFS MODIS/A	9 km	1998-2007 2003-Present	Monthly Monthly
Daily photoperiod (D_{irr})	h	Models	9 km	1998-Present	Monthly

ES.5 Selection of a Primary Productivity Model

Among the present generation of bio-optical models used to predict marine primary productivity from satellite-based chlorophyll concentration is what has become known as the VGPM, which is also called the NPP model. The VGPM is a sea surface temperature (SST) and irradiance-dependent, depth-resolved productivity model used to determine the maximum light-saturated rate of photosynthesis. The model uses SST, measurements of ocean color, and measurements of available light (i.e., light of the proper wavelength to support photosynthesis) to estimate chlorophyll.

From these monthly global data products, NPP monthly global maps were derived using the VGPM model. **Figure ES-2** shows an example of the four variables and the resulting NPP map for the month of April 2000.

The monthly NPP time-series from 1998 through 2009 was queried using each of the 26 OCS planning areas. For each planning area, the geographic information system (GIS)-shape file was used to generate a region-of-interest (ROI). Statistics of all images pixels within the ROI were performed to calculate the mean, standard deviation, and total (area integrated) monthly NPP.

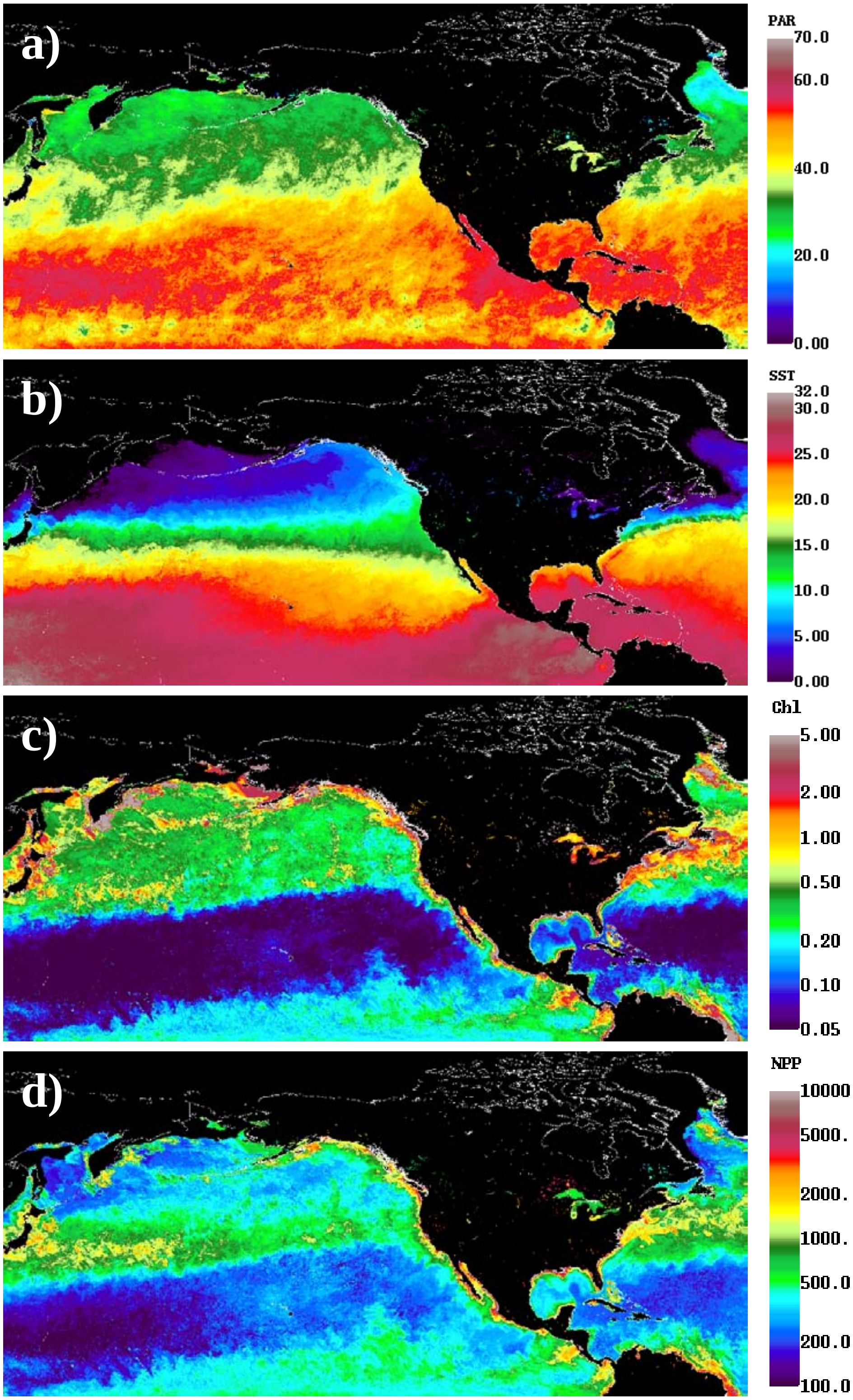

Figure ES-2. An example of inputs and output of the VGPM net primary productivity (NPP) model for April 2000. a) SeaWiFS PAR (Mol photons m^{-2} d^{-1}); b) AVHRR SST (^{o}C); c) SeaWiFS Chl (mg m^{-3}); and d) modeled NPP (mg C m^{-2} d^{-1}).

ES.6 Primary Productivity Estimates for OCS Planning Areas

Each of the 26 planning areas was characterized in terms of areal coverage, mean annual NPP, annual and monthly variance, and trend (i.e., increasing or decreasing productivity) over the 12-y period of 1998 through 2009. It is difficult to predict future trends, even if some of the planning areas showed an increasing or decreasing trend for the study period. This is because the controlling mechanism of primary productivity in each area is a complex function of many environmental factors, including climate change. A similar case can be found for global warming; even if the dominant temperature trend is increasing on a multi-decadal scale, on a decadal scale there may be a cooling trend. Graphic representations for each planning area included NPP (i.e., in units of milligrams C per square meter per day; mg C m^{-2} d^{-1}) and total NPP (i.e., in units of million tonnes of C per month; million tonnes C mo^{-1}) and annual NPP (million tonnes C); a representative figure is provided in **Figure ES-3**.

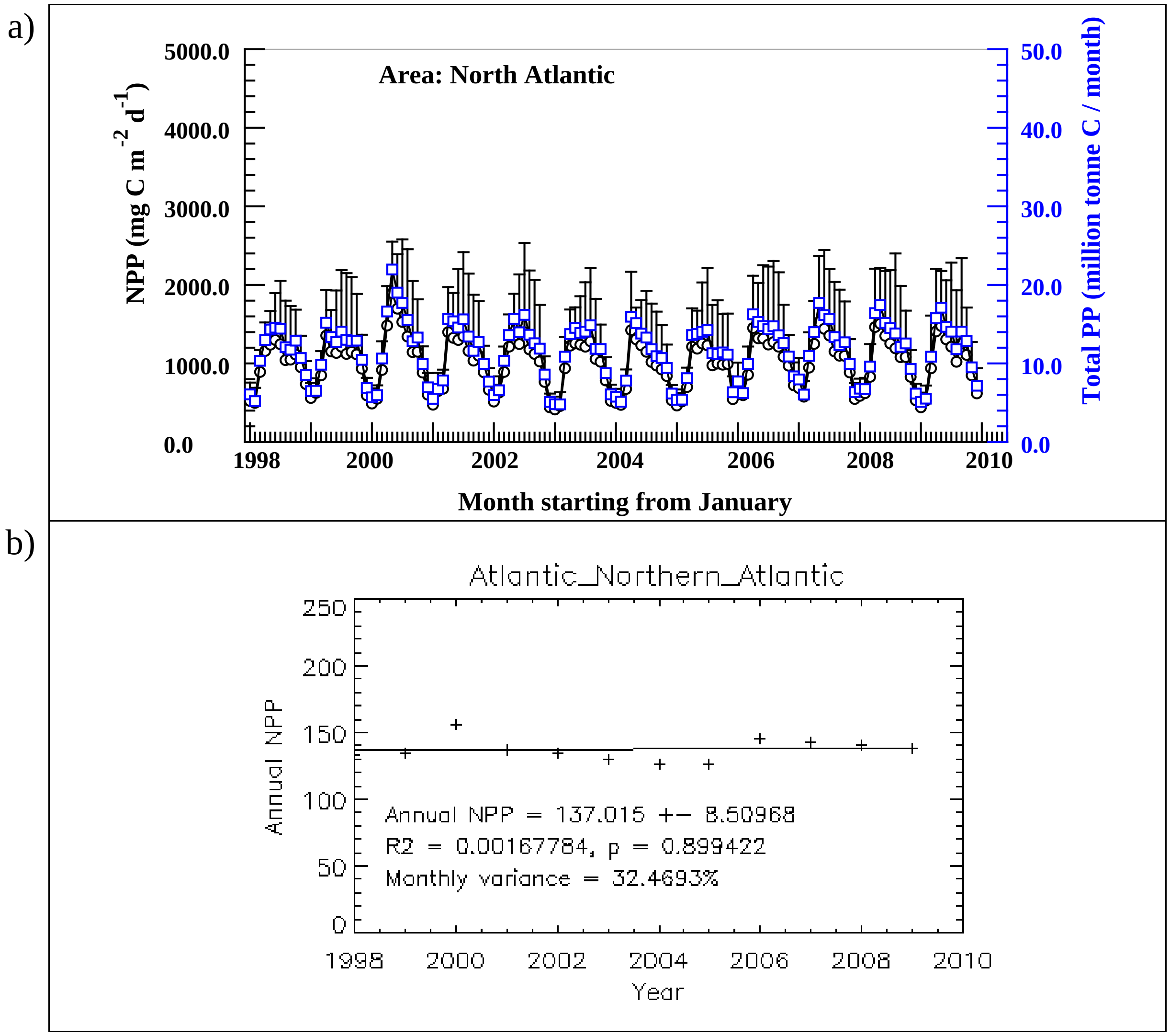

Figure ES-3. Representative figure of a) monthly net primary productivity (NPP) and monthly total NPP, and b) annual NPP statistics. This example is from the North Atlantic Planning Area.

Table ES-2 lists the summary primary productivity statistics for each planning area, including annual NPP (in million tons C), annual NPP variability (a measure of relative interannual variance), monthly NPP variability (a measure of seasonality), and annual NPP trend. The total integrated annual primary productivity varies substantially from area to area (**Figure ES-4**), ranging between 5.99±0.51 million tons C for the Straits of Florida and 195.07±14.98 million tons C for the Aleutian Arc, a change of >30 fold. Normalization to the acreage for each area yields annual primary productivity per acre, which shows less variability among the 26 areas (**Figure ES-5**). Except for the Chukchi Sea and Beaufort Sea planning areas in the Alaska Region, nearly all planning areas exhibited annual primary productivity between 0.5 and 1.7 million tons C acre^{-1}, a variation of ~<3-fold.

Table ES-2. Net primary productivity (NPP) statistics for the 26 OCS planning areas.

Region and Planning Area	Acreage (million acres)	Annual NPP[1] (million tons C)	Annual NPP (min–max)	Annual Variability[2] (%)	Monthly Variability[3] (%)	Annual Trend[4]
Atlantic Region						
North Atlantic	92.32	137.01±8.51	125.94 – 156.14	6.21	32.47	+, p=0.90
Mid-Atlantic	112.83	55.79±2.59	50.31 – 59.45	4.64	25.18	-, p=0.70
South Atlantic	54.34	49.59±4.44	41.15 – 58.51	8.95	26.86	-, p=0.97
Straits of Florida	9.64	5.99±0.51	5.40 – 7.11	8.51	22.50	-, p=0.23
Gulf of Mexico Region						
Eastern Gulf of Mexico	64.56	60.42±6.98	52.77 – 75.43	11.55	23.49	-, p=0.38
Central Gulf of Mexico	66.45	87.17±9.13	72.08 – 101.12	10.68	28.03	+, p=0.50
Western Gulf of Mexico	28.58	33.99±3.13	28.52 – 39.95	9.21	33.58	+, p=0.18
Pacific Region						
Southern California	88.98	100.45±10.95	78.51 – 117.93	10.90	21.38	**+, p<0.01**
Central California	43.68	60.23±6.70	48.22 – 75.99	11.12	25.82	**+, p=0.02**
Northern California	44.79	52.26±3.13	47.87 – 56.72	5.99	27.61	**+, p<0.01**
Washington-Oregon	71.00	89.89±7.43	78.08 – 100.97	8.26	43.59	**+, p<0.01**
Alaska Region						
Gulf of Alaska	112.10	124.97±4.82	117.36 – 131.80	3.86	50.10	+, p=0.74
Cook Inlet	5.36	8.97±0.61	7.95 – 9.75	6.80	58.30	-, p=0.63
Kodiak	89.00	82.73±4.18	74.66 – 88.42	5.05	49.11	-, p=0.05
Shumagin	84.65	78.19±6.04	65.35 – 86.87	7.72	53.98	-, **p=0.01**
Aleutian Arc	259.06	195.07±14.98	171.25 – 217.48	7.68	55.64	-, p=0.33
N. Aleutian Basin	32.45	39.73±6.90	28.97 – 50.08	17.37	43.93	-, p=0.88
St. George Basin	70.23	72.38±10.31	57.35 – 91.70	14.24	56.93	-, p=0.27
Bowers Basin	87.59	60.09±6.22	50.67 – 68.20	10.35	56.93	+, p=0.60
Aleutian Basin	41.33	30.96±4.17	25.10 – 37.71	13.47	69.29	-, p=0.90
Navarin Basin	34.02	26.75±6.26	17.97 – 37.32	23.40	58.83	-, p=0.71
St. Matthew-Hall	54.57	52.09±7.20	39.74 – 62.90	13.82	29.66	-, p=0.60
Norton Basin	24.25	34.07±4.00	26.81 – 40.69	11.74	44.27	**+, p=0.02**
Hope Basin	12.82	12.01±2.67	7.72 – 16.27	22.23	30.66	**+, p<0.01**
Chukchi Sea	62.59	10.64±5.41	2.93 – 21.63	50.85	38.02	**+, p=0.03**
Beaufort Sea	65.08	8.02±6.35	1.11 – 16.75	79.17	59.29	-, p=0.65

[1] Annual NPP is expressed in mean ± standard deviation;

[2] Annual NPP variability is expressed in (standard deviation/mean) x 100%;

[3] Monthly NPP variability is defined as (standard deviation/mean) x 100% for all valid months;

[4] Trend analysis is from linear regression between annual NPP and time. + indicates increasing trend, and – indicates decreasing trend. p < 0.05 (highlighted in bold font) indicates significant trend.

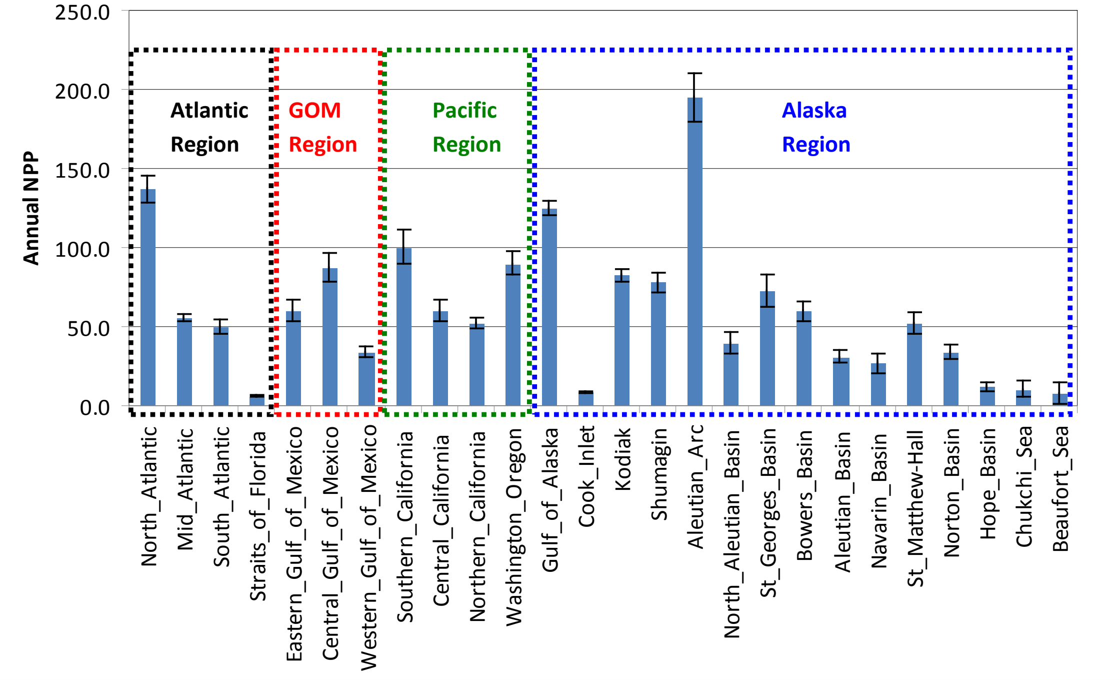

Figure ES-4. Total annual net primary productivity (NPP) (million metric tons C) between 1998 and 2009 for each of the 26 OCS planning areas. Values represent the mean + standard deviation of 12 annual values for the 1998-2009 period.

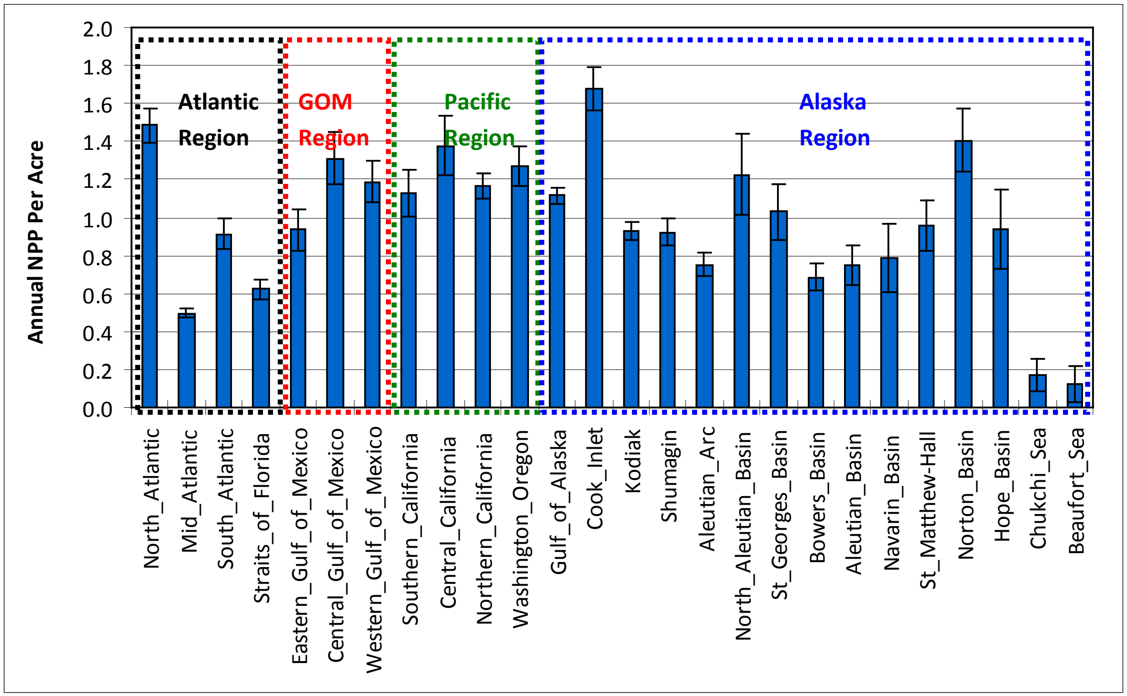

Figure ES-5. Total annual net primary productivity (NPP) (metric tons C) per acre between 1998 and 2009 for each of the 26 OCS planning areas. Values represent the mean + standard deviation of 12 annual values for the 1998-2009 period, standardized per unit area (acres).

Annual Primary Productivity

There are relatively small differences in annual primary productivity per acre across the regions. Significant findings included:

- Pacific Region: in general, exhibited the highest annual primary productivity per acre: >1.1 million tons C acre^{-1} for all four planning areas. Highest annual productivity per acre was evident in the Central California Planning Area; lowest productivity per acre was found in the Southern California Planning Area.

- Gulf of Mexico Region: exhibited high annual primary productivity per acre: >0.9 million tons C acre^{-1} for all three planning areas. Highest annual productivity per acre was evident in the Central Gulf of Mexico; lowest productivity per acre was found in the Eastern Gulf of Mexico Planning Area.

- Atlantic Region: showed variable results, with relatively low productivity: <0.9 million tons C acre^{-1}. Highest annual productivity per acre was noted for the North Atlantic Planning Area, while relatively low productivity was noted for the Mid Atlantic, South Atlantic, and Straits of Florida planning areas.

- Alaska Region: considerable variability was evident. Lowest annual primary productivity per acre was found in the Beaufort Sea (0.1) and the highest in Cook Inlet (>1.6).

The accuracy of primary productivity estimates for the Alaska Region may be substantially lower than in other regions due to several reasons. For example, the presence of turbid coastal waters may adversely affect remote sensing measurements (i.e., chlorophyll-*a* concentrations can be significantly overestimated [>100%] from satellite measurements due to algorithm artifacts in the atmospheric correction and bio-optical inversion). Variations in seasonal solar insolation effects may also result in reduced primary productivity (i.e., most of the areas in the Alaska Region are limited by sunlight).

While calculations are based on the VGPM model, based on various studies showing the validity of this model in assessing primary productivity in marginal seas and upwelling systems, some degree of uncertainty is expected from the model as applied to all 26 OCS planning areas.

Interannual Variability and Seasonality

Substantial interannual variability in primary productivity is found in several of the planning areas, with the highest interannual variability evident in the Alaska Region. Ten of the 15 Alaska planning areas exhibited interannual variability >10%, all of which occur in high latitudes (i.e., variability due to light limitation). In contrast, most of the remaining planning areas from the other three regions show interannual variability <10%. Low latitude areas are less sensitive to cloudiness as long as the cloud cover is not persistent over time.

Although interannual variability revealed no trend among the four regions (e.g., within the Alaska Region, the variability ranges from <4% to >50%, and the variability is similar among the other three regions), there is a clear trend in the seasonality (i.e., relative monthly variance) that increases from low-latitude areas to high-latitude areas. For the three regions of the contiguous U.S. (i.e., Atlantic, Gulf of Mexico, and Pacific), all planning areas exhibited <30% seasonality, with the exception of the Washington-Oregon, Western Gulf of Mexico, and North Atlantic planning areas. In contrast, in the Alaska Region, all areas (with the exception of the St. Matthew-Hall, Hope Basin, and Chukchi Sea planning areas) reflected >40% seasonality; highest seasonality (69%) was evident in the Aleutian Basin. This apparent trend in latitude-based seasonality is not simply a result of variability in solar insolation but is also influenced by several factors including water mixing and upwelling. Additional research into *in situ* data collection is needed to validate satellite-based observations, including the results of this analysis.

Comparisons Between 1990 and 2010 Primary Productivity Determinations

A majority of the data review and evaluation presented in the 1990 productivity summary focused on quantitative measurement (i.e., based on the Winkler oxygen technique, the Carpenter modification, or uptake of ^{14}C labeled bicarbonate [$H^{14}C0_3^-$]), as reported in the literature. The 1990 report presented daily and annual primary productivity estimates for each of the 26 OCS planning areas, with proper qualifications on data limitations.

Table ES-3 summarizes primary productivity information for each of the 26 OCS planning areas, comparing 1990 and 2010 primary productivity estimates on the basis of estimated annual production (g C m^{-2} y^{-1}). Estimates for 1990 were based exclusively on quantitative measurements conducted in the field or in the laboratory, as reported in the peer-reviewed and gray literature. The 2010 estimates are based on satellite-derived determinations using the NPP modeling approach.

Table ES-3. Comparison of 1990 and 2010 annual primary production determinations. Determinations were deemed similar if the range of annual production values overlapped. Bolded entries reflect those planning areas exhibiting dissimilar values between 1990 and 2010.

Region and Planning Area	Annual Primary Productivity (g C m^{-2} y^{-1})		Comparison Summary and Comments
	1990 Determinations	2010 Determinations	
Atlantic Region			
North Atlantic	260-455	337-418	Moderate seasonality, low interannual variability noted. 100% data coverage for the 12-y period analyzed.
Mid-Atlantic	**260-505**	**110-130**	Moderate seasonality, low interannual variability noted. 100% data coverage for the 12-y period analyzed. Large discrepancy between 1990 and 2010 estimates possibly due to insufficient sampling pre-1990.
South Atlantic	130-580	187-266	Moderate seasonality, low interannual variability noted. 100% data coverage for the 12-y period analyzed. 2010 estimates have a narrower range.
Straits of Florida	**7.6-35.4 (embayments)** **18.4 (coastal)**	**138-182**	Moderate seasonality, low interannual variability noted. 100% data coverage for the 12-y period analyzed. Large discrepancy between 1990 and 2010 estimates. Influence of the Gulf Stream noted. The 1990 estimates appear to be unreasonably low, when compared with the other Atlantic areas.

Table ES-3. (Continued).

Region and Planning Area	Annual Primary Productivity (g C m^{-2} y^{-1})		Comparison Summary and Comments
	1990 Determinations	2010 Determinations	
Gulf of Mexico Region			
Eastern Gulf of Mexico	50-800 (embayments) 89 (coastal, non-bloom) 164 (offshore)	202-289	Moderate seasonality, low interannual variability noted. 100% data coverage for the 12-y period analyzed. Generally comparable results between 1990 and 2010.
Central Gulf of Mexico	300-400 (coastal) 115-184 (offshore)	268-376	Moderate seasonality, low interannual variability noted. 100% data coverage for all 144 months (12 y).
Western Gulf of Mexico	**127-200 (embayments)** **103-176 (coastal)** **60-118 (offshore)**	**247-345**	Moderate seasonality, low interannual variability noted. 100% data coverage for the 12-y period analyzed. Large discrepancy between 1990 and 2010 estimates. The 1990 estimates appear to be unreasonably low when compared with the other Gulf of Mexico areas, perhaps due to uneven distribution of *in situ* measurements.
Pacific Region			
Southern California	275	218-327	Moderate seasonality, low interannual variability noted. 100% data coverage for the 12-y period analyzed. Significant annual trend (increasing).
Central California	275-325 (offshore-inshore gradient)	273-430	Moderate seasonality, low interannual variability noted. 100% data coverage for the 12-y period analyzed. Significant annual trend (increasing).
Northern California	300	264-313	Moderate seasonality, low interannual variability noted. 100% data coverage for the 12-y period analyzed. Significant annual trend (increasing).
Washington-Oregon	126->300 (river plume and oceanic to upwelling gradient)	272-351	Moderate seasonality, low interannual variability noted. 100% data coverage for the 12-y period analyzed. Significant annual trend (increasing).
Alaska Region			
Gulf of Alaska	**48-100 (offshore)** **200 (coastal)**	**259-291**	Strong seasonality, low interannual variability noted. Only 108 of the 144 months showed >75% data coverage. Large discrepancy between 1990 and 2010 estimates. The 1990 estimates are significantly lower than adjacent regions due to extremely limited database.
Cook Inlet	>300	367-449	Strong seasonality, low interannual variability noted. Only 108 of the 144 months showed >75% data coverage.
Kodiak	>300	207-245	Strong seasonality, low interannual variability noted. Only 108 of the 144 months showed >75% data coverage.
Shumagin	>300	191-254	Strong seasonality, low interannual variability noted. Only 119 of the 144 months showed >75% data coverage. Significant annual trend (decreasing).
Aleutian Arc	30-82 (waters S of the Aleutians) 100-200 (waters N of the Aleutians)	163-207	Strong seasonality, low interannual variability noted. Only 132 of the 144 months showed >75% data coverage.

Table ES-3. (Continued).

Region and Planning Area	Annual Primary Productivity (g C m^{-2} y^{-1})		Comparison Summary and Comments
	1990 Determinations	2010 Determinations	
N. Aleutian Basin	50-60 (Coastal Domain, non-upwelling) 220-240 (Coastal Domain, advection and upwelling) 166-188 (Central Domain) No annual production data available for the Outer Domain 1-2 (sea ice microalgae, est.)	221-381	Strong seasonality, moderate interannual variability noted. Only 100 of the 144 months showed >75% data coverage.
St. George Basin	200 (Central and Outer Domains; estimate extrapolated from N. Aleutian Basin data	202-323	Strong seasonality, moderate interannual variability noted. Only 105 of the 144 months showed >75% data coverage.
Bowers Basin	150-200	142-193	Strong seasonality, moderate interannual variability noted. Only 111 of the 144 months showed >75% data coverage.
Aleutian Basin	150-200	150-225	Extremely strong seasonality, moderate interannual variability noted. Only 108 of the 144 months showed >75% data coverage.
Navarin Basin	166-220	131-271	Strong seasonality, strong interannual variability. Only 88 of the 144 months showed >75% data coverage.
St. Matthew-Hall	50-70 (Coastal Domain) 160-200 (Central Domain)	180-285	Strong seasonality, moderate interannual variability noted. Only 74 of the 144 months showed >75% data coverage.
Norton Basin	50-70 (Norton Sound, AK Coastal Water) 285-324 (Anadyr/Bering Shelf Water)	273-415	Strong seasonality, moderate interannual variability noted. Only 70 of the 144 months showed >75% data coverage. Significant annual trend (increasing).
Hope Basin	50-70 (AK Coastal Water) 250-300 (Bering Sea Water) 13 (ice algae, Mar-June growth period)	149-313	Strong seasonality, strong interannual variability. Only 45 of the 144 months showed >75% data coverage. Significant annual trend (increasing).
Chukchi Sea	50-100 (AK Coastal Water, Cape Lisburne) 25-50 (AK Coastal Water, Pt. Barrow) 5 (ice algae, Mar-June growth period)	12-85	Strong seasonality, extremely strong interannual variability noted. Only 23 of the 144 months showed >75% data coverage. Significant annual trend (increasing). Limited coverage.
Beaufort Sea	1-20 (phytoplankton) 40 (shelf waters)	4-64	Strong seasonality, extremely strong interannual variability noted. Only 14 of the 144 months showed >75% data coverage. Limited coverage.

Overall, 22 of the 26 OCS planning areas exhibited similar productivity estimates in their minimal-maximal ranges between 1990 and 2010. Most planning areas exhibited 2010 productivity ranges that were comparable to the estimates developed in 1990. Given the completely different assessment and therefore independent methods between the two periods, this similarity provides strong support to the argument that model results (based on satellite data) provide excellent estimates of primary productivity (i.e., comparison of 1990 and 2010 primary productivity determinations indicate that the model-derived estimates are in good agreement with literature-based determinations). However, for the same reasons, it is impossible to determine whether or not there is a statistically significant trend between the two assessments. Further, because of differences in satellite instrumentation, algorithms, and spatial/temporal coverage, there remains continuing debate as to the potential for a consistent time series between the CZCS era (1978-1986) and the SeaWiFS/MODIS era (1998-present). Field data collection could provide validation of the current estimates and could be used as a baseline to evaluate future changes.

Four planning areas were identified where large discrepancies were evident (**Table ES-3**):

- Mid-Atlantic Planning Area: The current estimate of 110-130 g C m^{-2} y^{-1} is considerably lower than the 260-505 g C m^{-2} y^{-1} estimate developed in 1990;
- Straits of Florida Planning Area: The current estimate of 138-182 g C m^{-2} y^{-1} is considerably higher than the 1990 estimates of 7.6-35.4 g C m^{-2} y^{-1} (embayments) and 18.4 g C m^{-2} y^{-1} (coastal). No offshore annual estimate was provided in 1990;
- Western Gulf of Mexico Planning Area: The current estimate of 247-345 g C m^{-2} y^{-1} is considerably higher than the 1990 estimates of 127-200 g C m^{-2} y^{-1} (embayments), 103-176 g C m^{-2} y^{-1} (coastal), and 60-118 g C m^{-2} y^{-1} (offshore); and
- Gulf of Alaska Planning Area: The current estimate of 259-291 g C m^{-2} y^{-1} is considerably higher than the 1990 estimates of 48-100 g C m^{-2} y^{-1} (offshore) and 200 g C m^{-2} y^{-1} (coastal).

The primary reason for these discrepancies is attributed to differences in the sampling frequency and coverage. Satellites provide the most frequent measurements and synoptic coverage even after cloud screening for most areas, while *in situ* sampling is often limited in both space and time, and therefore more prone to spatial-temporal aliasing.

The limitations of using ^{14}C-based primary production to characterize large areas, as well as the uncertainty of scaling ^{14}C-based measurements (carbon uptake m^{-2} d^{-1}) to estimate annual production, are problematic. Because the modeled NPP uses monthly averages derived by averaging 9-km resolution data over a 12-y period for each planning area, the modeled NPP should provide a far more accurate estimate of primary production than is possible from a synopsis of literature for the various planning areas.

Using the same satellite data, several studies have shown a decreasing trend in surface chlorophyll in the subtropical gyres in the past decade and that the areas of low-chlorophyll gyres are expanding. These declines could be a result of enhanced surface-water stratification due to temperature increases. More recently, several authors have synthesized all available information in the past century to assess changes in phytoplankton biomass on decadal to centennial timescales, and over regional to global spatial scales. They showed statistically significant long-term decreases in surface chlorophyll in 8 of the 10 ocean basins, and for the global aggregate; most changes are on the order of 0.01 mg m^{-3} y^{-1}. They also found a strong correspondence between the chlorophyll change and changes in both leading climate indices (e.g., El Niño-Southern Oscillation [ENSO]) and ocean thermal conditions. However, on short-term scales, the "trends" depend heavily on the chosen years as well as on the algorithms. In the current assessment, the temporal span (i.e., 1990–2010) is relatively short. In addition, the methods used to derive primary productivity estimates were different between the 1990 and 2010 estimates. Therefore, only qualitative conclusions can be drawn from the 1990-2010 comparisons (i.e., 22 of the 26 OCS areas showed similar annual ranges, while the remaining four showed large differences). As satellite ocean color data become continuously available in the future, however, rigorous comparison between the current estimates and future estimates of primary productivity of the 26 OCS planning areas will be feasible.

ES.7 Primary Productivity Literature Updates

Review and summarization of available primary productivity data for the four major OCS regions – Atlantic, Gulf of Mexico, Pacific, and Alaska – for the period 1988 through 2009 provided an update of the water column primary productivity database initially established in 1990. Summary information from this literature review provided insight into the major oceanographic programs being conducted in nearshore and OCS waters, the relevance of acquired data to primary productivity determinations, and the nature of the research being conducted to determine mechanisms and processes affecting primary productivity.

ES.8 Secondary and Tertiary Productivity

There are only two software tools that are well developed and useful for estimating secondary and tertiary productivity: Atlantis and Ecopath. Atlantis is relatively new; there is only one recent effort to use this model in the U.S. (i.e., within Chesapeake Bay). In contrast, Ecopath has been in development since 1984 and there numerous users worldwide. In the U.S., the Ecopath model has been applied to all of the OCS regions, including many of the OCS planning areas. Other ecological modeling approaches are either focused on biogeochemical processes, only planktonic processes, or only portions of the biology of specific groups. Another possible approach is to use empirical data; such data can only estimate stocks, not production rates, because there are no methods for measuring secondary or tertiary production directly in the field. Consequently, the only approach that met the consideration criteria was Ecopath modeling.

Ecopath

Ecopath model results for U.S. OCS ecosystems were reviewed, and secondary productivity estimates were summarized for each planning area. Total system-wide productivity ranged from 410 t km^{-2} y^{-1} in the Gulf of Alaska to 15,466 t km^{-2} y^{-1} in Looe Key, FL (**Table ES-4**; **Figure ES-6**). This productivity estimate for Looe Key is clearly being driven by the high primary production and benthic production associated with coral reefs. Excluding the value from Looe Key and comparing only open ocean sites, the highest value is 2,817 t km^{-2} y^{-1}, found in the Eastern Subarctic Pacific Basin, which would include all or portions of the Gulf of Alaska, Kodiak, and Shumagin planning areas (**Table ES-5**).

Table ES-4. Characteristics of study areas where Ecopath models exist by region. Areas <100,000 km^2 were classified as local.

Study Area	Spatial Scale	Approximate Area (km^2)	Number of Functional Groups	Planning Area	System 2^o and 3^o Productivity (t km^{-2} y^{-1})	Data Time Frame
Atlantic						
Gulf of Maine	Local	NA	36*	NOA	1,361	1996-2000
Georges Bank	Local	NA	36*	NOA	1,641	1996-2001
Long Island Sound	Local	3,400	32	NOA	1,965	1995-2005
Mid-Atlantic Bight	Regional	111,200	55	NOA, MDA	1,587	1995-1998
SE U.S. continental shelf	Regional	174,300	42	MDA, SOA	1,076	1995-1998
Looe Key, Florida	Local	30	20	FLS	15,466	late 1980's - early 1990's
Gulf of Mexico						
Gulf of Mexico	Regional	Gulf-scale	63	WGM, CGM, EGM	764	1950-2004
West Florida Shelf	Regional	>170,000	59	EGM	1,078	2000
Pacific						
N California Current	Regional	NA	63	NOC, WAO	1,012	1990's
Alaska						
E Bering Sea, Gulf of Alaska	Regional	1,500,000	56	ALA, GEO, MAT, NAL, SHU, KOD, GOA, COK	1,184	1950-2005
E Bering Sea	Regional	NA	148*	NAL, GEO, MAT, NAV	614	1991
Gulf of Alaska	Regional	NA	138*	SHU, KOD, GOA	410	1990-1993
SE Alaska shelf	Regional	93,351	39	GOA	657	1999
E Bering Sea	Regional	495,218	148	NAL, GEO, MAT	613	1990-1994
Gulf of Alaska	Regional	291,840	138	SHU, KOD, GOA, COK	410	1990-1994
Aleutian Islands	Local	56,936	140	ALA	1,011	1990-1994
E Subarctic Pacific Basin	Regional	3,622,000	55	SHU, KOD, GOA	2,817	late 1980's - early 1990's
W and C Aleutian Islands	Local	56,936	40	ALA	862	1991

*Trophic groups for these models were aggregated into 17 common groups by the authors for comparison of ecosystems

Key to Planning Area abbreviations: North Atlantic (NOA), Mid-Atlantic (MDA), South Atlantic (SOA), Florida Straits (FLS), Eastern Gulf of Mexico (EGM), Central Gulf of Mexico (CGM), Western Gulf of Mexico (WGM), Northern California (NOC), Washington-Oregon (WAO), Chukchi Sea (CHU), Navarin Basin (NAV), North Aleutian Basin (NAL), St. Georges Basin (GEO), Cook Inlet (COK), Gulf of Alaska (GOA), Shumagin (SHU), Kodiak (KOD), Aleutian Arc (ALA), and St. Matthew-Hall (MAT).

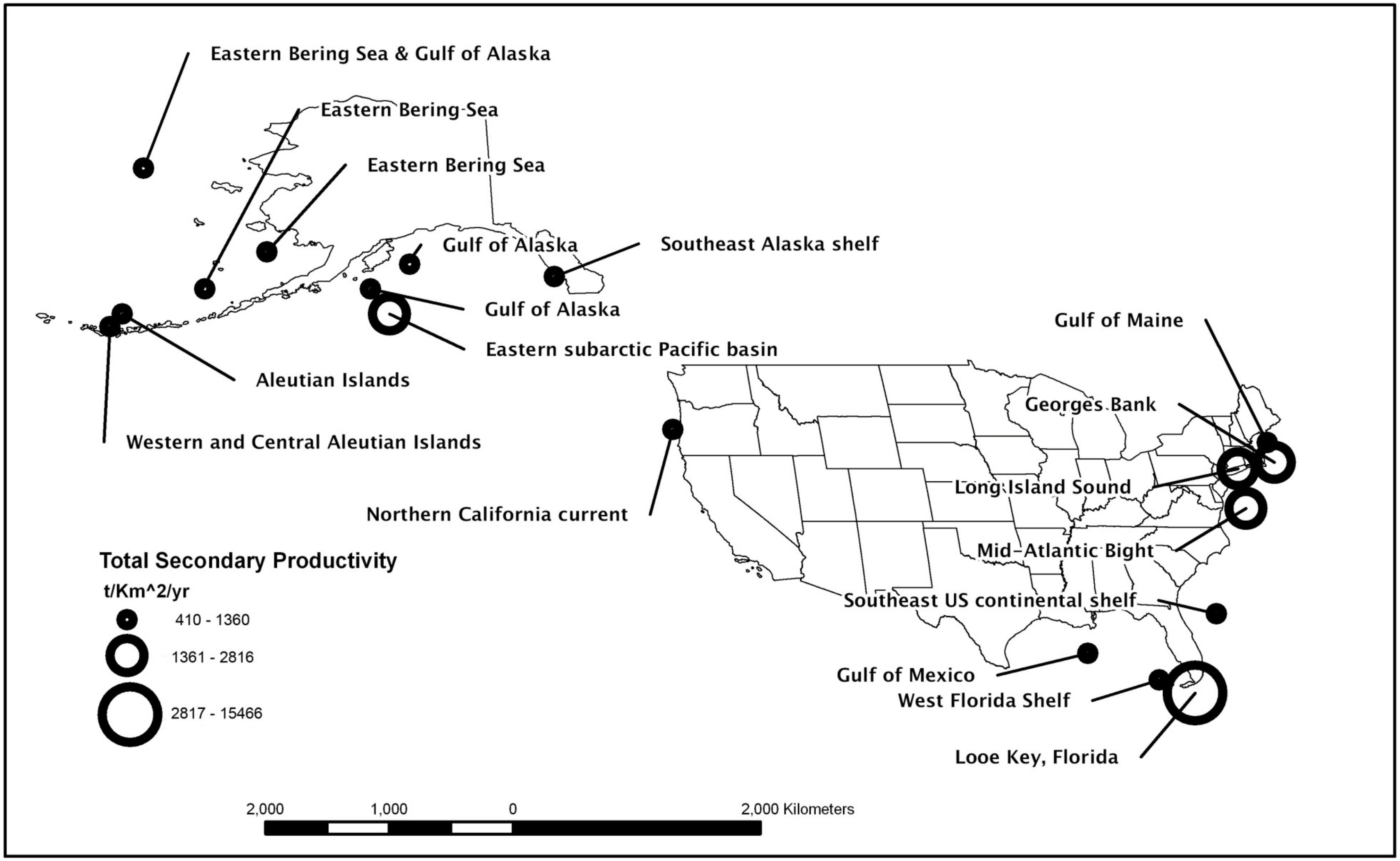

Figure ES-6. Bubble plot of productivity (t km^{-2} y^{-1}) values from Ecopath models in the Outer Continental Shelf regions. Values are from **Table ES-4**.

Table ES-5. Summary of the annual productivity data from Ecopath models. Mean values calculated from individual Ecopath modeling efforts by planning area, as presented in **Table ES-4**.

Study Area	Productivity (t km^{-2} y^{-1})								
	System	PEL	DEM	SKR	MAM	CMB	BEN	ZOP	PPD
Overall Mean	1,918	37	53	0.2	5	119	816	934	7,161
Overall Mean (w/o Looe Key)	1,121	15	14	0.2	5	49	216	836	5,810
Gulf of Mexico	921	24	15	1.15	0.00	53	348	481	6,934
Atlantic (w/o Looe Key)	1,526	15	8	0.05	0.02	60	293	1,149	6,695
Pacific	1,012	5	52	0.21	0.02	12	128	814	6,618
Alaska	953	14	13	0.06	8.19	46	146	743	4,979

Abbreviations: PEL = pelagic fishes, DEM = demersal fishes, SKR = sharks and rays, MAM = marine mammals, CMB = crustaceans, molluscs, and other mega-benthos, BEN = macro-, meio-, and micro-benthos, ZOP = zooplankton, PPD = primary producers, SYSTEM = total ecosystem secondary and tertiary productivity, excluding PPD.

On average, the Atlantic has the highest system productivity, followed (in descending order) by the Pacific, Alaska, and Gulf of Mexico regions. At the level of this broad comparison among regions, all of the values are in the same order of magnitude.

This study identified several significant limitations in the use of Ecopath modeling results for secondary and tertiary production comparisons among planning areas:

- Results are not available for all planning areas. Ecopath modeling studies were found that are applicable to all four Atlantic planning areas (especially North Atlantic), all three Gulf of Mexico planning areas, two Pacific planning areas (Northern California and Washington/Oregon), and parts of nine Alaska planning areas (Aleutian Arc, Cook Inlet, Gulf of Alaska, Kodiak, Navarin Basin, North Aleutian Basin, Shumagin, St. Georges Basin, and St. Matthew-Hall.)

- Most of the Ecopath modeling studies focused on a particular ecosystem and did not define a geographic delimited “study area.” To develop a secondary productivity estimate for an entire planning area, it would be necessary to model all of the ecosystems and develop a composite estimate based on the spatial extent of each ecosystem.

- Unlike the primary productivity modeling estimates derived in **Section 3**, the Ecopath modeling estimates would be difficult to validate by measuring secondary production directly in the field.

Empirical Measures

Zooplankton sampling coverage was extremely variable across the 26 OCS planning areas. Extensive, multiyear (and seasonal) sampling efforts were noted for the Southern California Planning Area (i.e., California Cooperative Oceanic Fisheries Investigations [CalCOFI]), North and Mid-Atlantic planning areas, and several of the southernmost Alaska planning areas (i.e., Gulf of

Alaska, Kodiak, Cook Inlet, and Shumagin). Other planning areas had very limited zooplankton sampling coverage (e.g., South Atlantic, Straits of Florida, Navarin Basin, St. Matthew-Hall, Norton Basin, Hope Basin) or no coverage at all (Chukchi Sea, Beaufort Sea). Disproportionate sampling (e.g., lack of multiyear and/or seasonal coverage; preference for shallow sampling) was also evident. Several planning areas have inconsistent coverage, where zooplankton data are available for some years but not for others, or where only selected seasons have been sampled.

Commercial fisheries landings were also considered as a potential indicator of tertiary production. In the Atlantic Region, Virginia (Mid-Atlantic Planning Area) and Massachusetts and Maine (North Atlantic Planning Area) reported the highest landings by weight. In the Gulf of Mexico Region, LA (Central Gulf of Mexico Planning Area), landings were dominant among the Gulf states. In the Pacific Region, California landings (including Southern California, Central California, and Northern California planning areas) were slightly higher than those shown for Washington and Oregon (Washington-Oregon Planning Area). Alaska statewide landings were exceptionally high compared to all other states.

Inherent difficulties in assessing all landings data were identified. While landings may be reported for a particular state, it is not easily determined where (i.e., from what planning area) fish were caught because landings (as required by Federal fisheries authorities) are recorded on the basis of port landed, not area fished. This problem is particularly acute in the Alaska landings data because of the high number of planning areas and their geographic coverage relative to the number of ports. These inherent issues with fisheries data utility, particularly as they related to estimating secondary and tertiary productivity on a planning area basis, are problematic. Given current reporting requirements, there are no solutions available to rectify this identified limitation.

ES.9 Secondary and Tertiary Productivity Methods and Literature Updates

In the past evaluation of biological productivity conducted in 1990, water column primary productivity served as the basis for a comparison of production among the 26 OCS planning areas. While using primary productivity alone is valid, and much can be learned by examining the processes of primary producers in ecosystems, it is also useful to examine productivity of higher trophic levels such as secondary and tertiary consumers of primary production. One objective of the current analysis was to evaluate current methods used to estimate secondary and tertiary productivity of marine ecosystems. Measurement methods (e.g., bioenergetics, allometric relationships) and modeling approaches (e.g., Atlantis, Ecopath, NPZ models) were reviewed and critically evaluated.

The Ecopath modeling approach was chosen for several reasons:

- Ecopath is a well developed modeling system that has many adherents, scientific acceptance, and much technical support;
- The data required for Ecopath are relatively available;
- There are already many Ecopath models available for OCS planning areas; and
- It would present a consistent approach for comparison across the nation as a whole.

Ecopath models were originally developed for fisheries management applications but have been extended to also serve as effective risk assessment and decision support tools. This approach can be used to estimate productivity at an ecosystem scale and enable ecosystem comparisons (e.g., when multiple modeling efforts have been conducted). This modeling approach can also be used to predict ecosystem and socioeconomic responses to oil and gas related activities, including exploration, production, shoreline development, and oil spills. While Ecopath enables risk assessment of oil and gas activities and spills by predicting the ecosystem responses to these various influences, the model can also be used as a support tool for making decisions about oil and gas leasing in the OCS planning areas by exploring various policy options via models implementation in the real world.

The Ecopath modeling approach is the most commonly used when characterizing secondary productivity, noted in approximately 350 publications. Its widespread use by scientists has demonstrated its capability in a number of applications.

ES.10 Empirical Measures Related to Secondary and Tertiary Production

Two empirical measures of secondary and tertiary production were evaluated, including zooplankton biomass and commercial fishery landings. Zooplankton biomass data are readily available from field sampling studies and are routinely monitored in some areas, however, there are database limitations evident, as noted previously. For zooplankton data, the Coastal and Oceanic Plankton Ecology, Production and Observation Database (COPEPOD) database was accessed and summarized. Commercial fisheries landings were also considered as a potential indicator of tertiary production. Landings reported to the National Marine Fisheries Service were accessed and summarized to characterize commercial fisheries information. Empirical measurements provide mainly stock assessments. By using allometric relationships, it is possible to convert biomass to productivity estimates, but there are inherent difficulties and assumptions about the use of constants in place of dynamic coefficients.

ES.11 Conclusions and Recommendations

Primary Production

Each of the 26 planning areas was characterized in terms of areal coverage, mean annual NPP, annual and monthly variance, and trend over the 12-y period of 1998 through 2009. Productivity determinations were depth-integrated, extending from the ocean surface to the euphotic depth (i.e., the depth where 1% of the surface light, or photosynthetically available radiation [PAR]), is available). This depth ranged from a maximum of 100 m (e.g., within ocean gyres) down to several meters (e.g., within eutrophic coastal waters). Graphic representations were developed for each planning area and included NPP, total NPP, and annual NPP. Comparison of 1990 and 2010 primary productivity determinations indicate that the model-derived estimates derived in the present analysis are in good agreement with literature-based determinations; 22 of the 26 OCS planning areas exhibited similar productivity estimates, based on minimal-maximal ranges. Given the completely different assessment and therefore independent methods between the two periods, this similarity provides strong support to the argument that model results (based on satellite data) provide excellent estimates of primary productivity.

Within the 1998-2009 primary productivity data set, significant variability in primary productivity determinations was evident, particularly in the Alaska Region. While some of this variability may be attributed to planning area-specific oceanographic features and/or local processes, some variability may be reflective of the data acquisition method. The accuracy of satellite-derived productivity estimates may be affected by one or more factors, including:

- chlorophyll-*a* concentration can be significantly overestimated (>100%) from satellite measurements (particularly in the Alaska Region) due to algorithm artifacts in the atmospheric correction and bio-optical inversion;
- Seasonal solar insolation effects are evident (i.e., predominantly in the Alaska Region); and
- Uniform application of the NPP model may be slightly problematic for marginal seas and areas of upwelling.

As a result of these identified limitations, future efforts should include extensive *in situ* data to validate satellite-based observations (including the results of this analysis) and application of the NPP model. This recommendation is particularly noteworthy of those planning areas at higher latitudes (i.e., within the Alaska Region).

Secondary Production

Ecopath

A total of 18 Ecopath models for U.S. OCS ecosystems was reviewed, and secondary productivity estimates were summarized. Data employed in the Ecopath modeling efforts extended from the 1950’s through 2005, although most data sources were from the 1990’s (**Table ES-4**). While not all planning areas fell within the area of study for the Ecopath model results, secondary productivity estimates for each region were available.

Data gaps were noted in regards to data/sampling effort and model development. Several important ecosystems have not been sampled adequately to provide reliable input data for Ecopath models, while many systems have not been modeled at all. There are also major problems associated with applying a productivity estimate and multiplying that value by total surface area to estimate total system productivity. Productivity at the ocean surface and productivity within the water column are different; it is difficult to estimate one based on the other, and accurate data are often difficult to obtain for total productivity within the water column. To further complicate this issue, some habitats are especially difficult to sample (e.g., deep benthic communities, Arctic habitats).

The challenges associated with parameter uncertainty are based on the current status of Ecopath model application and recognized limitations. Ecosystem modeling will be key for developing representative productivity estimates for each planning area, however, additional data acquisition and model revision are required. While Ecopath is currently the most popular and widely used ecosystem modeling approach, it still has major limitations. A model is only as good as the data used to estimate parameters. Thus, if quality data do not exist for an ecosystem, a scientifically sound ecosystem model cannot be developed. Also, many of the Ecopath models are recycling parameters from other models without further verification of the accuracy of model parameters. Further development and calibration of models is needed to increase confidence in model estimates of productivity.

NPZ

For broad-scale, comparable modeling, the NPZ approach may be very useful in the future. It is now possible to obtain maps of chlorophyll, biomass, and rates of primary production globally using satellite technology. Zooplankton biomass data are also widely available from field sampling studies, and are routinely monitored in some areas. Therefore, with sufficient high-resolution nutrient data, it should be possible to create secondary production maps for the whole globe (and OCS planning areas) at relatively fine-spatial scales.

Based on this most recent analysis of the NPZ modeling approach, there appear to be sufficient zooplankton data for most planning areas. However, the nutrient database is, at present, deficient. Identified limitations with the NPZ approach include the fact that only surface productivity would be calculated, leaving data gaps for fishes and benthos. It is suggested that coupling of NPZ and Ecopath in the future may be feasible.

Empirical Measures

Two empirical measures of secondary and tertiary production were evaluated as part of this analysis, including zooplankton biomass and commercial fishery landings. Zooplankton biomass data are widely available from field sampling studies and are routinely monitored in some areas. Based on access to the COPEPOD database, zooplankton sampling coverage was extremely variable across the 26 OCS planning areas. Disproportionate sampling (e.g., lack of multiyear and/or seasonal coverage; preference for shallow sampling) was also evident. Several planning areas have inconsistent coverage, where zooplankton data are available for some years but not for others, or where only selected seasons have been sampled.

Commercial fisheries landings were also considered as a potential indicator of tertiary production. Landings data were available for all regions, however, data limitations were evident. Further, inherent difficulties in assessing all landings data were identified. While landings may be reported for a particular state, it is not easily determined where (i.e., from what planning area) fish were caught. This problem is particularly acute in the Alaska landings data due to the high number of planning areas and their geographic coverage relative to the number of ports.

Table of Contents

Page

Page

Page

List of Figures

List of Figures
(Continued)

List of Tables

List of Abbreviations and Acronyms

ACC	Alaska Coastal Current
ACIA	Arctic Climate Impact Assessment
AVHRR	Advanced Very High Resolution Radiometer
BATS	Bermuda Atlantic Time Series
BOEMRE	Bureau of Ocean Energy Management, Regulation and Enforcement
C	carbon
CalCOFI	California Cooperative Oceanic Fisheries Investigations
CCE LTER	California Current Ecosystem Long-Term Ecological Research
CCS	California Current System
CDOM	colored dissolved organic matter
CO_2	carbon dioxide
COAST	Coastal Advances in Shelf Transport
CODE	Coastal Ocean Dynamics Experiment
CoOP	Coastal Ocean Processes
COPEPOD	Coastal and Oceanic Plankton Ecology, Production and Observation Database
CSA	Continental Shelf Associates, Inc.
CTZ	Coastal Transition Zone
CZCS	Coastal Zone Color Scanner
DIN	dissolved inorganic nitrogen
DMS	dimethylsulfide
EBM	ecosystem-based management
EcoFOCI	Ecosystems and Fisheries-Oceanography Cooperative Investigation Program
ECOHAB	Ecology and Oceanography of Harmful Algal Blooms
EcoMon-RV	Ecosystem Monitoring Research Vessel Surveys
ENSO	El Niño-Southern Oscillation
ESI	Environmental Sensitivity Index
ETS	electron transport system
EwE	Ecopath with Ecosim
FRRf	Fast Repetition Rate fluorometry
GAC	global area coverage
GIS	geographic information system
GLOBEC	Global Ocean Ecosystems Dynamics
GNATS	Gulf North Atlantic Time Series
GPP	gross primary production
GSFC	Goddard Space Flight Center
HICO	Hyperspectral Imager for the Coastal Ocean
HNLC	high-nutrient low-chlorophyll
HOT	Hawaii Ocean Time-series
HPLC	high performance liquid chromatography
IPCC	Intergovernmental Panel on Climate Change
ISO	intraseasonal oscillation
JGOFS	Joint Global Ocean Flux Study
JPL	(NASA) Jet Propulsion Laboratory
LAC	local area coverage
LME	large marine ecosystem
LTOP	Long Term Oceanographic Program
MERIS	Medium Resolution Imaging Spectrometer
MMbbl	million barrels
MMS	Minerals Management Service
MOBY	Marine Optical Buoy
MODIS	Moderate Resolution Imaging Spectrometers

N	nitrogen
NASA	National Aeronautics and Space Administration
NMFS	National Marine Fisheries Service
NOAA	National Oceanic and Atmospheric Administration
NPDES	National Pollutant Discharge Elimination System
NPP	net primary productivity
NPZ	nutrient-phytoplankton-zooplankton
NRC	National Research Council
NRL	U.S. Naval Research Laboratory
OCS	Outer Continental Shelf
OCSLA	Outer Continental Shelf Lands Act
ODP	Ocean Drilling Program
ORCAWALE	Oregon, California, and Washington Line-transect Expedition
P	phosphorus
P/B	production/biomass ratio
P*e*	production efficiency
PAR	photosynthetically available radiation
PDO	Pacific Decadal Oscillation
PNP	potential new production
PPD	primary producers
PROBES	Processes and Resources of the Bering Sea
RISE	River Influences on Shelf Ecosystems
RMS	root mean square
ROI	region-of-interest
ROMS	Regional Ocean Modeling System
SAB	South Atlantic Bight
SBF	synthetic-based drilling fluid
SEAMAP	Southeast Monitoring Assessment Program
SeaWiFS	Sea-viewing Wide Field-of-view Sensor
SNR	signal-to-noise ratio
SSC	sea surface chlorophyll
SST	sea surface temperature
USDOI	U.S. Department of the Interior
VGPM	Vertically Generalized Production Model
WBF	water-based drilling fluid
WEST	Wind Events and Shelf Transport

1.0 Introduction

This report presents marine productivity estimates for the 26 planning areas of the Federal Outer Continental Shelf (OCS). The study was sponsored by the Bureau of Ocean Energy Management, Regulation and Enforcement (BOEMRE; formerly Minerals Management Service [MMS]). By law, marine productivity is one of the factors that the agency must consider in its OCS Oil and Gas Leasing Program. The most recent estimates were prepared 20 y ago, and updated estimates are needed for ongoing decision-making and future program documents.

Marine primary production comes from three main sources: phytoplankton, microphytobenthos, and macrophytobenthos. Seagrasses, mangroves, and kelp are major primary producers in coastal and estuarine ecosystems. For the three major marine primary producers, production ranges from 50-300 g C m^{-2} y^{-1} for phytoplankton, from 20-300 g C m^{-2} y^{-1} for microphytobenthos, and from 500-2,000 g C m^{-2} y^{-1} for macrophytobenthos (Charpy-Roubaud and Sournia 1990). Habitat for phytoplankton is much more abundant as micro- and macrophytobenthic species are limited to benthic habitats. Thus, the majority of marine primary production is obtained through phytoplankton (Charpy-Roubaud and Sournia 1990). Consequently, phytoplankton has been considered to be a primary source for estimated primary productivity in marine ecosystems. Additionally, because the primary interest of BOEMRE is the Federal OCS and its 26 OCS planning areas, an emphasis has been placed on marine, rather than coastal, primary producers.

What is Marine Productivity?

Marine productivity is a broad term that can include water column and/or benthic sources. In this report, ***production*** is defined as the generation of biomass within the environment of interest – that is, biomass elaboration (Miller 2004).

Productivity is the rate of production (biomass elaborated per unit time). For primary producers such as phytoplankton, this is done by photosynthesis (primary production). Secondary production is the conversion of energy from primary producers by consumers to produce new biomass. Tertiary production is the conversion of energy from prey by higher-trophic level predators. In some studies, all production higher than primary is referred to as secondary production.

1.1 Background

Under the Outer Continental Shelf Lands Act (OCSLA), the U.S. Department of the Interior (USDOI) is responsible for the administration of mineral exploration and development of Federal lands. Within the USDOI, the BOEMRE is responsible for managing ocean energy and mineral resources on the OCS. The program is national in scope and includes 26 OCS planning areas within four regions (**Figure 1**): three in the Gulf of Mexico, four in the Atlantic, four in the Pacific, and 15 in Alaska.

Section 18(a)(2) of the OCSLA Amendments of 1978 specifies eight factors that the USDOI must consider in the timing and location of OCS oil and gas activities, including “the relative environmental sensitivity and marine productivity of different areas of the OCS.” To comply with this requirement, the MMS sponsored several studies of marine productivity.

Figure 1. Planning areas for the Outer Continental Shelf Oil and Gas Leasing Program.

Initial draft productivity estimates were prepared by the University of Maryland Eastern Shore (UMES) (UMES 1985). Continental Shelf Associates, Inc. (CSA) (CSA 1990) analyzed water column primary productivity data and prepared a report on benthic primary productivity (CSA 1991a) and a feasibility analysis of secondary productivity measures (CSA 1991b). The benthic productivity report included mangroves, coastal marshes, seagrasses, macroalgae, benthic diatoms, coral reefs, macroalgal turf, blue-green algae, and chemosynthetic associations.

The MMS selected water column primary productivity estimates from CSA (1990) as one of the factors for comparisons among planning areas. These data were used in the Proposed Revised Program for 2007–2012 (MMS 2007a) and the Draft Proposed Program for 2010–2015 (MMS 2009). USDOI has also considered productivity estimates in conjunction with its utilization of shoreline Environmental Sensitivity Index (ESI) characteristics within previous 5-y programmatic documents. Meaningful comparisons based on other productivity measures were found to be problematic. Benthic primary productivity comparisons are complicated by geographic differences in types and areal extent of producers as well as by methodological problems and inconsistencies (CSA 1991a). No suitable method was identified for consistently estimating total secondary or tertiary productivity (CSA 1991b).

The CSA (1990) report also estimated the areal extent of coastal and marine habitats for "environmental sensitivity" comparisons among planning areas. The MMS subsequently selected the ESI Shoreline database developed by the National Oceanic and Atmospheric

Administration (NOAA) for this purpose (MMS 2007a, 2009). Consequently, this study does not include updating the coastal and marine habitat acreage from the earlier report.

1.2 Objectives and Scope

The goal of this study was to provide the BOEMRE with current estimates of marine productivity for the 26 OCS planning areas. Specific objectives were to evaluate current methods of estimating marine productivity, to select the preferred method or methods, and, using the preferred method, to develop updated estimates for all OCS planning areas. This included updating the CSA (1990) report to the present state of knowledge on water column primary productivity and secondary/tertiary productivity.

1.3 Study Methods

Results of the 1990 productivity assessment indicated that water column primary productivity was an excellent metric for estimating marine productivity. The BOEMRE determined that a review of existing methodology for estimating water column primary productivity, including evaluation of the latest methods and available technology for data acquisition and interpretation, should be the main focus for updating productivity estimates. This methodology is sufficiently developed to offer the best chance of consistent, comprehensive estimates across planning areas. For secondary and tertiary productivity, the focus was on evaluating methods that hold the best promise for developing comprehensive estimates, and searching for published results applicable to the planning areas.

The study consisted of four main tasks, with the corresponding Principal Investigators:

- Evaluation of primary productivity methods – Douglas Biggs and Chuanmin Hu;
- Development of primary productivity estimates for OCS planning areas – Chuanmin Hu;
- Primary productivity literature updates – Douglas Biggs (Atlantic and Gulf of Mexico), Brian Balcom (Pacific), and Dean Stockwell (Alaska); and
- Secondary and tertiary productivity methods and literature updates – Paul Montagna.

A complete list of preparers and their affiliations is presented in **Appendix A**.

1.3.1 Evaluation of Primary Productivity Methods

Current methods for estimating marine primary productivity were evaluated, including a discussion of data sources (e.g., remote sensing and other methods) and data analysis or calculation methods. The evaluation of available modeling approaches included characterizing the various types of models currently used to estimate depth-integrated primary productivity from satellite measurements of the ocean. Important considerations included 1) scientific acceptance (whether the method has been published in peer-reviewed literature and been generally accepted and used in other studies); 2) data requirements; 3) spatial and temporal resolution (including whether the method can provide details of “hot spots” and seasonal productivity peaks within a planning area); 4) potential uncertainties and biases in the predictions; and 5) the degree to which the method lends itself to readily updating productivity estimates in the future.

1.3.2 Development of Primary Productivity Estimates for OCS Planning Areas

The earlier primary productivity review (CSA 1990) developed estimates by tabulating individual studies conducted in each planning area. The major problem noted in the report was "the lack of a consistent and uniform database," as evidenced by studies conducted in different areas employing different methodologies, sampling at different spatial scales, and/or sampling at different frequencies.

Because of advances in modeling, satellite imagery, and online databases that were not available 20 y ago, the approach in the current study was fundamentally different. Several models are now available to estimate photosynthetic rates from satellite-based measurements of chlorophyll concentrations. This study used the Vertically Generalized Production Model (VGPM) (Behrenfeld and Falkowski 1997a) to estimate net primary productivity (NPP) in each planning area as a function of chlorophyll, available light, and photosynthetic efficiency. NPP is gross primary productivity minus respiration. Data for input to the model were derived from satellite observations in each planning area. Methods are explained in **Section 2.6**.

1.3.3 Primary Productivity Literature Updates

The water column primary productivity database compiled by CSA (1990) was updated, with an emphasis on the published literature and reports for each planning area. A search of electronic databases was completed, and the data were reviewed and evaluated. Data sources of interest included 1) results from studies that measured rates of marine primary and secondary production; 2) results from studies that measured marine biomass or standing stocks; 3) relationships between marine biomass and productivity; and 4) relationships between size (length or marine biomass), respiration (or metabolism), and growth (or productivity).

A total of 11 electronic databases was queried, using search criteria largely similar to those reviewed during development of the 1990 report. The literature search included potential data sources dating back to 1988. Electronic databases included:

- Aquatic Sciences and Fisheries Abstracts (ASFA);
- BIOSIS Previews® (1926-present);
- Dissertation Abstracts Online;
- Enviroline®;
- GEOBASE™;
- Inside Conferences;
- National Technical Information Service (NTIS);
- Oceanic Abstracts;
- SciSearch® – a Cited Reference Science Database (1974-1989 and 1990-present); and
- Zoological Record Online®.

For marine primary productivity, the updated search criteria included

- ocean color;
- remote sensing;
- satellite;
- chlorophyll;
- marine primary production (productivity);
- phytoplankton production (productivity);
- VGPM; and
- SeaWiFS.

Geographic descriptors were used to narrow the search to U.S. Federal waters. Each of the OCS planning areas, or corresponding bodies of water, was used during the search.

Report authors were provided a list of titles from the initial computer literature search. Based on title review and author interest, abstracts were retrieved and reviewed. When an abstract indicated that a particular article or data source was relevant, the complete article was obtained. The search turned up 614 titles and from those, 319 full citations/abstracts were requested.

1.3.4 Secondary and Tertiary Productivity Methods and Literature Updates

Secondary and tertiary productivity measurement and calculation methods were reviewed and evaluated. This task included a consideration of new tools and approaches, such as allometric relationships and recent developments in modeling (e.g., the Ecopath model, the nitrogen-phytoplankton-zooplankton [NPZ] model). Important considerations in this review and evaluation were similar to those noted for primary productivity (i.e., scientific acceptance, data requirements, spatial and temporal resolution, potential uncertainties and biases in the predictions, and the degree to which each method lends itself to readily updating productivity estimates in the future.

As part of this task, a literature search was also conducted with the methods previously described. For secondary and tertiary productivity data sources, the following search terms were used:

- NPZ and/or N-P-Z;
- Ecopath;
- Ecosim;
- Ecospace;
- allometry;
- allometric relationships;
- bioenergetics;
- metabolism;
- secondary production (productivity);
- respiration;
- trophic dynamics; and
- food webs.

Based on the literature review and subsequent evaluation (**see Section 5**), the Ecopath modeling approach was chosen for further investigation. Eighteen Ecopath modeling studies were found that were applicable to one or more planning areas, and these modeling results were tabulated for comparison. Empirical methods available to address secondary productivity were also characterized through a review of pertinent data sources.

1.4 Report Organization

The report consists of six main sections:

- **Section 2** reviews and evaluates methods for estimating water column primary productivity.
- **Section 3** presents estimates of water column primary productivity for each planning area based on the VGPM modeling approach.
- **Section 4** updates the primary productivity literature for each planning area.
- **Section 5** reviews methods for estimating secondary and tertiary productivity and summarizes Ecopath modeling results applicable to the planning areas.
- **Section 6** outlines the empirical measures available to characterize secondary and tertiary production.
- **Section 7** compares productivity among planning areas, addresses the potential impacts of OCS activities and climate change on productivity, outlines study problems and limitations, and makes recommendations.

Literature cited is presented in **Section 8**. Additional supporting information is presented in **Appendices A** (List of Preparers), **B** (The Ecopath Model), **C** (Supporting Maps and Figures for Zooplankton Biomass and Fisheries Landings), and **D** (Analysis of Outer Continental Shelf Activities).

2.0 Evaluation of Primary Productivity Methods

2.1 Sources of Primary Productivity Data

Most of the data review and evaluation conducted by CSA (1990) focused on quantitative measurement of the evolution of oxygen using the Winkler oxygen technique and/or the Carpenter modification of that technique, and on the uptake of ^{14}C labeled bicarbonate ($H^{14}CO_3$). Both techniques have undergone continuous modification by limnologists and oceanographers since these methodologies were introduced in the mid-20th century as a means of quantifying changes in light bottle versus dark bottle evolution of O_2 and uptake of ^{14}C.

Because both the oxygen and ^{14}C methods are a mosaic of different methodologies, CSA (1990) identified an existing disagreement among primary productivity experts as to what these techniques actually measure. Most researchers felt that "standard" 24-h incubations with $H^{14}CO_3^-$ in fact measure something between net and gross primary productivity. Consequently, research conducted since 1990 has generally involved much shorter term (i.e., generally only 30-150 minutes) uptake experiments with $H^{14}CO_3^-$ in which smaller volumes of algal cultures and/or natural populations of phytoplankton from three or more different depths are exposed to a series of different light intensities. Results are subsequently used to describe photosynthesis versus irradiance behavior in order to generate "P vs. I" curves by the "photosynthetron" technique (i.e., Maranon and Holligan 1999; Prieto et al. 2008).

Moreover, measurements of primary production carried out in the 1960's and 1970's were usually done using $H^{14}CO_3^-$ stock solutions that likely had trace metal contamination. Subsequent researchers feared that by using these stocks for experimentation, the authors of classic papers had underestimated marine primary production (i.e., Marra and Heinemann 1984). Consequently, several groups of researchers repeated light bottle versus dark bottle uptake experiments at various locations in the 1980's and 1990's, this time using trace-metal free stock solutions of $H^{14}CO_3^-$. As detailed in the planning area-specific discussions that follow, these repeat measurements with trace-metal free $H^{14}CO_3^-$ solutions generally resulted in higher rates of regional primary productivity.

While the CSA (1990) report was being written, the oceanographic community was also debating how to reconcile some of the higher estimates of new production being reported by geochemists affiliated with the Transient Tracers in the Ocean program (Fanning 1992; Jenkins and Wallace 1992) with estimates from drawdown of nitrate and uptake of ^{14}C-labeled bicarbonate being reported by other scientists studying Planktonic Rate Processes in Oligotrophic Oceanic Systems (PRPOOS), off southern California and in the subtropical North Pacific (Eppley et al. 1985; Marra and Heinemann 1987). One outcome of this debate was a consensus recommendation to focus fieldwork during the Joint Global Ocean Flux Study (JGOFS) on characterizing the processes controlling the fluxes of carbon and related elements between the atmosphere, euphotic zone, and deep ocean (Platt et al. 1989).

CSA (1990) also noted that "Oceanic primary production can also be estimated from remote sensing of ocean color, bio-optical modeling, other biological models, and combinations of these techniques." The 37th Brookhaven Symposium in Biology, which produced a review of primary productivity and biogeochemical cycles in the sea (Falkowski and Woodhead 1992), was among the first to report on the many new tools that were developed or adapted at the close of the 20th century. These include satellite sensors of upper ocean color as a proxy for phytoplankton distributions, fluorescence and flow cytometry, molecular biological probes, sophisticated moored and shipboard instrumentation, and increased numerical modeling capabilities.

2.2 Measurement of Ocean Color from Space

As summarized in a recent review of technologies, techniques, and applications for remote sensing of coastal aquatic environments compiled by Müller-Karger et al. (2005), oceanographers have developed an extensive theoretical basis for assessment of ocean color and parameters that affect it, and they have proposed classification schemes to guide when to apply specific optical, bio-optical, and atmospheric correction algorithms. Decades ago, the dependence of color on water quality led Morel and Prieur (1977) to define two broad categories of ocean water types. Their "Case 1" waters were those in which water color was primarily a function of phytoplankton concentration. Their "Case 2" condition was everything else: environments where water color is strongly affected by terrigenous particulate and dissolved materials, resuspended sediment, marine colored dissolved organic matter (CDOM), or highly concentrated phytoplankton blooms like coccolithophore accumulations or red tides. Morel and Prieur (1977) also pointed out that in Case 2 waters, constituents were often independent of each other and did not co-vary with chlorophyll.

2.2.1 Coastal Zone Color Scanner (CZCS)

In 1978, the Coastal Zone Color Scanner (CZCS) (Hovis et al. 1980) was launched to begin collecting a global set of observations of visible radiation reflected by the ocean. The CZCS was an experimental sensor that provided an estimate of the water-leaving radiance originating in the first optical depth (Gordon et al. 1980). In a series of "sea-truth" reports following its launch, the average phytoplankton concentration in the first optical depth layer was empirically related to the water-leaving radiance. At low concentrations (i.e., clear Case 1 water, with 0.05-0.5 mg pigment m^{-3}), CZCS-derived parameters generally represented the optically-weighted average algal biomass within a surface layer of approximately 20-50 m depth (i.e., Müller-Karger et al. 1991). But at higher concentrations of pigment and in more turbid Case 2 water, CZCS algorithms usually overestimated actual phytoplankton concentration.

The CZCS acquired radiance data in five visible bands and one infrared band, each with a pixel size of about 1 km x 1 km (**Table 1**). However, only the first four of these bands proved useful for estimating phytoplankton concentration. Band 5 had a 100 nanometer (nm) bandwidth centered at 750 nm and a dynamic range that was more suited to land. Band 6 operated in the 10.5-12.5-µm region and sensed emitted thermal radiance for calculation of equivalent black body temperature. Unfortunately, this thermal band failed within the first year of the mission, so it was not used in the global processing effort.

Table 1. CZCS radiance bands (From: NASA 2010a).

Band Number	Wavelength Center	Bandwidth
1	443 nm	20 nm
2	520 nm	20 nm
3	550 nm	20 nm
4	670 nm	20 nm
5	750 nm	100 nm
6	10.5-12.5 µm	2 µm

nm = nanometer(s); µm = micrometer(s).

In 1980, the National Aeronautics and Space Administration (NASA) released the first image of chlorophyll standing stocks for the global biosphere, for which their CZCS team had composited the first 20 months of CZCS data acquired between 1978 and 1980 (http://www.nasaimages.org/luna/servlet/detail/nasaNAS~5~5~20968~125915; First-Composite-Image-of-the-Global). In 1990, after post-processing all available CZCS data for the period 1979-1986, Feldman used 60,000 CZCS images, plus 3 y of land vegetation data collected by the NOAA Advanced Very High Resolution Radiometer (AVHRR) instrument, to update NASA's global biosphere composite (**Figure 2**).

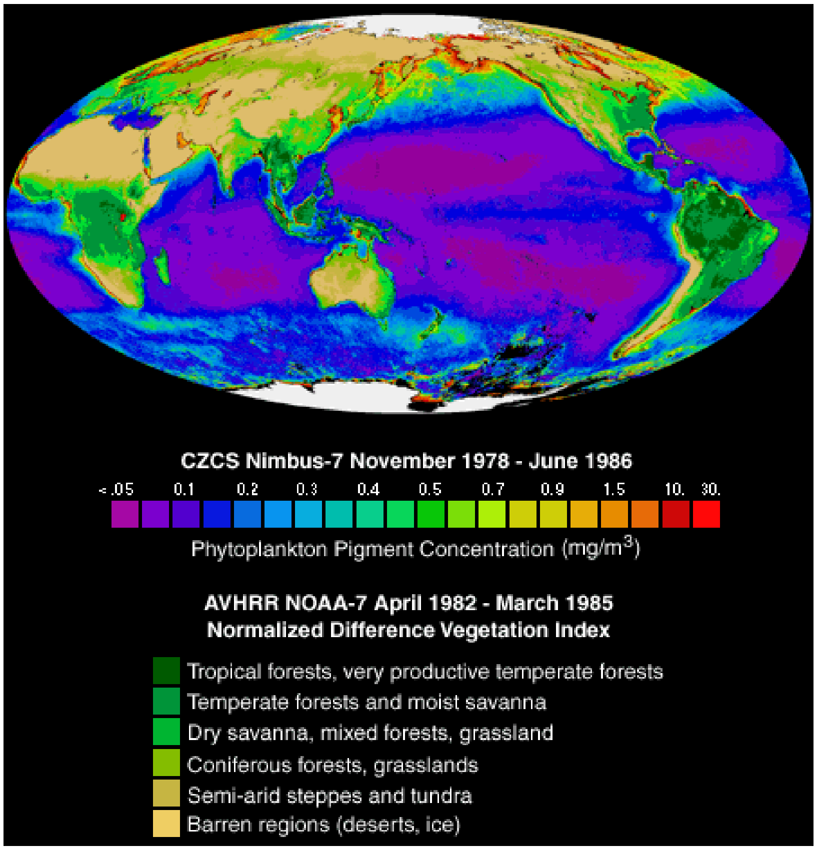

Figure 2. Phytoplankton pigment concentrations (mg m^{-3}) derived from Coastal Zone Color Scanner (CZCS) for the period November 1978-June 1986 (From: NASA 2010b).

Although a few papers that estimated chlorophyll concentration from CZCS data were included in the CSA (1990) report, more extensive synopses of phytoplankton biomass mean conditions using CZCS data were generally published after 1990. For example, Campbell and Aarup (1992) estimated the annual new production resulting from wintertime overturn of North Atlantic surface waters by using CZCS data collected during the period 1979-1983. Twelve monthly mean surface chlorophyll images, each based on 5-y averages of CZCS data, were used to identify three zones – subpolar latitude, mid latitude, and subtropical latitude – each with distinct seasonal patterns. New production in each of these three zones was estimated to average 43, 24, and 18 g C m^{-2} y^{-1}, respectively. Other synopses of CZCS data that authors used to estimate primary productivity for the OCS planning areas are discussed in the planning area-specific discussions of regional primary productivity of this report (**Section 4**).

A series of follow-on sensors were launched between 1997 and 2002 that have updated and upgraded the measurement of ocean color from space. These include 1) a Sea-viewing Wide Field-of-view Sensor (SeaWiFS), launched by NASA in 1997; 2) two Moderate Resolution Imaging Spectrometers (MODIS), launched by NASA in 1999 and 2002; and 3) a Medium Resolution Imaging Spectrometer (MERIS), launched in 2002 by the European Space Agency.

2.2.2 Sea-viewing Wide Field-of-view Sensor (SeaWiFS)

SeaWiFS collects water-leaving radiance data in eight channels, with five of these in the spectral range of 400-600 nm (http://oceancolor.gsfc.nasa.gov/SeaWiFS/). To supplement the 443 nm radiance band used in CZCS, **Table 2** shows that SeaWiFS has three other radiance bands for blue/green pigment determination plus a fifth band for in-water detritus correction.

Table 2. SeaWiFS radiance bands (From: Lewis 1992). SeaWiFS bands 1-6 are 20 nm wide, and bands 7 and 8 are 40 nm wide.

Band Number	Wavelength Center (nm)	Purpose
1	412	In-water detritus correction
2	443	Blue/green pigment algorithm
3	490	Blue/green pigment algorithm
4	510	Blue/green pigment algorithm
5	555	Blue/green pigment algorithm
6	670	Atmospheric correction
7	765	Atmospheric correction
8	865	Atmospheric correction

SeaWiFS was launched into a sun-synchronous orbit at an altitude of 705 km with re-visit time of approximately 1 d. SeaWiFS raw data are 10-bit digitization and have a nominal spatial resolution of 1.1 km (local area coverage, LAC) or 4.5 km (global area coverage, GAC). At one or more locations on the U.S. east coast, west coast, Gulf of Mexico coast, Alaska, and Hawaii, SeaWiFS data are captured in real-time using ground-based tracking antennae and are immediately processed, distributed, and archived. For example, SeaWiFS data for the Gulf of Mexico are captured at the Institute for Marine Remote Sensing at the University of South

Florida (IMARS) and at the Naval Research Laboratory at the Stennis Space Center (NRL). These data capture centers use NASA SeaDAS software to make chlorophyll concentration estimates, and they regularly incorporate improvements in calibration (i.e., Hu et al. 2003) and bio-optical algorithms (i.e., Hooker and Firestone 2003). SeaWiFS imagery shows the surface (to one optical depth, corresponding to a depth of 20-50 m in clear water and shallower in more turbid water) phytoplankton abundance (McClain et al. 1998), and it provides a means to effectively trace water circulation and oceanographic fronts (Hu et al. 2004a,b).

Two topical issues of *Deep-Sea Research II* published in 2004 summarized the views of ocean processes from the SeaWiFS mission. In 2007, NASA released a composite digital image of the SeaWiFS biosphere decadal average for which Feldman and Behrenfeld composited the first 10 y of SeaWiFS data (i.e., September 1997 – February 2007; http://svs.gsfc.nasa.gov/vis/a000000/a003400/a003451/index.html).

As of summer 2010, SeaWiFS is continuing its collection of ocean color data. NOAA has renewed a license to continue coverage from June 2010 until February 2011. This license includes the contiguous U.S. and adjacent waters.

2.2.3 Moderate Resolution Imaging Spectroradiometer (MODIS)

On 18 December 1999, NASA launched *Terra*, the first of a series of large satellites engineered to monitor the health of our planet (http://terra.nasa.gov). Among the suite of sensors on *Terra* is a MODIS. A second MODIS sensor was sent into orbit on 4 May 2002, when NASA launched *Aqua* (http://aqua.nasa.gov). MODIS-*Terra* is in descending sun-synchronous orbit, while MODIS-*Aqua* is in ascending sun-synchronous orbit.

In similar fashion to SeaWiFS, the MODIS sensors orbit at an altitude of 705 km. In another similarity to SeaWiFS, MODIS radiometers have five radiance bands in the 400-600-nm range (**Table 3**; bands 8-12). However, there are several important differences between MODIS and SeaWiFS. MODIS data are 12 bit (not 10 bit) digitization, and MODIS radiometers can measure chlorophyll fluorescence (**Table 3**; bands 13-14), as well as water-leaving radiance in the spectral range 400-600 nm, with 1 km resolution. **Table 4** identifies the other radiance bands available through MODIS and their uses. **Figure 3** shows examples of MODIS data products.

Table 3. MODIS radiance bands and their primary uses (From: http://modis.gsfc.nasa.gov/about/specifications.php).

Primary Use and Band	Bandwidth[1]	Spectral Radiance[2]	Required SNR[3]
Land/Cloud/Aerosols Boundaries			
1	620-670	21.8	128
2	841-876	24.7	201
Land/Cloud/Aerosols Properties			
3	459-479	35.3	243
4	545-565	29.0	228
5	1,230-1,250	5.4	74
6	1,628-1,652	7.3	275
7	2,105-2,155	1.0	110
Ocean Color/Phytoplankton/Biogeochemistry			
8	405-420	44.9	880
9	438-448	41.9	838
10	483-493	32.1	802
11	526-536	27.9	754
12	546-556	21.0	750
13	662-672	9.5	910
14	673-683	8.7	1,087
15	743-753	10.2	586
16	862-877	6.2	516
Atmospheric Water Vapor			
17	890-920	10.0	167
18	931-941	3.6	57
19	915-965	15.0	250

[1] Bands 1 to 19 are in nanometers (nm).

[2] Spectral radiance values are in units of watts/m^2-µm-sr (watts m^{-2}-µm-sr).

[3] SNR = Signal-to-noise ratio; performance goal is 30%-40% better than required.

Table 4. Other MODIS radiance bands (i.e., within the infrared spectrum) and their primary uses (From: http://modis.gsfc.nasa.gov/about/specifications.php).

Primary Use and Band	Bandwidth[1]	Spectral Radiance (Kelvin Temperature)[2]	Required NE[delta]T[3]
Surface/Cloud Temperature			
20	3.660-3.840	0.45 (300K)	0.05
21	3.929-3.989	2.38 (335K)	2.00
22	3.929-3.989	0.67 (300K)	0.07
23	4.020-4.080	0.79 (300K)	0.07
Atmospheric Temperature			
24	4.433-4.498	0.17 (250K)	0.25
25	4.482-4.549	0.59 (275K)	0.25
Cirrus Clouds Water Vapor			
26	1.360-1.390	6.00	150(SNR)
27	6.535-6.895	1.16 (240K)	0.25
28	7.175-7.475	2.18 (250K)	0.25
Cloud Properties			
29	8.400-8.700	9.58 (300K)	0.05
Ozone			
30	9.580-9.880	3.69 (250K)	0.25
Surface/Cloud Temperature			
31	10.780-11.280	9.55 (300K)	0.05
32	11.770-12.270	8.94 (300K)	0.05
Cloud Top Altitude			
33	13.185-13.485	4.52 (260K)	0.25
34	13.485-13.785	3.76 (250K)	0.25
35	13.785-14.085	3.11 (240K)	0.25
36	14.085-14.385	2.08 (220K)	0.35

[1] Bands 20-36 are in micrometers (µm).
[2] Spectral Radiance values are in units of watts/m^2-µm-sr (watts m^{-2}-µm-sr).
[3] NE(delta)T = Noise-equivalent temperature difference.

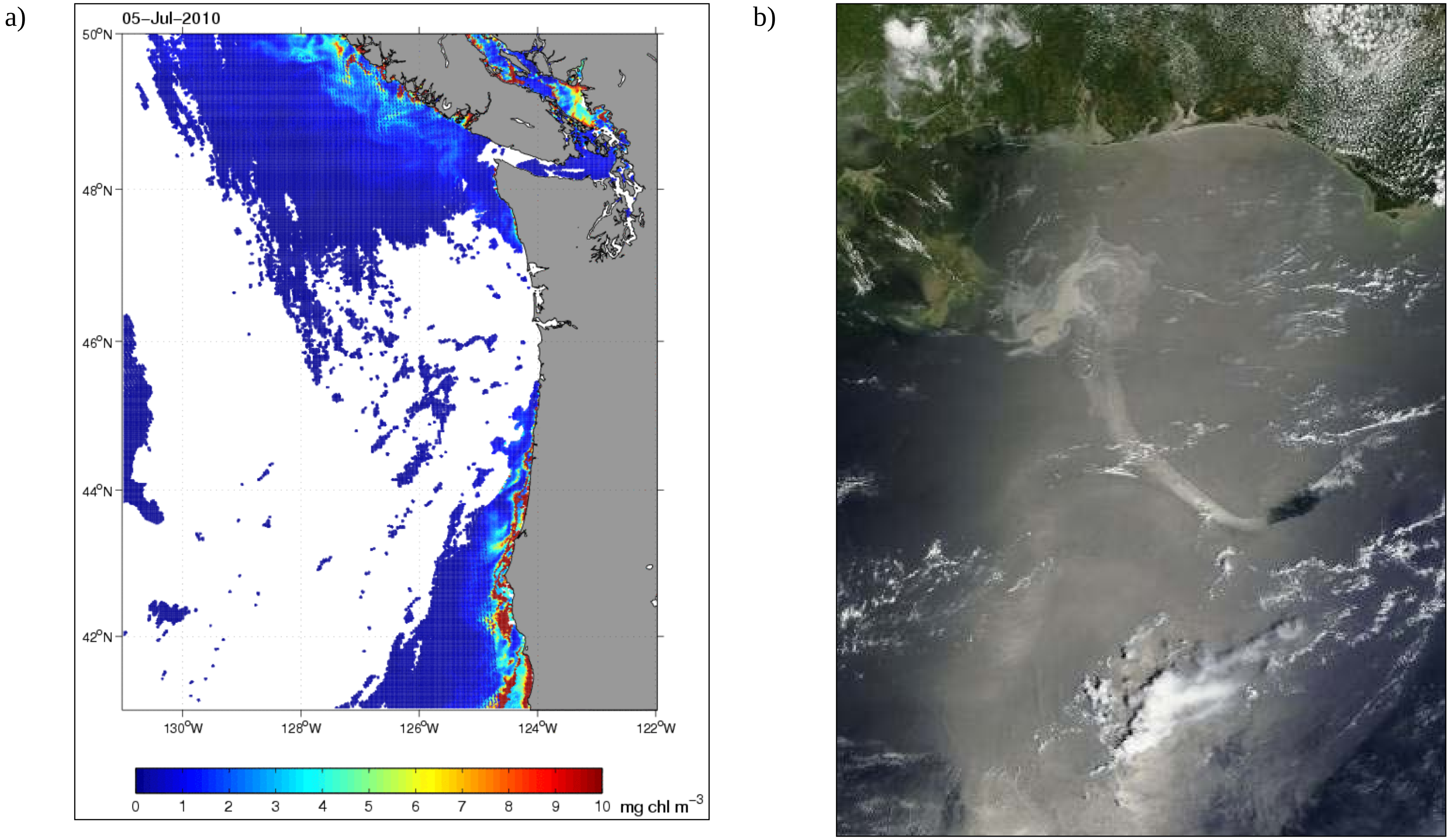

Figure 3. Examples of recent coastal ocean imagery from the Moderate Resolution Imaging Spectroradiometer (MODIS), in orbit on NASA's *Terra* and *Aqua* satellites. a) Chlorophyll *a* (4-km resolution) false-color image for 5 July 2010 for the Pacific Northwest coastal ocean, as reported by NOAA CoastWatch (http://www.nanoos.org/); areas close in to shore were largely cloud free, even though farther offshore much of the Pacific Northwest coastal ocean was covered by clouds (white). b) Oil spilled after an explosion aboard the drilling rig *Deepwater Horizon* visible near the Mississippi Delta in the Gulf of Mexico, 17 May 2010. NASA image by Jeff Schmaltz, MODIS Rapid Response Team.

2.2.4 SeaWiFS and MODIS Ocean Color Algorithm Validation

Ocean color algorithm validation is an important element ensuring that the data acquired via remote sensing techniques are properly ground-truthed. The Marine Optical Buoy (MOBY) project (http://www.star.nesdis.noaa.gov/sod/orad/mot/moce/overview.html), administered by NOAA, is an ongoing contribution to ocean color algorithm validation for SeaWiFS and MODIS. As described by NOAA, MOBY is a 14-m-long buoy developed and instrumented to measure upwelling radiance and downwelling irradiance at the sea surface and at three deeper depths. Submarine light is transmitted by fiber optics to the MOBY spectrograph for continuous energy measurements at subnanometer resolution from 340 nm (ultraviolet) to 950 nm (near-infrared). Standard meteorological observations are collected concurrent with the submarine light measurements, and supplemental oceanographic measurements, such as natural phytoplankton fluorescence, are also collected. MOBY transmits collected data to Marine Optical Characterization Experiment (MOCE) team members on a daily basis. These data are then processed and made available to SeaWiFS and MODIS Ocean Science Team members. MOBY is moored at 20°49.0′ N, 157°11.5′ W, west of Lanai, in the lee of the Hawaiian Islands.

Other bio-optical moorings at additional locations have been used as well to estimate seasonal and annual primary production. For example, Marra et al. (1992) summarized 240 d of moored data collected in 1987 on chlorophyll-*a* fluorescence and the scalar irradiance of photosynthetically available radiation (PAR), augmented by shipboard measurements of chlorophyll-*a* concentration, chlorophyll-*a* fluorescence, PAR, and net photosynthetic rate during four seasonal cruises to the mooring site in the western Sargasso Sea. They calculated the annual average gross primary production at the 1987 mooring as 12 mol C m^{-2} (144 g C m^{-2} y^{-1}).

When averaging imagery across fine scales of space and on days-weeks scales of time, many researchers try to minimize variance/mean statistics for ocean color digital data. Arnone et al. (2010), who summarized recent work by the U.S. NRL about variance versus mean for ocean color data, reported that variance often shows a positive functional relationship with mean, for SeaWiFS and for MODIS 1 km ocean color products. When using a 3 x 3 pixel box versus a 5 x 5 pixel box to do the averaging, centered on the 1 km x 1 km pixel in the center, they reported that the larger spatial area regions generally had more variance relative to mean. Similarly, Biggs et al. (2008) reported that when working with 4 y of biweekly-averaged SeaWiFS data for the period from 1998-2001 from 44 locations in the Gulf of Mexico, variance/mean ratio was lower at most locations when 3 x 3 pixel boxes that were centered on a 1 km x 1 km pixel in the center were contrasted with 5 x 5 pixel boxes used to do the same averaging.

2.2.5 Medium Resolution Imaging Spectrometer (MERIS)

In March 2002, the European Space Agency launched a polar-orbiting MERIS aboard their *Envisat* spacecraft. MERIS is a programmable imaging spectrometer that has 15 spectral bands in the range 412-900 nm that can be selected by ground command. Like MODIS, MERIS has a spatial resolution of about 1 km x 1 km over ocean, but MERIS spatial resolution is higher, to 260 m x 300 m, over land and coasts. Ocean color bands typically have a signal:noise ratio of 1,700 (i.e., about twice that of MODIS), and with a swath width of 1,150 km, MERIS can achieve global coverage every 3 d. At the most recent Ocean Sciences Meeting in 2010, Gower and King (2010) reported they used MERIS coastal zone data to delineate coastal phytoplankton blooms from weed-lines of floating aquatic vegetation being swept off-margin. *Envisat* also carries a synthetic aperture radar that, when used in conjunction with MERIS 412-900 nm data, allows researchers to effectively track ocean circulation and to delineate oceanographic fronts (**Figure 4**).

2.2.6 Hyperspectral Radiometers

To supplement their use of data from SeaWiFS, MODIS, and MERIS multispectral ocean color sensors that are flying now, the remote sensing community is getting quite interested in next-generation, hyperspectral radiometers. While the multispectral instruments measure reflection at a few relatively wide wavelength bands that are separated by segments where no measurements are taken, hyperspectral sensors measure reflection at a contiguous series of extremely narrow wavelength bands.

Because hyperspectral instruments are designed to survey the entire electromagnetic spectrum from 380-960 nm with over 120 bands each with bandwidth of just 5-6 nm, in theory they will be "spectrally overdetermined." However, hyperspectral radiometers should be able to measure reflection and emission of energy not only in high-resolution mode, but also with more accurate and detailed data than multispectral sensors can collect (Shippert 2004).

In September 2009, a Hyperspectral Imager for the Coastal Ocean (HICO) was added to the Japanese science module of the International Space Station. Several initial reports of its performance were presented at the 2010 Ocean Sciences Meeting. Davis et al. (2010) provided a synopsis of the initial performance of this spectrometer, which the U.S. NRL quickly developed "on the cheap" in just 16 months and is operating for the Japanese. HICO provides 90 m geostandardized data and has 128 spectral channels from 380-960 nm, with each spectral channel having an average width of 5.7 nm. Channel data can be combined to produce standard MODIS/MERIS products, to allow cross-calibration. Cross-calibration with other sensors is happening now, with MODIS/MERIS and also with SeaWiFS imagery, and with water column data collected in Hawaii by the MOBY program.

While MERIS has 15 channels of spectral information between 412 and 900 nm and the MERIS coastal zone footprint is 300 m, HICO has 128 spectral channels, each with a footprint of 90 m. At the 2010 Ocean Sciences Meeting, Arnone et al. (2010) reported that data from the two sensors were compared for an area off Newport, OR on 2 December 2009. Both sensors collected data along a 200-km distance, 15 km wide. HICO data show that MERIS overestimates irradiance in the spectral region <500 nm, but for the rest of the spectrum (500-900 nm), the two agree remarkably well. The MERIS 681 nm peak shows utility for detection of open-ocean algal blooms, while the 709 nm peak (max CHL method, as line height above baseline) is a better indicator for coastal algal blooms. At Oregon State University, a HICO website is expected go on-line later in 2010. Several other oral and poster presentations at the 2010 Ocean Sciences Meeting gave details of other HICO-MERIS comparisons.

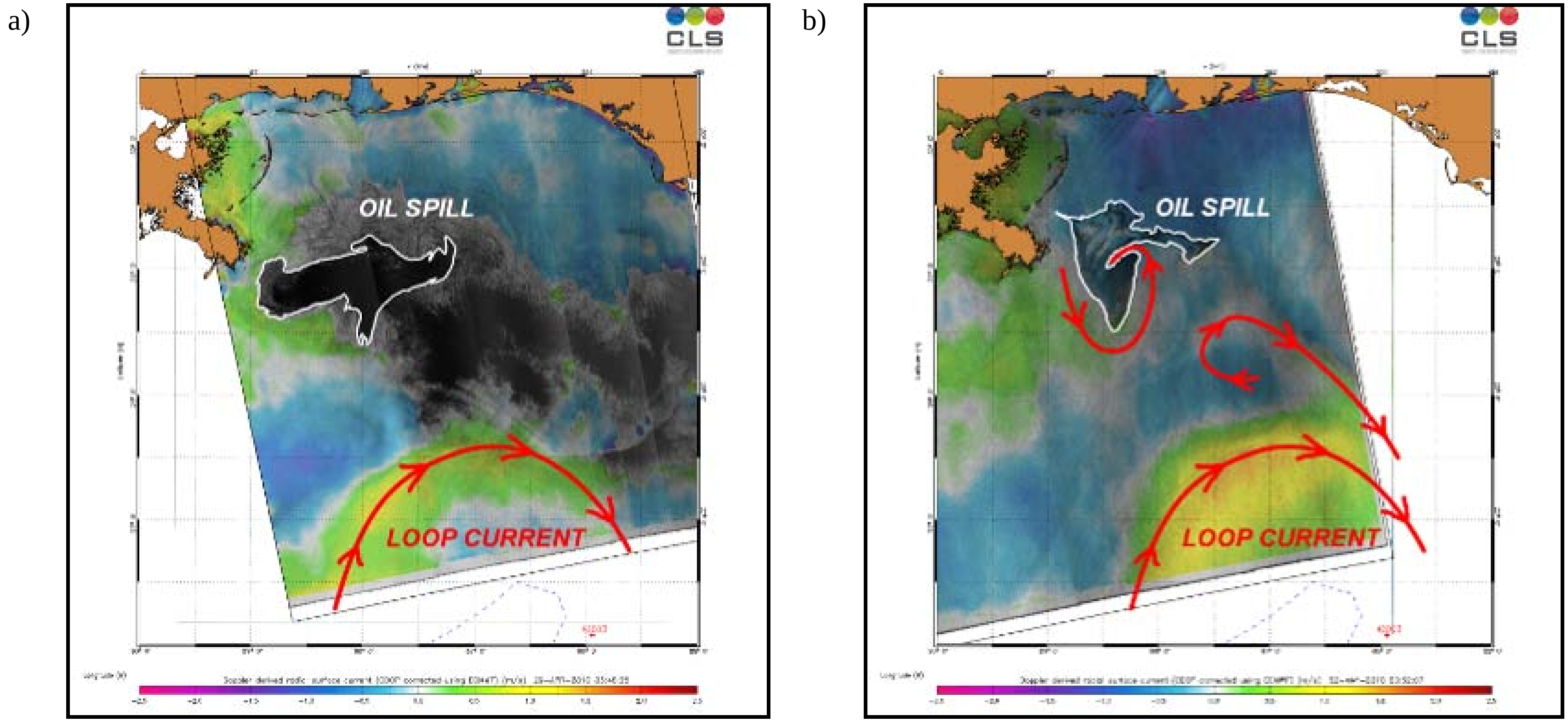

Figure 4. *Envisat* Advanced Synthetic Aperture Radar (ASAR) images from a) 29 April 2010 and b) 2 May 2010 tracking the *Deepwater Horizon* oil spill. By combining surface roughness and current flow information with data, SAR image analysts can detect the direction in which ocean color fronts or other ocean surface boundaries can drift. In these two images, ocean surface roughness variations and Doppler-derived ocean surface radial velocities show the dispersion of the oil spill in the Gulf of Mexico by upper ocean turbulent flow. a) In the 29 April image, smooth surfaces appear as black patches inside the oil spill and in the very low wind region east of the spill, where flow analysis is not possible. b) In the 2 May image, the overall shape of the spill appears to follow passively the flow derived from the Doppler measurements. In both images, the oil spill appears relatively confined around its point of origin. Most of the oil was still north of the Loop Current, a conveyor belt surface current circulation that circulates clockwise around the Gulf toward Florida before joining the Gulf Stream western North Atlantic boundary current. Image accessed at www.physorg.com/news192284227.html; credit: ESA/CLS; used with permission.

2.3 Calculating Primary Productivity from Measurement of Ocean Color from Space

The ability to derive basin-scale maps of phytoplankton chlorophyll in the upper ocean from satellite color sensors has led increasingly to the development of models relating biomass to primary production. Pioneering efforts by Eppley et al. (1985), Platt and Harrison (1985, 1986), and Platt and Sathyendranath (1988) were being reported at the time of the CSA (1990) report. But chlorophyll represents a pool size, while primary production is a flux; to derive a flux from a pool, a time-dependent variable must be incorporated (Falkowksi 1992). The simplest models relating carbon fixation to chlorophyll incorporate irradiance (Bidigare et al. 1992); the transfer function is a quantum yield. But because more complicated "light-chlorophyll models" (i.e., Cullen and Lewis 1995) are difficult to verify in the ocean, it becomes especially important to understand the underlying biological processes and how these processes are regulated in natural systems.

Among the present generation of bio-optical models used to predict marine primary productivity from satellite-based chlorophyll concentration is what has become known as the Vertically Generalized Production Model (VGPM), which is also called the net primary production (NPP) model. The model was proposed by Behrenfield and Falkowski (1997a), based on their investigation of the variability observed in phytoplankton primary production using a dataset of 11,283 ^{14}C-based measurements of daily carbon fixation collected at 1,698 oceanographic stations in open ocean and coastal waters. Behrenfield and Falkowski (1997a) noticed that a partial but strong negative exponential trend in the vertical distribution of primary production remained in their dataset after they removed the influences of euphotic depth, photoperiod, and chlorophyll concentration. This led them to develop a sea surface temperature (SST) and irradiance-dependent, depth-resolved productivity model to determine the maximum light-saturated rate of photosynthesis. The predictive parameter developed by their model was called PBmax (or PBopt). When they calculated PBopt using the ^{14}C-based measurements of daily integrated production, they reported their model accounted for 86% of observed variability in the 11,283 measured values of daily integral production. They also reported that when PBopt was estimated by means of the ensemble relationship developed from the dataset, their model still accounted for 58% of the observed variability. When they applied their model to monthly globally averaged CZCS chlorophyll images, Behrenfield and Falkowski (1997a) estimated marine net primary production was annually about 43.5 Pg C y^{-1} (43.5 x 10^9 metric tons). This estimate was in good general agreement with an estimate of 45-50 x 10^9 metric tons that had been published 2 y earlier by Longhurst et al. (1995), who had also used monthly mean near-surface chlorophyll fields for the period 1979-1986 from the CZCS data. Longhurst et al. (1995) binned the CZCS data into 57 different biogeochemical provinces that they had constructed based upon the regional oceanography and examination of the chlorophyll fields.

After SeaWiFS was launched later in the same year that Behrenfeld and Falkowski published their VGPM/NPP paper, subsequent researchers used VGPM methodology to estimate primary productivity with SeaWiFS (and later with MODIS, and with MERIS) ocean color data. In one such example, Müller-Karger et al. (2005) used the first 4 y of SeaWiFS ocean color data to recompute annual global net primary production (i.e., for the period 1998–2001). They calculated annual marine net primary production was globally about 48 Pg C y^{-1} (48 x 10^9 metric tons) and they estimated that areas bordering continents (bottom depth <2,000 m) support 10%-15% of this production.

According to Campbell et al. (2002), who summarized a round-robin comparison of algorithms for estimating ocean primary production from surface chlorophyll, temperature, and irradiance, the Behrenfeld and Falkowski VGPM/NPP technique was one of the top-performing models for estimating integrated daily primary production. Twelve algorithms, developed by 10 teams, were evaluated by comparing their ability to estimate depth-integrated daily production (IP, mg C m^{-2}) at 89 stations in geographically diverse provinces. The algorithms were furnished information about the surface chlorophyll concentration, temperature, photosynthetically available radiation, latitude, longitude, and day of the year. When algorithm results were compared with IP estimates derived from ^{14}C uptake measurements at the same stations, the best-performing algorithms generally predicted IP to within a factor of two of the ^{14}C-derived estimates.

2.4 Traditional and Satellite Measurements of New Production

New production (i.e., primary productivity supported by the uptake of newly available dissolved inorganic nitrogenous nutrients entering the photic zone from below (by upwelling or doming from midwater) and/or from above (by atmospheric sources) and regenerated production (i.e., primary productivity dependent on reduced nitrogen derived from excretion of organisms in the euphotic zone) are complementary quantities; their sum is the total primary production (Platt et al. 1992). Doming and upwelling both represent a cross-isopycnal introduction of nutrients from deeper, nutrient rich water; upwelled water breaks the ocean surface, whereas domed water does not. Both processes bring nutrients into the lower photic zone, where they are available for phytoplankton uptake. The ratio of new production to total primary production, which was called the *f*-ratio by Eppley and Peterson (1979), has proved to be a useful index of trophic status. If the export of organically-bound nutrient from the photic zone exceeds the rate at which that nutrient was supplied from outside the system, the excess of supply over export represents the capacity of the ecosystem to sustain secondary and higher levels of production (Platt et al. 1992; see also **Figure 5**). Export production and *f*-ratio are essential factors in productivity modeling (see **Section 5** discussions regarding NPZ and Ecosim models).

New production is generally estimated by comparing the uptake of nitrate with that of ammonium and other reduced forms of nitrogen. Uptake of nitrate can be estimated directly by measuring the rate of drawdown of NO_3^- standing stock in surface waters during a bloom (i.e., as done during the 1989 JGOFS North Atlantic Bloom Experiment) by measuring the shorter-term rate at which NO_3^- changes concentration using chemiluminescent nitrate analysis (McCarthy et al. 1992), or by incubating phytoplankton samples with ^{15}N-labeled nitrate and ^{15}N-labeled ammonium, using the method of Dugdale and Goering (1967).

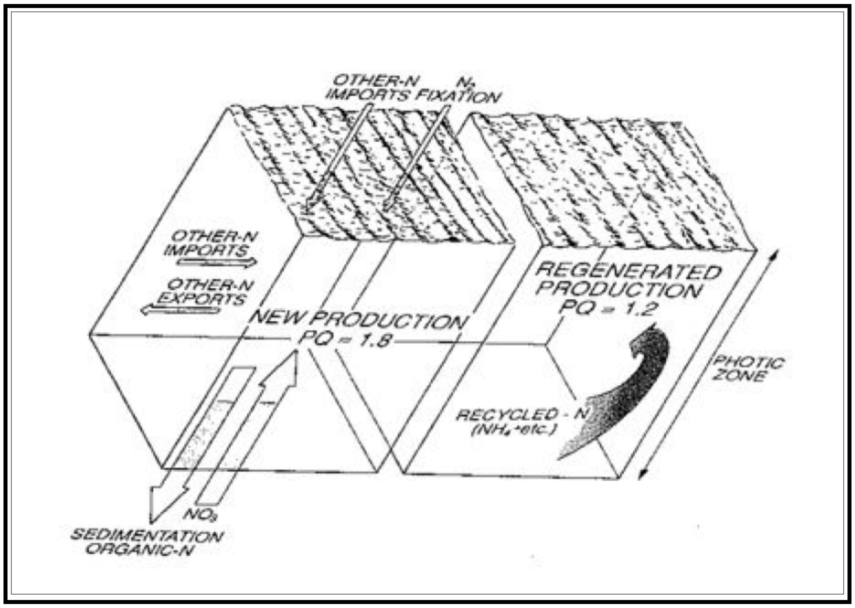

Figure 5. Schematic diagram showing the major fluxes for new and regenerated primary production (From: Platt et al. 1992).

Pena et al. (1992), who measured uptake of ^{15}N-labeled substrates along a meridional transect across the equatorial Pacific region at 135° W longitude from 15° S to 15° N in April 1988, reported the average euphotic zone *f*-ratio varied from 0.09 to 0.39 in this high-nutrient low-chlorophyll (HNLC) environment. Working a few months earlier along a different meridional transect at 150° W in the same HNLC environment, Wilkerson and Dugdale (1992) and Dugdale et al. (1992) reported an average *f*-ratio of 0.17. In the later paper, the authors also reported that the ratios of directly measured nitrate and carbon uptake and the ratios of ^{15}N-nitrate uptake to ^{15}N-nitrate plus ^{15}N-ammonium uptake agreed well. However, they cautioned that values of "*f*" calculated from a global ^{14}C versus *f* relationship (Eppley and Peterson 1979) or from a global nitrate versus *f* relationship (Platt and Harrison 1985) would have resulted in overestimates of new production for the HNLC equatorial Pacific upwelling region.

Others researchers are using remote sensing data to estimate new production. Most of them use a nitrate versus SST relationship to calculate seasonal inputs of new nitrogen into the photic zone (i.e., Eppley 1989; Abbott and Chelton 1991; for an update, see Silio-Calzada et al. 2008). However, Coles et al. (2004) reported a decoupling between chlorophyll *a* and vertical nutrient flux for a broad region of the tropical western North Atlantic Ocean, based on the positive relationship between sea surface height anomaly, SST, and ocean color. Instead, they speculated that development of a summertime chlorophyll-*a* surface maximum in this region was fueled by N_2 fixation rather than by uptake of nitrate doming or upwelling from below the photic zone.

Other methods for estimating new production use particulate organic carbon flux data from sediment traps coupled with estimates of the amount of new versus regenerated production to calculate primary production rates (Falkowski et al. 1994; Thunell et al. 2007). For example, Wefer and Fischer (1991) estimated that primary production for the Southern Ocean south of 50° S must be about 1 x 10^9 tons y^{-1} after using sediment trap data to calculate that the organic carbon flux out of the photic zone there averaged about 1.7 x 10^8 tons y^{-1}. Measurement of the disequilibrium between the particle-reactive tracer Th-234 and its soluble parent U-238 has also been advocated to quantify the export flux of organic matter (Buessler et al. 1992).

2.5 Other Methods

Fast Repetition Rate fluorometry (FRRf) is a sophisticated, non-intrusive method for probing oxygenic photosynthesis in algae, through detailed analysis of chlorophyll-*a* fluorescence. The instrumentation was developed from pump-probe fluorescence studies pioneered by Falkowski, Kiefer, and others who sought to quantitatively study the quantum yield and other aspects of molecular ecology of phytoplankton photosynthesis (i.e., Falkowski 1992; see also Kiefer and Reynolds 1992).

The relationship between the fluorescence of chlorophyll *a* and photosynthetic rate of planktonic photoautotrophs is most easily described in terms of the quantum yields of the two processes (Kiefer and Reynolds 1992). When the fluorescence emitted by chlorophyll *a* in a suspension of cells is excited by a flash of light that is sufficiently short, infrequent, and low in intensity, the redox state of the photosynthetic electron transport system (ETS) will be unaltered by the flash. The fluorescence that is induced by such a flash is called the “probe fluorescence,” and the dose of exciting photons is usually expressed as I (photons m^{-2} $flash^{-1}$). But when the probe flash is preceded by a “pump flash” whose dose (I_s) is sufficiently large to perturb the redox poise of the photosynthetic ETS, then the quantum yield of the fluorescence induced by the probe flash will differ from its natural value. The ability to systematically perturb the photosystem-II electron transport system with a pump flash and then to monitor the fluorescence response is the basis of the pump-probe measurement. In their review, Kiefer and Reynolds (1992) showed how the quantum yield of photosynthesis may be predicted from several measurements of pump-probe fluorescence in ambient light and in the dark. Yentsch et al. (2004) have argued that pump-probe variable fluorescence can also be interpreted as an analogue for nutrient stress.

Most researchers who use pump-probe research have focused on kinetics processes within photosystem II, since 95% or more of the *in vivo* fluorescence originates from the chlorophyll of the antenna of this photosystem (Kiefer and Reynolds 1992). In general, instantaneous photosynthetic rates measured by FRRf-excitation correlate well at sub-saturating light intensities with conventional ^{14}C-uptake rates, although they operate on different time-scales (Kaiblinger and Dokulil 2006).

Several kinds of FRRf instruments are commercially available for over-the-side use aboard research vessels, and/or on bio-optical moorings. These include a “FAST-tracka-II” second generation in-water instrument from Chelsea Instruments (http://www.chelsea.co.uk/Instruments%20FASTtracka.htm).

Flow cytometers are microspectrofluorometers that use laser light to measure the fluorescence and scattering cross-sections of individual cells, so in theory they can be used to estimate net primary productivity by individual algal cells. Conventional spectrofluorometers provide fluorescence excitation and emission spectra for natural assemblages of cells and particles, and flow cytometers provide such data for individual cells. As Kiefer and Reynolds (1992) pointed out in an early review of their capabilities, flow cytometers that have been operated in shore-based laboratories and/or taken to sea on research vessels have increased our understanding of the spatial distribution, temporal variability, and taxonomic composition of phytoplankton and cyanobacterial populations. They are routinely used for monitoring changes in picoplankton composition in the biweekly to monthly water samples that are taken at ocean time series stations in Hawaii and Bermuda (i.e., Vaulot et al. 1995; Cavendar-Bares et al. 2001). When combined with the amplification of cellular DNA by polymerase chain reaction or other cloning techniques, it is clear that the small cells that dominate photosynthetic biomass and primary production in most open ocean systems are not just prokaryotes. While the prokaryotic component of picoplankton is dominated by two genera (i.e., *Prochlorococcus* and *Synechococcus*), the eukaryotic fraction is much more diverse. Over six dozen species of eukaryotic phytoplankton <3 µm in size have now been described using molecular genetics (Vaulot et al. 2008). Species diversity of phytoplankton in the oligotrophic pelagic environment is detailed further in **Section 4.5**.

Semi-autonomous flow cytometers that are currently available include an “Imaging Flow Cytobot” developed by Olson and Sosik (2007) to make continuous measurements of plankton size, abundance and other characteristics, and to take video images of organisms for identification. When incorporated as one of the primary sensors of a coastal ocean observatory, the Flow Cytobot can be reprogrammed from an onshore laboratory to respond to changing conditions.

2.6 Conclusions and Selected Methodology

The VGPM primary productivity model (Behrenfeld and Falkowski 1997a) was selected for the primary productivity estimates in this report. The VGPM technique is one of the top-performing models for estimating integrated ocean primary production from surface chlorophyll, temperature, and irradiance. The model estimates the net primary productivity within the euphotic depth as

$$NPP_{eu} = 0.66125 \text{ x } P^{B}_{opt} \text{ x } [E_0/(E_0 + 4.1)] \text{ x } Z_{eu} \text{ x } C_{opt} \text{ x } D_{irr}$$

where

- P^{B}_{opt} (also called Assimilation Number) is the maximum C fixation rate within a water column (mg C (mg Chl)$^{-1}$ h^{-1});
- E_0 is the daily surface PAR (mol quanta m^{-2});
- Z_{eu} is the euphotic depth (m);
- C_{opt} is the chlorophyll concentration (mg mg^{-3}) at P^{B}_{opt}; and
- D_{irr} is the daily photoperiod (h).

For each location, the above variables were estimated from the satellite measurements in the following way. In the model, P^{B}_{opt} was derived from an empirical relationship with SST (T in °C):

$$P^{B}_{opt} = -3.27 \text{ x } 10^{-8}\, T^7 + 3.4132 \text{ x } 10^{-6}\, T^6 - 1.348 \text{ x } 10^{-4}\, T^5 + 2.462 \text{ x } 10^{-3}\, T^4 \\ - 0.0205\, T^3 + 0.0617\, T^2 + 0.2749\, T + 1.2956$$

In this application, T was obtained from satellite measurements. The valid range for the equation is -1 °C to 29 °C. Outside this range, P^{B}_{opt} is set to a constant of 1.13 for T <1 °C and 4.0 for T >29 °C. Recent research findings from subtropical and tropical oceans (Gong et al. 2000; Müller-Karger et al. 2004) suggest P^{B}_{opt} is underestimated for high-SST waters, and the revised relationship should be used. However, this relationship has not been verified in the global oceans, and the original coefficients were used to estimate P^{B}_{opt} in this analysis.

For other terms in the equation:

- E_0 was estimated using the satellite ocean color measurements and radiative transfer theory (Frouin et al. 2001);
- C_{opt} was obtained from satellite estimated surface chlorophyll concentration, C_{sat} (mg m^{-3});
- D_{irr} was obtained from daylight estimates, available from NASA/Goddard Space Flight Center (GSFC); and
- Z_{eu} was estimated using C_{sat} (mg m^{-3}) in the following way, per Behrenfeld and Falkowski (1997b):
  - Vertically integrated chlorophyll was modeled as $C_{tot} = 38.0\ C_{sat}^{0.425}$ for $C_{sat} < 1.0$ and $C_{tot} = 40.2\ C_{sat}^{0.507}$ for $C_{sat} \geq 1$.
  - Then, Z_{eu} was modeled as $568.2\ C_{tot}^{-0.746}$ for $Z_{eu} < 102$ and $200.0\ C_{tot}^{-0.293}$ for $Z_{eu} < 102$.

In summary, to estimate NPP at a given location, four parameters were required: SST, C_{sat}, PAR, and D_{irr}. All of these data were obtained from NASA.

SST monthly mean global data derived from AVHRR measurements from 1998 to date were obtained from NASA Jet Propulsion Laboratory (JPL), with the most recent reprocessing (V5) being used (http://podaac.jpl.nasa.gov/DATA_CATALOG/avhrrinfo.html). The algorithms and accuracy assessment can be found in Kearns et al. (2000) and Kilpatrick et al. (2001). Root mean square (RMS) difference between the satellite-estimated and *in situ* measured SST is often within °C, without significant bias.

C_{sat} (i.e., Chl in mg m^{-3}) and PAR monthly mean global data derived from SeaWiFS and MODIS estimates were obtained from NASA GSFC (International Ocean-Colour Coordinating Group [IOCCG] 2004), with the most recent reprocessing (SeaDAS6.1) being used. SeaWiFS data are continuous from 1998 to 2007, after which sensor degradation led to intermittent data flow. MODIS/Aqua data are from 2003 to date. Recent reprocessing and validation effort showed that they are comparable to each other (**Figures 6** and **7**).

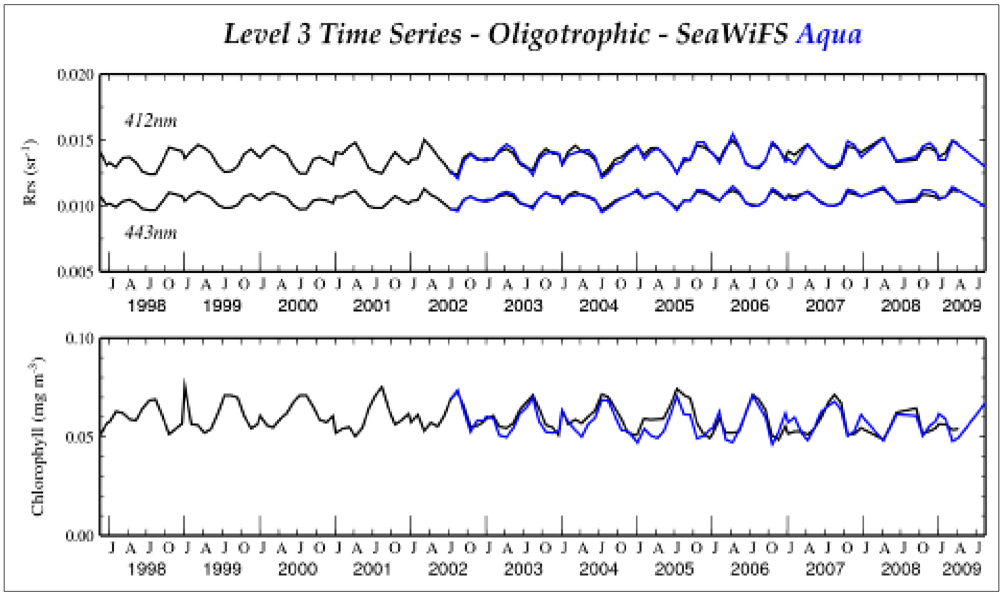

Figure 6. Excellent agreement is found between SeaWiFS and MODIS/Aqua derived remote sensing reflectance (R_{rs}, sr^{-1}) and chlorophyll-*a* concentration for the oligotrophic oceans. Figure courtesy of Bryan Franz (NASA/ Ocean Biology Processing Group) (Franz 2010).

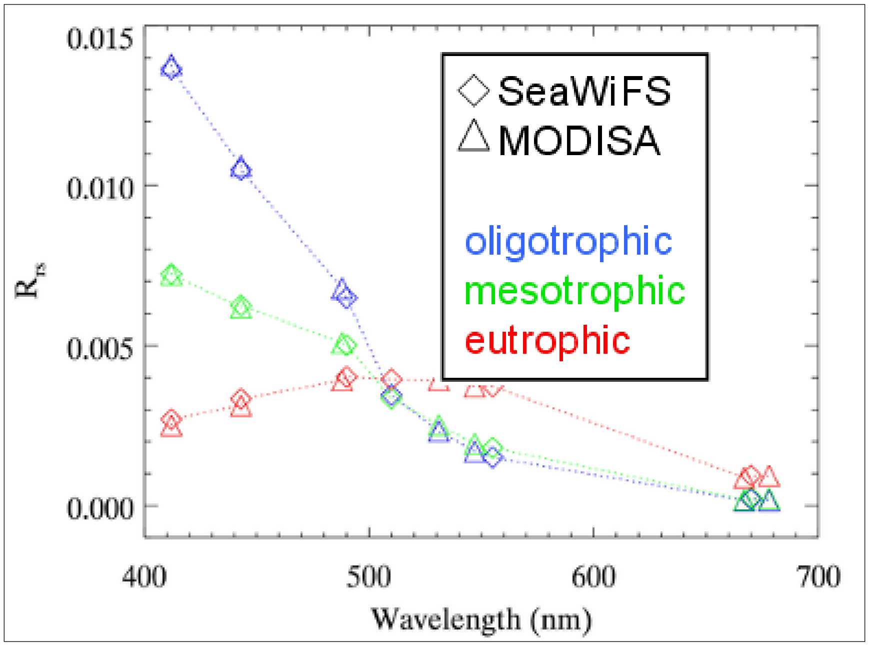

Figure 7. Excellent agreement is found between SeaWiFS and MODIS/Aqua derived spectral remote sensing reflectance (R_{rs}, sr^{-1}) for the global oceans. Figure courtesy of Bryan Franz (NASA/Ocean Biology Processing Group) (Franz 2010).

Global validation results showed that although the RMS difference between satellite-estimated and *in situ*-measured chlorophyll for open ocean waters is about 0.2 (in log scale; Gregg and Casey 2004), the mean ratio of the two is close to 1.0 (McClain et al. 2004a). PAR data on monthly scales have uncertainties within a few percent, as shown in Frouin et al. (2001). Daily hour (D_{irr}) data were obtained from Rutgers University.

Table 5 summarizes the data products used in estimating NPP. Note that although SeaWiFS provided continuous coverage from 1998 to date, in later years due to sensor errors there were several gaps that prevented accurate estimates of monthly or annual production. Therefore, for the complete time series of 1998-2009, SeaWiFS data were used between 1998 and 2004 and MODIS/Aqua data were used between 2005 and 2009.

Table 5. Data source characteristics used to estimate net primary productivity during this study.

Variable	Units	Sensor(s)	Source	Resolution	Period	Frequency
SST	°C	AVHRR	JPL	9 km	1998-Present	Monthly
C_{sat}	mg m^{-3}	SeaWiFS	GSFC	9 km	1998-2007	Monthly
C_{sat}	mg m^{-3}	MODIS/A	GSFC	9 km	2003-Present	Monthly
PAR	Mol photons m^{-2} d^{-1}	SeaWiFS	GSFC	9 km	1998-2007	Monthly
PAR	Mol photons m^{-2} d^{-1}	MODIS/A	GSFC	9 km	2003-Present	Monthly
D_{irr}	h	Models	Rutgers	9 km	1998-Present	Monthly

From these monthly global data products, NPP monthly global maps were derived using the VGPM model described above. **Figure 8** shows an example of the three variables and the resulting NPP map for the month of April 2000.

The monthly NPP time-series from 1998-2009 was queried using each of the 26 OCS planning areas. For each planning area, the geographic information system (GIS)-shape file was used to generate a region-of-interest (ROI). Statistics of all image pixels within the ROI were performed to calculate the mean, standard deviation, and total (area integrated) monthly NPP. To assure consistency between these shape-file defined ROIs and planning area-specific area coverage, as provided by BOEMRE, comparisons in area coverage between the two were conducted (**Table 6**). Most areas have differences of <1%. Two areas in the North of Alaska have differences of approximately 6.5%, attributed to map-projection induced artifacts. The shape-file defined ROIs were based on a geographic latitude-longitude or rectangular projection. When computing the total (i.e., area integrated) NPP, this slight difference has been accounted for by multiplying the mean NPP by the BOEMRE-specified area coverage.

Because of the rectangular projection used in NASA data, pixels within high-latitude regions have smaller area coverage than those in low-latitude regions (i.e., proportional to the cosine of the latitude). To account for this non-linear effect, the pixels have been weighted by cosine of latitude when computing the mean.

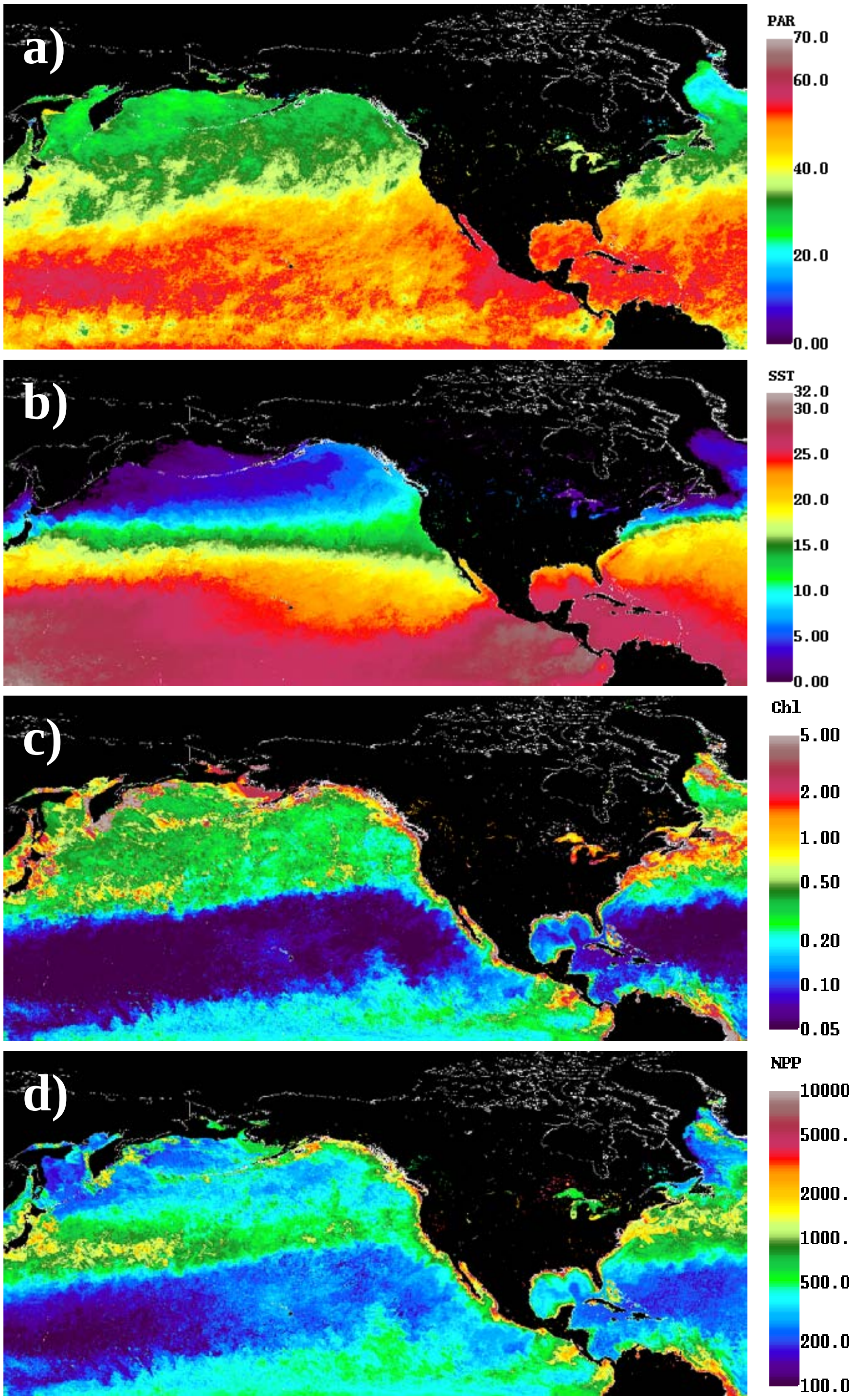

Figure 8. Examples of inputs and outputs of the VGPM NPP model for April 2000: a) SeaWiFS PAR (Mol photons m^{-2} d^{-1}); b) AVHRR SST (°C); c) SeaWiFS Chl (mg m^{-3}); and d) modeled NPP (mg C m^{-2} d^{-1}).

Table 6. Planning area statistics.

Region and Planning Area	Acreage (million acres)	Area (km^2)	Area (km^2) from shape files*	% Difference**
Atlantic Region				
North Atlantic	92.32	373,606.10	376,478.67	0.77
Mid-Atlantic	112.83	456,607.20	462,555.42	1.30
South Atlantic	54.34	219,906.36	222,698.03	1.27
Straits of Florida	9.64	39,011.73	39,047.03	0.09
Gulf of Mexico Region				
Eastern Gulf of Mexico	64.56	261,265.27	263,731.50	0.94
Central Gulf of Mexico	66.45	268,913.84	271,977.89	1.14
Western Gulf of Mexico	28.58	115,659.25	115,913.52	0.22
Pacific Region				
Southern California	88.98	360,089.59	363,527.05	0.95
Central California	43.68	176,766.84	177,706.12	0.53
Northern California	44.79	181,258.85	181,568.88	0.17
Washington-Oregon	71.00	287,327.05	289,754.92	0.84
Alaska Region				
Gulf of Alaska	112.10	453,652.99	462,373.86	1.92
Cook Inlet	5.36	21,691.17	22,100.61	1.89
Kodiak	89.00	360,170.53	364,754.15	1.27
Shumagin	84.65	342,566.69	344,199.49	0.48
Aleutian Arc	259.06	1,048,379.51	1,054,200.7	0.56
North Aleutian Basin	32.45	131,320.60	135,503.53	3.19
St. George Basin	70.23	284,210.97	287,539.02	1.17
Bowers Basin	87.59	354,464.45	359,560.12	1.44
Aleutian Basin	41.33	167,256.72	166,634.97	-0.37
Navarin Basin	34.02	137,674.17	139,271.85	1.16
St. Matthew-Hall	54.57	220,837.14	221,856.27	0.46
Norton Basin	24.25	98,136.35	104,618.28	6.61
Hope Basin	12.82	51,880.74	55,232.14	6.46
Chukchi Sea	62.59	253,292.96	253,131.22	-0.06
Beaufort Sea	65.08	263,369.64	263,026.24	-0.13

Notes: Acreage (million acres) from Planning Area Acreages for 2007-2012 5-Year Plan (PAstats.pdf);

* Area coverage calculated using shape files from BOEMRE (MMS) (www.boemre.gov/offshore/mapping).

** Percent difference between area coverage from calculation and from PAstats.pdf; most difference is within ±1%.

3.0 Primary Productivity Estimates for OCS Planning Areas

Figure 9 shows the geographic locations of all 26 OCS planning areas projected on a rectangular map. The primary productivity modeling results from each planning area are presented in the following subsections. Note that for the areas near Alaska, during (northern hemisphere) winter there is no or little data coverage. Under these circumstances, the following summaries only include data for those months where at least 75% of the planning area had valid satellite data coverage. The total monthly NPP for each planning area, however, is a result of integration over the entire planning area.

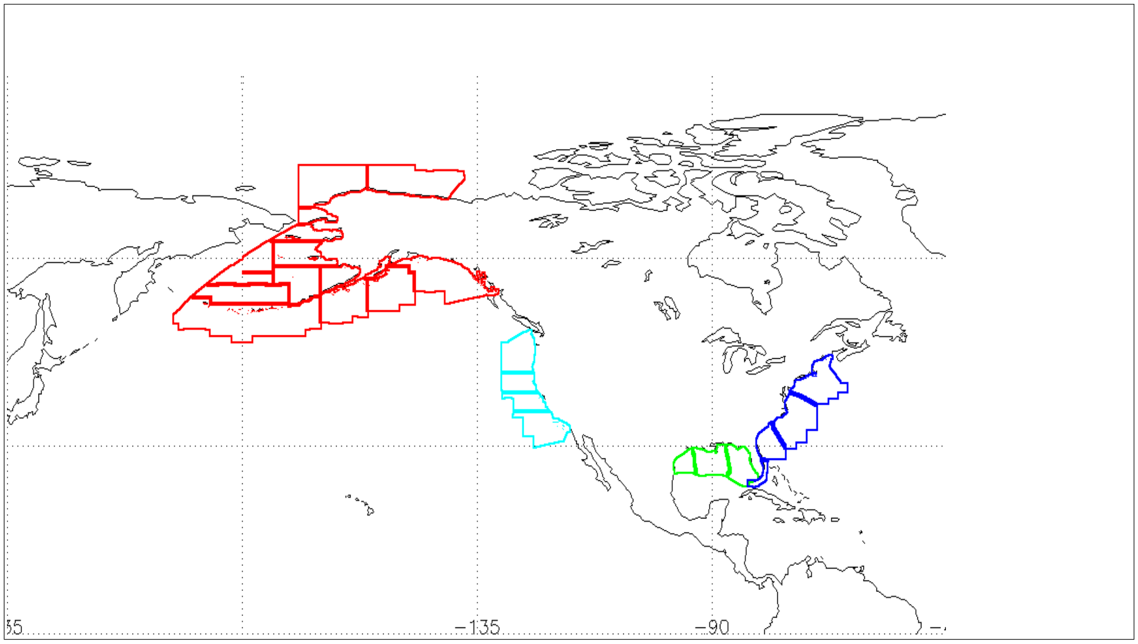

Figure 9. Locations of the 26 Outer Continental Shelf planning areas. Regions are color-coded as follows: Atlantic = blue; Gulf of Mexico = green; Pacific = cyan; Alaska = red.

Monthly and annual NPP statistics are provided for each planning area in graphical format. **Figures 10** through **13** show the Atlantic Region and its four planning areas. **Figures 14** through **16** cover the Gulf of Mexico and its three planning areas. **Figures 17** through **20** show the four planning areas of the Pacific Region. **Figures 21** through **35** depict the Alaska Region and its 15 planning areas. Brief summary discussions precede each figure.

The figures include information on monthly variations (i.e., seasonality) and annual variations (i.e., trend). For each month, both mean NPP (per area) and total NPP (integrated over area) are presented, with the former associated with standard deviations. Mean NPP is presented in units of mg C m^{-2} d^{-1}; total NPP is shown in units of million metric tons (tonnes) C mo^{-1}. The annual total NPP represents the sum of total monthly NPP in each individual year. It should be noted that, in order to show planning area-specific seasonality and interannual changes, the y-axis range has been customized for each area (i.e., the y-axis scale may be different among areas).

Productivity determinations were depth integrated, extending from the ocean surface to the euphotic depth (i.e., the depth where 1% of the surface light, or PAR, is available). This depth ranged from a maximum of 100 m (e.g., within ocean gyres) down to several meters (e.g., within eutrophic coastal waters).

3.1 Atlantic Region

3.1.1 North Atlantic

The North Atlantic Planning Area covers an area of 92.32 million acres. During the period 1998 through 2009, mean annual NPP was 137.01 million tons of carbon (standard deviation [s.d.] = ±8.51). Annual and monthly variance determinations were 6.21% and 32.47%, respectively. Over the period 1998 through 2009, trend analysis indicated no significant change in primary productivity (p = +0.90) (**Figure 10**).

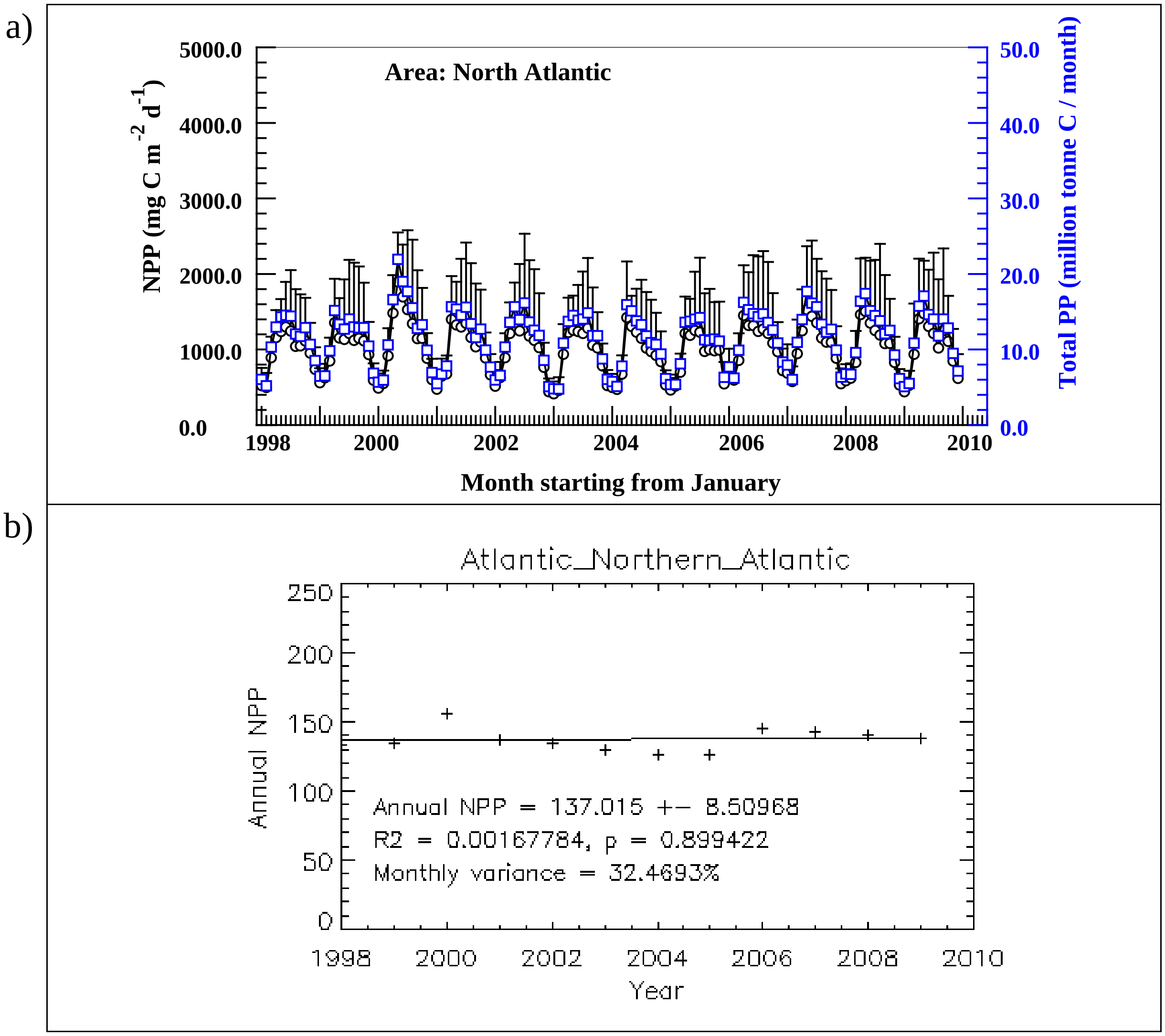

Figure 10. North Atlantic Planning Area a) monthly net primary production (NPP) statistics and b) annual NPP statistics (million tons C).

3.1.2 Mid-Atlantic

The Mid-Atlantic Planning Area covers an area of 112.83 million acres. During the period 1998 through 2009, mean annual NPP was 55.79 million tons of carbon (s.d. = ±2.59). Annual and monthly variance determinations were 4.64% and 25.18%, respectively. Over the period 1998 through 2009, trend analysis indicated a less than significant decrease in primary productivity (p = -0.70) (**Figure 11**).

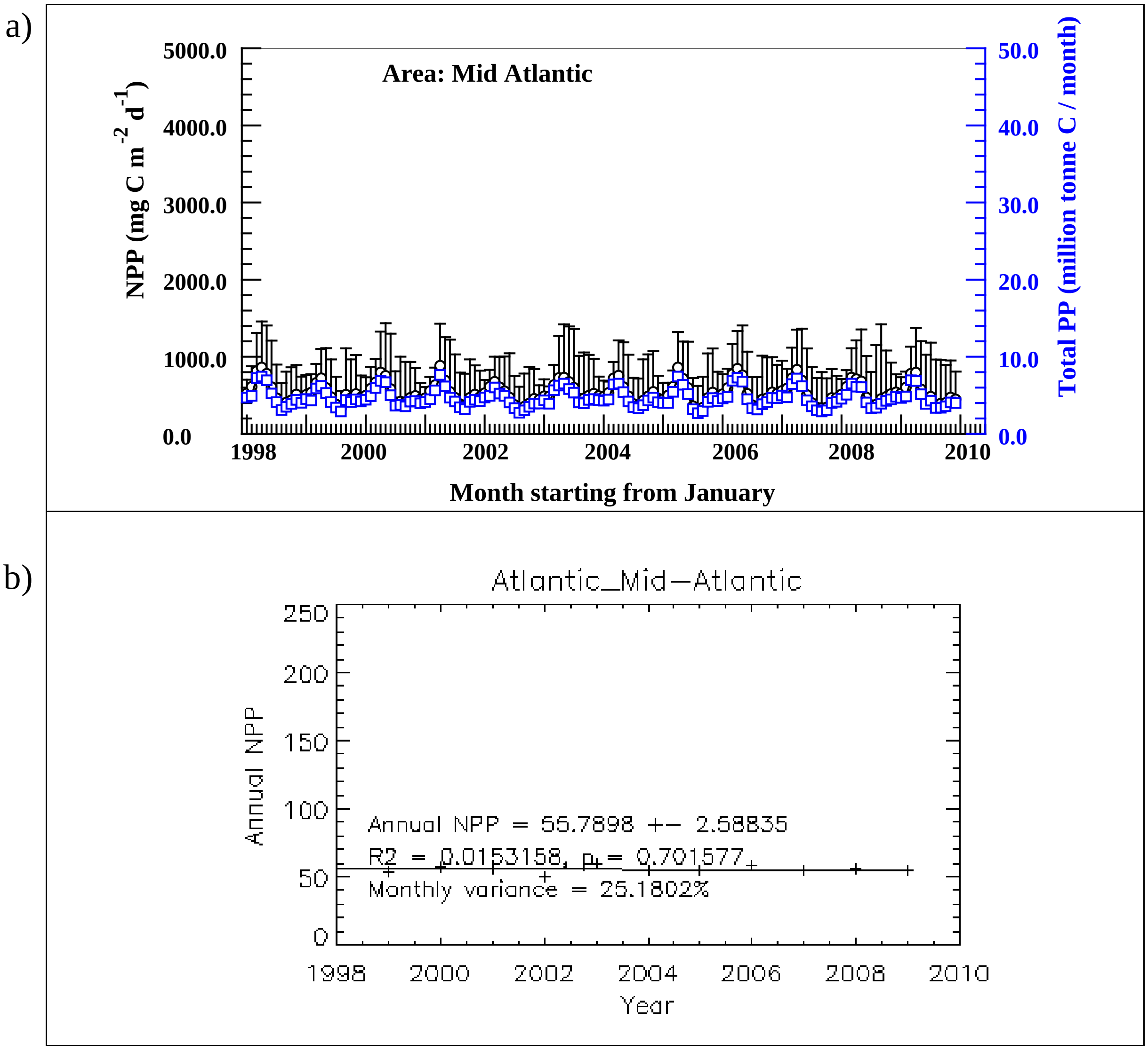

Figure 11. Mid-Atlantic Planning Area a) monthly net primary production (NPP) statistics and b) annual NPP statistics (million tons C).

3.1.3 South Atlantic

The South Atlantic Planning Area covers an area of 54.34 million acres. During the period 1998 through 2009, mean annual NPP was 49.59 million tons of carbon (s.d. = ±4.44). Annual and monthly variance determinations were 8.95% and 26.86%, respectively. Over the period 1998 through 2009, trend analysis indicated a less than significant decrease in primary productivity (p = -0.97) (**Figure 12**).

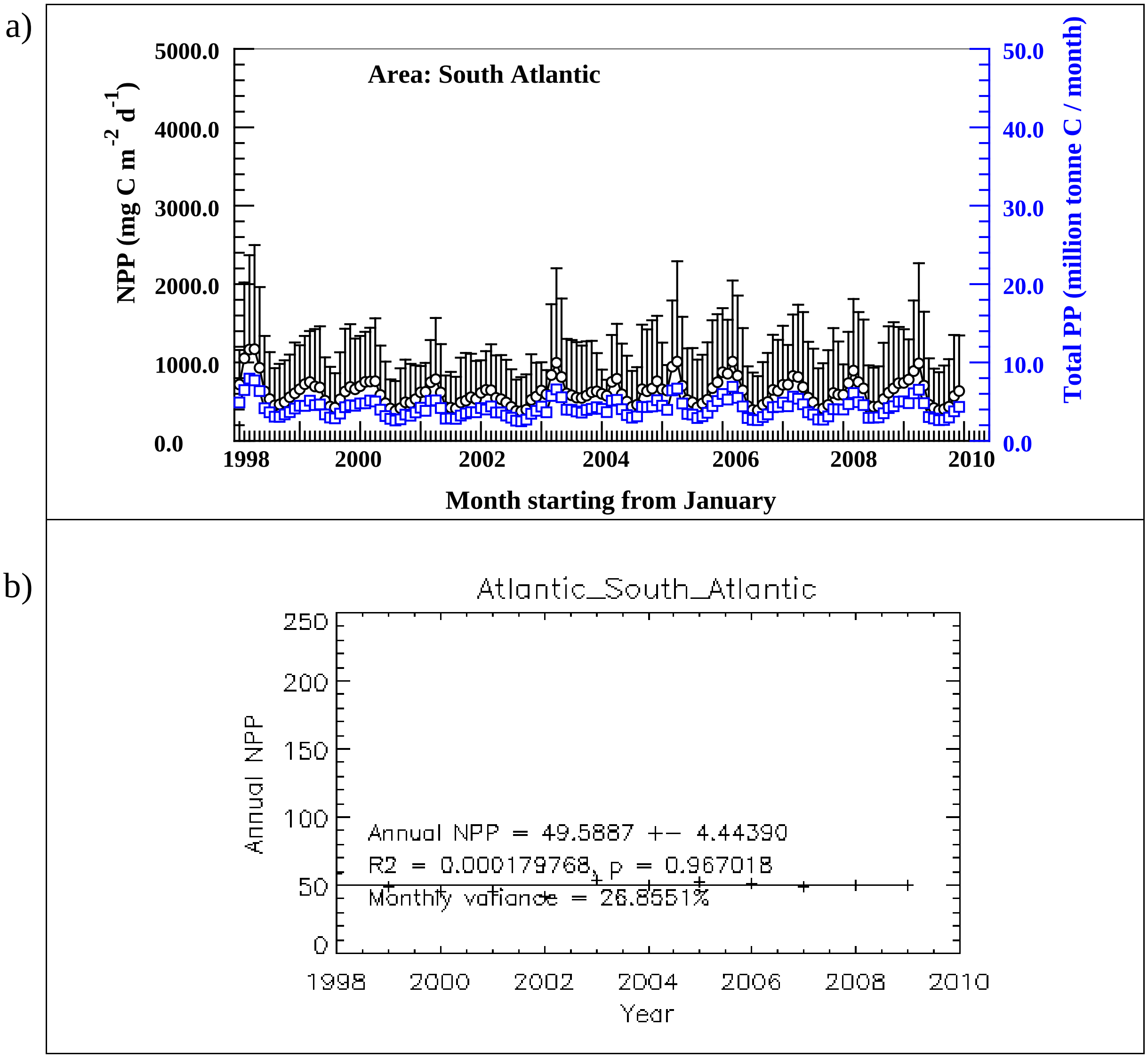

Figure 12. South Atlantic Planning Area a) monthly net primary production (NPP) statistics and b) annual NPP statistics (million tons C).

3.1.4 Straits of Florida

The Straits of Florida Planning Area covers an area of 9.64 million acres. During the period 1998 through 2009, mean annual NPP was 5.99 million tons of carbon (s.d. = ±0.51). Annual and monthly variance determinations were 8.51% and 22.50%, respectively. Over the period 1998 through 2009, trend analysis indicated a less than significant decrease in primary productivity (p = -0.23) (**Figure 13**).

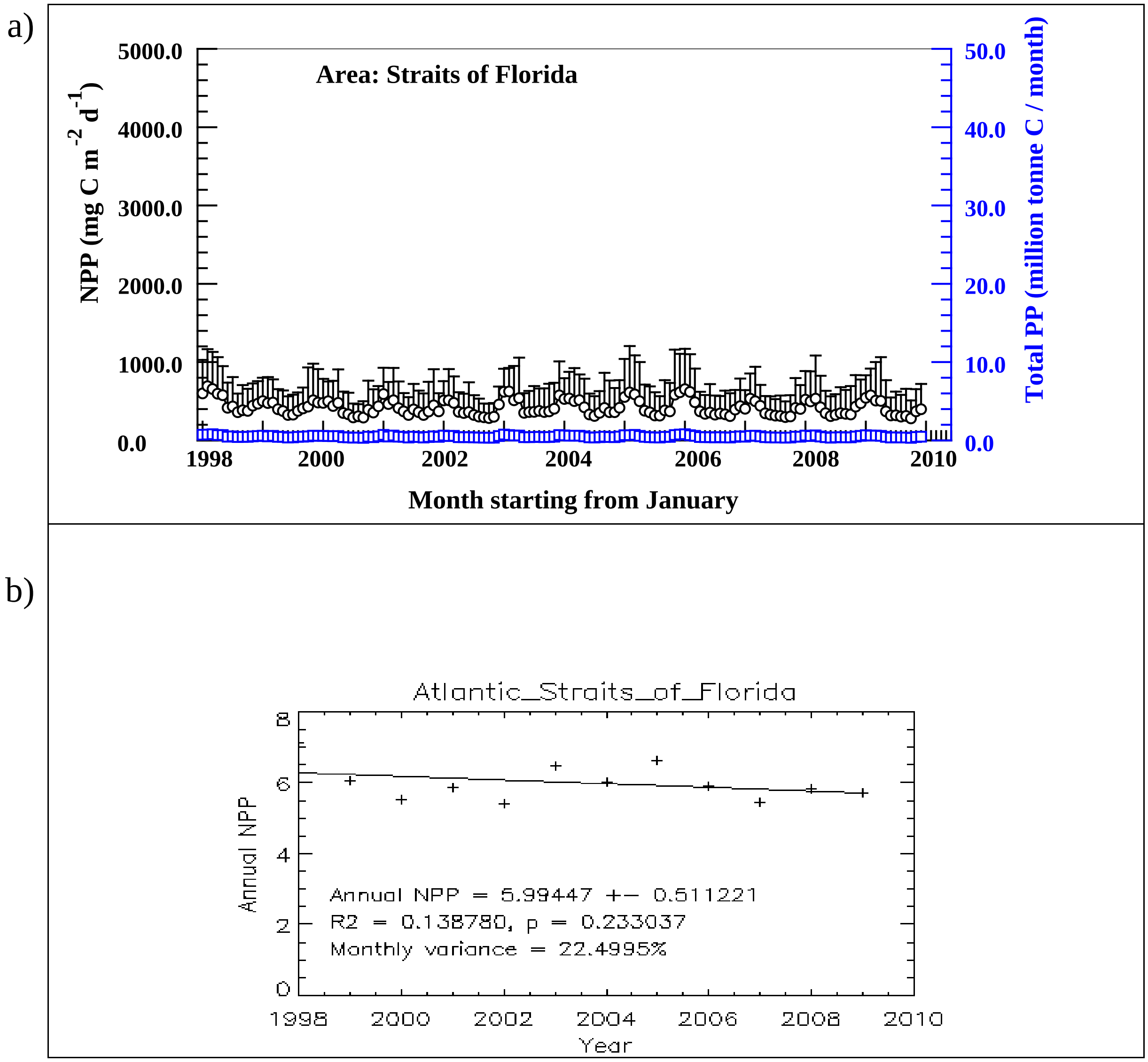

Figure 13. Straits of Florida Planning Area a) monthly net primary production (NPP) statistics and b) annual NPP statistics (million tons C).

3.2 Gulf of Mexico Region

3.2.1 Eastern Gulf of Mexico

The Eastern Gulf of Mexico Planning Area covers an area of 64.56 million acres. During the period 1998 through 2009, mean annual NPP was 60.42 million tons of carbon (s.d. = ±6.98). Annual and monthly variance determinations were 11.55% and 23.49%, respectively. Over the period 1998 through 2009, trend analysis indicated a less than significant decrease in primary productivity (p = -0.38) (**Figure 14**).

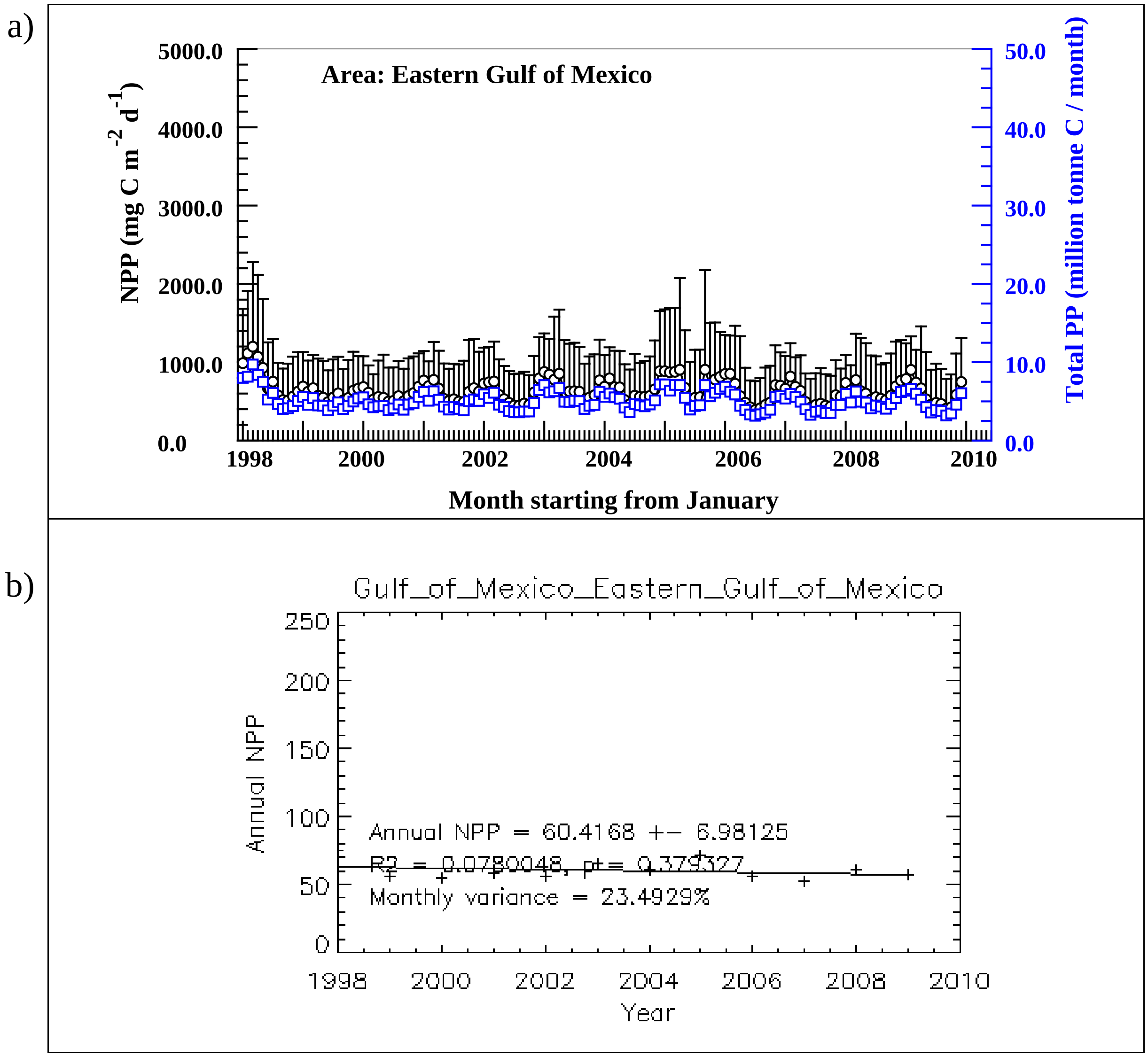

Figure 14. Eastern Gulf of Mexico Planning Area a) monthly net primary production (NPP) statistics and b) annual NPP statistics (million tons C).

3.2.2 Central Gulf of Mexico

The Central Gulf of Mexico Planning Area covers an area of 66.45 million acres. During the period 1998 through 2009, mean annual NPP was 87.17 million tons of carbon (s.d. = ±9.13). Annual and monthly variance determinations were 10.68% and 28.03%, respectively. Over the period 1998 through 2009, trend analysis indicated a less than significant increase in primary productivity (p = +0.50) (**Figure 15**).

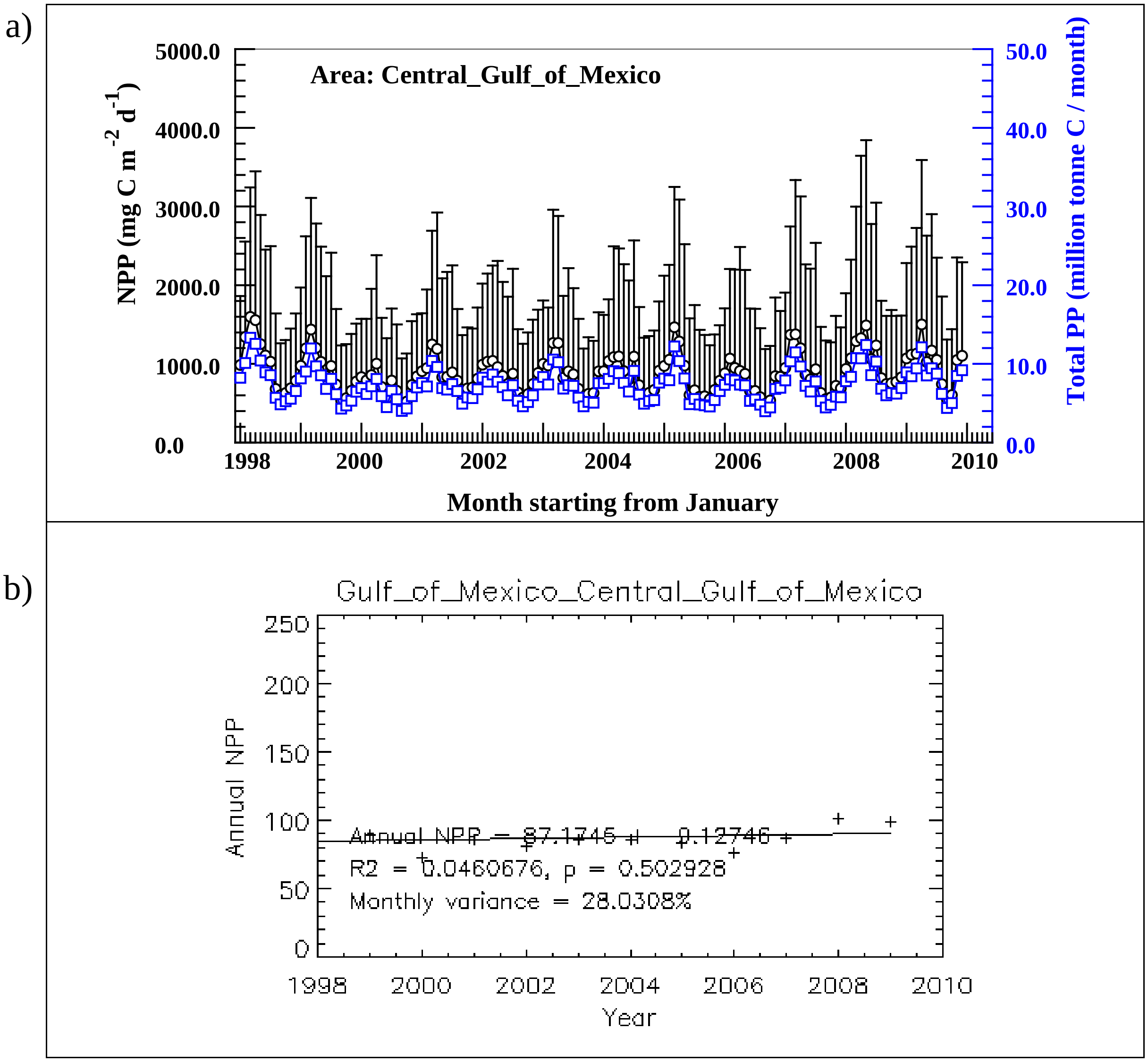

Figure 15. Central Gulf of Mexico Planning Area a) monthly net primary production (NPP) statistics and b) annual NPP statistics (million tons C).

3.2.3 Western Gulf of Mexico

The Western Gulf of Mexico Planning Area covers an area of 28.58 million acres. During the period 1998 through 2009, mean annual NPP was 33.99 million tons of carbon (s.d. = ±3.13). Annual and monthly variance determinations were 9.21% and 33.58%, respectively. Over the period 1998 through 2009, trend analysis indicated a less than significant increase in primary productivity (p = +0.18) (**Figure 16**).

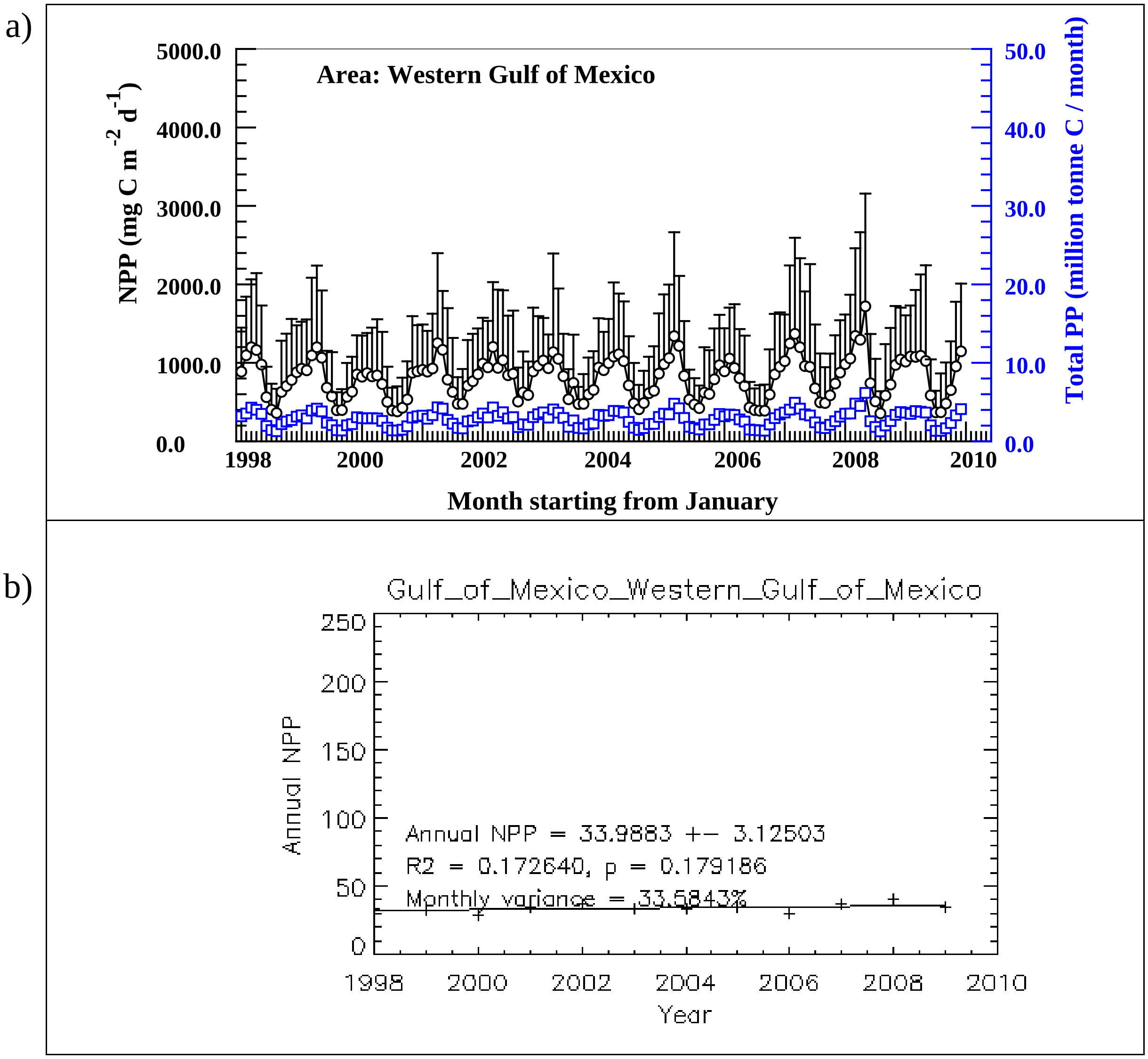

Figure 16. Western Gulf of Mexico Planning Area a) monthly net primary production (NPP) statistics and b) annual NPP statistics (million tons C).

3.3 Pacific Region

3.3.1 Southern California

The Southern California Planning Area covers an area of 88.98 million acres. During the period 1998 through 2009, mean annual NPP was 100.45 million tons of carbon (s.d. = ±10.95). Annual and monthly variance determinations were 10.90% and 21.38%, respectively. Over the period 1998 through 2009, trend analysis indicated a significant increase in primary productivity ($p<0.01$) (**Figure 17**).

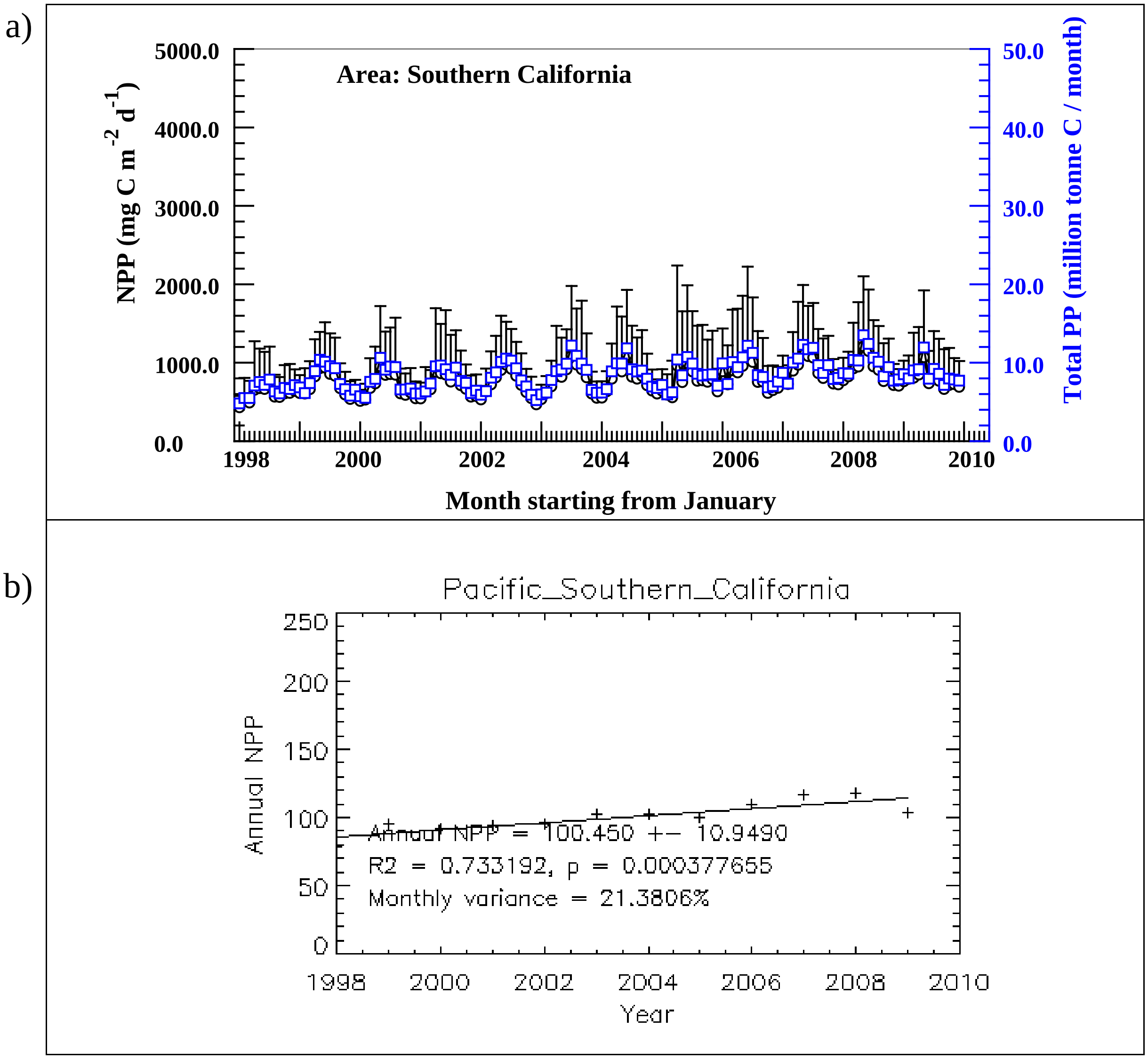

Figure 17. Southern California Planning Area a) monthly net primary production (NPP) statistics and b) annual NPP statistics (million tons C).

3.3.2 Central California

The Central California Planning Area covers an area of 43.68 million acres. During the period 1998 through 2009, mean annual NPP was 60.23 million tons of carbon (s.d. = ±6.70). Annual and monthly variance determinations were 11.12% and 25.82%, respectively. Over the period 1998 through 2009, trend analysis indicated a significant increase in primary productivity (p = +0.02) (**Figure 18**).

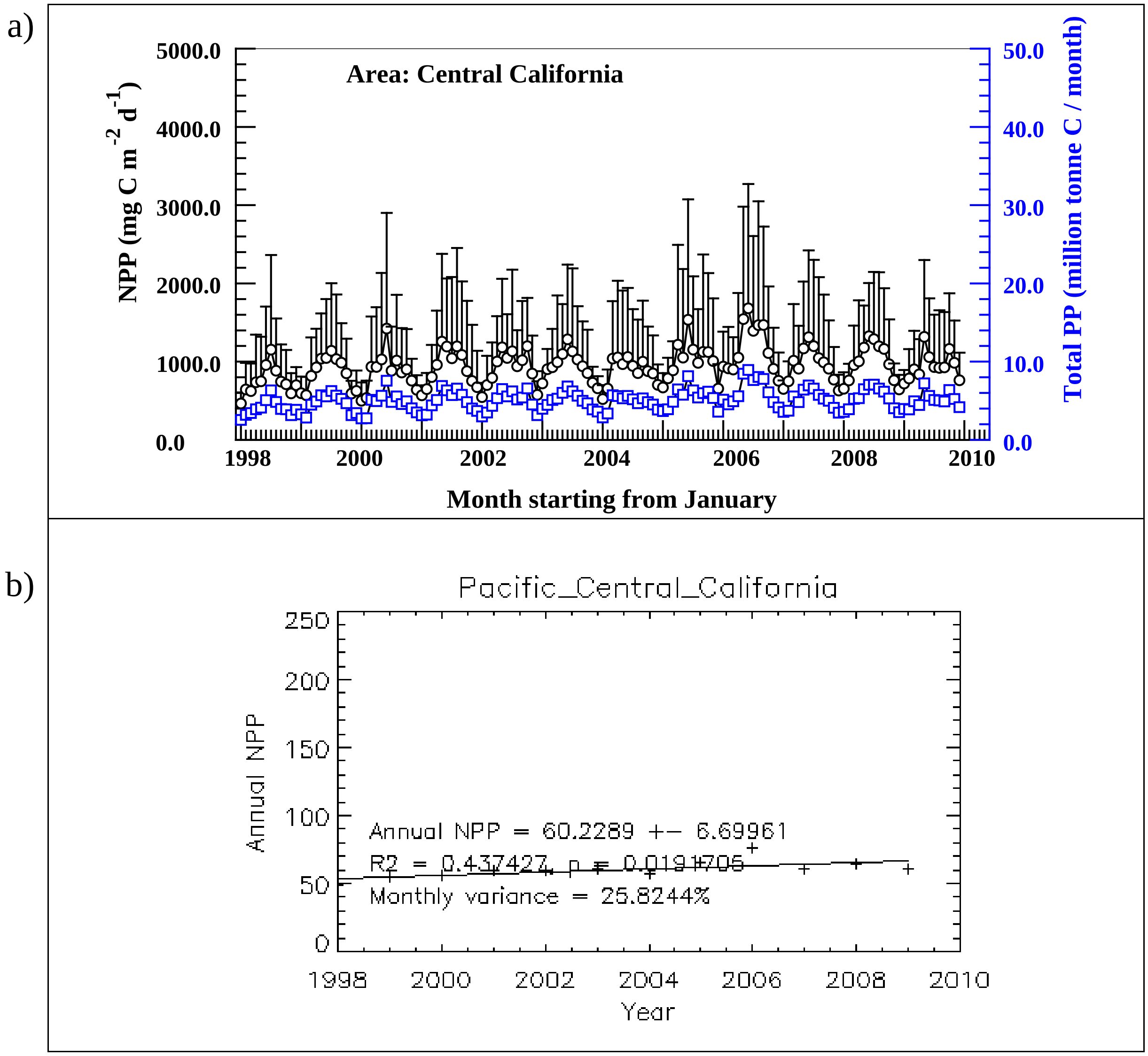

Figure 18. Central California Planning Area a) monthly net primary production (NPP) statistics and b) annual NPP statistics (million tons C).

3.3.3 Northern California

The Northern California Planning Area covers an area of 44.79 million acres. During the period 1998 through 2009, mean annual NPP was 55.26 million tons of carbon (s.d. = ±3.13). Annual and monthly variance determinations were 5.99% and 27.61%, respectively. Over the period 1998 through 2009, trend analysis indicated a significant increase in primary productivity ($p<0.01$) (**Figure 19**).

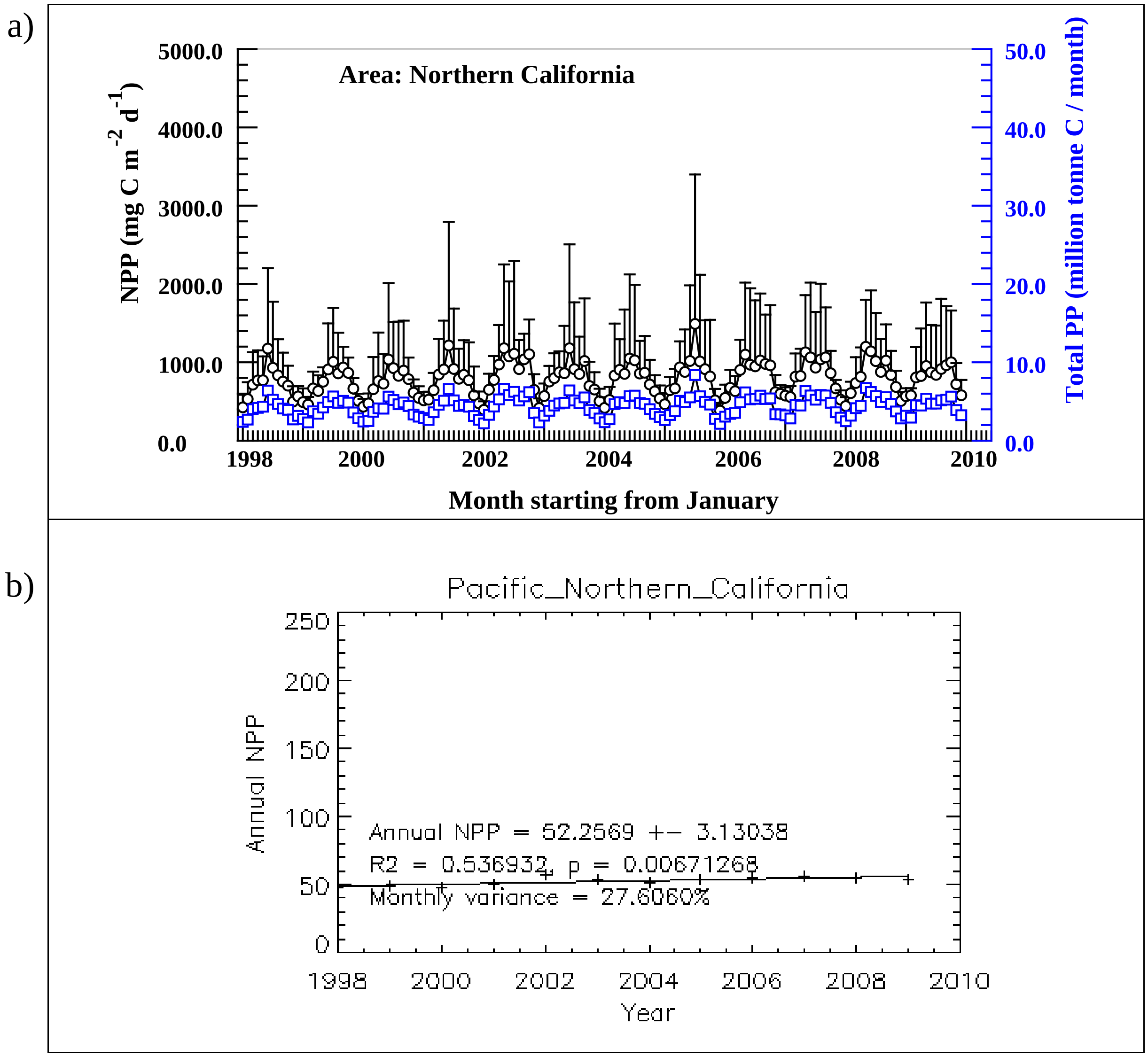

Figure 19. Northern California Planning Area a) monthly net primary production (NPP) statistics and b) annual NPP statistics (million tons C).

3.3.4 Washington-Oregon

The Washington-Oregon Planning Area covers an area of 71.00 million acres. During the period 1998 through 2009, mean annual NPP was 89.89 million tons of carbon (s.d. = ±7.43). Annual and monthly variance determinations were 8.26% and 43.59%, respectively. Over the period 1998 through 2009, trend analysis indicated a significant increase in primary productivity ($p<0.01$) (**Figure 20**).

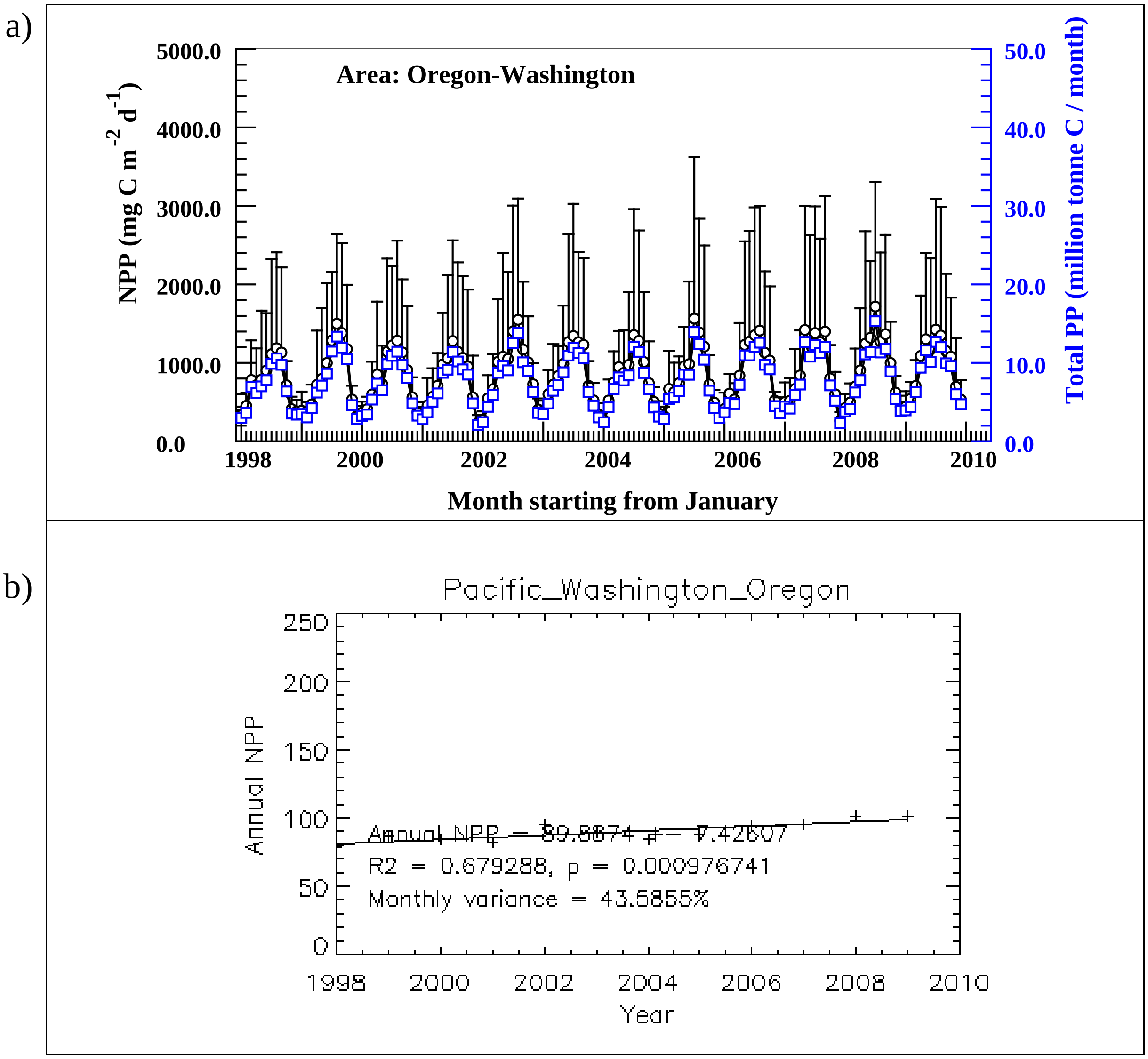

Figure 20. Washington-Oregon Planning Area a) monthly net primary production (NPP) statistics and b) annual NPP statistics (million tons C).

3.4 Alaska Region

3.4.1 Gulf of Alaska

The Gulf of Alaska Planning Area covers an area of 112.10 million acres. During the period 1998 through 2009, mean annual NPP was 124.97 million tons of carbon (s.d. = ±4.82). Annual and monthly variance determinations were 3.86% and 50.10%, respectively. Over the period 1998 through 2009, trend analysis indicated a less than significant increase in primary productivity (p = +0.74) (**Figure 21**).

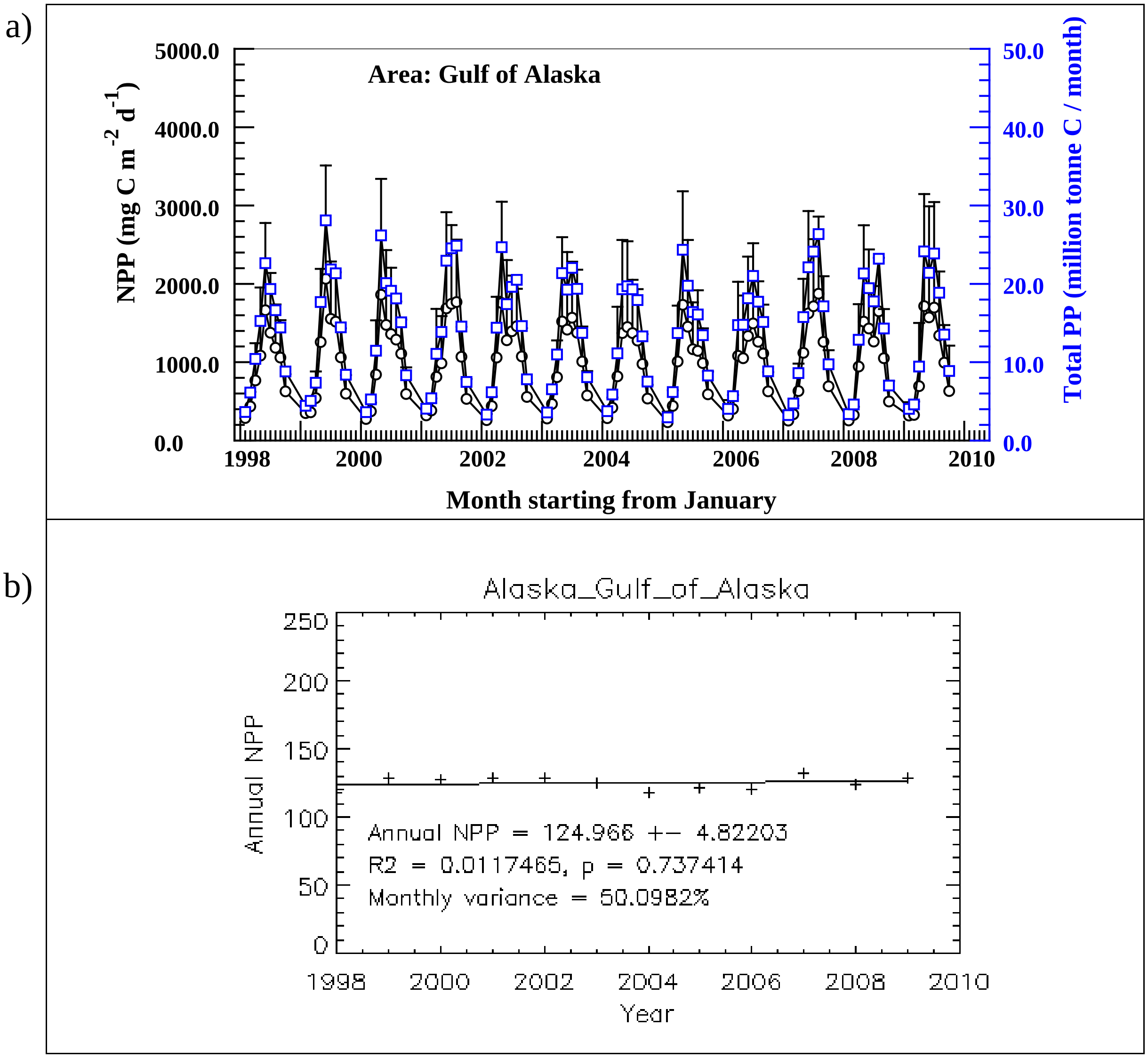

Figure 21. Gulf of Alaska Planning Area a) monthly net primary production (NPP) statistics and b) annual NPP statistics (million tons C).

3.4.2 Cook Inlet

The Cook Inlet Planning Area covers an area of 5.36 million acres. During the period 1998 through 2009, mean annual NPP was 8.97 million tons of carbon (s.d. = ±0.61). Annual and monthly variance determinations were 6.80% and 58.30%, respectively. Over the period 1998 through 2009, trend analysis indicated a less than significant decrease in primary productivity (p = -0.63) (**Figure 22**).

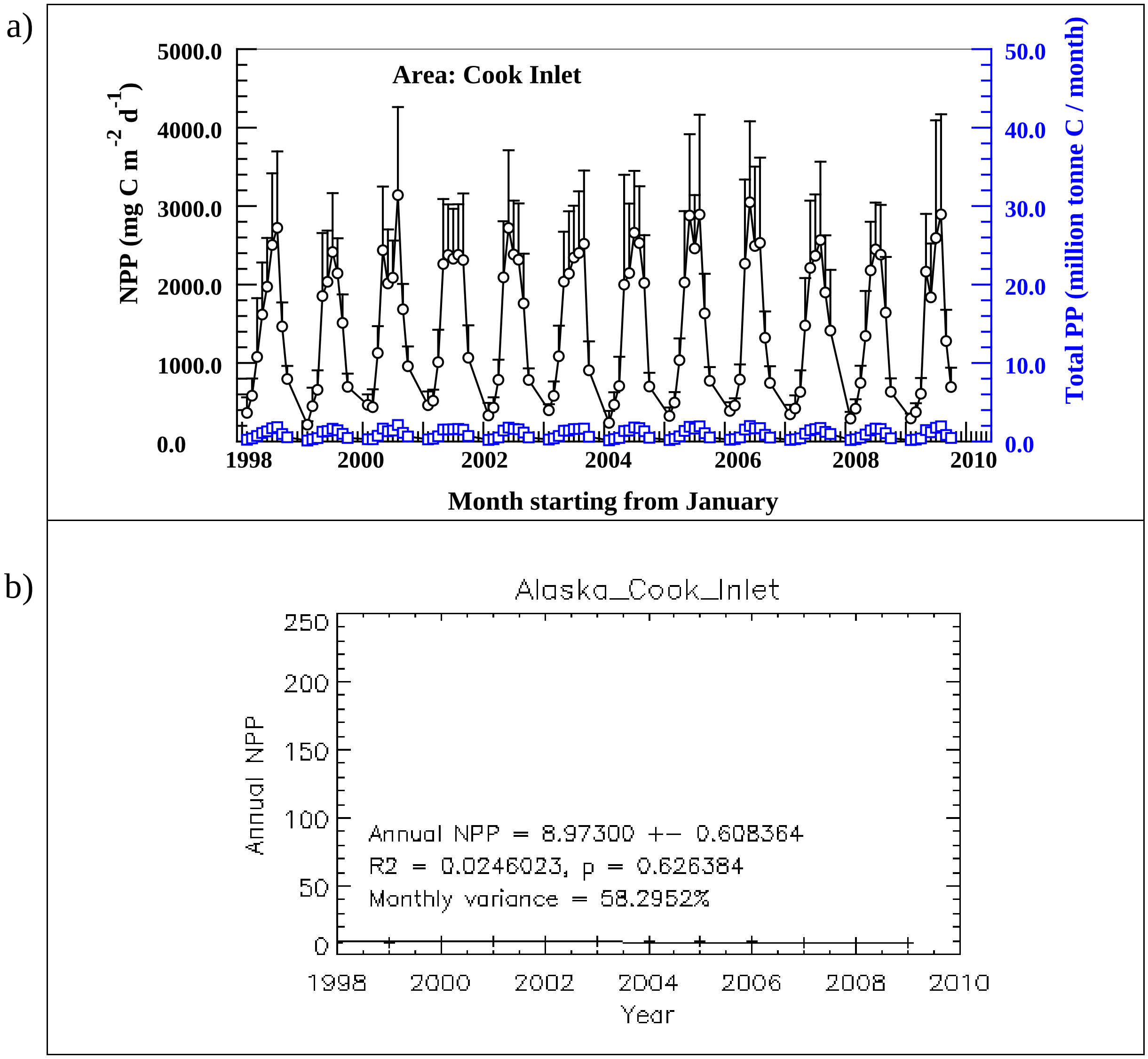

Figure 22. Cook Inlet Planning Area a) monthly net primary production (NPP) statistics and b) annual NPP statistics (million tons C).

3.4.3 Kodiak

The Kodiak Planning Area covers an area of 89.00 million acres. During the period 1998 through 2009, mean annual NPP was 82.73 million tons of carbon (s.d. = ±4.18). Annual and monthly variance determinations were 5.05% and 49.11%, respectively. Over the period 1998 through 2009, trend analysis indicated a less than significant decrease in primary productivity (p = -0.05) (**Figure 23**).

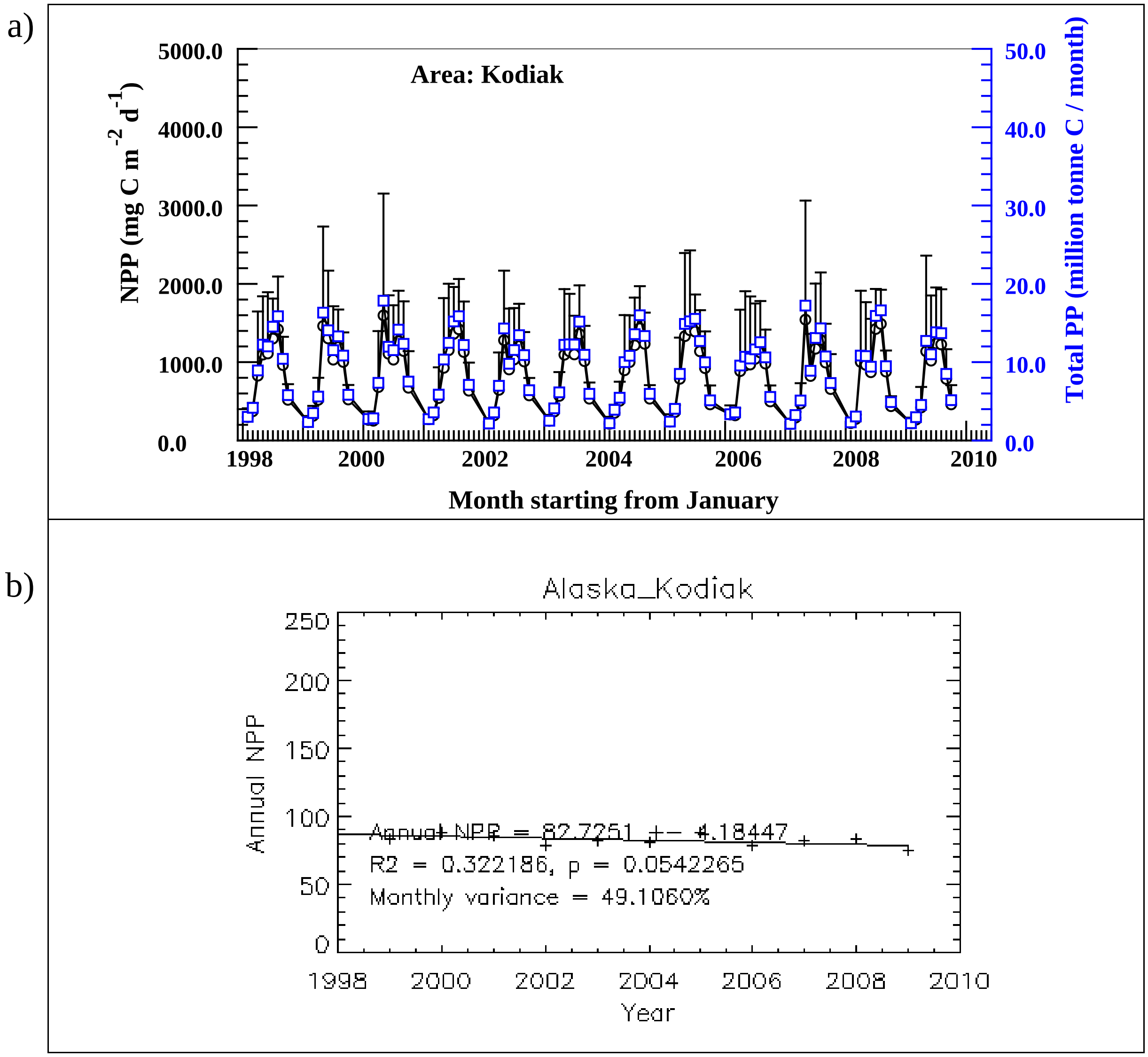

Figure 23. Kodiak Planning Area a) monthly net primary production (NPP) statistics and b) annual NPP statistics (million tons C).

3.4.4 Shumagin

The Shumagin Planning Area covers an area of 84.65 million acres. During the period 1998 through 2009, mean annual NPP was 78.19 million tons of carbon (s.d. = ±6.04). Annual and monthly variance determinations were 7.72% and 53.98%, respectively. Over the period 1998 through 2009, trend analysis indicated a significant decrease in primary productivity (p = -0.01) (**Figure 24**).

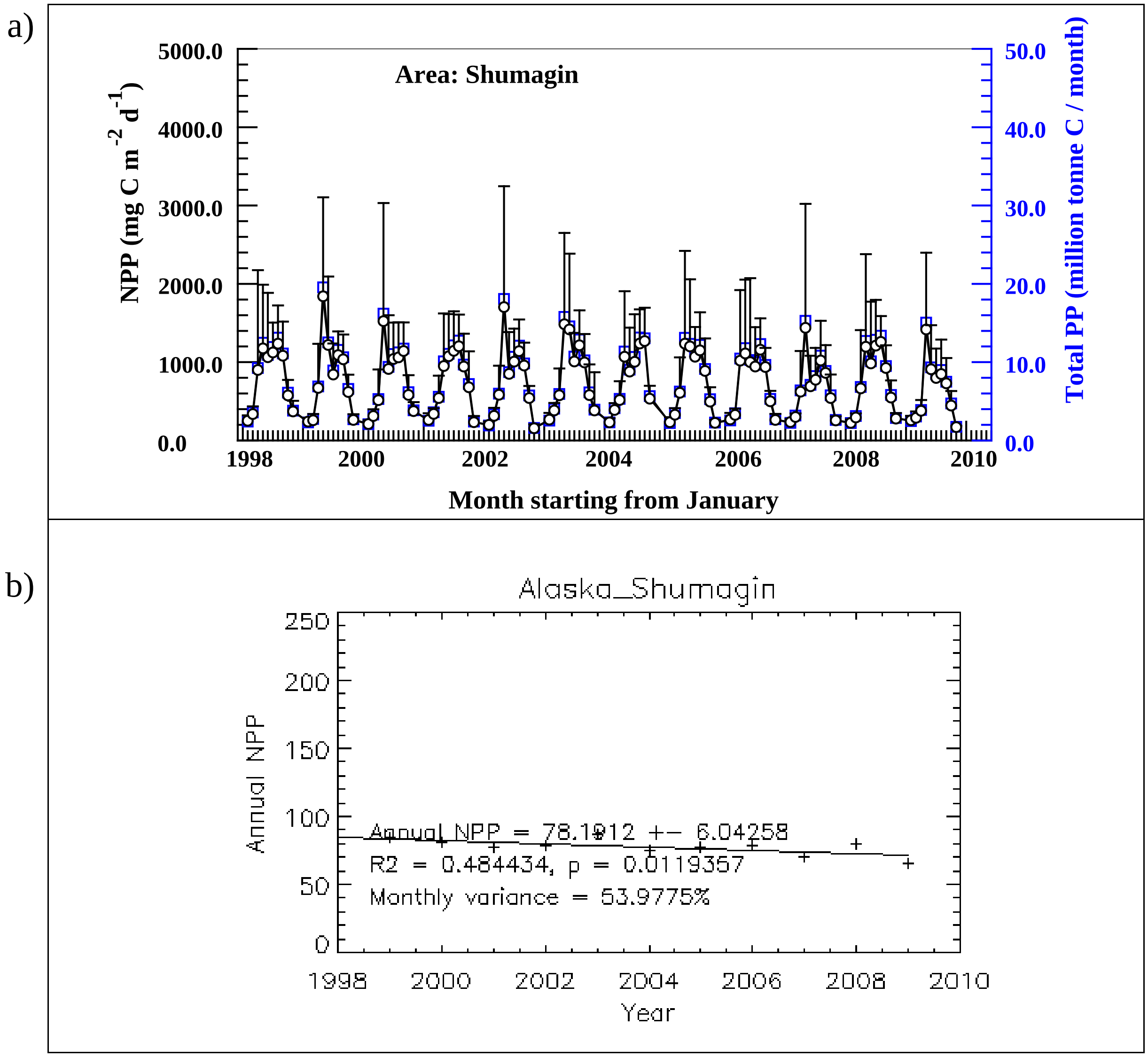

Figure 24. Shumagin Planning Area a) monthly net primary production (NPP) statistics and b) annual NPP statistics (million tons C).

3.4.5 Aleutian Arc

The Aleutian Arc Planning Area covers an area of 259.06 million acres. During the period 1998 through 2009, mean annual NPP was 195.07 million tons of carbon (s.d. = ±14.98). Annual and monthly variance determinations were 7.68% and 55.64%, respectively. Over the period 1998 through 2009, trend analysis indicated a less than significant decrease in primary productivity (p = -0.33) (**Figure 25**).

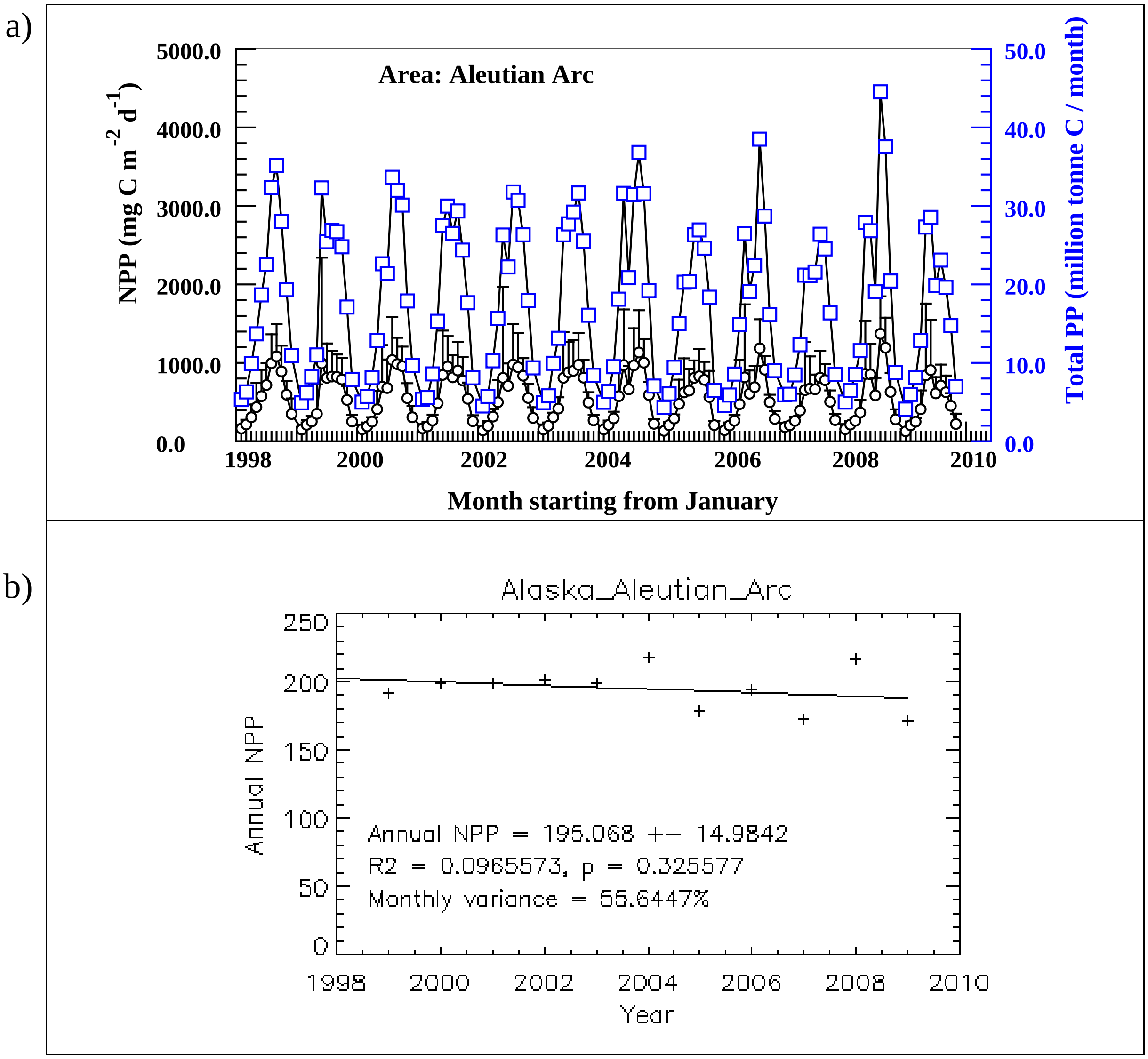

Figure 25. Aleutian Arc Planning Area a) monthly net primary production (NPP) statistics and b) annual NPP statistics (million tons C).

3.4.6 North Aleutian Basin

The North Aleutian Basin Planning Area covers an area of 32.45 million acres. During the period 1998 through 2009, mean annual NPP was 39.73 million tons of carbon (s.d. = ±6.90). Annual and monthly variance determinations were 17.37% and 43.93%, respectively. Over the period 1998 through 2009, trend analysis indicated a less than significant decrease in primary productivity (p = -0.88) (**Figure 26**).

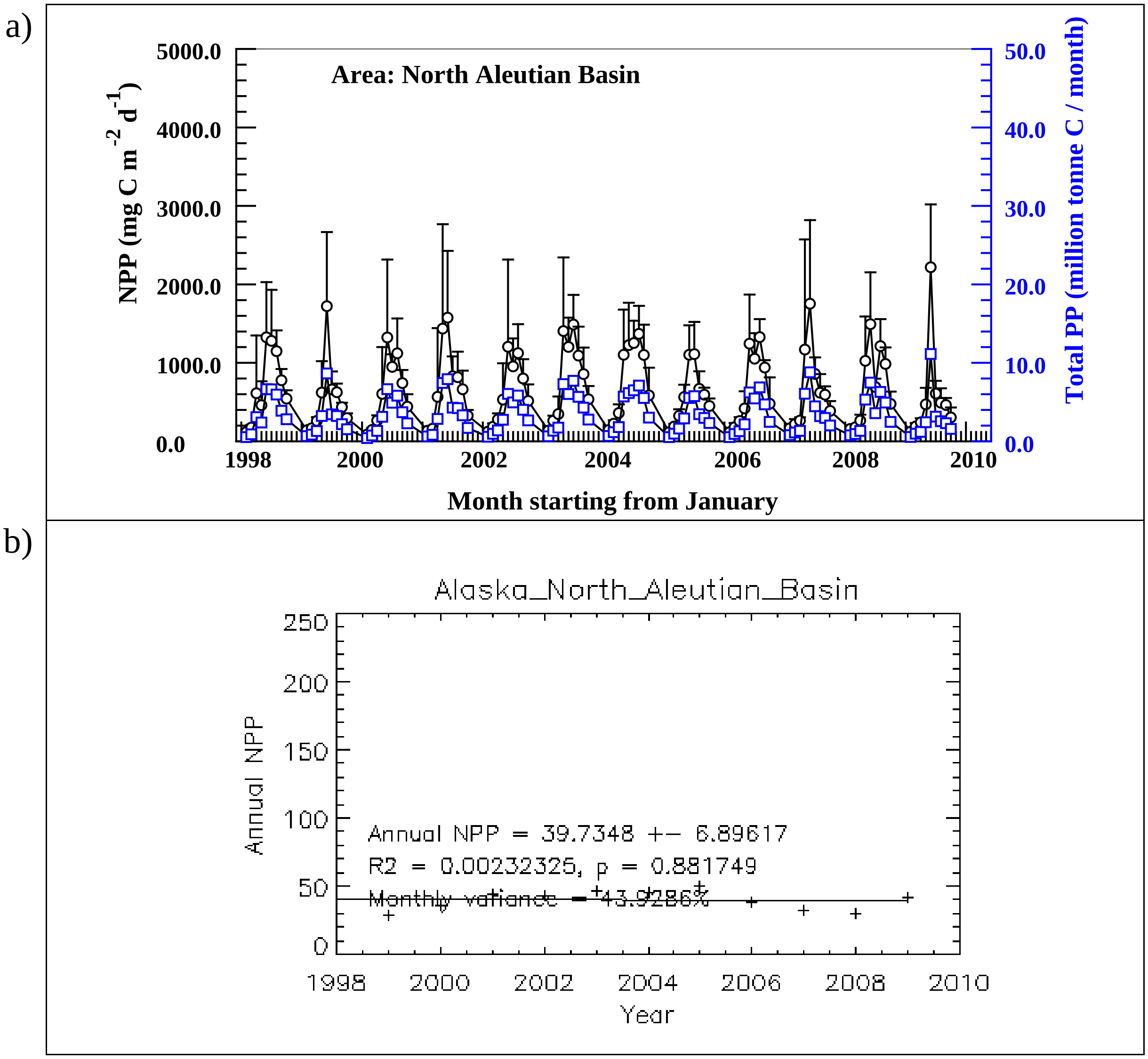

Figure 26. North Aleutian Basin Planning Area a) monthly net primary production (NPP) statistics and b) annual NPP statistics (million tons C).

3.4.7 St. George Basin

The St. George Basin Planning Area covers an area of 70.23 million acres. During the period 1998 through 2009, mean annual NPP was 72.38 million tons of carbon (s.d. = ±10.31). Annual and monthly variance determinations were 14.24% and 56.93%, respectively. Over the period 1998 through 2009, trend analysis indicated a less than significant decrease in primary productivity (p = -0.27) (**Figure 27**).

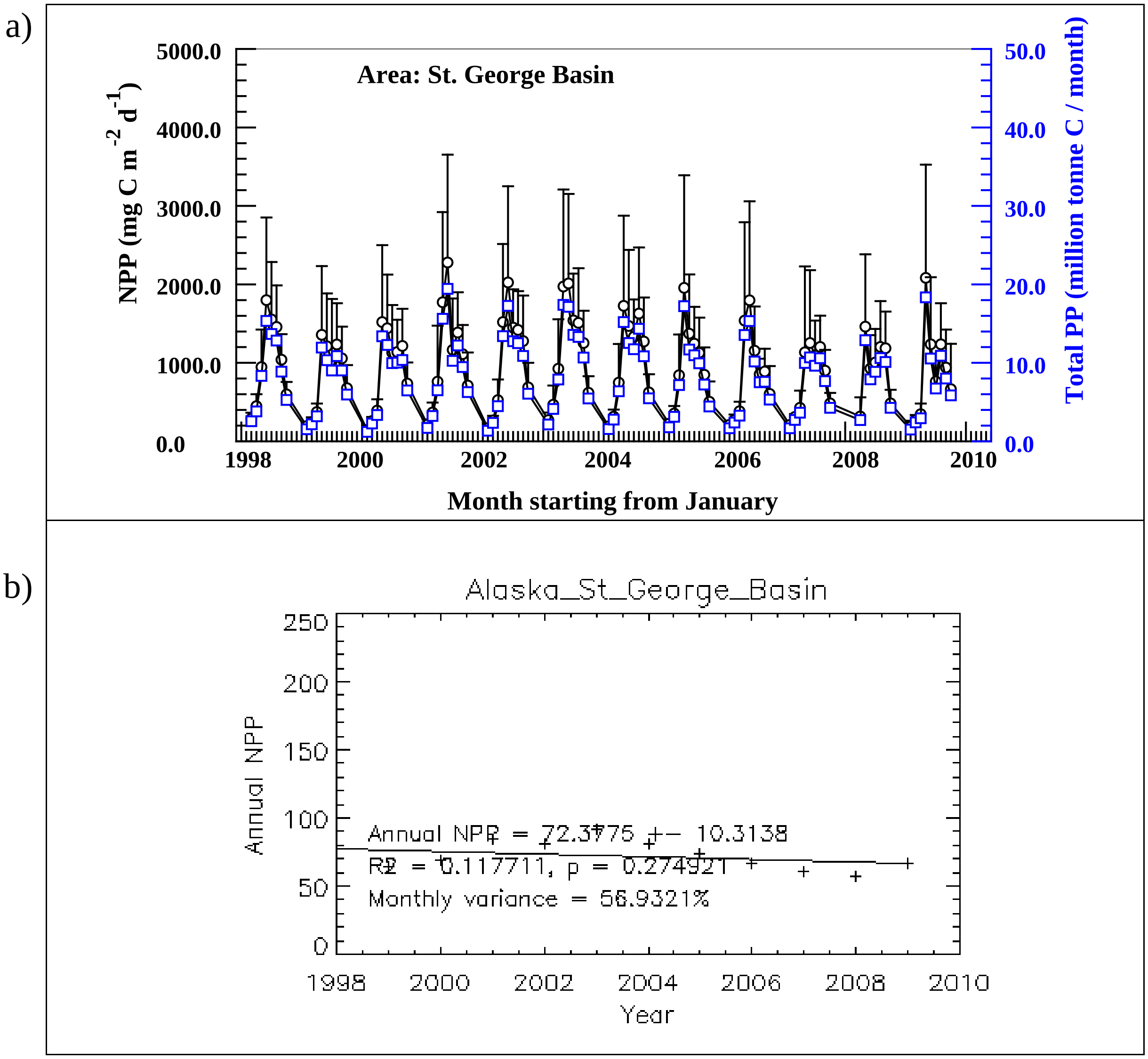

Figure 27. St. George Basin Planning Area a) monthly net primary production (NPP) statistics and b) annual NPP statistics (million tons C).

3.4.8 Bowers Basin

The Bowers Basin Planning Area covers an area of 87.59 million acres. During the period 1998 through 2009, mean annual NPP was 60.09 million tons of carbon (s.d. = ±6.22). Annual and monthly variance determinations were 10.35% and 56.93%, respectively. Over the period 1998 through 2009, trend analysis indicated a less than significant increase in primary productivity (p = +0.60) (**Figure 28**).

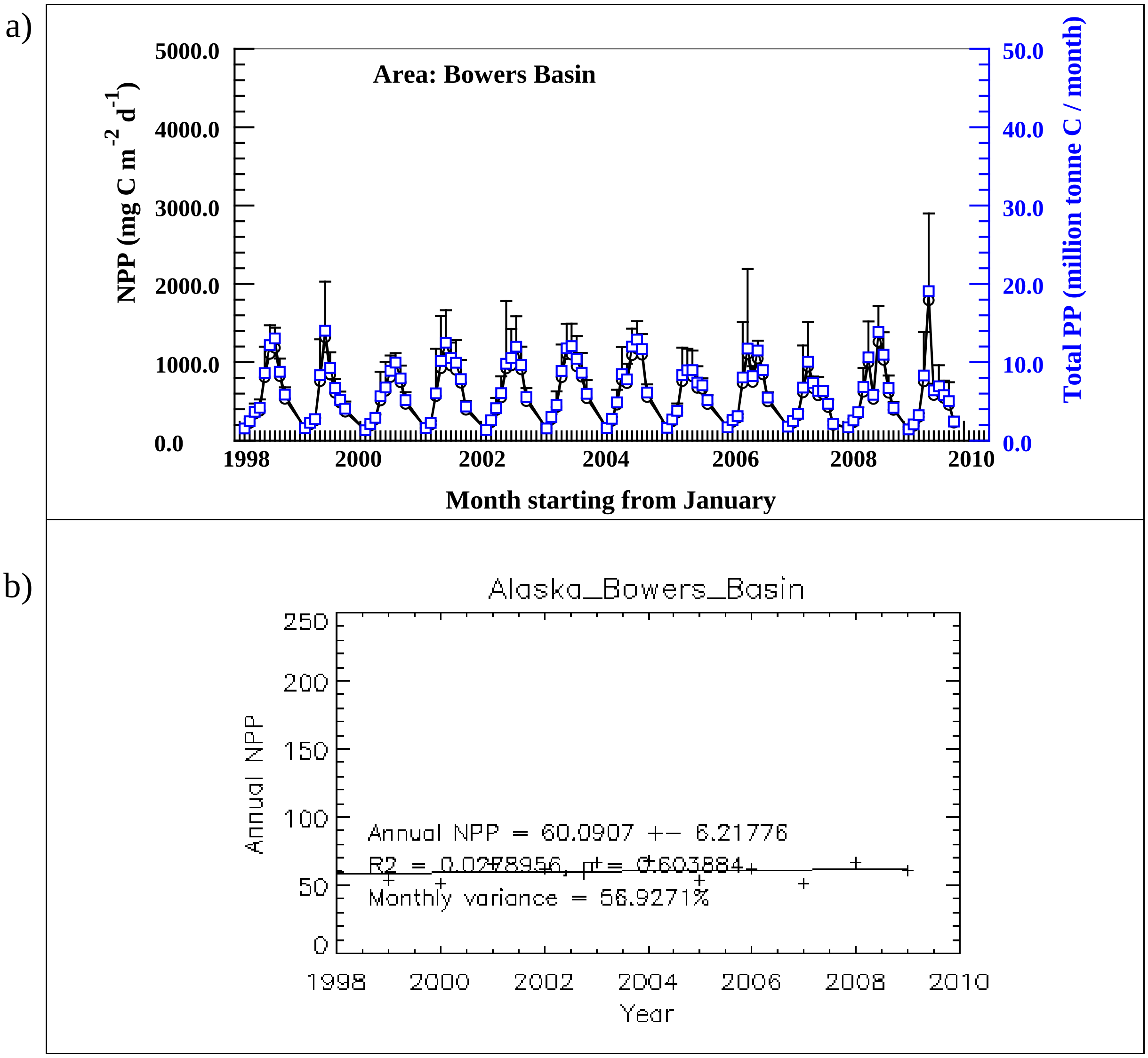

Figure 28. Bowers Basin Planning Area a) monthly net primary production (NPP) statistics and b) annual NPP statistics (million tons C).

3.4.9 Aleutian Basin

The Aleutian Basin Planning Area covers an area of 41.33 million acres. During the period 1998 through 2009, mean annual NPP was 30.96 million tons of carbon (s.d. = ±4.17). Annual and monthly variance determinations were 13.47% and 69.29%, respectively. Over the period 1998 through 2009, trend analysis indicated a less than significant decrease in primary productivity (p = -0.90) (**Figure 29**).

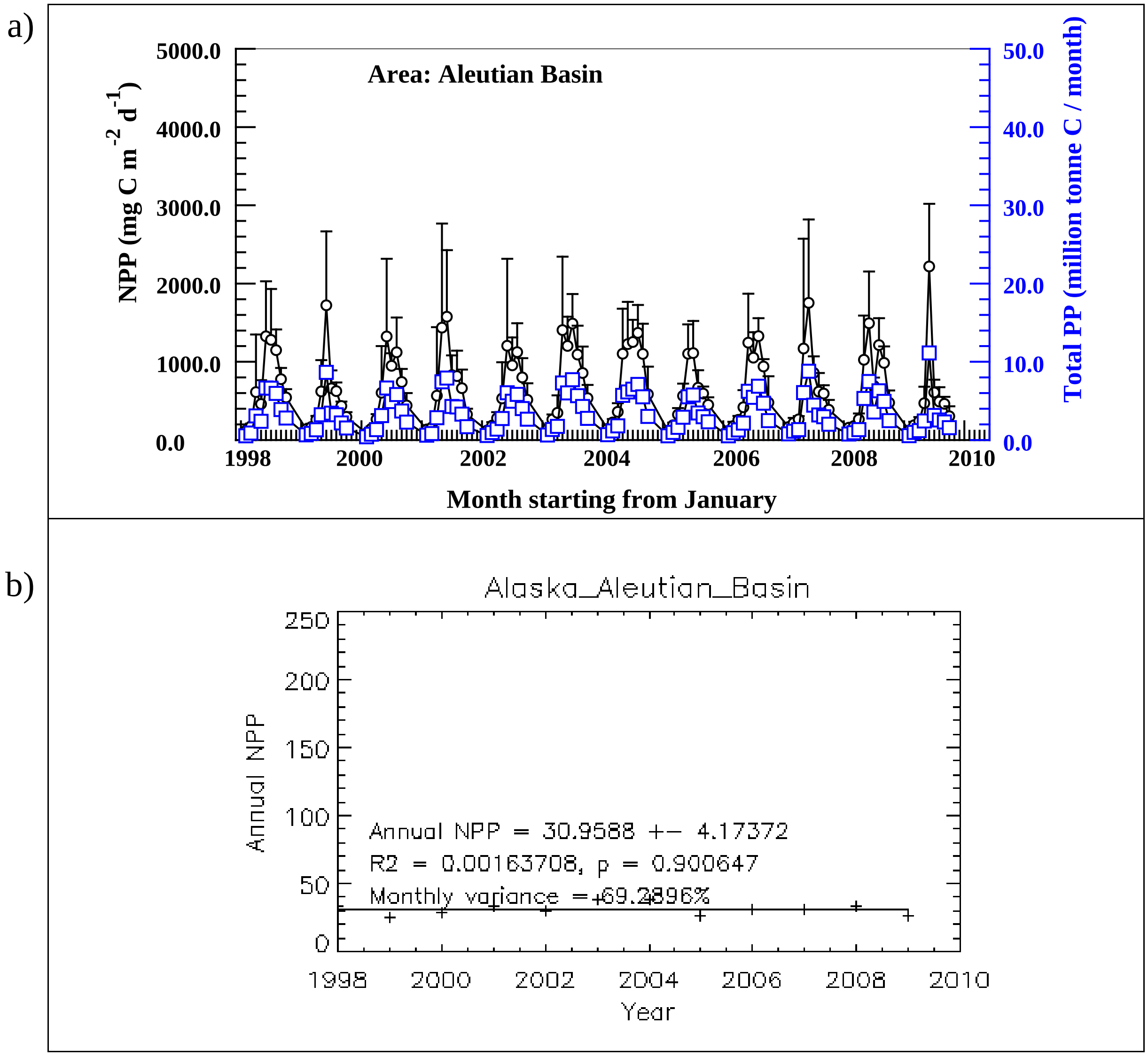

Figure 29. Aleutian Basin Planning Area a) monthly net primary production (NPP) statistics and b) annual NPP statistics (million tons C).

3.4.10 Navarin Basin

The Navarin Basin Planning Area covers an area of 34.02 million acres. During the period 1998 through 2009, mean annual NPP was 26.75 million tons of carbon (s.d. = ±6.26). Annual and monthly variance determinations were 23.40% and 56.83%, respectively. Over the period 1998 through 2009, trend analysis indicated a less than significant decrease in primary productivity (p = -0.71) (**Figure 30**).

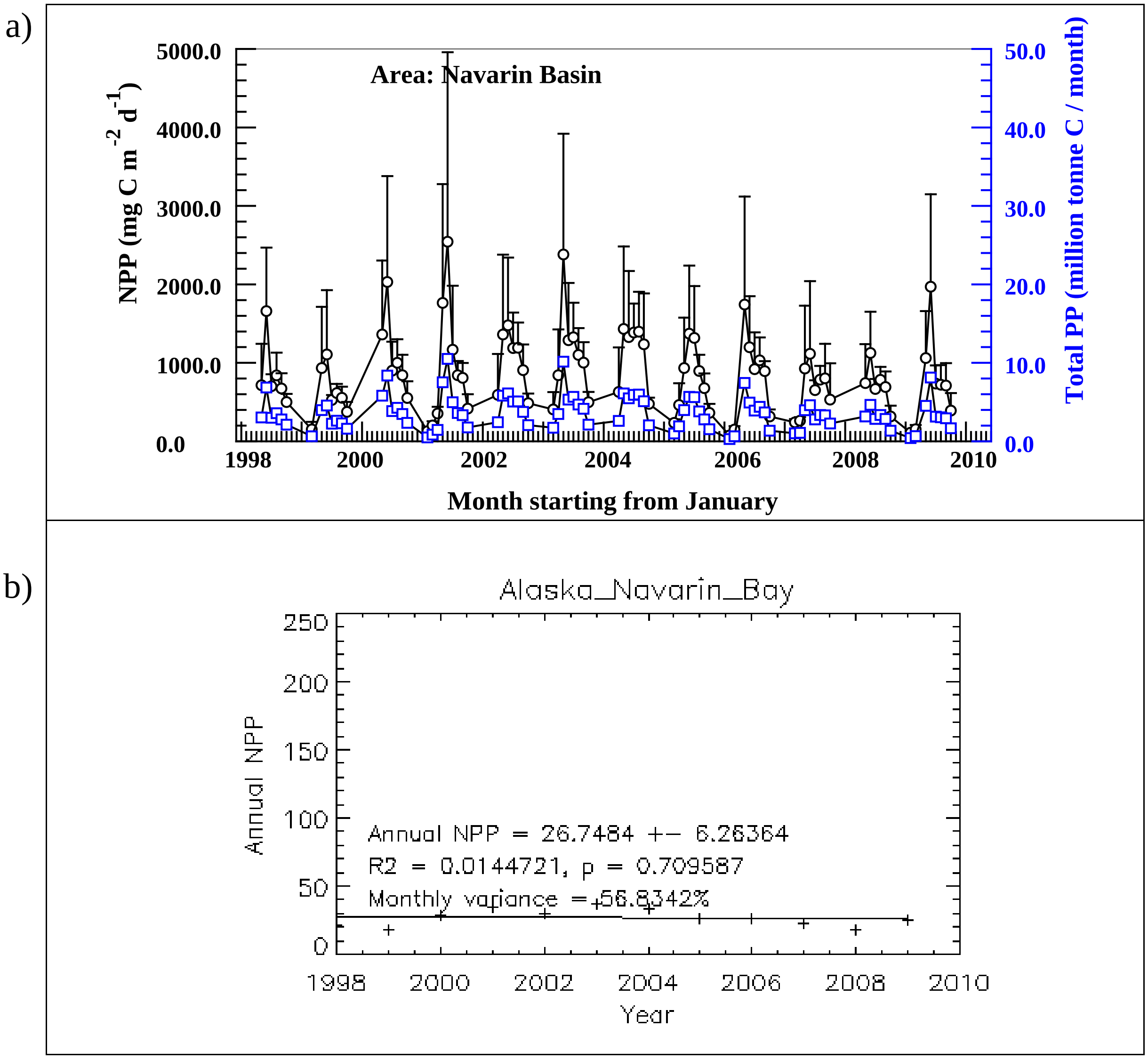

Figure 30. Navarin Basin Planning Area a) monthly net primary production (NPP) statistics and b) annual NPP statistics (million tons C).

3.4.11 St. Matthew-Hall

The St. Matthew-Hall Planning Area covers an area of 54.57 million acres. During the period 1998 through 2009, mean annual NPP was 52.09 million tons of carbon (s.d. = ±7.20). Annual and monthly variance determinations were 13.82% and 29.66%, respectively. Over the period 1998 through 2009, trend analysis indicated a less than significant decrease in primary productivity (p = -0.60) (**Figure 31**).

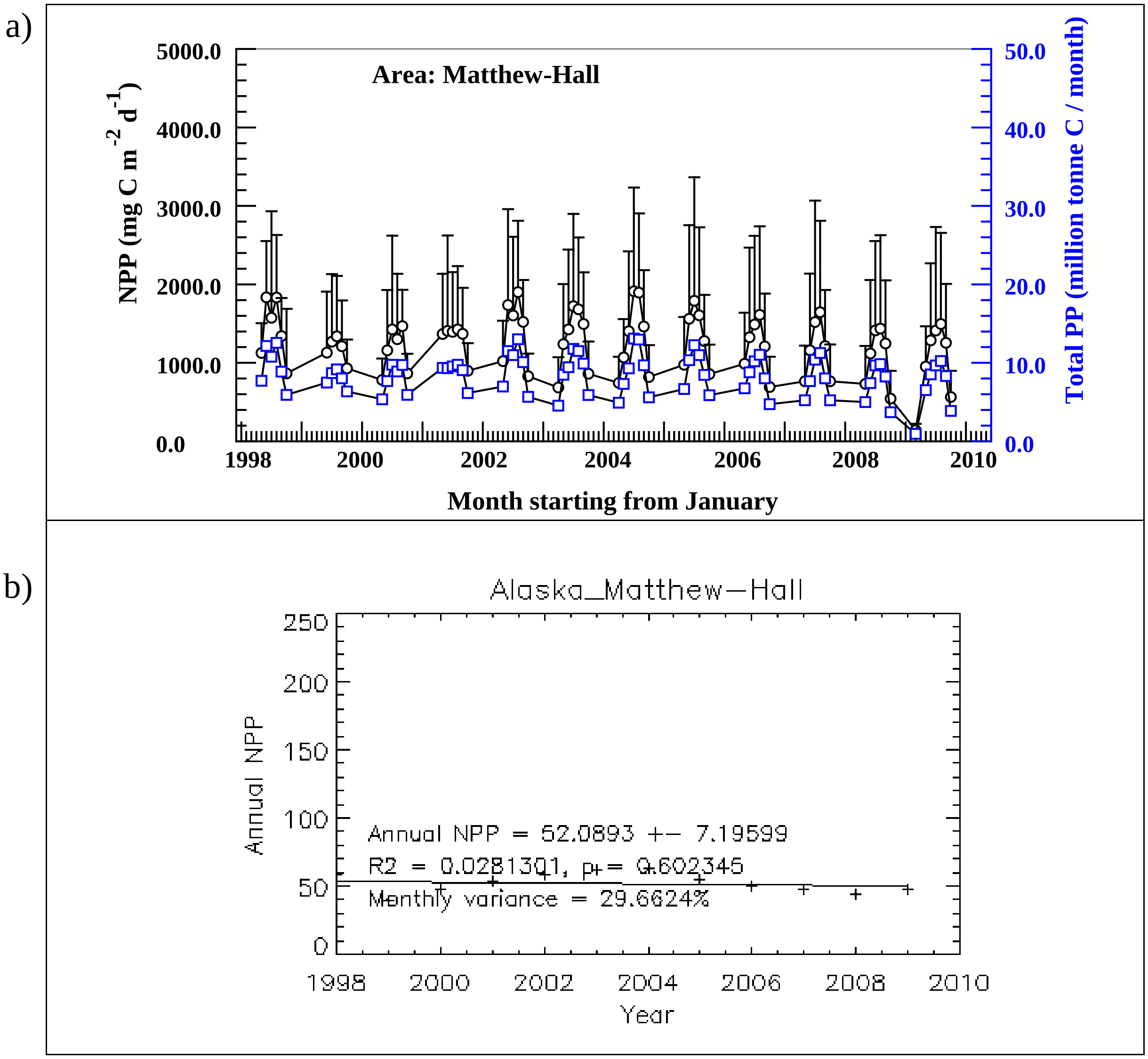

Figure 31. St. Matthew-Hall Planning Area a) monthly net primary production (NPP) statistics and b) annual NPP statistics (million tons C).

3.4.12 Norton Basin

The Norton Basin Planning Area covers an area of 24.25 million acres. During the period 1998 through 2009, mean annual NPP was 34.07 million tons of carbon (s.d. = ±4.00). Annual and monthly variance determinations were 11.74% and 44.27%, respectively. Over the period 1998 through 2009, trend analysis indicated a significant increase in primary productivity (p = +0.02) (**Figure 32**).

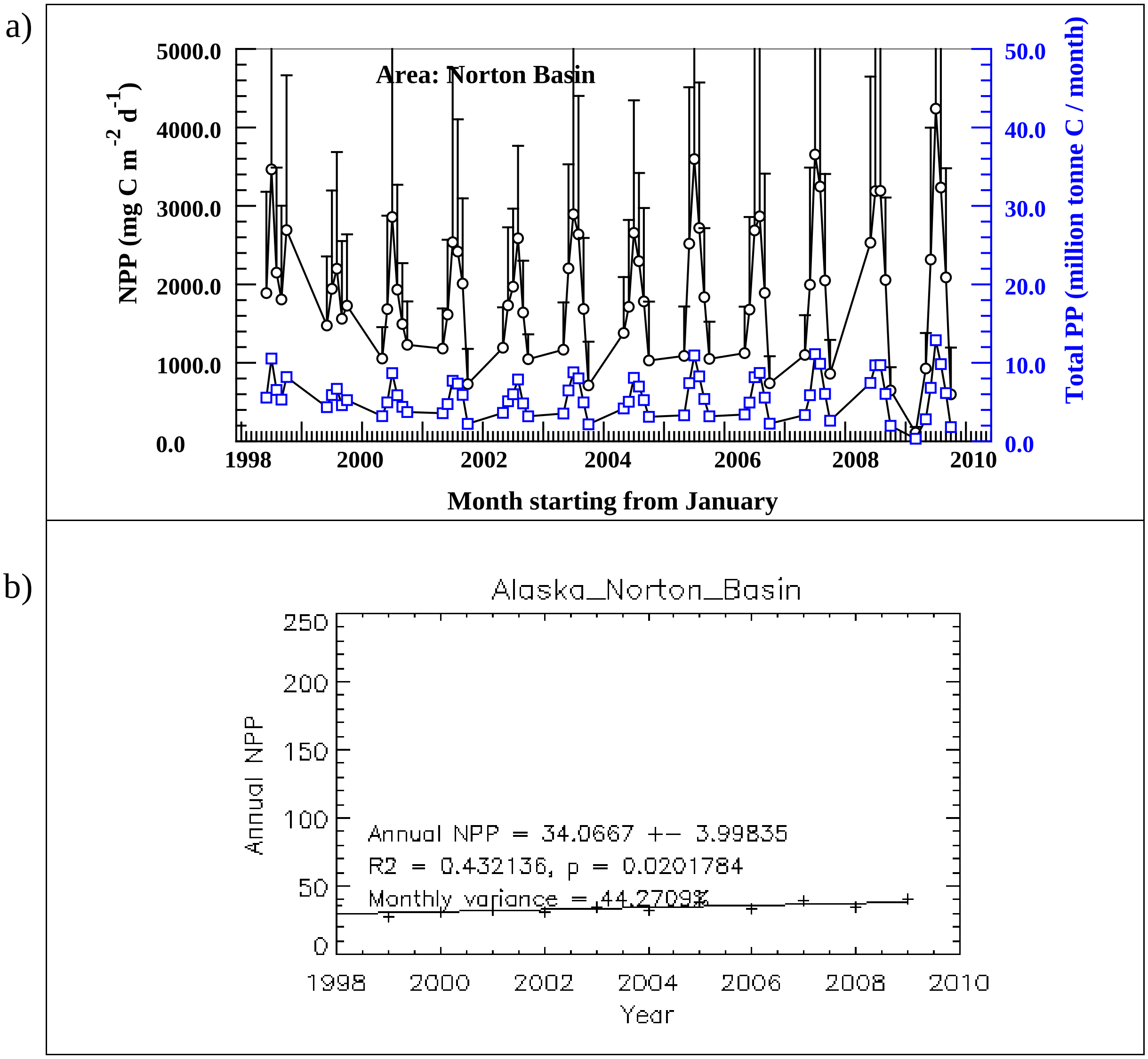

Figure 32. Norton Basin Planning Area a) monthly net primary production (NPP) statistics and b) annual NPP statistics (million tons C).

3.4.13 Hope Basin

The Hope Basin Planning Area covers an area of 12.82 million acres. During the period 1998 through 2009, mean annual NPP was 12.01 million tons of carbon (s.d. = ±2.67). Annual and monthly variance determinations were 22.23% and 30.66%, respectively. Over the period 1998 through 2009, trend analysis indicated a significant increase in primary productivity ($p<0.01$) (**Figure 33**).

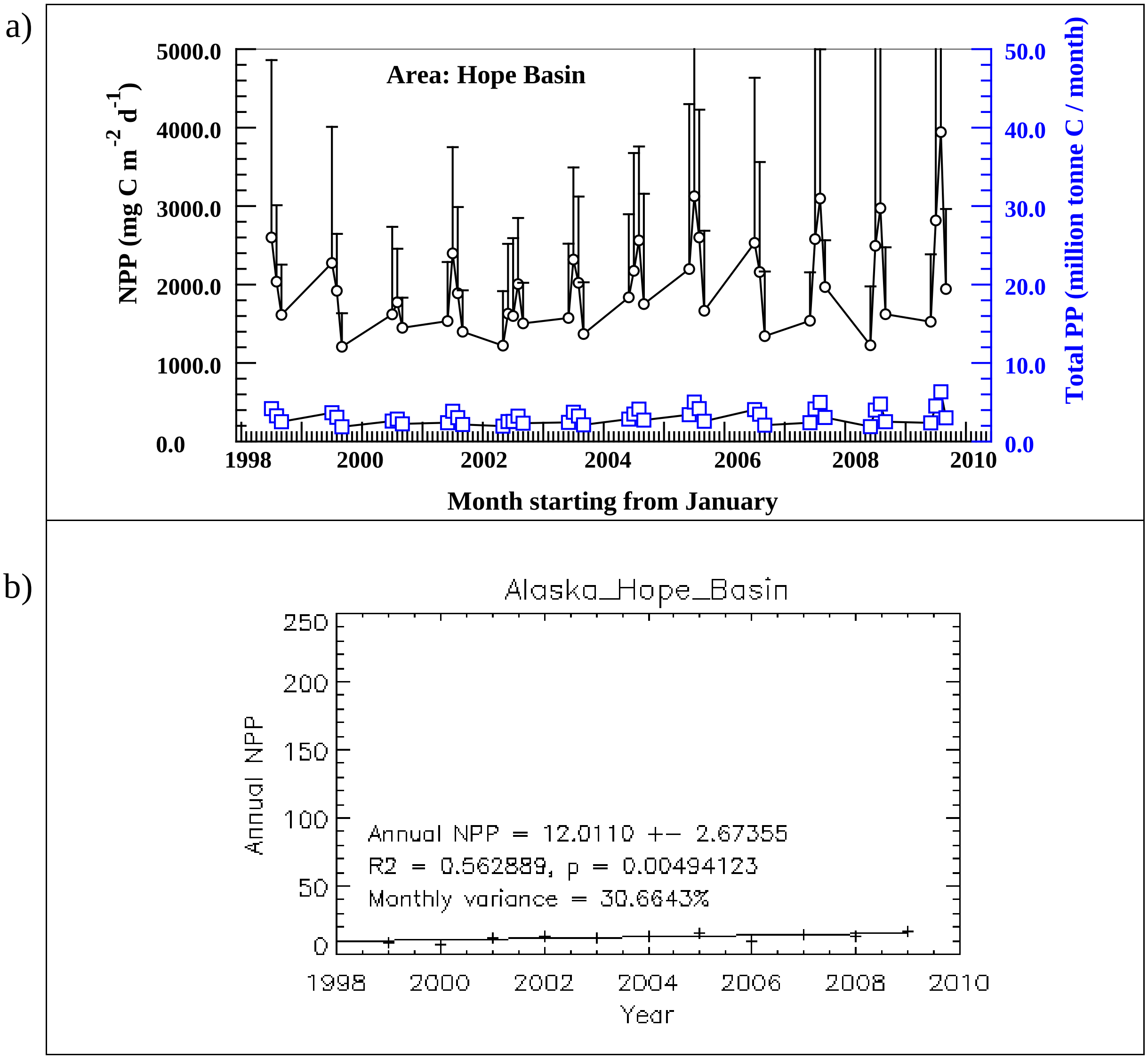

Figure 33. Hope Basin Planning Area a) monthly net primary production (NPP) statistics and b) annual NPP statistics (million tons C).

3.4.14 Chukchi Sea

The Chukchi Sea Planning Area covers an area of 62.59 million acres. During the period 1998 through 2009, mean annual NPP was 10.64 million tons of carbon (s.d. = ±5.41). Annual and monthly variance determinations were 50.85% and 38.02%, respectively. Over the period 1998 through 2009, trend analysis indicated a significant increase in primary productivity (p = -0.03) (**Figure 34**).

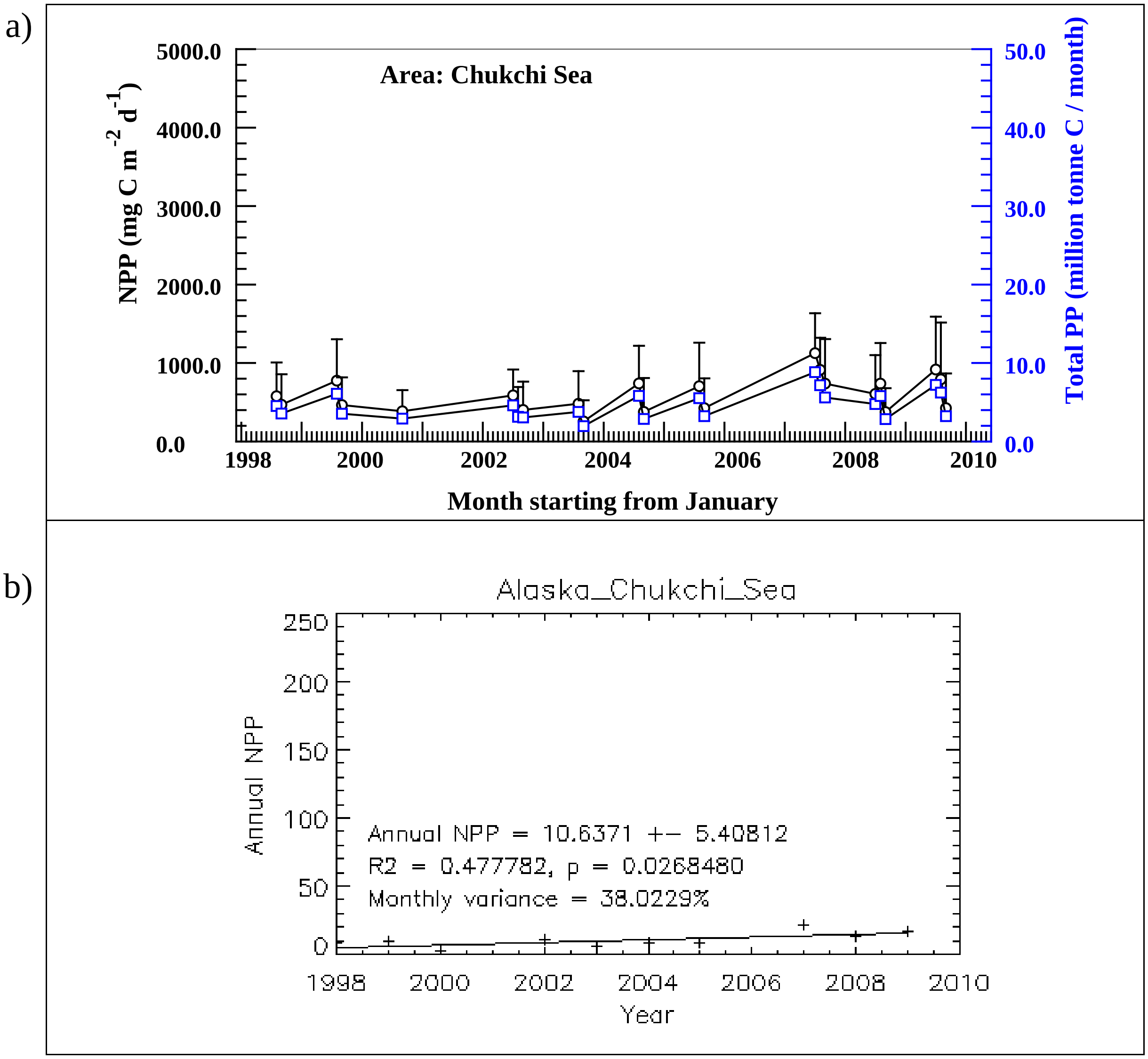

Figure 34. Chukchi Sea Planning Area a) monthly net primary production (NPP) statistics and b) annual NPP statistics (million tons C).

3.4.15 Beaufort Sea

The Beaufort Sea Planning Area covers an area of 65.08 million acres. During the period 1998 through 2009, mean annual NPP was 8.02 million tons of carbon (s.d. = ±6.35). Annual and monthly variance determinations were 79.17% and 59.29%, respectively. Over the period 1998 through 2009, trend analysis indicated an insignificant decrease in primary productivity (p = -0.65) (**Figure 35**).

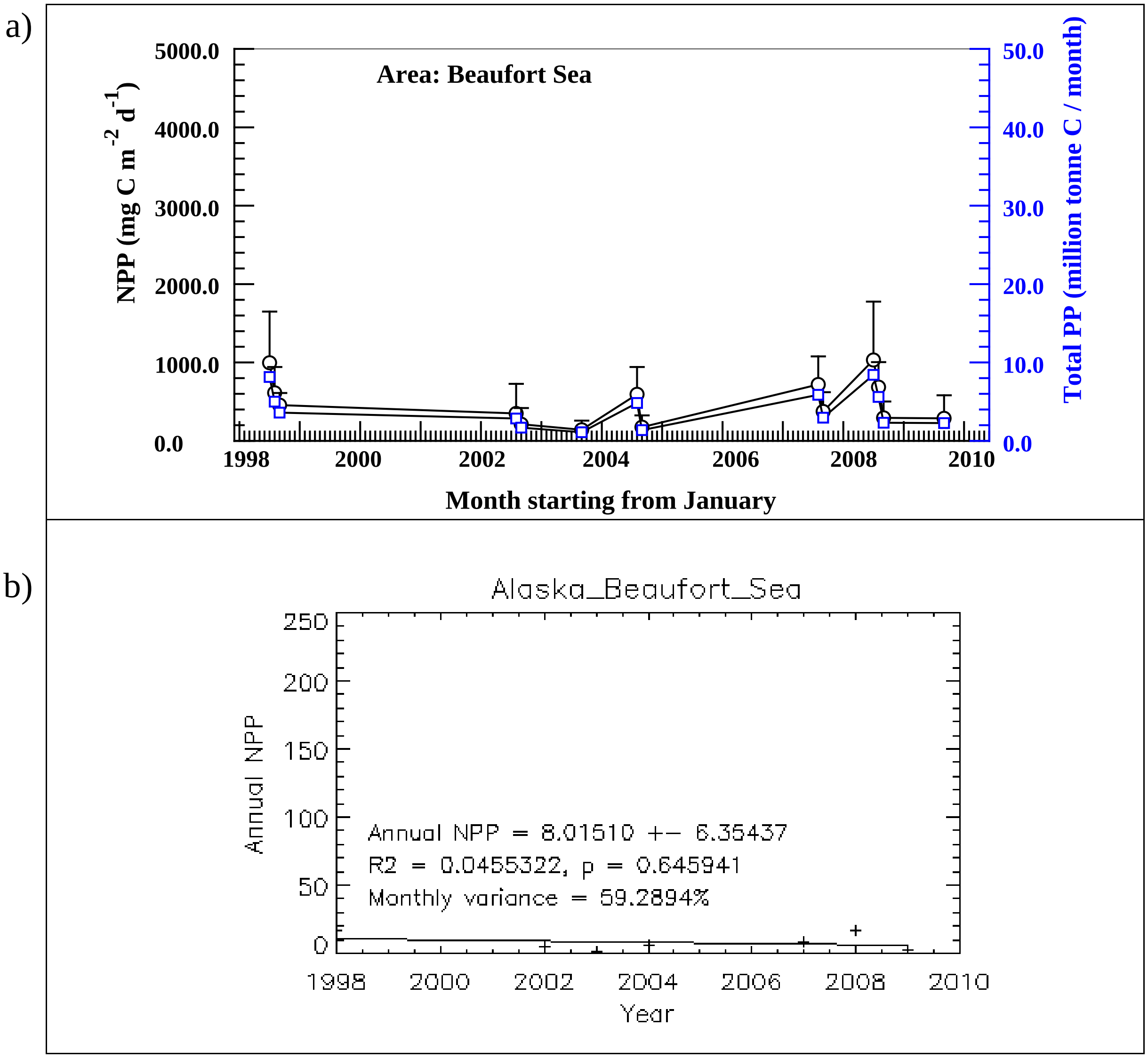

Figure 35. Beaufort Sea Planning Area a) monthly net primary production (NPP) statistics and b) annual NPP statistics (million tons C).

4.0 Primary Productivity Literature Updates

This section reviews and summarizes available primary productivity data for the four major OCS regions – Atlantic, Gulf of Mexico, Pacific, and Alaska – for the period 1988-2010, updating the water column primary productivity database initially established by CSA (1990), with an emphasis on the available published literature and reports applicable to OCS planning areas.

4.1 Atlantic Region

4.1.1 North Atlantic Planning Area

CSA (1990) emphasized that the North Atlantic Planning Area includes considerable habitat diversity, which in turn influences the magnitude of and regional variations in primary productivity. The principal sub-regional units that the 1990 report considered were Gulf of Maine, Scotian Shelf, and Georges Bank; the New York Bight and Hudson River discharge; and the Atlantic continental shelf off Long Island and New Jersey. But in the last 20 y, most of research on phytoplankton and primary production in this region has been focused mostly on the Gulf of Maine, Scotian Shelf, and Georges Bank.

The Gulf of Maine continued to be one of coastal ocean locations in which physical oceanographic drivers of coastal primary productivity (Townsend 1991) and bio-optical characteristics of coastal waters (Hoepffner and Sathyendranath 1992) were studied in detail after the CZCS mission ended in 1986. In his review, Townsend (1991) reported that increased phytoplankton productivity was tightly coupled to frontal regions where current shears are important, and that it was also enhanced where there was vertical diffusion of nutrients. Hoepffner and Sathyendranath (1992) reported that the specific absorption coefficient of phytoplankton at 440 nm changed dramatically from stratified waters in the central Gulf of Maine to the well-mixed area in the central part of Georges Bank. From pigment analysis conducted in conjunction with *in vivo* measurements of the specific absorption spectra of phytoplankton, they concluded that changes in specific absorption coefficient were linked to regional differences in the phytoplankton community. In other words, having information about taxonomy (i.e., knowing which phytoplankton species are present) is very important when trying to interpret remote sensing data. As a corollary, if logistics allow it is always desirable to have shipboard (and other *in situ* data) to supplement remote sensing data.

Coccolithophorid primary production can be quite important in the Gulf of Maine. Graziano et al. (2000) estimated that calcite production in summer can exceed 10% of total carbon production over deeper-water areas like Wilkinson Basin, the Northeast Channel, and the shelf break. But they also noted that the ratio of inorganic to organic carbon fixation, in general, was an order of magnitude lower in tidally mixed, high-nutrient regions of the Gulf of Maine, where diatoms are more abundant than coccolithophorid species.

Since 1998, spatial and temporal variability of phytoplankton standing stocks and primary production in the Gulf of Maine has been studied via the Gulf North Atlantic Time Series (GNATS). Measurements have been acquired along a transect between Portland, ME, USA, and Yarmouth, Nova Scotia, Canada (Balch et al. 2008). Scientific focus has been placed on differentiating differences between wet years, when greater than average riverine freshwater inputs decrease the density of the central basin mixed layer and thus cap the surface euphotic zone, reducing the upward diffusion of nutrients and lowering the phytoplankton biomass and productivity. Recent reports argue that interannual changes in the amount of low-salinity Scotian Shelf Water flowing over the Nova Scotia Shelf (Ji et al. 2007) and its subsequent inflow into the Gulf of Maine (Ji et al. 2008a,b) strongly impact water column stability and therefore control the winter-spring phytoplankton bloom dynamics.

The Howard-Yoder algorithm (see Campbell et al. 2002) is being used to predict primary production from remotely sensed ocean color data along the GNATS transect (Balch et al. 2008). These model studies conclude that total annual Gulf of Maine plus Georges Bank primary production averages 38 million metric tons of carbon, with Gulf of Maine plus Georges Bank coastal water (<60 m bottom depth) averaging 44% of the annual primary production (Balch et al. 2008). New primary production in the central Gulf of Maine is estimated to range from 20% (Townsend 1998) to 40% (Anderson 2009) of total annual primary production. If potential new production (PNP) is estimated as the difference between the time rate-of-change of vertically integrated nitrate in the euphotic zone and the vertical flux of nitrate into the base of this zone, then on the crest of Georges Bank it appears that PNP is quite low (<10%; see Bisagni 2003). This suggests that most of the nitrogen that fuels primary production over the shallow water of Georges Bank is largely recycled, and/or that nitrogen limitation there is common.

Away from the GNATS study area, a number of other researchers are also interested in Gulf of Maine estuary-plume systems. Salisbury et al. (2008) reported on pCO_2, chlorophyll fluorescence, and CDOM during seasonal surveys of the Kennebec (ME) and Merrimack (MA) estuary-plume systems. While both estuaries receive freshwater inputs from large New England rivers and are separated spatially by a distance of <150 km, Salisbury et al. (2008) found the two estuaries have marked differences in pCO_2 and optical variables. Results indicate that heterotrophic metabolism of high labile riverine carbon loads creates supersaturated pCO_2 conditions, while phytoplankton productivity is determined by the amount and type of riverine dissolved inorganic nitrogen (DIN). In the Damariscotta (ME) estuary, up to 23% of primary productivity can come from mixotrophic and autotrophic ciliates (Sanders 1995). When the autotrophic ciliates are present, they can dominate phytoplankton biomass (up to 35 µg C L^{-1}) but rather surprisingly, these autotrophs are usually absent in this estuary for most of the summer and autumn and are thus numerically important only for the spring bloom.

There are interannual differences in the start time for the spring bloom in the central Gulf of Maine. When phytoplankton blooms occur earlier than usual (i.e., when blooms begin while still in wintertime by the calendar), they apparently allow an extra generation of the copepod *Calanus finmarchicus* to develop, leading to an earlier buildup of this copepod population, which is in turn preyed upon by baleen whales and other third trophic level predators (Durbin et al. 2003). The authors emphasize that such earlier-than-usual increases in primary and secondary production have important effects on downstream regions such as Georges Bank (Ji et al. 2008a).

Primary production at Georges Bank is being studied using a three-dimensional ecosystem-physical model (e.g., NPZ model coupled to a detailed physical model forced by the M2 tides; see Franks and Chen 2001). The model suggests that high phytoplankton biomass and high *f*-ratios (i.e., new production/total primary production) develop in regions of strong vertical mixing such as on Georges Bank and on the eastern flank of the Nantucket Shoals, while lower biomass and lower new production occurs in the central Gulf of Maine. Interestingly, these model predictions of high new production run counter to the predictions of low PNP by Bisagni (2003). Further numerical experiments with the model have continued, which emphasize the importance of turbulence parameterization as well as tidal mixing (Tian and Chen 2006) for the prediction of primary production.

Harmful algal blooms in New England coastal waters continue to be a topic of interest. Townsend, Alexander, and others working with the Ecology and Oceanography of Harmful Algal Blooms (ECOHAB)-Gulf of Maine program are studying the distribution and abundance of dinoflagellates of the genus *Alexandrium* in the offshore waters of the eastern and the western portions of the Gulf of Maine (http://www.whoi.edu/science/B/ecohab/), while Tomas and Smayda are investigating blooms of the dinoflagellate genus *Cochlodinium* that occur frequently in Pettaquamscutt Cove, RI. During blooms in this Rhode Island cove, primary production by the dinoflagellate-dominated community there varies between 0.07 and 4.3 g C m^{-3} d^{-1} (Tomas and Smayda 2008). The harmful algal blooms are likely linked to eutrophication of the cove, since dissolved inorganic phosphate (DIP) was always present and DIN could reach concentrations of 140 µmol L^{-1}.

Beginning in the 1980's, NOAA's Northeast Monitoring Program (NEMP), regionally also known as NOAA's Ocean Pulse Program, routinely collected oceanographic data to allow NOAA scientists to monitor eutrophication and other forms of ocean pollution at over 100 stations along the continental shelf from the Gulf of Maine to Cape Hatteras, NC (Reid et al. 1987). But after 1987, as research priorities at NOAA's Northeast Fishery Center shifted away from routine monitoring of the water column and the seabed, phytoplankton composition was only occasionally determined and primary productivity was only occasionally measured at Ocean Pulse stations.

4.1.2 Mid-Atlantic Planning Area

The literature search for the Mid-Atlantic Planning Area resulted in identification of journal articles, the majority of which characterized primary productivity in nearshore coastal waters or open embayments. Only a limited number of documents have addressed primary production over the Mid-Atlantic continental shelf. The following discussion summarizes pertinent data sources for embayments and coastal waters adjacent to, as well as continental shelf waters of, the Mid-Atlantic Planning Area. The importance of data sources for the embayments and coastal waters inshore of the Mid-Atlantic Planning Area is based on the influence and degree of interaction between these waters and those overlying the adjacent continental shelf.

Primary productivity in Mid-Atlantic estuaries is strongly affected by water-column mixing, which can be attributed to currents, tides, and wind (Mallin and Paerl 1992). Mixing in shallow systems has the dual effect of increasing light attenuation in the water column through resuspension of particulate matter, while allowing entrained phytoplankton cells to experience a constantly varying light regime (Mallin and Paerl 1992). But the rivers that flow into these estuaries are also important sources of nitrogen (N) and phosphorus (P) that are needed to fuel primary production. It is estimated that five large rivers that discharge on the western North Atlantic continental shelf carry about 45% of the N and 70% of the P flux from the entire North

Atlantic watershed, including North, Central, and South America, Europe, and Northwest Africa (Howarth 1996). Denitrification is the major process responsible for removing N in most estuaries, and the fraction of total N input that is denitrified appears to be directly proportional to the log mean water residence time (Howarth 1996).

Since 1990, most regional studies have emphasized how much N and P eutrophication has occurred in the Mid-Atlantic region. Yoshiyama and Sharp (2006), for example, reported on the apparent inhibition of primary production by over-eutrophication in the Delaware Estuary. They examined a 26-y database that indicated a high-nutrient, low-growth situation now exists in the Delaware Estuary because of a combination of light limitation coupled with presumed toxic contamination in most areas of the estuary with large anthropogenic inputs.

In contrast, researchers working in Chesapeake Bay have reported that N and P addition generally stimulates phytoplankton growth. Larsen et al. (2001) reported excess phytoplankton production there contributes to hypoxic conditions, especially in summer months when phytoplankton production in Chesapeake Bay is new-nitrogen limited. Vincent (1992) pointed out that uptake of “new” versus “regenerated” forms of nitrogen can influence the daily pattern of nitrogen uptake and metabolism. Glibert and Garside (1992), who contrasted new production that is fueled by the uptake of nitrate with recycled production that is fueled by the uptake of reduced nitrogen sources in Chesapeake Bay, also reported that diel patterns exist and generally varied with season. During winter months, rates of nitrate uptake were often higher during the first part of the day, while rates of reduced nitrogen compounds were higher in afternoon and at night. But in summer, maximum observed rates of nitrate uptake only occurred 9-16 h after the maximum observed peak in the uptake of reduced nitrogen. The authors interpreted their findings in terms of seasonal shifts in nitrogen nutritional status of the assemblages, and they cited species-specific differences in the ability for a given stimulus (i.e., a nitrogen pulse at the mouth of the Bay) to manifest as an uptake response.

Harding et al. (1992) used aircraft remote sensing to describe the distribution of phytoplankton chlorophyll in the Chesapeake Bay, as the winter-spring diatoms bloom gave way to late-spring and summer dinoflagellate blooms. The instrument they used, NASA’s Ocean Data Acquisition System (ODAS), provided important validation for some of the radiometer settings that were later incorporated into NASA’s SeaWiFS. Conley and Malone (1992) suggested that dissolved silicate controls the magnitude of diatom production during the spring bloom, and that its eventual limitation causes the collapse of the spring bloom.

Monthly and annual phytoplankton productivity rates in four Virginia tidal rivers were reported by Nesius et al. (2007) to summarize a 12-y monitoring study with sampling stations in tidal freshwater, oligohaline, and mesohaline regions of each river. The estimated mean annual primary productivity over the study period for the four Virginia rivers in this study ranged from 49-230 g C m^{-2} y^{-1} (Nesius et al. 2007). Because estimating the rate of biogeochemical pumping of CO_2 from atmosphere to surface ocean by phytoplankton represents an alternative mechanism for measuring phytoplankton primary productivity, and because the coastal ocean is a region with highly variable physical processes, there is considerable interest in describing CO_2 fluxes into and out of this environment (Boehme et al. 1998). For example, a time-series of CO_2 measurements along with water column measurements of temperature, salinity, total alkalinity, oxygen, and nutrients was made approximately monthly at seven stations along a 32-km transect across the inner continental shelf off New Jersey. In general, surface waters were a source of CO_2 to the atmosphere in the summer and fall, offset by large fluxes of CO_2 into the surface waters during the winter to early spring (Boehme et al. 1998).

To continue and extend the CO_2 flux studies, Redalje et al. (2002) examined the spatial and temporal variability in primary production and phytoplankton pigments during two cruises to the shelf waters beyond the Chesapeake Bay and Cape Hatteras. They reported that primary production was positively correlated with light and temperature, while chlorophyll biomass was positively correlated with dissolved inorganic nitrite and nitrate and negatively correlated with temperature. These differences in correlation, they suggested, indicate that temperature plays a major role in the phytoplankton dynamics in this shelf ecosystem.

Other researchers have emphasized that atmospheric nitrogen deposition is responsible for 26% to over 70% of "new" nitrogen input to North Carolina estuaries and coastal waters (Paerl et al. 1990; Paerl and Fogel 1994). When they looked specifically at rainfall as a source of DIN, these researchers found it stimulated primary production off North Carolina (Paerl et al. 1999). They speculated that natural rain may supply both limiting DIN and co-limiting micronutrients like iron, contributing to the eutrophication potential of waters downwind of urban, industrial, and agricultural emissions. On the other hand, some of the same authors reported that bioassay experiments indicated that addition of hydrogen peroxide in concentrations similar to those in natural rain sometimes decreased chlorophyll-*a* production in surface ocean water off the coast of North Carolina (Willey et al. 1999). They therefore concluded that rainwater plays a complex role in primary productivity in surface seawater, with the specific effect dependent upon rainwater concentrations of nitrate, ammonium, trace metals, and hydrogen peroxide, as well as on the extent of nitrogen limitation and the oxidant concentration in the surface seawater.

In a subsequent publication, Paerl et al. (2006) contrasted the effects of anthropogenic perturbations on Chesapeake Bay with those impacting the Neuse River Estuary/Pamlico Sound. They noted that both estuarine systems have experienced large post-World War II increases in nitrogen and phosphorus loading, and that in both systems nutrient reductions have been initiated to alleviate symptoms of eutrophication. In both systems, variability in water residence time strongly influenced seasonal and longer-term patterns of phytoplankton biomass and community composition. Especially in the longer residence time of the Neuse River Estuary/Pamlico Sound system, fast-growing diatoms were favored during years of high freshwater discharge.

As an important component of this review of primary production in the Mid-Atlantic Planning Area, it is important to mention the paleoproductivity records collected by the Ocean Drilling Program (ODP). Geologists who examined cores of Late Cretaceous to early Paleogene age (71-36 million years ago) from the Blake Nose (ODP Leg 171B, Sites 1050, 1051, and 1052) pointed out that phosphorus and biogenic barium were good export productivity indicators (Faul et al. 2003). Both of these indicators were locally high in ODP Leg 171B cores from 69-61 million years ago, a time of proposed global high relative organic carbon burial. In other words, rates of carbon sequestration over the Mid-Atlantic shelf have varied dramatically over geologic time; present estimates of carbon export and burial there will be imperfect predictors of paleoproductivity.

4.1.3 South Atlantic Planning Area

In contrast to the Mid-Atlantic region, where there is a strongly seasonal variation of CO_2 flux into and out of continental shelf waters, on the U.S. southeastern continental shelf during most of the year there is oversaturation of pCO_2 and very strong CO_2 flux to the atmosphere (Wang et al. 2005). On the southeastern continental shelf, also known as the South Atlantic Bight (SAB), coastal and estuarine waters are generally highly productive, with annual primary production typically 600-700 g C m^{-2} y^{-1} (Verity et al. 1998). In salt-marsh estuaries, tidal flow causes strong temporal variability in environmental properties that impact primary production (Wetz et al. 2006), and temperature strongly regulates rates of photosynthesis and respiration following the Arrhenius law (Pomeroy et al. 2000).

Intrusions of nutrient-rich cold water can also be driven on to the SAB shelf by atmospheric forcing (i.e., anomalously strong and persistent upwelling-favorable winds). When these occur in summer, the resulting pool of anomalously cold water may constitute more than 50% of the water on the SAB shelf. When the excess nutrient flux onto the shelf associated with one such cold event in summer 2003 was estimated using published nitrate-temperature proxies, there seems to have been increased primary production over most of the SAB shelf (Aretxabaleta et al. 2007).

Continental shelf sediments of the SAB consist of relict sands that, at depths of 14-45 m, fall within the photic zone, and so significant rates of benthic primary production are sometimes measured there (Marinelli et al. 1998). Relatively high concentrations of diatom pigments extend to at least 2-3 cm in the sediments; high concentrations of chlorophyll *a* in the top 0.5 cm of the sands often exceeds the depth-integrated chlorophyll in the entire overlying water column (Nelson et al. 1999).

4.1.4 Straits of Florida Planning Area

In similar fashion to predominant physical processes occurring in the South Atlantic region, intrusions of nutrient-rich water onto the continental shelf stimulate locally enhanced primary productivity in the Florida Straits and Florida Current. The western boundary of the Florida Current is delineated from the inshore waters by a sharp rise in SST. When its movements were studied using satellite imagery for a 2-month period during January to March 1998, the Florida Current made five incursions inshore of its mean position during this period (Fornshell 2000). Such dynamic activity represents a major source of nutrients for primary productivity in this region.

Numerical model studies of the Florida Current in the Straits of Florida and along the east Florida continental shelf also show weekly to seasonal variability in nitrate inputs on to the shelf, due to bottom Ekman transport as the Florida Current jet interacts with the continental shelf topography and summer coastal upwelling favorable winds (Fiechter and Mooers 2007).

4.2 Gulf of Mexico Region

For this analysis, studies conducted on primary productivity measurements and mechanisms in the Gulf of Mexico region since 1990 have not been binned into Eastern, Central, and Western

Gulf of Mexico planning areas. Rather, in this section the Gulf of Mexico will be considered to be a subtropical mediterranean sea in which phytoplankton primary productivity is influenced primarily by physical processes expressed on basin-wide scales (Biggs and Ressler 2001). For example, oceanographic features (e.g., eddies) or seasonal characteristics (e.g., stratification) which affect primary production occur across planning area boundaries. As a result, these post-1990 results are not readily conducive to organization by individual planning area; the following Gulf of Mexico literature review summary reflects that fact.

Studies in the eastern Gulf of Mexico have reported that river and coastal waters on the southwest Florida shelf were supersaturated with CO_2 with respect to the atmosphere (Clark et al. 2004). They pointed out that pCO_2 levels generally decreased with increasing salinity, but at different gradients for the different river systems. They also noted that a positive correlation of pCO_2 levels with CDOM and chlorophyll was observed in all systems examined, so they concluded that CO_2 in natural waters may be produced from the photochemical degradation of CDOM, microbial respiration, or via shifts in the carbonate equilibrium. Biggs and Ressler (2001) reviewed phytoplankton distribution and abundance in the Gulf of Mexico, and they summarized previous studies of regional primary productivity. In their review, they noted that the Gulf of Mexico, like other subtropical seas, has large areas of oligotrophic (very low nutrient concentrations, or "ocean desert"-like) surface waters. From historical reports included in the review (e.g., light bottle versus dark bottle ^{14}C uptake measurements in the 1960's and 1970's), Biggs and Ressler (2001) noted that primary production in Gulf of Mexico oligotrophic regions typically averaged 100-150 mg C m^{-2} d^{-1}. Conversely, on the continental shelf of the northern Gulf near the Mississippi River delta and off Atchafalaya Bay, there are high inputs of nutrients from freshwater discharge (Dinnel and Bratkovich 1993). Biggs and Ressler (2001) pointed out that historical reports that measured ^{14}C uptake in the 1960's and 1970's noted primary production in these nutrient-rich continental margin areas of the Gulf of Mexico generally ranged 250-500 mg C m^{-2} d^{-1}, and they summarized that productivity was seasonally higher there during the winter-spring months when river flow is at its highest annual values.

The Gulf of Mexico has a total area of about 1.57 million km^2 (Lynch 1954), which is 0.43% of the total 362 million km^2 surface area of all the world's oceans. If 25% of the Gulf of Mexico area has extremely low primary production (100-150 mg C m^{-2} d^{-1}), 25% of the Gulf area has high production (250-500 mg C m^{-2} d^{-1}), and the rest of the area has intermediate values of primary production (150-250 mg C m^{-2} d^{-1}), then total annual primary productivity of the Gulf of Mexico can be estimated at approximately 129 million metric tonnes (**Table 7**).

Table 7. Estimated annual primary productivity of the Gulf of Mexico. Daily production averages derived from Biggs and Sanchez (1997).

Production Level	Daily Range (mg m^{-2})	Daily Average (mg m^{-2})	Annual Average (g m^{-2})	Total Area (km^2)	Total Primary Productivity (million metric tonnes)
High	250-500	375	137	392,500	54
Medium	150-250	200	73	785,000	57
Low	100-150	125	46	392,500	18
Total all regions				1,570,000	129

However, because this estimated annual total is only 0.26% of the estimated 50 gigatonnes of annual net primary production of the world ocean (Sabine et al. 2004), it implies the Gulf of Mexico is, on average, less productive than the rest of the world ocean. This characterization uses three different daily averages, multiplied by the basin area of each of the three regimes, to estimate the annual production of the entire Gulf of Mexico. A comparison of this annual estimate of phytoplankton primary production with remote-sensing estimates of annual NPP for the northern Gulf is discussed later (see **Section 7**).

Because measurements of primary production carried out in the 1960's and 1970's were done using $H^{14}CO_3^-$ stock solutions that likely had trace-metal contamination, subsequent researchers feared that by using these stocks for experimentation, the authors of classic papers had underestimated marine primary production. So several groups of researchers repeated light bottle versus dark bottle uptake experiments at various locations in the Gulf of Mexico in the 1980's and 1990's, this time using trace-metal free stock solutions of $H^{14}CO_3^-$. They sought to test the historical paradigm that much of the Gulf has lower-than-average primary production (Biggs 1992; Lohrenz et al. 1997, 1999).

At three locations within an anticyclonic eddy that was surveyed in October 1988 in the deepwater western Gulf of Mexico, primary production was measured during 4-6 h ^{14}C uptake experiments using the light bottle-dark bottle incubation method with trace-metal free stock solutions of $H^{14}CO_3^-$ (Biggs 1992). Highest rates of production occurred in the upper 30 m, where under conditions of full sunlight, 69% I_o, and 40% I_o, gross primary production (GPP) ranged from 0.12-0.46 mg C m^{-3} h^{-1}. While GPP declined exponentially as depth increased, there was usually a secondary peak in GPP within the deep chlorophyll maximum layer, at around 3% I_o. When integrated to the depth of 1% surface irradiance, GPP ranged from 14-23 mg C m^{-2} h^{-1}. When there are 12 h of daylight of sufficient intensity to support this hourly range of primary production, the daily average is 222 mg C m^{-2}. Productivity measured using the same technique was higher at two locations closer to the periphery of the eddy, where cooler, more nutrient-rich water was closer to the base of the surface mixed layer. Rates of production in the high light regime nearest the surface at these two locations reached 0.8 mg C m^{-3} h^{-1}, and GPP integrated to the 1% light level ranged from 30-35 mg C m^{-2} h^{-1}, for a daily average of 390 mg C m^{-2}. Assuming that these levels of productivity can be sustained 365 days per year because the average daytime light intensity received per square meter in this subtropical ocean from October-April does not fall to less than 50% of the average received per square meter from May-September, annual productivity inside versus near the periphery of the eddy works out to be, on average, 81-142 g C m^{-2} y^{-1}. Hence, these repeat light bottle versus dark bottle uptake experiment data argue that only *inside* deepwater anticyclonic eddies is Gulf of Mexico primary production substantially lower than global average primary productivity for most open ocean areas, which according to Smith and Hollibaugh (1993) is about 130 g C m^{-2} y^{-1}.

When these “ocean desert” anticyclonic eddies reach the western margin of the Gulf of Mexico, though, they influence the surface circulation over the continental slope and rise (Biggs and Müller-Karger 1994). And especially when cyclone-anticyclone eddy pairs or cyclone-anticyclone-cyclone triads impinge on the continental slope, they can act like counter-rotating gears to entrain shelf surface water and transport it off-margin. A review of 1979-1986 CZCS imagery showed that some eddy geometries over the continental slope in the western Gulf of Mexico transported high-chlorophyll shelf water seaward at least 100-200 km off shelf (Biggs and Müller-Karger 1994). Subsequent review of SeaWiFS imagery for the period 1997-2004 produced similar examples of off-margin transport of high-chlorophyll shelf water out over the continental slope in the north-central and northeastern Gulf of Mexico (Biggs et al. 2005).

Chlorophyll standing stocks and primary productivity on the continental margin of the northern Gulf of Mexico vary seasonally, with low values from April through early November when surface waters are usually stratified and higher values when surface waters cool and then deep-mix during the rest of the year (Müller-Karger et al. 1991). But major meteorological events can create anomalies in the seasonal cycle of pigment concentrations; during the El Niño-Southern Oscillation (ENSO) event of 1982–1983, positive anomalies were observed in CZCS pigment concentrations in the Gulf of Mexico and elsewhere in the Intra-Americas Sea during winter months (Melo-Gonzalez et al. 2000). These anomalies apparently formed after intense mixing of the water column by higher-frequency and stronger winds associated with cold fronts (so the ENSO of 1982–1983 therefore had a fertilizing effect on the region). Another positive anomaly was observed in 1980–1981, a non-ENSO period that featured higher hurricane and extratropical low-pressure activity (Melo-Gonzalez et al. 2000). ENSO events also result in greater summertime precipitation over the Mississippi River watershed, as what is usually a continental area of high atmospheric pressure changes to an area of lower atmospheric pressure. When this results in greater summer river outflow, higher loads of nutrients are discharged on to the inner shelf system. While this should lead in turn to greater summertime primary production, it also raises concerns (Justic et al. 2005) that such low frequency climatic variations might feed back to increase the size of a large inner shelf hypoxic zone (>2 x 10^4 km^2).

Primary productivity measured during the stratified part of the year (July and October) using the light bottle-dark bottle technique with trace-metal free stock solutions of $H^{14}CO_3^-$ for 4-6 h incubations averaged 93 mg C m^{-2} h^{-1} (1.1 g C m^{-2} d^{-1}) at three middle shelf locations, and 42 mg C m^{-2} h^{-1} (0.5 g C m^{-2} d^{-1}) at three outer shelf locations (Biggs and Sanchez 1997). Because nutrient concentrations on the continental shelf are spatially variable (Sahl et al. 1993) as well as seasonally variable, the average primary production of the northern Gulf of Mexico continental margin is also quite variable. It can range from 0.3-3.8 g C m^{-2} d^{-1} for the eastern and central regions, and 0.6-3.3 g C m^{-2} d^{-1} for the western region (Lohrenz et al. 1997). Inshore and closer to the Mississippi River delta, integrated carbon production often ranges between 4 and 8 g C m ^{2} d^{-1} (Biggs and Sanchez 1997; Lohrenz et al. 1997). However, nitrogen and/or silica limitation can also occur in the Mississippi River plume (Dortch and Whitledge 1992), and when/where this nutrient limitation occurs it is expressed as a reduction in primary production rates (Lohrenz et al. 1999). In Pensacola Bay, and presumably in other shallow bays that ring the Gulf of Mexico, benthic primary production can average 16%-32% of total system productivity (Murrell et al. 2009).

Variations in phytoplankton taxonomic composition from nine hydrographic cruises conducted during the period 1997-2000 were summarized by Qian et al. (2003)**,** who used chlorophyll and carotenoid pigment distributions that they analyzed by high performance liquid chromatography (HPLC) to describe spatial and temporal variations in phytoplankton biomass on the continental shelf of the northeast Gulf of Mexico. Qian et al. (2003) reported that on average, prymnesiophytes made up 25%-40% of total chlorophyll in the water column over the shelf during this 3-y period, while prokaryotes averaged 14%-38% of chlorophyll *a*. Diatoms generally contributed just 6%-13% of chlorophyll *a* and usually were abundant only in inner shelf coastal waters. Pelagophytes generally occurred in higher abundance in subsurface water, while dinoflagellates reached greater concentrations in near-surface waters.

The HPLC methodology did not resolve the presence of blue-green algae, but *Trichodesmium* (*Oscillatoria*) blooms are not uncommon in the Gulf of Mexico. These diazotrophs have a high iron requirement that is consistent with the biochemical demand for iron in the enzyme nitrogenase. Summer delivery of iron, in the form of Saharan dust, may provide an explanation for the frequent occurrence of *Trichodesmium* blooms in offshore waters of the West Florida shelf and elsewhere in the Gulf (Lenes et al. 2001).

Using SeaWiFS ocean color data to estimate sea surface chlorophyll (SSC) and in turn using a VGPM calculation to estimate primary production from SSC and SST, Biggs et al. (2008) reported that mean primary production was about 0.5 g C m^{-2} d^{-1} for a group of 22 continental margin stations in water depths of 200-3,000 m in the northwest Gulf of Mexico, 0.7 g C m^{-2} d^{-1} for another group of 22 continental margin stations in similar water depths in the northeast Gulf of Mexico, and 0.3 g C m^{-2} d^{-1} for a group of six oligotrophic open-ocean stations in water depths of >3,000 m in the central Gulf of Mexico. Because they used SeaWiFS data from January 1998 through December 2000 to compile monthly averages, Biggs et al. (2008) were able to compare seasonal with interannual changes in SSC and calculated primary production. While the annual average SSC was 0.19 mg m^{-3}, this ranged at most locations from annual highs of about 0.3 mg m^{-3} in November-February to lows of about 0.1 mg m^{-3} in May-August. Comparison of 3 y of monthly data showed little interannual variation at the northwest Gulf stations. In contrast, at the 22 northeast Gulf sites (north of 26° N and east of 91° W), average SSC was 2.8 times higher than in the northwest Gulf and also exhibited strong interannual variation. Maximum SSC values in the northeast region were observed in November-February and also during summers. The summer maxima were associated with Mississippi River water transported offshore to the east and southward by anticyclonic eddies in the northeast Gulf. The apparent increases in SSC in June-August at northeast Gulf stations reached average monthly concentrations >50% greater than those in the less stratified and deeper-mixed months of November-February.

Other plumes of low salinity high chlorophyll water can also extend hundreds of kilometers offshore into oligotrophic waters, particularly on the west Florida Shelf. Paul et al. (2000) combined HPLC pigment analysis, flow cytometry, and $H^{14}CO_3^-$ uptake to characterize the biological productivity of picophytoplankton in a “Green River” plume they sampled a few hundred kilometers west of Tampa Bay. They reported finding an abundance of *Prochlorococcus* cells ($>10^5$ L^{-1}) at depths of 20-70 m in this “Green River” that graded at deeper depths to a picoeukaryote community composed of diatoms, prymnesiophytes, and pelagophytes associated with the subsurface chlorophyll maximum. Other researchers, working off Charlotte Harbor (FL) in 2008, measured the uptake of a mix of 15-N labeled dissolved nitrogen compounds by a mixed community of picoplankton and diatoms, as part of field work for the ECOHAB project (Wawrik et al. 2009). Flow cytometric analysis of surface water from this coastal location indicated the presence of the genus *Synechococcus*, and direct microscopic observations during the time of sampling indicated that there were large populations of diatoms of the genera *Rhizosolenia*, *Pseudonitzschia*, *Cetoceros*, and *Thalassionema*.

Belabbassi et al. (2005) used data from three summertime oceanographic surveys of the northeast Gulf of Mexico 1998-2000 to quantify the amount of nutrients brought onto the shelf by deepwater eddies. From measurements at approximately 100 stations on each of the three summer cruises, nitrate and silicate were measured in the upper 15 m of the water column and in the depth interval from 15-60 m, the nominal depth of the euphotic zone. Belabbassi et al. (2005) pointed out that standing stocks of nitrate and silicate in the 15-60 m layer were between two and six times those measured in the upper 15 m on all three cruises and appeared to depend on the strength and relative proximity of local anticyclonic features to the shelf break. Belabbassi et al. (2005), measuring nutrient concentrations using standard autoanalyzer methods, judged that the nitrate and silicate in the near-surface interval of 0-15 m largely resulted from riverine discharge and subsequent advection, while these nutrients between 15 and 60 m resulted from uplift of waters by circulation features, and so Belabbassi et al. (2005) concluded that these deepwater eddies were very significant in supplying nutrients to the euphotic zone of the outer continental shelf of the northeastern Gulf of Mexico during summertime.

4.3 Pacific Region

The Pacific Region encompasses four OCS planning areas, which, from south to north, include Southern California, Central California, Northern California, and Washington-Oregon. Aside from site- or area-specific studies, many of the recent oceanographic research efforts conducted since 1990 have crossed planning area boundaries. The following summary provides an overview of the relevant primary productivity-related research conducted along the U.S. west coast or across several planning areas, followed by summary information available for each individual planning area within the Pacific Region.

A major, long-term oceanographic sampling effort, the California Cooperative Oceanic Fisheries Investigations (CalCOFI), has been conducted offshore California since 1949. A partnering of several government agencies (i.e., California Department of Fish and Game, NOAA National Marine Fisheries Service [NMFS]) and academia (i.e., Scripps Institution of Oceanography), the current focus of the program lies with characterizing the marine environment off the coast of California and monitoring the indicators of El Niño and climate change. CalCOFI conducts quarterly cruises off southern and central California, collecting a suite of hydrographic and biological data on station and underway (**Figure 36**).

Data collected at depths down to 500 m include temperature, salinity, oxygen, phosphate, silicate, nitrate and nitrite, chlorophyll, transmissometer, PAR, ^{14}C primary productivity, phytoplankton biodiversity, zooplankton biomass, and zooplankton biodiversity. Chlorophyll measurements have been acquired by CalCOFI since 1973. In 1984, ^{14}C primary productivity incubations were added to their survey protocols.

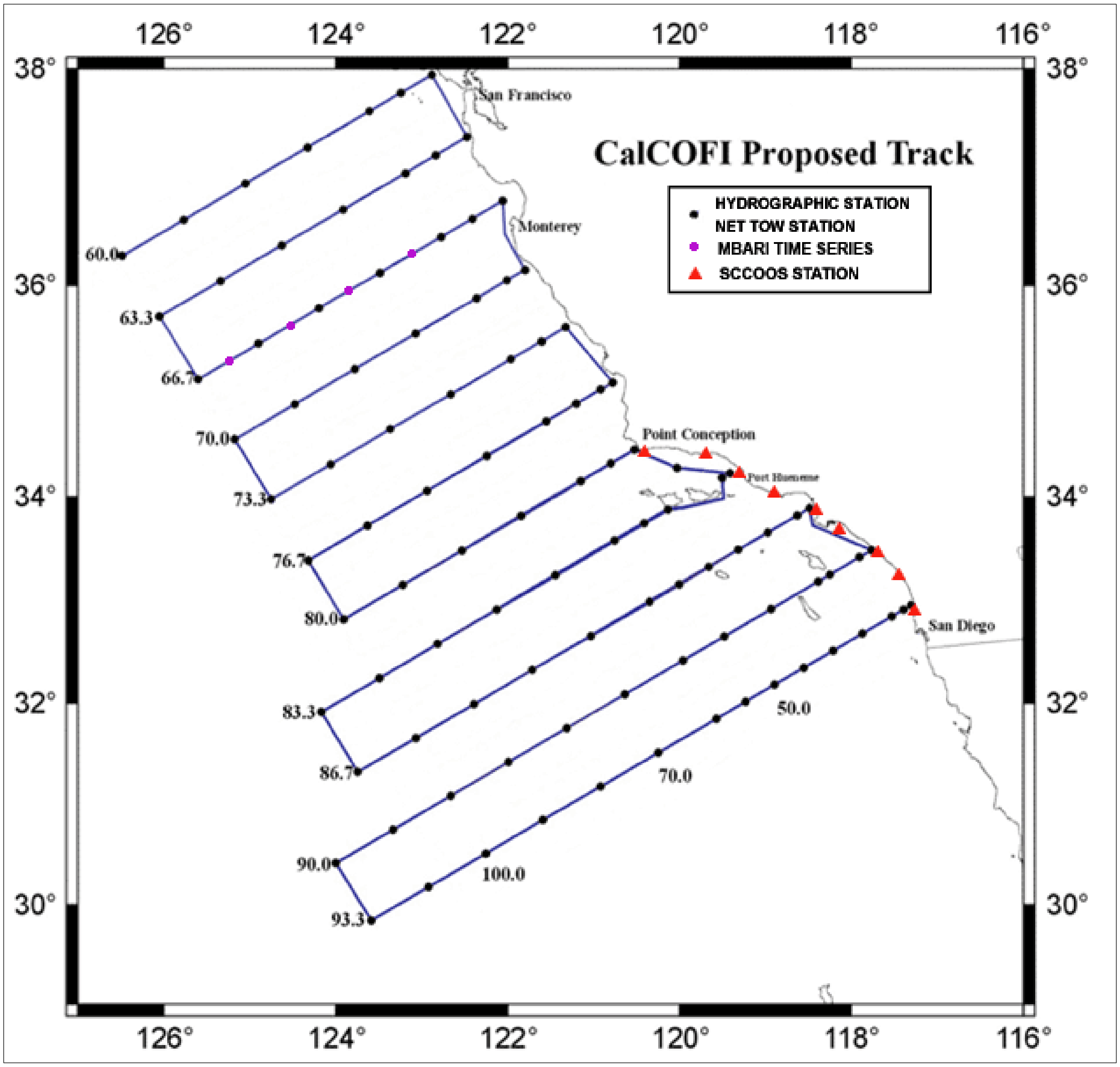

Figure 36. Location of CalCOFI transects, southern and central California (From: CalCOFI 2010).

CalCOFI prepares annual summaries of the state of the California Current (e.g., Goericke et al. 2007; McClatchie et al. 2008, 2009), normally inclusive of survey results for southern California and central California (CalCOFI North grid). More recently, survey work offshore northern California (Trinidad Head line) and offshore Oregon (Newport line) have also been summarized (McClatchie et al. 2009). While the emphasis of the annual reports lies with all aspects of sampling (e.g., primary and secondary productivity; seabirds, marine mammals), results of primary productivity sampling are routinely included. Of particular note are the physical-biological linkages developed for each annual report (e.g., regional and local effects of El Niño, La Niña, etc.). Online access is also available for CalCOFI survey data (http://data.calcofi.net/publications/calcofi-data-reports.html), including primary productivity data for 1996-2008.

The California Current System (CCS) is the predominant oceanographic feature in the Pacific Region. Several reviews and compendia have been completed characterizing various aspects of the CCS, including Hickey (1979), who evaluated seasonal variation of the currents of the CCS, and more recently characterized the northern portion of the CCS (Hickey and Banas 2008); Chelton et al. (1982), who analyzed variation of time series of physics and plankton of the CCS; and Huyer (1983), who characterized coastal upwelling. Hickey (1998) described the oceanography of the CCS over a range of time scales, and Checkley and Barth (2009) defined the patterns and processes of the CCS.

Checkley and Barth (2009) also summarized a series of process studies historically or currently being conducted within the CCS:

- Coastal Upwelling Ecosystem Analysis (CUEA) program (Huyer 1976) – investigations of the physical basis and biological effects of upwelling;

- Coastal Ocean Dynamics Experiment (CODE) – characterized the physics of the coastal ocean (e.g., Hickey 1998);

- Coastal Transition Zone (CTZ) program – evaluating the processes linking the coastal and oceanic domains (Brink and Cowles 1991);

- Partnership for Interdisciplinary Studies of Coastal Oceans (PISCO) – focuses on the diverse processes in nearshore and coastal ocean waters (www.piscoweb.org);

- Global Ocean Ecosystems Dynamics (GLOBEC) program (http://www.globec.org) – off the west coast of the continental U.S., GLOBEC researchers focused on investigating the biological oceanography of the CCS, with an emphasis on processes affecting higher-trophic levels (www.globec.oce.orst.edu/). The GLOBEC International Programme completed its activities in January 2010 after 10 y of sustained and coordinated research;

- California Current Ecosystem Long-Term Ecological Research (CCE LTER) program – implemented to augment California Cooperative Fisheries Investigations (CalCOFI) monitoring with process studies in the southern CCS (www.cce.lternet.edu/); and

- Coastal Ocean Processes (CoOP) program – focusing on air-sea interactions and the influence of winds and river input on the functioning of coastal upwelling ecosystems. In the northeast Pacific, most CoOP research has focused on understanding the Columbia River plume (http://www.skio.usg.edu/?p=research/coop/index).

A considerable amount of research during the past 20 y has concentrated on the CCS, due in part to its upwelling and oceanographic complexity (e.g., presence of eddies and jets), various nutrient sources, and associated elevations in primary productivity. Many of these efforts have concentrated on characterizing the mechanisms and physical processes of the CCS. The predominant perception of the physical and biological processes present in the CCS has evolved in recent years. Previously, the concept of a two-dimensional "conveyor belt" was preferred; in this approach, upwelling produced cold, nutrient-rich water near the coast (Dugdale and Wilkerson 1989) and resulted in a coastal phytoplankton bloom composed primarily of diatoms, which were subsequently fed upon by mesozooplankton (e.g., copepods, krill), which support a diverse community of planktivorous fish, birds, and marine mammals. As noted by Kudela et al. (2008), these highly productive surface waters are transported offshore, while plankton can sink into the upwelling return flow, completing the conveyor belt analogy. While this view of coastal upwelling may be appropriate for relatively straight coastlines, researchers have questioned whether such a simplified concept is appropriate for coastlines where topography is complex and where other mechanisms may have an influence (e.g., freshwater inflow).

Research on the physical-biological coupling within the CCS has been extensive, particularly in the northern portions of the CCS. Major research efforts, as summarized by Kudela et al. (2008), have included:

- Air-Sea Chemical Exchange Experiment (CASCEX), conducted in 1995 in the vicinity of Monterey Bay, CA;

- Wind Events and Shelf Transport (WEST), conducted from 2000-2003 in northern California, examining the role of upwelling;

- Coastal Advances in Shelf Transport (COAST), similar to WEST, conducted off Oregon from 2001-2003; COAST benefited from additional sampling and analysis in the northern California Current as part of the U.S. GLOBEC program; and

- River Influences on Shelf Ecosystems (RISE) project, conducted from 2004-2006, assessing the influence of the Columbia River discharge on the coastal upwelling ecosystem off Oregon and Washington.

Figure 37 shows the location of the physical-biological coupling research efforts summarized by Kudela et al. (2008), as well as the location of the previously noted GLOBEC effort.

Kudela et al. (2008) addressed a series of CCS attributes being evaluated by various research programs, including nutrients, the role of nitrogen in the CCS, the concept of nutrient retention over the shelf, site-specific analyses of winds, currents, and submarine topography and their effects on primary productivity, and the potential limiting factors associated with iron. Evidence suggests that toward the northern portions of the CCS, iron becomes less important in controlling phytoplankton production. Per Kudela et al. (2008), nitrogen may be the ultimate limiting nutrient controlling total productivity, while iron controls the pattern of the mosaic, as evidenced by the work of Brzezinski et al. (1997) and Kudela et al. (1997) in central California (Monterey Bay), by Dugdale et al. (2006) in the WEST region, by Huyer et al. (2005) in the COAST region, and by Bruland et al. (2008) and Kudela and Peterson (2009) in the RISE region.

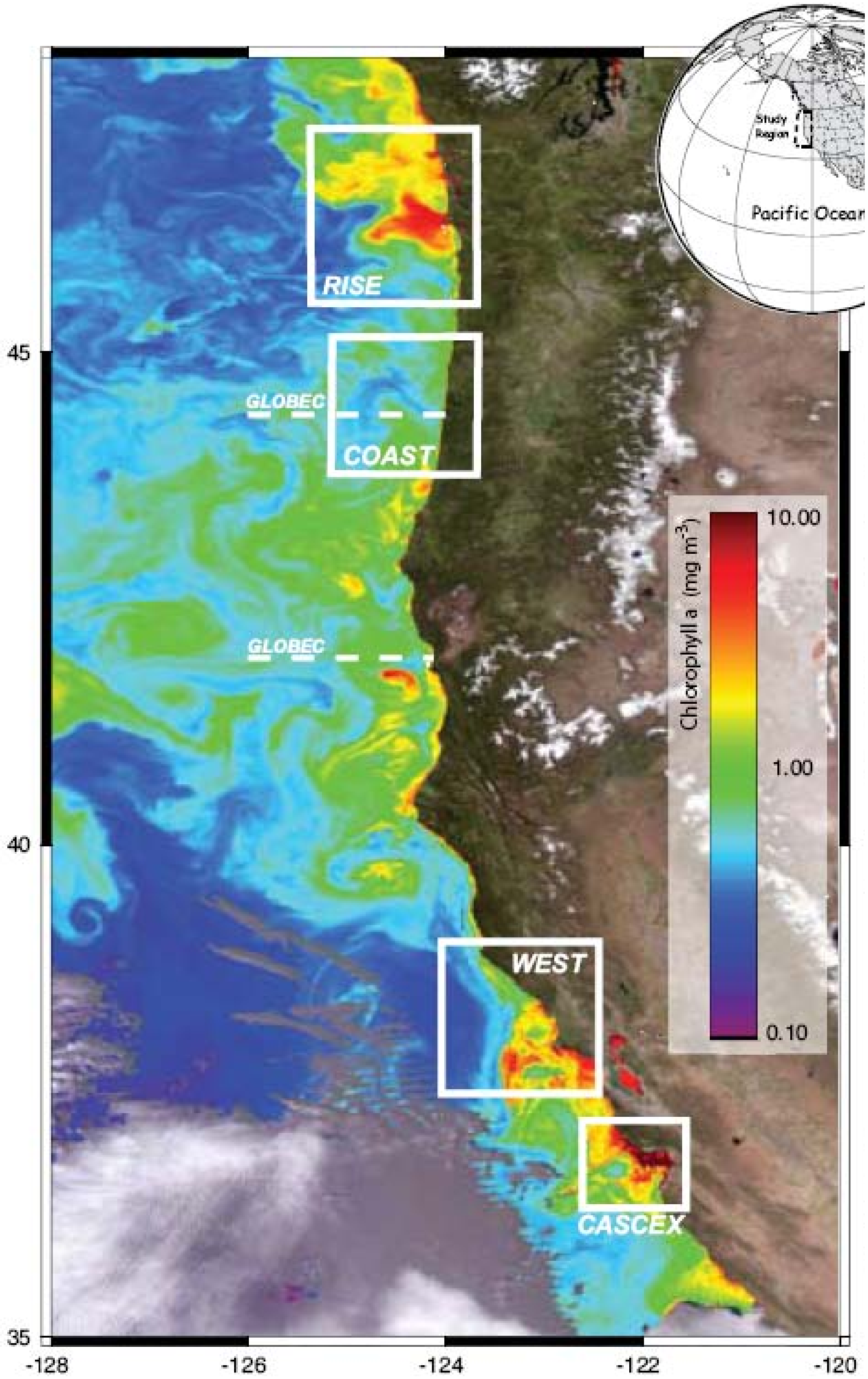

Figure 37. Location of four coastal ocean processes projects along the U.S. west coast, plus GLOBEC transects. Image from MODIS Aqua satellite instrumentation, 25 April 2004 (From: Kudela et al. 2008).

It has been hypothesized, per Kudela et al. (2008), that productivity of the WEST region is strongly controlled by the input of iron from the continental shelf (Kudela et al. 2006), by the availability of upwelled nitrate (Dugdale et al. 2006), and by effects of wind forcing (Botsford et al. 2003, 2006; Wilkerson et al. 2006). In the COAST study area, Chase et al. (2005a) measured iron in upwelling regions, noting the presence of steep iron gradients latitudinally and across the shelf, higher surface concentrations of iron in spring, greater particle-associated iron at depth in summer, and no evidence of iron limitations on phytoplankton production. Bruland et al. (2008) supported the findings of Chase et al. (2005a), failing to find evidence of iron limitation off Washington and Oregon. The relative contribution of outflow from the Columbia River to local primary productivity, particularly off Washington, was also highlighted by Ware and Thomson (2005).

Chase et al. (2007) assessed the potential linkage between river runoff and associated iron content with shelf width and their impacts on phytoplankton biomass along the U.S. west coast. They noted an increase in phytoplankton biomass from south to north (i.e., poleward) along the U.S. west coast attributed to increasing river runoff towards the north portions of the CCS (e.g., Columbia River discharge). They combined stream flow measurements and shelf width data with satellite-derived estimates of phytoplankton biomass to quantify the relationship between these variables, determining that a combination of winter streamflow and shelf width accounted for over 80% of the spatial variance in summer chlorophyll within 50 km of the coast. In those portions of the U.S. west coast characterized by the presence of a relatively broad shelf and large riverine inputs (i.e., along the Washington and Oregon coasts), phytoplankton productivity is not limited by iron (Chase et al. 2005a; Lohan and Bruland 2006); nearly all available NO_3 and considerable amounts of CO_2 are consumed within about 20 km of the coast (Hales et al. 2005, 2006). Further south, within those areas were the shelf is narrower and where there is a significant decrease in the amount of riverine discharge (e.g., off California), phytoplankton experience incomplete macronutrient uptake and iron-limited productivity (Hutchins and Bruland 1998; Bruland et al. 2001; Chase et al. 2005b).

Recent studies of phytoplankton communities in the CCS have addressed diverse topics, including characterizing the scales of variability (Henson and Thomas 2007a,b), the influence of El Niño and regime shifts on primary production (Kahru and Mitchell 2000; McGowan et al. 2003), identification of biological “hotspots” (Reese and Brodeur 2006), and seasonal changes and interannual variability in productivity (Legaard and Thomas 2006).

Remote sensing and interpretation of primary production within the CCS have also been recently summarized (e.g., Kahru et al. 2009), while the spatial variability in phytoplankton pigment concentrations in the CCS has also been characterized using older CZCS data (Thomas and Strub 1990, 2001). More recently, Kahru et al. (2009), in their analysis of SeaWiFS satellite data for the period 1997-2007 and comparisons to CalCOFI survey data, noted a significant increase in the annual NPP maxima along most of the coast of the CCS. Related increases in annual maxima in chlorophyll *a* along the coasts of the California Current as well as along the coasts of other major eastern boundary currents had been reported earlier (Kahru and Mitchell 2008). Kahru et al. (2009), in identifying an increasing trend of coastal NPP and chlorophyll *a* along most of the coast of the California Current, indicated that 1) in Central California, this trend is associated with decreased upwelling and increased sea surface temperatures, and 2) in southern California and northern Baja regions, there was no correlation with sea surface temperature or upwelling. This suggests that the increased trend in chlorophyll *a* and NPP is not explained by seasonal upwelling intensity. In the California Current, previous studies have indicated that increased upwelling is almost always associated with increased chlorophyll *a*, and increases in primary and secondary production (Botsford et al. 2006; Pennington et al. 2006; Rykaczewski and Checkley 2008).

Research on the CCS pertinent to primary productivity has also addressed a variety of topics since 1990. For example, Barth et al. (2007) characterized nearshore coastal ocean ecosystems in the northern portions of the CCS resulting from delayed upwelling. Barlow et al. (2008) assessed cetacean biomass and prey consumption concurrently with primary production requirements in the CCS. Kim and Miller (2006) evaluated the effects of stratification on primary production in the CCS. Hayward, in a series of articles, has evaluated the relationship between physical structure, chlorophyll concentrations, and planktonic communities within the CCS (Hayward and Venrick 1998; Hayward 1993, 1998).

Primary productivity measurements for the U.S. west coast are also available in real time through the NOAA CoastWatch program. This program identifies primary productivity measurements acquired remotely based on PAR values (derived from SeaWiFS sensor aboard the Orbview-2 satellite), chlorophyll-*a* concentrations (from MODIS Aqua), and blended SST measurements from multiple sensors. NOAA CoastWatch primary productivity from this region is an experimental dataset, distributed for scientific evaluation. Primary productivity data are available in near real time on the Southwest Fisheries Science Center OceanWatch Live Access Server (http://las.pfeg.noaa.gov/OceanWatch.html), as well as the NOAA CoastWatch West Coast Regional Node website (http://coastwatch.pfeg.noaa.gov/coastwatch/CWBrowser.jsp).

4.3.1 Southern California Planning Area

The Southern California Planning Area includes the area between the U.S.-Mexico border and Cape San Martin. The physical and biological structure of this region is strongly influenced by two predominant oceanographic features – the circulation of the CCS (Hickey 1979), composed of the low-salinity, southward flow of the core of the California Current, and the northward flow of the California Undercurrent, which is located inshore of California Current. In the southern portions of the Southern California Planning Area, within the region known as the Southern California Bight (between Pt. Conception and the U.S.-Mexico border), another dominant oceanographic feature is the Southern California Eddy. The Southern California Eddy is formed as a result of predominant current flow (i.e., the California Current) and the radical change in coastal orientation at Pt. Conception. The California Current moves southward, separating from the coast and allowing for formation of counterclockwise circulation formed by the California Current and the northward flow inshore, the Southern California Counter Current.

As noted by CSA (1990), the Southern California Planning Area is one of the best-sampled areas of the ocean for primary production. There are large data sets of direct measurements of water column primary production made by ^{14}C uptake. Prior to 1990, primary production was documented by 1) multiyear survey efforts undertaken by the CalCOFI program (Hewitt 1988; Bograd et al. 2003) and 2) the Southern California Bight Study (SCBS) (Eppley 1986) programs.

Since the last primary productivity summary (CSA 1990) was completed, continuing sampling efforts have been conducted under the CalCOFI program, as well as process-oriented research efforts noted previously (e.g., CODE, CTZ, GLOBEC, CoOP). Several researchers have also investigated the controlling mechanisms of primary productivity in the Southern California Bight.

Mantyla et al. (2008) evaluated patterns and controls of chlorophyll *a* and primary productivity cycles in the Southern California Bight. Using the long-term CalCOFI data set, they determined that the phytoplankton biomass in the Bight region exhibits considerable spatial and temporal heterogeneity, with mechanisms for nutrient input only weakly expressed (i.e, they are not easily identified). The maximum chlorophyll in the water column is most often found near the top of the nitracline, with maximum concentration largely dependent upon the ambient irradiance at depth (i.e., indicative of a nutrient and light limited system). A major influence on the concentration of chlorophyll at the depth of the maximum is the proximity of the nitracline to the surface; one common mechanism for the transport of nutrients into the photic zone is upwelling, the latter of which is generally lacking in the Bight except in the vicinity of Pt. Conception. Other factors contributing to spatial and temporal heterogeneity in the CalCOFI data set included isopycnal shoaling effects and winter convection.

Mantyla et al. (2008) also noted that while the amplitude of seasonal cycles of mixing and irradiance produces a strong cycle of primary production in several oceanic ecosystems outside of the Southern California Bight region, the amplitude of seasonal cycles within the Bight (i.e., in the CalCOFI area) is reduced, producing less pronounced fluctuations in phytoplankton biomass and contributing to spatial and temporal heterogeneity. However, wind-driven convection may still be a significant source of nutrients because of the absence of stronger mechanisms of nutrient input.

According to Lynn and Simpson (1987), the mean timing of the maximum surface density (minimum SST) varies spatially, occurring anywhere from 1 to 5 months after the winter solstice, depending upon the relative importance of winter convection and spring coastal upwelling in elevating deeper waters. The mean maximum surface density around Pt. Conception and the inner edge of the California Current occurs from mid-April to mid-May, largely in response to the Ekman offshore transport. The offshore California Current and the nearshore southern California regions have the mean maximum surface density between mid-January and mid-February. This pattern is consistent with the different annual cycles of chlorophyll in these areas (Hayward and Venrick 1998).

Citing a representative CalCOFI station offshore southern California (Station 90.03), Mantyla et al. (2008) noted the mean annual cycle of primary productivity is similar to that of chlorophyll *a*, with highest production from late winter to early summer, peaking at 1.3 g C m^{-2} d^{-1} in March. Minimum values of 0.4 g C m^{-2} d^{-1} occur in January (**Figure 38**).

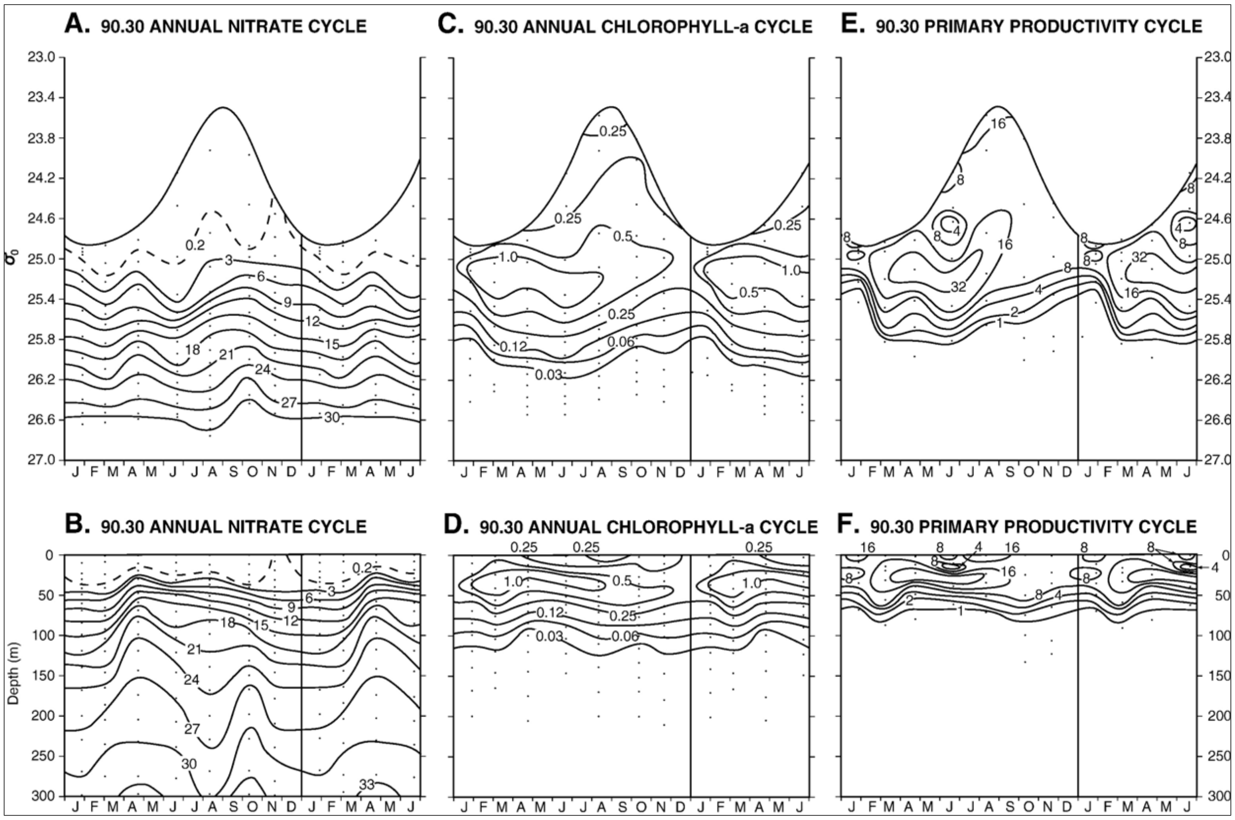

Figure 38. Annual cycle of nitrate, chlorophyll *a*, and primary productivity at CalCOFI Station 90.30. Plots appear in pairs, the first with respect to density (σt=23.0-27.0) and the second with respect to depth (0-300 m). A) nitrate vs. σt, B) nitrate vs. depth; C) chlorophyll *a* vs. σt, D) chlorophyll *a* vs. depth; E) primary productivity vs. σt; and F) primary productivity vs. depth (From: Mantyla et al. 2008). Image used with the approval of Elizabeth Vennrick.

Recent observations of phytoplankton iron limitation in central and northern California nearshore waters (i.e. within several kilometers from shore; Johnson et al. 1997; Hutchins et al. 1998) have suggested that both nitrate and iron might be limiting factors in primary productivity. King and Barbeau (2007), addressing the question of iron limitations to phytoplankton growth, infer that iron likely plays a role in the discrepancy between unused nitrate and low phytoplankton biomass observed in the 20-y CalCOFI dataset. The authors, however, did not dismiss alternate factors that may prevent phytoplankton from utilizing available nitrate (e.g., grazing; light limitation). As noted by King and Barbeau (2007), a series of articles addressing the question of iron limitation in California offshore waters, including those of the Southern California Planning Area, and similar eastern boundary current systems has been published (e.g., Johnson et al. 1997; Hutchins et al. 1998; Bruland et al. 2001; Firme et al. 2003; Fitzwater et al. 2003). In spite of upwelling, such high nutrient, low chlorophyll systems exhibit low phytoplankton growth attributed, in varying degrees, to iron limitation.

Landrey et al. (2009) conducted experimental studies of phytoplankton growth and grazing over a 2-y period within a coastal upwelling system off Point Conception to characterize phytoplankton dynamics. Rates of phytoplankton growth and microzooplankton grazing were determined by daily *in situ* dilution incubations at eight depths within the euphotic zone. Mesozooplankton grazing was determined by gut fluorescence analysis. Comparisons were made of net change rates (i.e., observed for the ambient phytoplankton community) versus net growth rates. The resulting relationship accounted for 91% of the variability observed. Per Landrey et al. (2009), grazing by mesozooplankton was high and variable, driving a substantial positive to negative shift in phytoplankton net change rate between years despite comparable environmental conditions and similar high growth rates. Their results suggested a strong potential for top-down control within this upwelling system.

Hopkinson (2007) described the role of iron as a limiting factor, and of light as a co-limiting factor, for phytoplankton growth in subsurface chlorophyll maxima zones of the Southern California Bight. The response of phytoplankton found in the mesotrophic waters of the Bight were indicative of iron-light co-limitation. The addition of iron produce changes in both the size and structure of the phytoplankton community (i.e., large diatoms became dominant over relatively small phytoplankton). Iron limitation was particularly acute when light levels changed rapidly, mimicking normal oceanographic processes (i.e., eddy events, strong internal waves). Results indicated that iron influences phytoplankton community structure within subsurface maxima zones.

Primary productivity measurements (e.g., chlorophyll *a*, phaeopigment, integrated primary production) from the CCE LTER program at Scripps Institution of Oceanography are available online. Sampling conducted between May 2006 and October 2008 resulted in 975 samples analyzed for chlorophyll *a* and phaeopigments and 46 measurements of integrated primary production. Chlorophyll-*a* determinations ranged from 0.02-8.86 µg L^{-1}. Measurements of integrated primary production ranged from 293-7,060 mg m^{-2} d^{-1} and averaged 1,609 mg m^{-2} d^{-1} (Scripps Institution of Oceanography 2010).

Picophytoplankton is composed of three groups and includes the cyanobacteria *Prochlorococcus* spp., *Synechococcus* spp., and small eukaryotic algae. Picophytoplankton contribute >50% of the biomass and production in warm oligotrophic tropical and subtropical open oceans (Agawin et al. 2000). *Prochlorococcus* spp. has been found to be more abundant in oligotrophic water than in eutrophic water, and *Synechococcus* spp. is ubiquitous in the upper layers of temperate and warm oceans (Zhao et al. 2010). The vast majority of picophytoplankton studies are within oligotrophic open ocean systems, including the Pacific, Indian, Arctic, and Atlantic oceans, as well as the Arabian, Red, and Mediterranean seas (Zwirglmaier et al. 2008). These two phytoplankton groups, along with picoeukaryotes, represent fundamental components of marine ecosystems; they display fast growth rates and high mortality losses and are significant factors in nutrient cycling and regeneration. In spite of their importance, only a few studies of picophytoplankton have been completed in the Pacific region.

Tai (2009) determined that *Synechococcus* with unique ecological niches are distributed along a coastal to offshore transect within the Southern California Bight. The composition of the *Synechococcus* communities generally changed with the nitricline, thermocline, and chlorophyll maximum depths, each of which deepened as sampling moved offshore. Distinct drops in these features at mesotrophic and oligotrophic sampling locations were matched by noticeable changes in *Synechococcus* community composition (i.e., changes in *Synechococcus* clades). Based on flow cytometry observations, *Synechococcus* also exhibited distinct fluorescence and scattering changes from coastal to open ocean environments and with depth in the Southern California Bight (Collier and Palenik, 2003). Tai (2009) suggests that these changes are linked to genetic differences in the *Synechococcus* community and not solely due to physiological conditions (e.g., light, nutrient levels).

Metagenomic analyses of *Synechococcus* have also been conducted by Palenik et al. (2008, 2009) in the southern portions of Southern California Bight. This research has been concentrated on the coastal clades of *Synechococcus* (i.e., lying well inshore of the Southern California Planning Area).

Primary productivity work in the southernmost reaches of the Southern California Planning Area includes the efforts of Mexican researchers operating off Baja California. Several of these data sources have relevance to productivity determinations in U.S. waters. Aguirre-Hernández et al. (2004) and Espinosa-Carreon et al. (2004) have published recent summaries of primary productivity in this area.

Espinosa-Carreon et al. (2004) examined mean fields, seasonal cycles, and interannual variability for satellite-derived chlorophyll pigment concentrations, sea surface height, and sea surface temperature during 1997-2002. Three dynamic regions were identified, including an upwelling zone next to the coast, the Ensenada Front in the north (in the southern portions of the Southern California Planning Area), and regions of repeated meanders and/or eddy variability west and southwest of Point Eugenia. High chlorophyll values were measured in the upwelling zone and diminished offshore, with the exception along the Ensenada Front (north of 31° N latitude), where higher chlorophyll values were noted about 150 km offshore.

4.3.2 Central California Planning Area

The Central California Planning Area extends between Cape San Martin in the south to Pt. Arena in the north. Primary productivity research in waters of the Central California Planning Area has not been as extensive since 1990 as compared to the Southern California Planning Area.

Chavez et al. (2002) have characterized the biological and chemical effects resulting from the 1997-1998 El Niño in central California waters. Starting in June 1997, an influx of warm southerly waters, with weak signatures on coastal sea level and thermocline depth, marked the onset of El Niño off central California. By late 1997, a stratified ocean condition predominated – deep thermocline, high sea level, and warm sea surface temperatures. During the first half of 1998, the California Current had moved closer to shore. Low salinity, low nutrient water was dominant; high nutrient, productive waters that occur in a north-south band from the coast to approximately 200 km offshore during cool years disappeared during El Niño. Nitrate concentrations in surface waters were less than 20% of normal; new production was reduced by close to 70%. La Niña began in the fall of 1998 when sea surface temperatures dropped below normal and ocean productivity increased to higher than normal levels. The reduction in coastal California primary productivity associated with El Niño was estimated to be 50 million metric tons of carbon (5×10^{13} g C).

Site-specific studies by Pennington and Chavez (2000) have characterized the seasonal fluctuations in physical oceanographic parameters and nutrient characteristics over an 8-y time period (1989-1996), and their subsequent influences on chlorophyll concentrations and primary production in Monterey Bay. During spring and summer, upwelling brings high-nutrient water to the surface of Monterey Bay. Nutrients, sunlight, and some degree of water column stratification lead to high primary production and elevated chlorophyll values during the upwelling period. During the upwelling period, flora within the Bay are dominated by diatoms, especially *Chaetoceros* spp.

Hutchins et al. (1998) proposed the idea of an “iron limitation mosaic,” based on sampling conducted within the nearshore waters, just inshore of the Central California Planning Area. Shipboard incubation experiments were conducted to evaluate the potential for limited phytoplankton growth due to limited iron availability, demonstrating that a lack of iron prevents the complete biological utilization of ambient nitrate and influences phytoplankton species composition in open-ocean HNLC regimes, including those sampled off central California. Addition of iron to nearshore HNLC waters promotes blooms of large chain-forming diatoms. Iron limitation effects ranged from subtle influences on phytoplankton species composition that would be missed by nutrient measurements alone, to a dramatic enhancement of nutrient drawdown and a comprehensive increase in productivity at all trophic levels. The silicic acid:nitrate (Si:N) uptake ratios in control incubations were two to three times higher than those in iron incubations. They determined that diatoms, stressed by a lack of iron, should deplete surface waters of silicic acid before nitrate, leading to a secondary silicic acid limitation of the phytoplankton community (Hutchins and Bruland 1998).

4.3.3 Northern California Planning Area

The Northern California Planning Area extends between Pt. Arena in the south to the California-Oregon border. Recent research on primary productivity in this planning area has been reported from the WEST and GLOBEC programs.

Wilkerson et al. (2006) analyzed a 3-y data set (2000-2003) of nearshore upwelling events off Bodega Bay (California). As part of the CoOP WEST study, nutrients, CO_2, size-fractionated chlorophyll, and phytoplankton community structure were measured. The ability of the ecosystem to assimilate nitrate (NO_3) and silicic acid/silicate ($Si(OH)_4$) and accumulate particulate material (i.e., phytoplankton) was realized in all 3 y, following short events of upwelling-favorable winds followed by periods of relaxed winds. This was observed as phytoplankton blooms, dominated by chlorophyll in cells greater than 5 µm in diameter that reduced ambient nutrient levels to below detection limits (i.e., reported as zero by Wilkerson et al. 2006). Seasonal wind-driven upwelling supplies abundant nutrients to support increased phytoplankton productivity. Maximum chlorophyll values of 32.1 mg L^{-1} for the study area were noted in 2000.

Sherr et al. (2005) described the spatial distribution patterns of coccoid cyanobacteria (*Synechococcus*) and small photosynthetic eukaryotes within the upwelling ecosystem off the coast of northern California and Oregon as part of the GLOBEC Northeast Pacific Long Term Oceanographic Program (LTOP). Because the majority of the samples collected were acquired off the Oregon coast and the results addressed Oregon upwelling, a more comprehensive summary of the results is presented in the next subsection.

4.3.4 Washington-Oregon Planning Area

The Washington-Oregon California Planning Area extends between the California-Oregon border and the Washington-British Columbia (Canada) border. Recent research on primary productivity in this planning area has been reported from the RISE, COAST, and GLOBEC programs, among others.

As part of the RISE program, Frame and Lessard (2009) recently characterized the composition and biomass of phytoplankton communities off the Washington and Oregon coasts and the effects of the Columbia River plume. The authors determined the taxonomic composition, size structure, and biomass of phytoplankton assemblages in near-surface shelf waters during four 3-week cruises in spring and/or summer of 2004-2006. In whole data-set comparisons, there were no significant differences in chlorophyll, carbon biomass, or diatom community structure between regions or between plume and non-plume samples. Over the entire data set, chlorophyll was similar off the Washington coast (median 5.4 mg L^{-1}) and within the Columbia River plume (median 5.6 mg L^{-1}). The median chlorophyll level off Oregon was lower (median 3.6 mg L^{-1}) but not significantly different, likely due to sample size. However, regional and plume differences in chlorophyll and biomass were evident. While diatom community composition differed between cruises, community composition within a cruise was similar across regions and in plume/non-plume samples, indicating there was no unique plume community. Diatoms typically accounted for over 65% of the total photosynthetic biomass in all samples, with notable variations evident in summer 2005 (when diatoms accounted for 86% of biomass) and in spring 2006 (when diatoms were a very small percentage of biomass in about half the samples). Median biomass determinations for Washington and Oregon were similar (86.3 and 85.0 mg C L^{1}), while the Columbia River plume biomass level was lower (75.6 mg C L^{-1}). Over broader scales, the Columbia River plume produces a more homogeneous phytoplankton community along the Washington and Oregon coasts. On finer temporal and spatial scales, differences in community structure as well as biomass were evident between samples in and outside of specific plumes.

Kudela and Peterson (2009) evaluated the influence of the Columbia River plume on phytoplankton rates and biomass accumulation using deckboard incubations as part of the RISE program in August 2005. While the authors noted the potential for problems associated with "bottle effects'' (e.g., elimination of important physical effects such as advection, diffusion, and light limitation), they argued that nutrient addition bioassay experiments provide control over physical and biological parameters that are not readily manipulated in true field experiments. They were able to examine the potential role of nitrate alone by comparing results with those where nitrate plus all other dissolved compounds, particularly iron and silicic acid, was evaluated. They assessed how nitrate alone versus nitrate with other dissolved compounds modulated the physiological and biomass response to a simulated plume mixing with Washington, near-field plume, and Oregon coastal waters. For all experiments, nitrogen (nitrate) was clearly controlling both biomass accumulation and growth rates. Despite the apparent south-north trend toward increasing biomass in this region, there were no obvious differences in phytoplankton physiological capacity, nor were there any indications of iron limitation in the short term. Kudela and Peterson (2009) concluded that phytoplankton in this region are predominantly nitrogen-limited but that upon release from this limiting factor, phosphorous and/or silicic acid (in waters not influenced by the Columbia River plume) would quickly become limiting. Evidence suggests that the mesoscale differences in phytoplankton biomass between the Oregon and Washington coasts result from a combination of enhanced grazing downstream (i.e., offshore and northward, southward, or bidirectional, depending upon prevailing winds) and the physically retentive and dispersive effects of the plume itself.

Banas et al. (2009) developed a biophysical model of planktonic nutrient cycling and plankton dynamics as part of the RISE efforts. The high-resolution hindcast circulation model covering the Oregon-Washington coast was designed to characterize the effects of Columbia River plume on regional-scale patterns of phytoplankton biomass and productivity. Their model tracks nitrogen in four phases – as dissolved nutrients, phytoplankton biomass, zooplankton biomass, and detritus. Large-scale winds in this area are highly variable in all seasons, with summer dominated by southward, upwelling-favorable winds and winter by northward, downwelling-favorable winds. These prevalent wind patterns are interspersed with strong, event-scale reversals that last from 2-10 d and may occur any time during the year. Banas et al. (2009) noted two patterns: 1) upwelling winds advect the Columbia River plume south past Oregon and offshore via Eckman transport; and 2) downwelling winds advect the plume northward and onshore along the Washington coast, with remnants of the northward plume water evident on the Washington shelf for many days after each downwelling event. Both upwelling and downwelling plumes have complex effects on coastal productivity.

Additional productivity data acquired as part of the RISE program was reported by Lessard and Frame (2008), who examined the spatial and temporal patterns and controls of phytoplankton growth, microzooplankton grazing, and chlorophyll associated with the Columbia River plume. Rates were measured on four cruises in the summers of 2004-2006. Upwelling conditions were highly variable within cruises and between years. The authors noted that phytoplankton growth rates ranged from <0 to 1.8 d^{-1} and appeared to be limited by nitrate; however, substantial rates were sometimes maintained when no nitrate was analytically detectable, supported by plume-supplied regenerated nitrogen (i.e., nitrogen regenerated from dead algae and zooplankton fecal material). Shelf-wide, grazing rates on larger phytoplankton were significant but lower than growth rates, contributing to phytoplankton biomass accumulation patterns. Growth rates were not consistently higher off the Washington coast than off the Oregon coast; the often higher chlorophyll in Washington waters was due, in part, to differential grazing and differences in carbon-to-chlorophyll ratios. New plume water was conducive to phytoplankton growth but unfavorable to microzooplankton. The highest growth and lowest grazing rates were found in the new plume, contributing to the formation of very high chlorophyll often observed near the river mouth.

Bane et al. (2007), reporting on efforts from the COAST program, characterized intraseasonal oscillations (ISOs) within the central Oregon upwelling system and their effects on primary and secondary production. The authors characterized ISOs with periods from ~15-40 d, as well as shorter timeframe fluctuations (2-6-d ‘‘weather-band’’ and 1-d diurnal time scales). Coastal upwelling of cool, nutrient-rich water is driven by extended periods of equator-ward alongshore winds. During the upwelling event evident off Oregon in summer 2001, 20-d ISOs exhibiting alongshore wind stress were dominant. These wind stress ISOs resulted from north-south positional ISOs of the atmospheric jet stream. Upper ocean temperature, phytoplankton, and zooplankton generally varied on the ~20-d time scale, and these correlated with the ISOs in alongshore wind stress and jet stream position, even though there also were weather-band stress fluctuations of comparable magnitude. Wind stress ISOs are typical along Oregon in the summer upwelling season, occurring in 10 of the 12 y examined by Bane et al. (2007).

Eisner and Cowles (2005) characterized spatial variability in phytoplankton pigment ratios, optical properties, and environmental gradients in Oregon coastal waters in August 2001, with sampling extending from 3-70 km offshore and 130 km north-south in the vicinity of Newport, OR. The authors noted that certain optical tools can be used in conjunction with discrete water samples to determine the characteristics and taxonomic composition (i.e., pigment ratios, relative particle size distribution, chlorophyll-*a* concentrations) of phytoplankton populations off the Oregon coast. In general, nutrients supplied by episodic upwelling, in conjunction with light provided by incident solar radiation and stratification of the upper water column from warming and the injection of less saline water masses, result in high phytoplankton photosynthesis and growth rates and high primary production over the Oregon shelf.

Sherr et al. (2005) described the spatial distribution patterns of small-sized phytoplankton, including coccoid cyanobacteria (*Synechococcus*) and small photosynthetic eukaryotes, within the upwelling ecosystem off the coasts of Oregon and northern California during nine cruises of the GLOBEC Northeast Pacific LTOP from March 2001 to December 2002. The authors found a consistent pattern of lowest abundance of small-sized phytoplankton in shelf regions, despite high nutrient and chlorophyll concentrations in recently upwelled water. Seaward of the upwelling front, the region of transition between inshore vertical sigma-t surfaces characteristic of upwelling and offshore horizontal sigma-t surfaces characteristic of vertical stratification, there were high abundances of both *Synechococcus* (5-58 x 10^4 cells mL^{-1}) and of photosynthetic eukaryotes (1-8.6 x 10^4 cells mL^{-1}) in the upper 50 m of the water column. Comparisons of cyanobacteria and small photosynthetic eukaryote abundances versus nitrate+nitrite concentration showed a negative relationship between abundance and nutrient concentration. At chlorophyll-*a* concentrations of <~2 mg L^{-1}, small cells typically comprised most of the carbon biomass of the phytoplankton. The pattern of phytoplankton distribution suggested a dramatic spatial shift in the structure of pelagic food webs in the Oregon upwelling ecosystem, from shelf upwelling blooms dominated by large diatoms, to slope and basin food webs dominated by <5-µm-sized phototrophic cells. No explanation was available as to why the abundances of small-sized phytoplankton, and especially of coccoid cyanobacteria, were low in high-nutrient, high-chlorophyll shelf waters.

4.4 Alaska Region

The Alaska Region encompasses 15 separate planning areas and a wide range of oceanic systems. These planning areas range from narrow, seasonally ice-covered shelves that border the Arctic Basin (Beaufort Sea), through one of the largest and most productive Mediterranean-type seas (Bering Sea), to a predominantly down-welling system of the subarctic North Pacific.

4.4.1 Gulf of Alaska Planning Area

The northern Gulf of Alaska shelf is a productive coastal region that supports several commercially important fisheries. The annual yields of numerous fish and shellfish stocks within this region are linked with variations in climate conditions, including the Pacific Decadal Oscillation (PDO) in the North Pacific basin (see Strom et al. 2010). The inner-shelf circulation is driven by the Alaska Coastal Current (ACC), which is locally forced by buoyant freshwater discharge and regional along-shore winds (Royer 1981). Outer-shelf circulation is dominated by the Alaskan Stream, an extension of the eastern Pacific gyre system. Both circulation patterns are further complicated by a complex bathymetry, tidal mixing, freshwater discharge, and cross-shelf exchange (**Figure 39**).

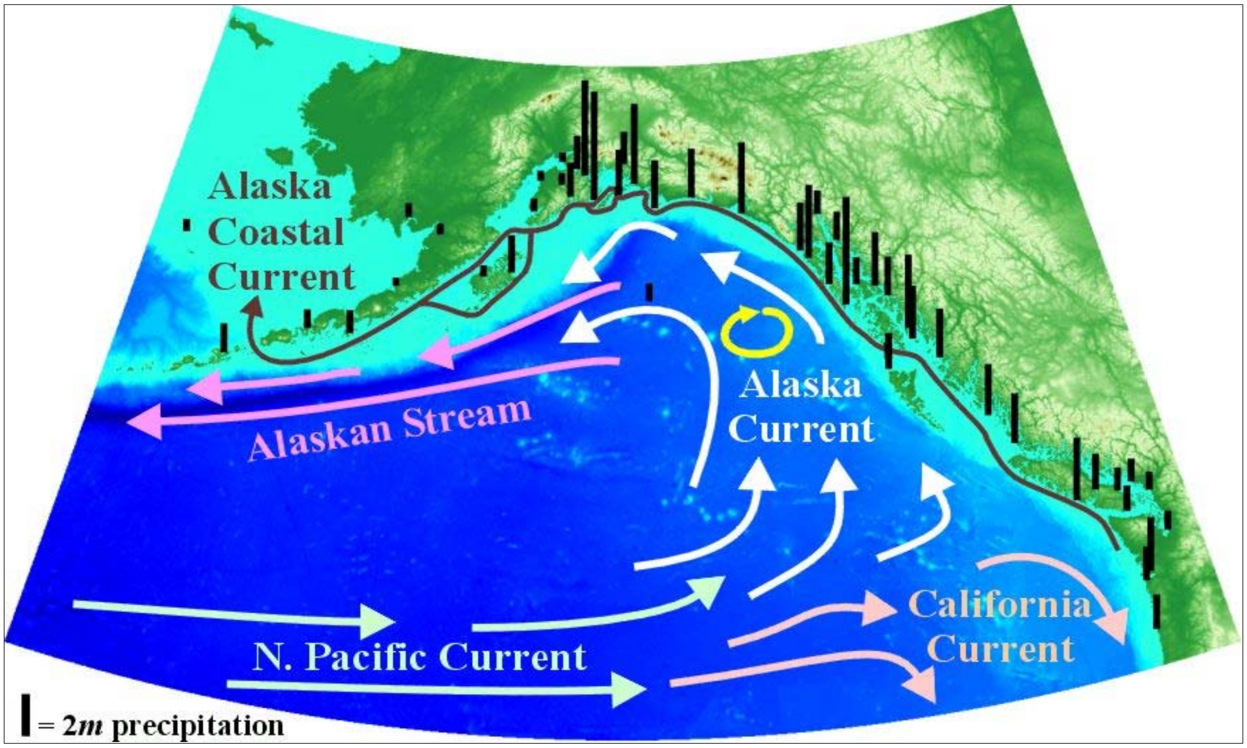

Figure 39. A circulation schematic of the Gulf of Alaska showing the major current systems, including the Alaska Coastal Current (ACC). The vertical bars are estimates of the annual precipitation rates measured at active and inactive coastal sites (From: Weingartner et al. 2005; with the authors' permission).

In addition, mesoscale variability along the entire southern coast of Alaska is seasonally influenced by the presence of southwestwardly propagating eddy fields (for reviews see Okkonen et al. 2003; Ladd et al. 2005; Janout et al. 2009). The mechanisms supporting such high levels of productivity over this shelf, however, are not fully understood since it is primarily a downwelling-dominated shelf (see Childers 2005). These shelf systems skirt an HNLC system characterized by low concentrations of phytoplankton. Typically, this community is dominated by small cells whose growth is iron-limited; at times, silicate-limited growth is also evident. The low plant biomass as well as the absence of a spring bloom is attributed to the balanced trophic relationships prevailing in the Subarctic Pacific (Frost 1987). Alternatively, Martin et al. (1989) suggested that the phytoplankton community in the Subarctic Pacific might be iron-limited (see Banse 1991 and Miller et al. 1991 for a critical discussion). Fiechter et al. (2009) have developed a model of iron limitation of primary production in coastal Gulf of Alaska and can differentiate between nitrate-limited and iron-limited growth conditions. In general, coastal waters become nitrate-limited during the phytoplankton growing season, whereas productivity in the Gulf of Alaska is limited by iron and dissolved silicate (Whitney et al. 2005). During a summer-time investigation, Strom et al. (2010) found that small phytoplankton (<20 μm) were responsible for most of the daily production in coastal waters, due both to their dominance of total chlorophyll content at most stations and to their higher chlorophyll-specific photosynthesis rates. Estimated primary productivities ranged from 359-909 mg C m^{-2} d^{-1}. These Gulf of Alaska productivities are considered moderate and generally less than those measured in coastal North Pacific regions having greater nutrient supply. Summertime production was sensitive to light availability, suggesting light limitation, although nutrient limitation and microzooplankton grazing are also considered important controlling factors (Strom et al. 2010).

Neuer (1992), in one of the few field and culture studies of cyanobacteria in subarctic waters, characterized the growth dynamics of *Synechococcus* spp. at two stations in the Gulf of Alaska. One of the two stations sampled occurs in very close proximity to the outer boundaries of the Gulf of Alaska and Kodiak planning areas. Abundance, specific growth rates, and overall contribution to phytoplankton carbon and productivity were determined based on field results from Subarctic Pacific Ecosystem Research cruises in June and September 1987. Specific growth rates were measured by the frequency-of-dividing-cells method. Culturing results indicated a division duration of 10.5 h. Neuer (1992) reported that the vertical distribution of *Synechococcus* spp. varied seasonally, with cells evenly distributed in the mixed layer at the beginning of June but concentrated in and below the pycnocline (40-60 m) in September. Instantaneous growth rate determinations 1) reached a maximum (0.7 d^{-1}) in surface waters in June; 2) were reduced (0.25 d^{-1}) in September within the mixed layer at the surface and 3) were lowest (~0.16 d^{-1}) below the pycnocline. The contribution of *Synechococcus* spp. to phytoplankton carbon and total primary production was estimated to be 21% and 8%, respectively, in surface waters in June. While September contributions were lower, they increased with depth, reaching maximum values (i.e., 31% and 68%, respectively) at and below the 1% light level. Field and laboratory culture growth rates were within the range of values noted for *Synechococcus* spp. found at lower latitudes, strongly suggesting that low temperatures found in the Gulf of Alaska do not inhibit growth of *Synechococcus*.

Within this region of the Gulf of Alaska, the euphotic zone undergoes an annual cycle of nutrient drawdown and replenishment in response to the local physical dynamics and phytoplankton activity. During the spring and summer, nutrient concentrations in the upper water column are reduced to limiting or near-limiting conditions by seasonally high phytoplankton chlorophyll biomass. In the fall and winter, wind mixing replenishes nutrient concentrations in surface waters (Childers et al. 2005). The entire region undergoes large degrees of interannual variability in the physical, chemical, and biological distributions throughout the subarctic Pacific in concert with various phases of the ENSO, the PDO and variable eddy fields (Childers et al. 2005). Comprehensive reviews of primary productivity and phytoplankton standing stock are yet to be made.

4.4.2 Cook Inlet Planning Area

Primary productivity and phytoplankton biomass reports for Cook Inlet are of limited scope and are only mentioned in assessments of either bird or fish populations. This evaluation attempts to relate chlorophyll fluorescence (typically *in vivo* measurements) to changes in seabird and/or fish stocks (Speckman et al. 2005). Speckman et al. (2005) concluded that the abundance and distribution of chlorophyll and thus both zooplankton and forage fish in Cook Inlet were affected much more by spatial variability in physical oceanography than by interannual variability. The high turbidity found within Cook Inlet reduces light availability and ultimately limits primary productivity. Over a 2-y project, estimated chlorophyll values ranged from approximately 2-12 μg L^{-1} during a July/August sampling period.

4.4.3 Kodiak Planning Area

Using 4 y of SeaWiFS data, Brickley and Thomas (2004) saw a strong cross-shelf gradient in average chlorophyll values. Their data showed elevated chlorophyll concentrations on the shelf and in association with submarine banks and canyons near Kodiak Island. The area to the south and east of Kodiak Island is characterized by a complex topography and strong tidal mixing, which in turn generates higher standing stocks of phytoplankton than the shelf area to the northeast (Ladd et al. 2005). The wide shelf region in the vicinity of Kodiak Island is among the most biologically productive in the Northeast Pacific (Brickley and Thomas 2004).

Spatial patterns also illustrated strong seasonal cycles and interannual variability both on the shelf and within ~300 km of the shelf break. Furthermore, spatial patterns evident in the imagery suggested that the elevated chlorophyll concentrations occurring along the shelf break and immediately seaward are associated with mesoscale eddies. It is evident that eddies have the potential to control a significant proportion of the spatial pattern and temporal variability of phytoplankton biomass in regions of the Northeast Pacific. This is consistent with previously published work documenting the position and dynamics of both cyclonic and anticyclonic eddies in the Alaska Current and the Alaskan Stream (see Okkonen et al. 2003; Ladd et al. 2007; Janout et al. 2009). Examining the summertime photosynthetic potential of phytoplankton and iron concentrations across the subarctic Pacific Ocean, Suzuki et al. (2002) observed near-Kodiak samples to have the highest concentrations of chlorophyll (~3.75 μg Chl L^{-1}) and total dissolvable iron (~1.0 nmol L^{-1}).

4.4.4 Shumagin Planning Area

Atmospheric, topographic forcing and freshwater runoff dominate the currents in the Gulf of Alaska (Royer 1981). This flow is modified by bathymetry along a dynamic shelf and by variability in winds. The main currents over the Shumagin regional shelf are the nearshore ACC and the Alaskan Stream flowing over the outer shelf and slope. Complexity of the ACC as it flows through Shelikof Strait, the sea valley, and shelf region downstream is further accentuated by upwelling, eddies, meanders, episodes of flow reversal, and cross-shelf eddies (see Bailey et al. 2005). This region’s numerous frontal systems commonly generate areas of phytoplankton blooms as a result of nutrient enhancement, as noted by Incze et al. (1996). A key species in northern North Pacific ecosystems, the walleye pollock (*Theragra chalcogramma*), has generated numerous ecological studies. Again, comprehensive primary productivity studies within this area are lacking.

4.4.5 Aleutian Arc Planning Area

A chain of more than 300 volcanic islands form part of the Aleutian Island Archipelago in the Northern Pacific Ocean, interspersed by a series of passes that permit interchange and transport of heat, salts, and nutrients between the Pacific Ocean and the Bering Sea. In addition, within these passes, deep vertical mixing occurs that introduces nutrients into the euphotic zone.

In a recent overview of production estimates in the Aleutians and Bering Sea, Springer et al. (1996) provided very general annual production rates of 150-200 g C m^{-2} y^{-1} across the entire Aleutian Island Archipelago. Assuming a 4-month growing season (Hansell et al. 1993), averaged daily production rates for Springer et al. (1996) were 1,230-1,640 mg C m^{-2} d^{-1}, results similar to the average production found in this study (1,510 ± 120 mg C m^{-2} d^{-1}). However, primary production rates identified in the current analysis varied widely, ranging from a low estimate of 40 ± 30 mg C m^{-2} d^{-1} to a high estimate of 6,810 ± 920 mg C m^{-2} d^{-1}, spanning far beyond the generalized rates given by Springer et al. (1996). This variability is due primarily to increased coverage. The results of Springer et al. (1996) were generalized and based on a small data set with limited time coverage. It is very difficult to get adequate satellite and ship coverage in this area, but as additional information is collected, researchers are observing increased variability when compared to the original assessment of Springer et al. (1996). Suzuki et al. (2002) have also noted an east-west gradient in photosynthetic potential of phytoplankton and iron concentrations across the entire Alaska OCS Region.

4.4.6 North Aleutian Basin Planning Area

During the last three decades, several studies of primary production were conducted on the southeastern Bering Sea shelf to understand the development of the spring bloom and the amount of primary production in the Bering Sea. Based on Processes and Resources of the Bering Sea (PROBES) data and that of Rho (2004), annual primary production estimates are 133 g C m^{-2} y^{-1} over the inner shelf and 144 g C m^{-2} y^{-1} over the middle shelf. There are two types of blooms over the southeastern Bering Sea shelf: ice-edge blooms and open water blooms. As the ice edge recedes, providing cold, low salinity water, strong stratification promotes phytoplankton blooms (Alexander and Niebauer 1981; Niebauer et al. 1981). When there is no sea ice, the spring phytoplankton bloom occurs when solar radiation increases and wind mixing decreases (Sambrotto et al. 1986). A new hypothesis, the Oscillating Control Hypothesis (OCH), provides a conceptual model of the responses of the Bering Sea primary production to alternating warm and cold periods (Hunt et al. 2002). The pelagic ecosystems in the southeastern Bering Sea, according to this hypothesis, will alternate between primarily bottom-up control in cold regimes and primarily top-down control in warm regimes. A model (1-D ecosystem model) was developed and successfully reproduced the observed ice-associated blooms in 1997 and 1999 at the NOAA/Pacific Marine Environmental Laboratory mooring M2 (Jin et al. 2007). The results of this model suggest that the ice-associated blooms were seeded by sea ice algae released from melting sea ice. Yet, these ice-associated blooms were seen to have had little impact on the annual primary production.

Some of the studies used the ^{14}C method to measure winter production on the shelf and summer production along the Aleutian chain (McRoy et al. 1972) and to measure summer production around the Pribilof Islands (Kopylov et al. 2005). Other studies estimated primary production indirectly from nitrate depletion in the euphotic zone or from nitrate uptake experiments (Sambrotto et al. 1986; Whitledge et al. 1986; Hansell et al. 1993; Rho et al. 2005). Instead of year-round measurements of primary production, most of the studies were focused either on specific seasons such as the ice-edge bloom (Niebauer et al. 1995), the spring bloom (Sambrotto et al. 1986; Whitledge et al. 1986), and the winter and summer periods (McRoy et al. 1972) or on a specific location of the shelf region (Sambrotto et al. 1986; Whitledge et al. 1986). From 1997 to 1999, Rho et al. (2005) also conducted primary production measurements in the southeastern Bering Sea shelf. Rho and Whitledge (2007) found data suggesting that a gradual progression of spring bloom development occurs from the inner shelf toward the shelf break. The authors note that the response of primary production to climate change can be misunderstood without proper temporal and seasonal measurements.

4.4.7 St. George Basin Planning Area

Classically, the hydrography and currents differentiate the cross-shelf oceanographic structure of the southeastern Bering Sea shelf into three domains with distinct characteristics (Coachman 1986; Schumacher and Stabeno 1998; Stabeno et al. 2008). Because of the shoaling bathymetry around the islands and their proximity to the shelf break, this region has characteristics that are unique on the shelf. Sullivan et al. (2008) have proposed that this domain be referred to as the ‘‘Pribilof Domain.’’ The Pribilof Domain is characterized by enhanced mixing, particularly the area between St. Paul and St. George Islands; organized anti-cyclonic flow around the island group; strong tidal currents; and is a location where nutrient-rich water from the bottom layer of the middle shelf and deeper water from the slope are vertically mixed to sustain production throughout the summer (Sullivan et al. 2008). A recent study around St. Paul Island showed that the summer values of phytoplankton abundance and primary production in the shelf break frontal region are similar to those of the shelf region during the spring bloom (Flint et al. 2002). Strom and Fredrickson (2008) report rates of phytoplankton growth in summer 2004 were strongly nutrient-limited (nitrogen) at nearly all sites. Hunt et al. (2008) discuss the patterns of spatial and temporal variation in the Pribilof Domain in terms of warm versus cold years. Using maps of SST, chlorophyll *a*, and PAR, Mizobata et al. (2008) derived summer primary production from 1998-2003. Comparing these satellite multi-sensor derived data estimates to mesoscale eddy fields, the distribution of high primary production was found to roughly coincide with the high variability area of the eddy field. Therefore, in addition to intense tidal mixing, Mizobata et al. (2008) demonstrate the importance of eddy-induced on-shelf nutrient flux. These exchanges probably contribute to the primary productivity at the western shelf of the Pribilof Islands, where the Bering Sea physics are highly variable.

4.4.8 Bowers Basin Planning Area

The deepwater (>3,000 m) part of the Bering Sea (Bering Sea Basin) is divided into three physiographic areas – the Aleutian, Bowers, and Komandorsky Basins. Bowers Basin is the deepwater basin that lies north of the Aleutian Islands adjacent to the Bering Sea continental shelf. Very little information exists on primary production estimates within this region. The direction of the surface water flow is clockwise in this basin, and the paleoceanography of the system has been reviewed by Takahashi (2005). Aizawa et al. (2005) examined living diatom assemblages in the surface waters of this region and waters near the Aleutian Arc. Centric diatoms dominate abundance profiles in shallow coastal waters and through island passes, while raphid pennate diatoms, although less numerous, dominate the oceanic regions. Coyle et al. (1998) studying zooplankton distributions within this region found elevated biomass in the Bering Sea (Bowers Basin) relative to the Pacific as, at least, partially due to episodic flow regimes.

4.4.9 Aleutian Basin Planning Area

In the central Bering Sea (the Aleutian Basin), a shelf-slope front marking the boundary between relatively fresh shelf water and more saline basin water extends ~1,000 km northwestward from Unimak Pass to near Cape Navarin (see review by Okkonen et al. 2004). This front coincides with the Bering Sea "Green Belt," a region of enhanced primary production that supports an extensive variety of consumer species (Springer et al. 1996). High surface chlorophyll-*a* concentrations (>10 mg m^{-3}) have been observed within an ~200-km wide band adjacent to and seaward of the shelf break. These bands of elevated chlorophyll are observed to be associated with anticyclonic eddy groups, propagating along the continental slope (Okkonen et al. 2004). These observations suggest that eddies are important, if not the principal, agents that cause variability in the distribution of chlorophyll and primary productivity during the spring bloom in the central Bering Sea. Variability in the structure and location of the frontal system and eddy fields defining the Green Belt region introduces variability to the advective pathways that support the production and distribution of phytoplankton assemblages, which in turn influence the distribution of upper trophic levels.

Summer productivity in the Bering Sea is well characterized and generally comprises low productivity in the surface oceanic domain, elevated and sustained productivity at the shelf break, and decreasing productivity moving shoreward from the shelf break (Springer et al. 1996; Rho 2004). Annual primary production of this outer shelf area, based on PROBES data and that of Rho (2004), is estimated to be ~138 g C m^{-2} y^{-1}. Nitrogen availability regulates middle shelf and inner shelf phytoplankton populations (Springer, et al. 1996; Rho 2004), yet iron concentrations have been shown to be particularly important where frontal processes promote vertical mixing, while eddies in the surface waters allow for the transport of iron-rich water into the Green Belt at the outer shelf-break front (see Aguilar-Islas et al. 2007; Hurst et al. 2010).

4.4.10 Navarin Basin Planning Area

No available references specifically focused on this region, nor were broader studies identified as being applicable to this planning area.

4.4.11 St. Matthew-Hall Planning Area

No available references specifically focused on this region, nor were broader studies identified as being applicable to this planning area.

4.4.12 Norton Basin Planning Area

The Bering Sea consists of several regions with distinct water masses (Takenouti and Ohtani 1974). It has a broad continental shelf in the east that contrasts sharply with a deep basin in the western region. Each of these regions has their own unique ecological characteristics of physical oceanographic parameters that drive the biological community composition (National Research Council [NRC] 1996). Norton Sound, a large gulf to the south of the Seward Peninsula and to the east of St. Lawrence Island, is located under the less productive Alaska Coastal Water and is influenced by Yukon River discharge (Springer 1988). Depth of Norton Sound averages about 20 m, with the region being ice-covered during much of the winter-spring. Storms in ice-free periods and strong bottom currents are key factors that influence the sedimentary and biological structure of the area (Grebmeier et al. 1988). To date, little information exists on Norton Sound primary productivity and phytoplankton biomass estimates within the Sound. The interdisciplinary oceanographic study ISHTAR (Inner Shelf Transfer and Recycling) provided supporting data on water mass features and water column productivity while examining the interannual variability of physical forcing on the cycle of carbon and nutrients within the Norton Basin (McRoy 1993). The Norton Basin is a highly advective system, with plumes of Anadyr Current water (i.e., high in phytoplankton biomass and primary productivity) dominating the western boundary and nutrient poor ACC water moving north through Shpanberg Straits. The high chlorophyll regions along the western boundary can generate 12-16 g C m^{-2} d^{-1}. These production rates are noted to be some of the highest values in the world for pristine waters (McRoy et al. 1987). Modeling spatial distributions of chlorophyll and primary productivity, Shuert and Walsh (1993) noted that the strength of advection and the east-west nitrate gradient determined distributions. It should be noted that the southeast Bering Sea has the highest primary and secondary productivity, whereas Norton Sound, reportedly, has the lowest (NRC 1996).

A study of the distribution of chlorophyll and suspended sediments in Norton Sound in May and July 1979 and 1980 was made using imagery from both raw and processed data collected by the Nimbus-7 CZCS (Maynard and Clark 1987; Maynard et al. 1987). One of the most prominent features in these images is the area of high pigment concentration and river sediment in the Norton Sound region where the seasonal ice edge is beginning to melt and pull away from shore near the Yukon River delta. To date, separation of chlorophyll signals from the heavy sediment burden of the Yukon River is under-studied. This early attempt to use satellite data for chlorophyll determinations was problematic; for example, it became evident that the Yukon River and other rivers strongly influenced patterns in chlorophyll and suspended sediment concentrations for shallow water systems.

4.4.13 Hope Basin Planning Area

The Hope Basin is a geological structure of the Chukchi Sea, and discussions of primary productivity and chlorophyll distributions will follow in the Chukchi Sea section (**Section 4.4.14**). Distributions of integrated chlorophyll have been shown for the Chukchi and Beaufort Seas, including the Hope Basin, Bering Straits, Norton Basin, and parts of the St. Matthews-Hall region (Dunton et al. 2005; **Figure 40**).

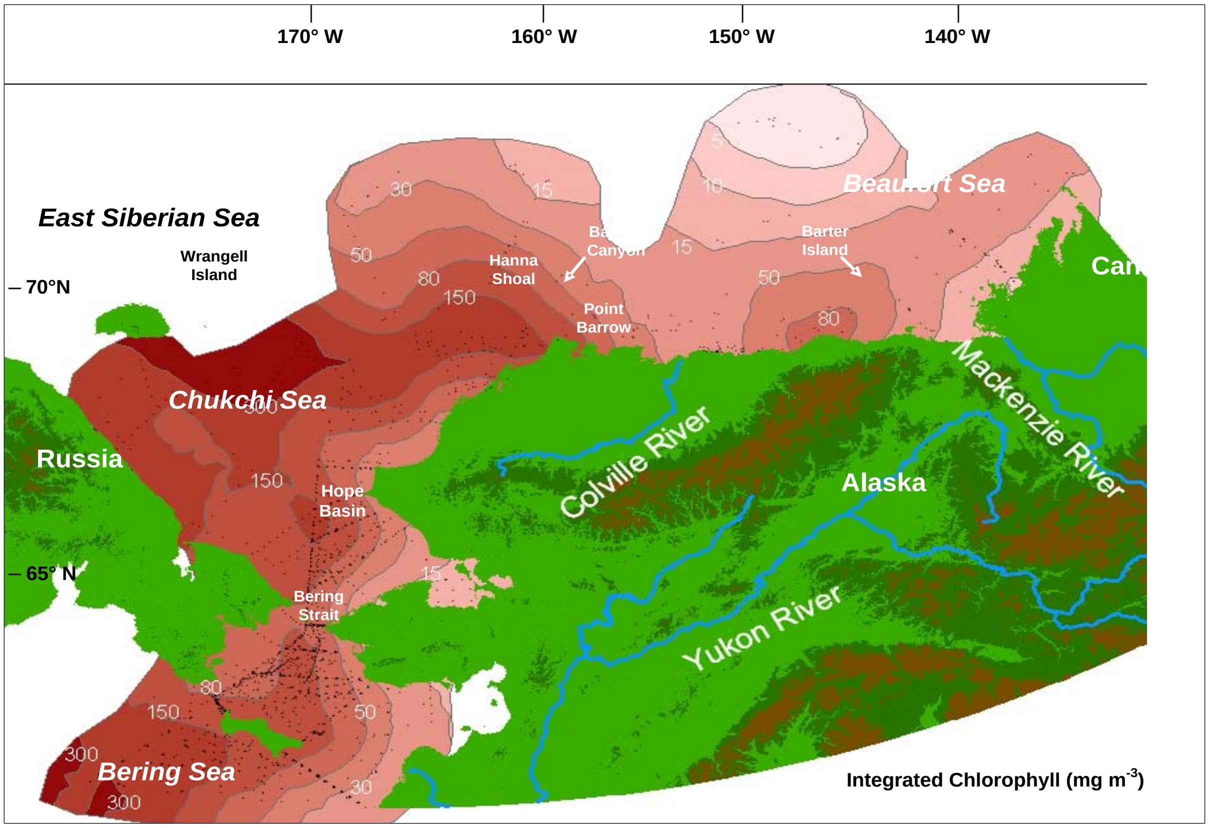

Figure 40. Contours of integrated chlorophyll-*a* concentrations (mg m^{-2}) based on discreet measurements collected during the period 1974-1995 (From: Dunton et al. 2005; with permission of the author).

4.4.14 Chukchi Sea Planning Area

Ice coverage, wind fields, and water movement impart strong seasonality to biological processes and distributions throughout the relatively shallow Chukchi Sea. Within this limited region, ice coverage varies from seasonally moderate ice in the south to extensive multiyear ice along the shelf break and northern boundaries with the Arctic Basin (Cota et al. 1996). Like Norton Basin, the Anadyr Current brings nutrient-rich water through the straits along the western boundary of the Chukchi Sea, while the ACC brings relatively fresher and more oligotrophic waters along the Alaskan coastline. Looking at late summer conditions in the Chukchi, Cota et al. (1996) found chlorophyll values to be relatively low (i.e., 0.1 mg m^{-3} within Arctic basin waters to 1.0 mg mg^{-3} over the shelf). These late summer conditions were characterized by low concentrations of both chlorophyll and nitrate in the upper column. Likewise, primary productivity values ranged from 0.7-1.5 g C m^{-2} d^{-1}, and averaged 0.75 g C m^{-2} d^{-1}. The advective field influencing the Chukchi Sea is seasonally variable as are biological distributions (Hill and Cota 2005). Chlorophyll biomass in the area is greatly reduced by ice cover in the spring, but intense blooms are observed concurrently with ice edge retreat (Wang et al. 2005). Summertime production rates for the Chukchi Sea region just north of the Bering Strait have some of the highest primary production rates observed in the Arctic, at 15 g C cm^{-2} d^{-1} (Springer and McRoy 1993). During late summer, average euphotic zone integrated production rates of 0.3 g C m^{-2} d^{-1} were measured in the northwest Chukchi Sea (Cota et al. 1996). In comparison, primary production was measured during an Arctic Ocean Section cruise as high as 2.57 g C m^{-2} d^{-1} on the Chukchi shelf at the end of July (Gosselin et al. 1997), and decreased to 0.1 g C m^{-2} d^{-1} over the Canada Basin. Concentrations of nitrate were high in July 1994, while in August 1993 nitrate was observed to be much lower in the surface waters. Cota et al. (1996) concluded that they had missed the spring bloom and were observing conditions symptomatic of a post-bloom environment. Observations suggest that spring rates are light-limited, averaging <0.03 g C cm^{-2} d^{-1}, while surface blooms during ice retreat approached 8 g C cm^{-2} d^{-1}. Thus, spatial variation in productivity during the spring is controlled by light and ice coverage, while summer distributions appear to be dictated by the chemical characteristics of the inflow through the Bering Strait. There is an east–west gradient in water mass properties across the Chukchi shelf, with the highest nutrient concentrations found in the west as Anadyr-influenced water flows from Bering Strait to Herald Valley (Codispoti et al. 2005). The high biological productivity in the waters north of the Bering Strait region is maintained by high nutrient Pacific water inflow. The Western Arctic Shelf-Basin Interactions (SBI) project is a 10-y Arctic environmental change program, producing two special issue volumes in *Deep-Sea Research II* in 2005 and 2009 (e.g., see Hill et al. 2005; Gradinger 2009).

Ultimately, the integration of these results, with continuing synthesis and modeling activities, will serve to help understand carbon fluxes across both the Chukchi and Beaufort Seas. More recently, Lee et al. (2007) reported mean annual primary production of phytoplankton for the whole Chukchi Sea, using a ^{13}C–^{15}N dual-isotope technique, as 55 g C m^{-2} with a value of 145 g C m^{-2} for the plume of Anadyr–Bering Shelf Water in the central Chukchi Sea. Chlorophyll concentrations during this time ranged from 200-500 mg chl m^{-2} and dominated typically larger phytoplankton (>5 µm).

Ice algal production, although not often studied, has been estimated to be responsible for up to 3% of total production within shelf areas (Gosselin et al. 1997). In an analysis of ice algae consisting of two ice cores, von Quillfeldt et al. (2003) noted high species abundance and complex assemblage composition (i.e., species representing seawater filtration ice, seeding from the seafloor, and freshwater input). Gradinger (2009) noted that sea-ice algae were a prime source of algal biomass and productivity in the SBI region in May/June 2002, which significantly exceeded phytoplankton values for both parameters. These data suggest that the ice algae community of these Chukchi Sea assemblages had a complex history compared to many other Arctic areas and are an important component when considering ecosystem impacts.

Works by Sukhanova et al. (2009) and Sergeeva et al. (2010) examined the phytoplankton community structure north of the Bering Strait and over the shelf, continental slope, and deepwater zones of the Chukchi and Beaufort Seas during the spring and summer. The phytoplankton community of the western Arctic during the spring/summer season is characterized by distinct spatial patchiness in qualitative and quantitative parameters. These spatial distributions were explained by variations in local conditions of ice melting, water stratification, water temperature, and nutrient supply (primarily the availability of nitrogen). Water inflow dynamics through the Bering Strait and Barrow Canyon influences were seen as major modifiers of community structure.

4.4.15 Beaufort Sea Planning Area

The Beaufort shelf is primarily forced by local wind stress, buoyancy, and deep-ocean interactions applied along the continental slope (Dunton et al. 2006). In reviewing distributions of terrestrial carbon in arctic coastal food webs, Dunton et al. (2006) consider the Beaufort Sea shelf as consisting of the Alaskan Beaufort and the Canadian Beaufort shelves. Both shelves are tightly linked to the annual cycles involving changes in regional sea ice and freshwater discharge. Yet, the amount of freshwater discharge influencing these shelves differs greatly.

The southern Beaufort Sea is characterized by the presence of the Mackenzie shelf having a depth of less than 80 m and receiving large amounts of freshwater from the Mackenzie River. This flux contributes to the overall heat and nutrient supply of the Arctic Ocean (Aagaard and Carmack 1989) and sustains substantial phytoplankton productivity (Carmack and Macdonald 2002). While this region is beyond the scope of this review, readers are referred to the primary productivity modeling effort (Lavoie et al. 2009), the phytoplankton physiology study (Matsuoka et al. 2009), and a community structure paper (Schloss et al. 2008).

Primary production in the Alaskan Beaufort is controlled by seasonal environmental changes, including solar irradiation, ice cover, water temperature, and vertical stratification, as well as the Pacific inflow from the south via the Bering Straits. The narrow shelf of the Beaufort Sea receives considerable coastal runoff, which lowers the salinity of nearshore waters and supplies a large amount of terrigenous material and nutrients (Sukhanova et al. 2005). A pronounced spatial difference was observed as a characteristic feature of the phytoplankton community in the western Arctic, coinciding with the seasonal shift from ice-covered sea to open water. Phytoplankton in these waters provide >90% of the total primary production over the shelf and continental slope in the Chukchi and Beaufort Seas, while ice algae are important only during a short period at the beginning of the vegetation season (Hill and Cota 2005). Gradinger (2009), however, stresses the importance of sea-ice algae production, suggesting a spatial estimate of areal production (based only on activity in the lowermost 10 cm of sea ice) of 20-30 mg C m^{-2} d^{-1} on the Chukchi shelf and 4-9 mg C m^{-2} d^{-1} on the western edge of the Beaufort shelf.

Information on phytoplankton community structure in the both the Chukchi and Beaufort Seas is limited, with studies in the western Beaufort Sea between 1973 and 1978 providing most of the information on phytoplankton community on the shelf near shore to the east of Barrow Canyon (Horner 1984; Outer Continental Shelf Environmental Assessment Program [OCSEAP]). Two recent papers (Sukhanova et al. 2009 and Sergeeva et al. 2010) focusing primarily in the Chukchi Sea and the very western edge of the Beaufort Sea found that the highest values of phytoplankton cell density and biomass were recorded in regions influenced by the inflow of Bering Sea waters or characterized by intense hydrodynamics, such as either the Bering Strait or Barrow Canyon. Thus, the spatial distribution of phytoplankton was dependent mainly on local features of hydrological and nutrient regimes.

4.5 Other Relevant Regional Measurements of Primary Production

Primary production data summarized in the previous sections was acquired from locations within one or more of the 26 OCS planning areas. However, there are other pertinent databases in which marine primary production was measured during multidisciplinary oceanographic research cruises and/or estimated from ocean color. The findings and implications from these regional studies have relevance to primary productivity measurements and determinations in U.S. OCS waters. These include time series stations in the subtropical North Atlantic and subtropical North Pacific Ocean (Bermuda Atlantic Time Series and Hawaii Ocean Time-series, respectively) and several JGOFS process studies:

- Bermuda Atlantic Time Series (BATS);
- Hawaii Ocean Time-series (HOT);
- JGOFS North Atlantic Spring Bloom Experiment;
- JGOFS Process Study in the Equatorial Pacific;
- JGOFS Arabian Sea Expedition; and
- JGOFS Southern Ocean Studies and follow-on iron addition experiments.

4.5.1 Bermuda Atlantic Time Series (BATS) and Hawaii Ocean Time-series (HOT)

Since 1988, hydrographic and biogeochemical data have been collected at the BATS site in the Sargasso Sea (31°50′ N, 64°10′ W) and since 1991 at HOTS station Aloha (22°45′ N, 158°00′ W). At both locations, biogeochemists have used diurnal oxygen changes from *in situ* measurements as well as uptake of ^{14}C to study primary production (i.e., Emerson et al. 2002). Lohrenz et al. (1992) initially summarized the relationship between primary production and sediment trap-derived downward flux of particulate organic carbon during the first 2 y of data collection at BATS (1989 and 1990). They reported the annual integrated primary production was 9.2 mol C m^{-2} y^{-1} (110 g C m^{-2} y^{-1}) in 1989 and 12 mol C m^{-2} y^{-1} (144 g C m^{-2} y^{-1}) in 1990. Two topical issues of *Deep-Sea Research II*, published in 1996 and 2001, synopsized additional results from the Hawaii and Bermuda research programs. Karl et al. (2001), who compared 10 y of monthly measurements of primary production at BATS and HOT, emphasized the strong seasonality in NPP at both sites and the wide range of e-values for export production, but they also noted that at both of these subtropical central gyre locations the average annual primary production was quite similar.

Pelegri et al. (2006) remarked on the duality in primary production of the North Atlantic, calling attention to the fact that the central subtropical gyre is surrounded at its margins by smaller cyclonic high-production regions. They were particularly interested in the importance of upward, along-pycnal advection of nutrient-rich subsurface layers (which they called "nutrient irrigation") into the euphotic layers. But at BATS it is the wintertime cross-pycnal mixing that is responsible for most of the new nitrogen input: the monthly data set of BATS primary production clearly shows that following winters in which deep mixing proceeds to greater than average depths, spring primary production is higher than average at BATS.

Recently, Luo et al. (2010) reported a summary of HOT (Station Aloha) primary production for the 15-y period 1991-2005. Luo et al. (2010) noted that data collection at Station Aloha is continuing and now has passed the 20-y mark. For his synopsis, Luo used the Variational Adjunct Method (VAM). The analysis of Luo et al. (2010) suggested that while annual productivity mostly ranges from 500-600 g C m^{-2} y^{-1}, the average is increasing with time. Luo pointed out that the mixed layer seems to be getting deeper at Station Aloha, and he speculated that with this deepening there is also an increase in nitrogen-recycling efficiency via the microbial loop. In other words, more primary production → more semi-labile dissolved organic matter losses → more heterotrophic bacteria → more NH_4^+ excretion → more phytoplankton photosynthesis.

4.5.2 JGOFS North Atlantic Spring Bloom Experiment, 1989

GPP was calculated from ^{14}C uptake rates and gross oxygen production rates determined using an ^{18}O tracer (Bender et al. 1992). In 1993, Hugh Ducklow and R.P. Harris edited a topical issue of *Deep-Sea Research II* to summarize the principal results of the 1989 North Atlantic Spring Bloom Experiment (NABE). For that topical issue, Harrison et al. (1993) and Li et al. (1993) summarized the taxonomic composition of the spring bloom phytoplankton and their primary productivity, not only along the cruise track but at the locations of two process studies carried out for 2 weeks each at 40° N and 45° N. At 40° N, they reported almost all of the phytoplankton standing stock was in the form of pico- and nano-size cells, whereas at 45° N about half the phytoplankton stock was in the form of diatoms and other larger-size (microphytoplankton-size) cells. Where these larger-size cells dominated phytoplankton carbon biomass, silicate depletion in surface waters was clearly evident. Heterotrophic bacteria production during the spring was estimated to metabolize 16%-36% of daily primary production within the euphotic zone, or 24%-78% in the upper 100 m of the water column.

The following spring (1990), the UK Biogeochemical Ocean Flux Study (BOFS) project was carried out for 7 weeks in the northeast Atlantic between 46° and 50° N, and 14° and 22° W (Savidge et al. 1992). Sampling and measurement of primary production was carried out adjacent to a Lagrangian buoy drogued at a depth of 30 m. Mesoscale eddies were observed to have a major influence on the development sequence of the spring bloom in this area of the northeast Atlantic.

4.5.3 JGOFS Process Study in the Equatorial Pacific, 1992-1993

During 1992, three research vessels conducted seven cruises in support of the U.S. EqPac Process Study, and in 1993 a fourth research vessel carried out a sediment trap recovery cruise. Fieldwork focused on a repeat meridional section (12° N-12° S) along 140° W, but two ships also surveyed 10° N-10° S at 95° W, 110° W, 125° W, and 170° W (http://www1.whoi.edu/datasys/mrg/eqpac_proc_study.html). The scientific objectives of the EqPac study were to characterize the processes controlling the fluxes of carbon and related elements between the atmosphere, euphotic zone, and deep ocean. The fieldwork window coincided with the beginning of the 1992-1993 El Niño event. Three topical issues of *Deep-Sea Research II*, released one per volume year from 1995-1997, presented the principal results of JGOFS EqPac. Five years later, in 2002, *Deep-Sea Research II* released another topical issue to report “The Equatorial Pacific JGOFS Synthesis.”

Bender et al. (1999) compared gross and net O_2 production measured *in vitro* with ^{14}C uptake. They reported that ^{14}C productivities in samples incubated 24 h were only about 45% of gross carbon production rates they calculated from gross O_2 production, but they recognized this difference was not incompatible with expected rates of photorespiration, excretion, and community mitochondrial reaction. More unexpected, however, was their finding that net carbon production rates were 4-20 times greater than estimates from drifting sediment traps and tracer transport studies. They speculated such a major imbalance might reflect their exclusion of macro-grazers from ^{14}C uptake bottles.

4.5.4 JGOFS Arabian Sea Expedition, 1994-1996

Five topical issues of *Deep-Sea Research II*, released one per volume year from 1998-2002, synopsized the principal results of the 1994-1996 Arabian Sea Expedition. A few years later, Marra and Barber (2005) wrote a summary of primary productivity in the Arabian Sea in which they sought to review the principal insights from all the JGOFS biogeochemical data. After reminding readers that temporal and spatial variations in phytoplankton biomass exist in the Arabian Sea at all scales from the diurnal to the seasonal, and from fine to large scale, Marra and Barber (2005) presented the paradigm that physiological rate parameters and productivity measurements suggest that Arabian Sea phytoplankton are not strongly limited by either irradiance or nutrient supply. Instead, they suggested, it is grazing upon this primary production that, in most cases, regulates the biomass of phytoplankton standing stock in the Arabian Sea. They accept the premise that differences in vertical mixing associated with the monsoonal circulation and with the mesoscale eddy field regulate the supply of irradiance and nutrients, but they also point out that vertical mixing is never deep enough to limit phytoplankton productivity. In other words, they argue, nitrogen does not appear to be a factor limiting phytoplankton growth. Rather, they propose that vertical mixing affects grazing by diluting micro-grazers along with phytoplankton. In other words, mixed layer deepening acts as a natural dilution experiment that allows phytoplankton to escape grazing losses and grow, and thereby create the observed variability in Arabian Sea phytoplankton biomass.

4.5.5 JGOFS Southern Ocean Studies

After IronEx-I and IronEx-2 iron-enrichment experiments were performed in HNLC environments near the Galapagos Islands in 1993 and 1995 (Coale et al. 1998), many JGOFS researchers were convinced that primary production in Southern Ocean, as in the equatorial Pacific, is similarly iron-limited, so JGOFS continued/extended iron enrichment process studies in HNLC environments of the sub-Antarctic and Antarctic. Six topical issues of *Deep-Sea Research II*, published 2000-2003, summarized the principal results of the JGOFS Alaska Environmental Satellite Oceanography (AESOP) project and the Southern Ocean Iron Release Experiment (SOIREE). Boyd et al. (2007), who published a synthesis of mesoscale iron experiments conducted during the period 1993-2005, recommended future directions for open ocean trials of ocean iron fertilization.

Most recently, in 2009 German researchers working from R/V *Polarstern* carried out the LOHAFEX iron-enrichment experiment (i.e., the LOHA [Hindi for iron] Fertilization Experiment) in the Atlantic sector of the Southern Ocean. They fertilized a 300-km^2 patch of ocean inside a cyclonic eddy with 6 metric tons of dissolved iron and then followed the effects of the fertilization on the plankton community there for 39 d. As expected, the iron enrichment initially stimulated primary production, but zooplankton grazers quickly moved in and consumed most of the new production. In doing so, these herbivores limited the amount of CO_2 that the phytoplankton community was able to draw down from the atmosphere.

5.0 Secondary and Tertiary Productivity Methods and Literature Updates

In the past evaluation of biological productivity (CSA 1990), water column primary productivity served as the basis for a comparison among the 26 OCS planning areas. While using primary productivity alone is valid, and much can be learned by examining the processes of primary producers in ecosystems, it is also useful to examine productivity of higher trophic levels such as secondary and tertiary consumers of primary production. The objective of this section of the report is to evaluate current methods used to estimate secondary and tertiary productivity of marine ecosystems. Few tools and approaches are available for evaluating secondary and tertiary production. For this analysis, only those approaches that 1) produce estimates of secondary production, and 2) are in general use, have been evaluated. Measurement methods (e.g., bioenergetics, allometric relationships) and modeling approaches (e.g., Ecopath, NPZ models) are reviewed and evaluated in the following discussion. Major advantages and disadvantages of each approach are also summarized.

Assessing the status and health of an ecosystem requires an examination of the system's structure and function. Insight into the structure of an ecosystem can be gained by examining the components of the trophic organization of the ecosystem, while analyzing rates and energy flows through a system can improve understanding of an ecosystem's functionality. These structural and functional characteristics are fundamental to how marine ecosystems are organized and provide vital benefits such as food to mankind. One important functional component of ecosystems is production of higher trophic levels, often referred to as secondary production.

5.1 Definitions and Background

Secondary productivity is the rate of conversion of energy obtained from primary producers by consumers to produce new organic material (e.g., biomass). Tertiary productivity refers to the rate of conversion of energy obtained from prey (i.e., consumers) by higher-trophic level predators. Thus there is a hierarchy of primary producers to secondary producers to tertiary producers. In most sections of this report, we will simultaneously examine secondary and tertiary productivity, and no distinction will be made between these two trophic levels. Thus, all productivity occurring higher than primary level will be referred to as secondary productivity.

It is also important to clarify what secondary productivity is not. Often, people refer to harvest, such as fisheries harvest, as productivity. While it is true that economic productivity occurs when resources are harvested, this is not the same as ecological productivity. In the current analysis, productivity is reviewed based on its ecological meaning in the context of energy flow through food chains, food pyramids, and food webs.

Light energy provided by the Sun is used by plants, as well as by phytoplankton in the ocean, to create organic matter via photosynthesis. These photoautotrophic organisms convert inorganic carbon (C), usually in the form of carbon dioxide (CO_2), into organic carbon, $n(CH_2O)$, and produce oxygen O_2 as a by-product through the reaction:

$$nCO_2 + 2nH_2O + \mathit{energy} \rightarrow n(CH_2O) + nO_2 + nH_2O$$

While this reaction is the only source of organic carbon production on land, there is a second energy source in oceans, and that is chemical energy from the oxidation of electron donors seeping from submarine geological formations. Using this same reaction equation, microbial chemoautotrophs can fix CO_2 using chemical energy from reduced ions such as such as hydrogen sulfide, elemental sulfur, ferrous iron, molecular hydrogen, and ammonia. The discovery of these chemosynthetic communities near hydrothermal vents in the deep parts of the oceans was a major discovery of the 1970's that completely changed our understanding of energy dynamics in the deep oceans. While the organization and dynamics of chemosynthetic communities in and near hydrothermal vents, hydrocarbon seeps, and brine seeps is an exciting area of deep sea research, secondary production at these sites will not be discussed in the current report.

While organic carbon is produced by either photoautotrophs or chemoautotrophs, all heterotrophic organisms consume the organic carbon and synthesize new organic matter via respiration. Thus, stored energy from photosynthesis is released by respiration. Respiration involves breaking down carbon bonds ($n\mathrm{CH_2O}$) to produce energy. Aerobic respiration requires O_2, and produces CO_2 and H_2O:

$$n(\mathrm{CH_2O}) + n\mathrm{O_2} \rightarrow n\mathrm{CO_2} + n\mathrm{H_2O} + energy$$

Where oxygen is lacking (especially in sediments), anaerobic respiration is the main pathway for the production and synthesis of new organic matter. Animals and protists generally do not use anaerobic respiration to consume organic matter. Anaerobic respiration is a process carried out primarily by bacteria. Examples of anaerobic respiration include sulfate reduction, nitrate reduction (i.e., denitrification), iron reduction, manganese reduction, and methanogenesis (i.e., carbon dioxide reduction). Anaerobic respiration requires oxidized ions to replace oxygen as the electron acceptor, e.g., sulfate reduction:

$$n(\mathrm{CH_2O}) + n\mathrm{SO_4^{2-}} \rightarrow n\mathrm{CO_2} + n\mathrm{S^{2-}} + energy$$

While much of the productivity of a system can be metabolism via anaerobic respiration, this process is primarily microbial and primarily takes place in sediments. For these reasons, no attempt has been made to review secondary production for anaerobes, and this topic will not be discussed further in this report.

In general, the rate of respiration is increased as temperature increases because the rate of catalytic enzyme reactions increases. Respiration can also be affected by environmental conditions, such as salinity or the presence of toxic chemicals. Stressed organisms must respire faster to maintain proper cell function.

The rate of secondary production is known as secondary productivity and is always expressed in units of biomass (or energy) for a given area and given time frame. The most common units of productivity are grams per square meter per day ($\mathrm{g\ m^{-2}\ d^{-1}}$), but these units are commonly scaled to kilograms, hectares, or years. Productivity, whether by one organism or groups of organisms, can be measured in terms of energy content (calories), chemical elements (carbon, nitrogen), or in biomass (wet weight, dry weight, or total organic carbon).

Growth alone is not productivity. This is true for either an organism or a population. An organism's growth has to be balanced by basal metabolism maintenance, and population growth is balanced by death. Thus, it is important to distinguish between gross production and net production. Gross production is the total productivity, whereas net production is the remaining portion of the total productivity after organism maintenance or population losses are accounted for.

5.1.1 Trophic Structure

Marine ecosystems are open, yet the components of the ecosystems are intricately connected via food chains and food webs. While the primary producers are essentially at one trophic level and mainly composed of a few taxonomic groups (the phytoplankton, microphytobenthos, macrophytes, and macroalgae), secondary producers are enormously diverse and dispersed throughout the oceans. Therefore, accurately estimating secondary productivity is a complicated process because many factors can influence ecosystem productivity. These factors include complexity of the biological systems (i.e., ecosystem structure and function), environmental characteristics (e.g., light, nutrients, salinity, temperature, etc.), and biogeographical patterns of organism distributions. In this subsection, focus will be on structure of the biological communities; function will be addressed in the next subsection.

Ecosystem structure has a strong influence on the overall function and productivity of a system. Marine ecosystems are composed of a variety of organism groups, ranging from primary producers (e.g., phytoplankton) to apex predators (e.g., sharks or killer whales). All organisms can be classified into trophic levels based on the source of energy supporting that group (i.e., its diet composition). Trophic level is often reported on a scale of 1-5, with the lowest level representing primary producers and the highest level reserved for apex predators. Organisms can also be classified into functional groups, which includes consideration of more specific details (e.g., feeding behavior or ecological niche). Each species possesses unique adaptations and physiological tolerances (responses) that enable the animal to function competitively by occupying a niche, enabling survival and reproduction. These structure classifications indicate the function of a species in an ecosystem and assist in construction of food chains or food webs.

Food chains are the simplest representation of the relationships between producers and consumers and are useful for organizing information at the productivity level. The best example of a simple food chain is the grazing food chain:

$$\text{Phytoplankton} \rightarrow \text{Zooplankton} \rightarrow \text{Anchovy}$$

In this example, the zooplankton is eaten by a specific species of fish that does not prey on other organisms. This simple relationship can be represented in terms of productivity as follows:

$$1^0 \rightarrow 2^0 \rightarrow 3^0$$

In this representation, the number is the trophic level, where 1 is primary, 2 is secondary, 3 is tertiary, and the superscript 0 (^{0}) represents the word producer (and also production or productivity). While this simplicity is useful at the trophic level, it is not useful to represent species interactions because typically organisms feed on many different organisms and often at multiple trophic levels.

Food webs that illustrate the interconnections among many individual species do represent the complexity of interactions among herbivores and predators and are useful tools for ecosystem studies because each ecosystem has a unique trophic structure. It is important to include all functional groups when building a food web diagram so that a clear understanding of energy flow within the ecosystem is achieved.

Ecological pyramids (or food pyramids) are another illustrative tool used in ecosystem studies (**Figure 41**). The concept of food pyramids was introduced nearly a century ago. Ecological pyramids can be constructed from various types of information: abundance, biomass, or energy. Pyramids constructed from abundance are typically not very useful because of the large range of size differences among organisms, so biomass data are preferred. Energy pyramids illustrate the energy flow or productivity at each successive level.

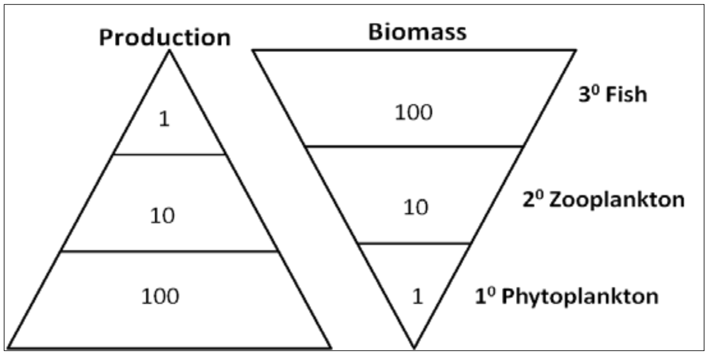

Figure 41. Ecological pyramids for production (g L^{-1} y^{-1}) and biomass (µg L^{-1}).

The typical biomass food pyramid is larger at the bottom with each level above becoming smaller and smaller, representing a large biomass of primary producers supporting fewer herbivores, and even fewer carnivores. However, in aquatic ecosystems, the biomass pyramid structure is usually inverted. The biomass of phytoplankton (the major primary producer) is much smaller compared to each subsequent higher trophic level group. A small biomass of phytoplankton can support a larger biomass of consumers and predators because they have a high turnover time, that is they have a short life cycle and reproduce rapidly, and are consumed by zooplankton and other consumers very rapidly (Fath and Killian 2007). Thus, a small biomass multiplied by a high turnover time can produce higher productivity than a large biomass turning over much slower.

Energy pyramids cannot be inverted. A trophic-dynamic approach to ecosystem studies emphasizes these trophic processes and relationships (Lindeman 1942). Energy is transferred from the bottom level up through the food web as organisms are consumed. Energy is lost during each transfer, with each subsequent level receiving less energy (Fath and Killian 2007). The production efficiency (P*e*) is the percentage of food energy not used for respiration and is represented by:

$$Pe = \text{Net } 2^0 \text{ production/Assimilation of } 1^0 \text{ production}$$

Net secondary production is the amount of energy stored in biomass (used for growth and reproduction), and assimilation is the total amount of energy coming in used for growth, reproduction, and respiration. The total assimilation of a trophic level represents the energy flow through that level. Larger organisms respire more, and thus have smaller production efficiencies. Production efficiency represents the percentage of production transferred to each successive trophic level, and generally decreases with increasing body size. For example, the production efficiency of most fish is about 10%, while production efficiencies of birds and mammals are in the range of 1%-3% (Campbell and Reece 2002). Turnover time (T_t) is defined as:

$$T_t\ (d^{-1}) = \text{Standing crop biomass (mg m}^{-2})/\text{Production (mg m}^{-2}\ d^{-1})$$

The turnover time is also referred to as the biomass:production ratio (B/P); it is in units of reciprocal time (days in this example).

5.1.2 Trophic Function

Energy flow through an ecosystem is a fundamental process for ecological health, sustainability, and maintaining characteristic species. Energy flows through oceanic ecosystems at the surface when primary producers convert solar energy to chemical energy via photosynthesis. Herbivores consume primary producers, extracting a percentage of the energy available from that trophic level. Consumers of these organisms then extract a percentage of these organisms, with the largest predators effectively obtaining the smallest amounts of energy.

Energy is never lost, it is simply transformed or recycled. For this reason, it is always important to include detritus, detrital feeders, and microbes in the food web. These important groups of the ecosystem are responsible for the energy recycling necessary in any environment. In oceans, a major pathway for productivity is through the microbial loop (Azam and Fuhrman 1984; **Figure 42**). Pomeroy (1974) was the first person to formulate the idea that a substantial amount of primary production was consumed by microbes and not utilized in the grazer food chain. The term for these interacting processes however, the “Microbial Loop,” was coined by Azam et al. (1983). Dissolved organic carbon is liberated by the bacterial decomposition of dead plankton, feces, and exuvia, and this carbon is reintroduced into the microbial part of the food web because bacteria are consumed by protists (e.g., ciliates and flagellates), which are in turn consumed by zooplankton. Thus, in oceans, there is a shunt for energy to flow within a microbial food web rather than to higher trophic levels. While the microbial loop is responsible for very high amounts of energy flow and productivity in oceans, it will not be discussed further in this report.

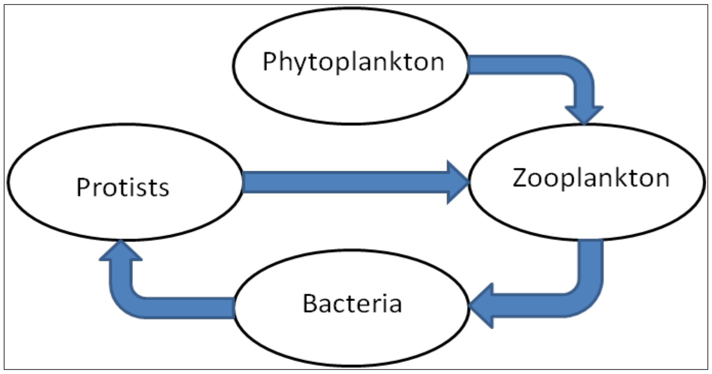

Figure 42. The microbial loop for recycling dissolved organic matter.

The ideal way to estimate productivity is to measure energy flow through an ecosystem, but this is very difficult to do. During transfer between trophic levels, energy is lost to the environment as heat. Energy does not circulate, but materials do. Therefore, carbon or nutrients (e.g., nitrogen or phosphorous) are commonly used as currency for modeling energy flow through ecosystems. Biogeochemical cycles illustrate the movement (i.e., flow or circulation) of basic elements as they move through ecosystem components. Carbon and nitrogen are the most commonly used elements for modeling energy flow in marine ecosystems. Carbon is an abundant and essential element and can be easily measured in all organisms. Nitrogen is most often the limiting nutrient in marine ecosystems. Carbon, nitrogen, and phosphorous cycles in oceans are fairly well understood and will not be reviewed here. These three elements typically exist in a characteristic ratio, termed the Redfield ratio (Redfield et al. 1963), with 106 carbon (C) atoms and 16 nitrogen (N) atoms for each phosphorous (P) atom (C:N:P = 106:16:1). These ratios are used in ecological modeling to convert various components of the ecosystem to a common currency.

5.2 Measurement Methods

Secondary production is difficult to estimate and nearly impossible to directly measure. It is possible to directly measure primary production by measuring CO_2 uptake or O_2 production. With animals, however, simply measuring respiration of all the diverse organisms is difficult, and measures of assimilation would also be needed. Respiration would be a measure of only net metabolism and not gross productivity. Others have tried using population dynamic models to measure population growth, but again it is difficult to measure cohort (or age-specific) growth, mortality, and reproductive success, and fecundity and mortality of adults, which are other parameters necessary to calculate productivity using a life-table approach. However, secondary productivity estimates can be made indirectly via measurement methods and application of coefficients or ratios derived from energetic relationships, such as bioenergetic and/or allometric relationships.

Although biomass can be used to indicate production in an ecosystem, it is not the same as productivity because the turnover times of organisms are different. Also, the major primary producers in marine systems are very small organisms with rapid turnover rates, and all organisms are constantly being consumed and produced in productive ecosystems. Therefore, biomass alone may not accurately indicate the productivity of an ecosystem without information on turnover times or energetic relationships (Odum 1959).

Many common ecosystem measurements can indicate the productivity of marine systems, e.g., biomass, respiration, and species distributions. But these measures must be coupled with modeling studies. Biomass is possibly the most often-used indicator of productivity in models. Examination of the biomass of even one trophic level can provide insight into the productivity of an ecosystem. For example, the distribution and biomass of zooplankton alone can reveal a lot about the productivity occurring in different ecosystems.

5.2.1 Allometric Relationships

It is generally well known that many aspects of an organism's biology vary with their body size (Whitfield 2001). This concept can be modeled using allometric scaling. A typical allometric scaling equation can be written as follows:

$$Y = aM^b$$

where

- Y is the dependence of a biological variable (such as metabolic rate);
- M is body mass;
- b is the scaling exponent; and
- a is an organism-specific constant.

One fundamental concept of allometric scaling is that an organism's metabolic rate is proportional to an organism's body size (Kleiber 1932; Oikawa and Itazawa 1993; Enquist et al. 1998). Pioneer research determined that an animal's metabolic rate is proportional to its body mass to the power of ¾ (b = ¾ in the above equation; Kleiber 1932). Building on this pioneering research, West et al. (1997) proposed that most biological phenomena scale as quarter powers of body mass. However, these scaling generalizations are sometimes deemed oversimplified and not universally applicable (Whitfield 2001; Kozlowski and Konarzewski 2004). Scaling exponents and constants vary greatly, depending on which taxonomic groups and measure of production is used (**Table 8**).

Production is proportional to respiration, and therefore respiration is often used as a proxy for production. Respiration and specific production (i.e., the production/biomass [P/B] ratio) are inversely proportional to the size of an organism of an individual species or taxa (Valiela 1995). This inverse relationship is generally true when making interspecific comparisons, although P/B ratios vary slightly among taxonomic groups of similar biomass. Using doubling time as a measure of production, Sheldon et al. (1972) determined that microbes and algae (1–100 µm) double in less than 10-100 h, zooplankton (100 µm-1 cm) double in less than 100-1,000 h, and fishes (1 cm-1 m) double in 100-1,000 h.

Table 8. Allometric scaling coefficients for different organisms in different locations. $Y = aM^b$, where a is a productivity variable and M is organism body mass.

Taxa	Location	*a*	*b*	Production Measure	Biomass Unit	Reference
All organisms	Global	-	-0.25	Generalized growth rate	NA	West and Brown 2005
	Global	-	0.75	Generalized metabolic rate	NA	West and Brown 2005
Zooplankton	Tropical species	3.027	-0.405	Respiration/Biomass (μL O_2 mg dry wt^{-1} h^{-1})	mg	Ikeda 1974
	Subtropical species	2.094	-0.336	Respiration/Biomass (μL O_2 mg dry wt^{-1} h^{-1})	mg	Ikeda 1974
	Temperate	1.340	-0.244	Respiration/Biomass (μL O_2 mg dry wt^{-1} h^{-1})	mg	Ikeda 1974
	Boreal	1.140	-0.217	Respiration/Biomass (μL O_2 mg dry wt^{-1} h^{-1})	mg	Ikeda 1974
Maximum abundance of terrestrial plants	Global	948	-0.757	Abundance (individuals m^{-2})	g	Belgrano et al. 2002
Maximum abundance of terrestrial plants and marine phytoplankton	Global (terrestrial), Sweden (marine)	1,020	-0.765	Abundance (individuals m^{-2})	g	Belgrano et al. 2002
Range of taxa from meiofauna to fish	Deep sea (global)	0.0074	-0.24	Mass-dependent respiration rate	mg C	Mahaut et al. 1995
Mammals	Terrestrial	0.0182	0.737	Basal metabolic rate	NA	Savage et al. 2004
	Terrestrial	0.146	0.878	Maximal metabolic rate	NA	Savage et al. 2004
	Terrestrial	274.16	-0.254	Resting respiratory rate (breaths min^{-1})	NA	Savage et al. 2004
Phytoplankton and terrestrial plants	Global	0.0008	-0.22	Carbon turnover rate (d^{-1})	g	Brown et al. 2004

Table 8. (Continued).

Taxa	Location	*a*	*b*	Production Measure	Biomass Unit	Reference
Benthic stream invertebrates	Global	-	0.469	Production (g dry weight m^{-2} y^{-1})	g	Statzner and Lévêque 2007
	Global	-	-0.435	Production/biomass	g	Statzner and Lévêque 2007
Benthic macrofauna (intertidal and subtidal)	Japan and Australia	0.038	0.8	Production (µg d^{-1})	mg (ash-free dry weight)	Edgar 1990
Fishes	Global	2.75	-0.26	Production/biomass	kcal equivalent	Banse and Mosher 1980
Mammals	Global	12.88	-0.33	Production/biomass	kcal equivalent	Banse and Mosher 1980
Aquatic and terrestrial invertebrates	Global	0.65	-0.37	Production/biomass	kcal equivalent	Banse and Mosher 1980
Fish (marine teleost; red seabream snapper, *Pagrus major*) tissues	Japan	-	-0.25 to -0.05	Tissue respiration (µL g^{-1} min^{-1})	body mass (g)	Oikawa and Itazawa 1993
Benthic macrofauna	Canada - intertidal	0.525	-0.304	Production/biomass	kcal equivalent	Schwinghamer et al. 1986
Benthic meiofauna	Canada - intertidal	0.073	-0.337	Production/biomass	kcal equivalent	Schwinghamer et al. 1986
Benthic macrofauna and meiofauna	Canada - intertidal	0.696	-0.208	Production/biomass	kcal equivalent	Schwinghamer et al. 1986

Marine secondary productivity rates and P/B ratios vary depending on an organism's taxa and its location (**Table 9**). In addition to limiting factors such as nutrient and food, production is largely affected by temperature (Edgar 1990). Increased temperature increases specific production and can also increase the rate that production changes with biomass (Ikeda 1974, 1985; Valiela 1995; Miller 2004). For marine zooplankton, 1-mg zooplankton individuals respire three times as fast in tropical regions relative to subarctic regions, whereas differences in respiration rates between the two regions are negligible for 100-mg individuals (Miller 2004). Production and respiration rates differ less among latitudinal regions than for a single species that experiences large temperature changes because species from different latitudinal regions are adapted behaviorally and physiologically to better suit their region (Miller 2004).

Table 9. Biomass and production of microzooplankton and fishes from various marine regions (From: Valiela 1995).

Taxa	Location	Sampling Depth (m)	Biomass (g dry wt m^{-3})	Biomass (g C m^{-2})	Production (g C m^{-2} y^{-1})
Zooplankton	Inshore waters	1-30	122	-	15.3
	Continental shelf	30	25	-	6.4
	Shelf break	200	108	-	5.5
	Open sea	200	20	-	5.7
Benthos	Estuaries	0-17	-	5.3-17	5.3-17
	Coastal seas	18-80	-	1.7-4.8	0.7-12
	Continental shelf	0-180	-	23	2.6
	Continental slope	180-730	-	18	2.4
	Deep sea	>3,000	-	0.02	-
Pelagic fishes	Continental shelf	0-180	-	2.6	0.3
	Continental slope	180-730	-	10.6	1.3
Demersal fishes	Continental shelf	0-180	-	8.6	0.3
	Continental slope	180-730	-	4	0.2

5.2.2 Bioenergetics

Bioenergetic models can be used to estimate food consumption and to explore relationships between consumption and body size (or population size) (Winship et al. 2002). Quantifying energy transfer in ecosystems is important to various components in ecological studies, and various methods exist to estimate feeding rates in animals (Rice and Cochran 1984; Ney 1993). For example, stomach content analysis (Murie and Lavigne 1991; Ohizumi and Miyazaki 1998) can provide a direct measure of food consumption, but data collection can be difficult and time-consuming and the animal must often be sacrificed, but non-lethal methods to obtain stomach contents exist for large predators such as sharks (Cortés and Gruber 1990; Barnett et al. 2010). Another technique is inferring wild feeding rates of captive marine animals (Perez et al. 1990; Nordøy et al. 1995), which can also be difficult to ascertain. Unlike these methods, bioenergetics modeling can provide an efficient and cost-effective means for quantifying the allocation of consumed energy over respiratory metabolism, excreted wastes, and growth (Kitchell et al. 1977) and determine the flow and the transformation of that energy in and between living organisms and their environment.

Bioenergetic models originated from work conducted by Winberg (1956) and are based on the first principle of thermodynamics: energy and matter are conserved. Bioenergetics models are useful for addressing a variety of ecological questions, such as nutrient regeneration (Kraft 1993; Chipps and Bennett 2000), food web interactions (He et al. 1993), benthic productivity (Kim and Montagna 2009; Montagna and Li 2010), larval fish consumption rates, habitat suitability, predator-prey interactions, consumption of resources by fish populations, optimizing aquaculture conditions, zinc pollution effects (Montagna and Li 1997), and mercury bioaccumulation (Cerino 2010). These models are often simple in structure, and the model input data needed are data most frequently collected by biologists. Bioenergetics models also assemble individuals in age- or size-based populations and specify trophic ontogeny of predator-prey interactions. In turn, these models are more widespread and increasingly popular in research studies, especially in fisheries research but have recently been applied to other aquatic animals such as invertebrates.

5.2.2.1 Key Studies and Results

In recent years, bioenergetic models have undergone improvements, including corrections for errors and improved calibration procedures. Such improvements have increased the accuracy of these models, resulting in model estimates closer to values observed in the field. Recently, bioenergetics models have been updated in order to correct for compensation-dependent errors (Bajer et al. 2004a,b; Cui and Wootton 1989; Chipps et al. 2000). Whitledge et al. (2006) found mean percent errors for predicting final weights of hybrid sunfish (F1 hybrid of female green sunfish [*Lepomis cyanellus*] crossed with male bluegill [*L. macrochirus*]) were significantly lower using the corrected model developed by Bajer et al. (2004a) rather than an uncorrected model (Whitledge et al. 1998). A regression-based procedure to correct for systematic sources of error in model output is a recalibration procedure developed by Bajer et al. (2004b) that uses regression equations to predict and subsequently correct model predictions of consumption rate error. Using a recalibration approach, Bajer et al. (2004b) significantly improved model estimates of growth and consumption for white crappie (*Pomoxis annularis*). Schoenebeck et al. (2008) also used a regression-based approach similar to that of Bajer et al. (2004b) to evaluate factors influencing the prediction errors in a bioenergetics model applied to juvenile (age-0) tiger muskellunge (*Esox masquinongy* x *E. lucius*). Estimates of food consumption derived from the model that incorporated the regression-based correction were also found to be more accurate (i.e., closer to observed consumption) than estimates derived from the uncorrected models. A study by Chizinski et al. (2008) used a simultaneous whole-model approach specified by Munch and Conover (2002) to construct a bioenergetics model for zebrafish (*Danio rerio*) in order to predict toxicological effects on development. In this experiment, the whole-model approach appeared to work considerably better than the approach of borrowing multiple bioenergetics coefficients from other species (Bajer et al. 2003, 2004a).

Bioenergetic models have also been used to estimate benthic secondary production. One study was performed in the Western Gulf of Mexico Planning Area to identify the zone of metal toxicity adjacent to production platforms (Montagna and Li 1997). Biomass of deposit feeding nematodes was used to calibrate a model of four processes: food intake, assimilation, loss by predation, and biological loss (which includes respiration, excretion, and non-predatory death). The average productivity for deposit-feeding nematodes on the Gulf of Mexico shelf is about 8 g C wet-weight m^{-2} d^{-1}. On average, deposit-feeding nematodes in the Gulf of Mexico (from depths of 29-157 m) have a production efficiency level of around 30%, compared to values of about 75% in estuaries. At stations within 50-100 m of the platforms, contamination was shown to decrease production efficiency to less than 15% (Montagna and Li 1997).

A similar bioenergetic modeling approach has been used in estuaries for macrofauna and with the addition of suspension feeders as well as deposit feeders (Kim and Montagna 2009; Montagna and Li 2010). In this approach, biomass production is simulated by using a Lotka-Volterra growth model where biomass is a function of the maximum net growth rate of benthos, the carrying capacity for a population that is limited by space, and predation loss. It was found that reducing freshwater inflow causes the upper and lower bay communities to respond in different ways. The models showed that reduced inflow to upper bays near the river resulted in decreasing benthic biomass, whereas biomass increased in lower bays near the Gulf of Mexico inlet. Also, functional diversity decreased in both bays with decreasing inflow because suspension feeders decrease with decreasing inflow and deposit feeders increase. These effects are probably due to the benthic community acclimating to different salinity regimes, or more (or less) salt-tolerant species populating the area. P/B ratios ranged from 1.2 to 3.2, and production rates ranged from 1 to 23 g dry-weight C m^{-2} y^{-1}.

5.2.2.2 Evaluation

Bioenergetic models are often simple in structure, and the model input data needed are commonly collected during field and laboratory studies (e.g., water temperature, habitat [thermal history and response], size at age [growth curves], size or age at sexual maturity, and mortality rates). These data can be easily accessed from previously conducted studies or new field and laboratory studies but must be species-specific in order to obtain accurate input into the model. For example, there are over 40 species-specific models that have been developed and are now accessible for use in popular software programs (Hanson et al. 1997), but most of these models are targeted to fishes and mammals. Invertebrate bioenergetics models are less common but are currently being developed (Chipps and Bennett 2002).

As for the actual process, bioenergetics models must include an observed growth rate and the physiological parameters such as temperature dependence, thermal tolerance, size dependence, etc. that can be accurately measured in a laboratory setting. The effects of temperature, body size, and food quality on maximum feeding rates that will in turn affect overall growth in the animal are also essential input components to the model; the allocation of energy is also an important component to consider. Consumed energy is first allocated to catabolic processes (maintenance and activity metabolism), then to waste losses (feces, urine), and the remaining is directed toward body growth and gonad development. Brett and Groves (1979) expressed this concept as an equation that can be modified to meet the goals and objectives of the study being conducted. The energy budget is stated as follows:

$$\textit{Energy Consumed} = \textit{Respiration} + \textit{Waste} + \textit{Growth}$$

Other components of the process include assembling parameter tables and input data and structuring analyses to address specific key questions in order to produce conditions such as those for maximum possible growth (Walters 1986).

The use of bioenergetics models has increased in recent years because of their usefulness in evaluating questions concerning energy flow through a system. However, there are still some issues that need further work, such as accurately estimating growth and consumption by way of the model output (Ney 1993; Bajer et al. 2004a). For example, bioenergetics models have shown that the accuracy of model predictions can vary with feeding and growth rates (Chipps et al. 2000; Bajer et al. 2004b) because growth efficiency is not a constant and growth rates are highly variable. These models must consider factors that constrain growth (e.g., diet quality or environmental stressors) or use the measured growth to estimate how much a predator has affected its prey populations. Methods to minimize error in model estimates are a key component of current and future research in bioenergetic modeling.

5.3 Modeling Approaches

> *"Scientists have broken down many kinds of systems. They think they know most of the elements and forces. The next task is to reassemble them, at least in mathematical models that capture the key properties of the entire ensembles."* E.O. Wilson 1998
>
> *"All models are wrong, some are useful."* G.E.P. Box 1976

Modeling secondary productivity is important because it is so difficult to directly measure production by animals. As the preceding quotations imply, we have a good understanding of components and processes organizing ecosystems, but that does not mean we have good models to assemble these processes and make good predictions of the net system response. In general, modeling is limited by three major factors: 1) lack of good mathematical representations of the rates, flows, and processes; 2) the enormous number of ecosystem components and the complex interactions between them; and 3) data to calibrate and validate models.

Marine ecosystems are more difficult to study via direct observation than terrestrial ecosystems, and what knowledge that does exist for marine ecosystems is fragmented. Modeling has become a popular approach used to experiment with ecosystems on a large scale without affecting the natural environment. The construction of ecosystem models has been the focus of numerous research efforts over the past 30 y (Morissette 2007).

Estimating productivity is valuable for many reasons. Production can be used as a measure of ecosystem health, and productivity estimates are crucial for modeling energy flow and constructing energy or elemental budgets for ecosystems. Estimates of production are useful for predicting potential yields for fishery species (Cowley and Whitfield 2002). Modeling approaches can be used to supplement capabilities of direct measurements and observations in marine ecosystems. Models also provide important tools to guide ecosystem and fisheries management. For example, recent shifts in fisheries management from the traditional, single-species approach to an ecosystem-based management (EBM) approach has been made possible by the development of ecosystem models. Unfortunately, obtaining direct measurements or calculations of productivity in the field takes considerable effort (labor, time, and money) (Cowley and Whitfield 2002). For this reason, recent advances in ecosystem modeling need to be explored to assess the various applications and possible uses of these models.

Ecosystem models, by definition, include more than one species or component of an ecosystem and incorporate external influences such as chemical, climatological, or physical factors. In the end, all ecological models represent a set of hypotheses as to how the ecosystem works. Many ecosystem modeling approaches utilize path analysis statistics to study ecological pathways. Path models examine input and output between compartments within a system (Lenzen 2007). Compartments can represent species, trophic groups and even fishery fleets. Energy or nutrients are often used as model currency. Thus, path analysis is useful for estimating the strength and direction of all factors that affect the functioning of an ecosystem. Modeling approaches can be used to conduct large-scale ecosystem experiments without affecting the natural environment. Thus, ecosystem models provide important tools for making informed decisions on how to manage oceans and their resources.

Many models are available, some more widely used than others. Each modeling approach has its own advantages and disadvantages, and they vary in their degree of complexity. Numerous aspects must be considered when choosing or developing a model to accurately describe the system of interest. The model structure and spatial resolution must be appropriate for the ecosystem and the research or management objectives. Sometimes a suite of models will be most appropriate, though not always the most practical. An appropriate modeling approach must be used in order to develop a better understanding of an ecosystem.

General types of ecosystem models include the following:

- *Dynamic Multispecies Models* generally focus only on interactions between species, though some models can incorporate physical or environmental forcing (Plaganyi 2007).
    - e.g., Minimally Realistic Models (MRM), Multispecies Virtual Population Analysis (MSVPA), Individual-Based Models (IBM), Globally Applicable Area-Disaggregated General Ecosystem Toolbox (GADGET).
- *Dynamic System Models* typically incorporate lower trophic levels and environmental factors. Higher trophic levels are usually left out, or included with minimal detail only. Some models also incorporate age structure and/or spatial aspects (Plaganyi 2007).
    - e.g., NPZ, Atlantis.
- *Whole Ecosystem Models* include all trophic levels in an ecosystem, aiming to represent each system component in a mass-balanced way (Plaganyi 2007).
    - e.g., Ecopath with Ecosim (EwE) and Ecospace.

Generally, more complex models are thought to be more realistic. However, with the addition of complexity comes the addition of uncertainty. As the number of parameters in a model increases, so does the associated range of uncertainty and error. Also, adding more parameters may force the model to fit the data, even if this does not accurately describe the system. Each parameter has its own associated range of error, and the additive effect of multiple parameters can be staggering, leading to inaccurate descriptions of ecosystems.

Good models have three basic requirements (Pauly et al. 2000):

- They must be effective in describing flows (e.g., biomass, energy) between different ecosystem components.
- They should be able to predict the outcomes of alternative management policies and strategies.
- They should be fast and easy to assemble, even when there may be a lack of data. This is especially important when considering models for management objectives.

Recent advances in ecosystem modeling need to be explored and evaluated to assess the various applications and possible uses of these models. In the current review, two modeling approaches will be evaluated in detail: NPZ and EwE. These approaches were selected for in-depth review because they are the only two modeling approaches that are in wide enough use to provide productivity estimates for comparisons among most of the 26 OCS planning areas.

5.3.1 Nutrient-Phytoplankton-Zooplankton Models

5.3.1.1 Overview

NPZ models are commonly used to describe plankton dynamics in oceans. They are compartment, or box, models containing at least three state variables: nutrients, phytoplankton, and zooplankton. Nitrogen is the most commonly used model currency to represent nutrient flow through an ecosystem. NPZ models are simple and offer many advantages. They contain few parameters and state variables, thereby increasing the likelihood that data will be available. They are relatively easy to understand and can be applied in ways that would be difficult with more complex models. Although NPZ models are not as realistic as more complex models with more components (i.e., boxes), they can provide realistic insight into the dynamics of an ecosystem (Franks 2002; Cloern 2007). This is because the models represent well known dynamics in the most fundamental part of the food web: nutrient uptake by primary producers, and herbivory by the first step of the consumer food web. The major concern about NPZ models is that they simply do not include top-down control of ecosystem processes.

When studying complex natural systems it is difficult to trust that simple compartmental models could accurately describe these systems. Therefore, many scientists have moved toward the use of more complex models (Fulton et al. 2003; Plaganyi 2007). Approaching problems with a simple model first, then increasing complexity only when necessary, is often the best approach to ecosystem modeling (Fulton et al. 2003). One approach to increasing the complexity of NPZ models is to simply add more boxes. For example, Arismendez et al. (2009) recently performed a study in the Texas coast using a six-compartment model with phytoplankton, zooplankton, and four species of nitrogen so that the detrital and grazing food chain could be represented. Another approach to increasing complexity of NPZ models is demonstrated in the North Pacific Ecosystem Model for Understanding Regional Oceanography (NEMURO). Additional state variables were included to better represent all species in the ecosystem. The concept was extended further when higher trophic groups (i.e., fish) were included, leading to NEMURO.FISH (Werner et al. 2007).

The extent of model simplification depends on the goals of the study. There are advantages to using simple models, e.g., faster processing time and easier parameterization. Also, simpler models require fewer assumptions, reducing the likelihood of errors. Thus, they are generally more robust models with predictable results (Flynn 2003). If the objective of a study is to examine “what-if” scenarios, then more complex, inclusive models are recommended (Flynn 2003).

A set of equations is assembled to model nutrient, phytoplankton, and zooplankton dynamics in the system.

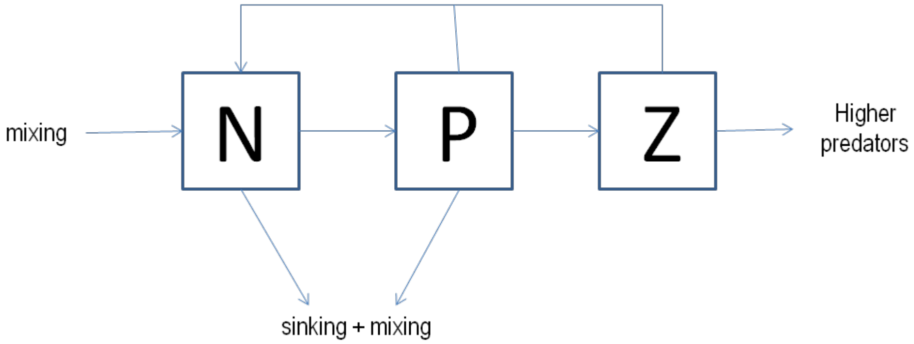

It is important to simulate the dynamics of nutrient consumption by organisms within an ecosystem because nutrient consumption is directly related to growth, which affects the biomass of each organism group and the entire ecosystem. A simple relationship can be described as follows: organisms consume resources, and total organism biomass subsequently increases (Flynn 2003).

After death, the nutrients contained in the phytoplankton or zooplankton are recycled into the system. It is thus that nitrogen is recycled and available to be taken up again during photosynthesis (Franks 2002).

Another important consideration when working with models, especially NPZ models, is export production, which is the transfer of biogenic material from one zone in the ocean system to another (Riebesell and Wolf-Gladrow 1992). For example, if vertical sinking of nutrients and phytoplankton occurs, then this process must be incorporated into the model; or, if lateral movement of materials occur due to currents, then multiple boxes can be created to model this transport.

NPZ models have been coupled to physical models (Franks 2002). Physical models can be one-, two-, or three-dimensional, and coupling is achieved by an advection-diffusion equation. In addition to advection and diffusion, biological and physical models can be coupled via depth or temperature dynamics, and the effect these physical forces have on the biological community and dynamics of the state variable in the system. NPZ models can also be coupled with additional NPZ models to examine connectivity and production transport between ecosystems (Cloern 2007).

Main types of data for comparing to model output include biomasses of phytoplankton and zooplankton; photosynthesis, nutrient uptake, and grazing rates; and derived quantities (Franks 2002). Although agreement between field-measured biomasses and the values of the state variables is an important requirement for accepting a model as a description of the system under investigation, it is not the only requirement.

NPZ models, or ecological models in general, can be applied in a theoretical, heuristic, or predictive framework (Franks 2002). NPZ models are most commonly used for theoretical applications, to ask questions like “what would happen if…?” Recently, NPZ models have been increasingly used for heuristic applications, to ask “how did this happen?” Very rarely are NPZ models used for predictive purposes, or to ask questions like “what will happen…?”.

5.3.1.2 Top-Down and Bottom-Up Control of Ecosystems

Ecosystems can be controlled from the bottom-up or top-down. This means that components of an ecosystem are either controlled by flow from components that support it or by components that consume it. For example, phytoplankton are controlled by limiting factors such as nutrients, an example of bottom-up control. However, phytoplankton are also controlled by zooplankton that consume them, which is an example of top-down control.

It is generally believed that top-down control is more prevalent in coastal benthic systems (Power et al. 1996) and bottom-up control is more prevalent in oceanic surface systems; many studies have focused on bottom-up processes (or limiting factors) when examining productivity at higher trophic levels (Franks 2002). This is in fact the case in many areas, but not all. Top-down effects are the driving factor in some areas (Jackson et al. 2001). Therefore, it can be useful in general to estimate productivity at higher trophic levels by examining nutrient, phytoplankton, and zooplankton dynamics. However, one must keep in mind that this approach may not provide an accurate description of every area, and it is important to have some general knowledge of biomass and production at higher trophic levels before jumping to a conclusion based on NPZ models.

Most often, complex marine ecosystems cannot be accurately described by top-down or bottom-up forces alone. Systems are affected by both forces simultaneously, in addition to other forces, depending on geographical or temporal location.

Frank et al. (2006) suggest evidence to support top-down control as the driving force in areas of low productivity, while highly productive areas are characterized by bottom-up control. Bottom-up analysis (e.g., NPZ models) should not be used as the only means to manage areas for oil and gas exploration and drilling. Areas appearing to have low production may be some of the most important areas supporting some higher trophic level species. Also, many areas with top-down control are at greater risk under fishing pressure (Jackson et al. 2001; Frank et al. 2006).

5.3.1.3 Evaluation

For broad-scale, comparable modeling, the NPZ approach may be very useful in the future. As seen in **Section 3**, it is now possible to obtain maps of chlorophyll, biomass, and rates of primary production globally using satellite technology. Zooplankton biomass data are also widely available from field sampling studies, and are routinely monitored in some areas (see **Appendix C**). Therefore, with sufficient high-resolution nutrient data, it should be possible to create secondary production maps for the whole globe (and OCS planning areas) at relatively fine-spatial scales. Efforts to assemble a nutrient database are ongoing at various locations. One important limitation of the NPZ approach is that it would estimate only surface productivity, modeling mainly just bottom-up control. For example, an NPZ model tells us nothing about fish feeding on zooplankton, nor any components of the benthos.

5.3.2 Ecopath Modeling Approaches

5.3.2.1 Overview

The Ecopath software suite is designed to construct and analyze mass-balance trophic models of entire ecosystems (i.e., all trophic groups, from primary producers to apex predators), providing an “ecosystem snapshot” (Plaganyi 2007). Ecopath is being used in 164 countries by nearly 6,000 people, and over 3,500 publications using Ecopath are listed on the Ecopath web page (Ecopath 2010). A recent computer search (January 14, 2011) found 172 papers on Ecopath in electronically indexed journals. Thus, it is important to evaluate the Ecopath modeling approach in this review as it is the best source of secondary and tertiary productivity information because it covers the most areas, and is performed in a consistent fashion across all areas making comparisons among areas and taxa valid.

The majority of Ecopath models are constructed for marine ecosystems (>80%), while freshwater (18%) and terrestrial (1.5%) environments are represented by less than 20% of the models (Morissette 2007). Ecopath models have been used to evaluate the effect of fishing on marine ecosystems and to guide fisheries assessment and management. The modeling approach can also be used to address other ecological and environmental questions. Ecosystem responses can be predicted for a variety of influences, including management policy options, placement of protected areas, and climate and environmental changes. Ecopath models enable ecosystem comparisons and have become important tools for EBM and marine spatial planning (MSP). Future applications and direction for research have been proposed in these areas as well as others.

Appendix B provides a detailed explanation of Ecopath model development, assumptions, data requirements, software tools, and outputs.

Initial Development: The French Frigate Shoals

Ecopath was developed in the 1980’s to gain insight into the structure and function of complex tropical ecosystems. The model was initially applied to the French Frigate Shoals (FFS), a coral reef ecosystem in the northwestern Hawaiian Islands (Polovina 1984a).

Overall, the initial development and use of the Ecopath model was successful in accurately depicting the structure and function of the FFS coral reef ecosystem. The model estimates were in close agreement with field estimates, indicating the potential of Ecopath to serve as a tool for enhancing understanding of the structure and function of complex ecosystems (Atkinson and Grigg 1984).

Further Developments

The initial success of Ecopath prompted scientists and managers to further evaluate the model, primarily within the context of how it could be used to study ecosystem dynamics. Christensen and Pauly (1992) were instrumental in the advancement of the original model by Polovina (1984b) and have been continuously updating Ecopath since the 1990's.

The introduction of Ecosim in 1995 added a temporal component to the Ecopath approach, enabling dynamic simulation of ecosystems over time (Walters 1996; Walters et al. 1997, 2000). In 1998, Ecospace was introduced, adding a geographical component to the Ecopath software suite, which enabled spatial analysis (Walters et al. 1999). Increased developments and use of the Ecopath modeling software led to the development of an integrated software package, Ecopath with Ecosim (EwE).

5.3.2.2 Model Description and Approach

Ecopath models incorporate two approaches. The first, based on Polovina (1984a,b), estimates biomass and food consumption for each ecosystem group. The second approach, based on Ulanowicz (1986), is used to analyze flows between the ecosystem groups and calculate various ecosystem indices.

Ecopath originally required the assumption of steady-state, or equilibrium, conditions, e.g., inputs must equal outputs for each group. The steady-state assumption demonstrated that model outputs should only be applied to the time period of the input values (Christensen and Pauly 1992). The steady-state assumption has been replaced with an assumption of mass balance for a given time period. Ecopath can now include rates of biomass accumulation (or depletion), and is thus considered “time-invariant” rather than “steady-state” (Christensen et al. 2008). This assumption was implemented as a way to ensure compatible energy flow estimates. Input data must pass the “mass balance filter” before energy flow in an ecosystem can be modeled (Christensen et al. 2008).

When Ecopath models are constructed, ecosystem groups (e.g., boxes or compartments) are established. Groups can be specific or broad, depending on modeling objectives, user knowledge, and data availability (Polovina 1984a,b). Typically, groups are composed of functionally similar species at the same trophic level. Ecosystem groups can be defined based on function, trophic level, food source, and life-history characteristics. Groups can consist of different species, single species, species aggregates, or linked age groups (“multi-stanza” groups). Functional groups should represent the whole ecosystem, from detritus and phytoplankton to sharks and whales.

The Ecopath model consists of two master equations, representing production and consumption, as follows:

Master Equation 1: Production

$$\begin{aligned} Production = {} & Catches + Predation\ Mortality + Net\ Migration \\ & + Biomass\ Accumulation + Other\ Mortality \end{aligned}$$

Master Equation 2: Consumption

$$Consumption = Production + Respiration + Unassimilated\ Food$$

The second master equation represents consumption of a group, and ensures energy balance within each group. The consumption equation is essentially the same as the bioenergetic model and is based on the principle that matter is conserved within each group. Energy balance is performed to estimate respiration from the consumption master equation. Estimates are made because measurements of respiration are rarely included in fisheries data. A routine is also included to estimate the energy balance from any combination of terms from the consumption equation (Christensen et al. 2008).

The two master equations, representing production and consumption, are linked via the predation mortality term. The predation mortality of a prey organism equals the consumption of its predators. Thus, the production of each group (master equation #1) is linked to the consumption of all applicable predator groups (master equation #2). Missing parameters are estimated by utilizing these linkages, because the mass balance assumption requires that the production of a group is not lost, but is transferred within the system (Christensen et al. 2008).

Input data requirements for each group in the model include estimates of biomass, consumption and total mortality, diet composition, and fishery catch. Generally, three of the following four input parameters are required for each functional group in the model biomass, P/B ratio (or total mortality), consumption/biomass ratio, or ecotrophic efficiency. Ecopath will then estimate the missing parameter. If data are available to satisfy all four input parameters for a group, the model is then able to estimate biomass accumulation or net migration.

5.3.2.3 Ecopath Modules

Ecopath software also contains a suite of modules for specific application. The modules that may be of use in managing OCS activities are described below. While these modules were created primarily for fisheries management, they can be modified to examine the effects of OCS activities on ecosystem function.

Ecosim

Ecosim adds a temporal component to the Ecopath software, enabling dynamic simulations at the ecosystem level. Ecosim is used mainly for policy exploration purposes and has become an important tool as fishery management strategies have shifted to an ecosystem approach (Pauly et al. 2000). Ecosim can also be useful for examining impacts of behavior. This can include organismal behavior (e.g., predator avoidance, etc.) but can also include human behaviors (e.g., fisheries impacts, oil and gas activities and spills) (Walters and Kitchell 2001; NOAA 2007; Overholtz and Link 2009).

Ecospace

The development of Ecospace introduced a spatial component to the Ecopath software suite (Walters et al. 1999). Ecospace was primarily designed to explore the impact and placement of Marine Protected Areas. The Ecospace module is able to integrate various data from GIS, including maps, and enables spatial optimization capabilities. New modules within Ecospace include Ecoseed and Importance Layers (Christensen et al. 2008).

EcoTroph

The EcoTroph module applies a theoretical approach to examining trophic dynamics in an ecosystem. The functioning of marine ecosystems is guided by a continuous trophic flow, from low to high trophic levels (Gascuel 2009). EcoTroph models the biomass trophic spectrum based on equations from physics flux, providing a continuous representation of biomass distribution according to trophic level (Gascuel et al. 2009). The flow of biomass through trophic levels provides a simple and useful picture of ecosystem functioning. Input parameters can be obtained from an Ecopath model or independent estimates. Input parameters include biomass, production, and catch (Gascuel et al. 2009).

Ecost

Ecost is a socioeconomic module that incorporates social and economic aspects into the Ecopath modeling approach. It is essentially a value chain model, describing the value of fish products from the sea to consumers. Economic flow is modeled as a continuation of the food web. Units (currency) commonly used in Ecost include landings, monetary value, and the number of jobs. Two major uses of Ecost include policy optimization (sector, fleet) and management strategy evaluation (closed loop simulation).

5.3.2.4 Evaluation

Advantages and Capabilities

Models can be designed to address ecological questions and examine ecosystem responses to various influences, such as fishing and management policy options concerning oil and gas activities. The ability to examine ecosystems over time and explore policy options and questions are key reasons that support the high number of EwE users worldwide. The most-cited reasons for constructing Ecopath models are to describe ecosystem structure (42%), examine fishery management issues (30%), answer theoretical ecology questions (11%), address policy matters (9%), and assist in the creation or management of Marine Protected Areas (Morissette 2007).

Ecopath is a widely used and common approach to modeling ecosystems. Thus, construction of Ecopath models has brought together multidisciplinary groups such as scientists (and data) from state and federal levels of government, international research organizations, universities, public interest groups, and private contractors. This collaborative effort is key for identifying data gaps and common goals and objectives of those involved. The collaborative model construction process can also highlight overlapping efforts by multiple users. This is essential for avoiding duplication of effort and work, which can hinder model development and progression.

EwE has become a popular ecosystem modeling approach, attracting a large, broad community of users. The Ecopath model enables users to develop an accurate understanding of the structure and function of an ecosystem. Equations are simplified, and smaller amounts of data are required in Ecopath compared to many other modeling approaches.

Disadvantages and Limitations

It is difficult to define a natural, complex system in such a way to satisfy the requirements of an ideal ecosystem box model. Several issues of particular importance need to be considered when using the Ecopath modeling approach, as described below.

Ecopath can provide inaccurate predictions that result from poor estimates of a few key parameters. This problem can be exacerbated by the fact that model builders often recycle parameters from one Ecopath model to another. In this way, the biggest advantage of Ecopath (i.e., that a model can be built quickly) also becomes a disadvantage.

A problem in all trophic-dynamic models is describing the effects of predators. A predator can have a large controlling effect on a prey group, even though they may not actually consume a large amount of this prey item. This is the classic keystone species concept (Paine 1966). Also, even though a prey type may not seem important for a predator, this predation may be an important controlling factor on the population of the prey item. Thus, it is important not to ignore small or rare components of a predator's diet when constructing an ecosystem model. If these species are not included in an Ecopath model, then the model will likely not yield a correct estimate of the prey productivity.

Mediation effects, or indirect trophic effects, exist when a third functional group is responsible for impacting (positively or negatively) the interaction between two other functional groups in an ecosystem. Ignoring these effects in an Ecopath model will often result in incorrect predictions regarding responses of organism groups to various ecosystem changes.

Ecopath does not handle bottom-up interactions very well. Occasionally, users intentionally underestimate the predation vulnerability of functional groups as a means of mimicking bottom-up control in an ecosystem; this tactic can lead to risky or misleading assumptions. By default, Ecosim assumes the foraging arena theory is true for all functional groups in an ecosystem. This, however, is not always the case, and foraging arenas are often shared by functional groups. Thus, removal of any one predator may simply result in the vulnerable prey individuals being taken just as fast, but by other predators.

When Ecosim models are fit to time series data, changes in functional groups can be seen over time. Changes, subtle or dramatic, can usually be attributed to trophic interactions or fishing effects. In some cases, however, the cause of a change is unknown. It is important to remember that changes in habitat can also occur that result in significant ecosystem changes, however, EwE does not consider the effect of habitat changes on trophic relationships. Thus, EwE may identify patterns as responses to trophic or fishing effects that may actually be the result of habitat changes.

The simplicity and ease of use of EwE can present problems, as noted previously. As with any ecosystem model, quick and easy construction often results in development of poor models. These models may be misleading, and thus impede understanding of an ecosystem.

EwE is not effective for estimating parameters within those ecosystems that exhibit high variability between seasons. Ecopath does not allow consideration of detailed energetic relationships. Additional problems have been encountered when trying to model populations of marine mammals (Plaganyi 2007). Further development, including better parameterization, is needed to improve the ability to explore policy options and resulting ecosystem responses. The incorporation of all functional groups increases the number of parameters and, thus, the difficulty in building and parameterizing a model. This is a problem with all ecosystem models. Major simplifications and assumptions are often made to simplify the models in order to decrease the number of parameters.

Ecopath is not the ultimate, all-inclusive model because it does not fully incorporate all bottom-up processes, especially those controlled by biogeochemical processes (e.g., the microbial loop). In addition, EwE cannot directly assess climate change scenarios, large increases in predator biomass, or simultaneous major system changes. Thus, additional dynamic approaches must be considered (Overholtz and Link 2009). Coupling of models can help to eliminate some of the disadvantages of each modeling approach.

Potential Uncertainties and Biases

There are many reasons why predictive approaches, such as EwE (and ecosystem modeling in general), are uncertain. Long-term monitoring data, especially on non-target species and various life stages, are lacking. Interaction effects (e.g., trophic, habitat) are difficult to monitor and quantify, especially the effects on recruitment of early life stages. Determining the source for various effects is difficult, especially when examining historical data. Our capabilities are limited when it comes to examining ecosystem dynamics at a large scale, and models and time series data can only provide so much insight. Also, increasing pressure on marine ecosystems is causing novel situations and problems. Anticipation of new problems and situations is difficult when these changes are often unpredictable. Failure to anticipate these new changes and problems can result in useless modeling attempts.

Even when parameters may be highly uncertain, Ecopath models may still provide important value. For example, policy options can be screened via the use of such models. Also, they provide starting points for further, more focused research (Walters et al. 2006).

Data Requirements and Availability

One advantage of the Ecopath modeling approach is that the required input values are often readily available for many of the species or groups in many marine ecosystems. Thus, the Ecopath approach enables fairly rapid construction and evaluation of balanced ecosystem models. Most of the data required for input into Ecopath models are data that is commonly collected for other purposes (i.e., species assessments, other research). In general, the data required for input in an Ecopath model are relatively simple and can often be found in stock assessments, technical reports, and the primary literature. Public access databases are available for some sampling programs. However, as a whole-ecosystem model, Ecopath requires data for all trophic levels. This may pose a problem, especially in data-poor areas (Morissette 2007; EBMtools.org). Finally, reusing existing parameters without verifying their values for existing conditions (such as spatial or temporal variability) may pose additional problems.

Database-driven models (i.e., models that can extract data from many large databases to generate ecosystem models) are expected to see increased development and use. An Ecopath model to describe the world's 66 large marine ecosystems (LMEs) was built using this approach (Christensen et al. 2009). Thus, Ecopath can be used for very large spatial scales such as OCS planning areas.

Ease of Readily Updating Estimates

As new data and information becomes available, they can be easily integrated into an existing Ecopath model. This is important for quick updating of models and is especially advantageous for adaptive management strategies.

Scientific Acceptance

Ecopath is by far the most widely used approach for ecosystem and multi-species modeling (Plaganyi 2007). Ecopath has become the prominent ecosystem modeling approach in the literature, especially over the last decade. According to Christensen et al. (2008), more than half of all primary journal publications in the field are based on the EwE approach. The ease of use, and continued improvements and developments, will likely allow EwE to continue as a forerunner in the field of ecosystem modeling (Plaganyi 2007).

5.3.3 Atlantis

The Atlantis modeling framework is another whole-ecosystem box model gaining popularity (Fulton et al. 2003, 2005; Plaganyi 2007; Fulton 2010). Like Ecopath, Atlantis was originally developed as a tool to evaluate various fisheries management strategies. The model was initially applied to Port Philip Bay in Australia (Fulton 2001; Fulton et al. 2004). The Atlantis framework incorporates physical, chemical, ecological, and human dynamics into the model via submodels to represent human impacts, ecology, and hydrographic factors. Atlantis is more inclusive of ecosystem processes than Ecopath because of the incorporation of various biogeochemical and oceanographic factors. Atlantis also incorporates the basic biogeochemical principles behind NPZ models (Fulton et al. 2005).

Model area in Atlantis is represented by 3-dimensional spatial polygons that incorporate differences in habitat types and water depths. Increasing spatial complexity (i.e., adding polygons, vertices, faces) increases the number of calculations required, and thus increases model run time. Oceanographic data (i.e., salinity, temperature, etc.) must be obtained to match each specific face (i.e., line segment) of each spatial polygon. Other data (e.g., vertical flux of materials) must be specific for each depth layer within each polygon (Kaplan et al. 2010). Therefore, initial data needs are extensive and specific.

Approximately 60 functional groups can be included in the Atlantis model. Once groups are assembled, they are hard-wired into the code, allowing virtually no flexibility to make changes. There are many requirements associated with assigning functional groups that makes the Atlantis model framework more inclusive, but also more difficult to develop relative to Ecopath. Up to 10 groups can be invertebrates measured on a per-area basis, of which two must be primary producers. Up to 19 groups can be invertebrates measured on a per-volume basis, of which three must be primary producers and three must be detritus (labile, refractory, and carrion). Up to two invertebrate groups can be used to split them into juvenile/adult biomass pools. Up to 35 vertebrate groups can be included, and all are treated the same. Each vertebrate group is divided into 10 age categories, regardless of life span. Biomass of vertebrates is divided into reserve weight (meat + gonad) and structural weight (bone) (Kaplan et al. 2010).

Input data for biological parameters must include concentration (mg N m^{-3}) of invertebrates and nutrients, numbers-at-age for vertebrates (number of individuals per age class per spatial box), and reserve and structural weight-at-age for vertebrates (mg N per individual). Atlantis model output consists of biomass, density, reserve N, and structural N for each functional group, age class, and spatial box.

The abundance of each group is tracked within each 3-dimensional spatial box. The model time step can be 12 or 24 h. Nitrogen is the most often used currency to examine flow through the system. Silica and oxygen can also be used, though the methods for using these in the model are not as developed.

The density (mg N m^{-3}) of primary producers (PX) is tracked over time as follows:

$$\frac{\Delta PX}{\Delta t} = growth - lysis - linear\ mortality - quadratic\ mortality - predation$$

where linear mortality is density-independent and quadratic mortality is density-dependent.

Growth is calculated as:

$$growth_{PX} = maximum\ growth\ rate * light\ limitation * nutrient\ limitation \\ * space\ limitation * PX$$

Similar equations are used to model density (mg N m^{-3}) and growth of invertebrate groups (CX):

$$\frac{\Delta CX}{\Delta t} = growth - linear\ mortality - quadratic\ mortality - predation \\ - fishing\ (optional)$$

$$growth_{CX} = [growth\ efficiency\ when\ feeding\ on\ live\ prey \\ + growth\ efficiency\ when\ feeding\ on\ detritus] * space\ limitation \\ * oxygen\ limitation$$

Vertebrates are tracked by abundance (number of individuals), biomass (mg N m-3), weight-at-age, and condition (reserve weight/structural weight). Changes in density over time of vertebrate groups (FX) are modeled as follows:

$$\frac{\Delta FX}{\Delta t} = immigration - emigration - linear\ mortality - quadratic\ mortality \\ - predation - fishing\ (optional)$$

Vertebrate growth is calculated in the same form as for invertebrates, but for each specific age group. Growth is then apportioned to structural and reserve weights within each biomass group. Additionally, spawning and recruitment events over shorter time periods can affect various vertebrate pools (Kaplan et al. 2010).

The Atlantis modeling approach originated in Australia and has just recently been used to model marine systems in the U.S. Atlantis was applied to the California Current ecosystem to examine various fishing strategies. Trade-offs between maximizing fisheries harvest and maintaining ecological structure and function were evaluated. The model study area extends from Cape Flattery, Washington to Point Conception, California, thus covering parts of all Pacific OCS planning areas. The area was divided into 48 detailed spatial boxes, and 54 functional groups were modeled utilizing N as the common currency. The model simulated a 25-y period in which various ranges of fishing intensity were examined. These simulations generated different results than similar modeling efforts using Ecopath (Field 2004; Field et al. 2006). These differences could be the result of various influences but most likely result from the increased detail and complexity involved in the Atlantis model compared to the Ecopath approach (Brand et al. 2007; Kaplan and Levin 2009). This illustrates the differences in these two modeling approaches, and future work is needed to examine the accuracy of each approach (especially Atlantis, as the Ecopath approach was developed 20 y prior).

Atlantis was recently applied to the Northeast U.S. Continental Shelf LME. This model was developed as a preliminary exercise to examine the application and accuracy of Atlantis, as well as to identify data gaps and areas for improvement and future research (Link et al. 2010). The model area extends along the continental shelf from the Gulf of Maine to Cape Hatteras, NC, thus covering portions of all OCS planning areas for the U.S. Atlantic Coast (excluding Straits of Florida). The area is divided into 22 spatial polygons, each with up to four layers representing water column depth. A total of 45 functional groups was modeled with N as the model currency, and 18 fishery fleets were incorporated into the model. The model was run for 50 y (1964-2014) with a 12-h time step. Overall, the model produced reasonable results that fit within tolerance levels for the full array of included factors (e.g., ecological, biogeochemical, etc.). This preliminary exercise demonstrates that Atlantis is able to reasonably represent complex system dynamics in an interdisciplinary way, and serves as a useful starting point for further work (Link et al. 2010).

Preliminary efforts to develop an Atlantis model for the Gulf of Mexico are currently underway (H. Perryman, 2011, personal communication, Rosenstiel School of Marine and Atmospheric Science, University of Miami, Miami, FL). Overall, there are insufficient model results from Atlantis to compare it to Ecopath, especially in the context of all OCS planning areas.

Input data requirements for Atlantis are more extensive than for Ecopath because of the added complexity in the Atlantis model framework. While Atlantis is more detailed, and thus perhaps the most inclusive ecosystem modeling tool currently available, Ecopath is more flexible and models can be developed more rapidly. Atlantis is superior to Ecopath and other ecosystem models for various reasons. Atlantis does not require as many simplifying assumptions of less sophisticated models. Complete descriptions of detrital and bacterial loops are included. Atlantis also handles habitat and abiotic conditions better and easily links to oceanographic models (e.g., Regional Ocean Modeling System, ROMS; Fulton 2001, 2010). **Table 10** highlights some important differences between Atlantis and Ecopath modeling methods (Fulton et al. 2003; Plaganyi 2007; Kaplan and Levin 2009).

Table 10. Comparison of Atlantis and Ecopath model characteristics.

Issue/Characteristic	Atlantis	Ecopath
Ontogenetic age structure	Explicit	Equilibrium assumed
Chemistry and detritus loops	Detailed	Simplified
Climate	Incorporated (links to ROMS model)	Optional (model coupling)
Run time	6-12 h	Seconds
Build time	1-3 y	3-9 months
Spatial structure	Dedicated	Optional/Flexible
Optimizations	No	Yes
Handling of error	No	Optional

5.4 Conclusions and Selected Methodology

For the secondary productivity comparisons in this report, the Ecopath modeling approach was chosen for several reasons:

- Ecopath is a well developed modeling system that has many adherents and much technical support;
- The data required for Ecopath are relatively available;
- There are already many Ecopath models available for OCS planning areas; and
- It would present a consistent approach for comparison across the nation as a whole; it has already been applied globally.

There are only two Atlantis models for OCS planning areas, so it would not yet be useful to base an OCS-wide application on that approach. While empirical data exist for zooplankton and fisheries, and these biomass data could be used to make productivity estimates using an allometric approach, there are insufficient data on the parameters necessary to calculate productivity across all OCS planning areas.

Ecopath models are useful for broad comparisons because these models have been produced for many OCS areas. In addition, Ecopath models have become popular and effective for risk assessment and as decision support tools. For example, the modeling approach can be used to estimate productivity at an ecosystem scale and enable ecosystem comparisons. Ecopath can also be used to predict ecosystem and socioeconomic responses to oil and gas related activities, including exploration, production, shoreline development, and oil spills. Ecopath enables risk assessment of oil and gas activities and spills by predicting the ecosystem responses to these various influences. Ecopath models can be used as support tools for making decisions about oil and gas leasing in the OCS planning areas by exploring various policy options via models before implementation in the real world.

However, it is well recognized that no model can completely and accurately depict an ecosystem. Therefore, many have proposed using multiple models to fill in gaps that other models are incapable of modeling. An iterative process in which single-species analyses and EwE are used together can be useful for improving model estimates (Christensen et al. 2008). New models have been constructed (and continue to be constructed and developed) that are helping to address the gap between the Ecopath approach and more detailed models (e.g., Atlantis, Spatial Ecosystem and Populations Dynamics Model [SEAPODYM]) (Overholtz and Link 2009). EwE, and the newly developed Atlantis, are the best models for addressing broad ecological questions or goals (Plaganyi 2007).

For broad-scale, comparable modeling, the NPZ approach may also be useful in the future. As seen in the primary productivity sections (**Sections 2** and **3**) of this report, it is now possible to estimate rates of primary production globally using satellite technology. Zooplankton biomass data are also widely available from field sampling studies and are routinely monitored in some areas (**Appendix C**). Therefore, once nutrient data can be obtained over similar spatial and temporal scales, it would be possible to create secondary production maps for the whole globe. Such an approach could also be applied to the OCS planning areas at relatively fine-spatial scales.

5.5 Reported Ecopath Modeling Results for OCS Planning Areas

Ecopath models for U.S. OCS ecosystems were reviewed, and secondary productivity estimates are summarized for each planning area. A total of 18 Ecopath models were found, including many (but not all) OCS planning areas (**Figure 43**, **Table 11**), as described in the following summaries. Biomass (B), production (P), and production/biomass ratio (P/B) data were compiled for all ecosystem components in each Ecopath model. If one of the parameters was not given, it was calculated from the others. For example, if B and P/B were reported, P was calculated from those values. All model groups were assigned to one of nine general functional groups to enable comparison of ecosystems: pelagic fish (PEL), demersal fish (DEM), sharks and rays (SKR), marine mammals (MAM), seabirds (BRD), crustaceans, mollusks and other mega-benthos (CMB), macro-, meio-, and micro-benthos (BEN), zooplankton (ZOP), and primary producers (PPD). Functional groups were assigned based on trophic characteristics (i.e., where they feed trophically). Production from seabirds (BRD) was negligible, so it was not considered in the analysis. Although detritus (DET) was a common functional group, it does not contribute to productivity, and thus was not included in the analysis. If the model developers did not report a group, it was left out in this analysis; parameters were not estimated for any missing groups. Production for each functional group was calculated by adding the production from each contributing group. For example, if the original model included several crabs and mollusks, the B, P, and P/B values were summed to obtain a value for the CMB group in total. This was performed to facilitate comparison of models for this analysis. Estimated secondary productivity of the entire ecosystem (SYSTEM) was calculated by adding the productivities of each functional group (excluding PPD).

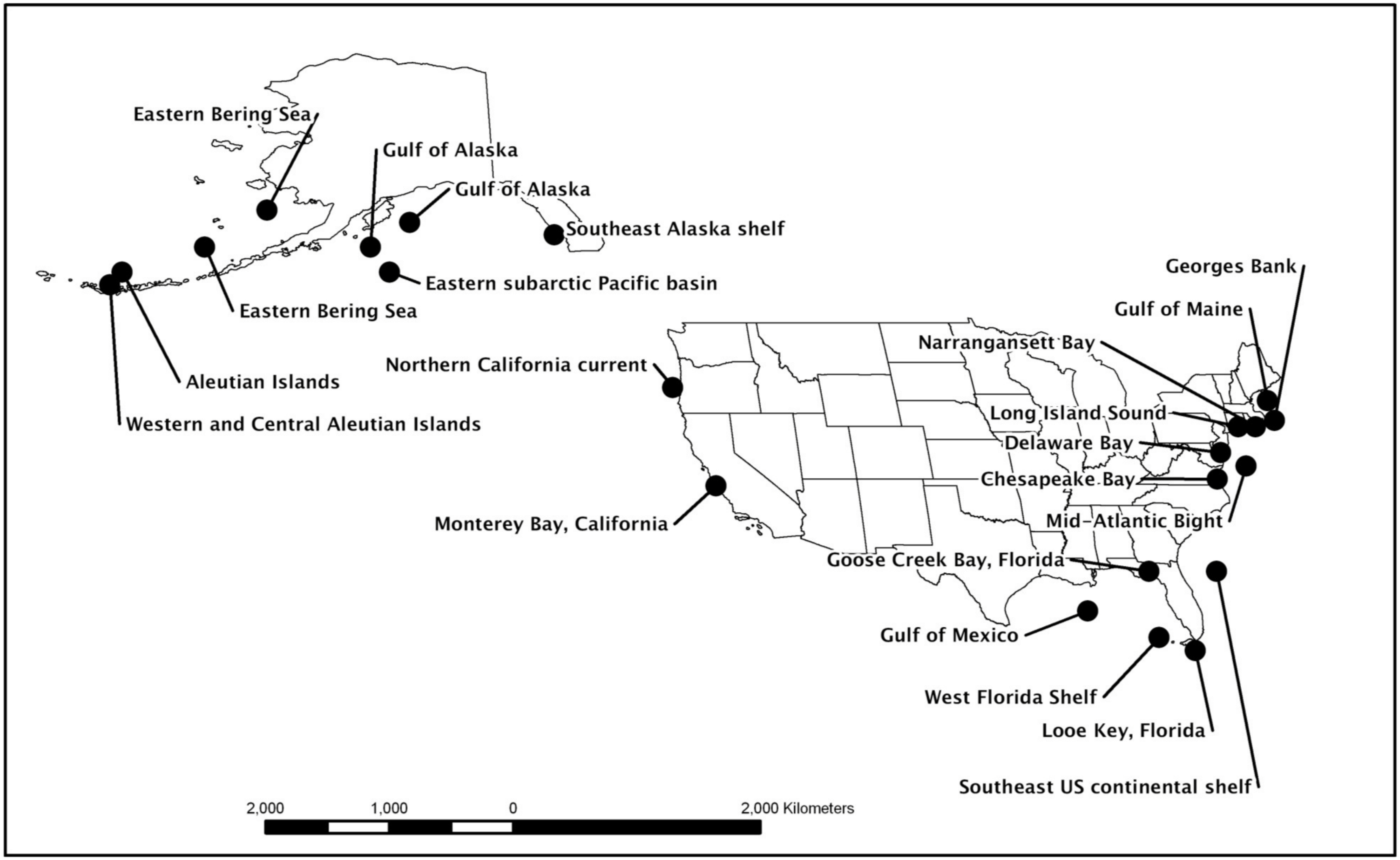

Figure 43. Locations of Ecopath modeling studies found in and near Outer Continental Shelf planning areas.

Table 11. Secondary productivity estimates from Ecopath models in the U.S. Outer Continental Shelf.

Region and Reference	Study Area	Planning Area(s)	Productivity (t km^{-2} y^{-1})								
			System	PEL	DEM	SKR	MAM	CMB	BEN	ZOP	PPD
Atlantic											
Gaichas et al. 2009	Gulf of Maine	North Atlantic	1,361	7.06	3.79	0.00	0.03	9.17	134.60	1,206.11	3,609.67
Gaichas et al. 2009	Georges Bank	North Atlantic	1,641	17.12	4.70	0.01	0.02	26.18	160.95	1,431.76	4,270.43
Zajac et al. 2008	Long Island Sound	none (near North Atlantic)	1,965	0.02	0.67	0.05	N/A	0.52	720.67	1,243.23	8,000.05
Okey 2001	Mid-Atlantic Bight	Mid-Atlantic	1,587	19.66	11.97	0.15	0.02	119.94	45.95	1389.50	13,259.07
Okey and Pugliese 2001	SE U.S. continental shelf	South Atlantic	1,076	32.03	21.09	0.04	0.01	143.00	404.84	474.50	4,335.90
Venier and Pauly 1997	Looe Key, Florida	none (near Straits of Florida)	15,466	411.93	711.55	0.32	N/A	1,321.11	10,420.84	2,600.00	30,123.75
Gulf of Mexico											
Walters et al. 2006	Gulf of Mexico	Western, Central, Eastern Gulf of Mexico	764	39.06	14.81	2.16	N/A	13.45	183.06	511.26	6,880.71
Okey et al. 2004	West Florida Shelf	Eastern Gulf of Mexico	1,078	8.01	14.55	0.13	0.00	91.66	513.67	449.84	6,986.94
Pacific											
Field and Francis 2005	N California Current	Washington-Oregon	1,012	5.47	52.04	0.21	0.02	11.78	128.40	814.10	6,618.00
Alaska											
Preikshot 2005	E Bering Sea, Gulf of Alaska	Alaska (multiple)	1,184	4.36	2.84	0.39	0.01	25.15	193.50	958.00	2,941.00
Gaichas et al. 2009	E Bering Sea	Alaska (multiple)	614	9.06	26.22	0.01	0.03	15.07	324.73	238.38	4,717.87
Gaichas et al. 2009	Gulf of Alaska	Alaska (Gulf of Alaska)	410	17.31	10.41	0.01	0.03	13.44	110.07	258.65	4,447.95
Guenette 2005	SE Alaska shelf	Alaska (multiple)	657	14.49	5.76	0.03	0.02	9.86	106.18	520.41	3,282.65
Aydin et al. 2007	E Bering Sea	Alaska (multiple)	613	4.16	27.99	0.01	0.03	176.73	166.21	238.08	4,717.86
Aydin et al. 2007	Gulf of Alaska	Alaska (multiple)	410	11.67	11.37	0.01	0.02	64.92	63.26	258.56	4,447.95
Aydin et al. 2007	Aleutian Islands	Alaska (Aleutian Arc)	1,011	38.80	18.12	0.00	73.50	75.50	73.50	731.81	5,203.93
Aydin et al. 2003	E Subarctic Pacific Basin	Alaska (multiple)	2,817	6.47	0.16	0.01	0.00	16.65	N/A	2,793.39	12,798.80
Heymans 2005	W and C Aleutian Islands	Alaska (Aleutian Arc)	862	22.21	13.36	0.03	0.03	12.76	126.89	686.99	2,252.15

Abbreviations: BEN = macro-, meio-, and micro-benthos; CMB = crustaceans, molluscs, and other mega-benthos; DEM = demersal fishes; MAM = marine mammals; N/A = not available; PEL = pelagic fishes; PPD = primary producers; SKR = sharks and rays; SYSTEM = total ecosystem secondary and tertiary productivity, excluding PPD; ZOP = zooplankton.

5.5.1 Atlantic Region

Six Ecopath models were reviewed for Atlantic OCS planning areas. In the North Atlantic, models have been developed for Long Island Sound (Zajac et al. 2008), the Gulf of Maine, and Georges Bank (Gaichas et al. 2009). All three ecosystems have comparable system productivity (1,965, 1,361, and 1,641 t km^{-2} y^{-1}, respectively). However, the major contributors of secondary production differ between the systems. Benthos contributes over 35% of the secondary productivity in Long Island Sound, but less than 10% in the Gulf of Maine and Georges Banks systems. This would be expected, as coastal and estuarine ecosystems are generally more productive. However, this could also represent a bias in sampling, as benthos samples are easier to collect in more shallow and enclosed environments. Georges Bank has the highest amount of productivity coming from pelagic fishes. Homarid lobsters and gadoid fishes are important commercial species in the North Atlantic region. Also, large attached algal species contribute significantly to primary productivity of the region (CSA 1991b).

Mid-Atlantic and South Atlantic planning areas are represented in models of the Mid-Atlantic Bight (Okey 2001) and the southeast U.S. continental shelf (Okey and Pugliese 2001). The study area for the Mid-Atlantic Bight model extends from Cape Cod, MA to Cape Hatteras, NC. The model includes 55 functional groups. Total secondary productivity of the system is estimated to be 1,587 t km^{-2} y^{-1}. The southeast continental shelf model covers the area between Cape Hatteras, NC and the Florida Keys. A transitional region around Cape Canaveral, FL separates the southeast shelf into two distinct areas. The model included 42 functional groups, and special interest was placed on baleen whales in the region. Secondary production for the ecosystem is approximately 1,076 t km^{-2} y^{-1} (Okey and Pugliese 2001). Important ecosystem and habitats in the Mid-Atlantic and South Atlantic planning areas are sensitive barrier island ecosystems and shellfish reefs. Penaeid shrimp and sciaenid fishes are commercially important species in the South Atlantic Planning Area (CSA 1991b).

A model of Looe Key (Venier and Pauly 1997) is representative of ecosystems in the Straits of Florida. The Looe Key National Marine Sanctuary (30 km^2 area) was used as a representative of an ecosystem to examine coral reefs in the Florida Straits (Venier and Pauly 1997). Before this model was developed, no ecosystem models existed for Florida coral reef systems. One goal of the study was to predict ecosystem response to management options. Twenty functional groups were included, and the model was compared to other coral reef ecosystem models from the Caribbean and elsewhere. Looe Key is significantly more productive than any other ecosystem modeled in the Atlantic OCS (15,466 t km^{-2} y^{-1}) and is actually the most productive of all ecosystems examined in the U.S. OCS; its high productivity is likely a result of high benthic productivity associated with coral reef habitats. Important commercial species in the region include palinurid lobsters and penaeid shrimp (CSA 1991b). High values for biomass and ecotrophic efficiency parameters indicate that Looe Key is a mature ecosystem (Venier and Pauly 1997).

5.5.2 Gulf of Mexico Region

Two Ecopath models covering planning areas in the Gulf of Mexico were reviewed. The Gulf of Mexico was modeled at the Gulf-scale, with an emphasis on coastal areas (Walters et al. 2006). The model included 63 functional groups and was developed to examine ecosystem response to changes in fisheries management and primary productivity rates over the 1950-2004 time period. Secondary production for the Gulf of Mexico (including Western, Central, and Eastern Gulf of Mexico planning areas) is estimated to be 764 t km^{-2} y^{-1} (Walters et al. 2006).

A series of simulations was conducted with Ecopath to evaluate the potential effects of shading by phytoplankton blooms on community organization of the West Florida Shelf (Okey et al. 2004). This model included 59 functional groups. Total secondary productivity for the West Florida Shelf (Eastern Gulf of Mexico Planning Area) is approximately 1,078 t km^{-2} y^{-1}. The eastern Gulf of Mexico supports productive coral reef habitats, thus, this region is expected to have the highest productivity of the three Gulf of Mexico planning areas.

The Gulf of Mexico is ecologically and economically important. The Gulf is home for a diverse and productive faunal community, and contains a significant percentage of U.S. salt marsh habitats. Fishing in the Gulf is a multi-billion dollar industry, supporting a large number of its coastal residents. The Gulf of Mexico accounts for a large percentage of the total U.S. landings, for shrimp (83% of total U.S. landings from Gulf), oysters (56%), and fish (14%) (NOAA 2008). The most productive fishing ports are located in Louisiana and Texas. Penaeid shrimp and sciaenid fishes are commercially important to the region (MMS 1991). Top species landed in the Gulf (by poundage) are menhaden, brown shrimp, white shrimp, blue crab, and the Eastern oyster (average for 2004-2006; NOAA 2008).

The Gulf of Mexico is also an important resource for oil and gas exploration and drilling activities, with more than half of the U.S. crude oil (52%) and natural gas (54%) production coming from the Gulf. Over 4,000 oil and gas platforms exist in the Gulf of Mexico. This is also an important industry for Gulf coast residents, with over $12 billion in wages earned by those employed by the oil and gas industry in the U.S. Gulf coast region (NOAA 2008).

5.5.3 Pacific Region

The U.S. Pacific includes four OCS planning areas: Washington-Oregon, Northern California, Central California and Southern California. The region is characterized by rocky intertidal shorelines and extensive kelp beds. Prominent functional groups in the region include marine mammals and salmonid fishes. The Northern California Current (NCC) is an important upwelling ecosystem located between Cape Mendocino, California and Cape Flattery, Washington and acts as a transition zone between California and the Aleutian Islands.

Two Ecopath models (representing 1960's and 1990's ecosystem characteristics) each containing 63 functional groups, were built for the Northern California Current ecosystem (Field and Francis 2005). Total secondary production for this ecosystem is approximately 1,012 t km^{-2} y^{-1} (based on the 1990 model). The Northern California Current ecosystem is of special interest as it represents habitat for many migratory species. Humpback whales and northern fur seals migrate between this region and Alaska, and many birds, including the sooty shearwater, migrate between the Northern California Current and the southern hemisphere (Field et al. 2006).

5.5.4 Alaska OCS Region

The waters surrounding Alaska are divided into 15 OCS planning areas: Chukchi Sea, Beaufort Sea, Hope Basin, Navarin Basin, North Aleutian Basin, St. George Basin, Norton Basin, Cook Inlet, Gulf of Alaska, Shumagin, Kodiak, Aleutian Arc, Aleutian Basin, Bowers Basin, and St. Matthew-Hall. Many Ecopath models have been constructed for Alaskan ecosystems, focusing on Eastern Bering Sea, Aleutian Islands, and Gulf of Alaska ecosystems. Common objectives for modeling Alaskan ecosystems include examining decline in marine mammal populations, especially Steller sea lions (Heymans 2005; Guenette 2005). Also, predicting ecosystem responses to fisheries management options and climate change is of special interest in Alaskan ecosystems (Aydin et al. 2003, 2007; Preikshot 2005).

Nine Ecopath models were reviewed for the Alaska Region. Eastern Bering Sea ecosystems are represented in three of the reviewed Ecopath models (Preikshot 2005; Aydin et al. 2007; Gaichas et al. 2009). The study area of the Preikshot model (2005) extends into the Gulf of Alaska as well. Four additional models cover ecosystems within the Gulf of Alaska region (Aydin et al. 2003, 2007; Guenette 2005; Gaichas et al. 2009). Two models focus on Aleutian Island ecosystems (Heymans 2005; Aydin et al. 2007). Estimates of total secondary production for Alaskan ecosystems range from 410 t km^{-2} y^{-1} in the Gulf of Alaska (Aydin et al. 2007; Gaichas et al. 2009) to 2,817 t km^{-2} y^{-1} in the eastern subarctic Pacific basin (Aydin et al. 2003).

Preikshot (2005) modeled the region from the eastern Bering Sea to the Gulf of Alaska, covering a total area of approximately 1,500,000 km^2. OCS planning areas included in the model area include Aleutian Arc, St. George Basin, St. Matthew-Hall, North Aleutian Basin, Shumagin, Kodiak, Gulf of Alaska, and Cook Inlet. The time frame for the model covers the 1950's to 2005, and 56 functional groups were included. The model was developed to organize available information and data about trophic dynamics of the ecosystem, and to examine the effects of fisheries and climate change. Total secondary productivity of the system is estimated at 1,184 t km^{-2} y^{-1} (Preikshot 2005).

Three Ecopath models were built to enable comparison of ecosystem structure in three Alaskan regions: eastern Bering Sea, Gulf of Alaska, and the Aleutian Islands (Aydin et al. 2007). The eastern Bering Sea model included 148 functional groups and covered an area of approximately 495,218 km^2 (including North Aleutian Basin, St. George Basin, and St. Matthew-Hall planning areas). The Gulf of Alaska model included 138 functional groups, covering an area of 291,840 km^2 in the Shumagin, Kodiak, Gulf of Alaska, and Cook Inlet planning areas. The model for the Aleutian Islands included 140 functional groups and covered approximately 57,000 km^2 in the Aleutian Arc Planning Area. The models were built with data for the years 1990-1994 (Aydin et al. 2007). The eastern Bering Sea and Gulf of Alaska have similar estimates for total secondary productivity, 613 and 410 t km^{-2} y^{-1}, respectively. The Aleutian Islands ecosystem is estimated to be more productive, with an estimated total secondary productivity of 1,011 t km^{-2} y^{-1}. Model comparisons show evidence of different food web structure in each ecosystem. This is an important consideration for fisheries management of these areas (Aydin et al. 2007).

The eastern subarctic Pacific basin was modeled to increase understanding of how the gyre ecosystem responds to changes (Aydin et al. 2003). This ecosystem is found within the

Shumagin, Kodiak, and Gulf of Alaska planning areas. Focus was on mammal, salmon, and squid functional groups; 55 total functional groups were included. The reference period of the data was from the late 1980's through the early 1990's. Total secondary production of the system is estimated to be 2,817 t km^{-2} y^{-1}, and represents the most productive system of those reviewed in this analysis.

A model of the southeast Alaska shelf (Gulf of Alaska Planning Area) was developed to examine the decline of Steller sea lions in the region (Guenette 2005). Data were obtained for 1999, and 39 functional groups were included in the model. Estimated secondary productivity of the system is 657 t km^{-2} y^{-1} (Guenette 2005).

Eastern Bering Sea and Gulf of Alaska ecosystems were also modeled by Gaichas et al. (2009). The eastern Bering Sea model included 148 functional groups, and the Gulf of Alaska model included 138 groups. These groups were aggregated into 17 common functional groups to facilitate ecosystem comparison. Both models utilized data from the early 1990's. The ecosystems were found to have similar system secondary productivity: 614 t km^{-2} y^{-1} in the eastern Bering Sea and 410 t km^{-2} y^{-1} in the Gulf of Alaska (Gaichas et al. 2009).

The cold, productive waters of Alaska attract populations of whales, sea lions, and other marine mammals. Abundant marine mammal populations are often an indicator of high primary productivity, and subsequently secondary productivity is higher in these areas (McRoy 1999). Alaska ecosystems are also home to several important commercial fishery species, including salmonid fishes and crabs (CSA 1991b). Overall, the reviewed Ecopath models indicate that the eastern subarctic Pacific basin is the most productive ecosystem within the Alaska OCS planning areas.

6.0 Empirical Measures Related to Secondary and Tertiary Production

Section 5 discussed the conceptual basis of secondary and tertiary production and provided estimates for several planning areas based on published Ecopath modeling studies. This section focuses on two empirical measures of secondary and tertiary production: zooplankton biomass and commercial fishery landings.

While it is difficult to measure secondary production, it is relatively easy to measure zooplankton biomass, which is a key component of models used to calculate production (Banse and Moser 1980). Zooplankton biomass data are widely available from field sampling studies, and are routinely monitored in some areas. These data can be used to estimate secondary productivity of the water column. Zooplankton biomass and data sources are discussed in **Appendix C**; a series of figures present zooplankton data, by region and period of sampling (e.g., average annual, seasonal, monthly).

Commercial fisheries landings can also be considered an indicator of tertiary production, although there are substantial caveats as noted below. Commercial fishery landing reports are required by Federal and State resource agencies, and these data are widely reported on the Internet. Data sources for commercial fisheries landings are discussed in **Appendix C**.

6.1 Zooplankton Biomass

The Coastal and Oceanic Plankton Ecology, Production and Observation Database (COPEPOD) contains zooplankton and phytoplankton data from samples collected globally. The database is managed by the NMFS and can be accessed online free of charge (http://www.st.nmfs.noaa.gov/plankton/). COPEPOD was created in an effort to make global plankton data readily available to scientists and managers. Data were obtained via Continuous Plankton Recorder (CPR) surveys, either by “ships of opportunity” or during designated research and sampling cruises.

In the current analysis, zooplankton data were obtained via the COPEPOD online database for each of the 26 OCS planning areas. More data were available for Alaska (2000-2008) than for other planning areas; data from the Atlantic (2000-2001) and Pacific (2006) were the most sparse. Yearly and/or seasonal zooplankton data are plotted individually in **Appendix C**, with the exception of 2008 data for Alaska. Overall, it is clear that the Alaska OCS Region, especially in the Chukchi Sea, had the highest average zooplankton biomass relative to other planning areas (**Figure 44**).

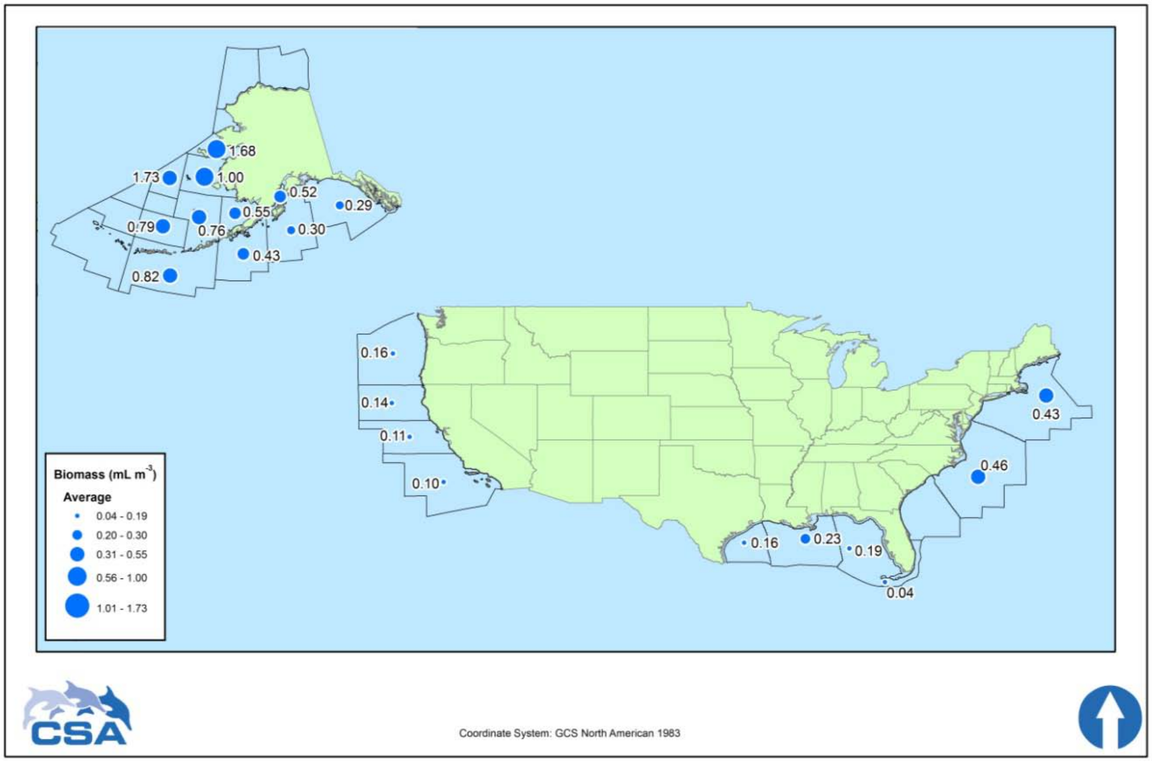

Figure 44. Average zooplankton biomass (displacement volume, mL m^{-3}) within the OCS planning areas. Zooplankton data periods include Alaska (2000-2007), Pacific (2006), California (2000-2006), Gulf of Mexico (2000-2003), and Atlantic (2000-2001). See **Appendix C** for data used to calculate the average by planning area.

Table 12 summarizes available zooplankton data by planning area, based on the data accessed via COPEPOD. Zooplankton data were characterized based on the temporal (i.e., monthly, seasonal, average annual; single year or multiyear) and spatial (i.e., extensive, moderate, or limited; nearshore vs. offshore) characteristics.

Several of the planning areas have extensive sampling coverage. For example, the Southern California Planning Area has an extensive multiyear, seasonal sampling effort (i.e., the CalCOFI grid) which covers a majority of the planning area. In other instances, other planning areas (e.g., South Atlantic, Straits of Florida) have virtually no zooplankton data archived within COPEPOD. Several planning areas have inconsistent coverage, where zooplankton data are available for some years but not for others, or where only selected seasons have been sampled.

The spatial distribution of zooplankton sampling efforts are also disproportionate. For example, several of the Alaska planning areas have extensive nearshore sampling, with only a limited number of stations in deeper water. Differences in sampling points are often by orders of magnitude from the others. Based on the review of the COPEPOD database, no zooplankton data are archived for the Beaufort and Chukchi Sea planning areas. In the North and Mid-Atlantic planning areas, offshore coverage is extensive to the north (e.g., Georges Bank), whereas zooplankton sampling is closer to shore as one moves south.

Table 12. Summary of zooplankton data sources accessed through COPEPOD.

Planning Area	Zooplankton Studies/Sources	Coverage Years	Spatial Coverage[1]	Comments
Atlantic				
North Atlantic	EcoMon-RV	2000-2001	Extensive	Seasonal (4 seasons); nearshore and offshore, with Georges Bank predominant
Mid-Atlantic	EcoMon	2000-2001	Extensive	Seasonal (4 seasons); nearshore and offshore, but predominantly nearshore
South Atlantic	EcoMon	2000-2001	Limited	Seasonal (4 seasons); very few samples
Straits of Florida	EcoMon	2000-2001	Limited	Seasonal (4 seasons)
Gulf of Mexico				
Eastern Gulf	SEAMAP	2000-2003	Moderate to Extensive	Mix of monthly, seasonal and average annual; inshore and offshore
Central Gulf	SEAMAP	2000-2003	Moderate to Extensive	Mix of monthly, seasonal and average annual; inshore and offshore
Western Gulf	SEAMAP	2000-2003	Moderate to Extensive	Mix of monthly, seasonal and average annual; inshore and offshore
Pacific				
Southern California	CalCOFI, ORCAWALE	2000-2006	Extensive	Annual average for 2000-2005; seasonal for 2006; inshore and offshore
Central California	CalCOFI, ORCAWALE	2000-2006	Extensive	Annual average for 2000-2005; seasonal for 2006; inshore and offshore
Northern California	EcoFOCI, ORCAWALE	2000-2006	Moderate to Extensive	Annual average for 2001 and 2006
Washington-Oregon	EcoFOCI, ORCAWALE	2000-2006	Moderate to Extensive	Annual average for 2001 and 2006
Alaska				
Gulf of Alaska	EcoFOCI	2000-2008	Extensive	Yearly average; predominantly shallow water
Cook Inlet	EcoFOCI	2000-2008	Extensive	Yearly average; predominantly shallow water
Kodiak	EcoFOCI	2000-2008	Extensive	Yearly average; predominantly shallow water
Shumagin	EcoFOCI	2000-2008	Extensive	Yearly average
Aleutian Arc	EcoFOCI	2000-2008	Moderate	Yearly average
N. Aleutian Basin	EcoFOCI	2000-2008	Moderate	Yearly average
St. George Basin	EcoFOCI	2000-2008	Moderate	Yearly average
Bowers Basin	EcoFOCI	2000-2008	Moderate	Yearly average
Aleutian Basin	EcoFOCI	2000-2008	Moderate	Yearly average
Navarin Basin	EcoFOCI	2000-2008	Limited	Yearly average
St. Matthew-Hall	EcoFOCI	2000-2008	Limited	Yearly average
Norton Basin	EcoFOCI	2000-2008	Limited	Yearly average
Hope Basin	EcoFOCI	2000-2008	Limited	Yearly average
Chukchi Sea	None	None	None	No zooplankton data archived in COPEPOD
Beaufort Sea	None	None	None	No zooplankton data archived in COPEPOD

[1] Spatial coverage descriptors for zooplankton data sets found within COPEPOD – none, limited, moderate, and extensive – for each respective planning area; categories based on professional judgment of the author.

6.2 Fisheries Landings

While it is common for many people to refer to fisheries harvest as productivity, it is not really the same as ecological productivity, and tertiary production can be very different from harvest. Fisheries harvest is driven primarily by economic and regulatory factors. Costs to capture fishery species (such as the price of fuel, equipment, insurance, labor, and supplies) have to be offset by the wholesale prices of the product, and the market changes continually.

State and Federal regulations, treaties, and international agreements govern how much, when, and where fishery species are harvested, and this is often without regard to the actual productivity of the ecosystem. Finally, fishery species go through boom-and-bust cycles, regime shifts, and dramatic alteration by fishing itself. Thus, there are ecological factors interacting with socioeconomic factors that drive fishery species growth, reproduction, and survival, and thus total gross and net tertiary productivity.

Commercial fishery landings data are obtained by NFMS from trip tickets, landing reports, logbooks, and examination of catches (NMFS Data Caveats). Total landings by state are the most accurate because confidential data are included. In more specific datasets (e.g., species landings), confidential data are handled in such a way as to maintain confidentiality. This may result in misleading data, as confidential landings are grouped with other data.

For the current analysis, commercial landings of fish and invertebrates data were obtained for 2008 for each state from NMFS. Landings are reported in aggregated groups of fishes and invertebrates, in pounds (live weight), and in pounds of meat for bivalves (excluding shells). Commercial fishery landings (millions of pounds) are also reported by port. Landings for major U.S. ports were obtained for 2008 from NMFS. Additional landings for the Gulf of Mexico shrimp fishery were also collected from NMFS. This dataset contains shrimp landings (i.e., headless, thousands of pounds) for the months January through May for the years 2006 through 2010.

Fisheries landings data by planning area, with the exception of the Alaska region, are graphically depicted in **Appendix C** (see **Figures C-42** through **C-44**). In the Atlantic Region, Virginia (Mid-Atlantic Planning Area) and Massachusetts and Maine (North Atlantic Planning Area) reported the highest landings by weight. In the Gulf of Mexico Region, Louisiana (Central Gulf of Mexico Planning Area) landings were dominant among the Gulf states. In the Pacific Region, California landings (including Southern California, Central California, and Northern California planning areas) were slightly higher than those shown for Washington and Oregon (Washington-Oregon Planning Area). Alaska statewide landings were exceptionally high compared to all other states.

The fishery landings data are reported by State, however, there are inherent difficulties in assessing all landings data – while landings may be reported for a particular state, it is not easily determined where (i.e., from what planning area) fish were caught. This problem is particularly acute in the Alaska landings data due to the high number of planning areas and their geographic coverage relative to the number of ports (**Figure 45**). While Alaska has the highest amount of finfish harvest, the Gulf of Mexico (especially the Central Gulf of Mexico Planning Area) has the highest amount of shrimp productivity.

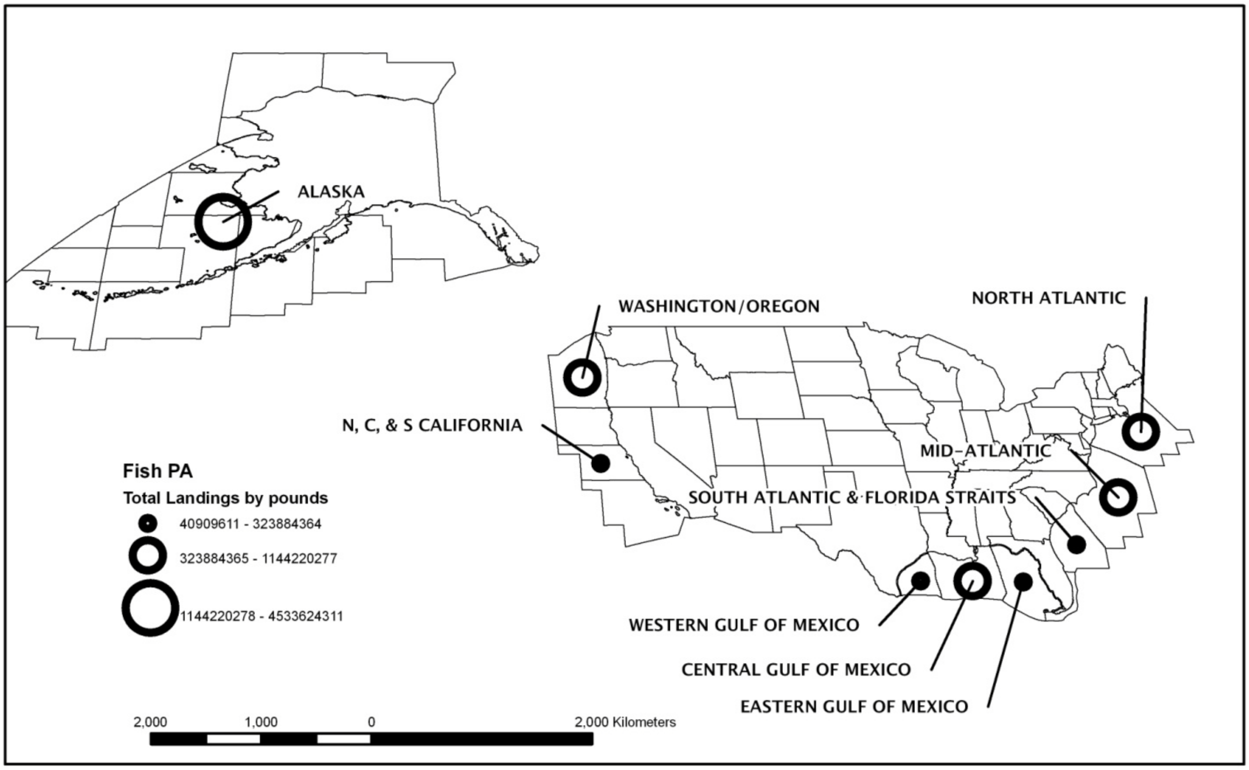

Figure 45. Fishery landings by state in 2008 reported by the National Marine Fisheries Service. Landings include finfishes and invertebrates (headless shrimp and meat for bivalves). See **Appendix C** for detailed data.

7.0 Discussion

7.1 Summary and Comparisons of Productivity Among Planning Areas

7.1.1 Primary Productivity

7.1.1.1 Satellite-Derived Productivity Estimates

Table 13 lists the summary primary productivity statistics for each planning area, including annual NPP (in million tons C), annual NPP variability (a measure of relative interannual variance), monthly NPP variability (a measure of seasonality), and annual NPP trend. The total integrated annual primary productivity varies substantially from area to area (**Table 13**, **Figure 46**), ranging between 5.99±0.51 million tons C for the Straits of Florida and 195.07±14.98 million tons C for the Aleutian Arc, a change of >30 fold. Normalization to the acreage for each area yield annual primary productivity per acre, which shows less variability among the 26 areas (**Figure 47**). Nearly all planning areas within the Alaska Region exhibited annual primary productivity between 0.5 and 1.7 million tons C acre^{-1}, a variation of ~<3-fold; the two exceptions were the Chukchi Sea and Beaufort Sea planning areas, where primary productivity levels were extremely low.

In general, small differences in annual NPP were noted between the regions. The Pacific Region exhibited the highest annual primary productivity per acre (>1.1 for all four planning areas). The Gulf of Mexico Region also exhibited high annual primary productivity per acre (>0.9) for its three planning areas, while the Atlantic Region showed diversified results, with relatively low productivity (<0.9) for all areas except the North Atlantic. Significant variability is found in the Alaska Region, with the lowest annual primary productivity per acre found in the Beaufort Sea (0.1) and the highest in Cook Inlet (>1.6). However, the accuracy of the primary productivity in this region may be substantially lower than in other regions due to several reasons described below.

First, it is well known that in turbid coastal waters, chlorophyll-*a* concentration can be significantly overestimated (>100%) from satellite measurements due to algorithm artifacts in the atmospheric correction and bio-optical inversion (Hu et al. 2003). Although there is lack of *in situ* data, most of the Cook Inlet waters are believed to be turbid coastal waters with biased chlorophyll-*a* estimates (Speckman et al. 2005). Thus, for Cook Inlet, the annual primary productivity may be overestimated. A similar argument may also apply to other areas where turbid coastal waters represent a significant portion of the planning area.

Second, due to seasonal solar insolation effects (i.e., extreme seasonal variability in solar radiation at higher latitudes), most of the areas in the Alaska Region are limited by sunlight. For example, for the Beaufort Sea, there is no single monthly measurement between 1999 and 2001 that met the 75% area coverage criteria, leading to no data during a 3-y period. A similar situation is found for the Chukchi Sea and Hope Basin. During several winter months, no monthly PAR data or chlorophyll data exist for the Navarin Basin, Matthew-Hall, and Norton Basin. This lack of data creates more uncertainty in the annual primary productivity estimates. Adding to this issue is the often persistent cloud cover in these high-latitude areas. Although monthly composites were used to minimize the cloud influence, persistent cloud cover may limit our ability to assess the “mean” state of ocean biomass (chlorophyll-*a* concentration).

Table 13. Net primary productivity statistics for the 26 Outer Continental Shelf planning areas.

Region and Planning Area	Acreage (million acres)	Annual NPP[1] (million tons C)	Annual NPP (min–max)	Annual Variability[2] (%)	Monthly Variability[3] (%)	Annual Trend[4]
Atlantic Region						
North Atlantic	92.32	137.01±8.51	125.94 – 156.14	6.21	32.47	+, p=0.90
Mid-Atlantic	112.83	55.79±2.59	50.31 – 59.45	4.64	25.18	-, p=0.70
South Atlantic	54.34	49.59±4.44	41.15 – 58.51	8.95	26.86	-, p=0.97
Straits of Florida	9.64	5.99±0.51	5.40 – 7.11	8.51	22.50	-, p=0.23
Gulf of Mexico Region						
Eastern Gulf of Mexico	64.56	60.42±6.98	52.77 – 75.43	11.55	23.49	-, p=0.38
Central Gulf of Mexico	66.45	87.17±9.13	72.08 – 101.12	10.68	28.03	+, p=0.50
Western Gulf of Mexico	28.58	33.99±3.13	28.52 – 39.95	9.21	33.58	+, p=0.18
Pacific Region						
Southern California	88.98	100.45±10.95	78.51 – 117.93	10.90	21.38	**+, p<0.01**
Central California	43.68	60.23±6.70	48.22 – 75.99	11.12	25.82	**+, p=0.02**
Northern California	44.79	52.26±3.13	47.87 – 56.72	5.99	27.61	**+, p<0.01**
Washington-Oregon	71.00	89.89±7.43	78.08 – 100.97	8.26	43.59	**+, p<0.01**
Alaska Region						
Gulf of Alaska	112.10	124.97±4.82	117.36 – 131.80	3.86	50.10	+, p=0.74
Cook Inlet	5.36	8.97±0.61	7.95 – 9.75	6.80	58.30	-, p=0.63
Kodiak	89.00	82.73±4.18	74.66 – 88.42	5.05	49.11	-, p=0.05
Shumagin	84.65	78.19±6.04	65.35 – 86.87	7.72	53.98	**-, p=0.01**
Aleutian Arc	259.06	195.07±14.98	171.25 – 217.48	7.68	55.64	-, p=0.33
N. Aleutian Basin	32.45	39.73±6.90	28.97 – 50.08	17.37	43.93	-, p=0.88
St. George Basin	70.23	72.38±10.31	57.35 – 91.70	14.24	56.93	-, p=0.27
Bowers Basin	87.59	60.09±6.22	50.67 – 68.20	10.35	56.93	+, p=0.60
Aleutian Basin	41.33	30.96±4.17	25.10 – 37.71	13.47	69.29	-, p=0.90
Navarin Basin	34.02	26.75±6.26	17.97 – 37.32	23.40	58.83	-, p=0.71
St. Matthew-Hall	54.57	52.09±7.20	39.74 – 62.90	13.82	29.66	-, p=0.60
Norton Basin	24.25	34.07±4.00	26.81 – 40.69	11.74	44.27	**+, p=0.02**
Hope Basin	12.82	12.01±2.67	7.72 – 16.27	22.23	30.66	**+, p<0.01**
Chukchi Sea	62.59	10.64±5.41	2.93 – 21.63	50.85	38.02	**+, p=0.03**
Beaufort Sea	65.08	8.02±6.35	1.11 – 16.75	79.17	59.29	-, p=0.65

[1] Annual NPP is expressed in mean ± standard deviation.

[2] Annual NPP variability is expressed in (standard deviation/mean) x 100%.

[3] Monthly NPP variability is defined as (standard deviation/mean) x 100% for all valid months.

[4] Trend analysis is from linear regression between annual NPP and time. + = increasing trend; – = decreasing trend. $p < 0.05$ (highlighted in bold font) indicates significant trend.

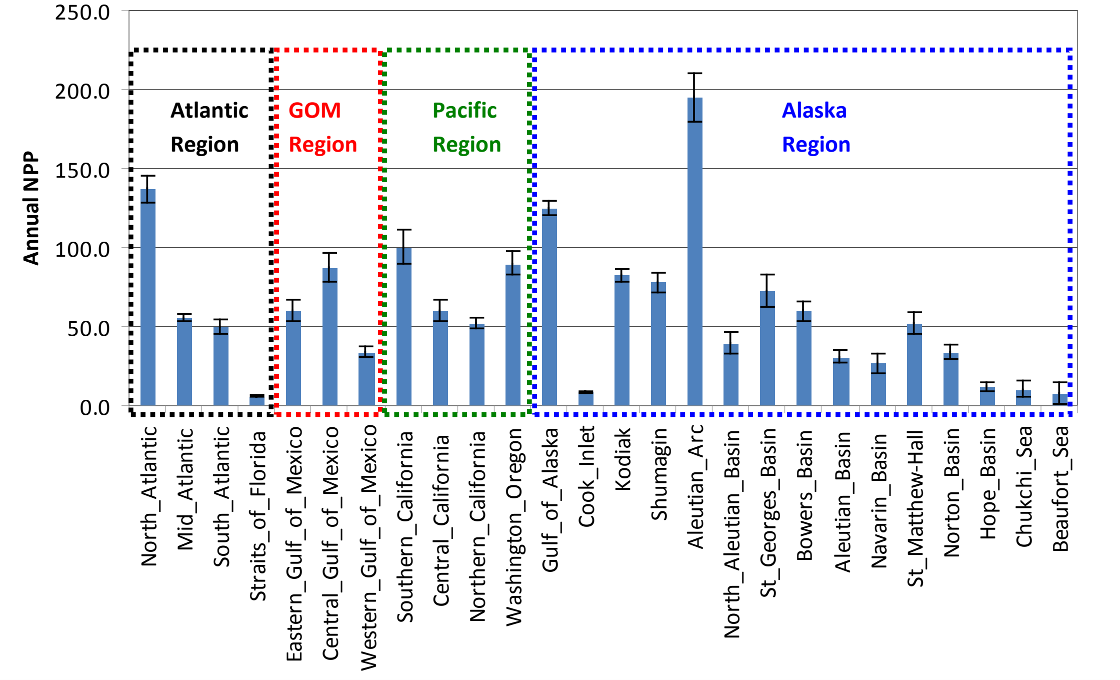

Figure 46. Total annual net primary production (NPP) (million metric tons C) between 1998 and 2009 for each of the 26 Outer Continental Shelf planning areas. Values represent the mean ± standard deviation of 12 annual values for the 1998-2009 period.

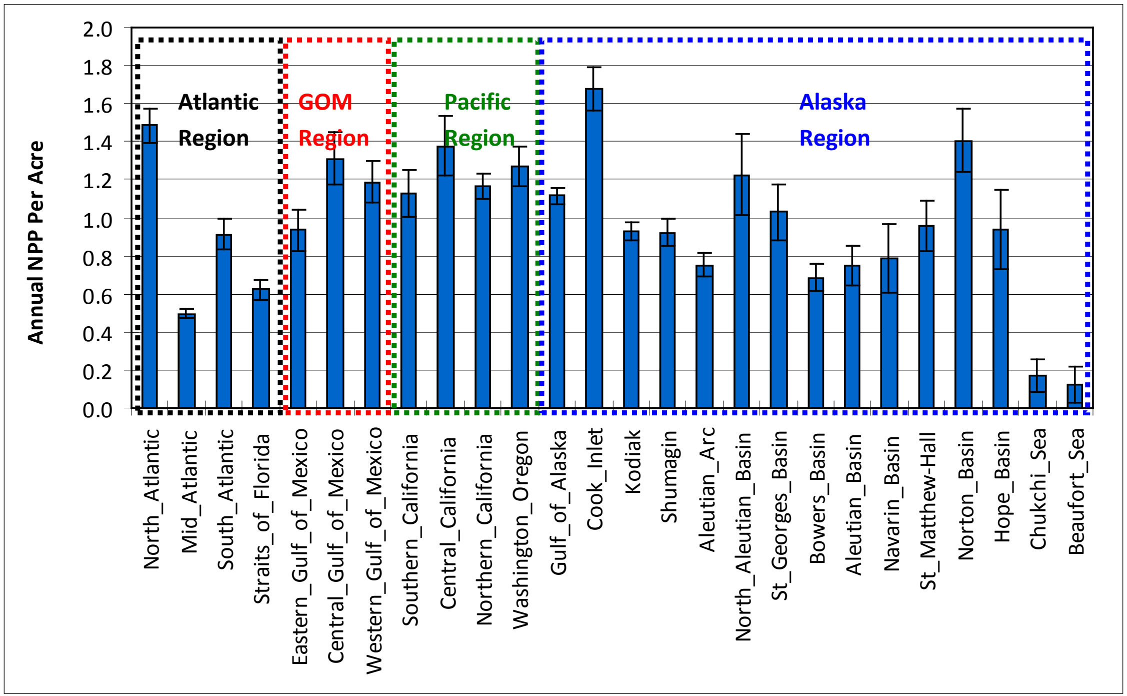

Figure 47. Total annual net primary production (NPP) (metric tons C) per acre between 1998 and 2009 for each of the 26 Outer Continental Shelf planning areas. Values represent the mean ± standard deviation of 12 annual values for the 1998-2009 period, standardized per unit area (acres).

For example, if only 1 of the 30 days is cloud-free, chlorophyll-*a* concentration from that day is used to represent the monthly mean. Clearly, this induces large uncertainties, often called "temporal aliasing." In low latitude areas, such uncertainties are minimized due to fast-changing clouds.

Third, the calculations are based on a community-accepted NPP model. Although various studies showed the validity of this model in assessing primary productivity in marginal seas (Gong et al. 2000) and upwelling systems (Müller-Karger et al. 2004), some degree of uncertainty is expected from the model as applied to all 26 OCS planning areas. Global assessments of satellite-based chlorophyll-*a* estimates suggest uncertainty (RMS difference from *in situ* data, not bias) of about 50% for most open ocean waters (Gregg et al. 2005). Without systematic *in situ* validation, the uncertainties in these annual primary productivity estimates are similar (i.e., 50% RMS difference). For areas with significant coverage of turbid coastal waters, in addition to this uncertainty, some positive bias may exist. In any case, however, the seasonality and annual variability results are valid and independent of these uncertainties and potential bias. This is because that although the absolute values of primary productivity may be biased due to a variety of reasons, these hidden errors are expected to be consistent in time, and therefore will not affect the temporal patterns observed above.

Substantial interannual variability in primary productivity is found in several of the planning areas, with the highest interannual variability evident in the Alaska. For example, interannual variability for the Beaufort Sea is 79.17%, with annual primary productivity varying by >10-fold (minimum: 1.11, maximum: 16.75). Similar interannual variability is found for the Chukchi Sea (2.93-21.63, with interannual variability = 50.85%). Ten of the 15 Alaska planning areas exhibited interannual variability >10%, all of which occur in high latitudes. In contrast, most of the remaining planning areas from the other three regions show interannual variability <10%. It is suggested that this difference is due to the fact that high-latitude areas are more light-limited. Persistent cloud cover may also present a significant influence on the available surface light (e.g., one cloud-free day and zero cloud-free days in a certain month will result in dramatic difference in the monthly mean PAR data). In contrast, low latitude areas are less sensitive to cloudiness as long as the cloud cover is not persistent over time.

Although interannual variability revealed no trend among the four regions (e.g., within the Alaska Region, the variability ranges from <4% to >50%, and the variability is similar among the other three regions), there is a clear trend in the seasonality (i.e., relative monthly variance) which increases from low-latitude areas to high-latitude areas. For the three regions of the contiguous U.S. (i.e., Atlantic, Gulf of Mexico, and Pacific), all planning areas exhibited <30% seasonality, with the exception of the Washington-Oregon, Western Gulf of Mexico, and North Atlantic planning areas. In contrast, in the Alaska Region, all areas reflected >40% seasonality (with the highest, 69%, in the Aleutian Basin), with the exception of the St. Matthew-Hall, Hope Basin, and Chukchi Sea planning areas. This apparent trend in latitude-based seasonality is not simply a result of variability in solar insolation, but may also be affected by several factors including water mixing and upwelling. For example, in the Gulf of Mexico, deep-mixing of nutrient-rich waters during winter results in high phytoplankton biomass and high primary productivity, while summer stratification leads to lower biomass and productivity (Müller-Karger et al. 1991). The coastal regions are also affected by coastal runoff from the Mississippi River and other rivers (Lohrenz et al. 1997). In contrast, in high-latitude areas of the Alaska Region, seasonal variations in primary productivity (i.e., summer highs and winter lows) appear to be driven by solar insolation and other factors including ice cover, circulation, vertical mixing, and nutrient availability (Coachman 1986; Brickley and Thomas 2004; Rho 2004; Childers et al. 2005; Kopylow et al. 2005; Jin et al. 2007). The seasonality of the Pacific Region is driven by solar insolation, local upwelling, circulation (e.g., California Current), coastal runoff, and other processes (Huyer 1983; Hayward 1998; Firme et al. 2003; Legaard and Thomas 2006; Kahru et al. 2009). The seasonality of the Atlantic Region is driven by solar insolation (for high latitude areas showing summer highs) and winter mixing (for low latitude areas showing winter highs), lateral transport, rainfall, and other processes (Li et al. 1993; Falkowski et al. 1994; Paerl et al. 1999; Gregg et al. 2005). Future effort should be made to collect extensive *in situ* data to validate these satellite-based observations.

7.1.1.2 Comparisons Between 1990 and 2010 Primary Productivity Determinations

As summarized in **Section 2.1**, a majority of the data review and evaluation presented in the previous productivity summary (CSA 1990) focused on quantitative measurement (i.e., based on the Winkler oxygen technique, the Carpenter modification, or uptake of ^{14}C labeled bicarbonate [$H^{14}C0_3^-$]), as reported in the literature. Limitations and qualifications to these data were identified by CSA (1990), concurrently with the evolution evident in measurement techniques (e.g., shorter-term uptake experiments, use of a series of different light intensities) and the reporting of "P vs. I" curves (i.e., the "photosynthetron" technique). Given these limitations, CSA (1990) presented daily and annual primary productivity estimates for each of the 26 OCS planning areas, often subdividing each planning area by regime/domain, upwelling/non-upwelling period, or season.

Table 14 summarizes primary productivity information for each of the 26 OCS planning areas, as presented in the CSA (1990) report, and compares those to the current 2010 primary productivity estimates on the basis of estimated annual production (g C m^{-2} y^{-1}). Estimates for 1990 were based exclusively on quantitative measurements conducted in the field or in the laboratory, as reported in the peer-reviewed and gray literature. The 2010 estimates are based on satellite-derived determinations using the NPP modeling approach. Estimates for 2010, as presented in **Table 14**, were derived from primary productivity ranges presented in **Table 13**.

Since 1990, there have been minor boundary adjustments to select planning areas. These boundary changes have little effect on these comparisons, given that they are being made on the basis of a standard unit (i.e., g C m^{-2} y^{-1}).

In **Section 2**, it was noted that results of the round robin test produced VGPM model predictions of integrated daily production (IP, mg C m^{-2}) within a factor of 2. More importantly, global assessments of satellite-based chlorophyll-*a* estimates suggest uncertainty (RMS difference from *in situ* data) of about 50% for most open ocean waters. For this comparison, it was simply assumed that the 1990 and 2010 values were similar if the range of annual production values overlapped.

Table 14. Comparison of 1990 and 2010 annual primary production determinations. Determinations were deemed similar if the range of annual production values overlapped. Bolded entries reflect those planning areas exhibiting dissimilar values between 1990 and 2010.

Region and Planning Area	1990 Primary Productivity Estimates			2010 Primary Productivity Estimates	
	Estimated Variability in Daily Production ($g\ C\ m^{-2}\ d^{-1}$)	Estimated Annual Production ($g\ C\ m^{-2}\ y^{-1}$)	Comments	Estimated Annual Production ($g\ C\ m^{-2}\ y^{-1}$)	Comments
Atlantic Region					
North Atlantic	<0.25-3.0	260-455	Regional sampling: high; high variability (10- to 12-fold variation) evident on a seasonal basis (spring, fall bloom); tidal mixing, estuarine input, and cross shelf exchange represent the major features influencing nutrient input and production; warm core rings exhibit elevated production levels compared to adjacent waters (2.4 $g\ C\ m^{-2}\ d^{-1}$ within vs. 0.14 $g\ C\ m^{-2}\ d^{-1}$ outside)	337-418	Moderate seasonality, low interannual variability. 100% data coverage for all 144 months (12 y). Results relatively reliable. Comparable results between 1990 and 2010.
Mid-Atlantic	<0.25-3.25	**260-505**	Regional sampling: moderate to high; high variability (11- to 13-fold variation) evident; estuarine input and cross shelf exchange represent the major features influencing nutrient input and production; warm core rings also contribute to regional variation in production values	**110-130**	Moderate seasonality, low interannual variability. 100% data coverage for all 144 months (12 y). Large discrepancy between 1990 and 2010 estimates possibly due to insufficient sampling pre-1990.
South Atlantic	0.05-2.70	130-580	Regional sampling: poor to moderate; exceptionally high variability (120-fold differences) noted between upwelling and non-upwelling production (upwelling production measured as high as 6 $g\ C\ m^{-2}\ d^{-1}$); Gulf Stream dynamics (e.g., meanders, eddies) regulate production over the shelf and slope; riverine inputs influence nearshore waters, with additional mediation via inshore embayments (e.g., Pamlico Sound)	187-266	Moderate seasonality, low interannual variability. 100% data coverage for all 144 months (12 y). Comparable results between 1990 and 2010, however, 2010 estimates have a narrower range.
Straits of Florida	0.021-0.128 (embayments) 0.004-0.020 (coastal) 0.19-0.50 (offshore)	**7.6-35.4 (embayments)** **18.4 (coastal)**	Regional sampling: very poor; data base restricted (Biscayne Bay and adjacent coastal waters, offshore Biscayne Bay, Dry Tortugas); high (>10-fold variation) to low-moderate (<3-fold variation) variability evident for daily and seasonal averages, respectively; Florida Current represents the major oceanographic feature influencing production; upwelling may also contribute, however, data are unavailable	**138-182**	Moderate seasonality, low interannual variability. 100% data coverage for all 144 months (12 y). Large discrepancy between 1990 and 2010 estimates. Influence of the Gulf Stream noted. The 1990 estimates appear to be unreasonably low, when compared with the other Atlantic areas.

Table 14. (Continued).

Region and Planning Area	1990 Primary Productivity Estimates			2010 Primary Productivity Estimates	
	Estimated Variability in Daily Production (g C m^{-2} d^{-1})	Estimated Annual Production (g C m^{-2} y^{-1})	Comments	Estimated Annual Production (g C m^{-2} y^{-1})	Comments
Gulf of Mexico Region					
Eastern Gulf of Mexico	1.0-4.0 (embayments) 0.125-0.400 (coastal, non-bloom) 0.50-3.8 (coastal, bloom) 0.15-0.94 (offshore)	50-800 (embayments) 89 (coastal, non-bloom) 164 (offshore)	Regional sampling: moderate (embayments and offshore) to poor (coastal waters); high variability (5- to 6-fold variation) in coastal waters attributed to red tide dinoflagellate bloom; low-moderate to high variability evident in offshore waters; Loop Current and associated eddies represent major oceanographic features influencing production	202-289	Moderate seasonality, low interannual variability. 100% data coverage for all 144 months (12 y). Generally comparable results between 1990 and 2010.
Central Gulf of Mexico	1.1-1.3 (coastal) 0.018-0.605 (offshore)	300-400 (coastal) 115-184 (offshore)	Regional sampling: poor; data base very limited; high seasonal and interannual variability (5- to 17-fold variation) evident in coastal waters; high spatial variability (≥5-fold variation) also evident; Mississippi River discharge influences nearshore (coastal) production	268-376	Moderate seasonality, low interannual variability. 100% data coverage for all 144 months (12 y). Comparable results between 1990 and 2010.
Western Gulf of Mexico	0.10-3.0 (embayments) 0.002-0.025 (coastal) 0.29-0.36 (offshore)	**127-200 (embayments)** **103-176 (coastal)** **60-118 (offshore)**	Regional sampling: moderate (embayments and coastal) to poor (offshore); high variability evident for coastal waters; low to moderate variability suggested for offshore waters; Loop Current-associated rings may represent regions of limited increases in production	**247-345**	Moderate seasonality, low interannual variability. 100% data coverage for all 144 months (12 y). Large discrepancy between 1990 and 2010 estimates. The 1990 estimates appear to be unreasonably low when compared with the other Gulf of Mexico areas, perhaps due to uneven distribution of *in situ* measurements.

Table 14. (Continued).

Region and Planning Area	1990 Primary Productivity Estimates			2010 Primary Productivity Estimates	
	Estimated Variability in Daily Production (g C m^{-2} d^{-1})	Estimated Annual Production (g C m^{-2} y^{-1})	Comments	Estimated Annual Production (g C m^{-2} y^{-1})	Comments
Pacific Region					
Southern California	0.30-0.80 (winter) 1.0-1.5 (summer) 0.5-1.5 (mean)	275	Regional sampling: high; high variability (>10-fold variation) evident on a seasonal and interannual basis; spatial variability (patchiness) also evident; CA Current System represents the primary mediator of production; El Niño and upwelling implicated in interannual productivity changes	218-327	Moderate seasonality, low interannual variability. 100% data coverage for all 144 months (12 y). Comparable results between 1990 and 2010. Significant annual trend (increasing).
Central California	0.80-3.2 (CalCOFI) 0.6-3.0 (offshore-inshore gradient)	275-325 (offshore-inshore gradient)	Regional sampling: moderate; high variability (>5- to 10-fold variation) evident on a seasonal and interannual basis; spatial variability (patchiness) also indicated; CA Current System represents the primary mediator of production; upwelling, eddies, and fronts implicated in production increases in coastal waters; El Niño events also noteworthy	273-430	Moderate seasonality, low interannual variability. 100% data coverage for all 144 months (12 y). Comparable results between 1990 and 2010. Significant annual trend (increasing).
Northern California	0.602-2.888 (shelf)	300	Regional sampling: poor; data base limited; high variability (>5-fold variation) suggested on a seasonal and interannual basis; spatial variability (patchiness), prompted by oceanographic events, strongly suggested; major oceanographic features include wind-driven coastal upwelling (particularly proximal to major promontories) and coastal forcing processes (eddies, coastal jets, advection)	264-313	Moderate seasonality, low interannual variability. 100% data coverage for all 144 months (12 y). Comparable results between 1990 and 2010. Significant annual trend (increasing).
Washington-Oregon	0.070-2.40 (shelf) 0.319-1.360 (slope) 0.385-0.960 (mean)	126->300 (river plume and oceanic to upwelling gradient)	Regional sampling: moderate (entire planning area) to high (coastal waters influenced by Columbia River plume); high variability evident; major oceanographic features include coastal upwelling and Columbia River discharge	272-351	Moderate seasonality, low interannual variability. 100% data coverage for all 144 months (12 y). Comparable results between 1990 and 2010. Significant annual trend (increasing).

Table 14. (Continued).

Region and Planning Area	1990 Primary Productivity Estimates Estimated Variability in Daily Production (g C m^{-2} d^{-1})	 Estimated Annual Production (g C m^{-2} y^{-1})	 Comments	2010 Primary Productivity Estimates Estimated Annual Production (g C m^{-2} y^{-1})	 Comments
Alaska Region					
Gulf of Alaska	0.05-0.50 (winter to summer, offshore) No daily production data available for coastal waters	**48-100 (offshore)** **200 (coastal)**	Regional sampling: poor; extremely limited data base; variability unknown; coastal (shelf) waters influenced by the AK Stream; freshwater input evident nearshore; offshore waters influenced by the AK Gyre and the Central Subarctic Domain	**259-291**	Strong seasonality, low interannual variability. Only 108 of the 144 months showed >75% data coverage. Large discrepancy between 1990 and 2010 estimates. The 1990 estimates are significantly lower than adjacent regions due to extremely limited database.
Cook Inlet	>2.0	>300	Regional sampling: poor to moderate; extremely high variability evident, attributed to seasonality (temperature extremes, seasonal fluctuations in light intensity); AK Current and AK Coastal Current produced advection and upwelling, respectively; tidal influences in CI result in both productivity enhancement (related to tidal fronts and associated nutrient increases) and diminution (related to increased levels of glacial silt)	367-449	Strong seasonality, low interannual variability. Only 108 of the 144 months showed >75% data coverage. Comparable results between 1990 and 2010.
Kodiak	>2.0	>300	Regional sampling: poor to moderate; extremely high variability evident, attributed to seasonality (temperature extremes, seasonal fluctuations in light intensity); AK Current and AK Coastal Current produced advection and upwelling, respectively	207-245	Strong seasonality, low interannual variability. Only 108 of the 144 months showed >75% data coverage. Generally comparable results between 1990 and 2010.
Shumagin	>2.0	>300	Regional sampling: poor to moderate; extremely high variability evident, attributed to seasonality (temperature extremes, seasonal fluctuations in light intensity); AK Current and AK Coastal Current produced advection and upwelling, respectively	191-254	Strong seasonality, low interannual variability. Only 119 of the 144 months showed >75% data coverage. Generally comparable results between 1990 and 2010. Significant annual trend (decreasing).

Table 14. (Continued).

Region and Planning Area	1990 Primary Productivity Estimates			2010 Primary Productivity Estimates	
	Estimated Variability in Daily Production (g C m^{-2} d^{-1})	Estimated Annual Production (g C m^{-2} y^{-1})	Comments	Estimated Annual Production (g C m^{-2} y^{-1})	Comments
Aleutian Arc	0.10-0.15 (waters S of the Aleutians) 0.34-0.63 (waters N of the Aleutians)	30-82 (waters S of the Aleutians) 100-200 (waters N of the Aleutians)	Regional sampling: poor; variability relatively unknown, although turbulence and upwelling proximal to islands and passes produces highly variable production; major oceanographic features include the AK Stream (S of the Aleutians) and Bering Sea waters (N of the Aleutians)	163-207	Strong seasonality, low interannual variability. Only 132 of the 144 months showed >75% data coverage. Comparable results between 1990 and 2010.
N. Aleutian Basin	2.60-6.70 (Coastal Domain, upwelling) No daily production data available for the Central Domain 0.10-5.00 (Outer Domain)	50-60 (Coastal Domain, non-upwelling) 220-240 (Coastal Domain, advection and upwelling) 166-188 (Central Domain) No annual production data available for the Outer Domain 1-2 (sea ice microalgae, est.)	Regional sampling: high (PROBES); high variability evident in all three domains; major oceanographic features include Coastal Domain (tidal action, advection-diffusion), Central Domain (tidal-driven diffusion), Outer Domain (advection-spring bloom); interannual variability attributed to storm and wind variation, particularly for the Outer Domain; sea ice microalgae contributions to total water column production $\leq$10%	221-381	Strong seasonality, moderate interannual variability. Only 100 of the 144 months showed >75% data coverage. Comparable results between 1990 and 2010.
St. George Basin	No daily production data available	200 (Central and Outer Domains; estimate extrapolated from N. Aleutian Basin data	Regional sampling: poor; variability unknown; major oceanographic features include Central Domain (tidal-driven diffusion), Outer Domain (advection-diffusion), island effect (proximal to Pribilof Islands); interannual variability attributed to storm and wind variation, particularly for the Outer Domain; characteristics extrapolated from N. Aleutian Basin data	202-323	Strong seasonality, moderate interannual variability. Only 105 of the 144 months showed >75% data coverage. Comparable results between 1990 and 2010.

Table 14. (Continued).

Region and Planning Area	1990 Primary Productivity Estimates			2010 Primary Productivity Estimates	
	Estimated Variability in Daily Production ($g\ C\ m^{-2}\ d^{-1}$)	Estimated Annual Production ($g\ C\ m^{-2}\ y^{-1}$)	Comments	Estimated Annual Production ($g\ C\ m^{-2}\ y^{-1}$)	Comments
Bowers Basin	0.160-0.630 (May-Sept) 0.490 (mean, May-Sept) 0.330 (mean, summer) 0.299-1.007 (July)	150-200	Regional sampling: poor; high variability suggested, based on inferences from other region, knowledge of Bering Sea oceanography; interannual variability dependent upon frequency and magnitude of storm events during any given year	142-193	Strong seasonality, moderate interannual variability. Only 111 of the 144 months showed >75% data coverage. Comparable results between 1990 and 2010.
Aleutian Basin	0.160-0.630 (May-Sept) 0.490 (mean, May-Sept) 0.330 (mean, summer) 0.299-1.007 (July)	150-200	Regional sampling: poor; high variability suggested, based on inferences from other region, knowledge of Bering Sea oceanography; interannual variability dependent upon frequency and magnitude of storm events during any given year	150-225	Extremely strong seasonality, moderate interannual variability. Only 108 of the 144 months showed >75% data coverage. Comparable results between 1990 and 2010.
Navarin Basin	0.109-0.534	166-220	Regional sampling: poor; variability unknown, although expected to be high; region influenced by the Bering Slope Current; characteristics extrapolated from other AK outer shelf region	131-271	Strong seasonality, strong interannual variability. Only 88 of the 144 months showed >75% data coverage. Comparable results between 1990 and 2010.
St. Matthew-Hall	0.30-0.50 (Coastal Domain) 0.002-0.005 (ice algae, Central Domain)	50-70 (Coastal Domain) 160-200 (Central Domain)	Regional sampling: poor; variability unknown, although expected to be high; major features affecting production include freshwater input from Kuskokwim and Yukon rivers; Central Domain features expected in distal waters of St. Matthew-Hall; characteristics extrapolated, in part, from N. Aleutian Basin	180-285	Strong seasonality, moderate interannual variability. Only 74 of the 144 months showed >75% data coverage. Comparable results between 1990 and 2010.
Norton Basin	0.330-0.470 (AK Coastal Water) No production data available for Anadyr/Bering Shelf Water	50-70 (Norton Sound, AK Coastal Water) 285-324 (Anadyr/Bering Shelf Water)	Regional sampling: poor (Norton Sound) to moderate (shelf waters); variability unknown, although expected to be high; region influenced by Anadyr Water, Bering Shelf Water, and AK Coastal Water; Yukon River input affects nearshore production; some characteristics of this region extrapolated from ISHTAR	273-415	Strong seasonality, moderate interannual variability. Only 70 of the 144 months showed >75% data coverage. Comparable results between 1990 and 2010. Significant annual trend (increasing).

Table 14. (Continued).

Region and Planning Area	1990 Primary Productivity Estimates			2010 Primary Productivity Estimates	
	Estimated Variability in Daily Production (g C m^{-2} d^{-1})	Estimated Annual Production (g C m^{-2} y^{-1})	Comments	Estimated Annual Production (g C m^{-2} y^{-1})	Comments
Hope Basin	0.50-1.57 (summer, ice free, AK Coastal Water) 1.0-16.0 (Bering Sea Water [Anadyr + Bering Shelf Water])	50-70 (AK Coastal Water) 250-300 (Bering Sea Water) 13 (ice algae, Mar-June growth period)	Regional sampling: moderate; variability unknown, although expected to be high; most of Kotzebue Sound is ice covered 60%-70% of the year; the contribution of ice algae to total water column productivity is potentially significant; storm surges affect circulation and nutrient distribution	149-313	Strong seasonality, strong interannual variability. Only 45 of the 144 months showed >75% data coverage. Comparable results between 1990 and 2010. Significant annual trend (increasing).
Chukchi Sea	0.10-0.32 (Aug) 0.66-1.51 (Sept)	50-100 (AK Coastal Water, Cape Lisburne) 25-50 (AK Coastal Water, Pt. Barrow) 5 (ice algae, Mar-June growth period)	Regional sampling: poor to moderate; variability unknown; major oceanographic feature of this region is AK Coastal Water, plus the presence of ice cover during most of the year	12-85	Strong seasonality, extremely strong interannual variability. Only 23 of the 144 months showed >75% data coverage. Comparable results between 1990 and 2010. Significant annual trend (increasing). Limited coverage.
Beaufort Sea	1.0-5.0 (ice algae, bloom [Apr-June])	1-20 (phytoplankton) 40 (shelf waters)	Regional sampling: poor to moderate; high variability evident; presence of ice cover during most of the year is a prevalent feature in this region	4-64	Strong seasonality, extremely strong interannual variability. Only 14 of the 144 months showed >75% data coverage. Comparable results between 1990 and 2010. Limited coverage.

Overall, 22 of the 26 OCS planning areas exhibited similar productivity estimates in their minimal-maximal ranges between 1990 and 2010. Given the completely different assessment and therefore independent methods between the two periods, this similarity provides strong support to the argument that model results (based on satellite data) provide valid estimates of primary productivity (i.e., comparison of 1990 and 2010 primary productivity determinations indicate that the model-derived estimates are in good agreement with literature-based determinations). However, for the same reasons, it is impossible to determine whether or not there is a statistically significant trend between the two assessments. Further, because of differences in satellite instrumentation, algorithms, and spatial/temporal coverage, there remains continuing debate as to the potential for a consistent time series between the CZCS era (1978-1986) and the SeaWiFS/MODIS era (1998-present). Field data collection could provide validation of the current estimates and be used as a baseline to evaluate future changes.

Four planning areas were identified where large discrepancies were evident:

- Mid-Atlantic Planning Area: The current estimate of 110-130 g C m^{-2} y^{-1} is considerably lower than the 260-505 g C m^{-2} y^{-1} estimate developed in 1990;
- Straits of Florida Planning Area: The current estimate of 138-182 g C m^{-2} y^{-1} is considerably higher than the 1990 estimates of 7.6-35.4 g C m^{-2} y^{-1} (embayments) and 18.4 g C m^{-2} y^{-1} (coastal). No offshore annual estimate was provided in 1990;
- Western Gulf of Mexico Planning Area: The current estimate of 247-345 g C m^{-2} y^{-1} is considerably higher than the 1990 estimates of 127-200 g C m^{-2} y^{-1} (embayments), 103-176 g C m^{-2} y^{-1} (coastal), and 60-118 g C m^{-2} y^{-1} (offshore); and
- Gulf of Alaska Planning Area: The current estimate of 259-291 g C m^{-2} y^{-1} is considerably higher than the 1990 estimates of 48-100 g C m^{-2} y^{-1} (offshore) and 200 g C m^{-2} y^{-1} (coastal).

There are several factors that could have led to the observed discrepancies in the two studies. In addition to differences in measurement methods (*in situ* versus satellites), the primary reason for these discrepancies is differences in the sampling frequency and coverage. Satellites provide the most frequent measurements and synoptic coverage even after cloud screening for most areas, while *in situ* sampling is often limited in both space and time, and therefore more prone to spatial-temporal aliasing. For example, in the 1990 estimates for the Mid-Atlantic region, high variability (11- to 13-fold variation) was evident from the samples. If the sampling frequency was biased towards coastal and shelf waters, the 1990 annual productivity estimates would be overestimated. Likewise, when *in situ* samplings in the western Gulf of Mexico were not evenly distributed throughout the year, annual integrated production might also be biased. Indeed, the 1990 estimates for Gulf of Alaska were derived from an "extremely limited database" (**Table 14**), subject to significant bias (e.g., solar insolation effects). Thus, it would be difficult to conclude that there is indeed a significant increase or decrease in annual primary productivity in these areas.

The 2010 modeled NPP (millions of tons C y^{-1}, from **Table 13**) indicates the literature survey of primary production by planning area (CSA 1990) certainly underestimated the productivity of the Gulf of Mexico. If one sums the annual NPP for the three Gulf of Mexico planning areas, as shown in **Table 13**, a total of approximately 181 million tons of C y^{-1} results (with a standard deviation of approximately 10 million tons of C y^{-1}); scaling up from the literature survey for the entire 1.57 million km^2 Gulf of Mexico basin, as determined by CSA (1990), it was concluded that total annual primary production of the entire basin was only about 129 million tons of C y^{-1} (**Table 7**, **Section 4.2**). Such comparisons illustrate the limitations of using broad averages for ^{14}C-based primary production (high, medium, low) to characterize large areas, as well as the uncertainty of scaling ^{14}C-based measurements (carbon uptake m^{-2} d^{-1}) to estimate annual production. Because the modeled NPP uses monthly averages derived by averaging 9-km resolution data over an 11-y period for each planning area, the modeled NPP should provide a far more accurate estimate of primary production than is possible from a synopsis of literature for the various planning areas.

Using the same satellite data, several studies have shown a decreasing trend in surface chlorophyll in the subtropical gyres in the past decade (Gregg et al. 2005) and that the areas of low-chlorophyll gyres are expanding (McClain et al. 2004b; Polovina et al. 2008). These declines could be a result of enhanced surface-water stratification due to temperature increases. More recently, Boyce et al. (2010) have synthesized all available information in the past century to assess changes in phytoplankton biomass on decadal to centennial timescales, and over regional to global spatial scales. They showed statistically significant long-term decreases in surface chlorophyll in 8 of the 10 ocean basins, and for the global aggregate. Most changes are on the order of 0.01 mg m^{-3} y^{-1}. They also found a strong correspondence between the chlorophyll change and changes in both leading climate indices (e.g., ENSO) and ocean thermal conditions. However, on short-term scales, the “trends” depend heavily on the chosen years as well as on the algorithms (Lee et al. 2010). In the current assessment, the temporal span (i.e., 1990–2010) is relatively short. In addition, the methods used to derive primary productivity estimates were different between the 1990 and 2010 estimates. Therefore, only qualitative conclusions can be drawn from the 1990-2010 comparisons (i.e., 22 of the 26 OCS areas showed similar annual ranges, while the remaining four areas showed large differences). As the emphasis of the current analysis has been heavily focused on continental margins, the conclusions from the published studies (Gregg et al. 2005; Polovina et al. 2008; Boyce et al. 2010) on basin-scale biomass cannot be extended here. As the available satellite ocean color database grows (i.e., a more extensive database is acquired over time), rigorous comparisons between the current estimates and future estimates of primary productivity of the 26 OCS planning areas will be feasible. Further, with a growing historical database, a more comprehensive trend analysis will be possible.

7.1.2 Secondary Productivity

7.1.2.1 Summary of Secondary Productivity Among Planning Areas

Ecopath

Ecopath models for U.S. OCS ecosystems were reviewed, and secondary productivity estimates summarized, as available, for each planning area. Total system-wide productivity ranged from 410 t km^{-2} y^{-1} in the Gulf of Alaska to 15,466 t km^{-2} y^{-1} in Looe Key, Florida (**Table 15**; **Figure 48**). This latter figure is clearly being driven by the high primary production and benthic production associated with coral reefs (Venier and Pauly 1997). Excluding the value from Looe Key and comparing only open ocean sites, the highest value is 2,817 t km^{-2} y^{-1}, found in the Eastern Subarctic Pacific Basin, which would include all or portions of the Gulf of Alaska, Kodiak, and Shumagin planning areas.

Table 15. Characteristics of study areas where Ecopath models exist by region. Areas <100,000 km^2 were classified as local.

Reference	Study Area	Spatial Coverage	Approximate Area (km^2)	Number of Functional Groups	Planning Area	System 2° and 3° Productivity (t km^{-2} y^{-1})	Data Time Frame
Atlantic							
Gaichas et al. 2009	Gulf of Maine	Local	NA	36*	NOA	1,361	1996-2000
Gaichas et al. 2009	Georges Bank	Local	NA	36*	NOA	1,641	1996-2001
Zajac et al. 2008	Long Island Sound	Local	3,400	32	NOA	1,965	1995-2005
Okey 2001	Mid-Atlantic Bight	Regional	111,200	55	NOA, MDA	1,587	1995-1998
Okey and Pugliese 2001	SE US continental shelf	Regional	174,300	42	MDA, SOA	1,076	1995-1998
Venier and Pauly 1997	Looe Key, Florida	Local	30	20	FLS	15,466	late 1980’s - early 1990’s
Gulf of Mexico							
Walters et al. 2006	Gulf of Mexico	Regional	Gulf-scale	63	WGM, CGM, EGM	764	1950-2004
Okey et al. 2004	West Florida Shelf	Regional	>170,000	59	EGM	1,078	2000
Pacific							
Field and Francis 2005	N California Current	Regional	NA	63	NOC, WAO	1,012	1990’s
Alaska							
Preikshot 2005	E Bering Sea, Gulf of Alaska	Regional	1,500,000	56	ALA, GEO, MAT, NAL, SHU, KOD, GOA, COK	1,184	1950-2005
Gaichas et al. 2009	E Bering Sea	Regional	NA	148*	NAL, GEO, MAT, NAV	614	1991
Gaichas et al. 2009	Gulf of Alaska	Regional	NA	138*	SHU, KOD, GOA	410	1990-1993
Guenette 2005	SE Alaska shelf	Regional	93,351	39	GOA	657	1999
Aydin et al. 2007	E Bering Sea	Regional	495,218	148	NAL, GEO, MAT	613	1990-1994
Aydin et al. 2007	Gulf of Alaska	Regional	291,840	138	SHU, KOD, GOA, COK	410	1990-1994
Aydin et al. 2007	Aleutian Islands	Local	56,936	140	ALA	1,011	1990-1994
Aydin et al. 2003	E Subarctic Pacific Basin	Regional	3,622,000	55	SHU, KOD, GOA	2,817	late 1980’s - early 1990’s
Heymans 2005	W and C Aleutian Islands	Local	56,936	40	ALA	862	1991

*Trophic groups for these models were aggregated into 17 common groups by the authors for comparison of ecosystems

Key to planning area abbreviations: North Atlantic (NOA), Mid-Atlantic (MDA), South Atlantic (SOA), Florida Straits (FLS), Eastern Gulf of Mexico (EGM), Central Gulf of Mexico (CGM), Western Gulf of Mexico (WGM), Northern California (NOC), Washington-Oregon (WAO), Chukchi Sea (CHU), Navarin Basin (NAV), North Aleutian Basin (NAL), St. Georges Basin (GEO), Cook Inlet (COK), Gulf of Alaska (GOA), Shumagin (SHU), Kodiak (KOD), Aleutian Arc (ALA), and St. Matthew-Hall (MAT).

NA = Not available.

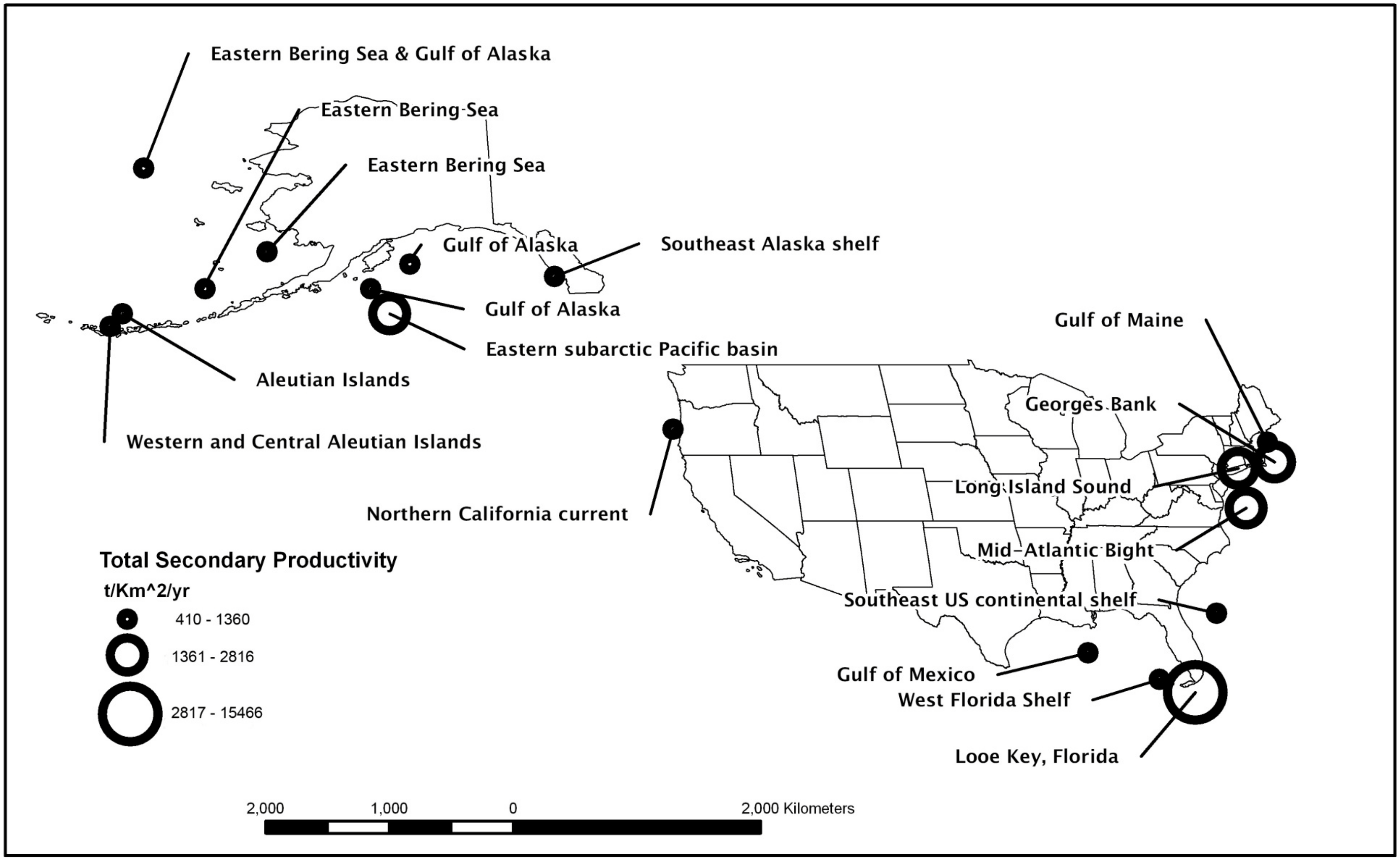

Figure 48. Bubble plot of productivity (t km^{-2} y^{-1}) values from Ecopath models in the Outer Continental Shelf regions. Values are from **Table 15**.

The overall average system productivity values, including and excluding Looe Key coral reef sites, is 1,918 and 1,121 t km^{-2} y^{-1}, respectively (**Table 16**). Excluding the highly productive coral reef value significantly lowers the average system productivity. On average, the Atlantic has the highest system productivity followed (in descending order) by the Pacific, Alaska, and Gulf of Mexico regions. At the level of this broad comparison among regions, all of the values are in the same order of magnitude.

When the components of the food web are arranged in an ecological pyramid (**Figure 49**), it appears the benthic food web is more efficient than the pelagic food web because higher tertiary and quaternary productivity can be supported by the water column productivity. This is likely because the benthic food web is also supported by falls of large dead marine mammals and fishes, which likely die of old age and are generally protected from predation by their large size.

Table 16. Summary of the annual productivity data from Ecopath models, as presented in **Section 5**.

Study Area	Productivity (t km^{-2} y^{-1})								
	System	PEL	DEM	SKR	MAM	CMB	BEN	ZOP	PPD
Overall Mean	1,918	37	53	0.2	5	119	816	934	7,161
Overall Mean (w/o Looe Key)	1,121,	15	14	0.2	5	49	216	836	5,810
Gulf of Mexico	921	24	15	1.15	0.00	53	348	481	6,934
Atlantic (w/o Looe Key)	1,526	15	8	0.05	0.02	60	293	1,149	6,695
Pacific	1,012	5	52	0.21	0.02	12	128	814	6,618
Alaska	953	14	13	0.06	8.19	46	146	743	4,979

Abbreviations: PEL = pelagic fishes, DEM = demersal fishes, SKR = sharks and rays, MAM = marine mammals, CMB = crustaceans, molluscs, and other mega-benthos, BEN = macro-, meio-, and micro-benthos, ZOP = zooplankton, PPD = primary producers, SYSTEM = total ecosystem secondary and tertiary productivity, excluding PPD.

Figure 49. Average productivity among all Ecopath models in OCS planning areas, excluding coral reefs (values from **Table 16**).

This study identified several significant limitations in the use of Ecopath modeling results for secondary and tertiary production comparisons among planning areas:

- Results are not available for all planning areas. Ecopath modeling studies were found that are applicable to all four Atlantic planning areas (especially North Atlantic), all three Gulf of Mexico planning areas, two Pacific planning areas (Northern California and Washington/Oregon), and parts of nine Alaska planning areas (Aleutian Arc, Cook Inlet, Gulf of Alaska, Kodiak, Navarin Basin, North Aleutian Basin, Shumagin, St. Georges Basin, and St. Matthew-Hall.)

- Most of the Ecopath modeling studies focused on a particular ecosystem and did not define a geographic delimited "study area." To develop a secondary productivity estimate for an entire planning area, it would be necessary to model all of the ecosystems and develop a composite estimate based on the spatial extent of each ecosystem.

- Unlike the primary productivity modeling estimates derived in **Section 3**, the Ecopath modeling estimates would be difficult to validate by measuring secondary production directly in the field.

Among the limitations noted above, the validation of secondary production estimates is particularly problematic. As with all ecosystem models that compute secondary and tertiary production, it is difficult to validate production estimates from Ecopath with direct field measurements. Secondary production by heterotrophs is the net biomass produced per unit area per unit time. Therefore, one would have to measure a rate as opposed to measuring a stock, the latter of which is relatively easy. There are field methods for measuring primary production by phytoplankton directly in the ocean, for example, oxygen production rates can be measured using dissolved oxygen determinations or carbon dioxide consumption by uptake of radioactive inorganic carbon. Measuring primary production is possible because of the small size of phytoplankton, which enables a scientist to perform experiments on small amounts of water. In contrast, the size spectrum of heterotrophs is dramatic, ranging from bacteria to whales. While it is possible to incubate small samples of water to measure bacterial production, the methods are actually based on DNA synthesis, so the method only indirectly estimates production and requires knowing conversion factors for DNA synthesis to carbon production. One method to estimate animal production is by measuring oxygen consumption, however, it is difficult to convert this measure to biomass production. While it is possible to incubate zooplankton, it is not possible to incubate larger animals, except in laboratory settings, so direct field measurements of oxygen consumption by a wide range of animals in the field is not possible. Also, the diversity of animals means that conversion factors needed to convert oxygen consumption rates to production rates would also be diverse. In the end, it is relatively easy to measure stocks, but not rates of production of animals in the sea. Thus, all production calculation methods for animals are model-based. Sometimes the models are simple, such as the bioenergetic approach, which relies on simple power functions to convert size into production. Sometimes the models are complex, such as Ecopath and Atlantis, which rely on complex trophic interactions and population dynamics to compute production estimates. The methodologies and models to estimate production have advanced dramatically since the mid-1980's and continue to advance today. Future advances are likely to come from extending

Ecopath or Atlantis, but it is equally possible that new discoveries will lead to new and improved approaches.

Empirical Measures

Two empirical measures of secondary and tertiary production were evaluated as part of this analysis, including zooplankton biomass and commercial fishery landings. Zooplankton biomass data are readily available from field sampling studies and are routinely monitored in some areas, however, there are database limitations evident. The COPEPOD database was accessed and summarized. Zooplankton sampling coverage was extremely variable across the 26 OCS planning areas. Extensive, multiyear (and seasonal) sampling efforts were noted for the Southern California Planning Area (i.e., CalCOFI), North and Mid-Atlantic planning areas, and several of the southernmost Alaska planning areas (i.e., Gulf of Alaska, Kodiak, Cook Inlet, and Shumagin). Other planning areas had very limited zooplankton sampling coverage (e.g., South Atlantic, Straits of Florida, Navarin Basin, St. Matthew-Hall, Norton Basin, Hope Basin) or no coverage at all (Chukchi Sea, Beaufort Sea). Disproportionate sampling (e.g., lack of multiyear and/or seasonal coverage; preference for shallow sampling) was also evident. Several planning areas have inconsistent coverage, where zooplankton data are available for some years but not for others, or where only selected seasons have been sampled.

Commercial fisheries landings were also considered as a potential indicator of tertiary production. In the Atlantic Region, Virginia (Mid-Atlantic Planning Area), and Massachusetts and Maine (North Atlantic Planning Area) reported the highest landings by weight. In the Gulf of Mexico Region, Louisiana (Central Gulf Planning Area) landings were dominant among the Gulf states. In the Pacific Region, California landings (including Southern California, Central California, and Northern California planning areas) were slightly higher than those shown for Washington and Oregon (Washington-Oregon Planning Area). Alaska statewide landings were exceptionally high compared to all other states.

Inherent difficulties in assessing all landings data were identified. While landings may be reported for a particular state, it is not easily determined where (i.e., from what planning area) fish were caught. This problem is particularly acute in the Alaska landings data due to the high number of planning areas and their geographic coverage relative to the number of ports.

Because of this general problem with fisheries landings data, any attempt to compute, estimate, or model secondary productivity based on these data has limitations in the spatial scale at which the data can be applied. For example, estimates would be valid only for very large regional scales because fish could potentially come from a range of distances from the port where the landings are reported.

Empirical measurements provide mainly stock assessments. By using allometric relationships, it is possible to convert biomass to productivity estimates, but there are inherent difficulties and assumptions about the use of constants in place of dynamic coefficients.

7.2 Potential Impacts of OCS Activities on Primary Productivity

To identify and assess potential impacts of OCS activities on primary productivity, two components must be identified or characterized – factors that control primary productivity and the nature of various OCS oil and gas activities that may influence those factors. Each of these components is discussed in further detail in the following subsections.

7.2.1 Factors Controlling Primary Productivity

Major factors that control marine primary productivity include nutrient availability, light, and temperature (Perry et al. 1981; Tilman et al. 1982; Howarth 1988; Falkowski 1994; Babin et al. 1995; Bouterfas et al. 2002; Sumich and Morrisey 2004). Of these factors, phytoplankton primary production in marine ecosystems is largely regulated by light intensity and nutrient availability (Perry et al. 1981). As noted by Pahlow (2005), several phytoplankton models have been derived from observations under conditions of balanced growth (i.e., constant chemical composition on a daily timescale, resulting in growth rate equal to loss rate). Under these conditions, phytoplankton are considered either nutrient- or light-limited when growth rate is determined by dilution rate or light intensity, respectively. Individual nutrient- or light-limited experiments have been modeled (e.g., see Shuter 1979; Laws and Bannister 1980; Laws and Chalup 1990; Baumert 1996; Geider et al. 1998). While a thorough analysis of nutrients, light, and temperature as regulators of phytoplankton growth and community dynamics is well beyond the scope of this analysis, a broad characterization of each provides the basis for identifying and discussing whether such components potentially result from OCS oil and gas activities. The occurrence, relative frequency, and spatial scale of various physical processes (e.g., upwelling, ring formation, seasonal freshwater inflow) also have potentially significant effects on primary productivity in OCS waters. The reader is referred to the literature update summaries provided previously for Region-specific discussions of those factors that influence local primary productivity.

7.2.1.1 Nutrient Limitation

Nutrients of concern to phytoplankton are regionally variable; however, four are of interest to this analysis: nitrogen (nitrate), phosphorus (phosphate), silica (silicate), and iron. **Section 2** provided summaries of both traditional and satellite measurements of new production and described several of the mechanisms by which nutrients influence primary productivity – doming and upwelling and from atmospheric sources. **Section 4** reviewed and summarized the available primary productivity data for the four major OCS regions – Atlantic, Gulf of Mexico, Pacific, and Alaska – for the period 1988-2010, updating the water column primary productivity database initially established by CSA (1990), with an emphasis on the available published literature and reports applicable to OCS planning areas. Many of the cited data sources detailed the planning area-specific mechanisms by which nutrients affect primary production. Research into phytoplankton communities and nutrient dynamics, by planning area, is well advanced for a majority of the planning areas. Major driving forces affecting nutrient concentrations are well defined for all OCS planning areas.

Within nearshore waters (i.e., inshore of the OCS Planning Areas), several recent research efforts have considered the effects on marine phytoplankton of various nutrient sources, including naturally occurring sources (e.g., riverine input into estuarine and coastal waters; see Kudela and Peterson 2009) and anthropogenic discharges (e.g., treated sewage into coastal waters; see Staehr et al. 2009). According to Cosgrove (2007), research into phytoplankton communities and nutrient dynamics in nearshore waters has been conducted, however, relatively few data are available regarding the response of phytoplankton and associated productivity to nutrient fluctuations (e.g., Lippemeier et al. 2001).

7.2.1.2 Solar Radiation and Light Intensity

In general, the intensity of light reaching the earth's surface, or irradiance (i.e., photons m^{-2} sec^{-1}) varies with season and the time of day, and may also be affected by local weather patterns (Wetzel and Likens 2000). Daily and seasonal differences are attributed to the angle at which photons arrive at the ocean surface.

Between solar altitudes of 90-45 degrees, reflective losses are only 2%-3%. Surface reflection rises from 13%-100% when the sun is lower than 20 degrees (Kirk 1992; Valiela 1995).

Some species of phytoplankton adapt to low light intensities by either increasing the size of the photosynthetic unit (Perry et al. 1981) or increasing the number of photosynthetic units (Kirk 1994). Phytoplankton may also alter their metabolism in response to light limitation. For example, cell cycle phase durations can be influenced by light limitation (e.g., see Olson et al. 1986). Phytoplankton may also acclimate to low irradiance levels by altering their cellular demand for iron (i.e., allowing for an increased synthesis of pigments) (Maldonado et al. 1999).

7.2.1.3 Temperature

Temperature has been noted as an important component in mediating planktonic communities (e.g., setting upper limits on physiological rate processes; Eppley 1972; Goldman and Carpenter 1974, as cited by Rose et al. 2009a). Interactions of temperature with other environmental variables (e.g., rising pCO_2, changes in irradiance, fluctuations in nutrient utilization) have been characterized in a limited number of field and laboratory research efforts (Goldman 1979; Lomas and Glibert 1999; Hare et al. 2007; Feng et al. 2009; Rose et al. 2009b). Redalje et al. (2002), assessing the spatial and temporal variability in primary production and phytoplankton pigments in shelf waters beyond the Chesapeake Bay and Cape Hatteras, reported that primary production was positively correlated with light and temperature, while chlorophyll biomass was positively correlated with dissolved inorganic nitrite and nitrate and negatively correlated with temperature. These differences in correlation, they suggested, indicate that temperature plays a major role in the phytoplankton dynamics in this shelf ecosystem. Rose et al. (2009a) have also noted that temperature has been hypothesized to constrain growth of heterotrophic protists relative to phototrophic protists at the extreme low temperatures characteristic of polar regions (Rose and Caron 2007).

7.2.2 Sources of Impact from OCS Oil and Gas Activities

Oil and gas operations comprise several different phases, including prospecting (i.e., seismic surveys, geotechnical sampling), exploration (i.e., exploratory drilling), and development/production (i.e., subsea completion; facility installation [platform; floating, production, storage, and offloading; pipelines; etc.], operation, and facility abandonment) (Regg et al. 2000; CSA 2004). **Appendix D** summarizes these phases of OCS oil and gas activity and identifies the activity-specific impact producing factors and the expected impact of each factor on plankton (including phytoplankton) and water quality, the latter of which affects plankton.

7.2.2.1 Number of Active Platforms and Drilling Activity

In the Gulf of Mexico, there are currently (as of 23 August 2010) 3,415 active platforms (**Table 17**), representing a mix of manned and unmanned facilities. In the Pacific Region, there are 23 active OCS platforms, all of which are manned facilities (**Table 18**). In the Alaska Region, there are three active OCS platforms and/or man-made (gravel) islands.

Between 1960 and 2006, MMS logged a total of 17,801 wells completed and 36,470 wells plugged and abandoned (**Appendix D**).

Table 17. Summary of active leases and platforms in OCS waters of the Gulf of Mexico, as of 23 August 2010 (From: BOEMRE 2010a).

Active Leases	Water Depth (m)	Approved Applications to Drill	Active Platforms
2,232	0-200	33,666	3,351
145	201-400	1,103	21
339	401-800	835	10
421	801-1,000	506	7
3,511	Above 1,000	1,635	26

Table 18. Summary of active leases and platforms in Federal OCS waters of the Pacific and Alaska Regions, as of 14 July 2010 and 12 August 2010, respectively (From: BOEMRE 2010b,c).

Active Leases/ Producing Leases	Total Development Wells Drilled	Total Exploration Wells Drilled	Active Platforms
Pacific Region			
49/43	1,020	328	23
Alaska Region			
675	-	-	3

7.2.2.2 Waste Streams

Offshore oil and gas operations produce a number of waste streams that are discharged into OCS waters following monitoring and/or treatment, some of which may have localized impacts to primary productivity. These waste streams include produced water, ballast water, displacement water, deck drainage, drilling muds, drilling cuttings, produced sand, cement residue, blowout preventer fluid, sanitary and domestic wastes, gas and oil processing wastes, slop oil, cooling water, and desalination brine (MMS 2007b). Discharges by OCS phase are outlined in **Table 19**.

Drilling muds and cuttings and produced water, because of their potential volumes and/or chemical constituents, pose the greatest potential threats to the marine environment, in general, and to planktonic communities, in particular. Both are released in large amounts from offshore drilling rigs and development platforms, although there are fundamental differences in the relative frequency and duration of these discharges.

Table 19. Summary of discharges from various oil and gas operations (Adapted from: MMS 2007b).

OCS Phase	Discharge	Summary Characteristics
Prospecting	Seismic survey vessel discharges	Low volumes of treated and/or monitored effluents; estimates: 100 L d^{-1} of sanitary waste and 220 L d ^{1} of domestic waste $person^{-1}$ d^{-1}; localized discharges at the ocean surface diluted to background levels within meters of discharge; extremely low potential for direct effects on phytoplankton
Exploration	Drilling muds and cuttings	Volumes dependent upon depth of well; both water-based drilling fluids (WBF) and synthetic-based drilling fluids (SBF) used; discharges only during or immediately following drilling (40-70 d per well); discharge volumes of muds and cuttings are variable, depending upon mud system used (WBF, SBF); WBF wells generate 7,000-9,700 bbl of drilling mud and 1,500-2,500 bbl of cuttings per well; SBF wells generate 1,184-1,901 bbl of cuttings per well; turbidity within 2 km of rig, with a return to ambient within minutes to hours of discharge cessation; rapid dilution within 1 km of discharges; low potential for direct effects on phytoplankton
	Treated sanitary wastes and gray water	Low volumes of treated and/or monitored effluents; estimates: 100 L of sanitary waste and 220 L of domestic waste $person^{-1}$ d^{-1}; localized discharges at the ocean surface diluted to background levels within meters of discharge; extremely low potential for direct effects on phytoplankton
	Deck drainage	Very low volumes, depending upon rig area and rainfall; estimated at 200 L $month^{-1}$; localized discharges at the ocean surface diluted to background levels within meters of discharge; extremely low potential for direct effects on phytoplankton
	Food wastes	Food waste discharge allowed when ground to 25 mm maximum diameter; volume generated dependent upon number of personnel aboard; localized increase in organic load to the ocean; extremely low potential for direct effects on phytoplankton
	Miscellaneous discharges[1]	Low volumes of discharge; localized discharges at the ocean surface diluted to background levels within meters of discharge; low potential for direct effects on phytoplankton
	Other chemicals[2]	Low volumes of treated and/or monitored effluents, typically associated with drilling muds and cuttings discharges; localized discharges at the ocean surface diluted to background levels within meters of discharge; low potential for direct effects on phytoplankton
	Cement	Excess cement released at the wellbore (i.e., localized discharges at the ocean floor); no potential for direct effects on phytoplankton

Table 19. (Continued).

OCS Phase	Discharge	Summary Characteristics
Development/ Production	Drilling muds and cuttings	Volumes dependent upon depth of well; both WBF and SBF used; discharges only during or immediately following drilling (40-70 d per well); discharge volumes of muds and cuttings are variable, depending upon mud system used (WBF, SBF); WBF wells generate 7,000-9,700 bbl of drilling mud and 1,500-2,500 bbl of cuttings per well; SBF wells generate 565-855 bbl of cuttings per well; turbidity within 2 km of rig, with a return to ambient within minutes to hours of discharge cessation; rapid dilution within 1 km of discharges; low potential for direct effects on phytoplankton
	Produced water	Discharge rates typically between 2 and 150,000 bbl d^{-1}; rapid dilution within 1 km of discharges; low potential for direct effects on phytoplankton
	Miscellaneous discharges[3]	Low volumes of discharge; localized discharges at the ocean surface diluted to background levels within meters of discharge; low potential for direct effects on phytoplankton
	Other chemicals[4]	Low volumes of discharge; localized discharges at the ocean surface diluted to background levels within meters of discharge; low potential for direct effects on phytoplankton
	Treated sanitary wastes and gray water	Low volumes of treated and/or monitored effluents; estimates: 100 L d^{-1} of sanitary waste and 220 L d^{1} of domestic waste $person^{-1}$ d^{-1}; localized discharges at the ocean surface diluted to background levels within meters of discharge; extremely low potential for direct effects on phytoplankton
	Food wastes	Food waste discharge allowed when ground to 25 mm maximum diameter; volume generated dependent upon number of personnel aboard; localized increase in organic load to the ocean; extremely low potential for direct effects on phytoplankton
	Cement	Excess cement released at the wellbore (i.e., localized discharges at the ocean floor); no potential for direct effects on phytoplankton

[1] Miscellaneous discharges during exploration include uncontaminated freshwater and seawater used for cooling water and ballast, desalination unit discharges, blowout preventer fluids, and boiler blowdown discharges.

[2] Other chemicals discharged during exploration include detergents, corrosion and scale inhibitors, emulsifiers, oxygen adsorbents, biocides, miscellaneous chemicals.

[3] Miscellaneous discharges during development/production include uncontaminated freshwater and seawater used for cooling water, desalination unit discharges, blowout preventer fluids, and boiler blowdown discharges.

[4] Other chemicals discharged during development/production include well treatment, workover, and completion fluids.

Drilling Muds and Cuttings

Drilling muds and cuttings are discharged only during well drilling, during either exploratory drilling or development drilling operations. During well intervals when water-based drilling fluids (WBF) are being used, both muds and cuttings are routinely discharged to the ocean. Cuttings and adsorbed WBF solids are discharged to the ocean at a rate of 0.2-2.0 m^3 h^{-1} (Neff 1987, 2005).

When nonaqueous base fluids (i.e., synthetic-based drilling fluid [SBF]) systems are used, the percentage of SBF retention on cuttings typically is subject to regulatory limits (Neff et al. 2000). SBF retention limit is dictated by National Pollutant Discharge Elimination System (NPDES) permit and varies by SBF used (see **Appendix D**). SBF base fluids include linear-α-olefins, poly-α-olefins, internal olefins, linear alkyl benzenes, ethers, esters, or acetals (Neff et al. 2000). MMS (2000) estimates that the average discharge of muds and cuttings for an OCS well is 4,286 bbl (180,000 gal.). As operators have moved into deeper water and drilled deeper wells, the use of SBF has become more prevalent, as has the drilling of the upper portions of a well with WBF and the lower portion of a well with SBF. For wells drilled using WBF, MMS (2007b) estimates that 7,000-9,700 bbl of drilling mud and 1,500-2,500 bbl of cuttings are discharged per well. For wells drilled using SBF, MMS (2007b) estimates that 565-855 bbl of cuttings are discharged for a development well, while 1,184-1,901 bbl of cuttings are discharged for an exploratory well. Well drilling, from spudding to completion, generally requires 40-70 d depending upon well complexity, water depth, drilling depth, and problems encountered during drilling.

A recent drilling mud discharge analysis evaluated the fate of the release of a low toxicity, mineral oil based drilling fluid (LTOBM) into the marine environment at a water depth of approximately 1,000 m (CSA International, Inc. 2010). Modeling, using both CORMIX and MUDMAP models, was based on the release of 584 bbl of drilling fluid with a density (fluid weight) of 9.8 ppg. The initial CORMIX modeling indicated that the plume of drilling fluid is rapidly dispersed to very low concentrations within a short distance from the discharge point. The plume sinks, since its density exceeds that of the ambient seawater. While the plume sinks, it also drifts in response to the ambient currents. Dilution was rapid, with the initial concentration diluted by a factor of 10,000 within a distance of 1 km from the discharge site, and by a factor of 100,000 by the time the plume reached the seabed. Additional details on modeling parameters and results are provided in **Appendix D**. There is a very low potential for direct impacts of drilling mud constituents affecting phytoplankton metabolism through hydrocarbon and/or trace metal exposure; this exposure would be limited to the immediate area of the discharge, with relatively rapid dilution expected.

Produced Water

Produced water discharges may begin upon initial production or may be delayed until a more mature stage has been reached within the field; produced water production is dependent upon the reservoir. Produced water generated during development and production typically increases as the age of the field increases. Produced and formation waters have been shown to contain oil, inorganic salts, processing or treatment chemicals, and trace metals. Discharges in both produced water and drilling muds and cuttings can include heavy metals (mercury, cadmium, zinc, chromium, copper, and others), biocides, corrosion and scale inhibitors, detergents, emulsifiers, and oxygen adsorbents (Neff 1987; International Association of Oil & Gas Producers 2005).

The discharge of produced water results in increased concentrations of some metals, hydrocarbons, and dissolved solids within an area of about 100 m adjacent to the point of discharge (MMS 2008). MMS (2007b) estimates that the annual volume of produced water discharged into the U.S. Gulf of Mexico from OCS facilities between 1996 and 2005 ranged between 431 and 686 million barrels (MMbbl), with an annual average of 596 MMbbl; daily discharge typically ranges between 2 and 150,000 bbl d^{-1}. MMS (2007b) estimated that produced water annually contributes 19,250 bbl (2,750 tonnes) of petroleum hydrocarbons to Gulf of Mexico waters. Offshore California, the existing NPDES discharge permit allows up to 7.46 MMbbl of produced water to be discharged annually from the 19 discharge locations in OCS waters.

Upon discharge, produced water is rapidly diluted, typically by 30- to 100-fold within tens of meters (International Association of Oil & Gas Producers 2005). At distances of 500-1,000 m from the discharge point, the dilution factor can be 1,000 to 100,000 or more. Some constituents will precipitate, and others, such as trace metals and aromatic hydrocarbons, will be scavenged onto particulate matter. There is a very low potential for direct impacts of produced water constituents affecting phytoplankton metabolism through hydrocarbon and/or trace metal exposure; this exposure would be limited to the immediate area of the discharge, with relatively rapid dilution expected.

Treated Sanitary Wastes

Volumes of treated sanitary wastes from an offshore platform, a fraction of those discharged from municipal wastewater facilities, are estimated at approximately 100 L $person^{-1}$ d^{-1}. An offshore facility manned by 25 personnel may be expected to discharge ~2,500 L d^{-1} of treated sanitary wastes. The maximum number of personnel aboard an offshore drilling rig is normally in the range of 100-120 personnel, with the potential to produce 10,000-12,000 L d^{-1} of sanitary wastes. The potential effects of platform sanitary waste discharges on phytoplankton would be expected to be influenced by the degree of mixing and total volume, with organic loading occurring only within tens of meters of the discharge.

7.2.3 Potential for Effects

Both negative and positive growth effects to phytoplankton communities may result from OCS oil and gas operations. Potentially negative effects on phytoplankton communities and associated primary productivity are associated with OCS facility discharges – primarily drilling muds and cuttings, produced water, and, to a lesser extent, treated sanitary wastes (Neff 1987, 2005; Neff et al. 2000). Based on the results of modeling studies, muds and cuttings and produced water discharge plumes either disperse rapidly in surface waters or sink and disperse through the water column. Only localized increases in either turbidity or nutrients are expected.

The volume and temporal characteristics of each of these discharges varies, resulting in differential impacts to plankton and water quality. Drilling muds and cuttings discharges occur only during or immediately after drilling, whether during exploratory or development drilling operations; most wells require 40-70 d to drill, with the discharge plume reaching a dilution factor of 10,000 within 1 km of the discharge, suggesting that only relatively short-term, localized impacts to phytoplankton are possible (Neff 1987, 2005). Further, chemical constituents of WBF discharges (muds and cuttings) and SBF discharges (cuttings only, with limited amounts of adhering muds) are regulated by NPDES permit. Produced water discharge volumes are extremely variable but tend to be continuous over the course of the life of a well or platform. Typically, new production wells generate only low volumes of produced water, the latter of which increases as the age of the field increases. Dilution to background levels occurs within 1 km of the discharge point, often within 100 m of the discharge, suggesting that only relatively localized, albeit continuous impacts to phytoplankton are possible.

The potential for beneficial effects from OCS activities also exists, particularly in association with the fouling community and associated fish populations that are known to inhabit permanent OCS facilities. Pseudofeces (e.g., from bivalves) and feces (e.g., from fish) released into the water column may provide a localized source of nutrients for planktonic biota located downcurrent from an OCS facility (Newell 2000).

In terms of OCS oil and gas activities that may adversely affect limiting factors of phytoplankton growth, the following sources or factors are noted:

- Nutrients: increased nutrient load from treated sanitary wastes and food wastes during all phases; highest volumes tend to occur during exploration; chronic discharges occur from development/production facilities;

- Light: minor amounts of shading from exploratory rigs (short term) and development/production facilities; localized turbidity from muds and cuttings discharges; and

- Temperature: minor amounts of cooling water during all phases; highest volumes noted for large production facilities.

There is also a very low potential for direct impacts of drilling muds and produced water constituents affecting phytoplankton metabolism through hydrocarbon and/or trace metal exposure. Drilling muds and cuttings discharges are limited to exploratory and development drilling periods. Produced water discharges are limited to production operations, tend to increase with increasing life of a producing field, and are typically continuous during production. Exposure to discharged drilling muds or produced water would be limited to the immediate area of the discharge, with relatively rapid dilution expected (Neff 1987).

7.3 Potential Impacts of Climate Change on Productivity

"There is high confidence, based on substantial new evidence, that observed changes in marine and freshwater biological systems are associated with rising water temperatures, as well as related changes in ice cover, salinity, oxygen levels and circulation. These include: shifts in ranges and changes in algal, plankton and fish abundance in high-latitude oceans."

– Intergovernmental Panel on Climate Change (IPCC 2007a)

According to IPCC (2007a), changes in both phytoplankton and zooplankton species and communities in the North Atlantic have been associated with northern hemisphere temperature trends and variations in the North Atlantic Oscillation index. These have included changes in species distributions and abundance, the occurrence of subtropical species in temperate waters, changes in overall phytoplankton biomass and seasonal length, changes in the ecosystem functioning and productivity of the North Sea, shifts from cold-adapted to warm-adapted communities, phenological changes, changes in species interactions, and an increase in harmful algal blooms (HABs) (Fromentin and Planque 1996; Reid et al. 1998; Edwards et al. 2001, 2002, 2006; Reid and Edwards 2001; Beaugrand et al. 2002, 2003; Beaugrand and Reid 2003; Edwards and Richardson 2004; Richardson and Schoeman 2004; IPCC 2007b). While these documented changes, as summarized by IPCC (2007a), address the entire North Atlantic, the potential exists that long-term changes in primary productivity for individual planning areas in the Atlantic Region might also have occurred or will be occurring, particularly within those portions of the North Atlantic Planning Area located at high latitudes.

In the north Pacific, Miller et al. (2007) have summarized the potential effects of climate change on ocean biology, including influences on the carbon cycle, affecting oceanic phytoplankton via changes in upper ocean absorption, and the influence of dimethylsulfide (DMS) production by phytoplankton on atmospheric aerosols. The authors also identified the primary influences of changes in physical climate on ocean biology. For example, changes in freshwater runoff and aoelian dust deposition patterns, both attributed to climate change, have been implicated in phytoplankton community structure changes. Specifically, the availability of macronutrients and trace elements (e.g., iron) are known controlling factors for phytoplankton photosynthesis (de Baar et al. 1995; Behrenfeld et al. 1996; Coale et al. 1996; Falkowski et al. 1998); any significant change in freshwater runoff or aeolian transport resulting from climate warming could change the inputs of nutrients and iron to the ocean, thereby affecting CO_2 sequestration. Miller et al. (2007) also note that climate change may also cause shifts in the structure of biological communities in the upper ocean (e.g., predicted changes in relative contributions of coccoliths and diatoms to the planktonic community).

There is also evidence that certain phytoplankton groups may have an advantage in highly stratified waters, where other groups are dominant when waters are more deeply mixed. Changes to ocean stratification could impact species composition and potentially affect the downward fluxes of organic carbon and consequently the efficiency of the biological pump.

Modeling climate change has been an area of research interest in recent years. Reichler and Kim (2008) evaluated available climate models, comparing model outputs against field observations. In all, 57 different national and international models developed over the past 20 y were evaluated, including the latest model generation cited by IPCC (2007a). Model output from three different climate model intercomparison projects were compared, including the initial Coupled Model Intercomparison Project (CMIP1) (Meehl et al. 2000), CMIP2 (Covey et al. 2003; Meehl et al. 2005), and CMIP3 (Program for Climate Model Diagnosis and Intercomparison 2007). CMIP was established to study the output of coupled atmosphere-ocean general circulation models.

According to Miller et al. (2007), a series of atmosphere-ocean models have been used to project the effect of climate change on marine biota (Sarmiento et al. 1998; Joos et al. 1999; Gabric et al. 2003; Pierce 2003). These models simulate various atmospheric and biological processes, including carbonate chemistry and gas exchange processes, physical and biological uptake of CO_2, and changes in temperature, salinity, wind speed, and ice cover. While these models may account for simple changes in biological productivity, they do not accommodate alterations in external nutrient supply, or changes in the biogeography of planktonic species. Coupled models need to be developed that simulate more complex biological feedbacks (Gabric et al. 2003).

In Alaska, the Arctic Climate Impact Assessment (ACIA) (ACIA 2005) notes that the impacts of warming temperatures on Alaska's marine ecosystems includes sea ice loss and changes in phytoplankton-based primary productivity, along with changes in species distribution, migration, and metabolism for indigenous fishes, marine mammals, and seabirds. In the Bering Sea, the annual ice melt controls the phytoplankton bloom, and two main patterns of spring plankton bloom are evident. During cold years, a late ice retreat results in a delayed phytoplankton bloom. For example, a late ice retreat in April coincides with enough sunlight for photosynthesis, and the bloom occurs in the cold, nutrient-rich melt-water. During a warm year, a non-ice associated bloom occurs where an early ice retreat does not coincide with sufficient sunlight or the conclusion of the winter storms (which introduce nutrients into the surface waters and prevent stratification), and phytoplankton cannot bloom. Under these conditions, the bloom is delayed until the winter winds have passed and the water has warmed enough to stratify. It has been predicted that SSTs could increase 1.8 °C (3.25 °F) in the Bering Sea and 1.0 °C (1.8 °F) in the Gulf of Alaska by the middle of the 21st century (Overland and Wang 2007). Extreme sea-ice loss could result in an ice free Arctic Ocean by summer 2100, and the Bering Sea will be ice-free year-round (ACIA 2005).

Increased CO_2 in the atmosphere increases ambient temperature (i.e., acting as a greenhouse gas). As atmospheric concentrations of CO_2 increase, the ocean absorbs additional CO_2, changing its pH. Since the industrial revolution, the pH of the world's oceans has dropped from 8.2 to 8.1, making it more acidic. Ocean acidification has been implicated in measured decreases in carbonate ion concentration, the latter of which is a crucial element in the construction of the exoskeleton of numerous marine calcifying organisms (i.e., corals, mollusks, and calcareous phytoplankton). The Secretariat of the Convention on Biological Diversity (2009), in their scientific synthesis of impacts arising from ocean acidification, noted the following pertinent to phytoplankton:

- Potential impacts to a major phytoplankton component – coccolithophores – are associated with ocean acidification. Coccolithophores secrete tests (plates made of calcite); massive blooms of this species have been documented, and decreasing rates of calcification of 40% have been observed in the coccolithophorid *Emiliania huxleyi* with increasing pCO_2, and up to 66% with pCO_2 values of 800 ppm. Most studies have focused on one coccolithophore species; variable results have been returned from observations of other coccolithophores that did not demonstrate a significant change in calcification rates with increased CO_2.

- Coccolithophores are major producers of DMS, which is oxidized to SO_4 in the atmosphere. DMS is an important component of aerosols and thought to influence the lifetimes and optical properties of clouds, and can be supersaturated in surface waters; it has been proposed that the resultant emissions to the atmosphere reduce the radiative flux to the Earth's surface.

Two trends in primary productivity have been recently documented, including

- decreasing trend in surface chlorophyll concentrations in the subtropical gyres in the past decade (Gregg et al. 2005); and
- areas of low chlorophyll gyres are expanding (McClain et al. 2004b; Polovina et al. 2008).

It has been suggested that one of the causes for these declines is the increase in surface-water stratification resulting from worldwide temperature increases. As noted previously, Boyce et al. (2010) have recently synthesized available information from the past century to assess changes in phytoplankton biomass, assessing various spatial (i.e., regional, global) and temporal (i.e., decadal, centennial) timescales. Results show statistically significant long-term decreases in surface chlorophyll within eight of the world's 10 ocean basins, and for the global aggregate, with most changes on the order of 0.01 mg m^{-3} y^{-1}. They also found a strong correspondence between the chlorophyll change and changes in both leading climate indices (e.g., ENSO) and ocean thermal conditions. However, on short-term scales, the "trends" depend heavily on the chosen years as well as on the algorithms (Lee et al. 2010).

7.4 Data Gaps and Recommendations

7.4.1 Primary Production

Significant variability in primary productivity determinations was evident, particularly in the Alaska Region. Accuracy of satellite-derived productivity estimates may be affected by one or more factors, including

- chlorophyll-*a* concentration can be significantly overestimated (>100%) from satellite measurements (particularly in the Alaska Region) due to algorithm artifacts in the atmospheric correction and bio-optical inversion;
- Seasonal solar insolation effects are evident (i.e., predominantly in the Alaska Region); and
- Uniform application of the NPP model may be slightly problematic for marginal seas and areas of upwelling; *in situ* validation in each of the planning areas is warranted.

The current atmospheric correction is the current state-of-the-art algorithm after several iterations within the ocean color community. However, it cannot address errors due to absorbing aerosols (e.g., dust, smoke, etc.) due to lack of ultraviolet bands. How often this occurs, and to what degree, requires ground measurements and detailed diagnosis of each individual scene (i.e., snapshot) instead of the monthly data. The same difficulty applies to bio-optical inversion, mainly due to the lack of *in situ* data. In the future, satellite ocean color instruments will have one or two ultraviolet bands that are designed to detect and correct absorbing aerosol effects, and more *in situ* data will be collected and available from the community. Therefore, future summary and synthesis efforts should include extensive *in situ* data to validate satellite-based observations and application of the NPP model.

7.4.2 Secondary Production

7.4.2.1 Ecopath

One of the prevalent observations noted during summarization of secondary productivity modeling was the different spatial scales evident among model results. In most ecosystem models, the "study area" is not clearly defined by boundaries or total area, but rather on ecosystem type. Thus, many of the studies do not indicate the total area of the ecosystem modeled, but rather assume that the model will effectively describe any site within the general area, and/or areas of identical ecosystem type. As a result, ecosystem modeling results were developed and/or reported for localized areas, while others were developed on broader, regional scales.

One of the more interesting questions that arose during review and summarization of secondary productivity modeling results was whether there is a reasonable prospect of eventually developing a representative secondary productivity estimate for each planning area and then multiplying by surface area to calculate total productivity. Such calculations are possible, however, two big challenges are evident: spatial resolution and parameter uncertainty.

The challenge associated with spatial uncertainty centers on major data gaps, the most significant of which is the disparity in data availability and model development. Several important ecosystems have not been sampled adequately to provide reliable input data for Ecopath models, while many systems have not been modeled at all. There are also major problems associated with applying a productivity estimate and multiplying that value by total surface area to estimate total system productivity. Productivity at the ocean surface and productivity within the water column are different; it is difficult to estimate one based on the other, and accurate data are often difficult to obtain for total productivity within the water column. To further complicate this issue, some habitats are especially difficult to sample (e.g., deep benthic communities, Arctic habitats).

The challenges associated with parameter uncertainty are based on the current status of Ecopath model application and recognized limitations. Ecosystem modeling will be key for developing representative productivity estimates for each planning area, however, additional data acquisition and model revision are required. While Ecopath remains the most prevalent and widely used ecosystem modeling approach in U.S. waters, it still has major limitations. A model is only as good as the data that go into it to estimate parameters. Thus, if quality data do not exist for an ecosystem, a high quality ecosystem model cannot be developed. Also, many of the Ecopath models are recycling parameters from other models with no verification that the parameters are correctly estimated. Further development and calibration of models is needed to increases confidence in model estimates of productivity.

7.4.2.2 NPZ

Based on this most recent analysis of the NPZ modeling approach, several questions have been raised regarding utility and technical rigor. The current analysis showed that high spatial resolution satellite data on chlorophyll (i.e., P, primary productivity estimates) are available. Remaining components necessary for the NPZ approach include high resolution data on nutrients (N) and zooplankton (Z). As reflected in **Appendix B**, there appears to be sufficient zooplankton data for most planning areas. However, the nutrient database is, at present, deficient. With a reasonable amount of effort, nutrient data can be compiled. Identified limitations with this approach include the fact that only surface productivity would be calculated, leaving data gaps for fish and benthos. It is suggested that coupling of NPZ and Ecopath in the future may be feasible.

There are efforts currently underway to use satellite data to estimate nutrient concentrations that would provide spatial resolution on the same scale as chlorophyll (i.e., Montagna NASA efforts off Texas; Hu efforts off Florida). The approach is based on the fact that nutrients flow from rivers into coastal waters along with sediments, thus there is a link between turbidity (which can be identified using satellite imagery) and nutrient concentrations. Identified limitations with this NPZ approach include the fact that only surface productivity and primary consumer productivity would be calculated, leaving data gaps for fish and benthos. It is suggested that coupling of NPZ and Ecopath in the future may be feasible.

8.0 Literature Cited

Aagaard, K. and E.C. Carmack. 1989. The role of sea ice and other fresh water in the arctic circulation. J. Geophys. Res. 94 (C10):14,485–14,498.

Abbott, M.R. and D.B. Chelton. 1991. Advances in passive remote-sensing of the ocean. Reviews of Geophysics 29:571-589.

Arctic Climate Impact Assessment (ACIA). 2005. Arctic climate impact assessment. Cambridge University Press. 1,042 pp.

Agawin, N.S.R.A., C.M. Duarte, and S. Agusti. 2000. Response of Mediterranean *Synechococcus* growth and loss rates to experimental nutrient inputs. Mar. Ecol. Prog. Ser. 206:97-106.

Aguilar-Islas, A.M., M.P. Hurst, K.N. Buck, B. Sohst, G.J. Smith, M.C. Lohan, and K.W. Bruland. 2007. Micro- and macronutrients in the southeastern Bering Sea: Insight into iron-replete and iron-depleted regimes. Progress in Oceanography 73(2):99-126.

Aguirre-Hernández, E., G. Gaxiola-Castro, S. Nájera-Martínez, T. Baumgartner, M. Kahru, and B.G. Mitchell. 2004. Phytoplankton absorption, photosynthetic parameters, and primary production off Baja California: Summer and autumn 1998. Deep-Sea Res. II 51:799-816.

Aizawa, C., M. Tanimoto, and R.W. Jordan. 2005. Living diatom assemblages from North Pacific and Bering Sea surface waters during summer 1999. Deep-Sea Res. II Top. Stud. Oceanogr. 52(16-18):2,186-2,205.

Alexander, V. and H.J. Niebauer. 1981. Oceanography of the eastern Bering Sea ice-edge zone in spring. Limnol. Oceanogr. 26(6):1,111-1,125.

Anderson, L.A. 2009. The seasonal nitrogen cycle in Wilkinson Basin, Gulf of Maine, as estimated by 1-D biological model optimization. J. Mar. Syst. 78:77-93.

Aretxabaleta, A., B.O. Blanton, H.E. Seim, F.E. Werner, J.R. Nelson, and E.P. Chassignet. 2007. Cold event in the South Atlantic Bight during summer of 2003: Model simulations and implications. J. Geophys. Res. C Oceans 112, C05022, doi:10.1029/2006JC003903.

Arismendez, S.S, H.-C. Kim, J. Brenner, and P.A. Montagna. 2009. Application of watershed analyses and ecosystem modeling to investigate land–water nutrient coupling processes in the Guadalupe Estuary, Texas. Ecological Informatics 4:243-253.

Arnone, R.A., S.D. Ladner, A. Lawson, Z. Lee, R.W. Gould, and C.O. Davis. 2010. Characterizing the spatial and temporal uncertainty in coastal ocean color products. Oral presentation BO 23A-08, Ocean Sciences Meeting, Portland, OR.

Atkinson, M.J. and R.W. Grigg. 1984. Model of a coral reef ecosystem II. Gross and net benthic primary production at French Frigate Shoals, Hawaii. Coral Reefs 3:13-22.

Aydin, K.Y., G.A. McFarlane, J.R. King, and B.A. Megrey, eds. 2003. The BASS/MODEL report on trophic models of the subarctic Pacific basin ecosystems. PICES-GLOBEC International Program on Climate Change and Carrying Capacity: PICES 25. 97 pp.

Aydin, K., S. Gaichas, I. Ortiz, D. Kinzey, and N. Friday. 2007. A comparison of the Bering Sea, Gulf of Alaska, and Aleutian Islands large marine ecosystems through food web modeling. NOAA Tech. Memo. NMFS-AFSC-178. 298 pp.

Azam, F. and J.A. Fuhrman. 1984. Measurements of bacterioplankton growth in the sea and its regulation by environmental conditions. In: Hobbie, J.E. and P.J.LeB. Williams, eds. Heterotrophic activity in the sea. New York: Plenum Press. Pp. 179-196.

Azam, F., T. Fenchel, J.G. Field, J.S. Gray, L.-A. Meyer-Reil, and F. Thingstad. 1983. The ecological role of water column microbes in the sea. Mar. Ecol. Prog. Ser. 10:257-263.

Babin, M., J. Therriault, L. Legendre, B. Nieke, R. Reuter, and A. Condal. 1995. Relationship between maximum quantum yield of carbon fixation and the minimum quantum yield of chlorophyll-a in vivo fluorescence in the Gulf of St. Lawrence. Limnol. Oceanogr. 40:956-968.

Bailey, K.M., L. Ciannelli, N.A. Bond, A. Belgrano, and N.C. Stenseth. 2005. Recruitment of walleye pollock in a physically and biologically complex ecosystem: A new perspective. Prog. Oceanogr. 67:24–42.

Bajer, P.G., W. Whitledge, and R.S. Hayward, and R.D. Zweifel. 2003. Laboratory evaluation of two bioenergetics models applied to yellow perch: Identification of a major source of systematic error. J. Fish Biol. 62:436-454.

Bajer, P.G., R.S. Hayward, G.W. Whitledge, and R.D. Zweifel. 2004a. Simultaneous identification and correction of systematic error in fish bioenergetics models: Demonstration with a white crappie (*Pomoxis annularis*) model. Can. J. Fish. Aquat. Sci. 61:2,168-2,182.

Bajer, P.G., W. Whitledge, and R.S. Hayward. 2004b. Widespread consumption-dependent systematic error in fish bioenergetics models and its implications. Can. J. Fish. Aquat. Sci. 61:2,158-2,167.

Balch, W.M., D.T. Drapeau, B.C. Bowler, E.S. Booth, L.A. Windecker, and A. Ashe. 2008. Space-time variability of carbon standing stocks and fixation rates in the Gulf of Maine, along the GNATS transect between Portland, ME, USA, and Yarmouth, Nova Scotia, Canada. J. Plank. Res. 30:119-139.

Banas, N.S., E.J. Lessard, R.M. Kudela, P. MacCready, T.D. Peterson, B.M. Hickey, and E. Frame. 2009. Planktonic growth and grazing in the Columbia River plume region: A biophysical model study. J. Geophys. Res. 114, C00B06.

Bane, J.M., Y.H. Spitz, R.M. Letelier, and W.T. Peterson. 2007. Intraseasonal oscillations in Oregon's coastal upwelling system: From the jet stream to zooplankton. Proc. Nat. Acad. Sci. USA 104:13,262-13,267.

Banse, K. 1991. Iron availability, nitrate uptake, and exportable new production in the subarctic Pacific. J. Geophys. Res. 96:741-748.

Banse, K. and S. Mosher. 1980. Adult body mass and annual production/biomass relationships of field populations. Ecol. Monogr. 50:355-379.

Barlow, J., M. Kahru, and B.G. Mitchell. 2008. Cetacean biomass, prey consumption, and primary production requirements in the California current ecosystem. Mar. Ecol. Prog. Ser. 371:285-295.

Barnett, A., K.S. Redd, S.D. Frusher, J.D. Stevens, and J.M. Semmens. 2010. Non-lethal method to obtain stomach samples from a large marine predator and the use of DNA analysis to improve dietary information. J. Exp. Mar. Biol. Ecol. 393:188-192.

Barth, J.A., B.A. Menge, J. Lubchenco, F. Chan, J.M. Bane, A.R. Kirincich, M.A. McManus, K.J. Nielsen, S.D. Pierce, and L. Washburn. 2007. Delayed upwelling alters nearshore coastal ocean ecosystems in the northern California current. Proc. Nat. Acad. Sci. USA 104:3,719-3,724.

Baumert, H. 1996. On the theory of photosynthesis and growth in phytoplankton. Part I: light-limitation and constant temperature. Int. Rev. Gesamten. Hydrobiol. 81:109-139.

Beaugrand, G. and P.C. Reid. 2003. Long-term changes in phytoplankton, zooplankton and salmon related to climate. Glob. Change Biol. 9:801-817.

Beaugrand, G., F. Ibanez, J.A. Lindley, and P.C. Reid. 2002. Diversity of calanoid copepods in the North Atlantic and adjacent seas: species associations and biogeography. Mar. Ecol. Prog. Ser. 232:179-195.

Beaugrand, G., K.M. Brander, J.A. Lindley, S. Souissi, and P.C. Reid. 2003. Plankton effect on cod recruitment in the North Sea. Nature 426:661-664.

Behrenfeld, M.J. and P.G. Falkowski. 1997a. Photosynthetic rates derived from satellite-based chlorophyll concentration. Limnol. Oceanogr. 42:1-20.

Behrenfeld, M.J. and P.G. Falkowski. 1997b. A consumer's guide to phytoplankton primary production models. Limnol. Oceanogr. 42:1,479-1,491.

Behrenfeld, M.J., A.J. Bale, Z.S. Kolber, J. Aiken, and P.G. Falkowski. 1996. Confirmation of iron limitation of phytoplankton photosynthesis in the equatorial Pacific Ocean. Nature 383:508-516.

Belabbassi, L., W.D. Nowlin, A.E. Jochens, P. Chapman, and D.C. Biggs. 2005. Summertime nutrient supply to near-surface waters of the northeastern Gulf of Mexico: 1998, 1999, and 2000. Gulf Mex. Sci. 23(2):137-160.

Belgrano, A., A.P. Allen, B.J. Enquist, and J.F. Gillooly. 2002. Allometric scaling of maximum population density: A common rule for marine phytoplankton and terrestrial plants. Ecol. Lett. 5:611-613.

Bender, M., H. Ducklow, J. Kiddon, J. Marra, and J. Martin. 1992. The carbon balance during the 1989 spring bloom in the North-Atlantic Ocean, 47°N, 20°W. Deep-Sea Res. Part A 39:1,707-1,725.

Bender, M., J. Orchardo, M.-L. Dickson, R. Barber, and S. Lindley. 1999. In vitro O_2 fluxes compared with ^{14}C production and other rate terms during the JGOFS Equatorial Pacific experiment. Deep-Sea Res. I 46:637-654.

Bidigare, R.R., B.B. Prezelin, and R.C. Smith. 1992. Bio-optical models and the problem of scaling. In: P.G. Falkowski and A.D. Woodhead, eds. Primary productivity and biogeochemical cycles in the sea. New York: Plenum Press. Pp. 175-212

Biggs, D.C. 1992. Nutrients, plankton, and productivity in a warm-core ring in the western Gulf of Mexico. J. Geophys. Res. 97:2,143-2,154.

Biggs, D.C. and F.E. Müller-Karger. 1994. Ship and satellite observations of chlorophyll stocks in interacting cyclone-anticyclone eddy pairs in the western Gulf of Mexico. J. Geophys. Res. 99:7,371-7,384.

Biggs, D.C. and P.H. Ressler. 2001. Distribution and abundance of phytoplankton, zooplankton, ichthyoplankton, and micronekton in the deepwater Gulf of Mexico. Gulf Mex. Sci. 19:7-29.

Biggs, D.C. and L.L. Sanchez. 1997. Nutrient enhanced primary productivity of the Texas-Louisiana continental shelf. J. Mar. Sys. 11:237-247.

Biggs, D.C., A.E. Jochens, M.K. Howard, S.F. DiMarco, K.D. Mullin, R.R. Leben, F.E. Müller-Karger, and C. Hu. 2005. Eddy forced variations in on- and off-margin summertime circulation along the 1000-m isobath of the northern Gulf of Mexico, 2000-2003, and links with sperm whale distributions along the middle slope. In: Sturges, W. and A. Lugo-Fernandez, eds. Circulation in the Gulf of Mexico: Observations and models. Amer. Geophys. Union Geophys. Monogr. Series. Pp. 71-85.

Biggs, D.C., C. Hu, and F.E. Müller-Karger. 2008. Remotely sensed sea surface chlorophyll and POC flux at Deep Gulf of Mexico Benthos sampling stations. Deep-Sea Res. II 55:2,555-2,562.

Bisagni, J.J. 2003. Seasonal variability of nitrate supply and potential new production in the Gulf of Maine and Georges Bank regions. J. Geophys. Res. C Oceans 108(11):16-1-16-22.

Boehme, S.E., C.L. Sabine, and C.E. Reimers. 1998. CO_2 fluxes from a coastal transect: A time-series approach. Mar. Chem. 63(1-2):49-67.

Bograd, S.J., D.A. Checkley, and W.S. Wooster. 2003. CalCOFI: A half century of physical, chemical, and biological research in the California current system. Deep-Sea Res. II 50(14-16):2,349-2,353.

Botsford, L.W., C.A. Lawrence, E.P. Dever, A. Hastings, and J. Largier. 2003. Wind strength and biological productivity in upwelling systems: An idealized study. Fish. Oceanogr.12:245-259.

Botsford, L.W., C.A. Lawrence, E.P. Dever, A. Hastings, and J. Largier. 2006. Effects of variable winds on biological productivity on continental shelves in coastal upwelling systems. Deep-Sea Res. II 53(25-26):3,116-3,140.

Bouterfas, R., M. Belkoura, and A. Dauta. 2002. Light and temperature effects on the growth rate of three freshwater algae isolated from a eutrophic lake. Hydrobiologia 489:207-217.

Box, G.E.P. 1976. Science and statistics. J. Amer. Statist. Assoc. 71:791-799.

Boyce, D.G., M.R. Lewis, and B. Worm. 2010. Global phytoplankton decline over the past century. Nature 466:591-596.

Boyd, P.W., T. Jickells, C.S. Law, S. Blain, E.A. Boyle, K.O. Buesseler, K.H. Coale, J.J. Cullen, H.J.W. de Baar, M. Follows, M. Harvey, C. Lancelot, M. Levasseur, N.P.J. Owens, R. Pollard, R.B. Rivkin, J. Sarmiento, V. Schoemann, V. Smetacek, S. Takeda, A. Tsuda, S. Turner, and A.J. Watson. 2007. Mesoscale iron enrichment experiments 1993-2005: Synthesis and future directions. Science 315:612-617.

Brand, E.J., I.C. Kaplan, C.J. Harvey, P.S. Levin, E.A. Fulton, A.J. Hermann, and J.C. Field. 2007. A spatially explicit ecosystem model of the California Current's food web and oceanography. U.S. Dept. Commerce, NOAA Tech. Memo. NMFS-NWFSC-84. 145 pp.

Brett, J.R. and T.D.D. Groves. 1979. Physiological energetics. In: Hoar, W.S., D.J. Randall, and J.R. Brett, eds. Fish Physiology. Volume 8. Bioenergetics and Growth. New York: Academic Press. Pp. 279-352.

Brickley, P. and A.C. Thomas. 2004. Satellite-measured seasonal and interannual chlorophyll variability in the Northeast pacific and coastal Gulf of Alaska. Deep-Sea Res. II Top. Stud. Oceanogr. 51:229–245.

Brink, K.H. and T.J. Cowles. 1991. The coastal transition zone program. J. Geophys. Res. 96:14,637-14,647.

Brown, J.H., J.F. Gillooly, A.P. Allen, V.M. Savage, and G.B. West. 2004. Toward a metabolic theory of ecology. Ecology 85:1,771-1,789.

Bruland, K.W., E.L. Rue, and G.J. Smith. 2001. Iron and macronutrients in California coastal upwelling regimes: Implications for diatom blooms. Limnol. Oceanogr. 46:1,661-1,674.

Bruland, K.W., M.C. Lohan, A.M. Aguilar-Islas, G.J. Smith, B. Sohst, and A. Baptista. 2008. Factors influencing the chemistry of the near-field Columbia River plume: Nitrate, silicic acid, dissolved Fe and dissolved Mn. J. Geophys. Res. doi:10.1029/2007JC004702.

Brzezinski, M.A., D.R. Phillips, F.P. Chavez, G.E. Friederich, and R.C. Dugdale. 1997. Silica production in the Monterey, California, upwelling system. Limnol. Oceanogr.42:1,694-1,705.

Buesseler, K.O., M.P. Bacon, J.K. Cochran, and H.D. Livingston. 1992. Carbon and nitrogen export during the JGOFS North-Atlantic bloom experiment estimated from Th-234-U-238 disequilibria. Deep-Sea Res. Part A 39(7-8A):1,115-1,137.

Bureau of Ocean Energy Management, Regulation, and Enforcement (BOEMRE). 2010a. Offshore statistics by water depth. http://www.gomr.mms/homepg/fastfacts/WaterDepth/WaterDepth.html.

Bureau of Ocean Energy Management, Regulation, and Enforcement (BOEMRE). 2010b. Pacific OCS platforms. http://www.boemre.gov/omm/pacific/offshore/platforms/platformintro.htm.

Bureau of Ocean Energy Management, Regulation, and Enforcement (BOEMRE). 2010c. Bureau of Ocean Energy Management, Alaska OCS Region, Detailed Active Leases. http://alaska.boemre.gov/lease/hlease/LeasingTables/detailed_active_leases.pdf.

California Cooperative Oceanic Fisheries Investigations (CalCOFI). 2010. Station maps, 113 stations. http://media.calcofi.org/graphs/stamaps.html. Accessed 23 August 2010.

Campbell, J.W. and T. Aarup. 1992. New production in the North-Atlantic derived from seasonal patterns of surface chlorophyll. Deep-Sea Res. Part A 39(10A):1,669-1,694.

Campbell, J., D. Antoine, R. Armstrong, K. Arrigo, W. Balch, R. Barber, M. Behrenfeld, R. Bidigare, J. Bishop, M.E. Carr, W. Esaias, P. Falkowski, N. Hoepffner, R. Iverson, D. Kiefer, S. Lohrenz, J. Marra, A. Morel, J. Ryan, V. Vedernikov, K. Waters, C. Yentsch, and J. Yoder. 2002. Comparison of algorithms for estimating ocean primary production from surface chlorophyll, temperature, and irradiance. Global Biogeochem. Cycles 16(3):1,035. doi:10.1029/2001GB001444.

Campbell, N.A. and J.B. Reece. 2002. Biology. 6th ed. San Francisco, CA: Benjamin Cummings.

Carmack, E.C. and R.W. Macdonald. 2002. Oceanography of the Canadian Shelf of the Beaufort Sea: A setting for marine life. Arctic 55:29–45.

Cavender-Bares, K.K., D.M., Karl, and S.W. Chisholm. 2001. Nutrient gradients in the western North Atlantic Ocean: Relationship to microbial community structure and comparison to patterns in the Pacific Ocean|. Deep-Sea Res. I Oceanogr. Res. Papers 48:2,373-2,395.

Cerino, D.S. 2010. Bioenergetics and trophic impacts of invasive Indo-Pacific lionfish. M.Sc. Thesis, East Carolina University.

Charpy-Roubaud, C. and A. Sournia. 1990. The comparative estimation of phtyoplanktonic, microphytobenthic and macrophytobenthic primary production in the oceans. Marine Microbial Food Webs 4:31-57.

Chase, Z., B. Hales, T. Cowles, R. Schwartz, and A. van Geen. 2005a. Distribution and variability of iron input to Oregon coastal waters during the upwelling season. J. Geophys. Res. 110, C10S12. doi:10.1029/2004JC002590.

Chase, Z., K.S. Johnson, V.A. Elrod, J.N. Plant, S.E. Fitzwater, L. Pickell, and C.M. Sakamoto. 2005b. Manganese and iron distributions off central California influenced by upwelling and shelf width. Mar. Chem. 95:235-254.

Chase, Z., P. Strutton, and B. Hales. 2007. Iron links river runoff and shelf width to phytoplankton biomass along the US west coast. Geophys. Res. Letters 34(L04607): doi:10.1029/2006GL028069.

Chavez, F.P., J.T. Pennington, C.G. Castro, J.P. Ryan, R.P. Michisaki, B. Schlining, P. Walz, K.R. Buck, A. McFadyen, and C.A. Collins. 2002. Biological and chemical consequences of the 1997-1998 El Niño in central California waters. Progr. Oceanogr. 54(1-4):205-232.

Checkley, C.M., Jr. and J.A. Barth. 2009. Patterns and processes in the California Current System. Progr. Oceanogr. doi:10.1016/j.pocean.2009.07.028.

Chelton, D.B., P.A. Bernal, and J.A. McGowan. 1982. Large-scale interannual physical and biological interaction in the California Current. J. Mar. Res. 40:1,095-1,125.

Childers, A.R., T.E. Whitledge, and D.A. Stockwell. 2005. Seasonal and interannual variability in the distribution of nutrients and chlorophyll *a* across the Gulf of Alaska shelf: 1998-2000. Deep-Sea Res. II Top. Stud. Oceanogr. 52:193-216.

Chipps, S. and D. Bennett. 2000. Zooplanktivory and nutrient regeneration by invertebrate (*Mysis relicta*) and vertebrate (*Oncorhynchus nerka*) planktivores: Implications for trophic interactions in oligotrophic lakes. Trans. Am. Fish. Soc. 129:569-583.

Chipps, S and D. Bennett. 2002. Evaluation of a *Mysis* bioenergetics model. J. Plankton Res. 4:77-82.

Chipps, S.R., L.M. Einfalt and D.H. Wahl. 2000. Growth and food consumption by tiger muskellunge: Effects of temperature and ration level on bioenergetic model predictions. Trans. Am. Fish. Soc. 129:186-193.

Chizinski, C.J., B. Sharma, K.L. Pope, K.L. Pope, and R. Patinos. 2008. A bioenergetic model for zebrafish *Danio rerio* (Hamilton). J. Fish Biol. 73:35-43.

Christensen, V. and D. Pauly. 1992. Ecopath II - A software for balancing steady-state ecosystem models and calculating network characteristics. Ecol. Model. 61:169-185.

Christensen, V. and C.J. Walters. 2004. Ecopath with Ecosim: Methods, capabilities, and limitations. Ecol. Model. 172:109-139.

Christensen, V., C.J. Walters, D. Pauly, and R. Forrest. 2008. Ecopath with Ecosim version 6: User Guide, November 2008 Edition. Lenfest Ocean Futures Project, Vancouver, 235 pp. (available online at www.ecopath.org).

Christensen, V., C.J. Walters, R. Ahrens, J. Alder, J. Buszowski, L.B. Christensen, W.W.L. Cheung, J. Dunned, R. Froese, V. Karpouzi, K. Kaschner, K. Kearney, S. Lai, V. Lam, M.L.D. Palomares, A. Peters-Mason, C. Piroddi, J.L. Sarmiento, J. Steenbeek, R. Sumaila, R. Watson, D. Zeller, and D. Pauly. 2009. Database-driven models of the world's large marine ecosystems. Ecol. Model. 220:1,984-1,996.

Clark, C.D., W.T. Hiscock, F.J. Millero, G. Hitchcock, L. Brand, W.L. Miller, L. Ziolkowski, R.F. Chen, and R.G. Zika. 2004. CDOM distribution and CO_2 production on the southwest Florida shelf. Mar. Chem. 89:145-167.

Cloern, J.E. 2007. Habitat connectivity and ecosystem productivity: implications from a simple model. Amer. Naturalist 169:E21-E33.

Coachman, L.K. 1986. Circulation, water masses, and fluxes on the southeastern Bering Sea shelf. Cont. Shelf Res. 5 (1-2):23–108.

Coale, K.H., K.S. Johnson, S.E. Fitzwater, R.M. Gordon, S. Tanner, F.P. Chavez, L. Ferioli, C. Sakamoto, P. Rogers, F. Millero, P. Steiberg, P. Nightingale, D. Cooper, W.P. Cochlan, M.R. Landry, J. Constantinou, G. Rollwagen, A. Trasvina, and R. Kudela. 1996. A massive phytoplankton bloom induced by an ecosystem scale iron fertilization experiment in the equatorial Pacific Ocean. Nature 383:495-501.

Coale, K.H., K.S. Johnson, S.E. Fitzwater, S.P.G. Blain, T.P. Stanton, and T.L. Coley. 1998. IronEx-I, an in situ iron-enrichment experiment: Experimental design, implementation and results. Deep-Sea Res. II Top. Stud. Oceanogr. 45:919-945.

Codispoti, L.A., C. Flagg, V. Kelly, and J.H Swift. 2005. Hydrographic conditions during the 2002 SBI process experiments. Deep-Sea Res. II Top. Stud. Oceanogr. 52 (24-26):3,199–3,226.

Coles, V.J., C. Wilson, and R.R. Hood. 2004. Remote sensing of new production fuelled by nitrogen fixation. Geophysical Research Letters 31:L06301. doi:10.1029/2003GL019018.

Collier, J.L. and B. Palenik. 2003. Phycoerythrin-containing picoplankton in the Southern California Bight. Deep-Sea Res. II 50:2,405-2,422.

Conley, D.J. and T.C. Malone. 1992. Annual cycle of dissolved silicate in Chesapeake Bay - Implications for the production and fate of phytoplankton biomass. Mar. Ecol. Prog. Series 81(2):121-128.

Continental Shelf Associates, Inc. (CSA). 1990. A comparison of marine productivity among Outer Continental Shelf Planning Areas. U.S. Dept. of the Interior, Minerals Management Service, Herndon, VA. OCS Study MMS 90-0070. 43 pp. + app.

Continental Shelf Associates, Inc. (CSA). 1991a. A comparison of marine productivity among Outer Continental Shelf Planning Areas. Supplement – An evaluation of benthic habitat primary productivity. U.S. Dept. of the Interior, Minerals Management Service, Herndon, VA. OCS Study MMS 91-0001. 245 pp. + app.

Continental Shelf Associates, Inc. (CSA). 1991b. A comparison of marine productivity among outer continental shelf planning areas. Feasibility analysis of secondary productivity measures. U.S. Dept. of the Interior, Minerals Management Service, Herndon, VA. OCS Study MMS 91-0031. 74 pp.

Continental Shelf Associates, Inc. (CSA). 2004. Geological and geophysical exploration for mineral resources on the Gulf of Mexico Outer Continental Shelf. Final Programmatic Environmental Assessment. U.S. Dept. of the Interior, Minerals Management Service, Gulf of Mexico OCS Region, New Orleans, LA. OCS EIS/EA 2004-054. https://www.gomr.mms.gov/PDFs/2004/2004-054.pdf.

Cortés, E. and S.H. Gruber. 1990. Diet, feeding habits and estimates of daily ration of young lemon sharks, *Negaprion brevirostris* (Poey). Copeia 1990:204-218.

Cosgrove, J.J. 2007. Marine phytoplankton primary production and ecophysiology using chlorophyll-*a* fluorescence. Ph.D. thesis, Murdoch University.

Cota, G.F., L.R. Pomeroy, W.G. Harrison, E.P. Jones, F. Peters, W.M. Sheldon, and T.R. Weingartner. 1996. Nutrients, primary production and microbial heterotrophy in the southeastern Chukchi Sea: Arctic summer nutrient depletion and heterotrophy. Mar. Ecol. Prog. Ser. 135:247-258.

Covey, C., K.M. AchutaRao, U. Cubasch, P. Jones, S.J. Lambert, M.E. Mann, T.J. Phillips, and K.E. Taylor. 2003. An overview of results from the Coupled Model Intercomparison Project (CMIP). Global Planet. Change 37:103-133.

Cowley, P.D. and A.K. Whitfield. 2002. Biomass and production estimates of a fish community in a small South African estuary. J. Fish Biol. 61:74-89.

Coyle, K.O., T.J. Weingartner, and G.L. Hunt, Jr. 1998. Distribution of acoustically determined biomass and major zooplankton taxa in the upper mixed layer relative to water masses in the western Aleutian Islands. Mar. Ecol. Prog. Ser. 165:95-108.

CSA International, Inc. 2010. Fate and potential effects: Drilling fluid accidental release at the Mahogany Deep-2 wellsite, West Cape Three Points Block, offshore Ghana. Prepared for Kosmos Ghana, LLC, Dallas, TX.

Cui, Y. and R. J. Wootton. 1989. Bioenergetics and growth of a cyprinid, *Phoxinus phoxinus* (L.): Development and testing of a growth model. J. Fish Biol. 34:47-67.

Cullen, J.J. and M.R. Lewis. 1995. Biological processes and optical measurements near the sea-surface - some issues relevant to remote-sensing. J. Geophys. Res.-Oceans 100(C7):13,255-13,266.

Davis, C.O., N. Tufillaro, R.A. Arnone, Z. Lee, D. Korwan, M. Corson, J. Nahorniak, M.J. Montes, B. Gao, R.L. Lucke, D. Lewis, R.W. Gould, and R.M. Letelier. 2010. On orbit calibration and product validation for the Hyperspectral Imager for the Coastal Ocean (HICO). Oral presentation BO 23A-07, Ocean Sciences Meeting, Portland, OR.

de Baar, H.J.W., J.T. de Jong, D.C.E. Bakker, B.M. Loscher, C. Veth, U. Bathmann, and V. Smetacek. 1995. Importance of iron for plankton blooms and carbon dioxide drawdown in the Southern Ocean. Nature 373:412-415.

Dinnel, S.P. and A. Bratkovich. 1993. Water discharge, nutrient concentration, and nitrate flux in the lower Mississippi River. J. Mar. Sys. 4:315-326.

Dortch, Q. and T.E. Whitledge. 1992. Does nitrogen or silicon limit phytoplankton in the Mississippi River plume and nearby regions? Cont. Shelf Res. 12:1,293-1,309.

Dugdale, R. and F. Wilkerson. 1989. New production in the upwelling center off Point Conception, California: Temporal and spatial patterns. Deep-Sea Res. 36:985-1,007.

Dugdale, R., F. Wilkerson, V. Hogue, and A. Marchi. 2006. Nutrient controls on new production in the Bodega Bay, California, coastal upwelling plume. Deep-Sea Res. II 53:3,049-3,062.

Dugdale, R.C. and J.J. Goering. 1967. Uptake of new and regenerated forms of nitrogen in primary production. Limnol. Oceanogr. 12:196-206.

Dugdale, R.C., F.P. Wilkerson, R.T. Barber, and F.P. Chavez. 1992. Estimating new production in the equatorial Pacific Ocean at 150 W. J. Geophys. Res.-Oceans 97(C1):681-686.

Dunton, K.H., J.L. Goodall, S.V. Schonberg, J.M. Grebmeier, and D.R. Maidment. 2005. Multi-decadal synthesis of benthic–pelagic coupling in the western arctic: Role of cross-shelf advective processes. Deep-Sea Res. II Top. Stud. Oceanogr. 52 (24-26):3,462–3,477.

Dunton, K.H., T. Weingartner, and E. Carmack. 2006. The nearshore western Beaufort Sea ecosystem: Circulation and importance of terrestrial carbon in arctic coastal food webs. Progress in Oceanography 71(2-4):362-378.

Durbin, E.G., R.G. Campbell, M.C. Casas, M.D. Ohman, B. Niehoff, J. Runge, and M. Wagner. 2003. Interannual variation in phytoplankton blooms and zooplankton productivity and abundance in the Gulf of Maine during winter. Mar. Ecol. Prog. Ser. 254:81-100.

Ecopath. 2010. http://www.ecopath.org/ Accessed 9/1/10.

Edgar, G.J. 1990. The use of the size structure of benthic macrofaunal communities to estimate faunal biomass and secondary production. J. Exper. Mar. Biol. Ecol. 137:195-214.

Edwards, M. and A.J. Richardson. 2004. Impact of climate change on marine pelagic phenology and trophic mismatch. Nature 430:881-884.

Edwards, M., P.C. Reid, and B. Planque. 2001. Long-term and regional variability of phytoplankton biomass in the north-east Atlantic (1960-1995). ICES. J. Mar. Sci. 58:39-49.

Edwards, M., G. Beaugrand, P.C. Reid, A.A. Rowden, and M.B. Jones. 2002. Ocean climate anomalies and the ecology of the North Sea. Mar. Ecol. Prog. Ser. 239:1-10.

Edwards, M., D.G. Johns, S.C. Leterme, E. Svendsen, and A.J. Richardson. 2006. Regional climate change and harmful algal blooms in the northeast Atlantic. Limnol. Oceanogr. 51:820-829.

Eisner, L. and T. Cowles. 2005. Spatial variations in phytoplankton pigment ratios, optical properties, and environmental gradients in Oregon coast surface waters. J. Geophys. Res. 110(C10S14): doi:10.1029/2004JC002614.

Emerson, S., C. Stump, B. Johnson, and D.M. Karl. 2002. *In situ* determination of oxygen and nitrogen dynamics in the upper ocean. Deep-Sea Res. I. 49:941-952.

Enquist, B.J., J.H. Brown, and G.B. West. 1998. Allometric scaling of plant energetics and population density. Nature 395:163-165.

Eppley, R.W. 1972. Temperature and phytoplankton growth in the sea. Fish Bull. 70:1,063-1,085.

Eppley, R.W., ed. 1986. Plankton dynamics of the Southern California Bight. Berlin and New York: Springer-Verlag. 373 pp.

Eppley, R.W. 1989. New production: History, methods, problems. In: V.S. Smetacek and G. Wefer, eds. Productivity of the ocean: Present and past. Report of the Dahlem Workshop, Berlin, 1988. John Wiley & Sons. Pp. 85-97.

Eppley, R.W. and B.J. Peterson. 1979. Particulate organic matter flux and planktonic new productivity in the deep ocean. Nature 282:677-680.

Eppley, R.W., E. Stewart, M.R. Abbott, and U. Heyman. 1985. Estimated ocean primary production from satellite chlorophyll. J. Plankton Res. 7:57-70.

Espinosa-Carreon, T.L., P.T. Strub, E. Beier, F. Ocampo-Torres, and G. Gaxiola-Castro. 2004. Seasonal and interannual variability of satellite-derived chlorophyll pigment, surface height, and temperature off Baja California. J. Geophys. Res. 109:C03039. doi:10.1029/2003JC002105.

Falkowski, P.G. 1992. Molecular ecology of phytoplankton photosynthesis. In: Falkowski, P.G. and A.D. Woodhead, eds. Primary productivity and biogeochemical cycles in the sea. New York: Plenum Press. Pp. 47-67.

Falkowski, P. 1994. The role of phytoplankton photosynthesis in global biogeochemical cycles. Photosynth. Res. 39:235-258.

Falkowski, P.G. and A.D. Woodhead, eds. 1992. Primary productivity and biogeochemical cycles in the sea. New York: Plenum Press. 550 pp.

Falkowski, P.G., P.E. Biscaye, and C. Sancetta. 1994. The lateral flux of biogenic particles from the eastern North American continental margin to the North Atlantic Ocean. Deep-Sea Res. II Top. Stud. Oceanogr. 41:583-601.

Falkowski, P.G., R.T. Barber, and V. Smetacek. 1998. Biogeochemical controls and feedbacks on ocean primary production. Science 281:200-206.

Fanning, K.A. 1992. Nutrient provinces in the sea - concentration ratios, reaction-rate ratios, and ideal covariation. J. Geophys. Res.-Oceans 97(C4):5,693-5,712.

Fath, B.D. and M.C. Killian. 2007. The relevance of ecological pyramids in community assemblages. Ecol. Model. 208:286-294.

Faul, K.L., L.D. Anderson, and M.L. Delaney. 2003. Late Cretaceous and early Paleogene nutrient and paleoproductivity records from Blake Nose, western North Atlantic Ocean. Paleoceanography 18(2):1,042.

Feng, Y., C.E. Hare, K. Leblanc, G. R. DiTullio, P. A. Lee, S.W. Wilhelm, J. Sun, J. M. Rose, N. Nemcek, I. Benner, and D.A. Hutchins. 2009. The effects of increased $p\mathrm{CO}_2$ and temperature on the North Atlantic Spring Bloom: I. The phytoplankton community and biogeochemical response.

Fiechter, J. and C.N.K. Mooers. 2007. Primary production associated with the Florida Current along the East Florida Shelf: Weekly to seasonal variability from mesoscale-resolution biophysical simulations. J. Geophys. Res. C Oceans 112, C12002, doi:10.1029/2006JC003576, 2007.

Fiechter, J., A.M. Moore, C.A. Edwards, K.W. Bruland, E. Di Lorenzo, C.V.W. Lewis, T.M. Powell, E.N. Curchitser, and K. Hedstrom. 2009. Modeling iron limitation of primary production in the coastal Gulf of Alaska. Deep-Sea Res. II Top. Stud. Oceanogr. 56 (24):2,503–2,519.

Field, J. 2004. Application of ecosystem-based fishery management approaches in the northern California Current. Ph.D. dissertation, University of Washington, School of Aquatic and Fishery Sciences, Seattle, WA. 418 pp.

Field, J. and R. Francis. 2005. Mass balance models of the Northern California Current. In: Guenette, S. and V. Christensen, eds. Food web models and data for studying fisheries and environmental impacts on Eastern Pacific ecosystems. Fisheries Centre Research Reports 13:207-216.

Field, J.C., R.C. Francis, and K. Aydin. 2006. Top-down modeling and bottom-up dynamics: Linking a fisheries-based ecosystem model with climate hypotheses in the Northern California Current. Prog. Oceanogr. 68:238-270.

Firme, G.F., E.L. Rue, D.A. Weeks, K.W. Bruland, and D.A. Hutchins. 2003. Spatial and temporal variability in phytoplankton iron limitation along the California coast and consequences for Si, N, and C biogeochemistry. Global Biogeochem. Cycles 17(1):1,016. doi:10.1029/2001GB001824.

Fitzwater, S.E., K.S. Johnson, V.A. Elrod, J.P. Ryan, L.J. Coletti, S.J. Tanner, R.M. Gordon, and F.P. Chavez. 2003. Iron, nutrient and phytoplankton biomass relationships in upwelled waters of the California coastal system. Cont. Shelf Res. 23:1,523-1,544.

Flint, M.V., I.N. Sukhanova, A.I. Kopylov, S.G. Poyarkov, and T.E. Whitledge. 2002. Plankton distribution associated with frontal zones in the vicinity of the Pribilof Islands. Deep-Sea Res. II Top. Stud. Oceanogr. 49 (26):6,069-6,093.

Flynn, K.J. 2003. Modelling multi-nutrient interactions in phytoplankton; balancing simplicity and realism. Prog. Oceanogr. 56:249-279.

Fornshell, J.A. 2000. Variability of the Florida Current offshore from Fort Pierce Florida as revealed by satellite imagery. Mar. Technol. Soc. J. 34(2):34-37.

Frame, E.R. and E.J. Lessard. 2009. Does the Columbia River plume influence phytoplankton community structure along the Washington and Oregon coasts? J. Geophys. Res. 114(C00B09). doi:10.1029/2008JC0049999.

Frank, K.T., B. Petrie, N.L. Shackwell, and J.S. Choi. 2006. Reconciling differences in trophic control in mid-latitude marine ecosystems. Ecol. Lett. 9:1,096-1,105.

Franks, P.J.S. 2002. NPZ models of plankton dynamics: Their construction, coupling to physics, and application. J. Oceanogr. 58:379-387.

Franks, P.J.S. and C. Chen. 2001. A 3-D prognostic numerical model study of the Georges Bank ecosystem. Part II: Biological-physical model. Deep-Sea Res. II Top. Stud. Oceanogr. 48(1-3):457-482.

Franz, B. 2010. SeaWiFS, MODIS Reprocessing, Ocean Biology Processing Group Update/IOP ISRO/ESA Collaborations. Presented at the NASA Ocean Color Research Group meeting, 11-13 May 2010, New Orleans, LA.

Fromentin, J.M. and B. Planque. 1996. *Calanus* and environment in the eastern North Atlantic. II. Influence of the North Atlantic Oscillation on *Calanus finmarchicus* and *C. hegolandicus*. Mar. Ecol. Prog. Ser. 134:111-118.

Frost, B.W. 1987. Grazing control of phytoplankton stock in the open subarctic Pacific Ocean: A model assessing the role of mesozooplankton, particularly the large calanoid copepods, *Neocalanus* spp. Mar. Ecol. Prog. Ser. 39:49-68.

Frouin, R., B. Franz, and M. Wang. 2001. Algorithm to estimate PAR from SeaWiFS data (2001). http://disc.sci.gsfc.nasa.gov/oceancolor/documentation/PDFs/seawifs_par_algorithm.pdf.

Fulton, E.A. 2001. The effects of model structure and complexity on the behavior and performance of marine ecosystem models. Ph.D. thesis, University of Tasmania, Hobart. 429 pp.

Fulton, E.A. 2010. Approaches to end to end ecosystem models. J. Mar. Syst. doi:10.1016/j.jmarsys.2009.12.012.

Fulton, E.A., A.D.M. Smith, and C.R. Johnson. 2003. Effect of complexity on marine ecosystem models. Mar. Ecol. Prog. Ser. 253:1-16.

Fulton, E.A., A.D.M. Smith, and C.R. Johnson. 2004. Biogeochemical marine ecosystem models I: IGBEM – a model of marine bay ecosystems. Ecol. Model. 174:267-307.

Fulton, E.A., A.D.M. Smith, and A.E. Punt. 2005. Which ecological indicators can robustly detect effects of fishing? ICES J. Mar. Sci. 62:540-551.

Gabric, A.J., R. Cropp, A. Hirst, and H. Marchant. 2003. The sensitivity of dimethylsulphide production to simulated climate change in the eastern Antarctic Southern Ocean. Tellus B 55:966-981.

Gaichas, S., G. Skaret, J. Falk-Petersen, J.S. Link, W. Overholtz, B.A. Megrey, H. Gjøsæterb, W.T. Stockhausen, A. Dommasnes, K.D. Friedland, and K. Aydin. 2009. A comparison of community and trophic structure in five marine ecosystems based on energy budgets and system metrics. Prog. Oceanogr. 81:47-62.

Gascuel, D. M. Leclerc, A. Valls, and S. Guénette. 2009. EcoTroph: A new tool in the EwE family. In: Deng, M.L., L. Palomares, A. Morissette, D. Cisneros-Montemayor, M. Varkey, M. Coll, and C. Piroddi, eds. Ecopath 25 years conference proceedings: Extended abstracts. Fisheries Centre Research Reports 17. Pp. 21-22.

Geider, R., H.L. MacIntyre, and T.M. Kana. 1998. A dynamic regulatory model of phytoplanktonic acclimation to light, nutrients, and temperature. Limnol. Oceanogr. 43:679-694.

Glibert, P.M. and C. Garside. 1992. Diel variability in nitrogenous nutrient-uptake by phytoplankton in the Chesapeake Bay plume. J. Plankton Res. 14(2):271-288.

Goericke, R., E. Venrick, T. Koslow, W. Sydeman, F. Schwing, S. Bograd, W.T. Peterson, R. Emmett, J.R. Lara, G. Gaxiola Castro, J. Gomez-Valdes, K.D. Hyrenbach, R.W. Bradley, M.J. Weise, J.T. Harvey, C. Collins, and N.C.H. Lo. 2007. The state of the California current, 2006-2007: Regional and local processes dominate. Calif. Coop. Oceanic. Fish. Invest. Rep. 48:33-66.

Goldman, J.C. 1979. Temperature effects on steady-state growth, phosphorus uptake, and the chemical composition of a marine phytoplankter. Microb. Ecol. 5:153-166.

Goldman, J.C. and E.J. Carpenter. 1974. A kinetic approach to the effect of temperature on algal growth. Limnol. Oceanogr. 19:756-766.

Gong, G.-C., F.-K. Shia, K.-K. Liu, Y.-H. Wen, and M.-H.Liang. 2000. Spatial and temporal variation of chlorophyll a, primary productivity and chemical oceanography in the southern East China Sea. Cont. Shelf Res. 20:411-436.

Gordon, H.R., D.K. Clark, J.L. Mueller, and W.A. Hovis. 1980. Phytoplankton pigments derived from the Nimbus-7 CZCS: Initial comparisons with surface measurements. Science 210:63-65.

Gosselin, M., M. Levasseur, P.A. Wheeler., R.A. Horner, and B.C. Booth. 1997. New measurements of phytoplankton and ice algal production in the Arctic Ocean. Deep-Sea Res. II 44:1,623-1,644.

Gower, J.F. and S.A. King. 2010. Validation of global observations of intense surface plankton blooms and floating vegetation using MERIS. Oral presentation BO 23A-06, Ocean Sciences Meeting, Portland, OR.

Gradinger, R. 2009. Sea-ice algae: Major contributors to primary production and algal biomass in the Chukchi and Beaufort Seas during May/June 2002. Deep-Sea Res. II Top. Stud. Oceanogr. 56 (17):1,201-1,212.

Graziano, L.M., W.M. Balch, D. Drapeau, B.C. Bowler, R. Vaillancourt, and S. Dunford. 2000. Organic and inorganic carbon production in the Gulf of Maine. Cont. Shelf Res. 20(6):685-705.

Grebmeier, J.M., C.P. McRoy, and H.M. Feder. 1988. Pelagic-benthic coupling on the shelf of the northern Bering and Chukchi seas. I. Food supply source and benthic biomass. Mar. Ecol. Prog. Ser. 48:57-67.

Gregg, W.W. and N.W. Casey. 2004. Global and regional evaluation of the SeaWiFS chlorophyll data set. Remote Sensing of Environment 93:463-479.

Gregg, W.W., N.W. Casey, and C.R. McClain. 2005. Recent trends in global ocean chlorophyll. Geophys. Res. Lett. 32, L03606. doi:03610.01029/02004GL021808.

Grigg, R.W., J.J. Polovina, and M.J. Atkinson. 1984. Model of a coral reef ecosystem III. Resource limitation, community regulation, fisheries yield and resource management. Coral Reefs 3:23-27.

Guenette, S. 2005. Models of Southeast Alaska. In: Guénette, S. and V. Christensen, eds. Foodweb models and data for studying fisheries and environmental impact on Eastern Pacific ecosystems: Vancouver, BC, Canada, Fisheries Centre, University of British Columbia, Fisheries Centre Research Reports 13:106-178.

Hales, B., L. Karp-Boss, A. Perlin, and P.A. Wheeler. 2006. Oxygen production and carbon sequestration in an upwelling coastal margin. Global Biogeochem. Cycles 20, GB3001. doi:10.1029/2005GB002517. doi:10.1029/2004GB002295.

Hales, B., T. Takahashi, and L. Bandstra. 2005. Atmospheric CO_2 uptake by a coastal upwelling system. Global Biogeochem. Cycles 19, GB1009.

Hansell, D.A., T.E. Whitledge, and J.J. Goering. 1993. Patterns of nitrate utilization and new production over the Bering-Chukchi shelf. Cont. Shelf Res. 13 (5-6):601-627.

Hanson, P.C., T.B. Johnson, D.E. Schindler, and J.F. Kitchell. 1997. Fish Energetics 3.0 University of Wisconsin Sea Grant Institute, Madison, WI.

Harding, L.W., E.C. Itsweire, and W.E. Esaias. 1992. Determination of phytoplankton chlorophyll concentrations in the Chesapeake Bay with aircraft remote-sensing. Remote Sensing of Environment 40(2):79-100.

Hare, C.E., K. Leblanc, G.R. DiTullio, R.M. Kudela, Y. Zhang, P.A. Lee, S.F. Riseman, and D.A. Hutchins. 2007. Consequences of increased temperature and CO_2 for phytoplankton community structure in the Bering Sea. Mar. Ecol. Prog. Ser. 352:9-16. doi:10.3354/meps07182, 2007.

Harrison, W.G., E.J.H. Head, E.P.W. Horne, B. Irwin, W.K.W. Li, A.R. Longhurst, M.A. Paranjape, and T. Platt. 1993. The western North Atlantic Bloom Experiment. Deep-Sea Res. II Top. Stud. Oceanogr. 40:279-305.

Hayward, T.L. 1993. Filaments in the California Current: Effects upon primary production. Final Report. 1 Oct 1988-40 Apr 1991. Accession Number: ADA263036.

Hayward, T.L. 1998. Linkages between physical structure and primary production in the California Current. Final Report A321853. Contract N00014-92-J-1675.

Hayward, T.L. and E.L. Venrick. 1998. Nearsurface pattern in the California Current: Coupling between physical and biological structure. Deep-Sea Res. II 45:1,617-1,638.

He, X., J.F. Kitchell, S.B. Carpenter, J.R. Hodgson, D.E. Schindler, and K.L. Cottingham. 1993. Food web structure and the long-term phosphorus recycling; a simulation model validation. Trans. Amer. Fish. Soc. 122:773-783.

Henson, S.A. and A. Thomas. 2007a. Phytoplankton scales of variability in the California Current System: 1. Interannual and cross-shelf variability. J. Geophys. Res. 112, C07017, doi:10.1029/2006JC004039.

Henson, S.A. and A. Thomas. 2007b. Phytoplankton scales of variability in the California Current System: 2. Latitudinal variability. J. Geophys. Res. 112, C07018, doi:10.1029/2006JC004040.

Hewitt, R.P. 1988. Historical review of the oceanographic approach to fishery research. CalCOFI Rept. 29:27-41.

Heymans, S.J.J. 2005. Ecosystem models of the Western and Central Aleutian Islands in 1963, 1979 and 1991. In: Guénette, S. and V. Christensen, eds. Foodweb models and data for studying fisheries and environmental impact on Eastern Pacific ecosystems. Vancouver, BC, Canada, University of British Columbia, Fisheries Centre Research Reports 13:8-82.

Hickey, B.M. 1979. The California Current system – hypotheses and facts. Prog. Oceanogr. 8:191-279.

Hickey, B.M. 1998. Coastal oceanography of western North America from the tip of Baja California to Vancouver Island. In: Robinson, A.R. and K.H. Brink, eds. The sea, the global coastal ocean, 11. New York: John Wiley & Sons. Pp. 345–393.

Hickey, B.M. and N.S. Banas. 2008. Why is the northern end of the California current system so productive? Oceanography 21(4):90-107.

Hill, V. and G. Cota. 2005. Spatial patterns of primary production on the shelf, slope and basin of the Western Arctic in 2002. Deep-Sea Res. II Top. Stud. Oceanogr. 52(24-26):3,344-3,354.

Hill, V., G. Cota, and D. Stockwell. 2005. Spring and summer phytoplankton communities in the Chukchi and Eastern Beaufort Seas. Deep-Sea Res. II Top. Stud. Oceanogr. 52(24-26):3,369-3,385.

Hoepffner, N. and S. Sathyendranath. 1992. Bio-optical characteristics of coastal waters - absorption-spectra of phytoplankton and pigment distribution in the western North-Atlantic. Limnol. Oceanogr. 37(8):1,660-1,679.

Hooker, S.B. and E.R. Firestone, eds. 2003. Algorithm updates for the fourth SeaWiFS data processing. SeaWiFS Postlaunch Technical Report Series 22:51-59.

Hopkinson, B.M. 2007. Oceanographic and ecological consequences of iron localization in phytoplankton photosystems. Ph.D. dissertation, University of California, San Diego, La Jolla, CA. 226 pp.

Horner, R. 1984. Phytoplankton abundance, chlorophyll a, and primary productivity in the western Beaufort Sea. In: Barnes, P., D. Schell, and E. Reimnitz, eds. The Alaskan Beaufort Sea: Ecosystems and environments. New York: Academic Press Inc. Pp. 295–310.

Hovis, W.A., D.K. Clark, F. Anderson, R.W. Austin, W.H. Wilson, E.T. Baker, D. Ball, H.R. Gordon, J.L. Mueller, S.Z. El-Sayed, B. Sturm, R.C. Wrigley, and C.S. Yentsch. 1980. Nimbus-7 coastal zone color scanner: System description and initial imagery. Science 201:60-63.

Howarth, R.W. 1988. Nutrient limitation of net primary production in marine ecosystems. Ann. Rev. Ecol. 19:89-110.

Howarth, R.W., ed. 1996. Nitrogen cycling in the North Atlantic Ocean and its watersheds. Kluwer Academic Publishers. 310 pp.

Hu, C., F.E. Müller-Karger, D.C. Biggs, K.L. Carder, B. Nababan, D. Nadeau, and J. Vanderbloemen. 2003. Comparison of ship and satellite bio-optical measurements on the continental margin of the NE Gulf of Mexico. Int. J. Remote Sens. 24:2,597-2,612.

Hu, C., E. Montgomery, R. Schmitt, and F.E. Müller-Karger. 2004a. The Amazon and Orinoco River plumes in the tropical Atlantic: Observation from space and S-floats. Deep-Sea Res-II 51:1151-1171.

Hu, C., F.E. Müller-Karger, G.A. Vargo, M.B. Neely, and E. Johns. 2004b. Linkages between coastal runoff and the Florida Keys ecosystem: A study of a dark plume event. Geophys. Res. Lett. 31: L15307.

Hunt, Jr., G.L., P. Stabeno, G. Walters, E. Sinclair, R.D. Brodeur, J.M. Napp, and N.A. Bond. 2002. Climate change and control of the southeastern Bering Sea pelagic ecosystem. Deep-Sea Res. II Top. Stud. Oceanogr. 49 (26):5,821-5,853.

Hunt, Jr., G.L., P.J. Stabeno, S. Strom, and J.M. Napp. 2008. Patterns of spatial and temporal variation in the marine ecosystem of the southeastern Bering Sea, with special reference to the Pribilof Domain. Deep-Sea Res. II Top. Stud. Oceanogr. 55(16-17):1,919-1,944.

Hurst, M.P., A.M. Aguilar-Islas, and K.W. Bruland. 2010. Iron in the southeastern Bering Sea: Elevated leachable particulate Fe in shelf bottom waters as an important source for surface waters. Cont. Shelf Res. 30(5):467-480.

Hutchins, D.A. and K.W. Bruland. 1998. Iron-limited diatom growth and Si:N uptake ratios in a coastal upwelling regime. Nature 393:561-564.

Hutchins, D.A., G.R. DiTullio, Y. Zhang, and K.W. Bruland. 1998. An iron limitation mosaic in the California upwelling regime. Limnol. Oceanogr. 43(6):1,037-1,054.

Huyer, A. 1976. A comparison of upwelling events in two locations: Oregon and northwest Africa. J. Mar. Res. 34(4):531-546.

Huyer, A. 1983. Coastal upwelling in the California Current system. Prog. Oceanogr. 12:259-284.

Huyer, A., J. Fleischbein, J. Keister, P. Kosro, N. Perlin, R. Smith, and P. Wheeler. 2005. Two coastal upwelling domains in the northern California Current system. J. Mar. Res. 63:901-929.

Ikeda, T. 1974. Nutritional ecology of marine zooplankton. Memoirs of the Faculty of Fisheries, Hokkaido University 22:1-97.

Ikeda, T. 1985. Metabolic rates of epipelagic marine zooplankton as a function of body mass and temperature. Marine Biology 85:1-11.

Incze, L.S., D.W. Siefert, and J.M. Napp. 1996. Mesozooplankton of Shelikov Strait, Alaska: Abundance and community composition. Cont. Shelf Res. 17:287–305.

Intergovernmental Panel on Climate Change (IPCC). 2007a. Climate Change 2007: Synthesis Report. In: Pachauri, R.K. and A. Reisinger, eds. Contributions of Working Groups I, II, and III to the Fourth Assessment Report of the Intergovernmental Panel on Climate Change. Geneva, Switzerland: IPCC. 104 pp.

Intergovernmental Panel on Climate Change (IPCC). 2007b. Climate Change 2007: The Physical Science Basis. In: Solomon, S.D., D. Qin, M. Manning, Z. Chen, M. Marquis, K.B. Averyt, M. Tignor, and H.L. Miller, eds. Contributions of Working Group I to the Fourth Assessment Report of the Intergovernmental Panel on Climate Change. Cambridge, UK and New York, NY: Cambridge University Press. 996 pp.

International Association of Oil & Gas Producers. 2005. Fate and effects of naturally occurring substances in produced water on the marine environment. Report No. 364. February 2005. http://www.ogp.org.uk/pubs/364.pdf.

International Ocean-Colour Coordinating Group (IOCCG). 2004. Guide to the creation and use of ocean-colour, level-3, binned data products. In: Antoine, D., ed. Reports of the International Ocean-Colour Coordinating Group, No. 4, IOCCG, Dartmouth, Canada.

Jackson, J.B.C, M.X. Kirby, W.H. Berger, K.A. Bjorndal, L.W. Botsford, B.J. Bourque, R.H. Bradbury, R. Cooke, J. Erlandson, J.A. Estes, T.P. Hughes, S. Kidwell, C.B. Lange, H.S. Lenihan, J.M. Pandolfi, C.H. Peterson. R.S. Steneck, M.J. Tegner, and R.R. Warner. 2001. Historical overfishing and the recent collapse of coastal ecosystems. Science 293:629-638.

Janout, M.A., T.J. Weingartner, S.R. Okkonen, T.E. Whitledge, and D.L. Musgrave. 2009. Some characteristics of Yakutat Eddies propagating along the continental slope of the northern Gulf of Alaska. Deep-Sea Res. II Top. Stud. Oceanogr. 56(24):2,444–2,459.

Jenkins, W.J. and D.W.R. Wallace. 1992. Tracer-based inferences of new primary production in the sea. In: Falkowski, P.G. and A.D. Woodhead, eds. Primary productivity and biogeochemical cycles in the sea. New York: Plenum Press. Pp. 299-316.

Ji., R., C.S. Davis, C. Chen, D.W. Townsend, D.G. Mountain, and R.C. Beardsley. 2007. Influence of ocean freshening on shelf phytoplankton dynamics. Geophys. Res. Lett. SO 34, L24607, doi:10.1029/2007GL032010.

Ji, R., C. Davis, C. Chen, and R. Beardsley. 2008a. Influence of local and external processes on the annual nitrogen cycle and primary productivity on Georges Bank: A 3-D biological physical modeling study. J. Mar. Syst. 73:31-47.

Ji, R., C.S. Davis, C. Chen, D.W. Townsend, D.G. Mountain, and R.C. Beardsley. 2008b. Modeling the influence of low-salinity water inflow on winter-spring phytoplankton dynamics in the Nova Scotian Shelf-Gulf of Maine region. J. Plankton Res. 30:1,399-1,416.

Jin, M., C. Deal, J. Wang, V. Alexander, R. Gradinger, S. Saitoh, T. Iida, Z. Wan, and P. Stabeno. 2007. Ice-associated phytoplankton blooms in the southeastern Bering Sea. Geophysical Research Letters 34:L06612, doi:10.1029/2006GL028849.

Johnson, K.S., R.M. Gordon, and K.H. Coale. 1997. What controls dissolved iron concentrations in the world ocean? Mar. Chem. 57:137-161.

Joos, F., G. Plattner, T.F. Stocker, O. Marchal, and A. Schmittner. 1999. Global warming and the marine carbon cycle feedbacks on future atmospheric CO_2. Science 284:464-467.

Justic, D., N.N. Rabalais, and R.E. Turner. 2005. Coupling between climate variability and coastal eutrophication: Evidence and outlook for the northern Gulf of Mexico. J. Sea Res. 54:25-35.

Kahru, M. and B.G. Mitchell. 2000. Influence of the 1997-98 El Niño on the surface chlorophyll in the California Current. Geophys. Res. Lett. 27:2,937-2,940.

Kahru, M. and B.G. Mitchell. 2008. Ocean color reveals increased blooms in various parts of the world. Eos Trans. AGU 89(18):170, doi:10.1029/2008EO180002.

Kahru, M., R. Kudela, M. Manzano-Sarabia, and B.G. Mitchell. 2009. Trends in primary production in the California Current detected with satellite data. J. Geophys. Res. 114:C02004. doi:10.1029/2008JC004979.

Kaiblinger, C. and M. Dokulil. 2006. Application of fast repetition rate fluorometry to phytoplankton photosynthetic parameters in freshwaters. Photosynthesis Research 88(1):19-30.

Kaplan, I.C. and P. Levin. 2009. Ecosystem-based management of what? An emerging approach for balancing conflicting objectives in marine resource management, pp. 77-95. In: R.J. Beamish and B.J. Rothschild (eds.), The Future of Fisheries Science in North America. Fish & Fisheries Series 31.

Kaplan, I., B. Fulton, I. Ortiz, and C. Ainsworth. 2010. How to build an Atlantis model: A living document. April 2010. 54 pp.

Karl, D.M., J.E. Dore, R. Lukas, A.F. Michaels, N.R. Bates, and A. Knap. 2001. Building the long-term picture: The U.S. JGOFS Time-Series Programs. Oceanography 14:6-17.

Kearns, E.J., J.A. Hanafin, R.H. Evans, P.J. Minnett, and O.B. Brown. 2000. An independent assessment of Pathfinder AVHRR sea surface temperature accuracy using the Marine Atmosphere Emitted Radiance Interferometer Interferometer (MAERI). Bull. Amer. Meteorol. Soc. 81:1,525-1,536.

Kiefer, D.A. and R.R. Reynolds. 1992. Advances in understanding phytoplankton fluorescence and photosynthesis. In: Falkowski, P.G. and A.D. Woodhead, eds. Primary productivity and biogeochemical cycles in the sea. New York: Plenum Press. Pp. 155-174.

Kilpatrick, K.A., G.P. Podesta, and R.E. Evans. 2001. Overview of the NOAA/NASA advanced very high resolution radiometer Pathfinder algorithm for sea surface temperature and associated matchup database. J. Geophys. Res. 106:9,179-9,197.

Kim, H. and A.J. Miller. 2006. How stratification changes affect primary production in the California Current System. American Geophysical Union, Fall Meeting 2006, abstract #OS11A-1469.

Kim, H.-C. and P.A. Montagna. 2009. Implications of Colorado River freshwater inflow to benthic ecosystem dynamics: A modeling study. Estuar. Coast. Shelf S. 83:491-504.

King, A.L. and K. Barbeau. 2007. Evidence for phytoplankton iron limitation in the southern California Current System. Mar. Ecol. Prog. Ser. 342:91-103.

Kirk, J.T.O. 1992. The nature and measurement of the light environment in the ocean, pp. 9-30. In: Falkowski, P.G. and A.D. Woodhead, eds. Primary productivity and biogeochemical cycles in the sea. Plenum Press.

Kirk, J.T.O. 1994. Light & Photosynthesis in Aquatic Ecosystems. 2nd Edition. Cambridge University Press, Cambridge, UK.

Kitchell, J.F., D.J. Stewart, and D. Weininger. 1977. Applications of a bioenergetics model to perch (*Perca flavescens*) and walleye (*Stizostedion vitreum*). J. Fish. Res. Board Can. 34:1,922-1,935.

Kleiber, M. 1932. Body size and metabolism. Hilgardia 6:315-353.

Kopylov, A.I., M.V. Flint, and A.V. Drits. 2005. Primary production of phytoplankton in the eastern part of the Bering Sea. Oceanology 42:215-225.

Kozlowski, J. and M. Konarzewski. 2004. Is West, Brown and Enquist's model of allometric scaling mathematically correct and biologically relevant? Functional Ecology 18:283-289.

Kraft, C.E. 1993. Phosphorus regeneration by Lake Michigan alewives in mid-1970s. Trans. Am. Fish. Soc. 122:749-755.

Kudela, R.M. and T.D. Peterson. 2009. Influence of a buoyant river plume on phytoplankton nutrient dynamics: What controls standing stocks and productivity? J. Geophys. Res. 114(C00B11). doi:10.1029/2008JC004913.

Kudela, R.M., W.P. Cochlan, and R.C. Dugdale. 1997. Carbon and nitrogen uptake response to light by phytoplankton during an upwelling event. J. Plank. Res. 19:609-630.

Kudela, R., N. Garfield, and K. Bruland. 2006. Bio-optical signatures and biogeochemistry from intense upwelling and relaxation in coastal California. Deep-Sea Res. II 53:2,999-3,022.

Kudela, R.M., N.S. Banas, J.A. Barth, E.R. Frame, D.A. Jay, J.L. Largier, E.J. Lessard, T.D. Peterson, and A.J. Vander Woude. 2008. New insights into the controls and mechanisms of plankton productivity in coastal upwelling waters of the northern California Current System. Oceanography 21(4):46-59.

Ladd, C., P. Stabeno, and N. Cockelet. 2005. A note on cross-shelf exchange in the northern Gulf of Alaska. Deep-Sea Res. II: Topical Studies in Oceanography 52(5-6):667-679.

Ladd, C., C.W. Mordy, N. Kachel, and P.J. Stabeno. 2007. Northern Gulf of Alaska eddies and associated anomalies. Deep-Sea Res. I: Oceanogr. Res. Pap. 54(4):487-509.

Landry, M.R., M.D. Ohman, R. Goericke, M.R. Stukel, and K. Tsyrklevich. 2009. Lagrangian studies of phytoplankton growth and grazing relationships in a coastal upwelling ecosystem off Southern California. Prog. Oceanogr. 83:209-216.

Larsen, R.K., III, J.C. Steinbacher, and J.E. Baker. 2001. Ammonia exchange between the atmosphere and the surface waters at two locations in the Chesapeake Bay. Envir. Sci. Tech. 35:4,731-4,738.

Lavoie, D., R.B. Macdonald, and K.L. Denman. 2009. Primary productivity and export fluxes on the Canadian shelf of the Beaufort Sea: A modelling study. J. Mar. Syst. 75 (1-2):17-32.

Laws, E.A. and T.T. Bannister. 1980. Nutrient and light-limited growth of *Thalassiosira fluviatilis* in continuous culture, with implications for phytoplankton growth in the ocean. Limnol. Oceanogr. 25:457-473.

Laws, E.A. and M.S. Chalup. 1990. A microalgal growth model. Limnol. Oceanogr. 35:597-608.

Lee, S.H., T.E. Whitledge, and S. Kang. 2007. Recent carbon and nitrogen uptake rates of phytoplankton in Bering Strait and the Chukchi Sea. Cont. Shelf Res. 27(17):2,231-2,249.

Lee, Z., S. Shang, C. Hu, M.R. Lewis, R. Arnone, Y. Li, and B. Lubac. 2010. Time series of bio-optical properties in a subtropical gyre: Implications for the evaluation of inter-annual trends of biogeochemical properties. J. Geophys. Res. 115, C09012, doi: 10.1029/2009JC005865.

Legaard, K.R. and A.C. Thomas. 2006. Spatial patterns in seasonal and interannual variability of chlorophyll and sea surface temperature in the California Current. J. Geophys. Res.-Oceans 111, C06032, doi:10.1029/2005JC003282.

Lenes, J.M., B.P. Darrow, C. Cattrall, C.A. Heil, M. Callahan, G.A. Vargo, R.H. Byrne, J.M. Prospero, D.E. Bates, K.A. Fanning, and J.J. Walsh. 2001. Iron fertilization and the *Trichodesmium* response on the West Florida shelf. Limnol. Oceanogr. 46(6):1,261-1,277.

Lenzen, M. 2007. Structural path analysis of ecosystem networks. Ecol. Model. 200:334-342.

Lessard, E.J. and E.R. Frame. 2008. The influence of the Columbia River Plume on patterns of phytoplankton growth, grazing and chlorophyll on the Washington and Oregon coasts. Paper presented at the 2008 Ocean Sciences Meeting, AGU/ASLO/ TOS/ERF, Orlando, FL.

Lewis, M.R. 1992. Satellite ocean color observations of global biogeochemical cycles. In: Falkowski, P.G. and A.D. Woodhead, eds. Primary productivity and biogeochemical cycles in the sea. New York: Plenum Press. Pp. 139-153.

Li, W.K.W., P.M. Dickie, W.G. Harrison, and B.D. Irwin. 1993. Biomass and production of bacteria and phytoplankton during the spring bloom in the western North Atlantic Ocean. Deep-Sea Res. II Top. Stud. Oceanogr. 40:307-327.

Lindeman, R.L. 1942. The trophic-dynamic aspect of ecology. Ecology 23:399-418.

Link, J. 2002. Does food web theory work for marine ecosystems? Marine Ecology Progressive Series 230:1-9.

Link, J.S., E.A. Fulton, and R.J. Gamble. 2010. The northeast U.S. application of ATLANTIS: A full system model exploring marine ecosystem dynamics in a living marine resource management context. Prog. Oceanogr. 87:214-234.

Lippemeier, S., R. Hintze, K. Vanselow, P. Hartig, and F. Colijn. 2001. In-line recording of PAM fluorescence of phytoplankton cultures as a new tool for studying effects of fluctuating nutrient supply on photosynthesis. Euro. J. Phycol. 36:89-100.

Lohan, M.C. and K.W. Bruland. 2006. Importance of vertical mixing for additional sources of nitrate and iron to surface waters of the Columbia River plume: Implications for biology. Mar. Chem. 98:260-273.

Lohrenz, S.E., G.A. Knauer, V.L. Asper, M. Tuel, A.F. Michaels, and A.H. Knap. 1992. Seasonal variability in primary production and particle-flux in the northwestern Sargasso Sea - United-States JGOFS Bermuda Atlantic Time-Series Study. Deep-Sea Res. Part A 39(7-8A):1,373-1,391.

Lohrenz, S.E., G.L. Fahnstel, D.G. Redalje, E.A. Lang, X. Chen, and M.J. Dagg. 1997. Variations of primary production of northern Gulf of Mexico continental shelf waters linked to nutrient inputs from the Mississippi River. Mar. Ecol. Prog. Ser. 155:45-54.

Lohrenz, S.E., G.L. Fahnstel, D.G. Redalje, E.A. Lang, M.J. Dagg, T.E. Whitledge, and Q. Dortch. 1999. Nutrients, irradiance, and mixing as factors regulating primary production in coastal waters impacted by the Mississippi River plume. Cont. Shelf Res. 19:1,113-1,141.

Lomas, M.W. and P.M. Glibert. 1999. Interactions between NH_{+4} and NO_{-3} uptake and assimilation: comparison of diatoms and dinoflagellates at several growth temperatures. Mar. Biol. 133:541-551.

Longhurst, A., S. Sathyendranath, T. Platt, and C. Caverhill. 1995. An estimate of global primary production in the ocean from satellite radiometer data. J. Plankton Res. 17:1,245-1,271.

Luo, Y., H. Ducklow, S.C. Doney, and M.A. Friedrichs. 2010. Investigating the decadal increase of primary production at Station ALOHA, Hawaii, using data assimilative model. Oral presentation CO31A-02, Ocean Sciences Meeting, Portland, OR.

Lynch, S.A. 1954. Geology of the Gulf of Mexico. In: Gulf of Mexico, its origin, waters and marine life. U.S. Dept. Interior Fishery Bull. 89(55):67-86.

Lynn, R.J. and J.J. Simpson. 1987. The California Current system: The seasonal variability of its physical characteristics. J. Geophys. Res. 92:12,947-12,966.

Mahaut, M.L., M. Sibuet, and Y. Shirayama. 1995. Weight-dependent respiration rates in deep-sea organisms. Deep-Sea Res. I 42:1,575-1,582.

Maldonado, M.T., P.W. Boyd, P.J. Harrison, and N.M. Price. 1999. Co-limitation of phytoplankton growth by light and Fe during winter in the NE subarctic Pacific Ocean. Deep-Sea Res. II Top. Stud Oceanogr. 46(11-12):2,475-2,485.

Mallin, M.A. and H.W. Paerl. 1992. Effects of variable irradiance on phytoplankton productivity in shallow estuaries. Limnol. Oceanogr. 37(1):54-62.

Mantyla, A.W., S.J. Bograd, and E.L. Venrick. 2008. Patterns and controls of chlorophyll-*a* and primary productivity cycles in the Southern California Bight. J. Mar. Systems 73:48-60.

Maranon, E. and P.M. Holligan. 1999. Photosynthetic parameters of phytoplankton from 50 degrees N to 50 degrees S in the Atlantic Ocean. Mar. Ecol. Prog. Series 176:191-203.

Marinelli, R.L., R.A. Jahnke, D.B. Craven, J.R. Nelson, and J.E. Eckman. 1998. Sediment nutrient dynamics on the South Atlantic Bight continental shelf. Limnol. Oceanogr. 43:1,305-1,320.

Marra, J. and R.T. Barber. 2005. Primary productivity in the Arabian Sea: A synthesis of JGOFS data. Prog. in Oceanogr. 65:159-175.

Marra, J. and K. Heinemann. 1984. A comparison between noncontaminating and conventional incubation procedures in primary production measurements. Limnol. Oceanogr. 29:389-392.

Marra, J. and K.R. Heinemann. 1987. Primary production in the North Pacific Central Gyre: Some new measurements based on ^{14}C. Deep-Sea Res. 34:1,821-1,829.

Marra, J., T. Dickey, W.S. Chamberlin, C. Ho, T. Granata, D.A. Kiefer, C. Langdon, R. Smith, K. Baker, R. Bidigare, and M. Hamilton. 1992. Estimation of seasonal primary production from moored optical sensors in the Sargasso Sea. J. Geophys. Res.-Oceans 97(C5):7,399-7,412.

Martin, J.H., R.M. Gordon, S. Fitzwater, and W.W. Broenkow. 1989. VERTEX phytoplankton-iron studies in the Gulf of Alaska, USA. Deep-Sea Res. Part A. Oceanogr. Res. Pap. 36(5):649-680.

Matsuoka, A., P. Larouche, M. Poulin, W. Vincent, and H. Hattori. 2009. Phytoplankton community adaptation to changing light levels in the southern Beaufort Sea, Canadian Arctic. Estuar. Coast. Shelf S. 82(3):537-546.

Maynard, N.G. and D.K. Clark. 1987. Satellite color observations of Spring blooming in Bering Sea shelf waters during the ice edge retreat in 1980. J. Geophys. Res. 92:7,121-7,139.

Maynard, N.G., V. Barale, and J. Svejkovsky. 1987. Satellite observed dynamics of chlorophyll and suspended sediments in a shallow, high latitude embayment. Adv. Space Res. 7(2):83-88.

McCarthy, J.J., C. Garside, and J.L. Nevins. 1992. Nitrate supply and phytoplankton uptake kinetics in the euphotic layer of a Gulf-Stream warm-core ring. Deep-Sea Res. Part A 39(1a):S393-S403.

McClain, C.R., M.L. Cleave, G.C. Feldman, W.W. Gregg, S.B. Hooker, and N. Kuring. 1998. Science quality SeaWiFS data for global biosphere research. Sea Tech. 39:10-16.

McClain, C.R., G.C. Feldman, and S.B. Hooker. 2004a. An overview of the SeaWiFS project and strategies for producing a climate research quality global ocean bio-optical time series. Deep-Sea Res. II 51:5-42.

McClain, C.R., S.R. Signorini, and J.R. Christian. 2004b. Subtropical gyre variability observed by ocean-color satellites. Deep-Sea Res. II 51:281-301.

McClatchie, S., R. Goericke, J.A. Koslow, F.B. Schwing, S.J. Bograd, R. Charter, W. Watson, N. Lo, K. Hill, J. Gottschalck, M. L'Heureux, Y. Xue, W.T. Peterson, R. Emmett, C. Collins, G. Gaxiola-Castro, R. Durazo, M. Kahru, B.G. Mitchell, K.D. Hyrenbach, W.J. Sydeman, R.W. Bradley, P. Warzybok, and E. Bjorkstedt. 2008. The State of the California Current, 2007-2008: La Niña conditions and their effects on the ecosystem. Calif. Coop. Oceanic Fish. Invest. Rep. 49:39-76.

McClatchie, S., R., Goericke, F.B. Schwing, S.J. Bograd, R. Charter, W. Watson, N. Lo, K. Hill, C. Collins, M. Kahru, B.G. Mitchell, J.A. Koslow, J. Gomez-Valdes, B.E. Lavaniegos, G. Gaxiola-Castro, J. Gottschalck, M. L'Heureux, Y. Xue, M. Manzano-Sarabia, E. Bjorkstedt, S. Ralston, J. Field, L. Rogers-Bennett, L. Munger, G. Campbell, K. Merkens, D. Camacho, A. Havron, A. Douglas, and J. Hildebrand. 2009. The State of the California Current, Spring 2008-2009: Cold conditions drive regional differences in coastal production. Calif. Coop. Oceanic Fish. Invest. Rep. 50:43-68.

McGowan, J.A., S.J. Bograd, R.J. Lynn, and A.J. Miller. 2003. The biological response to the 1977 regime shift in the California Current. Deep-Sea Res. II 50:2,567-2,582.

McRoy, C.P. 1993. ISHTAR, the project: An overview of inner shelf transfer and recycling in the Bering and Chukchi seas. Cont. Shelf Res. 13(5-6):473-479.

McRoy, C.P. 1999. Water over the bridge: A summing up of the contributions of the ISHTAR Project in the Northern Bering and Chukchi Seas. In: Loughlin, T.R. and Ohtani, K. (editors), 1999, Dynamics of the Bering Sea: A summary of physical, chemical, and biological characteristics, and a synopsis of research on the Bering Sea. University of Alaska Sea Grant, AK-SG; 99-03. 825 pp.

McRoy, C.P., J.J. Goering, and W.E. Shiels. 1972. Studies of primary production in the eastern Bering Sea. In: Takenouti, A.Y., ed. Biological oceanography of the North Pacific Ocean. Tokyo: Idemitsu-shoten. Pp. 199-216.

McRoy, C.P., D.A. Hansell, A.M. Springer, J.J. Walsh, and T.E. Whitledge. 1987. Global maximum of primary production in the north Bering Sea. Eos 68:L1727.

Meehl, G.A., G.J. Boer, C. Covey, M. Latif, and R.J. Stouffer. 2000. The Coupled Model Intercomparison Project (CMIP). Bull. Amer. Meteor. Soc. 81:313-318.

Meehl, G.A., C. Covey, B. McAvaney, M. Latif, and R.J. Stouffer. 2005. Overview of the coupled model intercomparison project. Bull. Amer. Meteor. Soc. 86:89-93.

Melo-Gonzalez, N., F.E. Müller-Karger, S. Cerdeira-Estada, R. Perez de los Reyes, I. Victoria del Rio, P. Cardenas-Perez, and I. Mitrani-Arenal. 2000. Near-surface phytoplankton distribution in the western Intra-Americas Sea: The influence of El Nino and weather events. J. Geophys. Res. C 96:12,645-12,665.

Miller, C.B. 2004. Biological Oceanography. Malden, MA: Blackwell Publishing. 402 pp.

Miller, C.B., B.W. Frost, P.A. Wheeler, M.R. Landry, N. Welschmeyer, and T.M. Powell. 1991. Ecological dynamics in the subarctic Pacific, a possibly iron-limited ecosystem. Limnol. Oceanogr. 36(8):1,600-1,615.

Miller, A.J., A.J. Gabric, J.R. Moisan, F. Chai, D.J. Neilson, D.W. Pierce, and E. Di Lorenzo. 2007. Chapter 2, Global Change and Oceanic Primary Productivity: Effects of Ocean-Atmosphere-Biological Feedbacks. Elsevier Oceanography Series 73:27-63.

Minerals Management Service (MMS). 2000. Gulf of Mexico deepwater operations and activities: Environmental assessment. U.S. Dept. of the Interior, Minerals Management Service, Gulf of Mexico OCS Region, New Orleans, LA. OCS EIS/EA MMS 2000-001.

Minerals Management Service (MMS). 2007a. Proposed Final Program: Outer Continental Shelf Oil and Gas Leasing Program, 2007-2012. April 2007.

Minerals Management Service (MMS). 2007b. Gulf of Mexico OCS Oil and Gas Lease Sales: 2007-2012. Western Planning Area Sales 204, 207, 210, 215, and 218; Central Planning Area Sales 205, 206, 208, 213, 216, and 222. Final Environmental Impact Statement. OCS EIS/EA MMS 2007-018. U.S. Dept. of the Interior, Minerals Management Service, Gulf of Mexico OCS Region, New Orleans, LA. 2 volumes.

Minerals Management Service (MMS). 2008. Gulf of Mexico OCS Oil and Gas Lease Sales: 2009-2010. Central Planning Area Sales 208, 213, 216, and 222. Western Planning Area Sales 210, 215, and 218. Final Environmental Impact Statement. OCS EIS/EA MMS 2008-041. U.S. Dept. of the Interior, Minerals Management Service, Gulf of Mexico OCS Region, New Orleans, LA. 485 pp.

Minerals Management Service (MMS). 2009. Draft Proposed Outer Continental Shelf (OCS) Oil and Gas Leasing Program 2010–2015 Considering Comments of Governors, Section 18 Factors and OCS Alternative Energy Opportunities. January 2009.

Mizobata, K., S. Saitoh, and J. Wang. 2008. Interannual variability of summer biochemical enhancement in relation to mesoscale eddies at the shelf break in the vicinity of the Pribilof Islands, Bering Sea. Bering Sea. Deep-Sea Res. II Top. Stud. Oceanogr. 55(16-17):1,717–1,728.

Monaco, M.E. and R.E. Ulanowicz. 1997. Comparative ecosystem trophic structure of three U.S. mid-Atlantic estuaries. Mar. Ecol. Prog. Ser. 161:239-254.

Montagna, P.A. and J. Li. 1997. Modeling contaminant effects on deposit feeding nematodes near Gulf of Mexico production platforms. Ecol. Model. 98:151-162.

Montagna, P.A. and J. Li. 2010. Effect of Freshwater inflow on nutrient loading and macrobenthos secondary production in Texas lagoons. In: Kennish, M.J. and H.W. Paerl, eds. Coastal lagoons: Critical habitats of environmental change, Boca Raton, FL: CRC Press, Taylor & Francis Group. Pp. 513-539.

Morel, A. and L. Prieur. 1977. Analysis of variations in ocean color. Limnol. Oceanogr. 22:709-722.

Morissette, L. 2007. Complexity, cost and quality of ecosystem models and their impact on resilience: A comparative analysis, with emphasis on marine mammals and the Gulf of St. Lawrence. Ph.D. dissertation, University of British Columbia. 278 pp.

Müller-Karger, F.E., J.J. Walsh, R.H. Evans, and M.B. Meyers. 1991. On the seasonal phytoplankton concentration and sea surface temperature cycles of the Gulf of Mexico as determined by satellites. J. Geophys. Res. 96:12,645-12,665.

Müller-Karger, F.E., R. Varela, R. Thunell, Y. Astor, H. Zhang, R. Luerssen, and C. Hu. 2004. Processes of coastal upwelling and carbon flux in the Cariaco Basin. Deep-Sea Res. 51:927-943.

Müller-Karger, F.E., R. Varela, R. Thunell, R. Luerssen, C. Hu, and J.J. Walsh. 2005. The importance of continental margins in the global carbon cycle. Geophys Res. Lett. 32:L01602. doi:10.1029/2004GL021346.

Munch, S.B. and D.O. Conover. 2002. Accounting for local physiological adaptation in bioenergetics models: Testing hypotheses for growth rate evolution by virtual transplant experiments. Can. J. Fish. Aquat. Sci. 59:393-403.

Murie, D.J. and D.M. Lavigne. 1991. Food consumption of wintering harp seals, *Phoca groenlandica*, in the St. Lawrence estuary, Canada. Can. J. Zool. 69:1289-1296.

Murrell, M.C., J.G. Campbell, J.D. Hagy III, and J.M. Caffrey. 2009. Effects of irradiance on benthic and water column processes in a Gulf of Mexico estuary: Pensacola Bay, Florida, USA. Estuar. Coast. Shelf Sci. 81:501-512.

National Aeronautics and Space Administration (NASA). 2010a. Coastal Zone Color Scanner specifications. http://oceancolor.gsfc.nasa.gov/CZCS.

National Aeronautics and Space Administration (NASA). 2010b. CZCS Nimbus-7, 7 November 1978-June 1986. Phytoplankton pigment concentrations (mg m^{-3}). http://disc.sci.gsfc.nasa.gov/oceancolor/documentation/scientific-documentation/CZCS_Starter_kit.shtml.

National Oceanic and Atmospheric Administration (NOAA). 2007. Large marine ecosystems: A breakthrough concept for ecosystem management. http://celebrating200years.noaa.gov/breakthroughs/ecosystems/welcome.html. Accessed 3/26/10.

National Oceanic and Atmospheric Administration (NOAA). 2008. Gulf of Mexico at a Glance. Washington, D.C.: U.S. Dept. of Commerce, National Oceanic and Atmospheric Administration, National Ocean Service.

National Research Council (NRC). 1996. The Bering Sea ecosystem. The National Academic Press. http://www.nap.edu/books/0309053455/html/index.html. Accessed 3/10/2004. 320 pp.

Neff, J.M. 1987. Biological effects of drilling fluids, drill cuttings and produced waters. In: Boesch, D.F. and N.N. Rabalais, eds. Long-term effects of offshore oil and gas development. London: Elsevier Applied Science Publishers. Pp. 469-538

Neff, J.M. 2005. Composition, environmental fates, and biological effects of water based drilling muds and cuttings discharged to the marine environment: a synthesis and annotated bibliography. Prepared for Petroleum Environmental Research Forum (PERF) and American Petroleum Institute. 83 pp.

Neff, J.M., S. McKelvie, and R.C. Ayers, Jr. 2000. Environmental impacts of synthetic based drilling fluids. Report prepared by Robert Ayers & Associates, Inc. U.S. Dept. of the Interior, Minerals Management Service, Gulf of Mexico OCS Region, New Orleans, LA. OCS Study MMS 2000-064. 118 pp.

Nelson, J.R., J.E. Eckman, C.Y. Robertson, R.L. Marinelli, and R.A. Jahnke. 1999. Benthic microalgal biomass and irradiance at the sea floor on the continental shelf of the South Atlantic Bight: Spatial and temporal variability and storm effects. Cont. Shelf Res. 19(4):477-505.

Nesius, K.K., H.G. Marshall, and T.A. Egerton. 2007. Phytoplankton productivity in the tidal regions of four Chesapeake Bay (USA) tributaries. Va. J. Sci. 58(4):191-204.

Neuer, S. 1992. Growth dynamics of marine *Synechococcus* spp. in the Gulf of Alaska. Mar. Ecol. Prog. Ser. 83:251-262.

Newell, C. 2000. Biology of certain mollusk species: Blue mussels; a case study, pp. 125-132. In: R.E. Martin, P.E. Carter, G.J. Flick, Jr., and L.M. Davis (eds.), Marine and Freshwater Products Handbook. Technomic Publishing Company, Inc., Lancaster, PA.

Ney, J.J. 1993. Bioenergetics modeling today: Growing pains on the cutting edge. Trans. Am. Fish. Soc. 122:736-748.

Niebauer, H.J., J. Roberts, and T.C. Royer. 1981. Shelf break circulation in the northern Gulf of Alaska. J. Geophys. Res. 86(C5):4,231–4,242.

Niebauer, H.J., V. Alexander, and S.M. Henrichs. 1995. A time-series study of the spring bloom at the Bering Sea ice edge. I. Physical processes, chlorophyll, and nutrient chemistry. Cont. Shelf Res. 15:1,859-1,877.

Nordøy, E.S., P.E. Mårtensson, A.R. Lager, L.P. Folkow, and A.S. Blix. 1995. Food consumption of the Northeast Atlantic stock of harp seals. In: Blix, A.S., L. Walløe, and Ø. Ulltang, eds. Developments in marine biology 4: Whales, seals, fish and man. Amsterdam: Elsevier Science. Pp. 255-260.

Odum, E. 1959. Fundamentals of ecology. Philadelphia: WB Saunders Co.

Ohizumi, H. and N. Miyazaki. 1998. Feeding rate and daily energy intake of Dall's porpoise in the northeastern Sea of Japan. Proceedings of the NIPR Symposium on Polar Biology 11:74-81.

Oikawa, S. and Y. Itazawa. 1993. Allometric relationship between tissue respiration and body mass in a marine teleost, porgy *Pagrus major*. Comp. Biochem. Physiol. 105:129-133.

Okey, T.A. 2001. A ‘straw-man’ Ecopath model of the Middle Atlantic Bight Continental Shelf, United States. Middle Atlantic Bight, U.S., Part II: Northwest Atlantic. In: Guenette, S., V. Christensen, and D. Pauly, eds. Fisheries impacts on North Atlantic ecosystems: Models and analyses. Fisheries Centre Research Reports 9(4):151-166.

Okey, T.A. and R. Pugliese. 2001. A preliminary Ecopath model of the Atlantic Continental Shelf adjacent to the southeastern United States. Southeastern United States, Atlantic Shelf. In: Guenette, S., V. Christensen, and D. Pauly, eds. Fisheries impacts on North Atlantic ecosystems: Models and analyses. Fisheries Centre Research Reports 9 (4):167-181.

Okey, T.A., G.A. Vargo, S. Mackinson, M. Vasconcellos, B. Mahmoudie, and C.A. Meyer. 2004. Simulating community effects of sea floor shading by plankton blooms over the West Florida Shelf. Ecol. Model. 172:339-359.

Okkonen, S.R., T.J. Weingartner, S.L. Danielson, D.L. Musgrave, and G.M. Schmidt. 2003. Satellite and hydrographic observations of eddy-induced shelf-slope exchange in the northwestern Gulf of Alaska. J. Geophys. Res. 108(C2):3,033-3,042.

Okkonen, S.R., G.M. Schmidt, E.D. Cokelet, and P.J. Stabeno. 2004. Satellite and hydrographic observations of the Bering Sea ‘Green Belt’. Deep-Sea Res. II Top. Stud. Oceanogr. 51(10-11):1,033-1,051.

Olson, R.J., D. Vaulot, and S.W. Chisholm. 1986. Effects of environmental stress on the cell cycle of two marine phytoplankton species. Plant Physiol. 80:918-925.

Olson, R.J. and H.M. Sosik. 2007. A submersible imaging-in-flow instrument to analyze nano- and microplankton: Imaging FlowCytobot. Limnol. Oceanogr. Methods 5:195-203.

Overholtz, W. and J. Link. 2009. A simulation model to explore the response of the Gulf of Maine food web to large-scale environmental and ecological changes. Ecol. Model. 220:2,491-2,502.

Overland, J.E. and M. Wang. 2007. Future climate of the North Pacific Ocean. Eos Trans. Amer. Geophys. Union 88(16):178-182.

Paerl, H.W. and M.L. Fogel. 1994. Isotopic characterization of atmospheric nitrogen inputs as sources of enhanced primary production in coastal Atlantic Ocean waters. Mar. Biol. (Berlin) 119:635-645.

Paerl, H.W., J. Rudek, and M.A. Mallin. 1990. Stimulation of phytoplankton production in coastal waters by natural rainfall inputs nutritional and trophic implications. Mar. Biol. 107:247-254.

Paerl, H.W., J.D. Willey, M. Go, B.L. Peierls, J.L. Pinckney, and M.L. Fogel. 1999. Rainfall stimulation of primary production in western Atlantic Ocean waters: Roles of different nitrogen sources and co-limiting nutrients. Mar. Ecol. Prog. Series 176:205-214.

Paerl, H.W., L.M. Valdes, B.L. Peierls, J.E. Adolf, and L.W. Harding. 2006. Anthropogenic and climatic influences on the eutrophication of large estuarine ecosystems. Limnol. Oceanogr. 51:448-462.

Pahlow, M. 2005. Linking chlorophyll-nutrient dynamics to the Redfield N:C ratio with a model of optimal phytoplankton growth. Mar. Ecol. Progr. Ser. 287:33-43.

Palenik, B., E. Latham, B. Brahamsha, V. Tai, Q. Ren, and I.T. Paulsen. 2008. Metagenomic analysis of plasmids in coastal marine cyanobacterial populations. Abstract. Metagenomics 2008. November 3-7, 2008. California Institute for Telecommunications and Information Technology (Calit2), University of California, San Diego, La Jolla, CA.

Palenik, B., Q. Ren, V. Tai, and I.T. Paulsen. 2009. Coastal *Synechococcus* metagenome reveals major roles for horizontal gene transfer and plasmids in population diversity. Env. Microbiol. 11:349-359.

Paul, J.H., A. Alfreider, J.B. Kang, R.A. Stokes, D. Griffin, L. Campbell, and E. Ornolfsdottir. 2000. Form IA rbcL transcripts associated with a low salinity/high chlorophyll plume ('Green River') in the eastern Gulf of Mexico. Mar. Ecol. Prog. Series 198:1-8.

Pauly, D. and V. Christensen. 1995. Primary production required to sustain global fisheries. Nature 374:255-257.

Pauly, D., V. Christensen, and C. Walters. 2000. Ecopath, Ecosim, and Ecospace as tools for evaluating ecosystem impact of fisheries. ICES Journal of Marine Science 57:697-706.

Pelegri, J.L., A. Marrero-Diaz, and A.W. Ratsimandresy. 2006. Nutrient irrigation of the North Atlantic. Prog. Oceanogr. 70:366-406.

Pena, M.A., W.G. Harrison, and M.R. Lewis. 1992. New production in the central equatorial Pacific. Mar. Ecol. Prog. Series 80(2-3):265-274.

Pennington, J.T. and F.P. Chavez. 2000. Seasonal fluctuations of temperature, salinity, nitrate, chlorophyll and primary production at station H3/M1 over 1989-1996 in Monterey Bay, California. Deep-Sea Res. II Top. Stud. Oceanogr. 47(5-6):947-973.

Pennington, J.T., K.L. Mahoney, V.S. Kuwahara, D.D. Kolber, R. Calienes, and F.P. Chavez. 2006. Primary production in the eastern tropical Pacific: A review. Prog. Oceanogr. 69:285-315. doi:10.1016/j.pocean.2006.03.012.

Perez, M.A., W.B. McAlister, and E.E. Mooney. 1990. Estimated feeding rate relationship for marine mammals based on captive animal data. NOAA Tech Memo NMFS F/NWC-184.

Perry, M., M. Talbot, and R. Alberte. 1981. Photoadaptation in marine phytoplankton: response of the photosynthetic unit. Mar. Biol. 62:91-101.

Pierce, D.W. 2003. Future changes in biological activity in the North Pacific due to anthropogenic forcing of the physical environment. Climatic Change 62:45-74.

Plaganyi, E.E. 2007. Models for an ecosystem approach to fisheries. FAO Fisheries Technical Paper No.477. 125 pp.

Platt, T. and W.G. Harrison. 1985. Biogenic fluxes of carbon and oxygen in the ocean. Nature 318:55-58.

Platt, T. and W.G. Harrison. 1986. Reconciliation of carbon and oxygen fluxes in the upper ocean. Deep-Sea Res. 33:273-276.

Platt, T. and S. Sathyendranath. 1988. Oceanic primary production: Estimation by remote sensing at local and regional scales. Science 241:1,613-1,620.

Platt, T., P. Jauhari, and S. Sathyendranath. 1992. The importance and measurement of new production. In: Falkowski, P.G. and A.D. Woodhead, eds. Primary productivity and biogeochemical cycles in the sea. Plenum Press. Pp. 273-284.

Platt, T., W.G. Harrison, M.R. Lewis, W.K.W. Li, S. Sathyendranath, R.E. Smith, and A.F. Vezina. 1989. Biological production of the oceans: The case for a consensus. Mar. Ecol. Prog. Ser. 52:77-88.

Polovina, J.J. 1984a. Model of a coral reef ecosystem I. The ECOPATH model and its application to French Frigate Shoals. Coral Reefs 3:1-11.

Polovina, J.J. 1984b. An overview of the Ecopath model. ICLARM Fishbyte 2:5-7.

Polovina, J.J., E.A. Howell, and M. Abecassis. 2008. Ocean’s least productive waters are expanding. Geophys. Res. Lett. 35(L03618), doi:10.1029/2007GL031745.

Pomeroy, L.R. 1974. The ocean's food web, a changing paradigm. BioScience 24:499-504.

Pomeroy, L.R., J.E. Sheldon, W.M. Sheldon, Jr., J.O. Blanton, J. Amft, and F. Peters. 2000. Seasonal changes in microbial processes in estuarine and continental shelf waters of the south-eastern U.S.A. Estuar. Coast. Shelf Sci. 51(4):415-428.

Power, M.E., D. Tilman, J.A. Estes, B.A. Menge, W.J. Bond, L.S. Mills, G. Daily, J.C. Castilla, J. Lubchenco, and R.T. Paine. 1996. Challenges in the quest for keystones. Bioscience 46:609-620.

Preikshot, D. 2005. Data sources and derivation of parameters for generalised Northeast Pacific Ocean Ecopath with Ecosim models. In: Guénette, S. and V. Christensen, eds. Foodweb models and data for studying fisheries and environmental impact on Eastern Pacific ecosystems. Fisheries Centre Research Reports 13(1):179-206.

Prieto, L., R.D. Vaillancourt, B. Hales, and J. Marra. 2008. On the relationship between carbon fixation efficiency and bio-optical characteristics of phytoplankton. J. Plankton Res. 30(1):43-56. doi:10.1093/plankt/fbm093.

Program for Climate Model Diagnosis and Intercomparison. 2007. IPCC Model Ouput. Accessed online at www-pcmdi.llnl.gov/ipcc/about_ipcc.php.

Qian, Y., A.E. Jochens, M.C. Kennicutt, and D.C. Biggs. 2003. Spatial and temporal variability of phytoplankton biomass and community structure over the continental margin of the northeast Gulf of Mexico based on pigment analysis. Cont. Shelf Res. 23:1-17. Redalje, D.G., S.E. Lohrenz, P.G. Verity, and C.N. Flagg. 2002. Phytoplankton dynamics within a discrete water mass off Cape Hatteras, North Carolina: The Lagrangian experiment. Deep-Sea Res. II Top. Stud. Oceanogr. 49(20):4,511-4,531.

Redfield, A.C., B.H. Ketchum, and F.A. Rickards. 1963. The influence of organisms on the composition of seawater. In: Hill, M.N., ed. The sea, Vol. 2. New York: J. Wiley & Sons. Pp. 26-77.

Reese, D.C. and R.D. Brodeur. 2006. Identifying and characterizing biological hotspots in the northern California Current. Deep-Sea Res. II 53:291-314.

Regg, J.B., S. Atkins, B. Hauser, J. Hennessey, B.J. Kruse, J. Lowenhaupt, B. Smith, and A. White. 2000. Deepwater development: A reference document for the deepwater environmental assessment Gulf of Mexico OCS (1998 through 2007). OCS Report MMS 2000-015. U.S. Dept. of the Interior, Minerals Management Service, Gulf of Mexico OCS Region, New Orleans, LA. https://www.gomr.mms.gov/PDFs/2000/2000-015.pdf.

Reichler, T. and J. Kim. 2008. How well do coupled models simulate today's climate? Bull. Am. Meteorol. Soc. 89:303-311.

Reid, P.C. and M. Edwards. 2001. Long-term changes in the pelagos, benthos and fisheries of the North Sea. In: Kröncke, M. Türkay, and J. Sündermann, eds. Burning issues of North Sea ecology. I. Senckenbergiana Maritima 31:107-115.

Reid, P.C., M. Edwards, H.G. Hunt, and A.J. Warner. 1998. Phytoplankton change in the North Atlantic. Nature 391:532-546.

Reid, R.N., M.C. Ingham, and J.B. Pearce. 1987. NOAA’s Northeast Monitoring Program (NEMP): A report on progress of the first five years (1979-1984). NOAA Tech. Memo. NMFS-F/NEC-44. 150 pp.

Rho, T. 2004. Primary production and nutrient dynamics of the southeastern Bering Sea shelf. Ph.D. dissertation, University of Alaska Fairbanks, Fairbanks, AK (unpublished).

Rho, T. and T.E. Whitledge. 2007. Characteristics of seasonal and spatial variations of primary production over the southeastern Bering Sea shelf. Cont. Shelf Res. 27 (1):2,556-2,569.

Rho, T., T.E. Whitledge, and J.J. Goering. 2005. Interannual variations of nutrients and primary production over the southeastern Bering Sea Shelf during the spring of 1997, 1998, and 1999. Oceanology 45(3):376-390.

Rice, J.A. and P.A. Cochran. 1984. Independent evaluation of a bioenergetics model for largemouth bass. Ecology 63:732-739.

Richardson, A.J. and D.S. Schoeman. 2004. Climate impact on plankton ecosystems in the Northeast Atlantic. Science 30(5):1,609-1,612.

Riebesell, U. and D.A. Wolf-Gladrow. 1992. The relationship between physical aggregation of phytoplankton and particle flux: A numerical model. Deep-Sea Res. 39:1,085-1,102.

Rose, J.M. and D.A. Caron. 2007. Does low temperature constrain the growth rates of heterotrophic protists? Evidence and implications for algal blooms in cold waters. Limnol. Oceanogr. 52:886-895.

Rose, J.M., Y. Feng, C.J. Gobler, R. Gutierrez, C.E. Hare, K. Leblanc, and D.A. Hutchins. 2009b. The effects of increased pCO_2 and temperature on the North Atlantic Spring Bloom. II. Microzooplankton abundance and grazing.

Rose, J.M., Y. Feng, G.R. DiTullio, R.B. Dunbar, C.E. Hare, P.A. Lee, M. Lohan, M. Long, W.O. Smith, Jr., B. Sohst, S. Tozzi, Y. Zhang, and D.A. Hutchins. 2009a. Synergistic effects of iron and temperature on Antarctic plankton assemblages. Biogeosciences (6):3,131-3,147.

Royer, T.C. 1981. Baroclinic transport in the Gulf of Alaska. Part II: Fresh water driven Alaskan Coastal Current. J. Mar. Res. 39:251-266.

Rykaczewski, R.R. and D.M. Checkley, Jr. 2008. Influence of ocean winds on the pelagic ecosystem in upwelling regions. PNAS 105(6):1965-1970. doi_10.1073_pnas.0711777105.

Sabine, C.L., R.A. Feely, N. Gruber, R.M. Key, K. Lee, J.L. Bullister, R. Wanninkhof, C.S. Wong, D.W.R. Wallace, B. Tilbrook, F.J. Milero, T-H Peng, A. Kozyr, T. Ono, and A.F. Rios. 2004. The oceanic sink for anthropogenic CO_2. Science 305:367-371.

Sahl, L.E., W.J. Merrell, and D.C. Biggs. 1993. The influence of advection on the spatial variability of nutrient concentrations on the Texas-Louisiana continental shelf. Cont. Shelf Res. 13:233-251.

Salisbury, J.E., D. Vandemark, C.W. Hunt, J.W. Campbell, W.R. McGillis, and W.H. McDowell. 2008. Seasonal observations of surface waters in two Gulf of Maine estuary-plume systems: Relationships between watershed attributes, optical measurements and surface pCO(2). Estuar. Coast. Shelf S. 77(2):245-252.

Sambrotto, R.N., H.J. Niebauer, J.J. Goering, and R.L. Iverson. 1986. The relationship among vertical mixing, nitrate uptake, and growth during the spring bloom on the southeast Bering Sea middle shelf. Cont. Shelf Res. 5:161-198.

Sanders, R.W. 1995. Seasonal distributions of the photosynthesizing ciliates *Laboea strobila* and *Myrionecta rubra* (*Mesodinium rubrum*) in an estuary of the Gulf of Maine. Aquatic Microbial Ecology 9:237-242.

Sarmiento, J.L., T.M.C. Hughes, R.J. Stouffer, and S. Manabe. 1998. Simulated response of the ocean carbon cycle to anthropogenic climate warming. Nature 393:245-249.

Savage, V.M., J.H. Brown, J.F. Gillooly, W.H. Woodruff, G.B. West, A.P. Allen, B.J. Enquist, and J.H. Brown. 2004. The predominance of quarter power scaling in biology. Functional Ecology 18:257-282.

Savidge, G., D.R. Turner, P.H. Burkill, A.J. Watson, M.V. Angel, R.D. Pingree, H. Leach, and K.J. Richards. 1992. The BOFS 1990 spring bloom experiment: Temporal evolution and spatial variability of the hydrographic field. Progress in Oceanography 29:235-281.

Schloss, I.R., C. Nozais, S. Mas, B. van Hardenberg, E. Carmack, J. Tremblay, S. Brugel, and S. Demers. 2008. Picophytoplankton and nanophytoplankton abundance and distribution in the southeastern Beaufort Sea (Mackenzie Shelf and Amundsen Gulf) during Fall 2002. J. Mar. Syst. 74 (3-4):978-993.

Schoenebeck, C.W., S. Chipps, and M. Brown. 2008. Improvement of an esocid bioenergetics model for juvenile fish. Trans. Am. Fish. Soc. 137:1,891-1,897.

Schumacher, J.D. and P.J. Stabeno. 1998. Continental shelf of the Bering Sea. In: Robinson, A.R. and K.H. Brink eds. The sea, vol. 11. Wiley. Pp. 789–822 (Chapter 27).

Schwinghamer, P., B. Hargrave, D. Peer, and C.M. Hawkins. 1986. Partitioning of production and respiration among size groups of organisms in an intertidal benthic community. Mar. Ecol. Prog. Ser. 31:131-142.

Scripps Institution of Oceanography. 2010. California Current Ecosystem LTER. 11. Chlorophyll. 176. Integrated primary production – process cruise dataset (CCELTER). http://oceaninformatics.ucsd.edu/datazoo/data/ccelter/datasets. Accessed 20 August 2010.

Secretariat of the Convention on Biological Diversity. 2009. Scientific synthesis of the impacts of ocean acidification on marine biodiversity. Technical Series No. 46. Montreal. 61 pp.

Sergeeva, V.M., I.N. Sukhanova, M.V. Flint, L.A. Pautova, J.M. Grebmeier, and L.W. Cooper. 2010. Phytoplankton community in the western Arctic in July–August 2003. Oceanology 50(2):184-197.

Sheldon, R.W., A. Prakash and W.H. Sutcliffe, Jr. 1972. The size distribution of particles in the ocean. Limnol. Oceanogr. 17:327-340.

Sherr, E.B., B.F. Sherr, and P.A. Wheeler. 2005. Distribution of coccoid cyanobacteria and small eukaryotic phytoplankton in the upwelling ecosystem off the Oregon coast during 2001 and 2002. Deep-Sea Res. II 52:317-330.

Shippert, P. 2004. Why use hyperspectral imagery? Photogrammetric Engineering and Remote Sensing 68(4):377-380.

Shuert, P.G. and J.J. Walsh. 1993. A one-dimensional ecological model of summer oxygen distributions within the Chukchi Sea. Cont. Shelf Res. 13(5-6):543-573.

Shuter, B. 1979. A model of physiological adaptation in unicellular algae. J. Theor. Biol. 78:519-552.

Silio-Calzada, A., A. Bricaud, and B. Gentili. 2008. Estimates of sea surface nitrate concentrations from sea surface temperature and chlorophyll concentration in upwelling areas: A case study for the Benguela system. Remote Sensing of Environment 112:3,173-3,180.

Smith, S. and J. Hollibaugh. 1993. Coastal metabolism and the oceanic organic carbon balance. Rev. Geophys. 31:75-89.

Speckman, S.G., J.F. Piatt, C.V. Minte-Vera, and J.K. Parrish. 2005. Parallel structure among environmental gradients and three trophic levels in a subarctic estuary. Progress in Oceanography 66:25-65.

Springer, A.M. 1988. The paradox of pelagic food webs on the Bering–Chukchi continental shelf. Ph.D. dissertation, University of Alaska Fairbanks, Fairbanks. 232 pp.

Springer, A.M. and C.P. McRoy. 1993. The paradox of pelagic food webs in the northern Bering Sea—III. Patterns of primary production. Cont. Shelf Res. 13(5-6):575-599.

Springer, A.M., C.P. McRoy, and M.V. Flint. 1996. The Bering Sea green belt: Shelf-edge processes and ecosystem production. Fisheries Oceanography 5:205-233.

Stabeno, P.J., N. Kachel, C. Mordy, D. Righi, and S. Salo. 2008. An examination of the physical variability around the Pribilof Islands in 2004. Deep-Sea Res. II Top. Stud. Oceanogr. 55(16-17):1,701- 1,716.

Staehr, P.A., A.M. Waite, and S. Markager. 2009. Effects of sewage water on bio-optical properties and primary production of coastal systems in western Australia. Hydrobiol. 620(1):195-205.

Statzner, B. and C. Lévêque. 2007. Linking productivity, biodiversity and habitat of benthic stream macroinvertebrate communities: Potential complications of worldwide and regional patterns. International Review of Hydrobiology 92:428-451.

Strom, S.L. and K.A. Fredrickson. 2008. Intense stratification leads to phytoplankton nutrient limitation and reduced microzooplankton grazing in the southeastern Bering Sea. Deep-Sea Res. II Top. Stud. Oceanogr. 55(16-17):1,761- 1,774.

Strom, S.L., E.L. Macri, and K.A. Fredrickson. 2010. Light limitation of summer primary production in the coastal Gulf of Alaska: Physiological and environmental causes. Mar. Ecol. Prog. Ser. 402:45-57.

Sukhanova, I.N., M.V. Flint, L.A. Pautova, D.A. Stockwell, J.M. Grebmeier, and V.M. Sergeeva. 2009. Phytoplankton of the western Arctic in the spring and summer of 2002: Structure and seasonal changes. Deep-Sea Res. II Top. Stud. Oceanogr. 56(1):1,223-1,236.

Sukhanova, I.N., M.V. Flint, L.A. Pautova, D.A. Stockwell, J.M. Grebmeier, and V.M. Sergeeva. 2009. Phytoplankton community of the western Arctic in the vegetation season of 2002: Structure and seasonal changes. Deep-Sea Res. II Top. Stud. Oceanogr. 52(24-26):1,223-1,236.

Sullivan, M.E., N.B. Kachel, C.W. Mordy, and P.J. Stabeno. 2008. The Pribilof Islands: Temperature, salinity and nitrate during summer 2004. Deep-Sea Res. II Top. Stud. Oceanogr. 55(16-17):1,729-1,737.

Sumich, J.L. and J.F. Morrisey. 2004. Chapter 2 – Phytoplankton. In: Biology of marine life. Sudbury, MA: Jones and Barlett Publishers.

Suzuki, K., H. Liu, T. Saino, H. Obata, M. Takano, K. Okamura, Y. Sohrin, and Y. Fujishima. 2002. East–west gradients in the photosynthetic potential of phytoplankton and iron concentration in the subarctic Pacific Ocean during early summer. Limnol. Oceanogr. 47(6):1,581–1,594.

Tai, V. 2009. Diversity and dynamics of *Synechococcus* populations in the Southern California Bight. Ph.D. dissertation, University of California, San Diego, La Jolla, CA. 255 pp.

Takahashi, K. 2005. The Bering Sea and paleoceanography. Deep-Sea Res. II Top. Stud. Oceanogr. 52(16-18):2,080-2,091.

Takenouti, A.Y. and K. Ohtani. 1974. Currents and water masses in the Bering Sea: A review of Japanese work. In: Hood, D.W. and E.J. Kelley, eds. Oceanography of the Bering Sea with emphasis on renewable resources. Seattle, WA: Univ. Wash.

Thomas, A.C. and P.T. Strub. 1990. Seasonal and interannual variability of pigment concentrations across a California Current frontal zone. J. Geophys. Res. 95:13,023-13,042.

Thomas, A. and P.T. Strub. 2001. Cross-shelf phytoplankton pigment variability in the California Current. Cont. Shelf Res. 21:1,157-1,190.

Thunell, R., C. Benitez-Nelson, R. Varela, Y. Astor, and F. Müller-Karger. 2007. Particulate organic carbon fluxes along upwelling-dominated continental margins: Rates and mechanisms. Global Biogeochemical Cycles 21(1):GB1022.

Tian, R. and C. Chen. 2006. Influence of model geometrical fitting and turbulence parameterization on phytoplankton simulation in the Gulf of Maine. Deep-Sea Res. II Top. Stud. Oceanogr. 53(23-24):2,808-2,832.

Tilman, D., S.S. Kilham, and P. Kilham. 1982. Phytoplankton community ecology: The role of limiting nutrients. Ann. Rev. Ecol. Syst. 13:349-372. doi:10.1146/annurev.es.13.110182.002025.

Tomas, C.R. and T.J. Smayda. 2008. Red tide blooms of *Cochlodinium polykrikoides* in a coastal cove. Harmful Algae 7(3):308-317.

Townsend, D.W. 1991. Influences of oceanographic processes on the biological productivity of the Gulf of Maine. Reviews in Aquatic Sciences 5:211-230.

Townsend, D.W. 1998. Sources and cycling of nitrogen in the Gulf of Maine. J. Mar. Syst. 16(3/4):283-295.

Ulanowicz, R.E. 1986. Growth and development: Ecosystem phenomenology. New York: Springer Verlag. 203 pp.

University of Maryland Eastern Shore (UMES). 1985. Federal OCS oil and gas activities: A relative comparison of marine productivity among the outer continental shelf Planning Areas. Draft report for the U.S. Dept. of the Interior, Minerals Management Service, Washington, DC. Cooperative Agreement No. 14-12-0001-30014. 1,450 pp.

Valiela, I. 1995. Marine ecological processes. 2nd ed. New York: Springer-Verlag. 686 pp.

Vaulot, D., D. Marie, R.J. Olson, and S.W. Chisholm. 1995. Growth of *Prochlorococcus*, a photosynthetic prokaryote, in the equatorial Pacific-Ocean. Science 268(5216):1,480-1,482.

Vaulot, D., W. Eikrem, M. Viprey, and H. Moreau. 2008. The diversity of small eukaryotic phytoplankton ($\leq$3µm) in marine ecosystems. FEMS Microbiol. Rev. 32:795-820.

Venier, J.M. and D. Pauly. 1997. Trophic dynamics of a Florida Keys coral reef ecosystem, pp. 915-920. In: Volume 1, Proceedings of the 8th International Coral Reef Symposium, June 24-29, 1996, Panama City. Smithsonian Tropical Research Institute, Balboa, Panama.

Verity, P.G., J.O. Blanton, J. Amft, C. Barans, D. Knott, B. Stender, and E. Wenner. 1998. Influences of physical oceanographic processes on chlorophyll distributions in coastal and estuarine waters of the South Atlantic Bight. J. Mar. Res. 56:681-711.

Vincent, W.F. 1992. The daily pattern of nitrogen uptake by phytoplankton in dynamic mixed layer environments. Hydrobiologia 238(Aug):37-52.

von Quillfeldt, C.H., W.G. Ambrose, Jr., and L.M. Clough. 2003. High number of diatom species in first-year ice from the Chukchi Sea. Polar Biology 26:806-818.

Walters, C.J. 1986. Adaptive management of renewable resources. New York: Macmillan.

Walters, C. 1996. Suggested improvements for Ecopath modeling. In: Pauly, D. and V. Christensen, eds. Mass-balance models of north-eastern Pacific ecosystems. Fisheries Centre Research Reports 4(1):82-86.

Walters, C. 2000. Impacts of dispersal, ecological interactions, and fishing effort dynamics on efficacy of marine protected areas: How large should protected areas be? Bulletin of Marine Science 66:745-757.

Walters, C. and J.F. Kitchell. 2001. Cultivation/depensation effects on juvenile survival and recruitment: Implications for the theory of fishing. Can. J. Fish. Aquat. Sci. 58:39-50.

Walters, C., V. Christensen, and D. Pauly. 1997. Structuring dynamic models of exploited ecosystems from trophic mass-balance assessments. Rev. Fish Biol. Fisheries 7:139-172.

Walters, C., D. Pauly, and V. Christensen. 1999. Ecospace: Prediction of mesoscale spatial patterns in trophic relationships of exploited ecosystems, with emphasis on the impacts of marine protected areas. Ecosystems 2:539-554.

Walters, C., D. Pauly, V. Christensen, and J.F. Kitchell. 2000. Representing density dependent consequences of life history strategies in aquatic ecosystems: EcoSim II. Ecosystems 3:70-83.

Walters, C., S.J.D. Martell, and B. Mahmoudi. 2006. An Ecosim model for exploring ecosystem management options for the Gulf of Mexico: Implications of including multistanza life history models for policy predictions. Presentation at the Mote Symposium No.6, Florida State University, November 2006. 23 pp.

Wang, Z.A., W.J. Cai, Y. Wang, and H. Ji. 2005. The southeastern continental shelf of the United States as an atmospheric CO_2 source and an exporter of inorganic carbon to the ocean. Cont. Shelf Res. 25(16):1,917-1,941.

Ware, D.M. and R.E. Thomson. 1991. Link between long-term variability in upwelling and fish production in the Northeast Pacific Ocean. Can. J. Fish. Aquat. Sci. 48:2,296-2,306.

Ware, D.M. and R.E. Thomson. 2005. Bottom-up ecosystem trophic dynamics determine fish production in the Northeast Pacific. Science 308:1,280-1 284.

Wawrik, B., A.V. Callaghan, and D.A. Bronk. Use of inorganic and organic nitrogen by *Synechococcus* spp. and diatoms on the west Florida shelf as measured using stable isotope probing. Appl. Environ. Microbiol. 75(21):6662-6670, doi:10.1128/AEM.01002-09.

Wefer, G. and G. Fischer. 1991. Annual primary production and export flux in the Southern-Ocean from sediment trap data. Mar. Chem. 35(1-4):597-613.

Weingartner, T.J., S.L. Danielson, and T.C. Royer. 2005. Freshwater variability and predictability in the Alaska Coastal Current. Deep-Sea Res. II Top. Stud. Oceanogr. 52(1-2):169–191.

Werner, F.E., S-I. Ito, B.A. Megrey, and M.J. Kishi. 2007. Synthesis of the NEMURO model studies and future directions of marine ecosystem modeling. Ecol. Model. 202:211-223.

West, G.B. and J.H. Brown. 2005. The origin of allometric scaling laws in biology from genomes to ecosystems: Towards a quantitative unifying theory of biological structure and organization. J. Exper. Biol. 208:1,575-1,592.

West, G.B., J.H. Brown, and B.J. Enquist. 1997. A general model for the origin of allometric scaling laws in biology. Science 276:122-126.

Wetz, M.S., K.C. Hayes, A.J. Lewitus, J.L. Wolny, and D.L. White. 2006. Variability in phytoplankton pigment biomass and taxonomic composition over tidal cycles in a salt marsh estuary. Mar. Ecol. Prog. Series 320:109-120.

Wetzel, R.G. and G.E. Likens. 2000. Limnological analyses. 3rd Edition. Springer Science+Business Media, Inc., New York, NY.

Whitfield, J. 2001. All creatures great and small. Nature 413:342-344.

Whitledge, G.W., R.S. Hayward, D.B. Noltie, and N. Wang. 1998. Testing bioenergetics models under feeding regimes that elicit compensatory growth. Trans. Am. Fish. Soc. 127:740-746.

Whitledge, G.W., P.G. Bajer, and R.S. Hayward. 2006. Improvement of bioenergetics model predictions for fish undergoing compensatory growth. Trans. Am. Fish. Soc. 135:49-54.

Whitledge, T.E., W.S. Reeburgh, and J.J. Walsh. 1986. Seasonal inorganic nitrogen distributions and dynamics in the southeastern Bering Sea. Cont. Shelf Res. 5(1-2):109-132.

Whitney, F.A., W.R. Crawford, and P.J. Harrison. 2005. Physical processes that enhance nutrient transport and primary productivity in the coastal and open ocean of the subarctic NE Pacific. Deep-Sea Res. II 52(2005):681-706.

Wilkerson, F., A. Lassiter, R. Dugdale, A. Marchi, and V. Hogue. 2006. The phytoplankton bloom response to wind events and upwelled nutrients during the CoOP-WEST study. Deep-Sea Res. II 53:3,023-3,048.

Wilkerson, F.P. and R.C. Dugdale. 1992. Measurements of nitrogen productivity in the equatorial Pacific. J. Geophys. Res.-Oceans 97(C1):669-679.

Willey, J.D., H.W. Paerl, and M. Go. 1999. Impact of rainwater hydrogen peroxide on chlorophyll a content of surface Gulf Stream seawater off North Carolina, USA. Mar. Ecol. Prog. Series 178:145-150.

Wilson, E.O. 1998. Consilience: The unity of knowledge. New York: Alfred A. Knopf Publishers. 322 pp.

Winberg, G.G. 1956. Rate of metabolism and food requirements of fishes. Belorussion State University, Minsk. (Translated from Russian by Fisheries Research Board of Canada. Translations Series No. 194, 1960.)

Winship, A.J., A.W. Trites, and D.A.S. Rosen. 2002. A bioenergetic model for estimating the food requirements of Steller sea lions *Eumetopias jubatus* in Alaska, USA. Mar. Ecol. Prog. Ser. 229:291-312.

Wolff, M., V. Koch, and V. Isaac. 2000. A trophic flow model of the Caete Mangrove Estuary (North Brazil) with considerations for the sustainable use of its resources. Estuar. Coast. Shelf S. 50:789-803.

Yentsch, C.S., C.M. Yentsch, D.A. Phinney, B.E. Lapointe, and S.F.W. Yentsch. 2004. The odyssey of new production. J. Exper. Mar. Biol. and Ecol. 300:15-30.

Yoshiyama, K. and J.H. Sharp. 2006. Phytoplankton response to nutrient enrichment in an urbanized estuary: Apparent inhibition of primary production by over-eutrophication. Limnol. Oceanogr. 51:424-434.

Zajac, R.N., K. Seals, and D. Simpson. 2008. Food webs in Long Island Sound: Review, synthesis and potential applications. U.S. EPA Long Island Sound Study, Final Report – United States Environmental Protection Agency Grant No. LI-97101401. 87 pp.

Zhao, S., J. Wei, H. Yue, and T. Xiao. 2010. Picophytoplankton abundance and community structure in the Philippine Sea, western Pacific. Chinese J. Oceanol. Limnol. 28(1):88-95.

Zwirglmaier, K., L. Jardillier, M. Ostrowski, S. Mazard, L. Garczarek, D. Vaulot, F. Not, R. Massana, O. Ulloa, and D.J. Scanlan. 2008. Global phylogeography of marine *Synechococcus* and *Prochlorococcus* reveals a distinct partitioning of lineages among oceanic biomes. Environ. Microbiol. 10(1):147-161, doi:10.1111/j.1462-2920.2007.01440.x.

Appendices

Appendix A
List of Preparers

Name	Affiliation	Role(s)	Section(s)
Principal Investigators			
Brian J. Balcom, M.S.	CSA International, Inc., Salinas, CA	Project manager; primary productivity literature updates for Pacific	Lead author of 1.0, 4.3, and Appendix D Co-author of 7.0
Douglas C. Biggs, Ph.D.	Texas A&M University, College Station, TX	Evaluation of primary productivity methods; primary productivity literature updates for Atlantic and Gulf of Mexico	Author of 2.1 – 2.4, 4.1, 4.2, and 4.5 Co-author of 7.0
Chuanmin Hu, Ph.D.	University of South Florida, St. Petersburg, FL	Development of primary productivity estimates for OCS Planning Areas	Author of 2.5 and 3.0
Paul Montagna, Ph.D.	Texas A&M University, Corpus Christi, TX	Secondary and tertiary productivity methods and literature updates	Lead author of 5.0, 6.0, Appendix B, and Appendix C; Co-author of 7.0
Dean A. Stockwell, Ph.D.	University of Alaska, Fairbanks, AK	Primary productivity literature updates for Alaska	Author of 4.4
Additional Contributors			
S.A. Arismendez, Ph.D.	Texas A&M University, Corpus Christi, TX	Secondary and tertiary productivity methods and literature updates	Co-author of 5.0, 6.0, Appendix B, and Appendix C
Brittany Blomberg, Ph.D. (cand.)	Texas A&M University, Corpus Christi, TX	Secondary and tertiary productivity methods and literature updates	Co-author of 5.0, 6.0, Appendix B, and Appendix C
S. Nanez-James, B.S.	Texas A&M University, Corpus Christi, TX	Secondary and tertiary productivity methods and literature updates	Co-author of 5.0, 6.0, Appendix B, and Appendix C
T.A. Palmer, M.S.	Texas A&M University, Corpus Christi, TX	Secondary and tertiary productivity methods and literature updates	Co-author of 5.0, 6.0, Appendix B, and Appendix C
D. Sholz, M.S.	Texas A&M University, Corpus Christi, TX	Secondary and tertiary productivity methods and literature updates	Co-author of 5.0, 6.0, Appendix B, and Appendix C
CSA Staff			
Neal W. Phillips, Ph.D.	CSA International, Inc., Philadelphia, PA	Technical review and senior editor	Complete document
Kristen L. Metzger, M.L.S.	CSA International, Inc., Stuart, FL	Literature search; journal article and document access	Complete document
Melody B. Powell, B.S.	CSA International, Inc., Stuart, FL	Technical editor	Complete document
Keith VanGraafeiland, B.S.	CSA International, Inc., Stuart, FL	GIS analyst	Complete document
Karen Stokesbury	CSA International, Inc., Stuart, FL	Document production coordinator	Complete document

Appendix B
The Ecopath Model

Appendix B Contents

B.1 Introduction

The Ecopath software suite is designed to construct and analyze mass-balance trophic models of entire ecosystems (i.e., all trophic groups, from primary producers to apex predators), providing an “ecosystem snapshot” (Plaganyi 2007). Ecopath is prevalent among modeling approaches because of its nearly universal applicability (i.e., it covers most areas; it treats secondary and tertiary productivity data in a consistent fashion) and provides a basis for comparisons among areas.

The majority of Ecopath models have been constructed for marine ecosystems (>80%), with application of the model to freshwater (18%) and terrestrial (1.5%) environments constituting the balance (Morissette 2007). Ecopath models have been used to evaluate the effect of fishing on marine ecosystems, and guide fisheries assessment and management. The model can also be used to address other ecological and environmental questions. Ecosystem responses can be predicted for a variety of influences, including management policy options, placement of protected areas, and climate and environmental changes (Ecopath 2010). Ecopath models enable ecosystem comparisons, and have become important tools for ecosystem-based management (EBM) and marine spatial planning. Future applications and direction for research have been proposed in these areas as well as others.

B.2 Initial Development: The French Frigate Shoals

By the 1980’s, a number of models had been developed to simulate ecosystem dynamics in temperate and polar seas. These systems were well understood and relatively data rich, so the models were fairly detailed and complex. However, tropical ecosystems were much less understood at the time. It would have been impractical, if not impossible, to develop a model of similar detail for a complex tropical ecosystem. Also, most temperate ecosystems are managed with a single-species approach. The single-species approach is not useful in the tropics because target species are more difficult to define and represent small fractions of total catch compared to temperate systems (Pauly 2009). Thus, a model was needed that could investigate ecosystem dynamics in tropical marine systems.

Ecopath was developed by Polovina and associates at the National Marine Fisheries Service (NMFS) Honolulu Laboratory in the 1980’s to gain insight into the structure and function of complex tropical ecosystems (Polovina 1984a). The Ecopath model was designed to estimate the biomass budget of each “box,” or organism group, assuming a steady-state ecosystem, and was the first model to utilize path analysis statistics. Path models, consisting of ecosystem boxes and flow between them, can be simple, and do not require significant detail or exhaustive inputs to provide important ecosystem insight (Polovina 1984b). Polovina applied his model to the French Frigate Shoals (FFS), a coral reef ecosystem in the Northwestern Hawaiian Islands.

Three publications described the initial development and use of Ecopath. The first explained the Ecopath model and its application to the FFS ecosystem (Polovina 1984b). The second compared estimates of benthic primary production from the Ecopath model and field studies (Atkinson and Grigg 1984). The third publication elaborated on how the model could be used to develop better understanding and management of coral reef ecosystems (Grigg et al. 1984). Overall, the initial development and use of the Ecopath model was successful in accurately depicting the structure and function of the FFS coral reef ecosystem. The model estimates were in close agreement with field estimates, indicating the potential of Ecopath to serve as a tool for enhancing understanding of the structure and function of complex ecosystems (Atkinson and Grigg 1984).

B.3 Further Developments

The initial success of Ecopath prompted scientists and managers to look closer at the model and how it could be used to study ecosystem dynamics. Christensen and Pauly (1992) were instrumental in the advancement of the original model by Polovina (1984a), and have been continuously updating Ecopath since the 1990's. Applying the same basic concepts, they reprogrammed the original model, expanding its capabilities and use. Ecopath II was introduced in 1992. The basic equation remained the same, but the new model provided more outputs than the original Ecopath (Christensen and Pauly 1992).

During the 1990's, Ecopath was applied to different ecosystems worldwide. Users came together at conferences and workshops to discuss the model. Problems were addressed, and directions for future research and model development were identified. Its use spread, and the Ecopath approach was established in the primary literature.

Walters et al. (1996, 1997, 2000) had a significant influence on the development of Ecopath, viewing the model as a starting point rather than an end product (Pauly 2009). The introduction of Ecosim in 1995 added a temporal component to the Ecopath approach, enabling dynamic simulation of ecosystems over time. In 1998, Ecospace was introduced, adding a geographical component to the Ecopath software suite, which enabled spatial analysis (Walters et al. 1999). Increased developments and use of the Ecopath modeling software led to the development of an integrated software package, "Ecopath with Ecosim" (EwE). The basic equations have not changed since Polovina (1984a), and have been critically examined for many years.

B.3.1 EwE Version 6

EwE Version 5 had reached its technical limitations, especially regarding the ability to link with other models. However, the need to update the EwE 5 software was met with hesitation. EwE Version 6 was developed under a 4-y project funded through the Lenfest Ocean Program and released in September 2007 (Ecopath 2010). Restructuring of EwE involved development of:

- Separate EwE components to increase maintainability and extensibility;
- Separate algorithms and a user interface to enable reuse of the computational code for different applications;
- A modern programming environment (.NET) to ensure compatibility and extensibility;
- Fully OOP-implementation;
- Components of EwE that would allow connections to other programming environments; and
- Localization.

Overhaul Goals:

- Preserve structure of existing computational code; and
- Ensure familiarity with complex models.

Extending EwE:

- Add variables to models;
- Add calculations to models;
- Change calculations in models;
- Add user interface elements;
- Change existing user interfaces;
- Use EwE output elsewhere; and
- Use other data as inputs for EwE.

Extension Strategies:

- Embedded: rewrite and extend existing code; and
- External: rewrite and extend functionality without affecting existing code.

B.3.2 Ecopath

Ecopath models incorporate two approaches. The first approach estimates biomass and food consumption for each ecosystem group. The second approach is used to analyze flows between ecosystem groups and to calculate various ecosystem indices.

The Ecopath model consists of two master equations, representing production and consumption, as follows:

Master Equation 1: Production

Production = Catches + Predation Mortality + Net Migration + Biomass Accumulation + Other Mortality

which can formally be expressed as (for group *i*):

$$P_i = Y_i + B_i M2_i + E_i + BA_i + P_i(1 - EE_i)$$

and can be re-expressed as:

$$B_i \cdot (P|B)_i - \sum_{j=1}^{n} B_j \cdot (Q|B)_j \cdot DC_{ji} - (P/B)_i \cdot B_i \cdot (1 - EE_i) - Y_i - E_i - BA_i = 0$$

or

$$B_i \cdot (P/B)_i \cdot EE_i - \sum_{j=1}^{n} B_j \cdot (Q/B)_j \cdot DC_{ji} - Y_i - E_i - BA_i = 0$$

The production of each group is represented by the above equation. Thus, for an ecosystem with n groups, n equations will be written. The result is a system of linear equations, as follows:

$$B_1 \cdot (P/B)_1 \cdot EE_1 - B_1 \cdot (Q/B)_1 \cdot DC_{11} - B_2 \cdot (Q/B)_2 \cdot DC_{21} \cdots - B_n \cdot (Q/B)_n \cdot DC_{n1} - Y_1 - E_1 - BA_1 = 0$$

$$B_2 \cdot (P/B)_2 \cdot EE_2 - B_1 \cdot (Q/B)_1 \cdot DC_{12} - B_2 \cdot (Q/B)_2 \cdot DC_{22} \cdots - B_n \cdot (Q/B)_n \cdot DC_{n2} - Y_2 - E_2 - BA_2 = 0$$

$$B_n \cdot (P/B)_n \cdot EE_n - B_1 \cdot (Q/B)_1 \cdot DC_{1n} - B_2 \cdot (Q/B)_2 \cdot DC_{2n} \cdots - B_n \cdot (Q/B)_n \cdot DC_{nn} - Y_n - E_n - BA_n = 0$$

The set of linear equations can be solved simultaneously via matrix algebra (Christensen and Pauly 1992). The production equation ensures mass balance of groups in the model (Christensen et al. 2008).

The second master equation represents consumption of a group, and ensures energy balance within each group:

Master Equation 2: Consumption

$$Consumption = Production + Respiration + Unassimilated\ Food$$

The consumption equation is essentially the same as the bioenergetic model and is based on the principle that matter is conserved within each group (Ecopath 2010). Energy balance is performed to estimate respiration from the consumption master equation. Estimates are made because measurements of respiration are rarely included in fisheries data. A routine is also included to estimate the energy balance from any combination of terms from the consumption equation (Christensen et al. 2008).

The two master equations, representing production and consumption, are linked via the predation mortality term. The predation mortality of a prey organism equals the consumption of its predators. Thus, the production of each group (Master Equation 1) is linked to the consumption of all applicable predator groups (Master Equation 2). Missing parameters are estimated by utilizing these linkages, because the mass balance assumption requires that the production of a group is not lost, but is transferred within the system (Christensen et al. 2008).

To use the Ecopath model, a number of input parameters must be entered by the user. Data requirements include (for each group in the model): estimates of biomass, consumption and total mortality, diet composition, and fishery catch (Ecopath 2010).

Generally, three of the following four input parameters are required for each functional group in the model: biomass, production/biomass ratio (or total mortality), consumption/biomass ratio, or ecotrophic efficiency (EE) (Ecopath 2010). Ecopath will then estimate the missing parameter. If data are available to satisfy all four input parameters for a group, the model is then able to estimate biomass accumulation or net migration (Ecopath 2010). It is preferable to let Ecopath estimate EE, rather than include it as one of three input parameters. EE is the most difficult parameter to estimate, and cannot be measured in the field. Local data are important for biomass estimations.

Ecopath parameters and other basic input include the following:

- Basic Parameters --
    - Biomass
    - Production/Biomass (P/B) ratio
        - When mass balance is assumed, the P/B ratio is equal to the total mortality rate (Z). The total mortality is actually the preferred input parameter for production, and should be used instead of P/B when possible. This ensures that recruitment to older age classes is accounted for. Z is the sum of fishing mortality (F) and natural mortality (M), where natural mortality represents loss by predation (M2) and other natural losses (M0),
    - Consumption/Biomass (Q/B) ratio
    - Ecotrophic Efficiency (EE)
        - Ecotrophic efficiency estimates provides information about how much of a group's production is consumed by predators each year. Values of EE must be between 0 and 1 (inclusive) under steady-state conditions. An EE value of 0 indicates that the group is not consumed by any other group, nor is it exported. EE values of 1 indicate that the group is heavily preyed upon (or grazed, or fished), preventing any organisms to die of old age. EE values greater than one would be impossible, as more biomass cannot be used than what is produced (Wolff et al. 2000). For most groups, EE values should be close to 1; top predators and primary producers are the two main exceptions. These results can be used to estimate primary production required by organisms at higher trophic levels (Polovina 1984a). Ecotrophic efficiency can provide insight into the role of predation in a system (Grigg et al. 1984). High ecotrophic efficiency levels resulting from the Ecopath model indicate that predation is the major driving force regulating secondary and higher production of coral reef ecosystems (Grigg et al. 1984).

- Additional Parameters --
    - Catch rate
    - Net Migration rate
    - Biomass Accumulation rate
    - Assimilation rate
    - Diet Composition
        - A diet composition matrix is used to identify the proportion of a predators (*j*) diet contributed by a prey species (*i*): j.

- Other Basic Input --
    - Habitat Area
    - Biomass in Habitat Area
    - Production/Consumption (P/Q) ratio
    - Unassimilated Consumption
    - Detritus Import
    - Detritus Fate.

- Additional Parameters Necessary for Multi-stanza Groups --
    - Curvature (K), von Bertalanffy growth rate
    - Recruitment Power
    - Relative Biomass Accumulation rate (BA/B)
    - Weight at Maturity/W_infinity
    - Forcing Function Number for Hatchery Stocking
    - Fixed Fecundity
    - Age, start (months).

- Fishery Parameters --
    - Definition of Fleets
        - Fixed Cost
        - Effort Related Cost
        - Sailing Related Cost
        - Profit
        - Total Value.
    - Landings
    - Discards
    - Discard Fate
    - Off-Vessel Price
    - Non-Market Price.

The parameterization of an Ecopath model is based on satisfying the two master equations. The parameterization routine in Ecopath includes algorithms that iteratively estimate as many missing parameters as possible before setting up the set of linear equations. Per Christensen and Walters (2004), the following loop is carried out until no additional parameters can be estimated:

- Estimate gross food conversion efficiency [equation];
- Estimate P/B ratio if possible [equation]; and
- Estimate EE [equation].

Most of the time, obtaining a balanced network with the Ecopath approach is left to trial and error, either in the form of user intervention or Monte-Carlo simulations. However, newer models use features such as autobalance to ease the process (Morissette 2007).

Key indices and outputs of Ecopath include the following:

- Trophic Level
- Biomass Accumulation (BA) and BA rate
- Net Migration
- Flow to Detritus (Non-assimilated Food)
- Net Efficiency
- Omnivory Index.

Additional indices include the following:

- Mortality Coefficients and Predation Mortality
- Consumption (Ecopath Parameterization)
- Respiration
    - Assimilation
    - Respiration/Assimilation ratio
    - Production/Respiration ratio
    - Respiration/Biomass (R/B) ratio
- Niche Overlap (O_{jk})
- Electivity
- Ivlev Electivity Index (E_i)
- Standardized Forage Ratio (S_i)
- Search Rates
- Fishery (Ecopath Parameterization)
    - Quantity
    - Market Value
    - Non-Market Value.

B.3.3 Ecopath Tools

Ecopath includes a tool to create flow diagrams, or food webs. The construction of a food web model for the ecosystem, including production and biomass estimates along with values for the predator consumption vectors (kg km^{-2}), provides an overview of the biomass budget schematic for major prey-predator pathways. From this schematic, ratios of production can be determined. It also provides information about trophic levels, with high amounts of internal predation indicating a group may actually consist of species at two trophic levels (Polovina 1984b).

Also, the Network Analysis Plug-in is available for Ecopath, and includes the following capabilities:

- Trophic level decomposition and relative flows
- Summary of flow data
    - Flow pyramid (transfer efficiency)
    - Biomass Pyramid (biomass by trophic level)
    - Catch Pyramid (catch by trophic level)
- Flows and biomasses from primary producers, detritus, and whole system
- Primary Production Required (PPR): These studies have enabled scientists to estimate the PPR to support global fish populations and continued commercial fisheries (Pauly and Christensen 1995; Pauly et al. 2000). The PPR for global fisheries was estimated at 8%, with estimates three to four times higher on continental shelves (Pauly and Christensen 1995), or 25%-35% (Pauly et al. 2000)
- Mixed Trophic Impact (MTI) analyses, which assesses the relative impact that the change in biomass of a given group would have on the biomass of other groups in the system (Jarre-Teichmann 1998). The major assumption is that the trophic structure does not change.

Therefore, we cannot use MTI for predictions, but can use it as a sensitivity analysis of cascading effects of changes in food webs (Jarre-Teichmann 1998)

- Ascendency (A), representing both size and organization of the flows (Wolff et al. 2000)
- Flow from Detritus
- Cycles and Pathways

B.3.4 Ecopath Modules

Ecosim

Ecosim adds a temporal component to the Ecopath software, enabling dynamic simulations at the ecosystem level (Ecopath 2010). Ecosim was used mainly for policy exploration purposes and has become an important tool as fishery management strategies have shifted to an ecosystem approach (Pauly et al. 2000).

Ecosim can be useful for examining/incorporating impacts of behavior. This can include organism behavior (e.g., predator avoidance, etc.), but may also include human behaviors such as fisheries impacts. The behavior of prey species limits the predation rate, efficiency, and effectiveness of their predators. Ecosim assumes that predation occurs primarily in specific spatial patches or foraging arenas where juveniles are forced to accept predation risk in order to forage, and predation rates are limited by the time juveniles spend in and out of the foraging areans, not by predator satiation (Walters and Kitchell 2001). Ecosim provides non-trophic mediation of interaction between a consumer and a prey group (Christensen et al. 2008). Ecosim has been useful for investigating the historic response of systems to harvesting and harvesting policies (Overholtz and Link 2009). Ecosim in its packaged form is only recommended for use in hypothesis exploration or first-order perturbation and sensitivity analyses as a supplement to other forecasting methods (NOAA 2007).

Initial parameters for Ecosim are obtained from the base Ecopath model. The mass-balance results from Ecopath are used to estimate parameters for Ecosim. Variable speed splitting enables efficient modeling of the dynamics of both fast (phytoplankton) and slow groups (whales). Top-down vs. bottom-up control are incorporated explicitly. Biomass and size structure dynamics can be included for key ecosystem groups, using a mix of differential and difference equations (Ecopath 2010). Ecosim uses coupled differential equations to express the biomass dynamics of an ecosystem (Pauly et al. 2000), of the form:

$$dB_i/dt = g_i \Sigma_j C_{ji} - \Sigma_j c_{ij} + I_i - (M_i + F_i + e_i)B_I$$

Before calculating rates of consumption, the biomass of each prey group is divided into a vulnerable and an invulnerable component (Pauly et al. 2000). This information can then be used to determine if the system is controlled by top-down or bottom-up forces, by examining the transfer rate (v_{ij}) between these two components (adjustable by the user) (Pauly et al. 2000). The consumption rate equation then becomes:

$$C_{ij} = v_{ij} a_{ij} B_i B_j / (v_{ij} + v'_{ij} + a_{ij} B_j)$$

In some systems, fishing alone is enough to drive the Ecopath model. However, for other systems, other mechanisms than those already included in Ecosim (fishing + predation) may be necessary to drive the model. Results of an Ecosim model also depend heavily on the vulnerabilities of each ecosystem group (Pauly et al. 2000).

The recommended procedure/approach for using Ecosim is to build two models. First, build a present day model by taking advantage of current available data. Then, use the present day model to build a past model, extending the model back to the designated first year in the chosen time series. Finally, run the past model and evaluate the parameters. Use this information together with the present day model to make predictions about ecosystem response to changes (Christensen et al. 2008). The two models also need to be parameterized. Data are often sparse for the time period of the past model, especially for diets. However, one can assume diet preference is the same in both past and present day models (Christensen et al. 2008).

Ecosim adds a temporal component to Ecopath by converting the steady-state trophic flows into dynamic, time-dependent predictions (Plaganyi 2007). Numbers of prey that are in vulnerable (V_{ij}) and non-vulnerable (N_i-V_{ij}) states are modeled as such:

$$d(N_i-V_{ij})/dt = -v_{ij}(N_i - V_{ij}) + v'_{ij}V_{ij}$$

$$dV_{ij}/dt = v_{ij}(N_i - V_{ij}) - v'_{ij}V_{ij} - a_{ij}V_{ij}N_j$$

Under the assumption that the dynamics of the V_{ij} are much faster than those of the N_i, dV_{ij}/d_t is set to zero, yielding (per Plaganyi 2007):

$$V_{ij} = v_{ij}N_i/(v_{ij} + v'_{ij} + a_{ij}N_j)$$

Therefore, the general term in Ecosim to describe the trophic flows between a prey (i) and predator (j) group becomes:

$$Q_{ij} = a_{ij}v_{ij}B_iB_j/(v_{ij} + v'_{ij} + a_{ij}B_j)$$

With further developments to the Ecosim model, this equation has evolved to the form:

$$Q_{ij} = (a_{ij}v_{ij}B_iP_jT_iT_jS_{ij}M_{ij}/D_j)/(v_{ij} + v'_{ij}T_iM_{ij} + a_{ij}M_{ij}P_jS_{ij}T_j/D_j)$$

where the handling time (Dj) is expressed as:

$$D_j = h_jT_j/(1 + \Sigma_k a_{kj}B_kT_kM_{kj})$$

Additional parameters in Ecosim include:

- duration of simulation (years);
- base proportion of free nutrients;
- nutrient loading forcing function number;
- fleet/effort dynamics; and
- contaminant tracing (Ecotrace).

Group parameters:

- maximum relative P/B;
- maximum relative feeding time;
- feeding time adjustment rate;
- fraction of other mortality sensitive to change in feeding time;
- predator effect on feeding time;
- density-dependent catchability;
- QBmax/QBo (handling time); and
- switching power parameter.

Vulnerabilities:

- Time series
    - historical comparison data; and
    - time forcing data.

Mediation (trophic mediation functions):
- facilitation; and
- protection.

Tools available in Ecosim include:
- Monte Carlo runs;
- Fishing Policy search; and
- Fit to time series.

Ecospace

The development of Ecospace introduced a spatial component to the Ecopath software suite (Walters et al. 1999). Ecospace was primarily designed to explore the impact and placement of marine protected areas (MPAs). The Ecospace module is able to integrate various data from GIS, including maps, and enables spatial optimization capabilities. New modules within Ecospace include Ecoseed and Importance Layers (Christensen et al. 2008).

Biomass in Ecospace cells can be determined by two methods:

- Ecopath base biomasses; and
- Habitat-adjusted biomasses.

Three approaches can be used for running simulations in Ecospace:

- EwE6 multi-stanza model;
- IBM (individual-based model); and
- EwE5 approach.

Spatial optimization tools are available in Ecospace, and utilize two methods: Seed Cell or Importance Layer methods.

EcoTroph

The EcoTroph module models the biomass trophic spectrum based on equations from physics flux, providing a continuous representation of biomass distribution according to trophic level (Gascuel et al. 2009). The flow of biomass through trophic levels provides a simple and useful picture of ecosystem functioning. Input parameters can be obtained from an Ecopath model, or independent estimates. Input parameters include biomass, production, and catch (Gascuel et al. 2009). EcoTroph includes four routines:

- ET-Transpose: looking at an Ecopath model using EcoTroph;
- ET-Diagnosis: using EcoTroph for simulation and global diagnosis;
- ET-CTSA (Catch Trophic Spectrum Analysis): estimating ecosystem biomass from catches and using EcoTroph in data-poor environments (CTSA is basically a VPA at the ecosystem scale); and
- ET-Dynamics: using EcoTroph with time series.

EcoTroph applies a theoretical approach to examining trophic dynamics in an ecosystem. The functioning of marine ecosystems is guided by a continuous trophic flow, from low to high trophic levels (Gascuel et al. 2009). The EcoTroph model is based on a few simple assumptions: biomass flow decreases with trophic level (trophic efficiency), flow speed is faster in low trophic levels, flow kinetics depend on predator abundance (top-down control), and secondary production partly comes from biomass recycling (Gascuel et al. 2009).

EcoRanger

Ecoranger is a module for semi-Bayesian parameter estimation (Christensen et al. 2008).

Data Pedigree

The data pedigree describes the origin of the data and their respective confidence intervals. This is fed into Ecoranger (and Ecosim). It is effective in describing the uncertainty associated with the data picked up by Monte Carlo routines (Christensen et al. 2008). Sometimes, it is of interest to know how well rooted the model is in local data. The data pedigree may soon be able to help address this question.

The ability to enter a pedigree for input parameters has increased the ability to determine the quality of an Ecopath model. The pedigree identifies the confidence of each input value, allowing distinction between precise estimates, estimates from similar systems, or guesses (Pauly et al. 2000). This allows the computation of an overall index of model quality, and provides prior distributions for Ecoranger, which incorporates a Bayesian approach for explicitly considering uncertainty in Ecopath inputs (Pauly et al. 2000).

EcoEmpire

Not yet available, this module will incorporate empirical relationships in the Ecopath approach (Christensen et al. 2008).

EcoTrace

This module enables tracking of bioaccumulation through ecosystems.

EcoSense

Ecosense routines provide a method for incorporating Ecopath thermodynamic constraints and model structure into dynamic ecosystem model projections within a Bayesian synthesis framework (NOAA 2007).

Network Analysis

Network analyses are used to explore ecosystem structure (Christensen et al. 2008), by quantifying a number of indices, including: input-output relationships, cycling, through-flows, storage, information theory indices, and diet relationships (Monaco and Ulanowicz 1997).

Ecost

Ecost is a socioeconomic module that incorporates economics into the EwE modeling approach. It is essentially a value chain model, describing the value of fish products from sea to consumer. Ecost is coupled with a base Ecopath model and accounts for social and economic aspects. Economic flow is modeled as a continuation of the food web. Units (currency) commonly used in Ecost include tons, dollars per ton over a total area, and number of jobs. The incorporation of Ecost in EwE is important for two major reasons: policy optimization (sector, fleet), and management strategy evaluation (closed loop simulation).

B.4 Ecopath Capabilities

Models can be designed to address ecological questions and examine ecosystem responses to various influences, such as fishing and management policy options concerning oil and gas activities. The ability to examine ecosystems over time and explore policy options and questions are key reasons that support the high number of EwE users worldwide. The most cited reasons for constructing Ecopath models are to: describe ecosystem structure (42%), examine fishery management issues (30%), answer theoretical ecology questions (11%), address policy matters (9%), and assist in the creation or management of MPAs (Morissette 2007). Ecopath has been used to model marine ecosystems world-wide, enabling comparisons between ecosystems (Overholtz and Link 2009).

EwE models are important tools for fisheries management that are capable of helping maintain ecosystem balance and avoid collapse of ecosystems and fisheries. Humans disproportionately affect top predators, causing unexpected trophic cascades. As the top predators are fished out, fishing down into the food web begins (e.g., moving down the trophic chain to target forage fish). Fishing down the food web can disrupt the balance and functioning of important, critical and often large areas of the ocean. EwE can provide a tool to examine the potential results of human activities, as well as fishery and management policies and/or changes (Christensen et al. 2008). EBM is one approach that can be used to prevent ecosystem degradation by fishing down the food web (Christensen et al. 2008). The ecosystem approach to fisheries (EAF) is of the same concept. Ecosystem modeling, especially simulation modeling, plays a fundamental role for EAF and EBM (Christensen et al. 2008).

Ecopath is a widely used and common approach to modeling ecosystems. Thus, construction of Ecopath models has brought together multidisciplinary groups such as scientists (and data) from state and federal levels of government, international research organizations, universities, public interest groups and private contractors (Ecopath 2010). This collaborative effort is key for identifying data gaps and common goals and objectives of those involved. The collaborative model construction process can also highlight overlapping efforts by multiple users. This is essential for avoiding duplication of effort and work, which can hinder model development and progression. The construction of Ecopath models provides another general and significant advantage: these models contribute to the global collection of ecological data and knowledge (Morissette 2007).

EwE has become a popular ecosystem modeling approach, attracting a large, broad community of users. The Ecopath model enables users to develop an accurate understanding of the structure and function of an ecosystem. Equations are simplified, and smaller amounts of data are required in Ecopath compared to many other modeling approaches. Parameterization of functional responses is much more flexible, and more advanced, in EwE than in many other published ecosystem modeling methods (Christensen et al. 2008). Improvements and additions to the original model have increased the ease of use and capabilities of the EwE software. EwE can be used to make simple (even meaningless) models, but can also be used to develop advanced ecosystem models by experienced users. No programming or mathematical skills are required to build a basic Ecopath model. However, advanced users find these skills beneficial for developing advanced models (Plaganyi 2007).

The Ecopath software is easily accessible, is free of charge, and runs on Windows PC. The Ecopath software suite provides a user interface, support, and training for users (Plaganyi 2007). The EwE software provides technical support to its users, including the ability for developers and users to communicate via an online Wiki and through a user list server. Ecopath workshops and training courses are offered. The unified format, flexibility, and ease of use are major strengths of EwE. The recent reprogramming of EwE (from Visual Basic 6 to .NET) has enabled easier access to code and has improved interoperability capabilities (e.g., coupling of models).

The EwE software suite enables presentation of model outputs. Enhanced visualization capabilities are in development. Extensive facilities are being developed to work on improving the presentation and visualization abilities of the EwE software.

B.5 References Cited

Atkinson, M.J. and R.W. Grigg. 1984. Model of a coral reef ecosystem II. Gross and net benthic primary production at French Frigate Shoals, Hawaii. Coral Reefs 3:13-22.

Christensen, V. and D. Pauly. 1992. Ecopath II - A software for balancing steady-state ecosystem models and calculating network characteristics. Ecological Modelling 61:169-185.

Christensen, V. and C.J. Walters. 2004. Ecopath with Ecosim: methods, capabilities, and limitations. Ecological Modelling 172:109-139.

Christensen, V., C.J. Walters, D. Pauly, and R. Forrest. 2008. Ecopath with Ecosim version 6: User Guide, November 2008 Edition. Lenfest Ocean Futures Project, Vancouver, 235 p. (available online at www.ecopath.org).

Ecopath. 2010. http://www.ecopath.org/ Accessed 9/1/10.

Gascuel, D., S. Guénette, and D. Pauly. 2008. The trophic-level based ecosystem modelling approach: theoretical overview and practical uses. ASC-ICES CM 2008/F:18, September 2008, Halifax, Canada. 16 pp.

Gascuel, D. M. Leclerc, A. Valls, and S. Guénette. 2009. EcoTroph: A new tool in the EwE family, pp. 21-22. In: M.L. Deng Palomares, L. Morissette, A. Cisneros-Montemayor, D. Varkey, M. Coll, and C. Piroddi (eds.), Ecopath 25 Years Conference Proceedings: Extended Abstracts. Fisheries Centre Research Reports 17.

Grigg, R.W., J.J. Polovina, and M.J. Atkinson. 1984. Model of a coral reef ecosystem III. Resource limitation, community regulation, fisheries yield and resource management. Coral Reefs 3:23-27.

Jarre-Teichmann, A. 1998. The potential role of mass balance models for the management of upwelling ecosystems. Ecological Applications 8:S93-S103.

Monaco, M.E. and R.E. Ulanowicz. 1997. Comparative ecosystem trophic structure of three U.S. mid-Atlantic estuaries. Marine Ecology Progress Series 161:239-254.

Morissette, L. 2007. Complexity, cost and quality of ecosystem models and their impact on resilience: A comparative analysis, with emphasis on marine mammals and the Gulf of St. Lawrence. Ph.D. dissertation, University of British Columbia. 278 pp.

National Oceanic and Atmospheric Administration (NOAA). 2007. Large marine ecosystems: A breakthrough concept for ecosystem management. http://celebrating200years.noaa.gov/breakthroughs/ecosystems/welcome.html. Accessed 3/26/10.

Overholtz, W. and J. Link. 2009. A simulation model to explore the response of the Gulf of Maine food web to large-scale environmental and ecological changes. Ecological Modelling 220:2,491-2,502.

Pauly, D. 2009. Ecopath: from the French Frigate Shoals to the Phillipines and the UBC. In: Palomares, M.L.D., L. Morissette, A. Cisnero-Montemayor, D. Varkey, M. Coll, and C. Piroddi, eds. Ecopath 25 Years Conference Proceedings: Extended Abstracts. Fisheries Centre Research Reports 17(3):17-19.

Pauly, D. and V. Christensen. 1995. Primary production required to sustain global fisheries. Nature 374:255-257.

Pauly, D., V. Christensen and C. Walters. 2000. Ecopath, Ecosim, and Ecospace as tools for evaluating ecosystem impact of fisheries. ICES Journal of Marine Science 57:697-706.

Plaganyi, E.E. 2007. Models for an ecosystem approach to fisheries. FAO Fisheries Technical Paper No.477. 125 pp.

Polovina, J.J. 1984a. Model of a coral reef ecosystem I. The ECOPATH model and its application to French Frigate Shoals. Coral Reefs 3:1-11.

Polovina, J.J. 1984b. An overview of the Ecopath model. ICLARM Fishbyte 2:5-7.

Walters, C. and J.F. Kitchell. 2001. Cultivation/depensation effects on juvenile survival and recruitment: Implications for the theory of fishing. Canadian Journal of Fisheries and Aquatic Science 58:39-50.

Walters, C. 1996. Suggested improvements for Ecopath modeling, pp. 82-86. In: D. Pauly and V. Christensen (eds.), Mass-Balance Models of North-Eastern Pacific Ecosystems. Fisheries Centre Research Reports 4(1).

Walters, C., V. Christensen, and D. Pauly. 1997. Structuring dynamic models of exploited ecosystems from trophic mass-balance assessments. Reviews in Fish Biology and Fisheries 7:139-172.

Walters, C., D. Pauly, and V. Christensen. 1999. Ecospace: Prediction of mesoscale spatial patterns in trophic relationships of exploited ecosystems, with emphasis on the impacts of marine protected areas. Ecosystems 2:539-554.

Walters, C., D. Pauly, V. Christensen, and J.F. Kitchell. 2000. Representing density dependent consequences of life history strategies in aquatic ecosystems: EcoSim II. Ecosystems 3:70-83.

Wolff, M., V. Koch, and V. Isaac. 2000. A trophic flow model of the Caete Mangrove Estuary (North Brazil) with considerations for the sustainable use of its resources. Estuar. Coast. Shelf S. 50:789-803.

Appendix C

Supporting Maps and Figures for Zooplankton Biomass and Fisheries Landings

Appendix C Contents

Page

List of Figures

Figure **Page**

List of Figures
(Continued)

Figure **Page**

List of Figures
(Continued)

Figure **Page**

Zooplankton Abundance and Fisheries Landings Data Sources

All data used were obtained from the National Oceanic and Atmospheric Administration National Marine Fisheries Service (NMFS) (www.st.nmfs.noaa.gov/st1).

NMFS COPEPOD. Online database: <http://www.st.nmfs.noaa.gov/plankton/data/>. (Online database containing plankton data from various sampling programs).

NMFS Commercial Landings by Group. Web query at: <http://www.st.nmfs.noaa.gov/st1/commercial/index.html>. Accessed 2 Jul 2010. (Commercial fish and invertebrate landings (pounds) for 2008 reported by state).

NMFS Commercial Fishery Landings by Port. Fisheries of the United States 2008: <http:/www.st.nmfs.noaa.gov/st1>. (Landings (millions of pounds) for the top U.S. ports for 2008).

NMFS Gulf of Mexico Shrimp Statistics. <http://www.st.nmfs.noaa.gov/st1/market_news/doc45.txt>. (Gulf of Mexico shrimp landings (headless, thousands of pounds) for each state for January – May, 2006-2010).

"Data Caveats for Commercial Fishery Landings." 18 Feb. 2009. NMFS. 2 Jul. 2010 <http://www.st.nmfs.noaa.gov/st1/commercial/landings/caveat.html>.

The Coastal and Oceanic Plankton Ecology, Production and Observation Database (COPEPOD) contains zooplankton and phytoplankton data from samples collected globally. The database is managed by the NMFS and can be accessed online free of charge (http://www.st.nmfs.noaa.gov/plankton/). The database was created in an effort to make global plankton data readily available to scientists and managers. Data were obtained via Continuous Plankton Recorder (CPR) surveys, either by "ships of opportunity" or during designated research and sampling cruises.

Zooplankton data were obtained via the COPEPOD online database for each of the planning areas. The following sampling programs include samples taken within the OCS planning areas:

- CalCOFI (U.S. Pacific coast), CALifornia Cooperative Oceanic Fisheries Investigations program
- EcoFOCI (Northern California, Oregon, Washington, and Alaska), ECOsystems and Fisheries-Oceanography Cooperative Investigation program
- EcoMon-RV (U.S. Atlantic coast), ECOsystem MONitoring Research Vessel surveys
- ORCAWALE (U.S. Pacific coast), Oregon, California, and Washington Line-transect Expedition marine mammal survey
- SEAMAP (Gulf of Mexico), SouthEAst Monitoring Assessment Program

Zooplankton data for recent years (2000-present) were collected from each of these programs. Data are reported as zooplankton displacement volume (mL m^{-3}), which is a measure of biomass.

Commercial fishery landings data are obtained by NFMS "from state-mandated fishery or mollusk trip tickets, landing weighout reports provided by seafood dealers, federal logbooks of fishery catch and effort, and shipboard and portside interview and biological sampling of catches" (NMFS Data Caveats). Total landings by state are the most accurate because confidential data are included. In more specific datasets (e.g., species landings), confidential data are handled in such a way to maintain confidentiality. This may result in misleading data, as confidential landings are grouped with other data.

Commercial landings of fish and invertebrates were obtained for 2008 for each state (NMFS). Landings are reported in aggregated groups of fish and invertebrates, and are reported in pounds (live weight), and pounds of meat for bivalves (excluding shells). Commercial fishery landings (millions of pounds) are also reported by port. Landings for major U.S. ports were obtained for 2008 (NMFS). Additional landings for the Gulf of Mexico shrimp fishery were collected (NMFS). This dataset contains shrimp landings (headless, thousands of pounds) for the months January through May for the years 2006 through 2010.

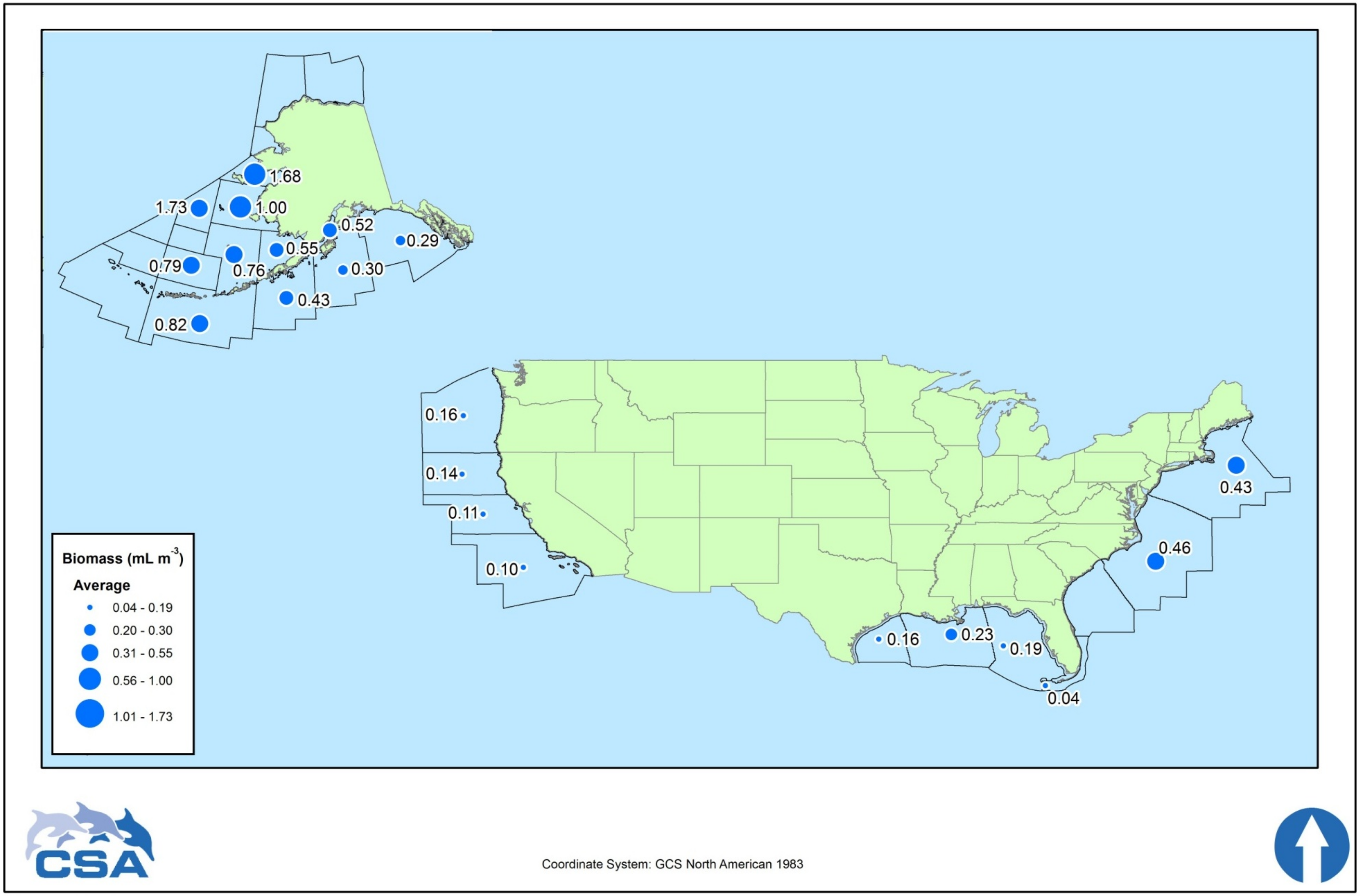

Figure C-1. Average zooplankton biomass in OCS planning areas: Alaska (2000-2007), Pacific (2006), California (2000-2006), Gulf of Mexico (2000-2003), and Atlantic (2000-2001).

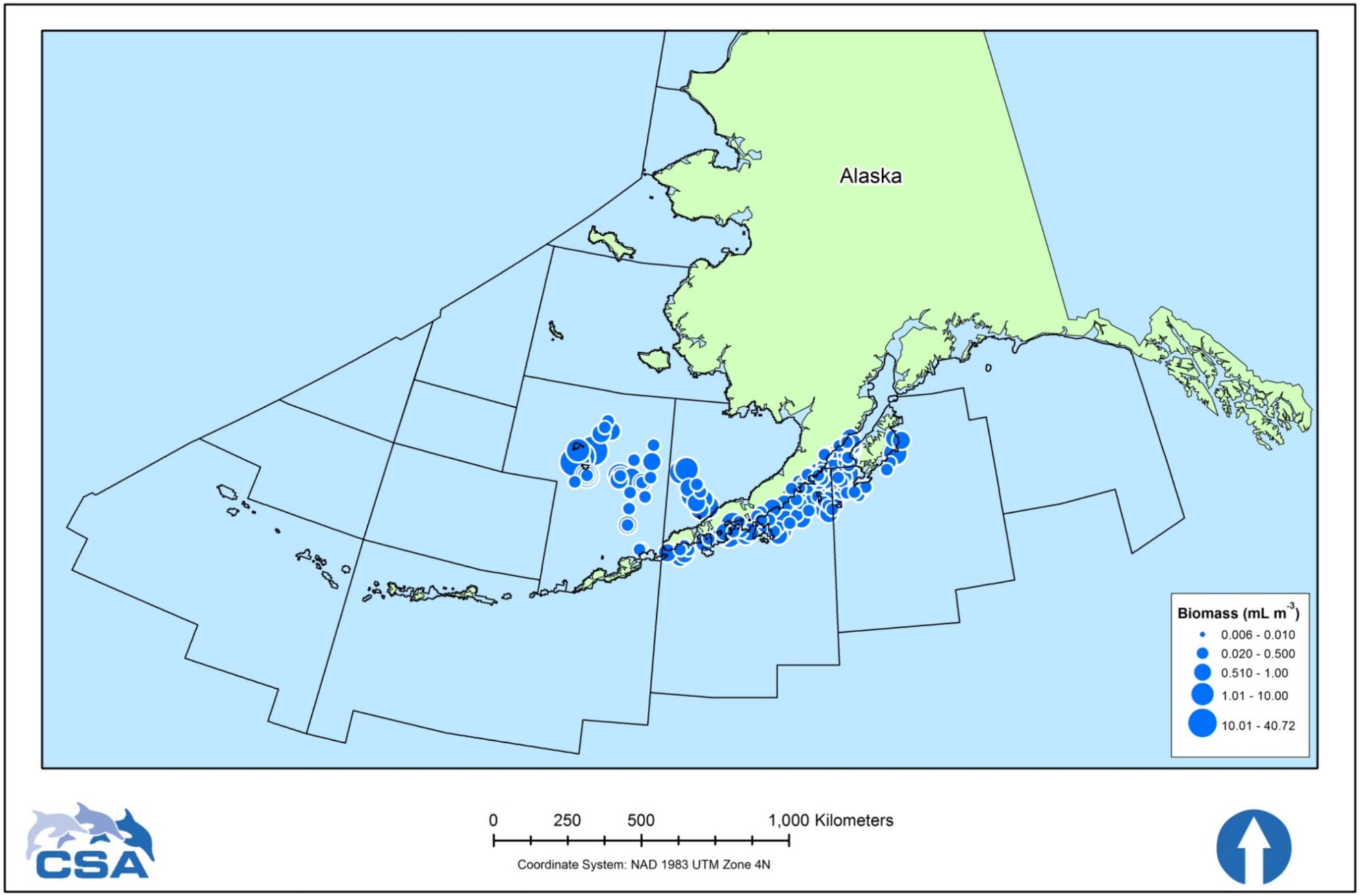

Figure C-2. Alaska Outer Continental Shelf Region annual average zooplankton biomass, 2000.

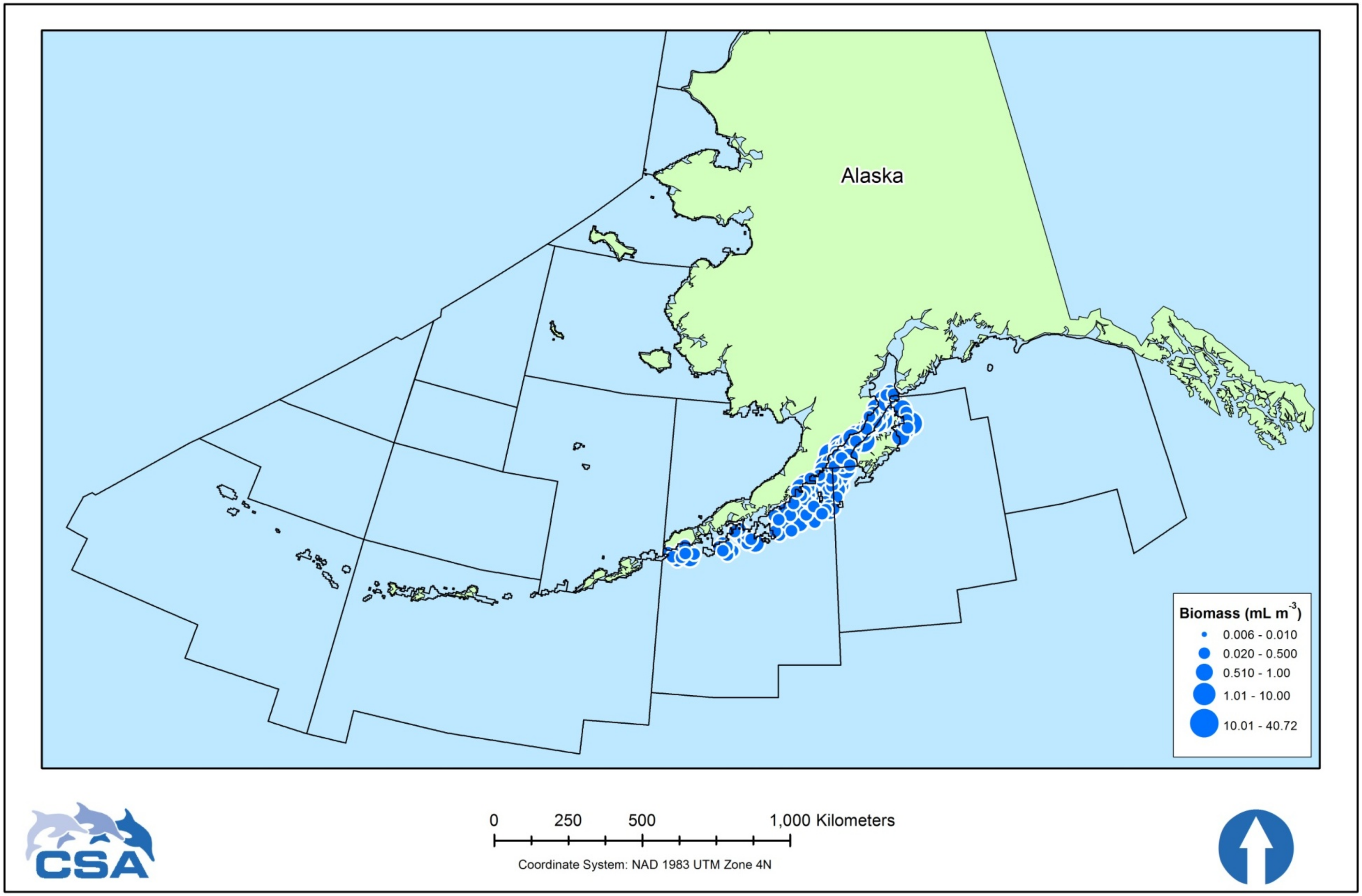

Figure C-3. Alaska Outer Continental Shelf Region annual average zooplankton biomass, 2001.

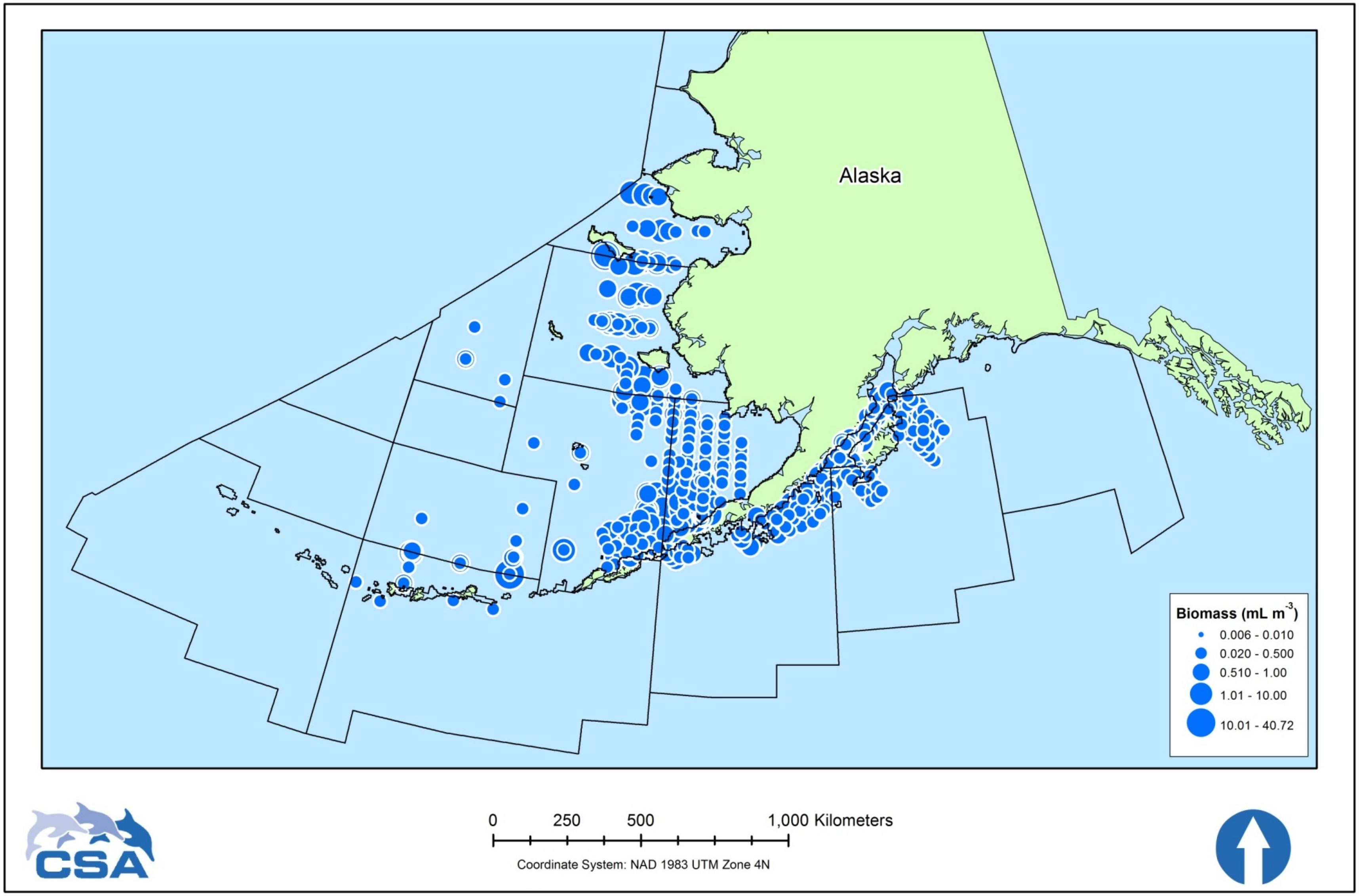

Figure C-4. Alaska Outer Continental Shelf Region annual average zooplankton biomass, 2002.

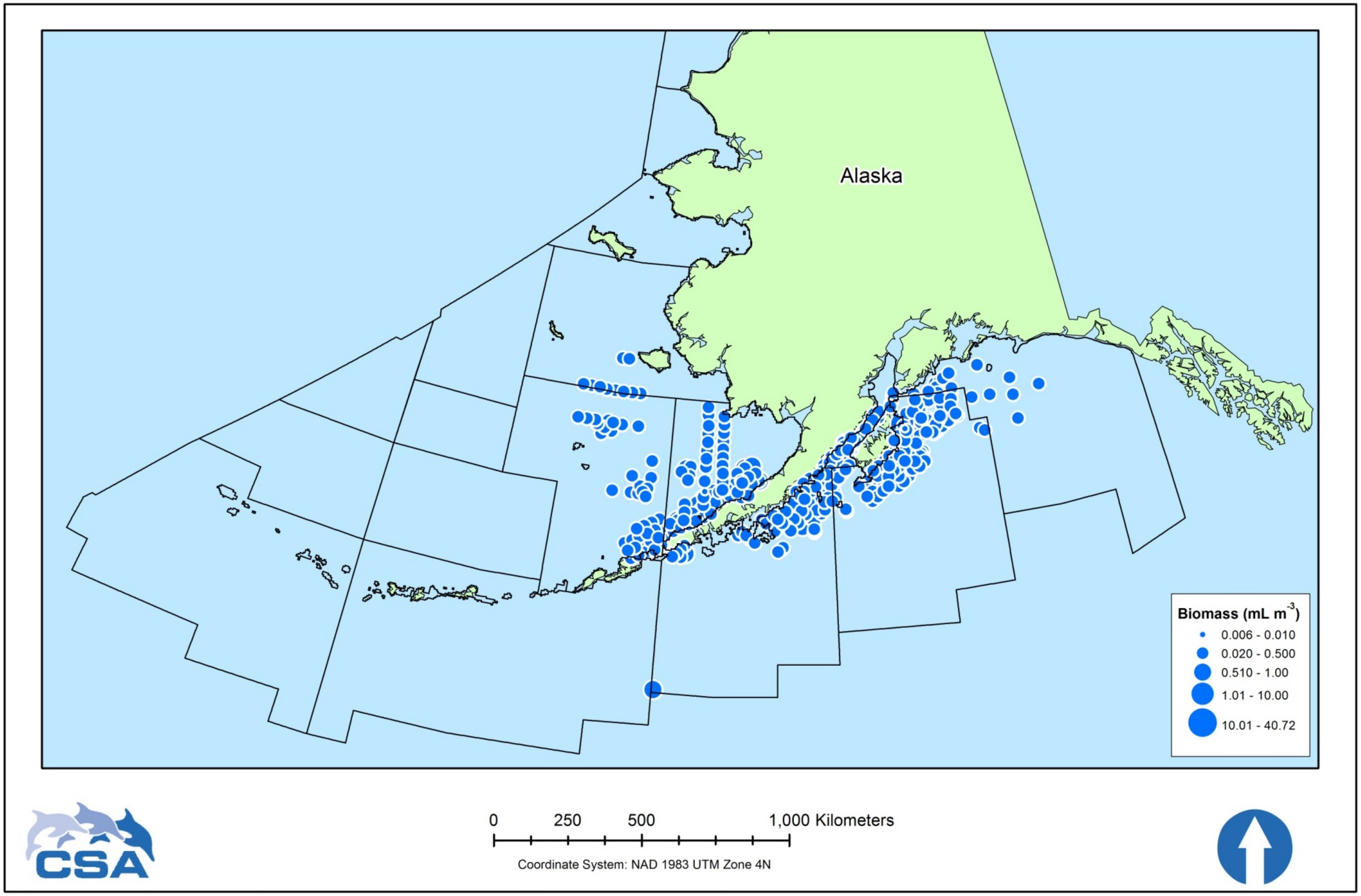

Figure C-5. Alaska Outer Continental Shelf Region annual average zooplankton biomass, 2003.

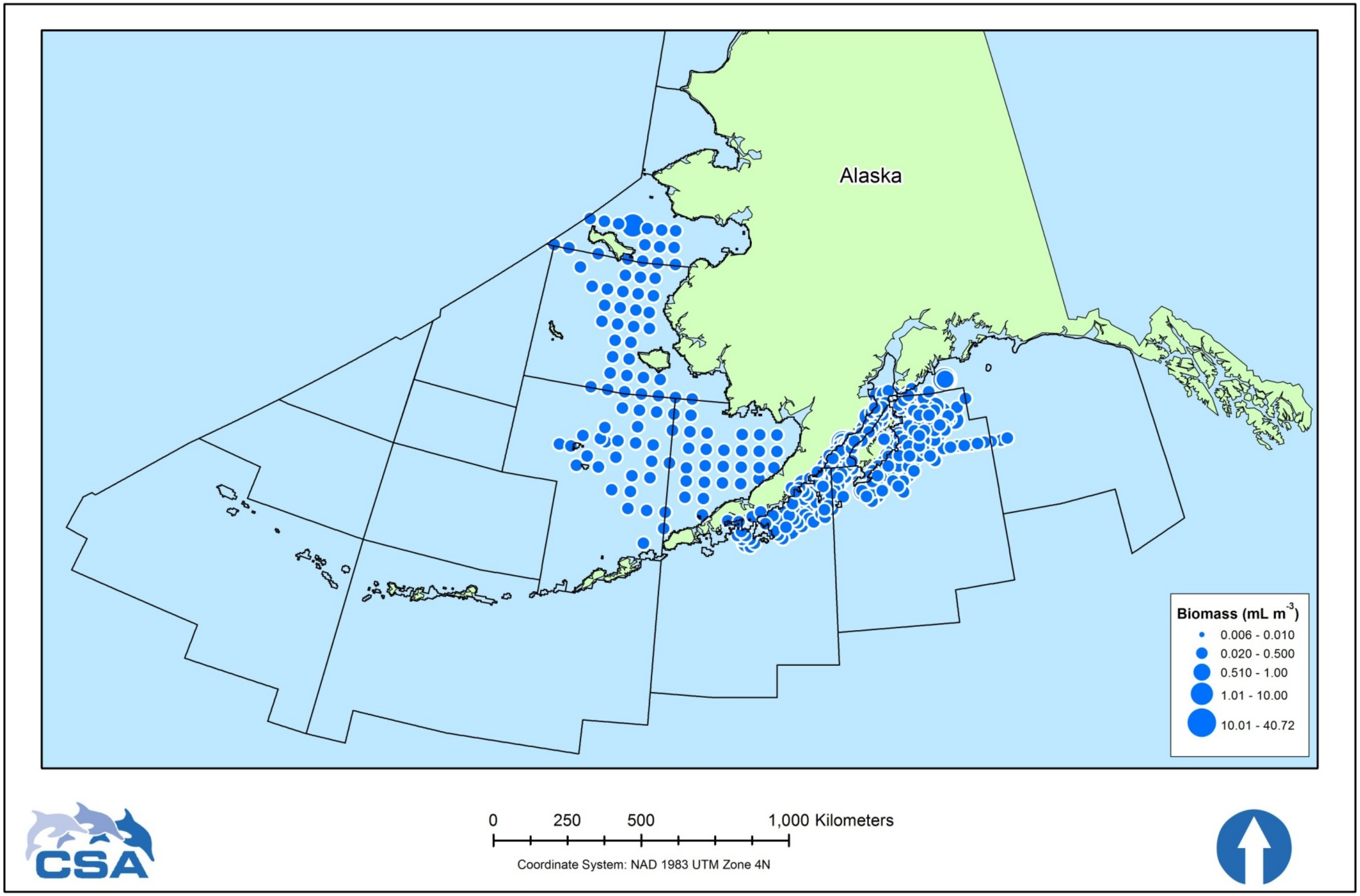

Figure C-6. Alaska Outer Continental Shelf Region annual average zooplankton biomass, 2004.

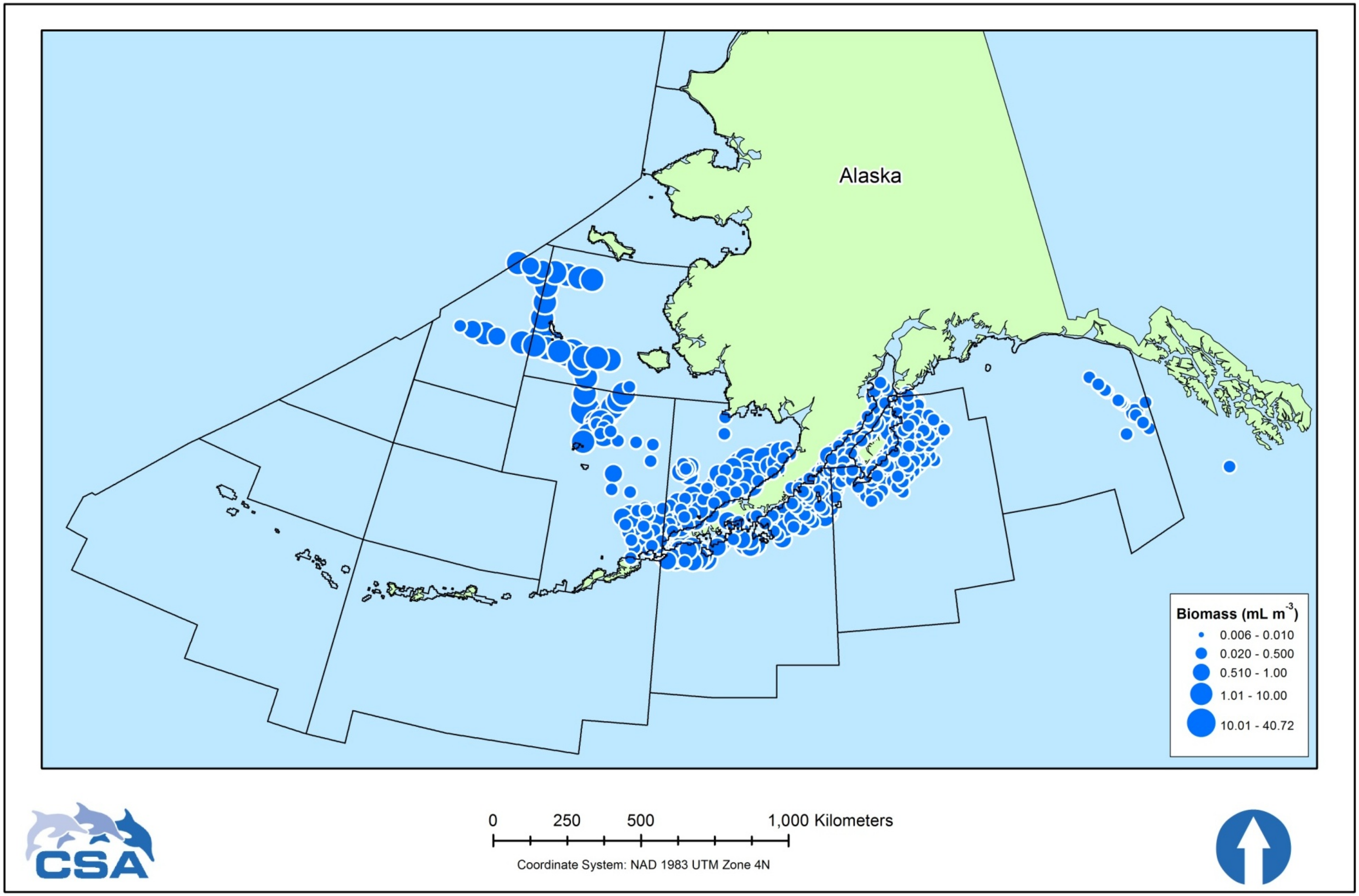

Figure C-7. Alaska Outer Continental Shelf Region annual average zooplankton biomass, 2005.

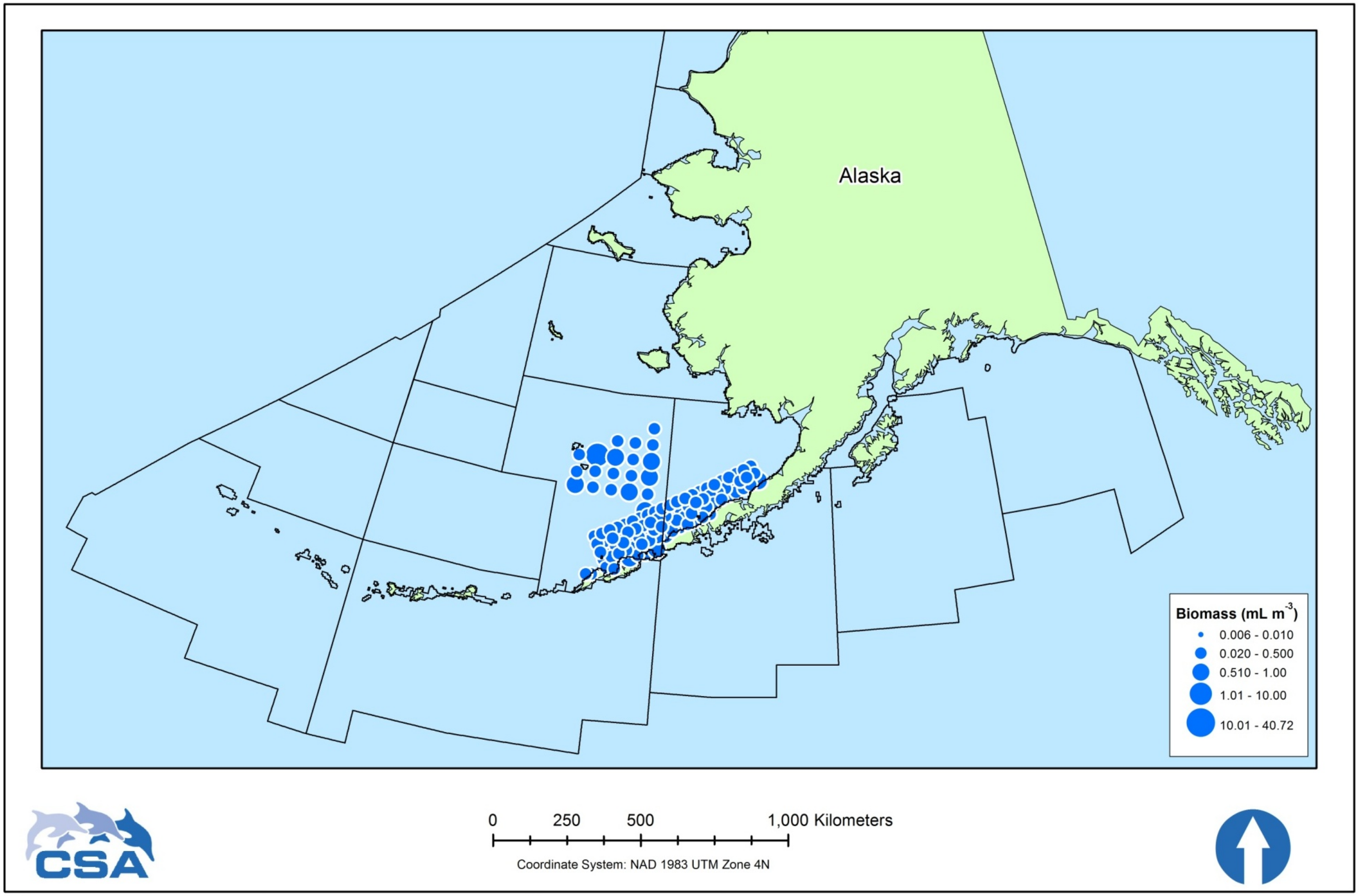

Figure C-8. Alaska Outer Continental Shelf Region annual average zooplankton biomass, 2006.

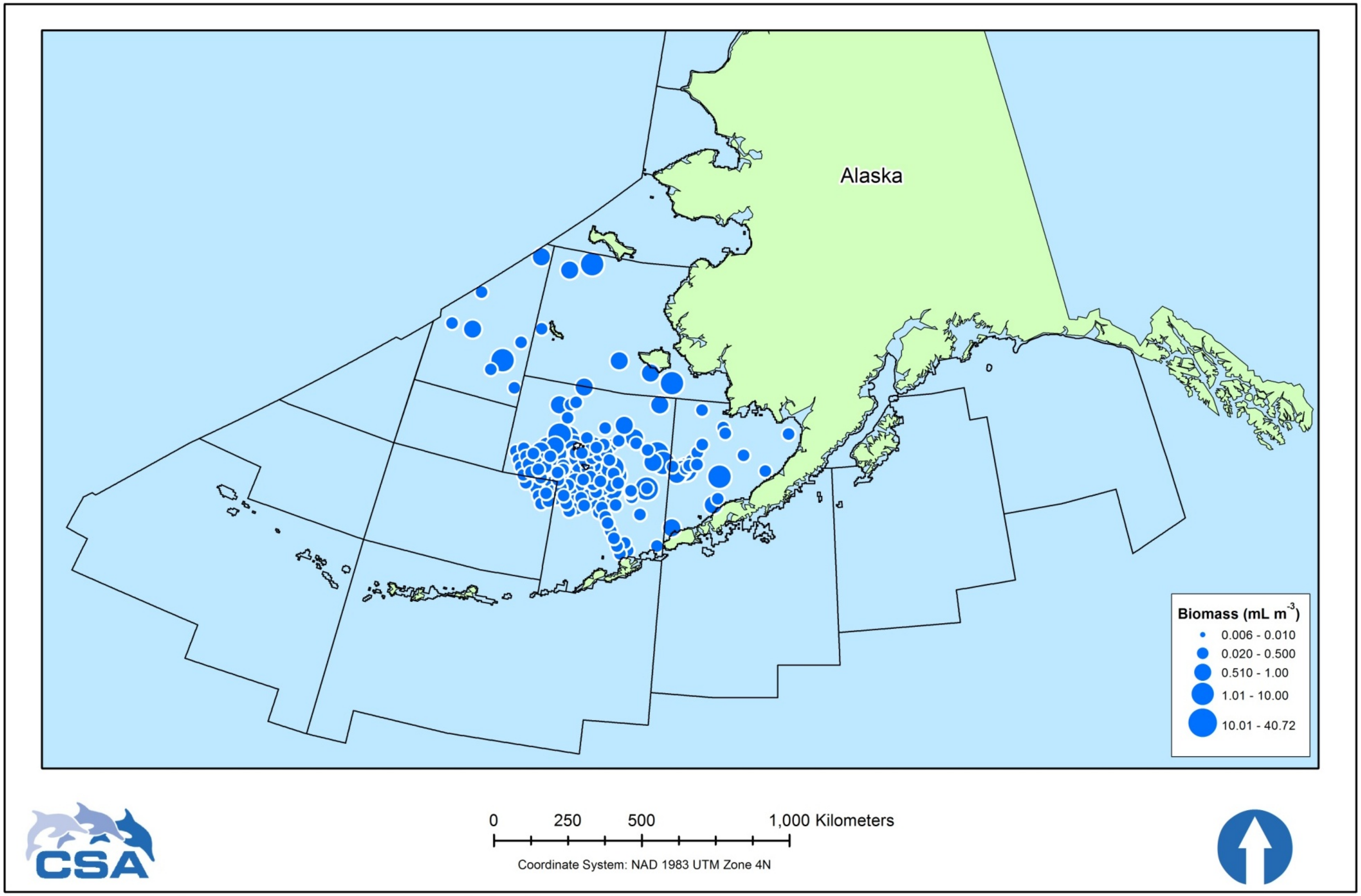

Figure C-9. Alaska Outer Continental Shelf Region annual average zooplankton biomass, 2007.

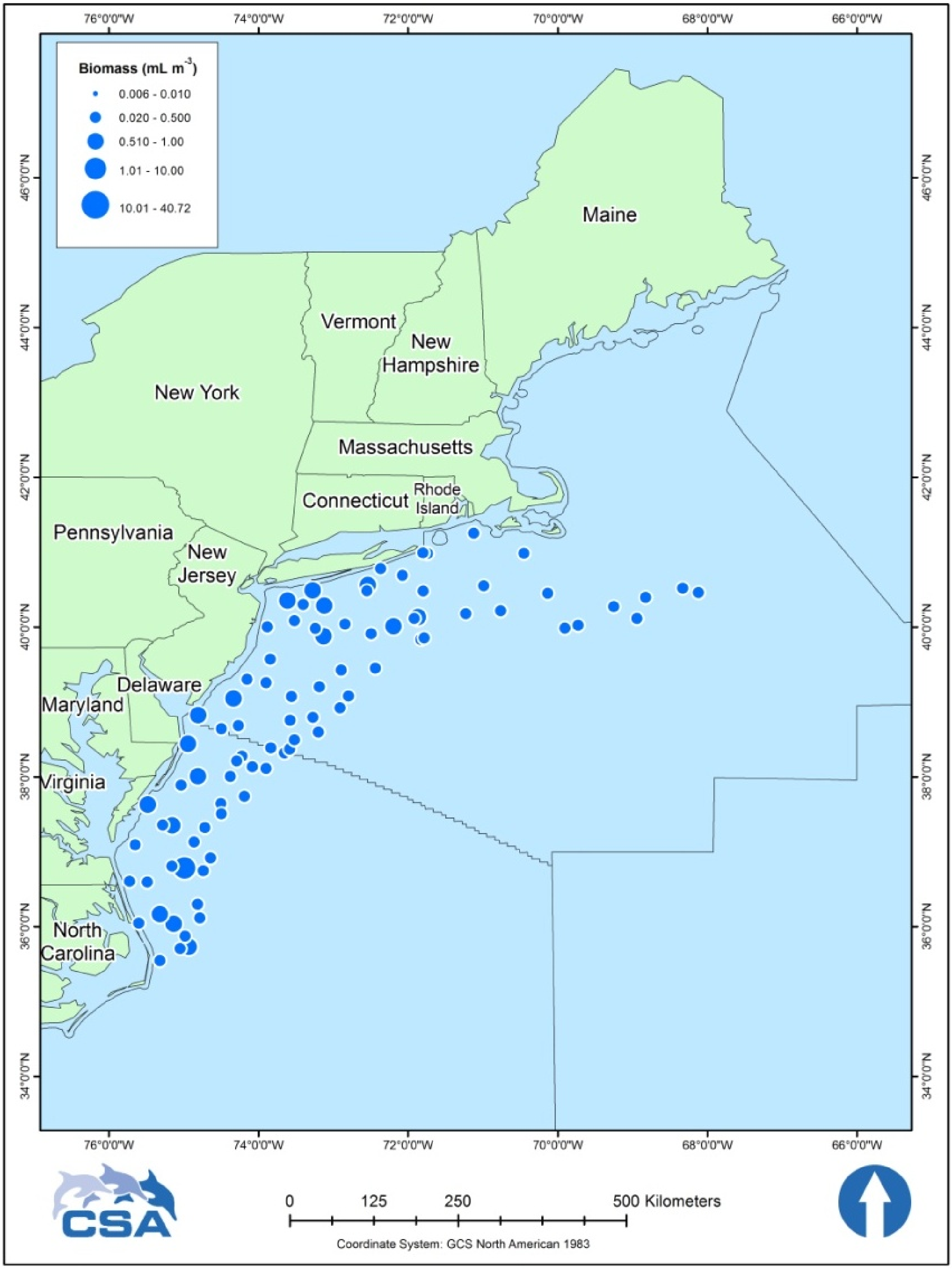

Figure C-10. Atlantic Outer Continental Shelf Region average zooplankton biomass, Winter 2000.

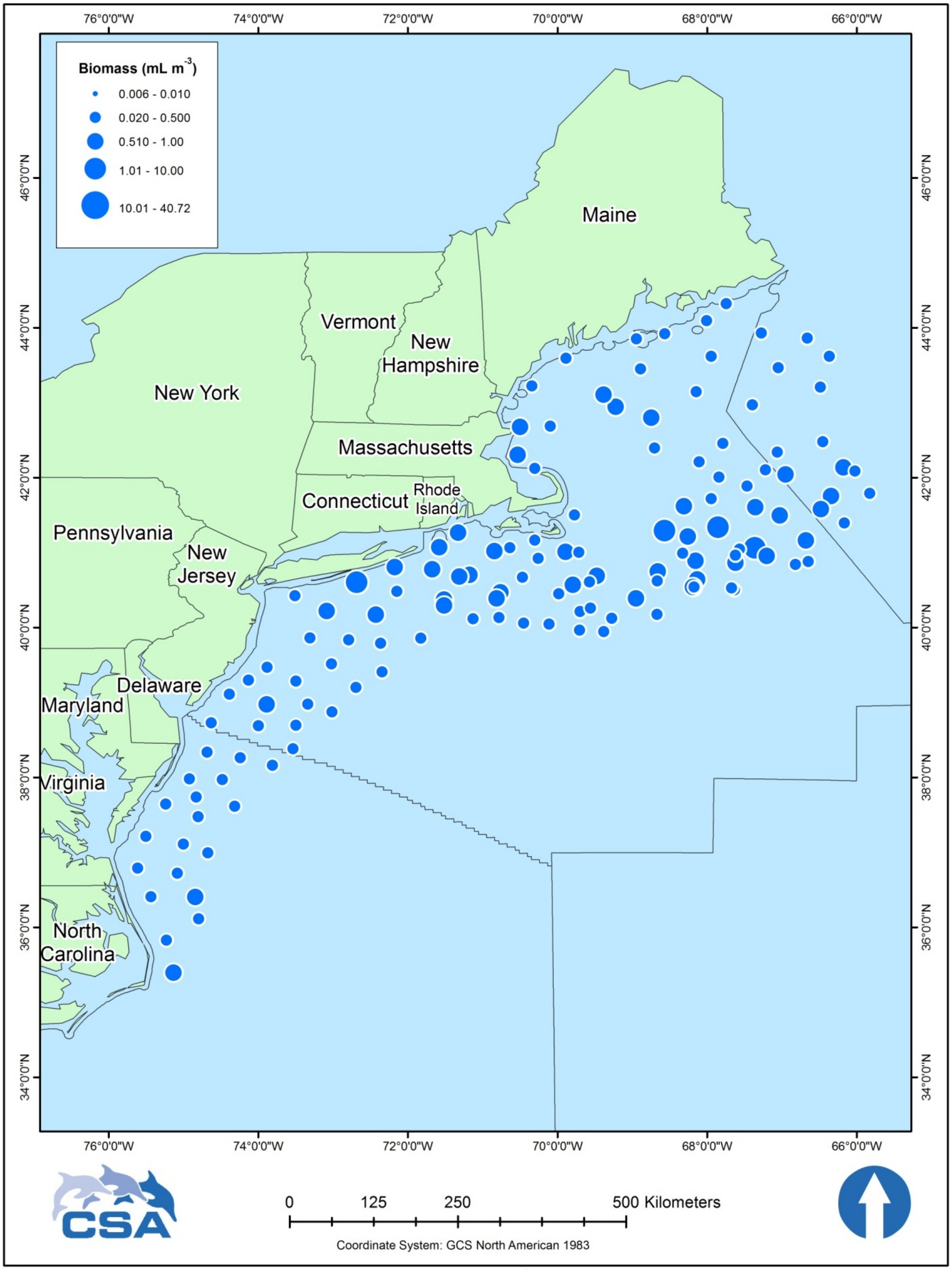

Figure C-11. Atlantic Outer Continental Shelf Region average zooplankton biomass, Spring 2000.

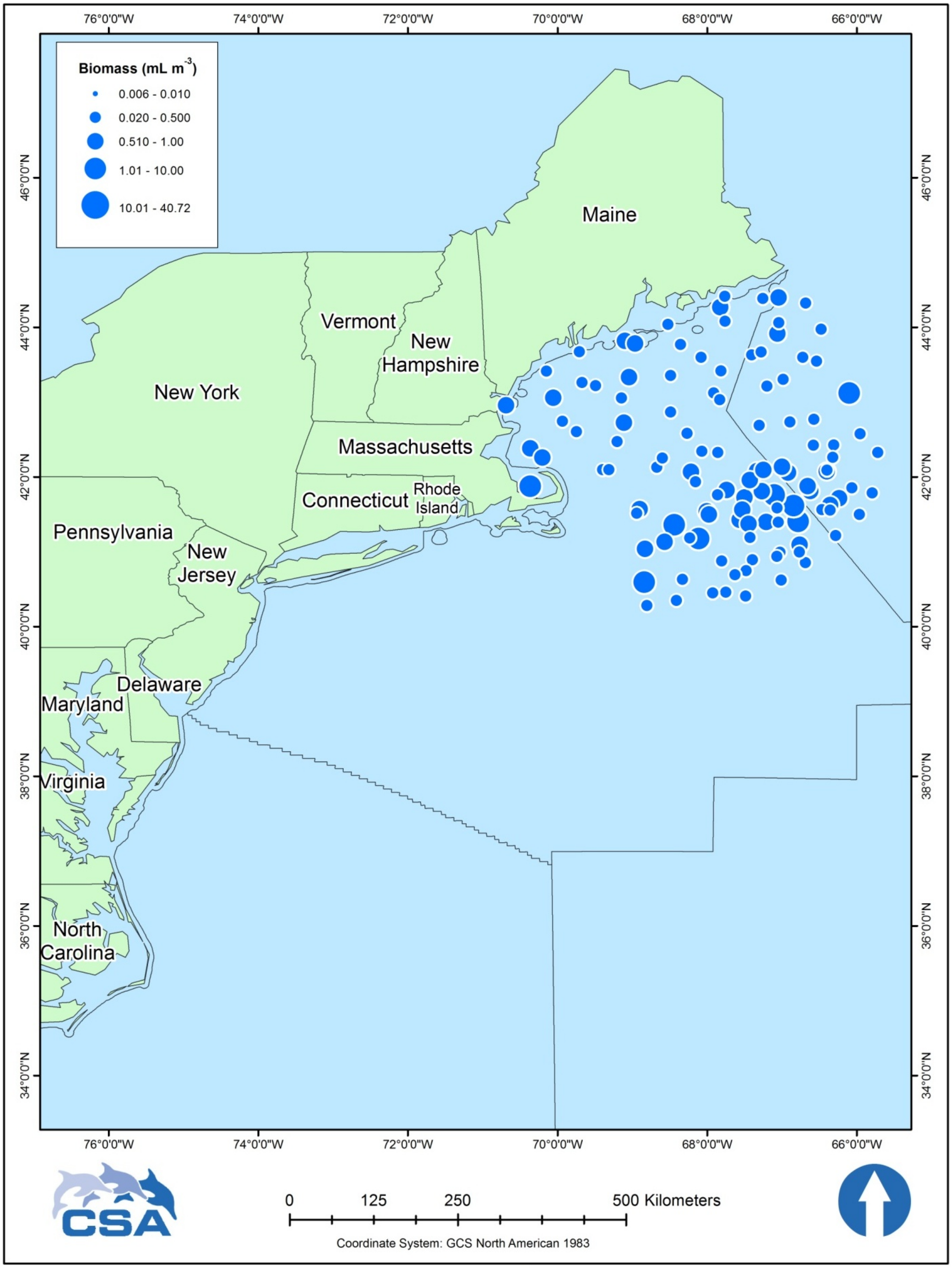

Figure C-12. Atlantic Outer Continental Shelf Region average zooplankton biomass, Summer 2000.

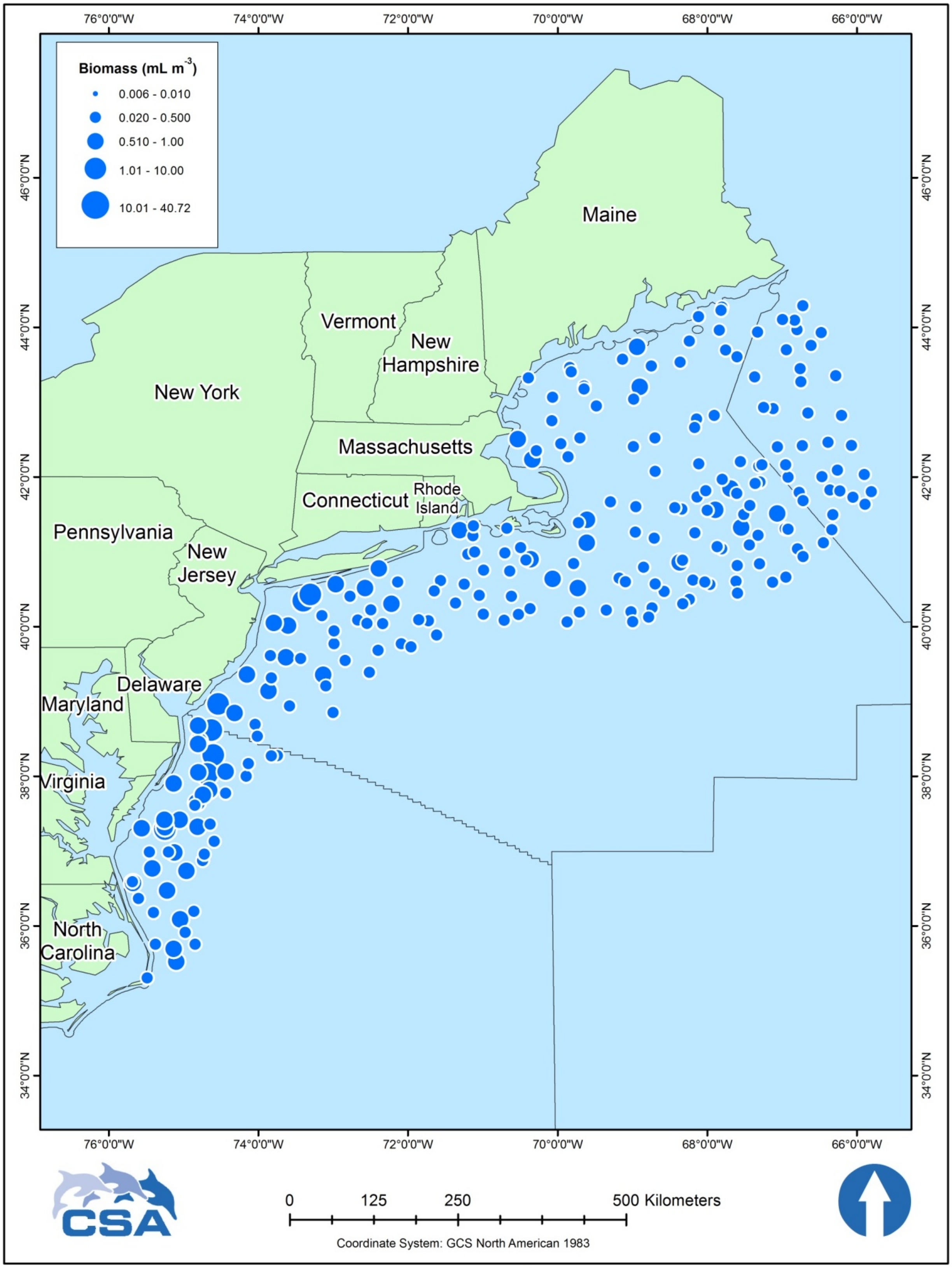

Figure C-13. Atlantic Outer Continental Shelf Region average zooplankton biomass, Fall 2000.

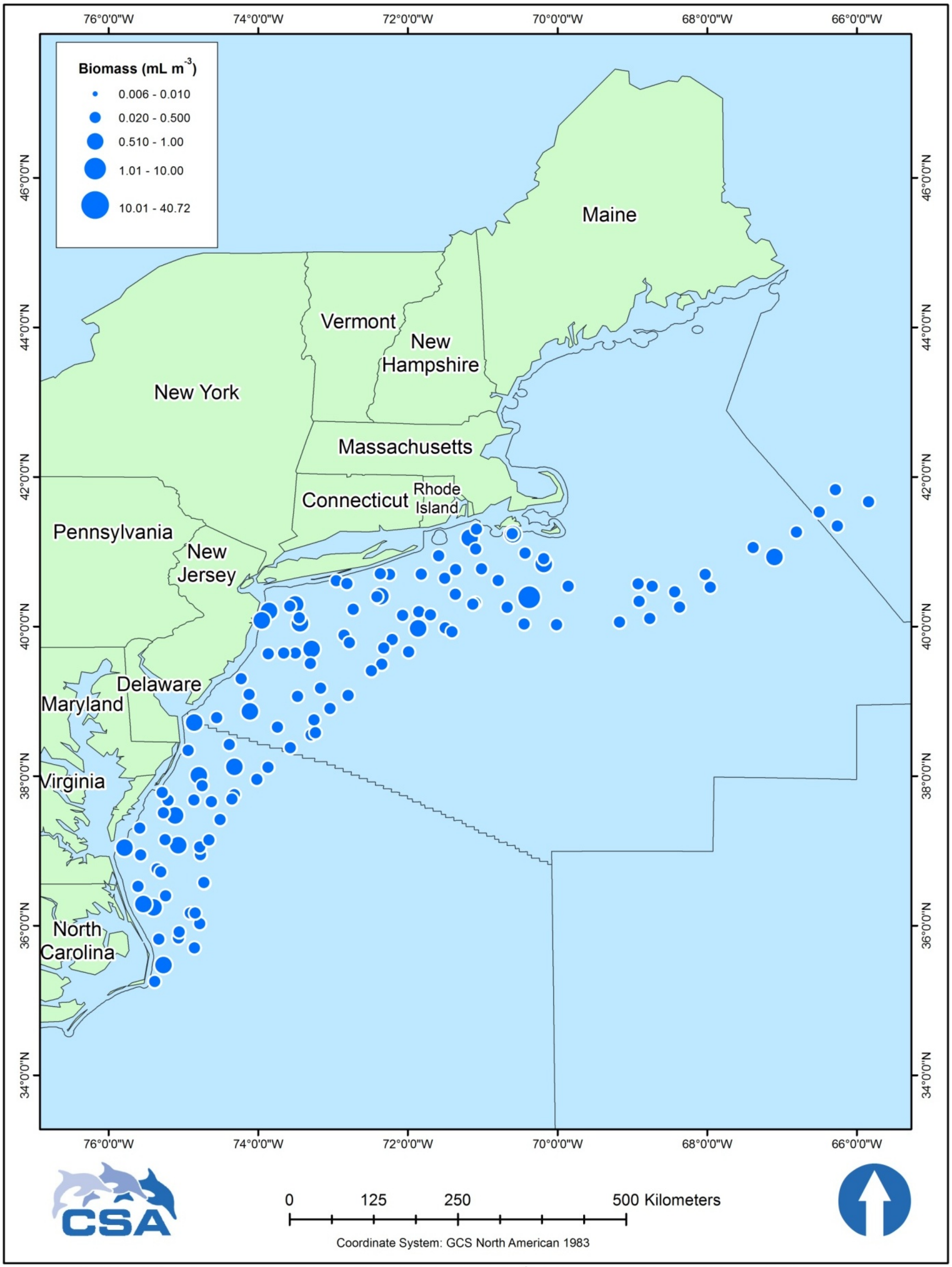

Figure C-14. Atlantic Outer Continental Shelf Region average zooplankton biomass, Winter 2001.

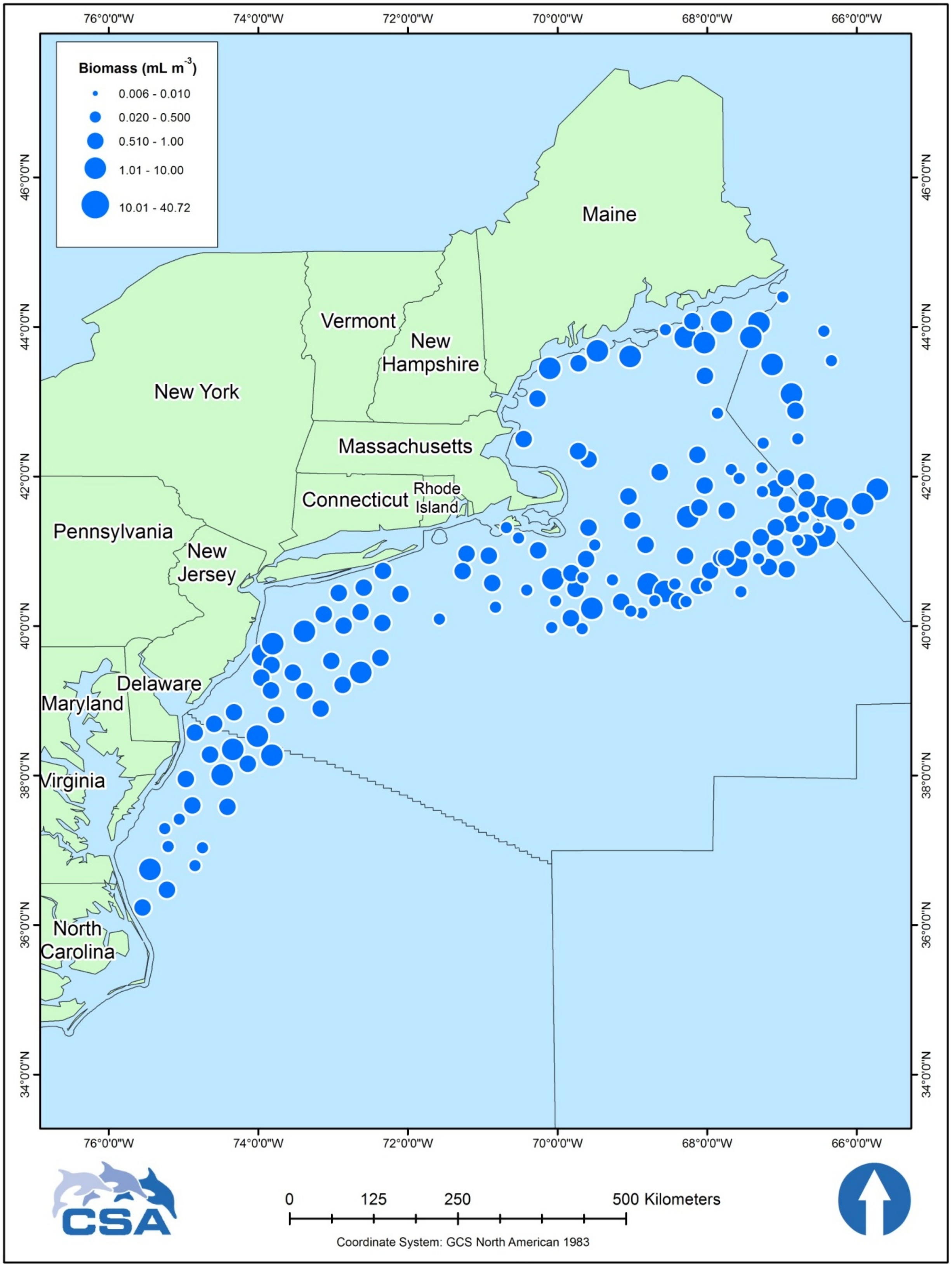

Figure C-15. Atlantic Outer Continental Shelf Region average zooplankton biomass, Spring 2001.

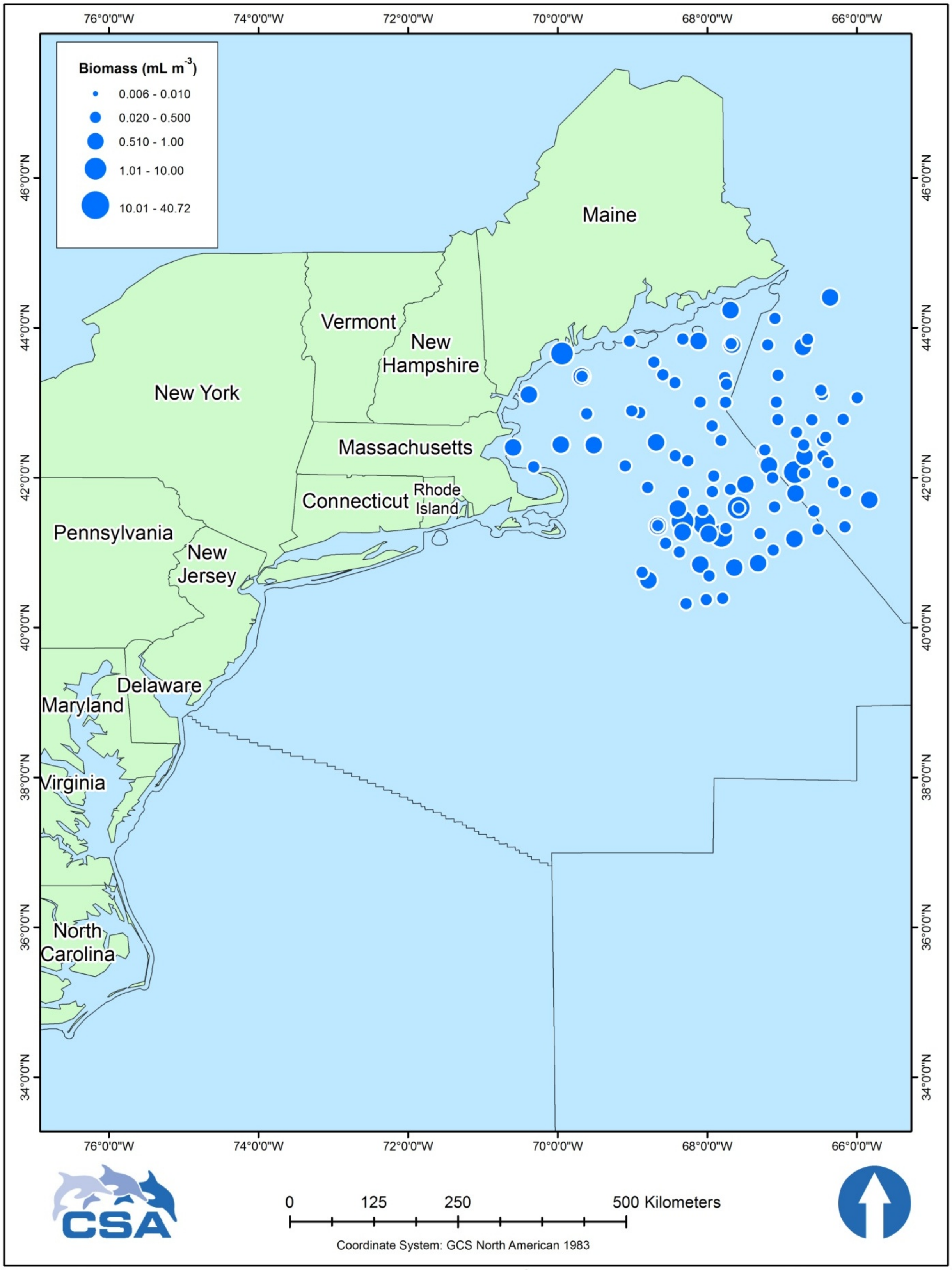

Figure C-16. Atlantic Outer Continental Shelf Region average zooplankton biomass, Summer 2001.

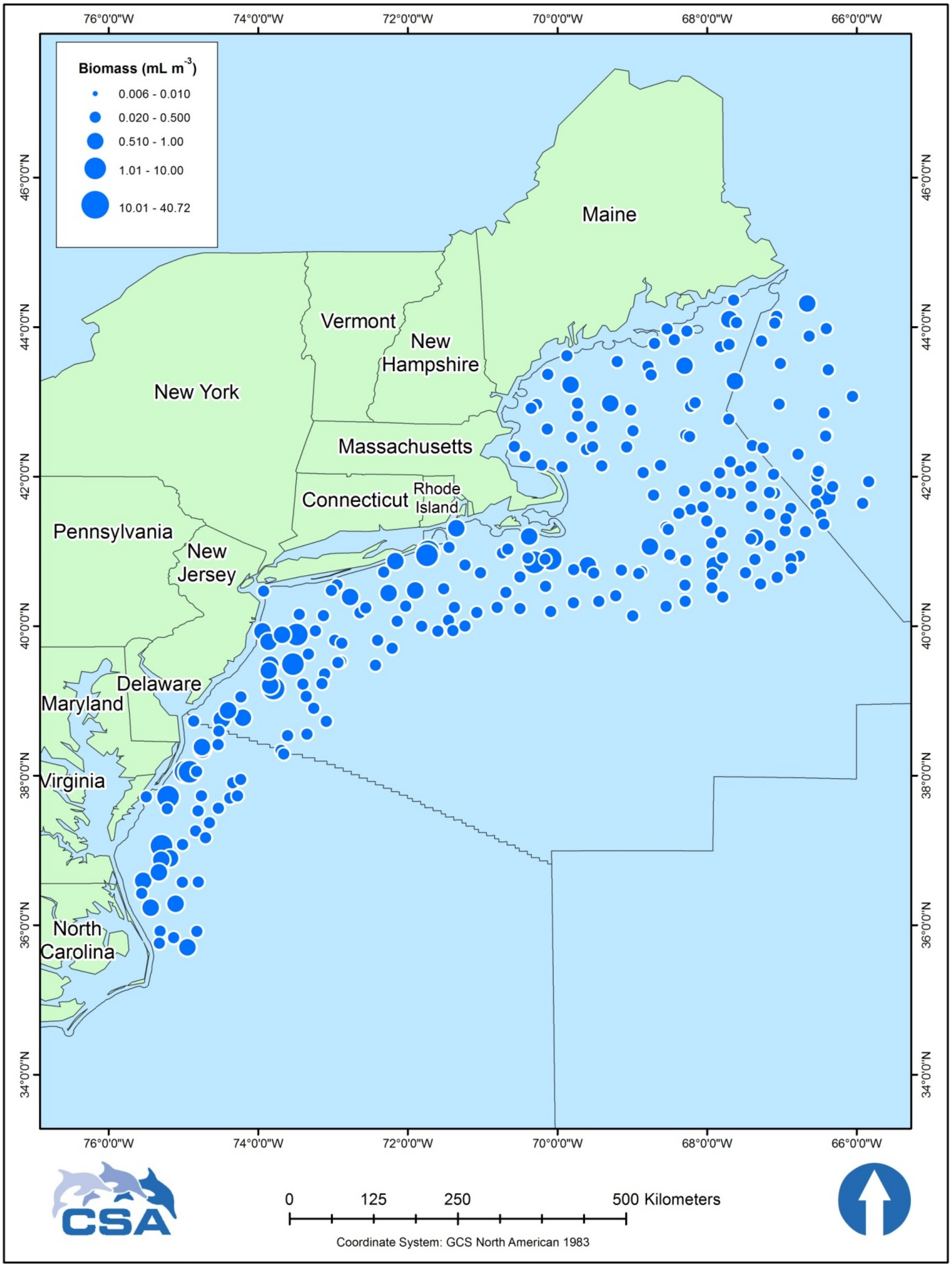

Figure C-17. Atlantic Outer Continental Shelf Region average zooplankton biomass, Fall 2001.

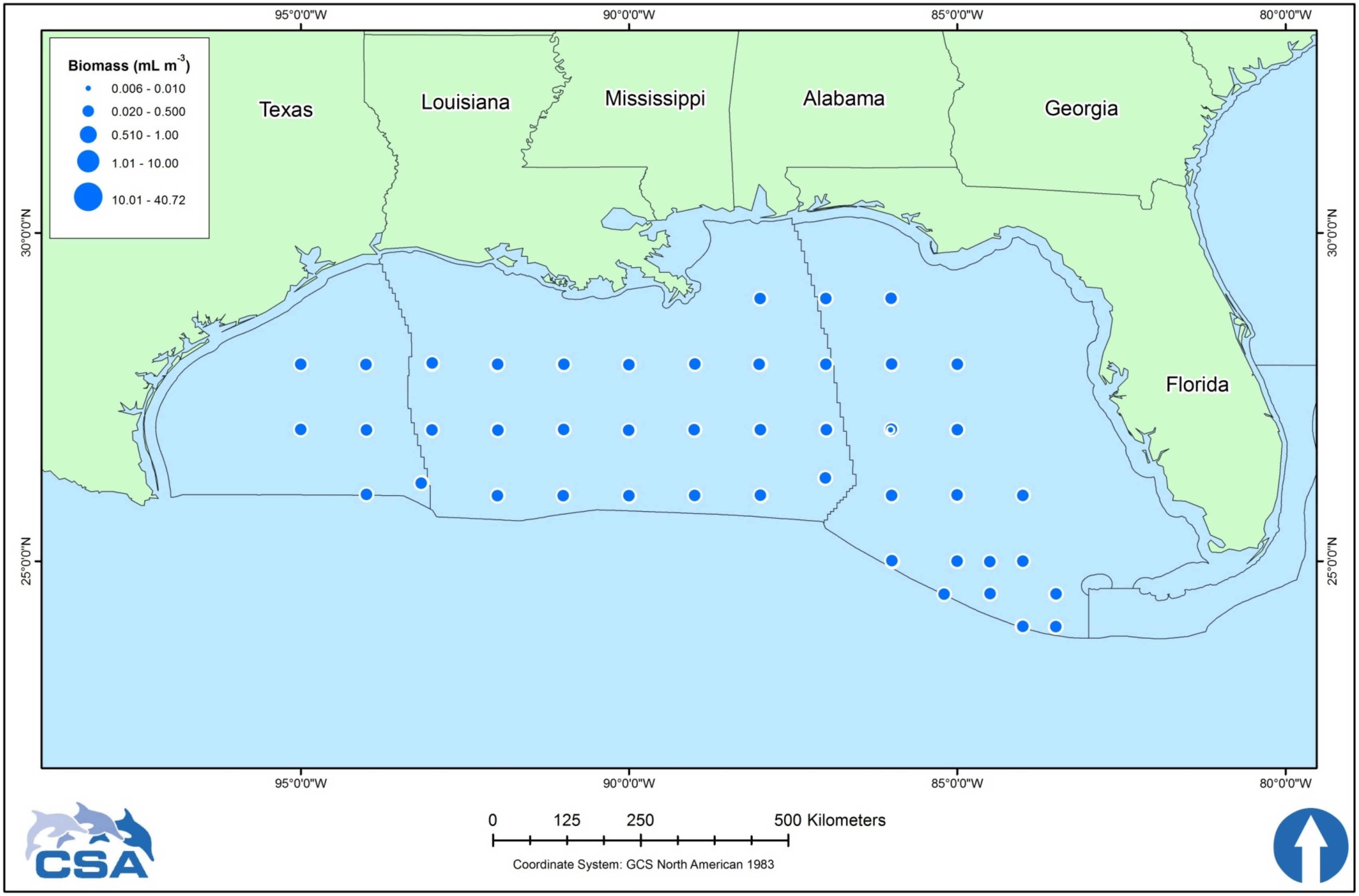

Figure C-18. Gulf of Mexico Outer Continental Shelf Region average zooplankton biomass, Spring 2000.

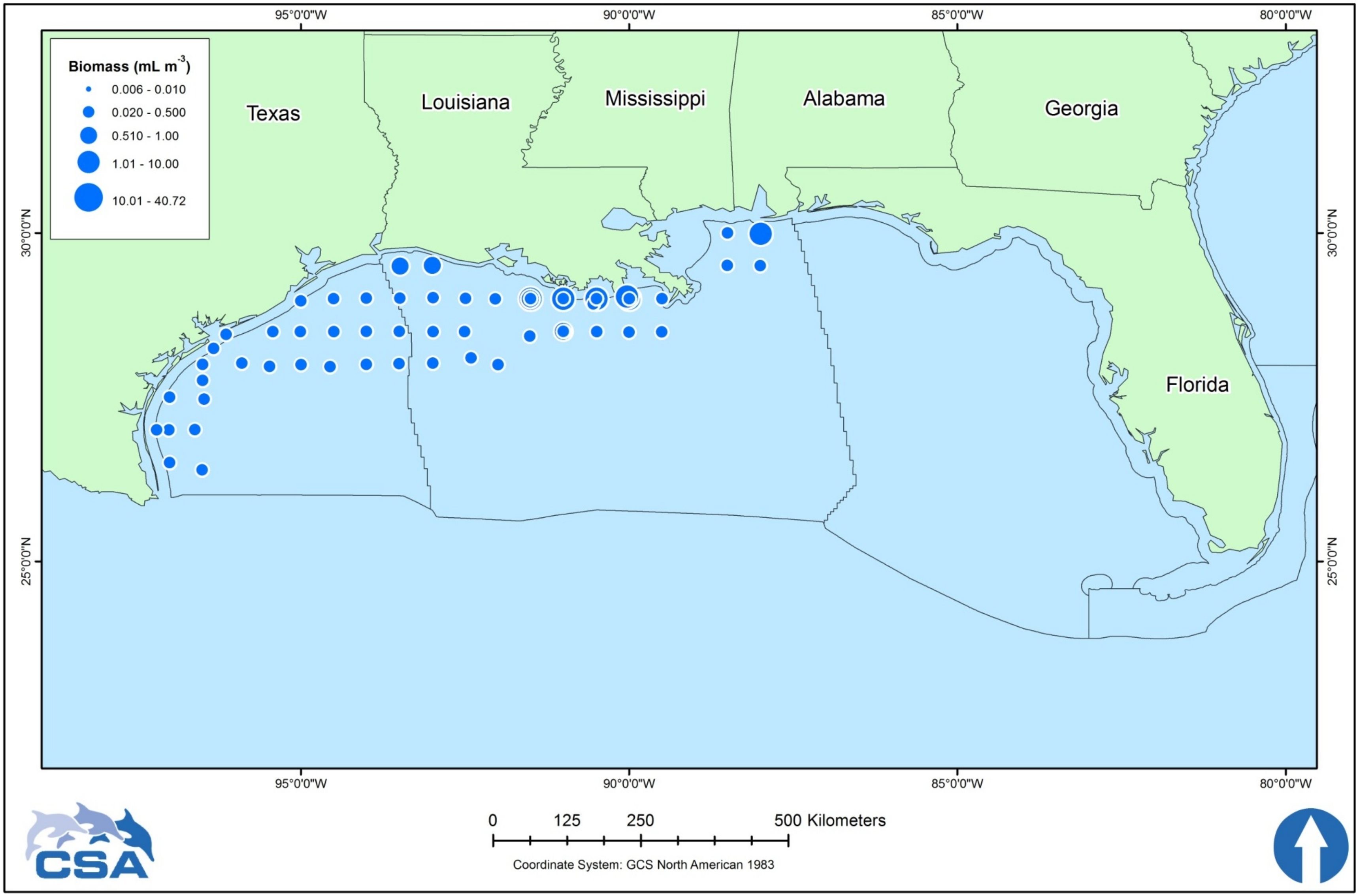

Figure C-19. Gulf of Mexico Outer Continental Shelf Region average zooplankton biomass, Summer 2000.

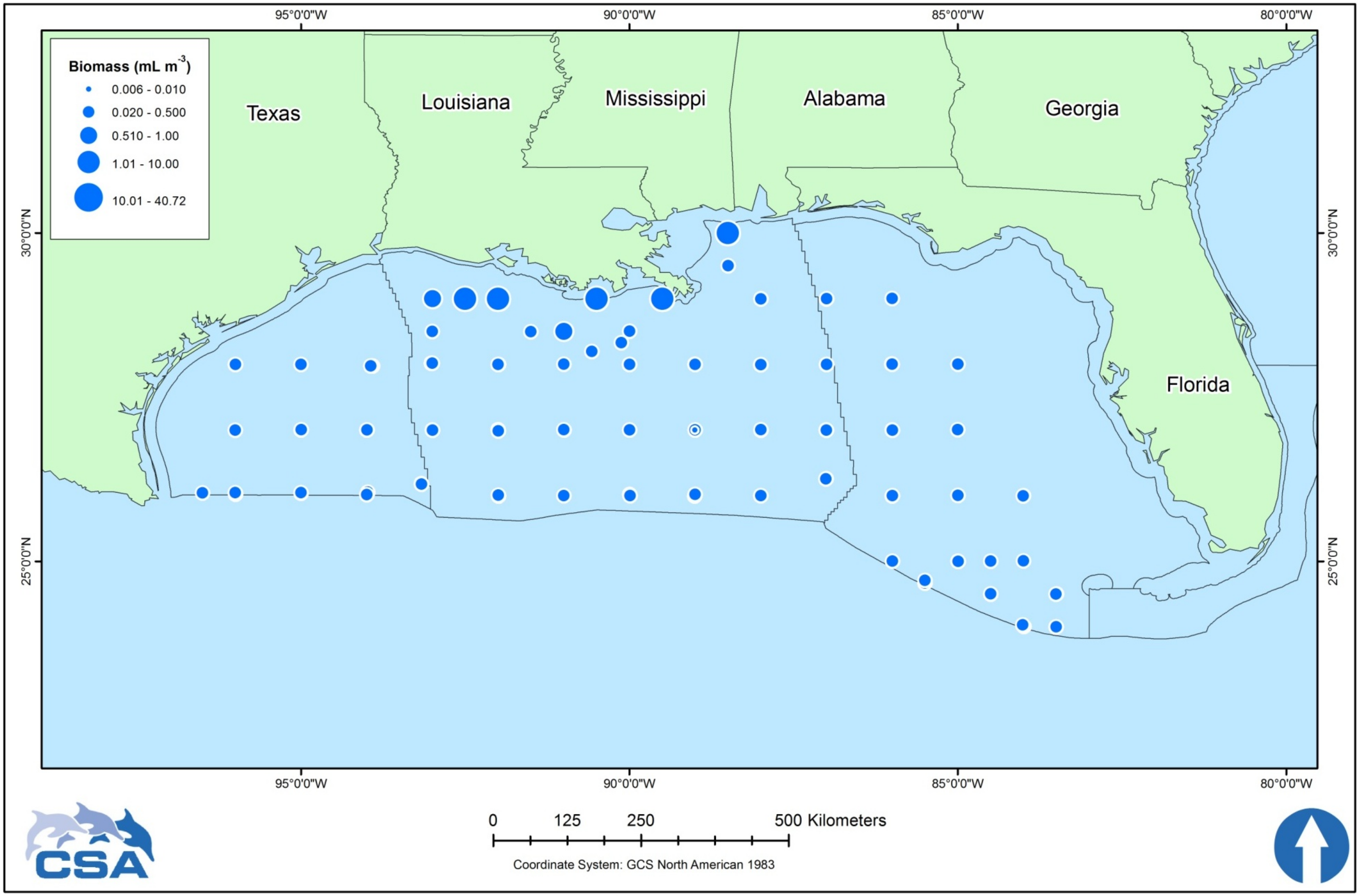

Figure C-20. Gulf of Mexico Outer Continental Shelf Region average zooplankton biomass, Spring and Summer 2001.

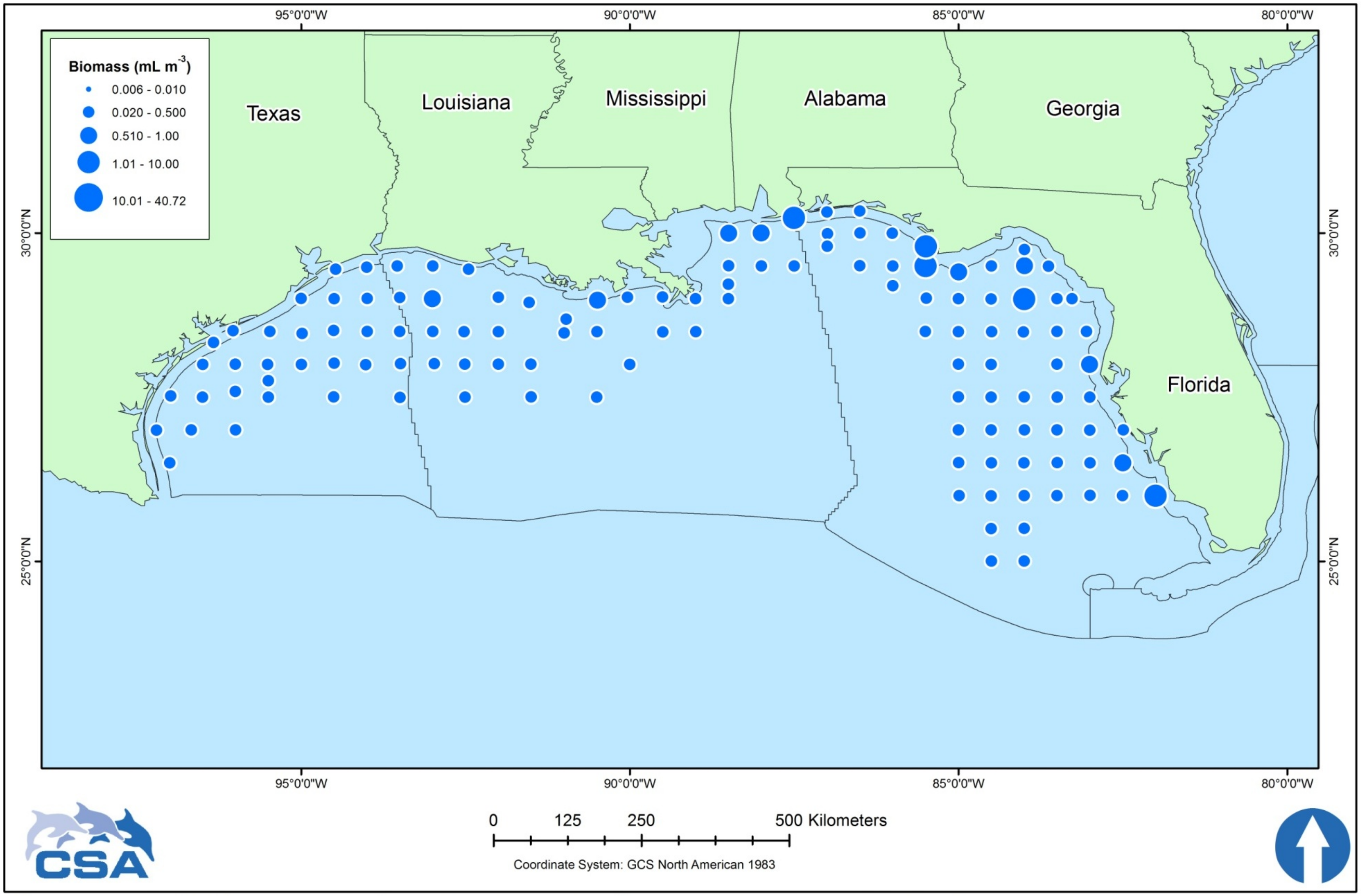

Figure C-21. Gulf of Mexico Outer Continental Shelf Region average zooplankton biomass, September 2001.

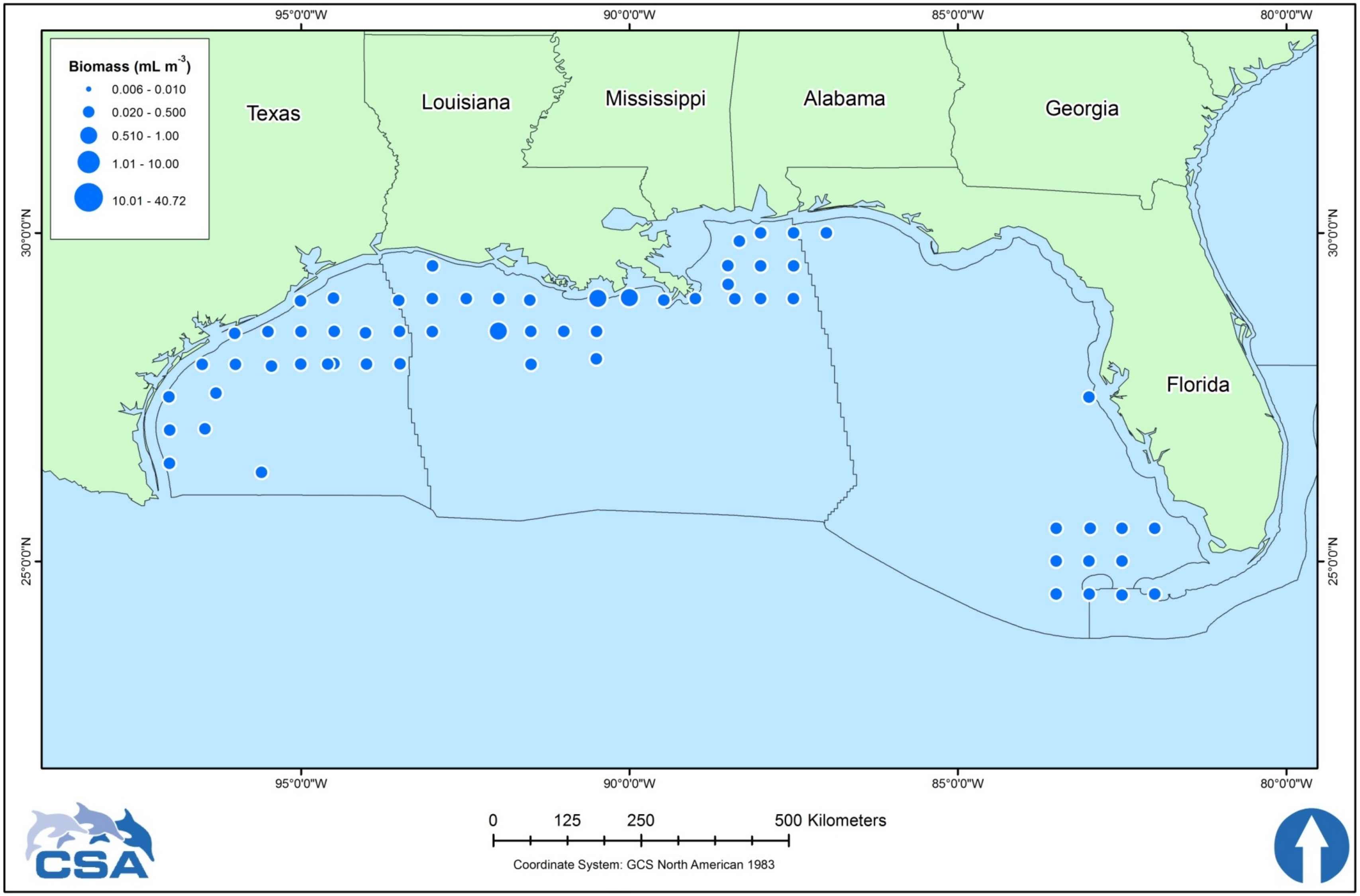

Figure C-22. Gulf of Mexico Outer Continental Shelf Region average zooplankton biomass, Fall 2001.

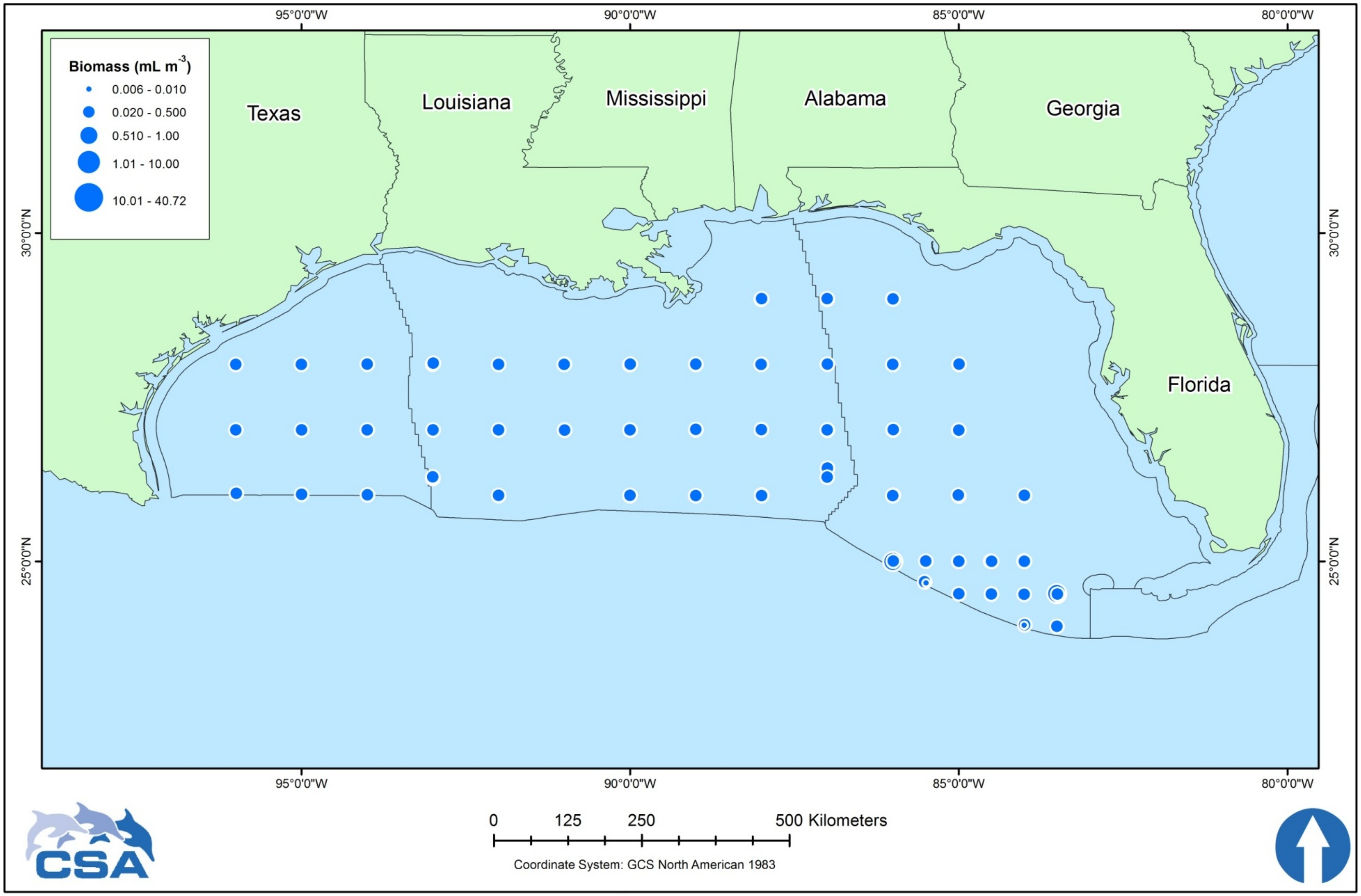

Figure C-23. Gulf of Mexico Outer Continental Shelf Region average zooplankton biomass, Spring 2002.

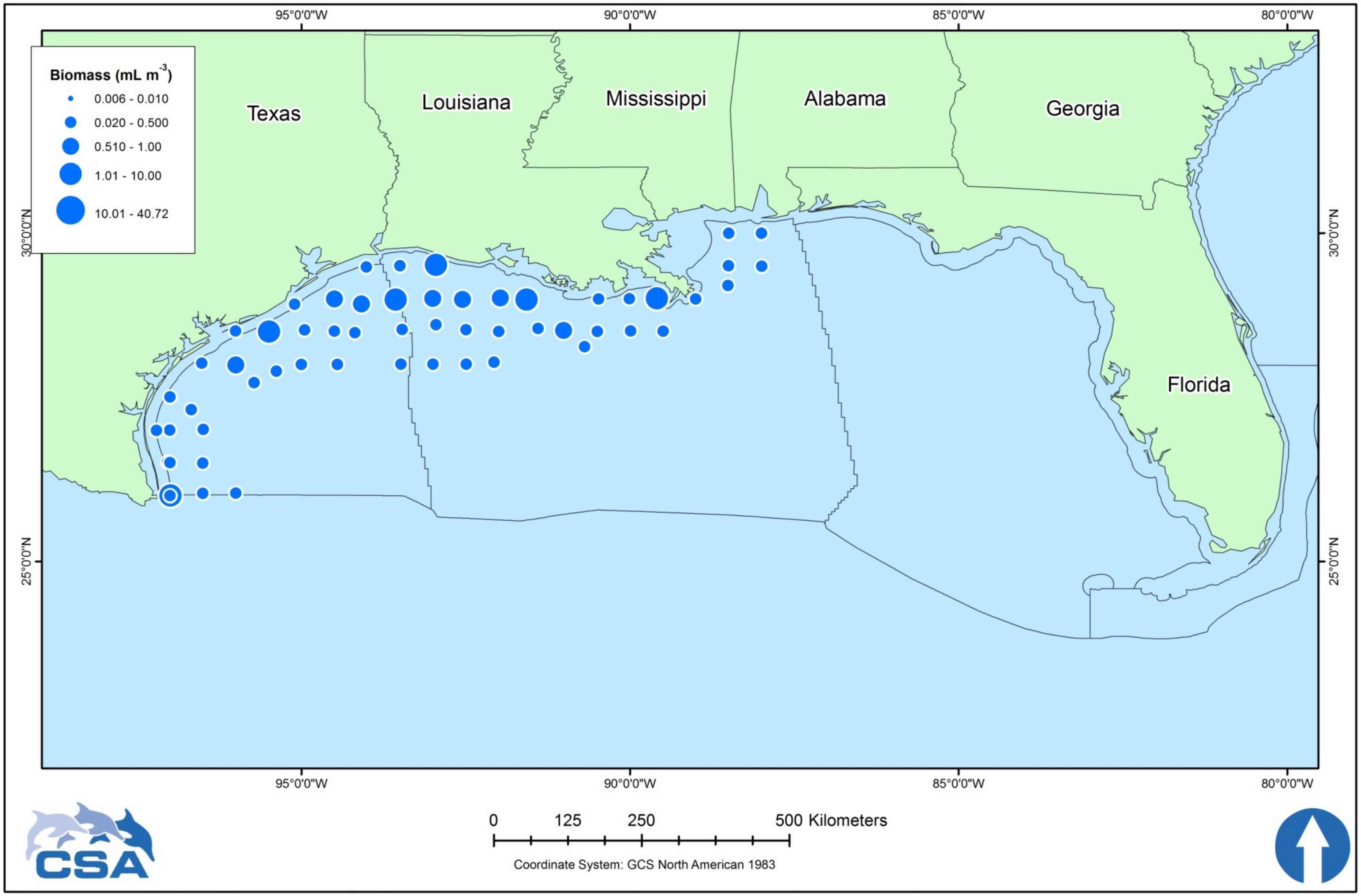

Figure C-24. Gulf of Mexico Outer Continental Shelf Region average zooplankton biomass, Summer 2002.

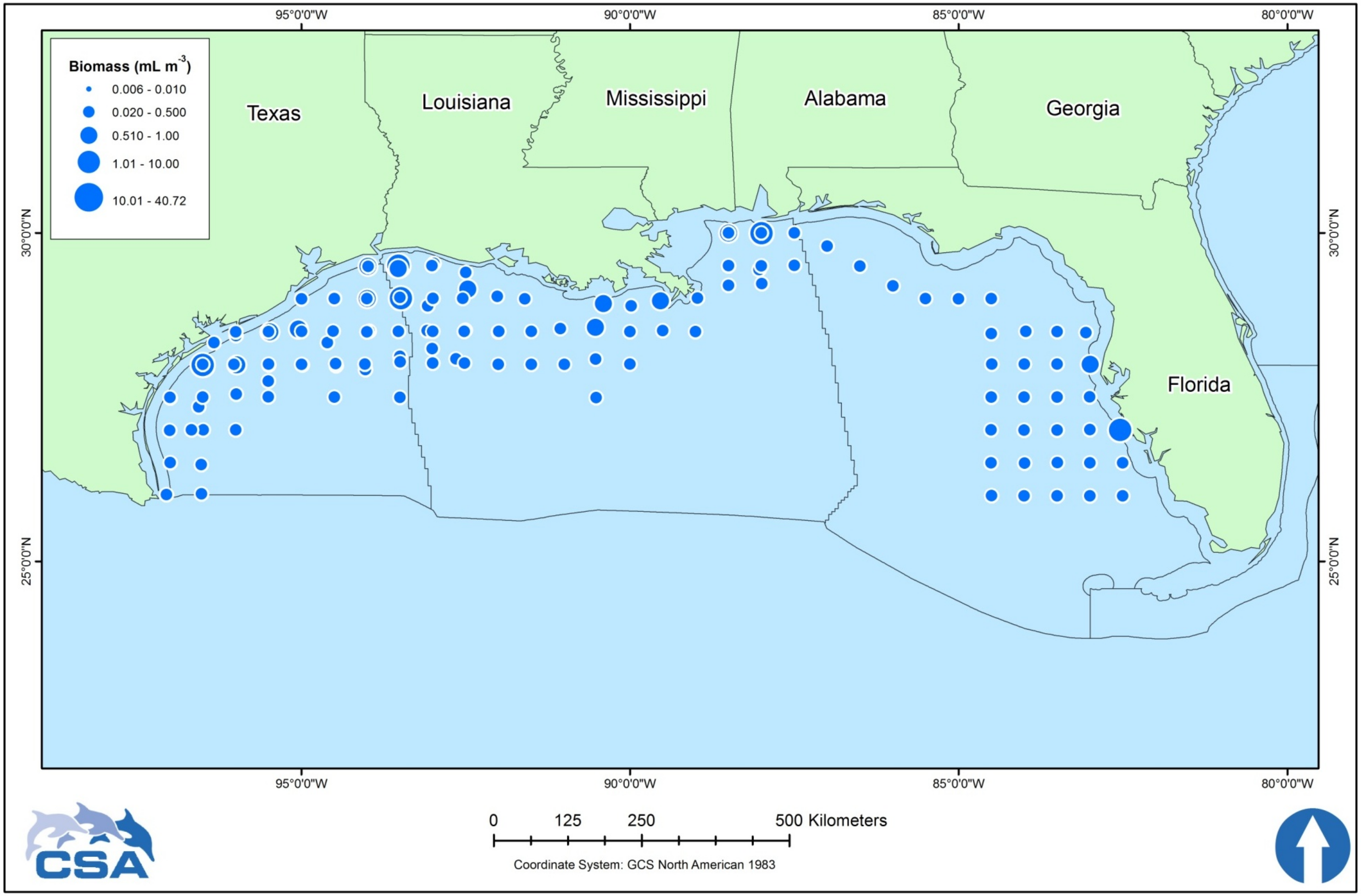

Figure C-25. Gulf of Mexico Outer Continental Shelf Region average zooplankton biomass, Fall 2002.

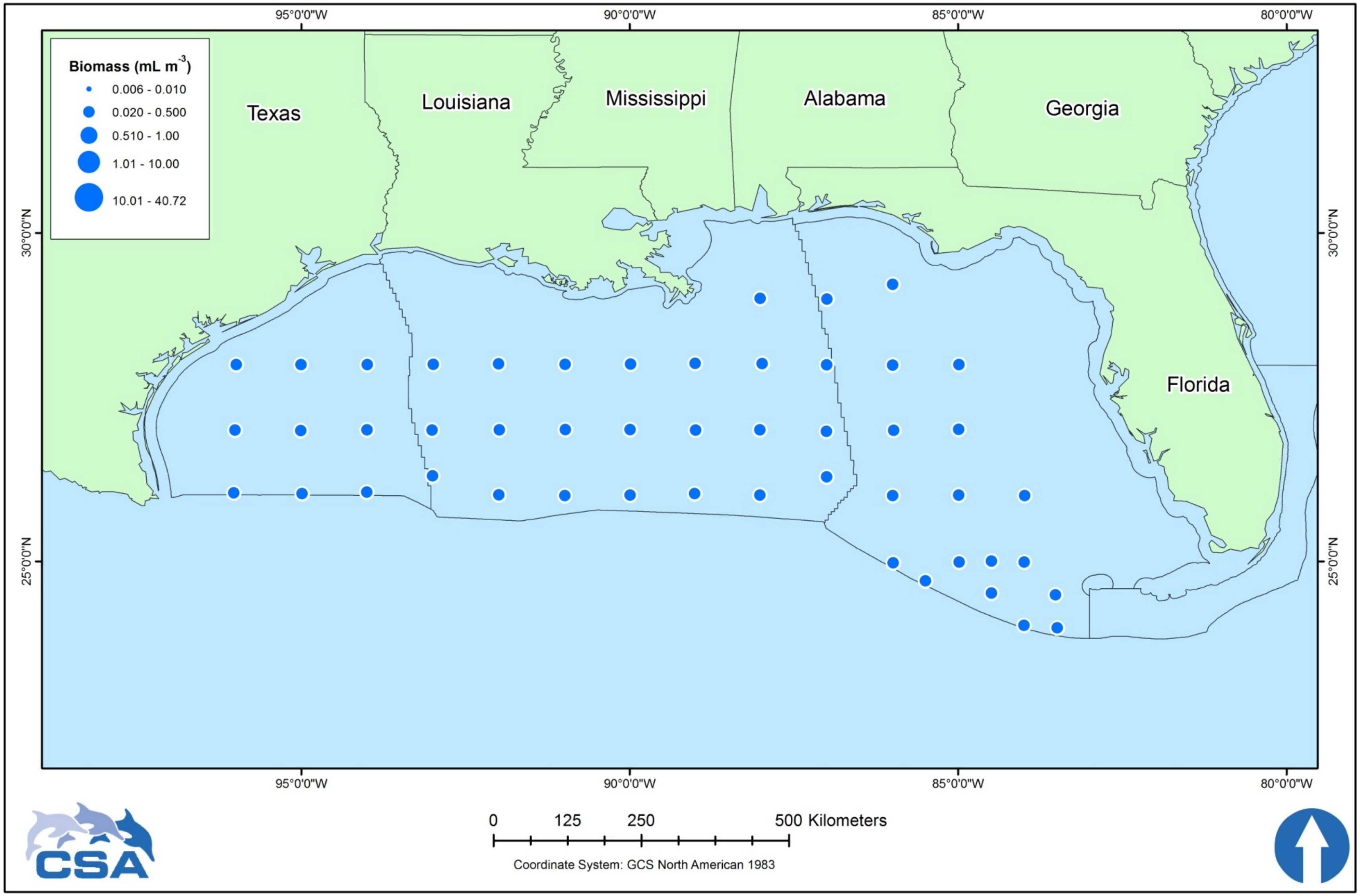

Figure C-26. Gulf of Mexico Outer Continental Shelf Region annual average zooplankton biomass, 2003.

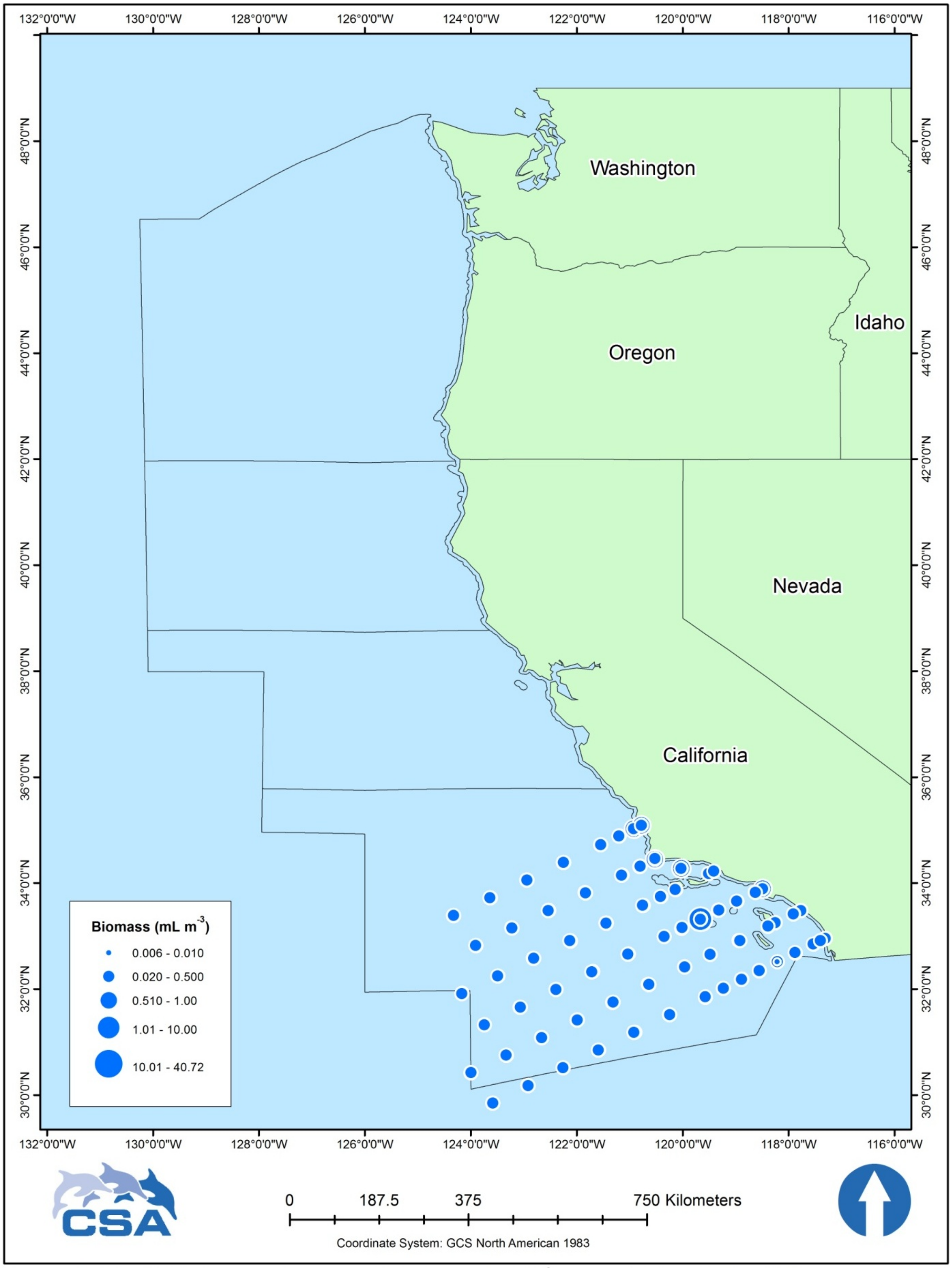

Figure C-27. Pacific Outer Continental Shelf Region annual average zooplankton biomass, 2000.

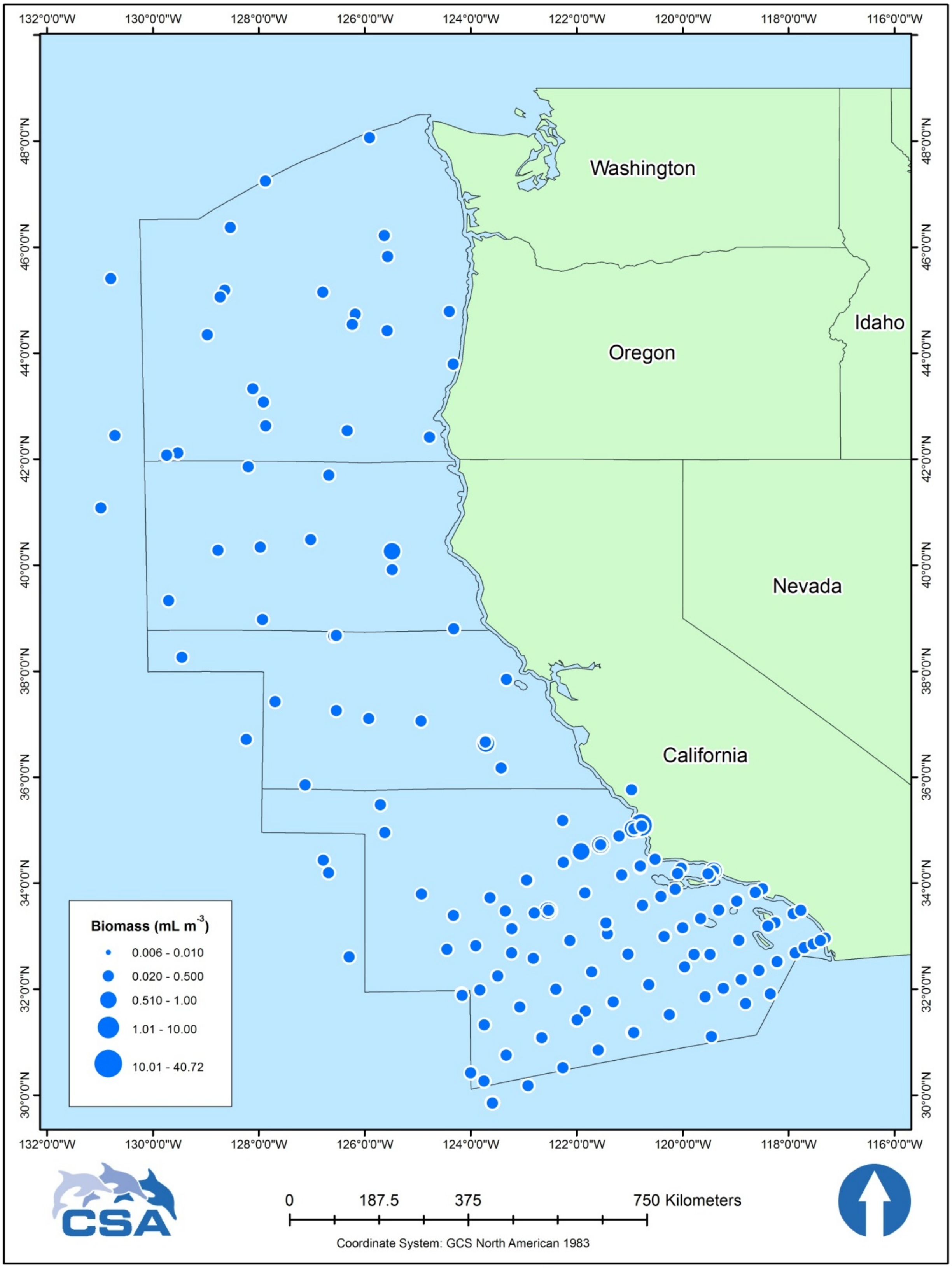

Figure C-28. Pacific Outer Continental Shelf Region annual average zooplankton biomass, 2001.

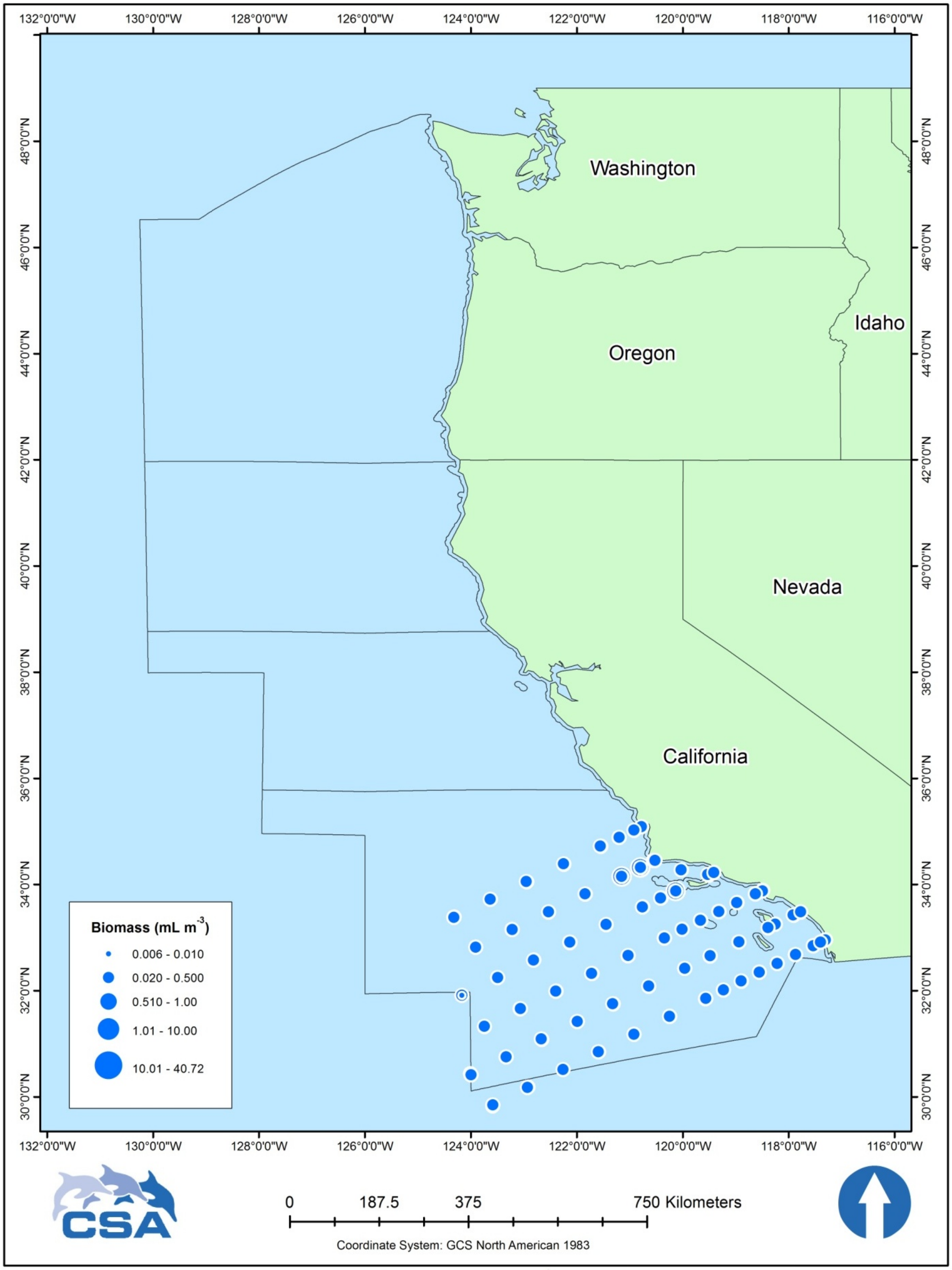

Figure C-29. Pacific Outer Continental Shelf Region annual average zooplankton biomass, 2002.

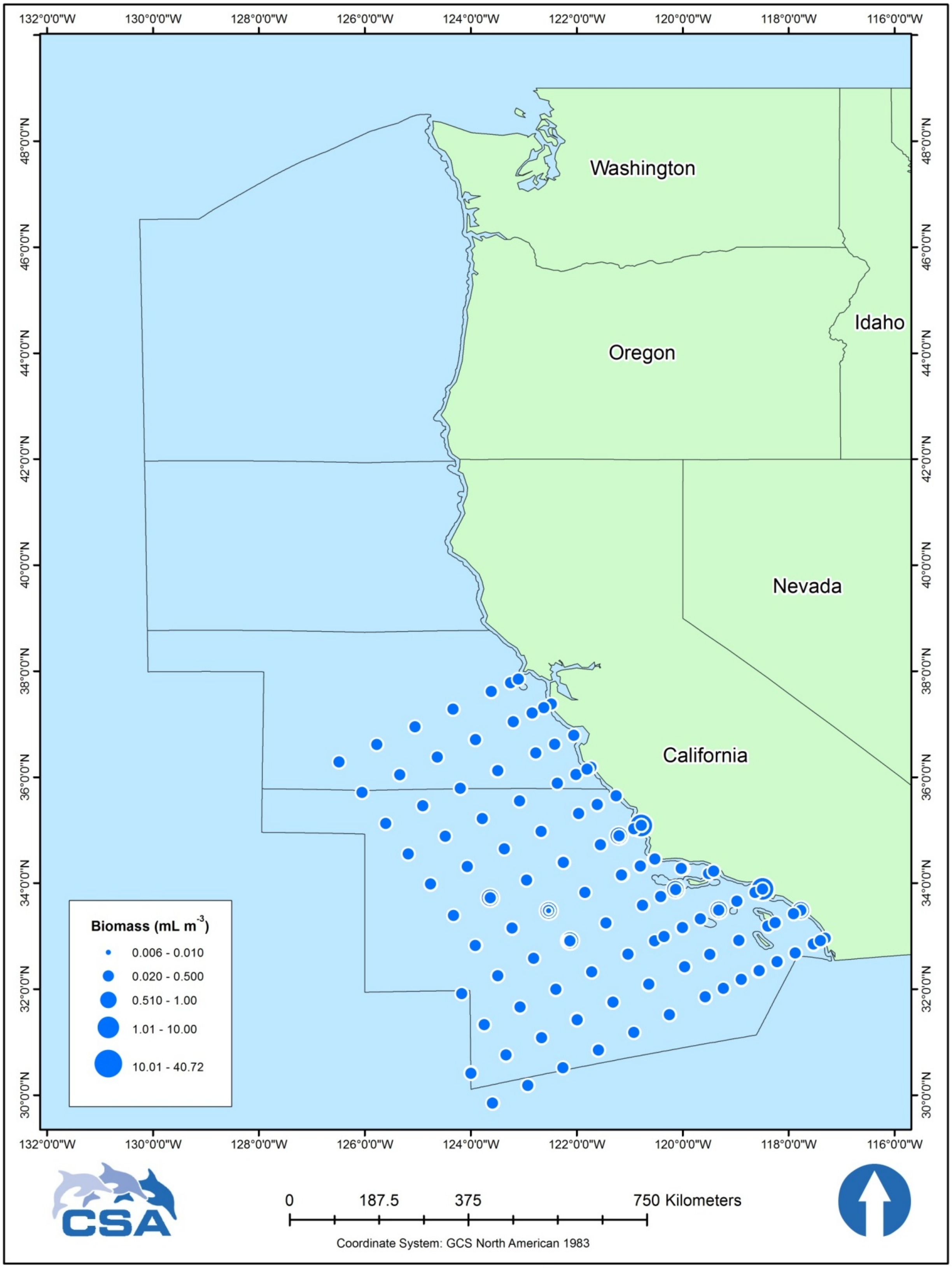

Figure C-30. Pacific Outer Continental Shelf Region annual average zooplankton biomass, 2003.

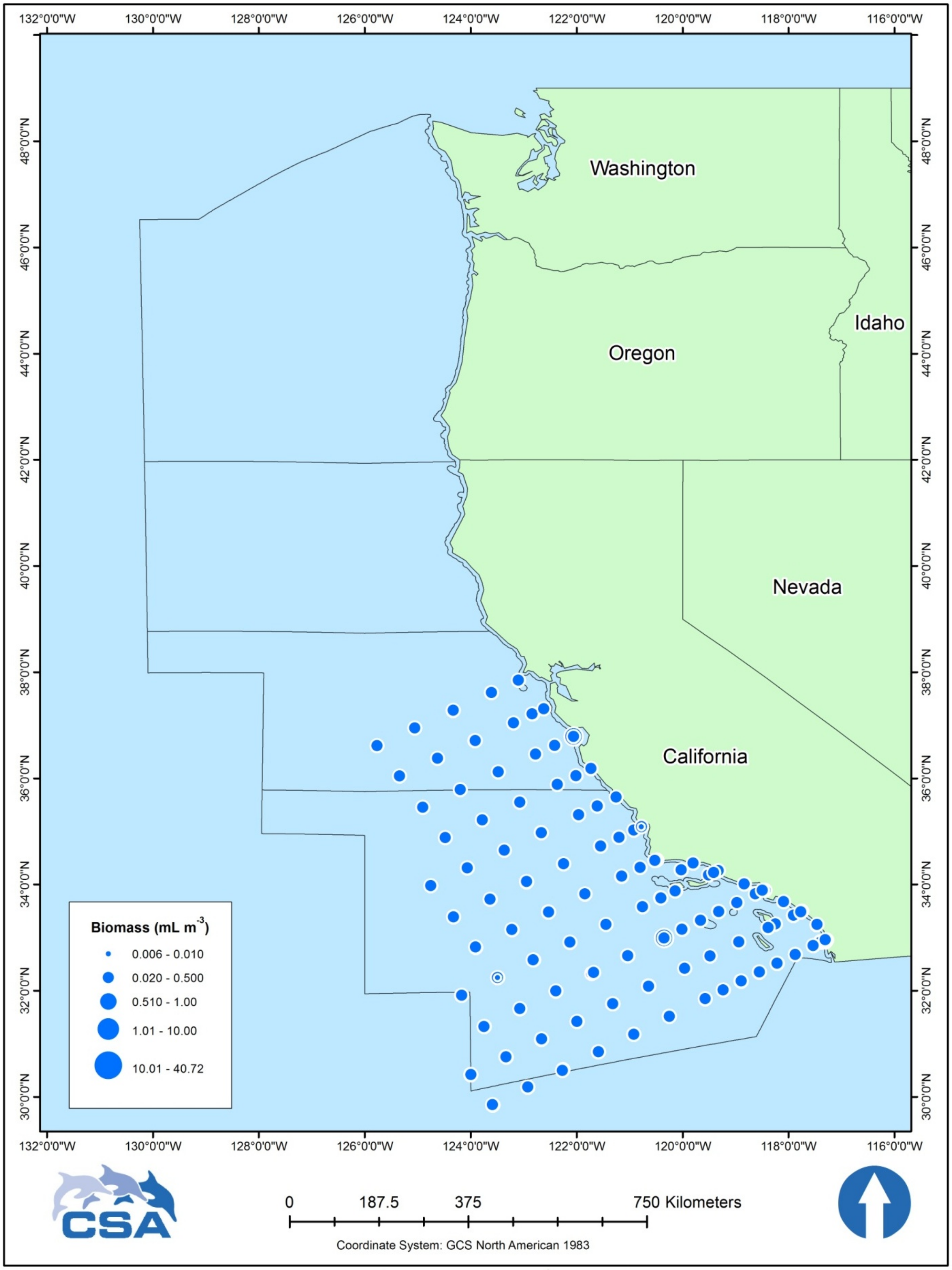

Figure C-31. Pacific Outer Continental Shelf Region annual average zooplankton biomass, 2004.

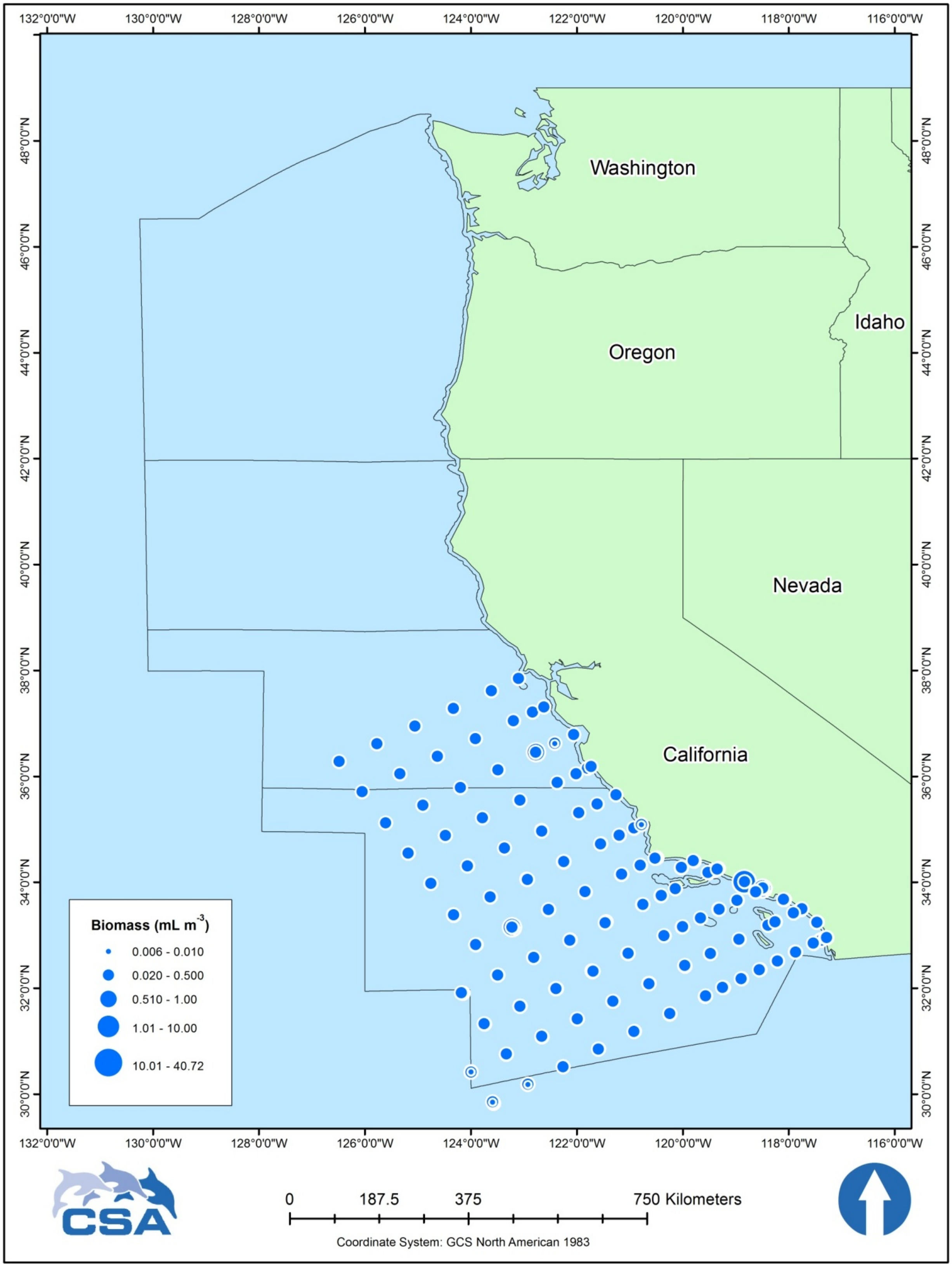

Figure C-32. Pacific Outer Continental Shelf Region annual average zooplankton biomass, 2005.

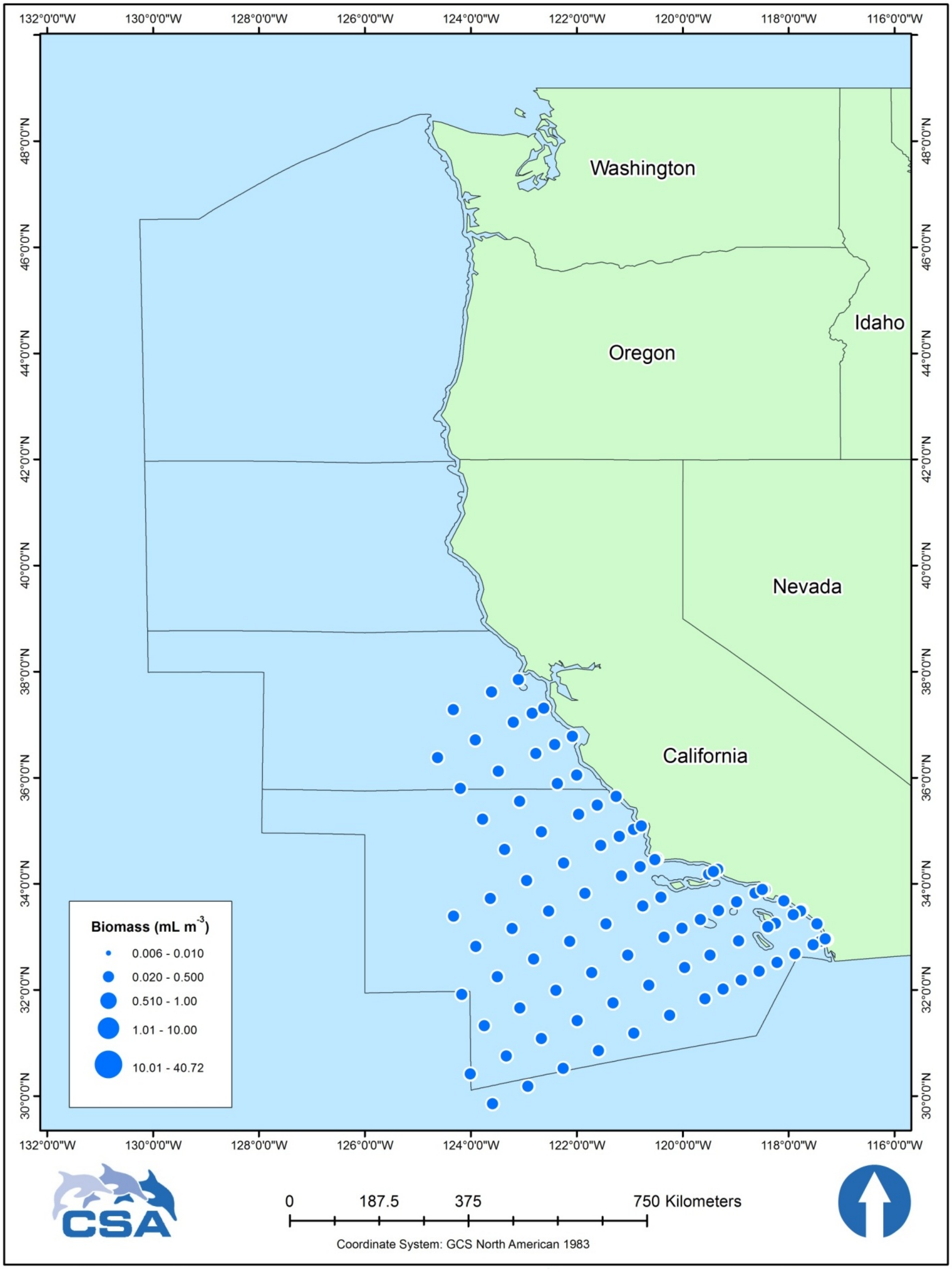

Figure C-33. Pacific Outer Continental Shelf Region average zooplankton biomass, Winter 2006.

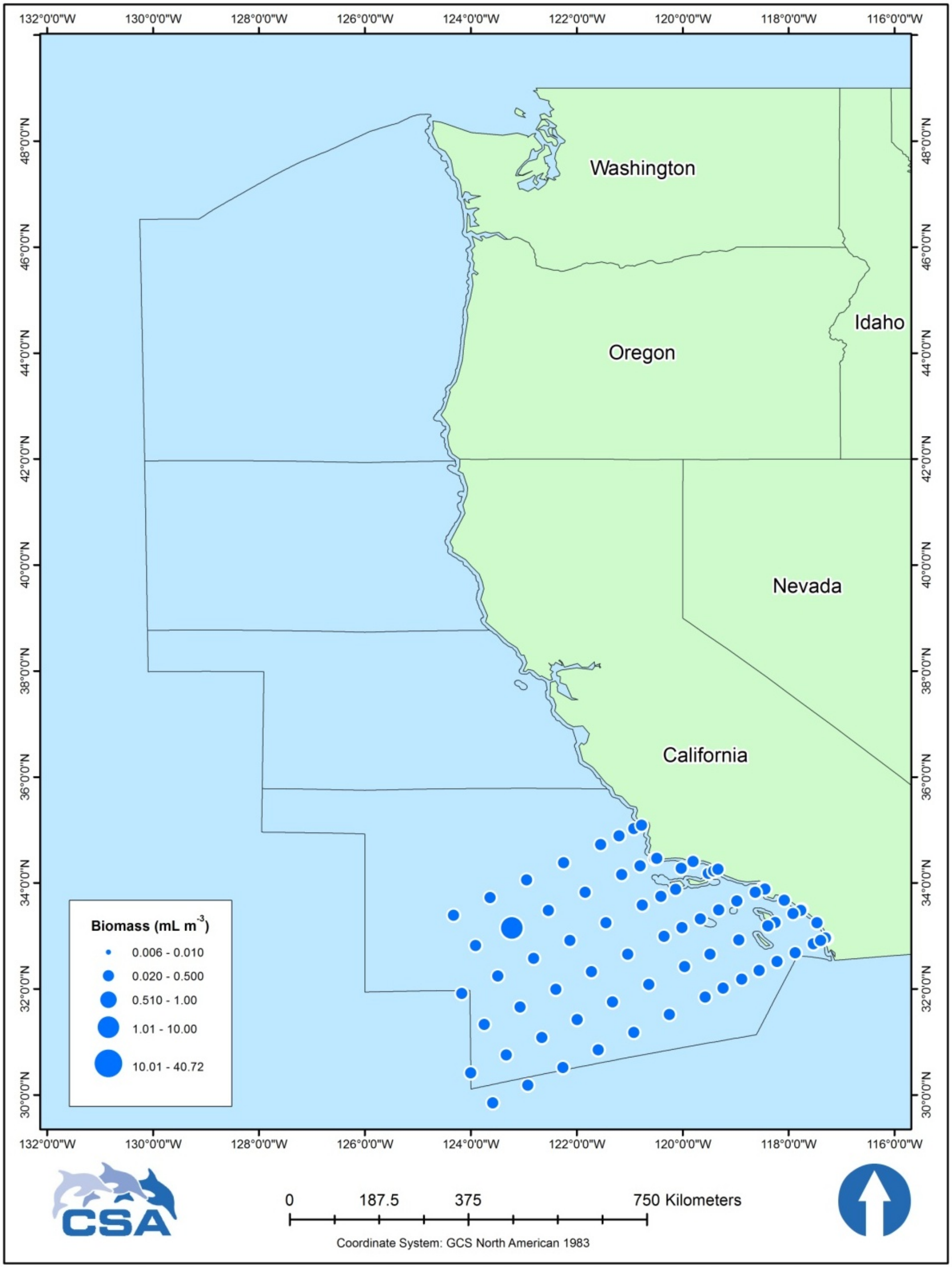

Figure C-34. Pacific Outer Continental Shelf Region average zooplankton biomass, Summer 2006.

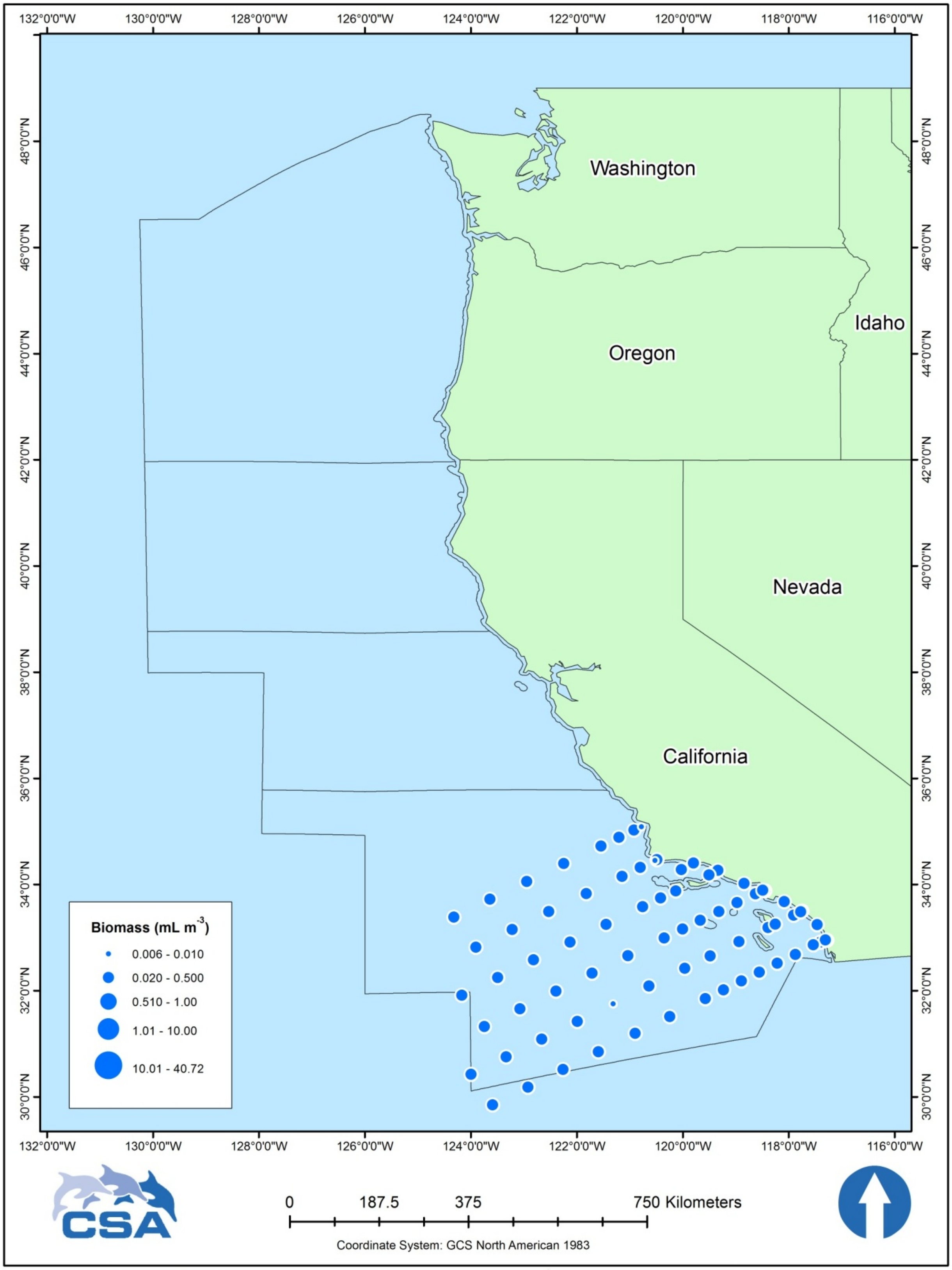

Figure C-35. Pacific Outer Continental Shelf Region average zooplankton biomass, Fall 2006.

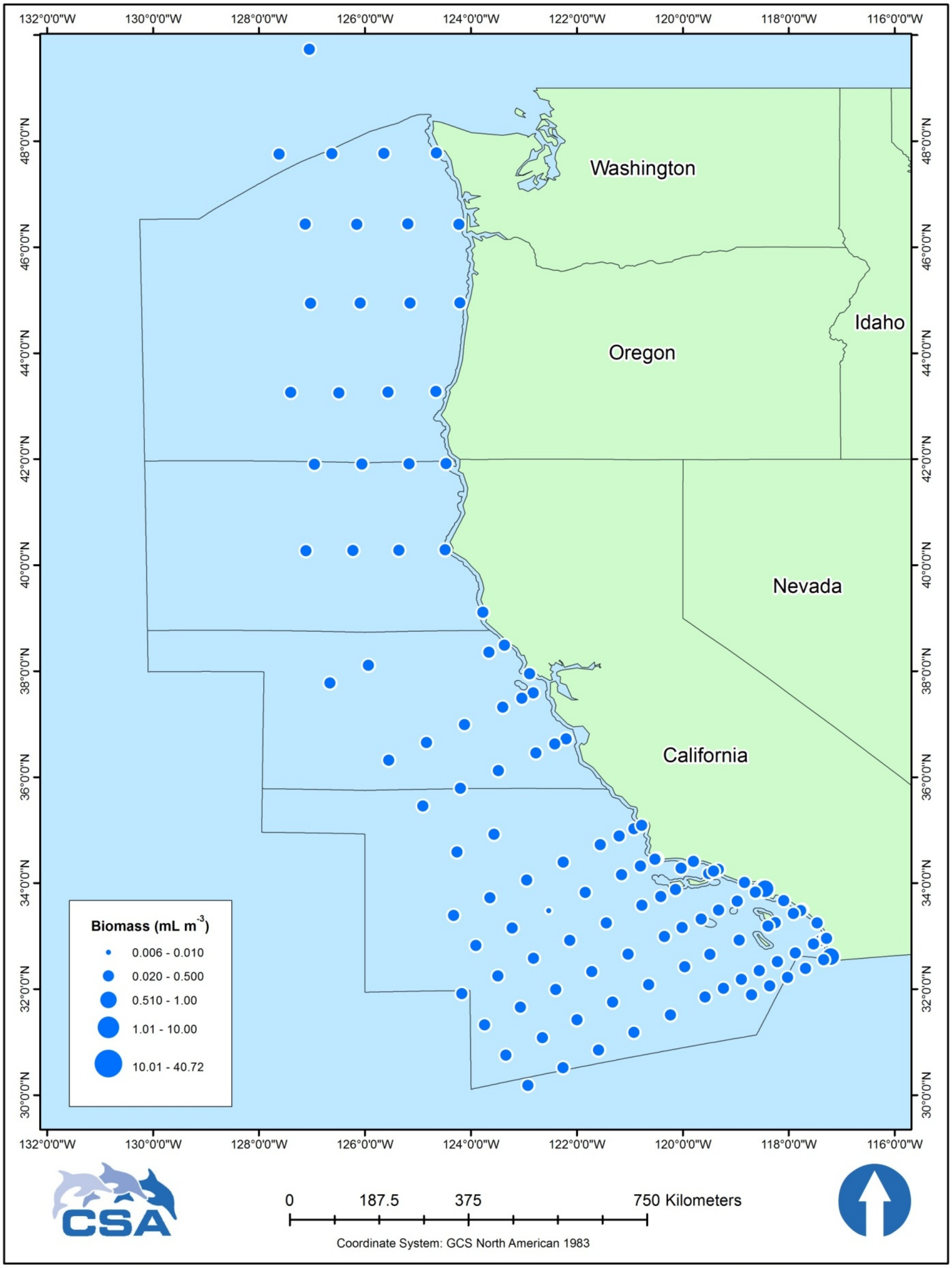

Figure C-36. Pacific Outer Continental Shelf Region average zooplankton biomass, Spring 2006.

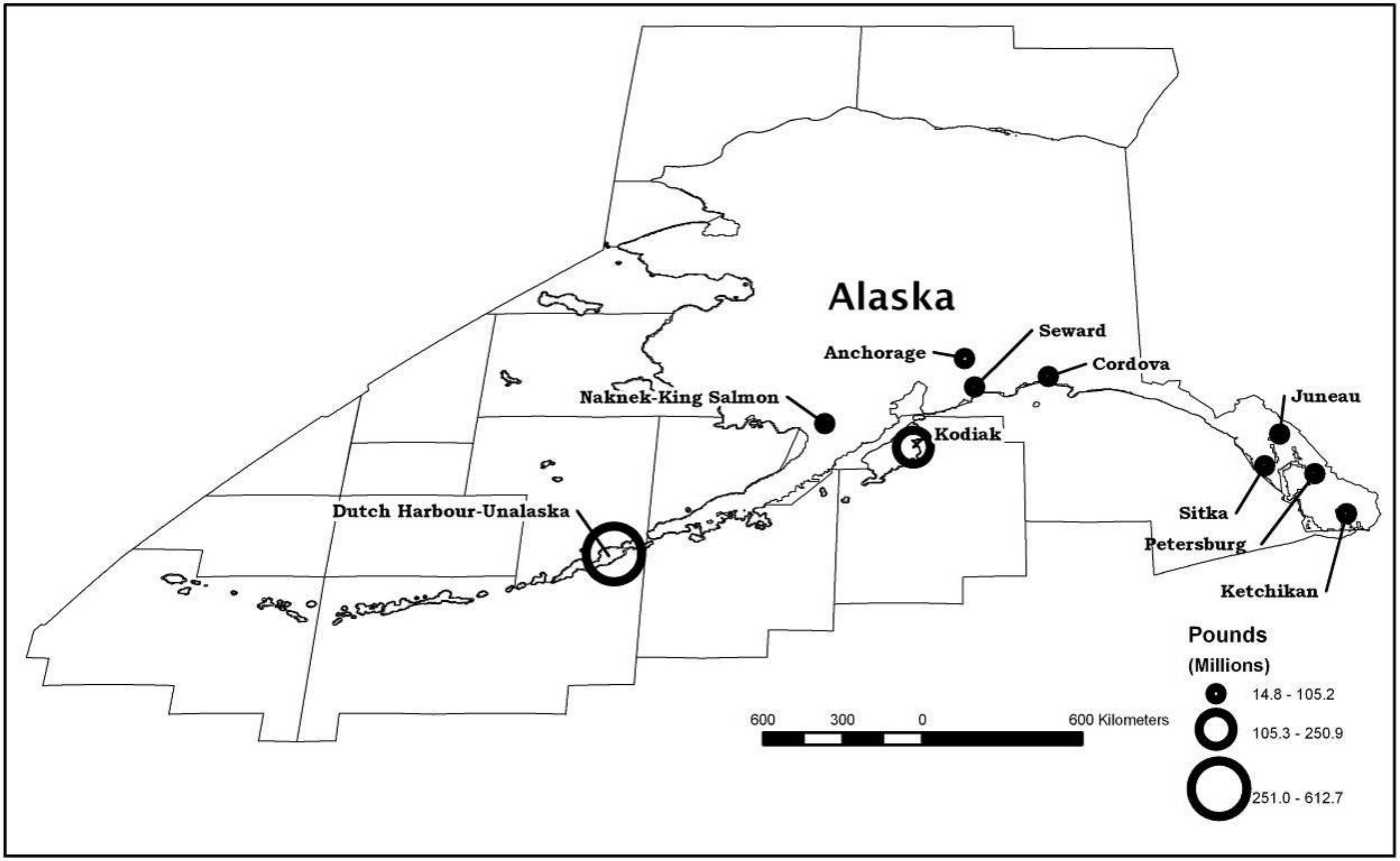

Figure C-37. Alaska Outer Continental Shelf Region fish landings by port (millions of pounds), 2008.

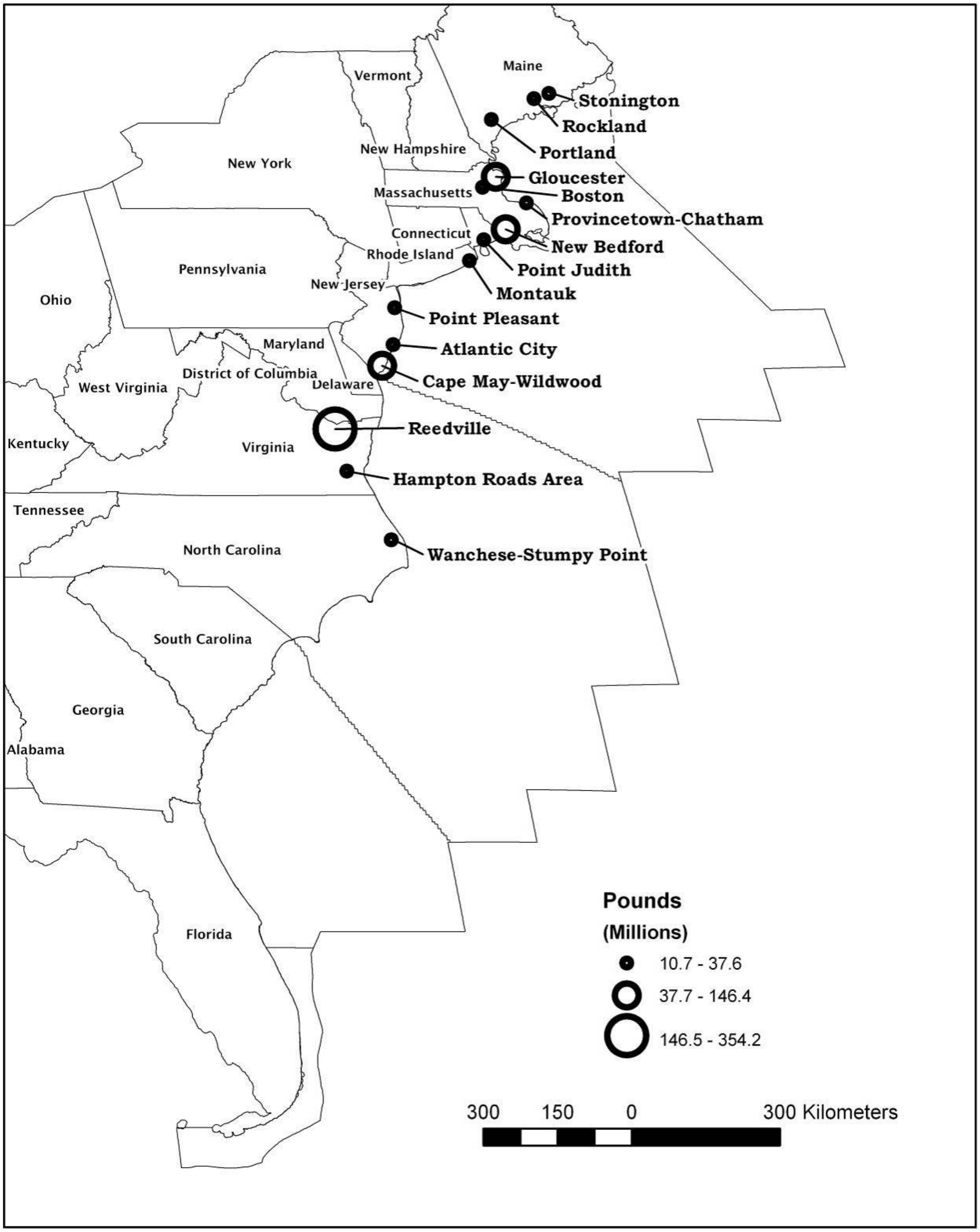

Figure C-38. Atlantic Outer Continental Shelf Region fish landings by port (millions of pounds), 2008.

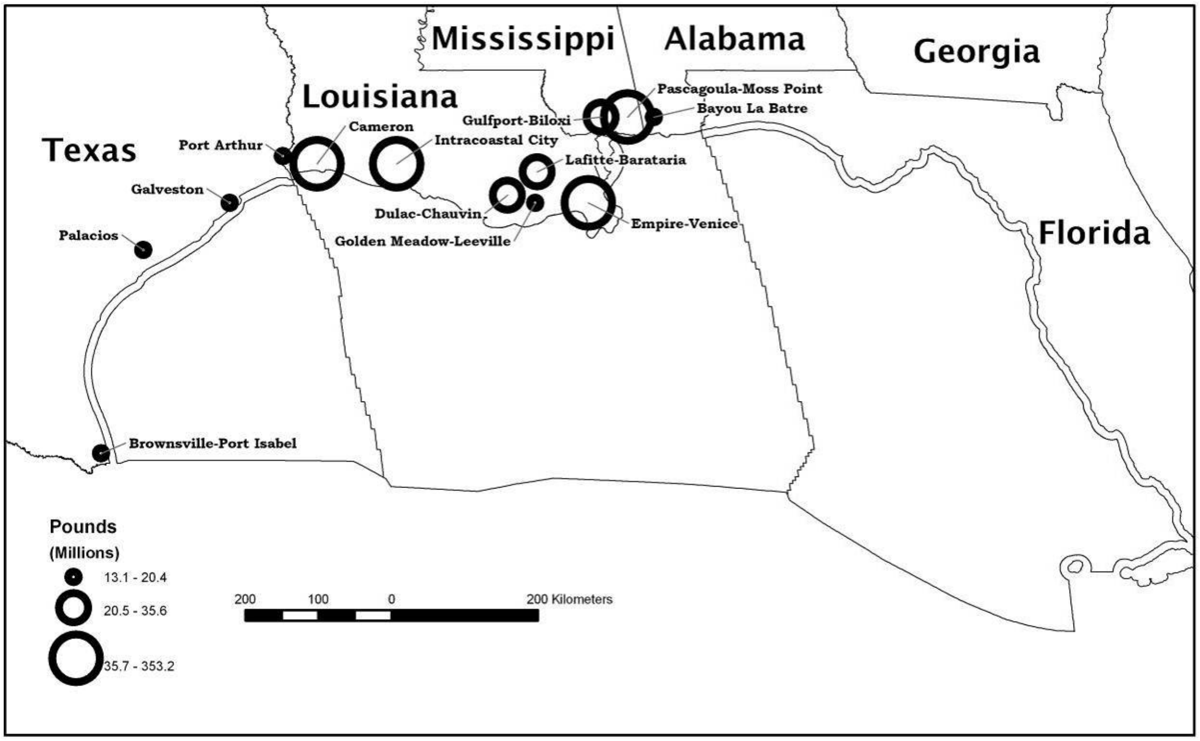

Figure C-39. Gulf of Mexico Outer Continental Shelf Region fish landings by port (millions of pounds), 2008.

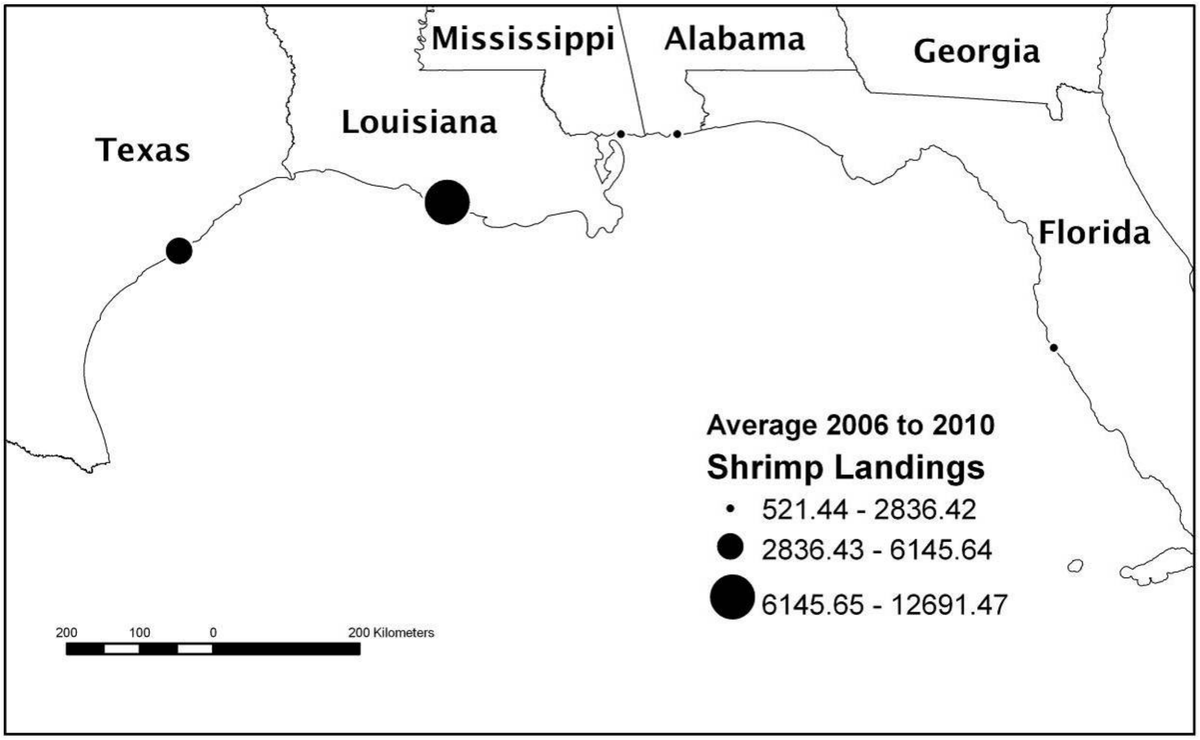

Figure C-40. Gulf of Mexico Outer Continental Shelf Region shrimp landings by state (thousands of pounds) averaged over 2006-2010 seasons.

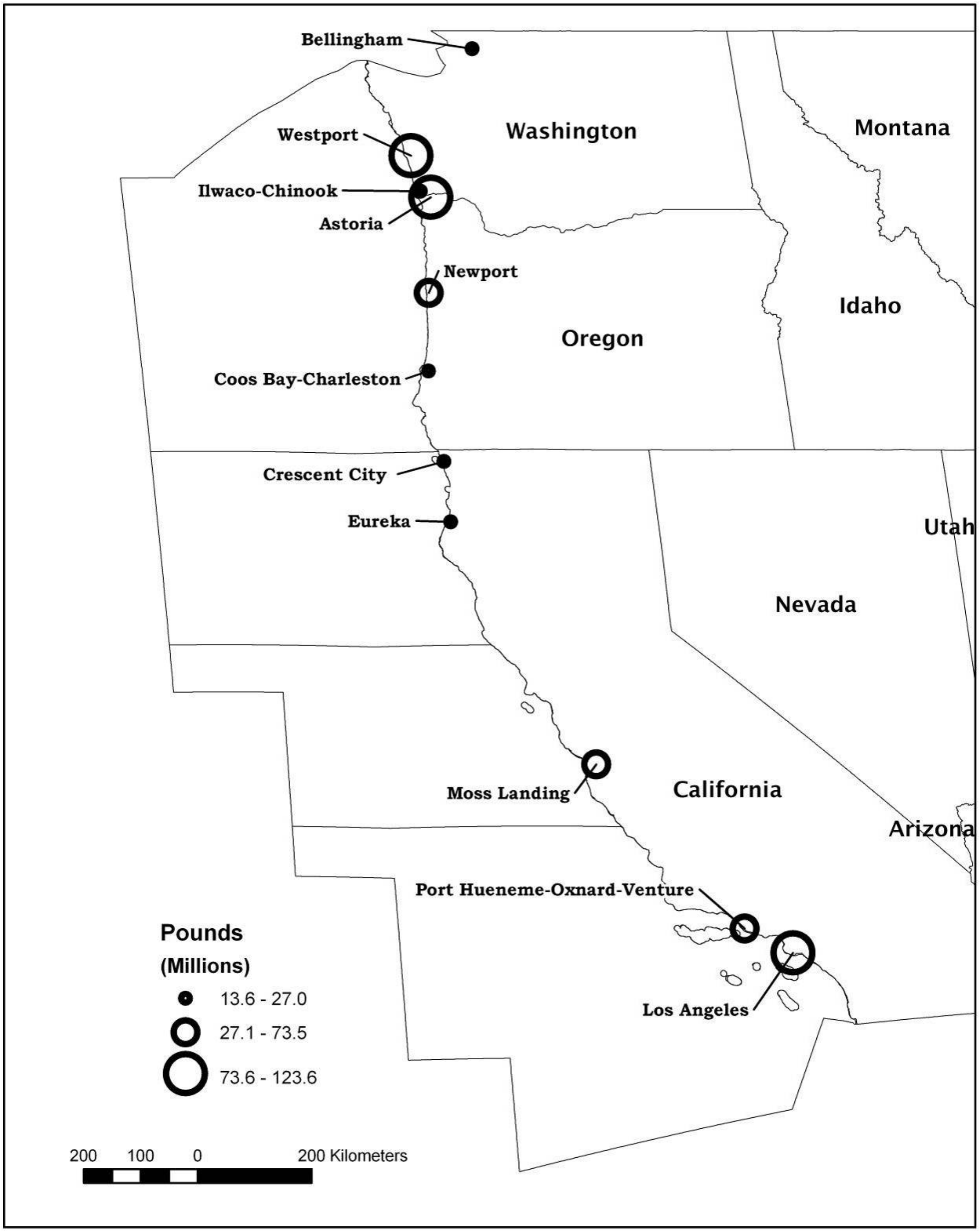

Figure C-41. Pacific Outer Continental Shelf Region fish landings (millions of pounds), 2008.

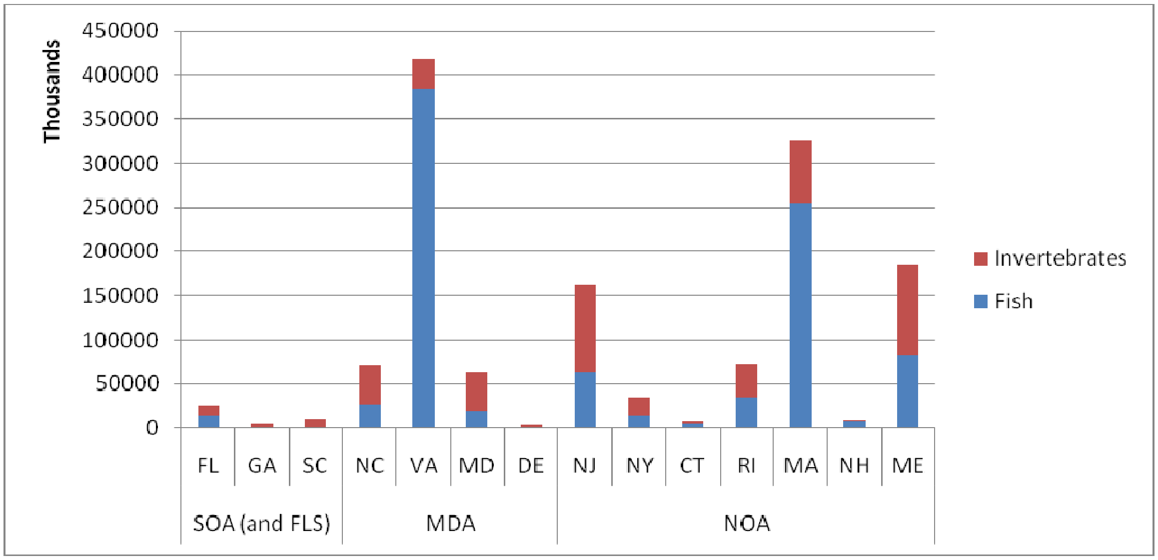

Figure C-42. Commercial fisheries landings (thousands of pounds) by state in the Atlantic Outer Continental Shelf Region planning areas, 2008. NOA = North Atlantic; MDA = Mid-Atlantic; SOA = South Atlantic; FLS = Straits of Florida.

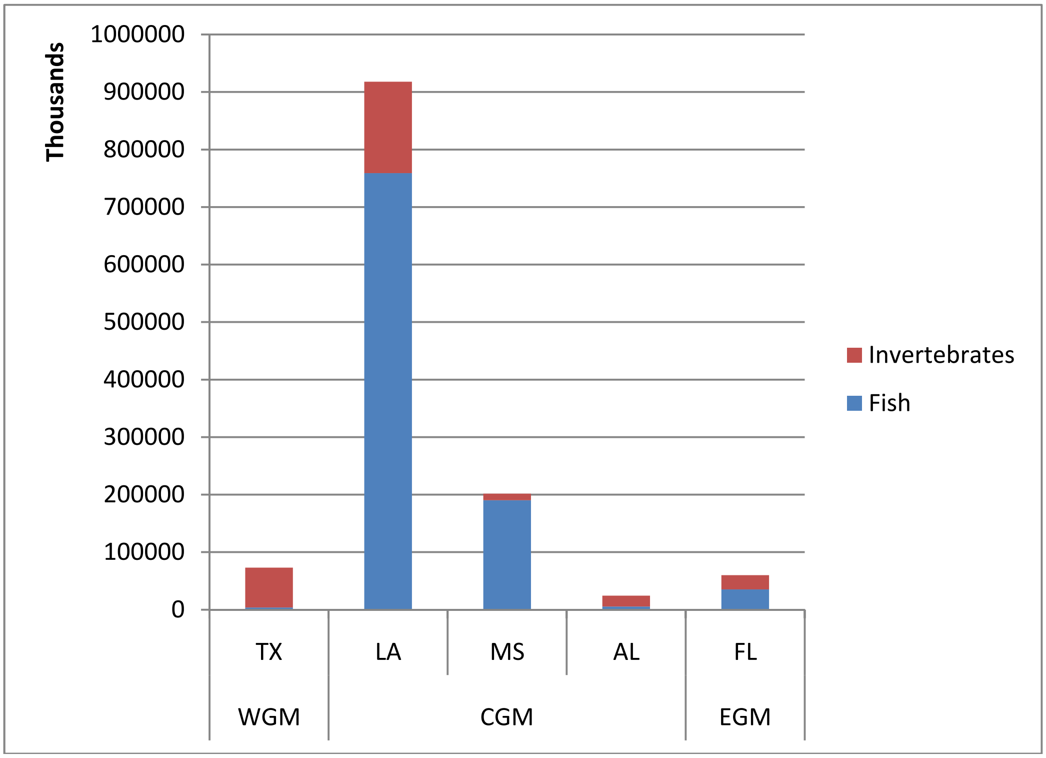

Figure C-43. Commercial fisheries landings (thousands of pounds) by state in the Gulf of Mexico Outer Continental Shelf Region planning areas, 2008. WGM = Western Gulf of Mexico; CGM = Central Gulf of Mexico; EGM = Eastern Gulf of Mexico.

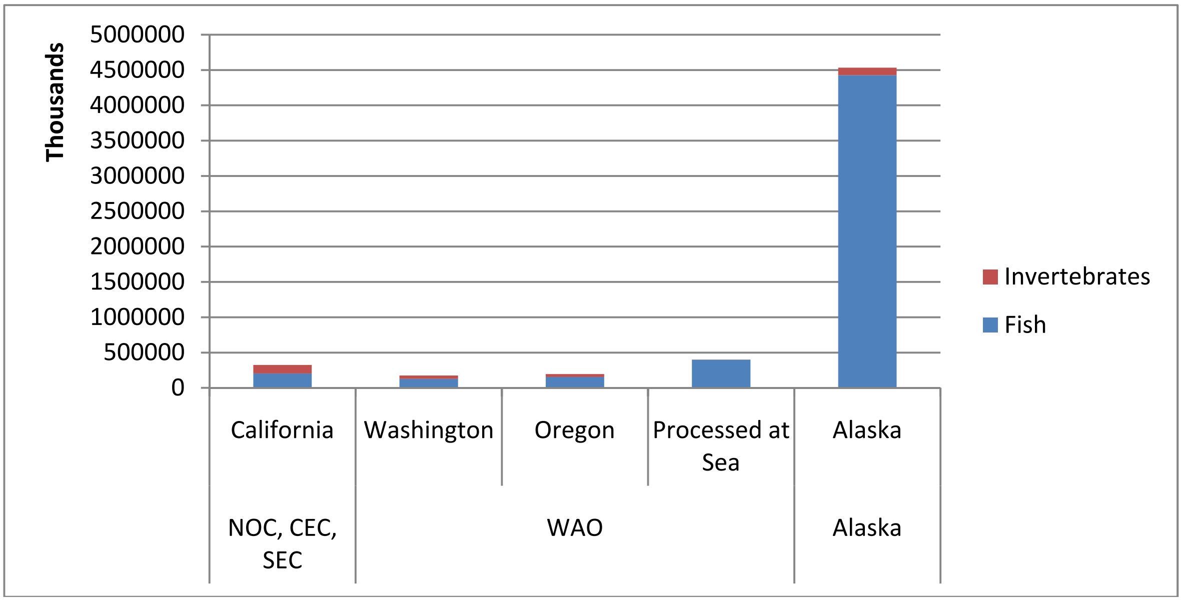

Figure C-44. Commercial landings (thousands of pounds) by state in the Pacific and Alaska region, by planning area, 2008. WAO = Washington-Oregon; NOC = Northern California; CEC = Central California; SOC = Southern California. Alaska landings are composite values (no planning areas differentiated).

Appendix D
Analysis of Outer Continental Shelf Activities

Appendix D Contents

Page

Characterization of Outer Continental Shelf Oil and Gas Activities and Associated Impacts Pertinent to Plankton Communities

The approach used in the analysis of Outer Continental Shelf (OCS) activities and their potential effects on primary productivity is from an impact assessment perspective – i.e., describing the phases of OCS activity, identifying impact producing factors for each phase, and narrowing the analysis to those factors which may affect plankton or the environment in which they live (i.e., water quality). Three phases of OCS oil and gas activity are noted:

- **Prospecting** – activities to locate hydrocarbons and/or evaluate hydrocarbon potential by methods other than drilling. Prospecting includes seismic surveys, geological and geochemical sampling, electromagnetic surveys, and remote sensing.

- **Exploration** – the process of drilling one or more exploratory wells in a block to determine whether commercially exploitable hydrocarbons are present.

- **Development and Production** – the process of exploiting commercial quantities of hydrocarbons. Key activities include drilling of development wells, installation of production facilities, installation of export facilities such as pipelines, routine operation of these systems, and eventual decommissioning.

For each of these phases, the activities and impacts associated with each phase are described.

D.1 Prospecting

D.1.1 Description of Activities

Prospecting for hydrocarbon resources in the marine environment encompasses a variety of techniques, including seismic surveys, geological and geochemical sampling, electromagnetic surveys, and remote sensing surveys (Continental Shelf Associates, Inc. 2004). In general, seismic surveys are the activities of most interest with respect to environmental impacts. The other techniques typically have little or no environmental impact. **Table D-1** summarizes the characteristics of potential prospecting survey activities that may occur. Several of these methods may also be used during other phases of offshore oil and gas activity (e.g., during exploration and/or development and production).

Table D-1. Characteristics of prospecting activities (Adapted from: Continental Shelf Associates, Inc. 2004).

Activity	Purpose	Description	Survey Platform and Sound Source	Type and Location of Activities
Seismic Surveys				
2D streamer surveys	Delineate oil and gas reservoirs	Receivers on streamer cables	Vessel; single array of airguns	Streamers passing through water column
3D streamer surveys	Delineate/monitor oil and gas reservoirs	Receivers on streamer cables	Vessel; dual array of airguns	Streamers passing through water column

Table D-1. (Continued).

Activity	Purpose	Description	Survey Platform and Sound Source	Type and Location of Activities
High-resolution site surveys	Locate shallow hazards, archaeological resources, sensitive benthic habitats	Receivers on streamer cables	Vessel; single or multiple airguns	Streamers passing through water column
Ocean bottom cable surveys	Delineate/monitor oil and gas reservoirs	Receivers on cables deployed on seafloor	Multiple vessels; dual array of airguns	Cables placed temporarily on seafloor
Vertical cable surveys	Delineate/monitor oil and gas reservoirs	Receivers on vertical cables anchored to seafloor	Two vessels; dual array of airguns	Vertical cables anchored temporarily on seafloor
Vertical seismic profile	Correlate geological data to seismic data	Receivers on vertical cables lowered into borehole	Suspended (e.g., by crane) from drilling rig or workboat; single or multiple airguns	Receivers inserted into borehole
Geological and Geochemical Sampling				
Bottom sampling	Obtain physical and chemical data on surficial sediments	Samples collected with a gravity or piston corer, grab, or dredge	Vessel; none	Removal of a sediment sample
Shallow coring	Obtain physical and chemical data on surficial sediments	Conventional rotary drilling from a boat or barge	Vessel; none	Removal of a sediment sample
Electromagnetic Surveys				
Magneto-telluric surveys	Delineate potential oil and gas reservoirs	Receivers placed on seafloor to detect natural electrical and magnetic fields	Vessel; none	Receivers placed temporarily on seafloor
Bi-pole surveys	Delineate potential oil and gas reservoirs	Receivers detect electrical signals sent into seafloor	Vessel; none	Receivers placed temporarily on seafloor
Remote Sensing				
Radar imaging	Delineate potential oil and gas reservoirs	Radar detects oil slicks indicating possible seep locations	Satellite; none	Remote sensing
Aeromagnetic surveys	Delineate potential oil and gas reservoirs	Magnetometer measures earth's magnetic field and/or its vertical gradient	Aircraft (fixed wing); none	Remote sensing
Gravity surveys	Delineate potential oil and gas reservoirs	Gravity meter measures earth's gravitational field	Vessel (or rarely, helicopter); none	Meter placed in water column
Gravity gradiometry	Delineate potential oil and gas reservoirs	Instrument measures earth's gravity gradient	Vessel; none	Instrument placed in water column
Marine magnetic surveys	Delineate potential oil and gas reservoirs	Magnetometer measures earth's magnetic field and/or its vertical gradient	Vessel; none	Meter placed in water column

D.1.2 Impact Factors

The following prospecting activities are expected to produce negligible or minor environmental impacts, as determined by Continental Shelf Associates, Inc. (2004):

- **Geological and geochemical sampling** – Bottom sampling and shallow coring could affect a small area of seafloor, resulting in surficial sediment disturbance, resuspension, and creation of minor surficial features (e.g., gouges, holes, depressions, etc.). The total seafloor area disturbed during these activities is generally a few square meters and the impact is similar to collecting sediment samples for scientific research. Impacts on sediments/geology and benthic communities are considered to be negligible.

- **Electromagnetic surveys** – In addition to small amounts of ship traffic (with associated discharges and emissions), these surveys involve only minor disturbance to the seafloor (temporary placement of receiver boxes on the bottom). Impacts on sediments/geology and benthic communities are considered to be negligible.

- **Remote sensing surveys** – These involve only a small amount of vessel and/or aircraft traffic (with associated discharges and emissions) and have little or no impact on any resource.

Therefore, seismic surveys are the only prospecting activity that should be analyzed in detail. Five impact factors (i.e., causes or sources) were identified: 1) airgun noise; 2) vessel traffic and towed streamers; 3) effluent discharges; 4) air pollutant emissions; and 5) seafloor disturbance. Of these impact factors, only effluent discharges have the potential to affect water quality. No impacts to plankton are expected from seismic survey operations. Relevant resources that may be affected by each impact factor are identified in **Table D-2**.

Table D-2. Impact factors associated with seismic surveys which potentially affect plankton and water quality resources.

Resource	Airgun Noise	Vessel Traffic and Towed Streamers	Effluent Discharges	Air Pollutant Emissions	Seafloor Disturbance
Water quality	---	---	o	---	---
Plankton	---	---	---	---	---

X = potentially significant impact with mitigation recommended; o = minor or negligible impact, no additional mitigation recommended; -- = no impact.

D.1.3 Impact Analysis

Effects of Effluent Discharges

Effluent discharges from survey vessels include treated sanitary waste, domestic waste, deck drainage, and bilge and ballast water. Impacts from seismic survey vessels are similar to those of effluent discharges from other ships in the region. For example, effluents may affect concentrations of suspended solids, nutrients, and chlorine, as well as generating biochemical oxygen demand (BOD). These discharges are expected to be diluted rapidly in the open ocean. Impacts are likely to be undetectable beyond tens of meters from the source and are considered to be negligible.

D.2 Exploration

D.2.1 Description of Activities

During oil and gas exploration, one or more exploratory wells are drilled in a block to determine whether commercially exploitable hydrocarbons are present. An operator may also conduct additional seismic surveys and/or other prospecting surveys to help select drilling locations and identify geohazards.

Drilling an exploratory well in the deepwater environment typically takes 70-90 d (Regg et al. 2000). However, the duration may range from 40-120 d, depending on the target well depth and any problems encountered during drilling. Typically, a self-contained, mobile drilling rig is brought into an area to drill a well. Based on the history of exploratory drilling in U.S. waters and the general trend of operators moving into deeper water, the most likely type of drilling rigs currently in use are semi-submersibles or drillships. Each well is drilled to a predetermined depth and either temporarily suspended or abandoned in accordance with industry standards. During drilling, the rig discharges drilling fluids and cuttings and other effluents in accordance with effluent limits established by OCS (and U.S. Environmental Protection Agency [USEPA]) region under the National Pollutant Discharge Elimination System (NPDES) permit.

If a hydrocarbon formation is discovered during exploratory drilling, a well test may be conducted. A well test is a procedure to determine the productive capacity, pressure, permeability, and/or extent of a hydrocarbon reservoir, and it may involve burning a small quantity of oil or gas. If a well is deemed productive, it may be suspended by installing cement or mechanical plugs to isolate the hydrocarbon intervals and fitting a well suspension cap to allow reentry of the well at a later date (for completion and production).

If no commercially exploitable reservoir is found during exploratory drilling, a well is permanently plugged with cement or mechanical plugs and abandoned. Typically, a site clearance survey is conducted to ensure that any debris from drilling activities is removed from the seafloor around each drillsite.

Types of Drilling Units

Several types of mobile offshore drilling units are used for exploratory drilling, including jack-up rigs, semi-submersibles, and drillships (**Figure D-1**). Because conventional jack-up rigs are limited to water depths of 110-120 m or less (Bennett 2008) and the vast majority of recent exploratory drilling activity has occurred in deeper water, they are not expected to be used. The three rig types are characterized as follows (from MMS 2008):

Figure D-1. Examples of mobile offshore drilling units: a) jack-up; b) semi-submersible; and c) drillship. Public domain images from the U.S. Department of Energy (jack-up; courtesy of Blake Offshore LLC; posted at www.apps1.eere.energy.gov), Baud et al. (2002; semi-submersible; courtesy of Diamond Offshore Drilling, Inc.), and NOAA (drillship; courtesy of Transocean; posted at www.noaa.gov).

- **Jack-up** – a mobile bottom-supported offshore drilling structure with columnar or open-truss legs that support the deck and hull. When positioned over the drilling site, the bottoms of the legs rest on the seafloor. A jack-up rig is towed or propelled to a location where the legs are lowered onto the seafloor, pushed into the sediment by the weight of the jack-up, and the hull of the jack-up is raised above the sea surface.

- **Semi-submersible** – a floating vessel that is supported primarily on large pontoon-like structures submerged below the sea surface. Most semi-submersibles are not self-propelled and must be towed to a drillsite by assisting vessels. Operating decks are elevated about 30 m or more above the pontoons on large steel columns. Semi-submersibles can operate in a wide range of water depths, including deep water. Conventionally moored semi-submersibles are held in place by 6-12 anchors placed radially around the rig and extending to distances of 3 km or more. Dynamically positioned semi-submersibles use a computer-controlled system that allows the rig to maintain position using thrusters, thereby avoiding the need for anchoring.

- **Drillship** – a vessel modified to include a drilling rig and special station-keeping equipment. Drillships are self-propelled, are capable of operating in deep water and ultra-deep water, and typically carry larger payloads than semi-submersible rigs. They typically use dynamic positioning rather than conventional moorings. A "moon pool" in the centre of the drillship provides access for a derrick from the deck surface through the centre of the vessel to the water column.

Operators select the type of drilling rig based on the characteristics of the physical environment (including water depth), expected drilling depth, and the mobility required based on expected weather and sea state conditions. Maximum water depth is a function of the length of the rig's riser – the bundled utility tubes through which drilling fluids and other material are conducted, enclosed in an outer tube, suspended from the semi-submersible to the seafloor. Semi-submersibles can usually operate in rougher seas than a drillship (Canadian Association of Petroleum Producers [CAPP] 2006).

While there are differences between jack-up rigs, semi-submersibles, and drillships with respect to capabilities, treatment facilities, and effluent discharge depths, the characteristic volumes, and types of wastes streams generated during drilling operations are similar. Also, all offshore drilling rigs, regardless of type, contain well drilling equipment, working and living quarters, crew and supply transfer capabilities (e.g., moorings/landing platforms for supply vessels, helidecks for helicopter landing and departure), and fire and rescue equipment.

Drilling Discharges

From an impact perspective, one of the key activities during exploratory drilling is the discharge of drilling fluids and cuttings. These discharges occur in accordance with the effluent limits summarized in **Table D-3**.

Cuttings are rock fragments that are displaced as the drill bit moves through geological formations. They are discharged more or less continuously during drilling.

Drilling fluids (also known as drilling muds) are special fluids that are pumped down into the well through nozzles on the drill bit. They are a complex mixture of clays, chemical additives, freshwater, and/or seawater that are used to lubricate and cool the drill bit, flush out cuttings, control formation pressures, seal permeable formations, and maintain well bore stability. Drilling fluids also help to minimize damage to reservoirs, prevent the formation of gas hydrates, assist in the transition of hydraulic energy to drill tools, assist in formation evaluation via logging equipment, control corrosion, and facilitate casing cementing (CAPP 2005). Drilling fluids are composed of several main ingredients (primarily water, barite, and clay minerals) and numerous special purpose additives (National Research Council 1983; Neff 1987).

Table D-3. Summary of U.S. OCS discharge requirements for drilling wastes.

Baseline Requirements

- No discharge of free oil (using a static sheen test) or diesel oil
- Acute toxicity must have a 96-h LC50 >30,000 ppm (using USEPA's mysid shrimp toxicity text)
- Metals concentrations in the barite added to mud must not exceed:
    - 1 mg/kg for mercury
    - 3 mg/kg for cadmium
- No discharge of drilling wastes allowed within 3 miles of shore (except for Alaskan facilities in the offshore subcategory)

Additional Requirements for Synthetic-Based Muds (SBMs)

- SBMs themselves may not be discharged
- Cuttings coated with up to 6.9% SBMs may be discharged
    - Ester SBMs can have up to 9.4% SBM on cuttings
- Polycyclic aromatic hydrocarbon (PAH) content:
    - Ratio of PAH mass to mass of base fluid may not exceed 1 x 10^{-5}
- Biodegradation rate of chosen fluid shall be no slower than that for internal olefin
    - Base fluids are tested using the marine anaerobic closed bottle test
- Base fluid sediment toxicity shall be no more toxic than that for internal olefin base fluid
    - Base fluid stocks are tested by a 10-d acute solid-phase test using amphipods (*Leptocheirus plumulosus*)
    - Discharged cuttings are tested by a 4-d acute solid-phase test using amphipods (*Leptocheirus plumulosus*)
- No discharge of formation oil
    - Whole muds are tested onshore by gas chromatography/mass spectrometry (GC/MS) analysis
    - Discharged cuttings are tested for crude oil contamination by fluorescence method
- Conduct seabed survey or participate in industry-wide seabed survey

There are two major types of drilling fluids: water-based fluids (WBFs) and nonaqueous base fluids (NABFs). WBFs consist of fresh or salt water, barite, clay, caustic soda, lignite, lignosulfonates, and/or water-soluble polymers. NABFs (also known as organic-phase fluids) are emulsions – a base fluid consisting of a liquid hydrocarbon or other water insoluble organic chemical forms the continuous external phase while calcium chloride brine forms the discontinuous internal phase (Neff et al. 2000). In the past, NABFs have contained diesel or conventional mineral oil as the primary component (Group I fluids). However, the industry has moved to NABFs using low-toxicity mineral oil (Group II fluids) and, more recently, enhanced mineral oils and synthetics (Group III fluids), also known as synthetic-based fluids (SBFs). SBF base fluids include linear-α-olefins, poly-α-olefins, internal olefins, linear alkyl benzenes, ethers, esters, or acetals (Neff et al. 2000). According to International Association of Oil & Gas Producers (2007), 90% of the NABF cuttings discharged in 2006 contained SBFs.

Both WBFs and SBFs are used during drilling. SBFs are typically used for drilling, directional drilling and in deep waters where hole stability and integrity are critical. No diesel oil-based fluids are used.

During the initial stage of drilling, a large diameter surface hole is “jetted” a few hundred meters into the seafloor. At this stage, the cuttings and seawater used as drilling fluid are discharged onto the seafloor. Surface casing is subsequently lowered into the hole and cemented in place.

A blowout preventer (BOP) is installed on the top of the surface casing to prevent water or hydrocarbons from escaping into the environment. Once the BOP is fully pressure tested, the next section of the well is drilled.

The marine riser is a pipe with special fittings that establishes a seal between the top of the wellbore and the drilling rig. After it is set, all drilling fluid and cuttings are returned to the drilling rig and passed through a solids control system designed to remove cuttings and silt so that the drilling fluids may be recirculated downhole. The drill cuttings, typically sand or gravel-sized with any residual drilling mud attached, are then discharged via the shale chute. Drilling fluid properties eventually become degraded, and the used fluids are periodically discharged in bulk (WBFs) or returned to the supplier for recycling (SBFs).

During well intervals when WBF systems are used, cuttings and adsorbed WBF solids are discharged to the ocean at a rate of 0.2-2.0 m^3 h^{-1} (Neff 1987, 2005). When SBF systems are used, the percentage of SBF retention on cuttings typically is subject to regulatory limits (Neff et al. 2000). SBF retention limit is dictated by NPDES permit and varies by SBF used (**Table D-3**). MMS (2000) estimates that the average discharge of muds and cuttings for an OCS well is 4,286 bbl (180,000 gal.). As operators have moved into deeper water and drilled deeper wells, the use of SBF has become more prevalent, as has the drilling of the upper portions of a well with WBF and the lower portion of a well with SBF. For wells drilled using WBF, MMS (2007) estimates that 7,000-9,700 bbl of drilling mud and 1,500-2,500 bbl of cuttings are discharged per well. For wells drilled using SBF, MMS (2007) estimates that 565-855 bbl of cuttings are discharged for a development well, while 1,184-1,901 bbl of cuttings are discharged for an exploratory well. Well drilling, from spudding to completion, generally requires 40-70 d depending upon well complexity, water depth, drilling depth, and problems encountered during drilling.

Table D-4 presents a broader picture of the annual and cumulative counts for wells completed and wells plugged and abandoned on the U.S. OCS. Between 1960 and 2006, 17,801 wells were completed and 36,470 wells were plugged and abandoned (BOEMRE 2010).

Table D-4. Oil and gas well drilling on Federal offshore leases, 1960-2006 (From: BOEMRE 2010).

Year	Well Drilling Status			Completed	P&A	Cumulative Total
	Active	Suspended	Other			
1960	58	53	N/A	1,923	686	2,720
1961	54	99	N/A	2,467	814	3,434
1962	56	107	N/A	3,091	1,002	4,256
1963	62	130	N/A	3,631	1,226	5,049
1964	73	193	102	4,313	1,372	6,053
1965	89	261	0	4,733	1,685	6,768
1966	82	0	444	3,305	1,871	5,702
1967	95	0	496	3,762	2,233	6,586
1968	133	0	592	4,258	2,592	7,575
1969	103	129	590	4,752	2,919	8,493
1970	106	115	534	5,359	3,278	9,392
1971	89	152	551	5,718	3,724	10,234
1972	79	263	537	6,032	4,168	11,079
1973	84	249	546	6,421	4,599	11,899

Table D-4. (Continued).

Year	Well Drilling Status			Completed	P&A	Cumulative Total
	Active	Suspended	Other			
1974	91	292	1,006	6,218	5,108	12,715
1975	97	292	977	6,104	5,617	13,087
1976	97	362	1,117	6,461	6,088	14,125
1977	169	496	N/A	7,914	6,610	15,189
1978	117	486	N/A	8,433	7,133	16,169
1979	175	603	N/A	8,964	7,576	17,318
1980	191	739	N/A	9,638	8,057	18,625
1981	173	724	N/A	10,308	8,704	19,909
1982	166	701	N/A	11,164	8,913	20,944
1983	134	597	N/A	11,990	9,374	22,095
1984	253	313	1,151	11,861	9,903	23,481
1985	195	348	1,166	12,285	10,487	24,481
1986	95	279	1,200	12,536	11,909	26,019
1987	142	265	1,275	12,736	12,373	26,791
1988	116	289	1,402	12,827	13,164	27,798
1989	123	361	1,441	12,938	13,846	28,709
1990	120	266	1,466	13,167	14,677	29,696
1991	64	249	1,436	13,184	15,430	30,363
1992	104	180	1,465	13,209	16,348	31,306
1993	129	193	1,433	13,181	16,709	31,645
1994	117	222	1,435	12,705	16,860	31,339
1995	124	247	1,522	13,475	18,089	33,457
1996	212	151	1,615	13,583	18,817	34,378
1997	268	149	1,792	13,546	19,956	35,711
1998	175	122	1,913	13,702	21,124	37,036
1999	219	110	2,026	13,011	22,034	37,400
2000	230	146	2,166	13,096	22,735	38,373
2001	153	73	2,032	13,930	24,474	40,662
2002	143	73	2,116	13,876	25,484	41,692
2003	204	50	3,138	18,424	32,251	54,067
2004	197	58	3,296	18,260	33,746	55,557
2005	242	67	3,601	18,001	34,878	56,789
2006	209	61	3,834	17,801	36,470	58,375

Notes: Other – other kinds of wells not yet plugged and abandoned (P&A), but standing awaiting work, are not separately reported from 1960-1963 and from 1977-1983. Before 1964 and from 1977-1983, wells or boreholes not yet P&A were listed as either completed or suspended; P&A – plugged and abandoned, includes wells and boreholes. Source: TIMS/Regional Quarterly Reports, as of June 2007.

D.2.2 Impact Factors

Eight impact factors are identified in association with exploratory drilling, including: 1) drilling rig installation and removal; 2) drilling rig presence; 3) drilling discharges; 4) other effluent discharges; 5) marine debris; 6) air pollutant emissions; 7) well testing; and 8) support activities. Of these impact factors, drilling rig presence, drilling discharges, other effluent discharges, marine debris, and well testing have the potential to affect water quality and/or plankton. **Table D-5** summarizes the environmental resources potentially affected by each impact factor.

Table D-5. Impact factors associated with exploratory drilling seismic surveys that potentially affect plankton and water quality resources.

Resource	Drilling Rig Installation/ Removal	Drilling Rig Presence	Drilling Discharges	Other Effluent Discharges	Marine Debris	Air Pollutant Emissions	Well Testing	Support Activities
Water quality	---	---	o	o	o	---	X	---
Plankton	---	o	o	---	---	---	---	---

X = potentially significant impact with mitigation recommended; o = minor or negligible impact, no additional mitigation recommended; -- = no impact.

D.2.3 Impacts

Effects of Drilling Rig Presence (including Noise and Lights)

Exploratory drilling rigs typically are onsite for approximately 70-90 d. During this time, the physical presence of the rig, as well as noise and lights from drilling activities, may affect marine biota including plankton (as well as fishes, marine mammals, sea turtles, and birds). For a single, temporary structure such as a drilling rig, the effects are negligible. The potential impact for permanent structures (e.g., production platforms) is discussed further under Development and Production.

The most obvious effect of drilling rig presence during exploratory drilling is the attraction of fishes (Gallaway and Lewbel 1982). Offshore structures typically attract epipelagic fishes such as tunas, dolphin, billfishes, and jacks (e.g., Holland et al. 1990; Higashi 1994). This "artificial reef effect" is generally considered a beneficial impact, however, it is unlikely to affect plankton.

Impacts on phytoplankton may occur from shading due to rig presence. However, phytoplankton will move with ambient currents and any reduction in photosynthesis will be short term in nature.

Effects of Drilling Discharges

The fate and effects of drilling discharges have been reviewed extensively (National Research Council 1983; Neff 1987; Hinwood et al. 1994; Neff et al. 2000; Neff 2005; International Association of Oil & Gas Producers 2003). To understand the fate of drilling discharges, it is helpful to recognize three types of discharges:

- Seafloor releases of cuttings, seawater, and excess cement slurry during initial jetting of wells. Most of this material settles within tens of meters around the wellsite, producing the thickest accumulations (several centimeters to tens of centimeters) of muds and cuttings on the seafloor;

- Discharges of water-based drilling fluids and cuttings from the drilling rig. These occur after the marine riser is set, allowing drilling fluids and cuttings to be returned to the drilling rig. The discharged cuttings tend to sink rapidly within a few hundred meters, whereas the drilling fluids may disperse over several kilometers, producing a thin or even undetectable layer on the seafloor (Boothe and Presley 1989);

- Discharges of SBF cuttings from the drilling rig. When SBF systems are used, the SBF itself is recycled, but cuttings are discharged along with small amounts of adhering drilling fluids. The SBF cuttings tend to clump together and sink rapidly near the wellsite, generally within a few hundred meters of the discharge (Neff et al. 2000; International Association of Oil & Gas Producers 2003) (**Figure D-2**).

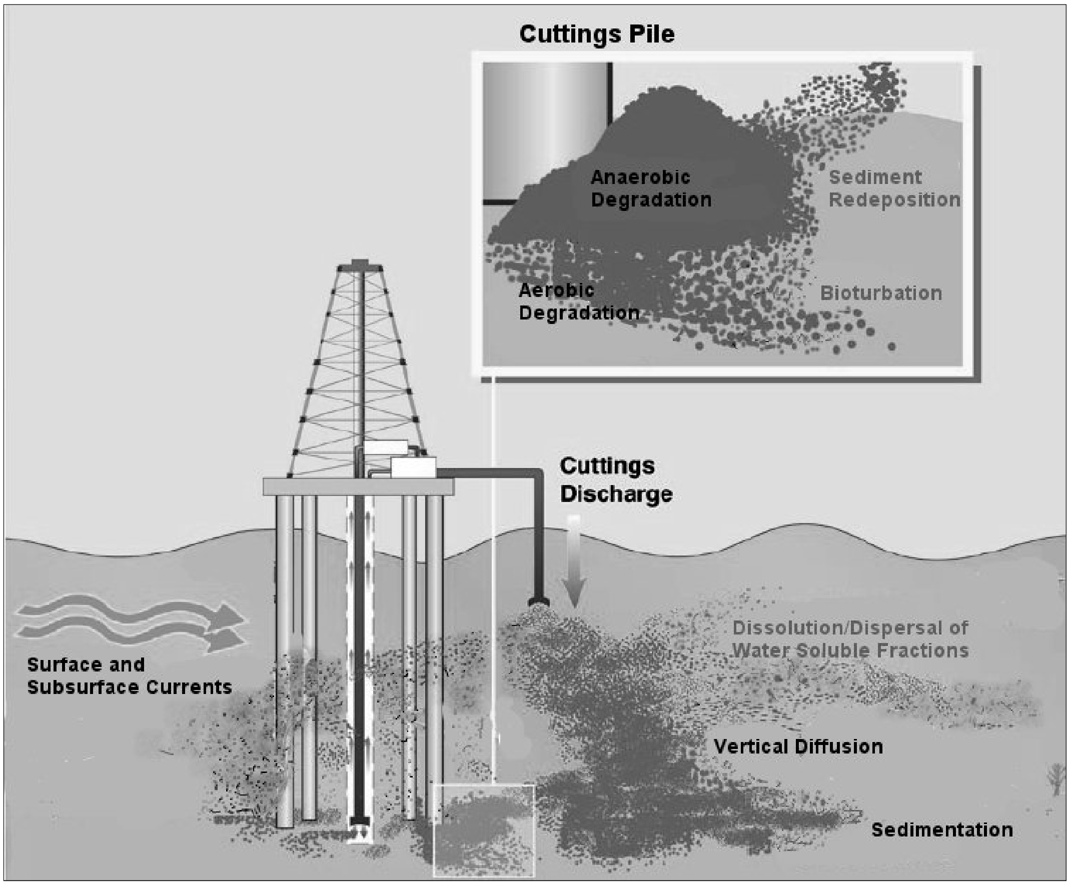

Figure D-2. Fate of cuttings discharges (Adapted from: International Association of Oil & Gas Producers 2003).

Effects on Water Quality and Plankton

Drilling fluid and cuttings discharges will produce a visible plume that will move with the currents as these materials are diluted and settle to the seafloor. In general, turbid water may extend between a few hundred meters and several kilometer down-current from the discharge point and to persist for several hours after each bulk discharge. Studies have demonstrated reductions in water clarity within a few hundred meters to about 2 km of drilling rigs during drilling fluid discharges (Ayers et al. 1980a,b; Ray and Meek 1980). Dispersion to background levels typically requires several minutes to several hours (Neff 1987).

During well intervals when SBFs are used, only the cuttings will be discharged, along with a low percentage of adhering drilling fluids. Drilling fluids associated with SBF cuttings typically adhere tightly to cuttings particles and do not produce much turbidity as the cuttings sink through the water column (Neff et al. 2000).

Discharges of drilling fluids and cuttings are likely to have little or no impact on plankton due to the low toxicity and rapid dispersion of these discharges (National Research Council 1983; Neff 1987; Hinwood et al. 1994). Water-based drilling fluids typically have low toxicity. Therefore, there is little chance of toxic effects on plankton and other water column organisms.

Effects of Other Effluent Discharges

Other routine discharges during exploratory drilling typically include treated sewage and domestic wastes (including food waste); deck drainage; and miscellaneous discharges. These are subject to BOEMRE regulations and NPDES permit limits.

Sewage, or sanitary waste, consists of human body wastes from toilets and urinals. Sanitary waste is routinely treated using a marine sanitation device that produces an effluent with a minimum residual chlorine concentration of 1.0 mg L^{-1} and no visible floating solids or oil and grease. Wastewater treatment sludge is transported to shore for disposal at an approved facility. Domestic waste, or “gray water,” includes water from showers, sinks, laundries, and galleys, safety showers, and eye-wash stations. Gray water does not require treatment before discharge. Service vessels are normally equipped with an approved marine sanitation device. Food waste, a type of domestic waste, is ground prior to discharge, in accordance with MMS requirements; in accordance with 33 CFR 151.73, no person may discharge garbage from a fixed or floating platform engaged in the exploration, exploitation, or associated offshore processing of seabed mineral resources or any ship within 500 m of a platform. Victual waste (any spoiled or unspoiled food waste) may be discharged if it passes through a grinder that meets requirements in 33 CFR 151.75 and the platform is beyond 12 nmi from nearest land.

Sanitary and domestic waste from drilling rigs and support vessels may affect concentrations of suspended solids, nutrients, and chlorine, as well as generating BOD. It is assumed that one person generates 100 L d^{-1} of sanitary waste and 220 L d^{-1} of domestic waste. It is predicted that sanitary wastes have an associated BOD of 240 mg L^{-1}. Assuming a typical crew complement of 130 persons, a drilling rig may be expected to generate about 13,000 L of sanitary wastewater, resulting in 3.1 kg of BOD and 28,600 L of domestic wastewater per rig on a daily basis. These discharges are expected to be diluted rapidly in the open ocean (USEPA 1993; MMS 2007). Impacts are likely to be undetectable beyond tens of meters from the source.

Deck drainage consists of all waste resulting from rainfall, rig washing, deck washings, tank cleaning operations, and runoff from curbs and gutters, including drip pans and work areas. Drilling rigs are designed to contain runoff and prevent oily drainage from being discharged. The flow is diverted to separation systems depending on the area collected. Regulations preclude the discharge of free oil in deck drainage that could cause a film, sheen, or discoloration of the surface of the water, or a sludge or emulsion to be deposited beneath the surface of the water. Only non-oily water (<15 ppm) can be discharged overboard. If the deck becomes contaminated, oily deck drainage is contained by absorbents or collected by a pollution pan under the rig floor for recycling and/or disposal. Because of the separation and treatment of water from oily areas prior to discharge, deck drainage is not expected to produce a visible sheen or any other detectable impacts on water quality.

The volume of deck drainage varies with the amount of rainfall. For example, considering a typical surface area of about 10,000 m^2 for a drillship and a maximum monthly rainfall of about

100 mm (3.9 in.) results in a monthly average deck drainage of 1,000 m^3 (6,290 bbl; 10^6 L). Rig washes may account for approximately another 200 L per month.

Additional miscellaneous discharges typically occur from numerous sources on a drilling rig. Examples include uncontaminated freshwater and seawater used for cooling water and ballast, desalination unit discharges, blowout preventer fluids, and boiler blowdown discharges (USEPA 1993). These discharges must meet MMS and NPDES requirements and are expected to be diluted rapidly in the open ocean. Impacts on water quality are likely to be undetectable beyond tens of meters from the source.

Effects of Marine Debris

Offshore oil and gas operations generate trash including paper, plastic, wood, glass, and metal. Most is associated with galley and food service operations and with operational supplies such as shipping pallets, containers used for drilling fluids and chemical additives (sacks, drums, and buckets), and protective coverings used on mud sacks and drilling pipes (MMS 2007). Some personal items, such as hardhats and personal flotation devices, are accidentally lost overboard from time to time. Generally, galley, operational, and household trash is collected and stored on the lower deck near the loading dock in large receptacles covered with netting. Drilling operations require the most supplies, equipment, and personnel, and therefore, generate more solid trash than production operations.

Solid waste generated during exploratory drilling is typically transported to shore by service vessels for disposal at approved landfill facilities. Based on historical data for a typical drillship, monthly solid waste transported to shore for disposal is expected to be about 40,000 kg.

Disposal of trash and debris in the ocean is prohibited under MMS regulations. Drilling rigs operate under a Garbage Management Plan to ensure adherence to these regulations. In addition, most petroleum companies have waste management programs that apply the principles of source reduction, reuse, and recycling to reduce the amount of waste generated.

Pieces of debris that fall overboard, such as welding rods, buckets, and pieces of pipe, are eventually colonized by epibiota. They also attract fishes due to their physical structure on the otherwise flat seafloor, resulting in a minor, local impact on the benthic community (Shinn et al. 1993) and no impacts to water quality or plankton. The impact is limited to a few meters to tens of meters of the wellbore.

Effects of Well Testing

If a hydrocarbon formation is discovered during exploratory drilling, well testing may be conducted. A well test is a procedure to determine the productive capacity, pressure, permeability, and/or extent of a hydrocarbon reservoir.

A conventional production test (drillstem test) is usually conducted with a tool that allows the well to be opened and closed at the bottom of the hole with a surface-actuated valve. One or more pressure gauges are customarily mounted into the tool and are read and interpreted after the test is completed. The most common test sequence consists of a short flow period, perhaps 5-10 minutes, followed by a buildup period of about an hour that is used to determine initial reservoir pressure. This is followed by a flow period of 4-24 h to establish stable flow to the surface, if possible, and followed by the final shut-in or buildup test that is used to determine permeability thickness and flow potential (Schlumberger 2008a).

If hydrocarbons are brought to the surface during the well test, they are disposed of by burning. The oil, water, and chemicals are pumped to a burner on a flare boom where the fluids are atomized in a chamber using compressed air and the mixture ignited. This combustion will result in emissions to the atmosphere. Gas from well testing is either flared or vented directly to the atmosphere.

In addition to the atmospheric emissions, burning of crude oil can result in some incomplete combustion and the fallout of unburned oil droplets to the sea surface. Production of a visible sheen on the sea surface would be a violation of water quality standards and should be avoided. High efficiency burners have been developed that minimize incomplete combustion and reduce the potential for hydrocarbon fallout (e.g., Schlumberger 2008b).

D.3 Development and Production

D.3.1 Description of Activities

Development and production is the process of exploiting commercial quantities of hydrocarbons. Key activities include drilling and completing development wells, installing production facilities and pipelines, routine operation of these systems, and eventual decommissioning. To date, no development or production activities have occurred in the license area.

A variety of development and production systems are available. The type of facilities selected by an operator depends on factors such as water depth, reservoir type, and proximity to existing oil and gas infrastructure and support operations. Examples could include conventional fixed platforms, compliant towers, floating production systems, or subsea systems controlled remotely from platforms in shallow water or on land. Design, fabrication, installation, and startup of an offshore development and production facility typically require 7 y or more from discovery to initial production (Regg et al. 2000).

Offshore production facilities conduct limited processing of oil and gas for transport. Examples include liquid/gas separation, H_2S removal, and gas compression. Once transported to shore, the oil or gas typically requires further processing by facilities such as oil refineries, gas processing plants, or petrochemical plants.

Development and production activities also typically include seismic operations such as high-resolution site surveys, vertical seismic profile surveys, and vertical cable surveys, all of which have been previously characterized.

Types of Production Facilities

Figure D-3 shows several development and production facility types. **Table D-6** summarizes the characteristics of development and production systems and their installation.

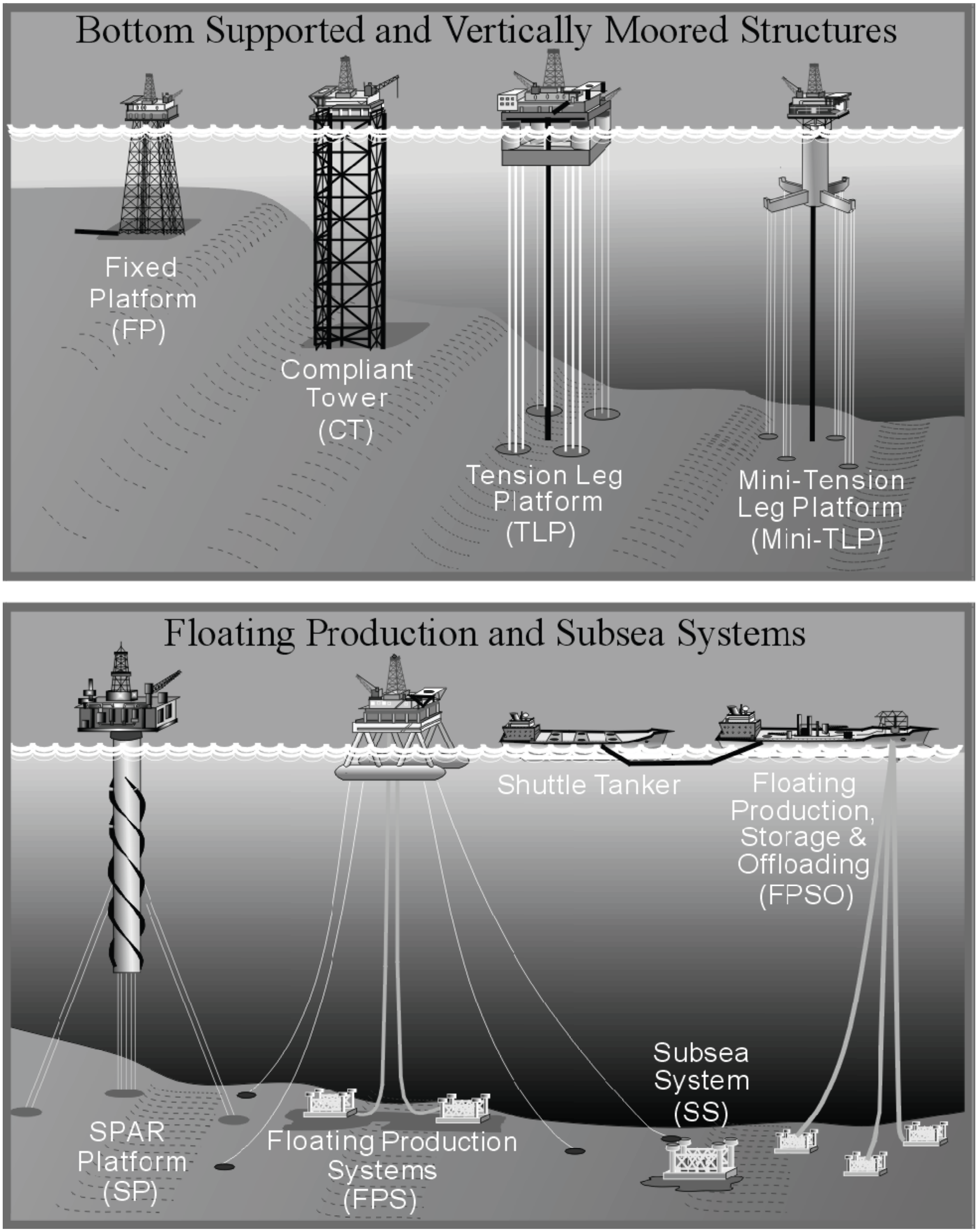

Figure D-3. Types of deepwater development and production systems (From: Regg et al. 2000).

Table D-6. Summary of offshore development and production facilities (Adapted from: Global Security 2008).

Facility and Depth Range	Construction	Seafloor Anchoring	Overview
Bottom-Founded Systems			
Fixed Platform (water depths less than 600 m)	Welded tubular steel jacket, deck, and surface facility Jacket - a tubular supporting structure for an offshore platform consisting of four, six, or eight 7- to 14-ft diameter tubulars welded together with pipe braces	Piles driven into the seafloor secure the jacket. The jacket is secured to the seafloor by weight and 2-m diameter piles that penetrate several 100 m or more below the mudline Typical base dimensions are 120 m by 150 m. Skirts may also be added to aid the jacket in fixing it to the seafloor. Dimensions can range up to 45 m on a side at the water line	Once the jacket is secured and the deck is installed, additional modules are added for drilling, production, crew operations, and accommodations. Large, barge-mounted cranes position and secure the jacket prior to the installation of the topsides modules. Surface facilities (topsides) are the part of the platform that contains the drilling, production, and crew quarter modules. Topsides dimensions could be 60 m by 60 m per deck level, with four decks, resulting in an overall height of 30 m.
Compliant Tower (water depths of 300-600 m)	Steel tubular jacket used to support surface facilities Typically, the jacket is composed of four leg tubulars that can range from 1-2 m in diameter and are welded together with pipe braces to form a space-frame-like structure	Secured to the seafloor with piles. Mooring is only used in the guyed-tower design. Clump weights may be attached to each mooring line, moving as the tower moves with the wind and wave forces. Base dimensions can range up to 90 m on a side	Similar to fixed platforms, but compliant towers yield to the water and wind movements in a manner similar to floating structures. A compliant tower jacket has smaller dimensions than a fixed platform and may consist of two or more sections; can also have buoyant sections in the upper jacket with mooring lines from jacket to seafloor (i.e., a guyed-tower design) or a combination of the two. The lower jacket is secured to the seafloor and acts as a base for the upper jacket and surface facilities. Large barge-mounted cranes position and secure the jacket and install the surface facility modules.
Tension Leg Platform (TLP) (water depths of 300-1,500 m)	Buoyant platform held in place by a mooring system	Mooring system – a set of tension legs or tendons attached to the platform and connected to a template or foundation on the seafloor. The template is held in place by piles driven into the seafloor	Similar to conventional fixed platforms except that the platform is maintained on location by moorings held in tension by hull buoyancy, which dampens vertical motion of the platform but allows for horizontal movement. Topside facilities and most daily operations are the same as for a conventional platform. Foundation secures the TLP to the seafloor; most foundations are templates laid on the seafloor, then secured by concrete or steel piles driven by use of a hydraulic hammer; other designs include a gravity foundation. As many as 16 concrete piles with dimensions of 30 m in diameter and 120 m long are used (one for each tendon).

Table D-6. (Continued).

Facility and Depth Range	Construction	Seafloor Anchoring	Overview
Floating Systems Spar (water depths up to 3,000 m)	Deep-draft floating caisson Caisson – a hollow cylindrical structure similar to a very large buoy	A lateral catenary system of 6-20 lines keeps the spar on location; mooring lines are a combination of spiral strand wire and chain. Because of its low motion, the spar can use a taut mooring system at a reduced scope and cost compared with a full catenary system. Each mooring line is anchored to the seafloor with a driven or suction pile. Depending on hull size and water depth, the moorings can vary in number up to 20 lines and contain 1,100 m of chain and wire. The footprint created by the mooring system can reach a half-mile or more in diameter measured on centre from the hull to the anchor piles	Consists of four major systems – hull, moorings, topsides, and risers. Spars rely on a traditional mooring system (anchor-spread mooring) to maintain position. About 90% of the structure is underwater. The number of wells, wellhead spacing, and facilities weight determine the size of the centre well and the diameter of the hull. Approximate hull diameter for a typical spar is 40 m, with an overall height, once deployed, of approximately 210 m. Spars use three basic types of risers: production, drilling, and export/import. The seafloor pattern (footprint) depends on the number of risers.
Semi-submersible production units (water depths from 150 to greater than 3,000 m)	Platform-shaped; purpose built or modified/retrofitted from an existing semi-submersible mobile offshore drilling units (MODU)	If moored, semi-submersible production units are anchored via 8-, 12-, or 16-point, semi-taut, chain-wire-chain or chain caternary system. Seafloor anchoring via tubular steel suction piles pressed into the seafloor, or via anchors	Semi-submersible production units can be either moored or can remain on site via dynamic positioning (DP). Lengths and widths variable, ranging from 100-165 m and 90-125 m, respectively. Semi-submersible designs are diverse. The lower hull is made up of three or four pontoons that form a triangular or rectangular ring at the base of the columns. Pontoons are either cylindrical or rectangular. Flowline steel catenary riser porches, located on the hull pontoons, support a variety of flowlines. Various utility risers are distributed around the outside of the hull on the columns.

Table D-6. (Continued).

Facility and Depth Range	Construction	Seafloor Anchoring	Overview
Floating production, storage, and offloading (FPSO) systems (water depths up to and beyond 3,000 m)	Ship-shaped; purpose built or modified/retrofitted from an existing tanker vessel Floating Storage and Offloading (FSO) units are considered a subset of FPSOs	Either seafloor anchored or dynamically positioned. Seafloor anchoring is via several 15-25 m long, large diameter anchor piles, coupled with wire and chain mooring lines, or via multiple drag anchors	FPSO systems are typically ship-shaped; they receive crude oil from deepwater wells and store it in their hull tanks until the crude can be pumped into shuttle tankers or oceangoing barges for transport to shore. FPSO turret structures are designed to anchor the vessel, allow "weather vaning" of the FPSO to accommodate environmental conditions, permit the constant flow of oil and production fluids to the vessel from an undersea field, all while being a structure capable of quick disconnect in the event of emergency. FPSOs may be used as production facilities to develop marginal oil fields or fields in deepwater areas remote from the existing OCS pipeline infrastructure. Alternatively, ship-shaped Floating Storage and Offloading (FSO) systems (vessels with no production processing equipment) can be used to support oil and gas developments. An FSO is typically used as a storage unit for production processed from other platforms that are remote from infrastructure and lack al pipeline to transport oil to the refinery.

Offshore production facilities may include either bottom-supported and vertically-moored structures, floating production systems, and subsea systems (Offshore 2007; Global Security 2008). Bottom-supported and vertically-moored structures include:

- Fixed platforms, which are used in shallow to deep water, with economic water-depth limits of about 610 m. They include both steel jacket platforms and concrete gravity base structures.
- Compliant towers, which are floating platforms that are permanently anchored to the seafloor and are feasible in water depths of about 300-600 m.
- Tension-leg platforms (TLPs), which are attached to the seafloor with tendons held in tension and are used frequently in water depths of about 300-1,500 m.

Floating production systems include:

- Spars, which are buoyant structures shaped like a single, large-diameter cylinder, with a functional deck mounted on top. Operational water depths range up to about 3,000 m.
- Semi-submersible production units, which are either modified from existing semi-submersible drilling rigs or purpose-built.

- Floating production, storage, and offloading (FPSO) systems, which are ship-shaped vessels with storage and limited treatment facilities. They support both floating and subsea production arrays. FPSOs may be used in water depths ranging up to and beyond 3,000 m.

Subsea systems are generally multi-component seafloor systems that allow for the production of hydrocarbons in water depths that would normally rule out installing conventional fixed or bottom-founded platforms (Regg et al. 2000). Through an array of subsea wells, manifolds, central umbilicals, and flowlines, a subsea system can be located many kilometers away in deeper water and tied back to existing host facilities in shallow water or onshore. Host facilities in deep water are likely to be one of several types of floating production systems.

Pipelines and Flowlines

Pipelines and flowlines are important components of development and production systems. Generally, pipelines transport hydrocarbons from a producing field to shore, whereas flowlines handle hydrocarbons and other chemicals within a field or between fields and offshore facilities. Flowlines that transport oil and/or gas to subsea manifolds, to a production facility, or between production facilities are considered gathering lines; pipelines that transport produced oil or gas to shore are considered trunklines (Cranswick 2001).

Pipelines vary in their specifications (i.e., diameter, wall thickness, internal and external pressure thresholds) depending upon factors including the physical and chemical characteristics of the hydrocarbon product, the physical environment (e.g., water depth, slope inclination, potential for span gap), and expected servicing and maintenance requirements, among other factors. Typical pipeline diameters range from 10-150 cm and wall thicknesses range from 1-4 cm. Pipelines may be configured as a single pipeline, as a pipe-in-pipe arrangement, as flexible pipe, or as a bundle (i.e., multiple pipelines or flowlines bundled and laid together).

Pipelines are thermal- or concrete-coated externally, may be coated internally, and are typically constructed of steel to reduce heat loss and increase stability (Cranswick 2001; Guo et al. 2005). Deepwater pipelines do not require a concrete weight coating due to the low wave and current conditions, but typically do require a high degree of thermal insulation. Pipelines may also be equipped with cathodic protection to protect the pipeline from external corrosion and leaks. Pipelines may also be outfitted with pressure sensors and remotely operated valves to protect the pipeline from overpressure and to detect abnormal low-pressure conditions (Cranswick 2001).

Pipelines can be installed by several different methods, including S-lay, J-lay, reel barge, and tow-in lay methods (Cranswick 2001; Guo et al. 2005) (**Figure D-4**), described as follows:

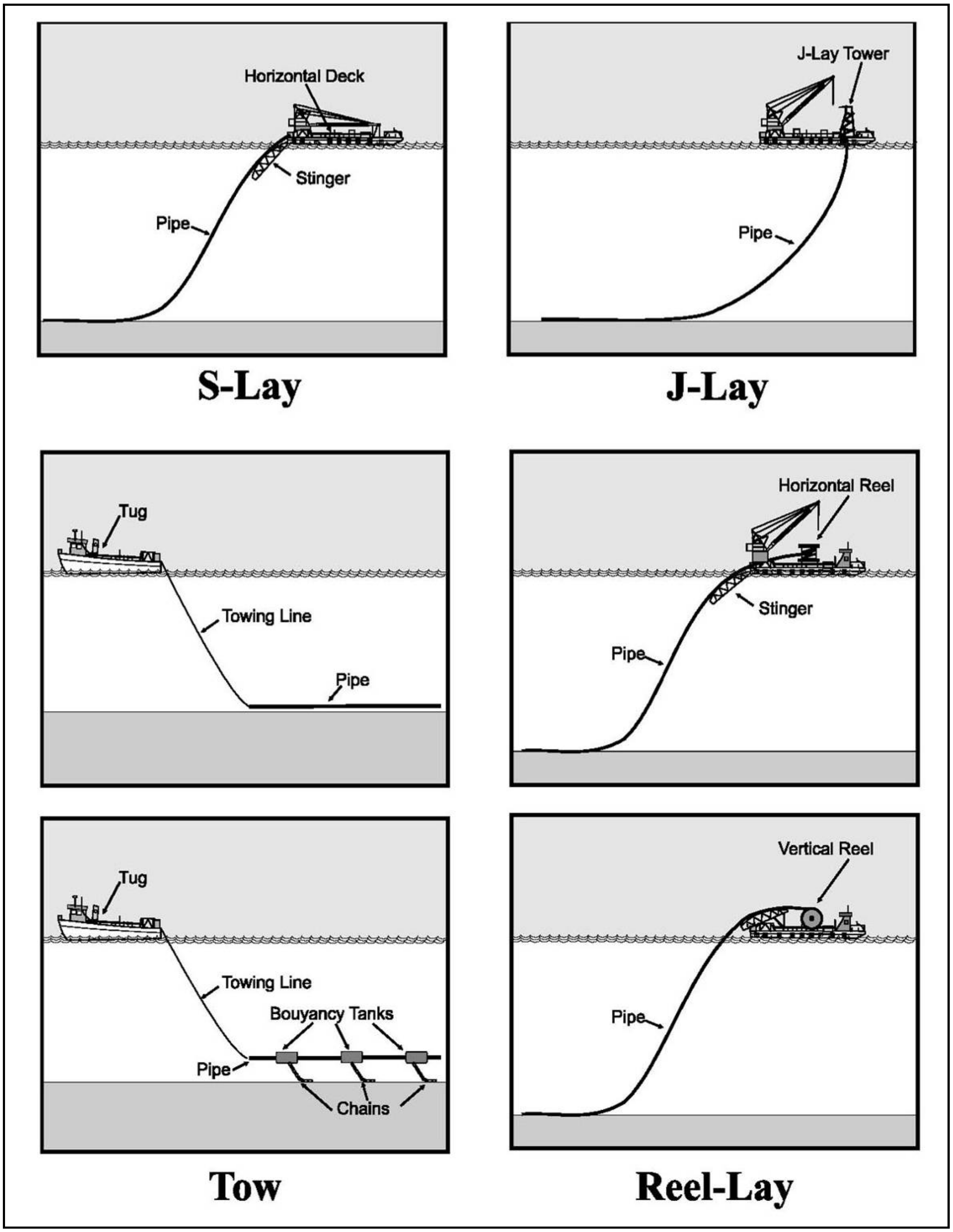

Figure D-4. Examples of offshore pipelaying methods (From: Cranswick 2001).

- S-lay – sections 12-25 m long are welded together on the lay barge and then coated. The lay barge moves forward and the completed sections of pipe enter the water, reaching the seafloor as more sections are welded. A stinger is used to control the degree of pipe bending during deployment. This method is used in shallow to deep water.

- J-lay – sections up to 75 m in length can be handled; J-lay barges have a tall tower on the stern for welding and coating. J-lay deployment of pipe is nearly vertical; J-lay can be used in deeper water than S-lay, but is typically not used in waters 60-150 m deep due to limited pipe angle and the bending stress imposed on the pipe.

- Reel-barge – typically involves small diameter pipelines; the pipe is welded, coated and wound on a reel onshore, then deployed offshore for installation. Horizontal reels lay pipe using S-lay deployment; vertical reels most commonly use a J-lay deployment, although an S-lay deployment is possible.

- Tow-in method – four variations possible: surface tow, mid-depth tow, off-bottom tow, and bottom tow, all of which require a tow vessel. Buoyancy modules are secured to the pipeline, allowing it to float on the sea surface. Floating pipeline is towed to the installation site from shore, then buoyancy modules are removed or the pipeline is flooded, allowing it to sink to the seafloor. Mid-depth tow requires fewer buoyancy modules; off-bottom tow requires the addition of chains to weigh the pipeline down. Bottom tow places the pipeline on the seafloor, where it is dragged into position.

Lay barges can be either conventionally moored (i.e., anchored) or dynamically positioned. Smaller lay barges (i.e., 120 m long by 30 m wide) typically require 8 anchors weighing 14,000 kg each. Larger barges operating in 300 m of water typically requires 12 anchors (3 anchors per quarter), each weighing 25,000 kg or more. In general, the larger the lay barge the greater the anchor requirements (Cranswick 2001).

To deploy and recover the anchors of a S-lay barge operating in 300 m of water, two anchor handling vessels are required. A smaller lay barge operating in shallower water requires only one smaller anchor-handling vessel. The number of anchor-handling vessels associated with a J-lay barge is essentially the same as for a similar size barge using the S-lay method. The number of anchor relocations per kilometer of offshore pipeline constructed is a function of the size of the lay barge, water depth, ocean floor conditions in the vicinity of the pipeline installation, and the amount of anchor line that can be stored, deployed, and retrieved by the lay barge.

The practical water depth limit for a large conventionally moored lay barge that uses the S-lay method is about 300 m, based on a ratio of anchor line length to water depth of about five to one. For pipelines supporting deepwater production facilities, installation by conventionally moored lay barges will probably be limited to those portions of the pipeline routes located in water depths less than 300 m.

Pipeline trenching and burial may also be required in areas heavily used by bottom-founded fishing activities (e.g., trawling), in regions where near bottom conditions are sufficiently rigorous to produce spanning or significant sediment movement, or where regulations require this practice. Trenching methods include conventional excavation with dredging, plowing, jetting, and mechanical trenching (Cranswick 2001). The area of seafloor disturbance and sedimentation varies depending on the trenching method and variations in bottom topography, sediment density, and currents.

Pipeline installation activities in deepwater areas can be difficult both in terms of route selection and construction. Depending on the location, the seafloor surface can be extremely irregular. Engineering challenges include high hydrostatic pressure, cold temperatures, darkness, and variable subsurface current velocities and directions. Accurate, high-resolution geophysical surveying becomes increasingly important in areas with irregular seafloor. Operators may be expected to analyze high resolution data to minimize pipeline length and avoid areas of unstable seafloor geologic structures and obstructions that might cause excessive pipe spanning, and potentially adverse effects to sensitive benthic communities.

Development Drilling Activities

The development and production phase includes drilling of delineation and production wells, which are sometimes collectively termed development wells (MMS 2007). Delineation wells are drilled to help define the extent and location of a hydrocarbon reservoir, and may or may not ultimately become production wells. Development wells may be drilled from movable structures, such as semi-submersibles or drillships (either anchored or dynamically positioned drilling vessels). The number of wells per structure varies according to the type of production structure used, the prospect size, and the drilling/production strategy.

Exploratory drilling activities have been described previously. Development drilling is a similar process except the duration is usually shorter (e.g., 40- 60 d vs. 70-90 d for an exploratory well; Regg et al. 2000) and includes well completion. Completion is a term used to describe the assembly of downhole tubulars and equipment required to enable safe and efficient production from an oil or gas well. The process typically includes setting and cementing the production casing, installing some downhole production equipment, perforating the casing and surrounding cement, treating the formation, setting a gravel pack (if needed), and installing production tubing. After a production test determines the desired production rate to avoid damaging the reservoir, the well is ready to go online and produce (MMS 2007).

Operational Discharges

Effluent discharges generated during development drilling include drilling fluids and cuttings, deck drainage, sanitary wastes, and domestic wastes. These discharges are similar to those described previously. Additional waste streams during production include produced water, produced sand, and well treatment, workover, and completion fluids (MMS 2007). Minor additional discharges occur from numerous sources such as desalination unit discharges, blowout preventer fluids, boiler blowdown discharges, excess cement slurry, and uncontaminated freshwater and saltwater (USEPA 1993).

Produced water is formation water that is brought to the surface during production, and it is often the largest volume discharge. Rates of produced water release can vary widely among fields and over time within a field. Generally, the fraction of produced water is low when production begins, increasing over time to a maximum near the end of the field life. In a nearly depleted field, production may be as high as 95% water and 5% petroleum, and over a life of a producing field, the volume of produced water may be 10 times greater than the volume of petroleum.

Volumes of produced water discharged are variable, depending upon the maturity of the producing formation, the type of hydrocarbon being produced, the volume of water required for injection, and the rate of hydrocarbon production realized at the offshore facility. Discharge rates are typically between 2 and 150,000 bbl d^{-1} (MMS 2007). MMS (2007) estimates that the annual volume of produced water discharged into the U.S. Gulf of Mexico from OCS facilities between 1996 and 2005 ranged between 431 and 686 million barrels (MMbbl), with an annual average of 596 MMbbl. Offshore California, the existing NPDES discharge permit allows up to 7.46 MMbbl of produced water to be discharged annually from the 19 discharge locations in OCS waters.

Selected chemical characteristics of produced water discharges are presented in **Table D-7**. Produced water contains a variety of chemicals that have been dissolved from the geologic formations in which the produced water resided for millions of years. These chemicals include inorganic salts from the relic seawater in the formation, metals, organic compounds, and radionuclides. Most produced waters from offshore sources have salinities (total dissolved solid concentrations) greater than that of seawater. In addition, a number of specialty chemicals may be added to produced water during the treatment process.

Table D-7. Chemical characteristics of produced water discharges from eight production platforms in the U.S. Gulf of Mexico, April 2003 to May 2005 (From: Veil et al. 2005).

Parameter and Unit of Measure	Concentration			
	Mean	Median	Maximum	Minimum
Biochemical oxygen demand (BOD) (mg L^{-1})	957	583	11,108	80
Dissolved BOD (mg L^{-1})	498	432	1 128	132
Suspended BOD (mg L^{-1})	76	57	146	16
Total organic carbon (TOC) (mg L^{-1})	564	261	4 880	26
Dissolved TOC (mg L^{-1})	216	147	620	67
Suspended TOC (mg L^{-1})	32	13	127	5
Nitrate (mg L^{-1})	2.15	1.15	15.8	0.60
Nitrite (mg L^{-1})	0.05	0.05	0.06	0.05
Ammonia (mg L^{-1})	74	74	246	14
Total Kjeldahl nitrogen (mg L^{-1})	83	81	216	17
Orthophosphate (mg L^{-1})	0.43	0.14	6.6	0.10
Total phosphorus (mg L^{-1})	0.71	0.28	7.9	0.10
Conductivity (µmhos cm^{-1})	87,452	86,480	165,000	360
Salinity (ppt)	100	84	251	0
Temperature (°C)	38	32	80	20
pH	6.29	6.50	7.25	1.77

Upon discharge, produced water is diluted rapidly, typically by 30- to 100-fold within tens of meters (International Association of Oil & Gas Producers 2005). At distances of 500-1,000 m from the discharge point, the dilution factor is 1,000-100,000 or more. Some constituents will precipitate, and others such as trace metals and aromatic hydrocarbons, will be scavenged onto particulate matter.

Produced water discharges are subject to regulatory limits for oil content. The effluent limits for produced water vary by OCS region. Summary effluent limits for the U.S. OCS are provided in **Table D-8**.

Table D-8. Summary of NPDES discharge prohibitions and other limits for produced water discharges, by region (Adapted from: Veil et al. 2004; Veil 2006).

Permit	Discharge Prohibition	Other Limits	Other Requirements
Region 4, proposed, under review	No discharges within 1,000 m of Area of Biological Concern	- Oil and grease: 29 mg L^{-1} monthly avg.; 42 mg L^{-1} daily max. - No visible sheen - Whole effluent toxicity (WET) testing	Produced water discharges allowed in water depths $\geq$200 m Notification before using new chemicals
Region 6, OCS	No discharges within Area of Biological Concern or National Marine Sanctuary	- Oil and grease: 29 mg L^{-1} monthly avg.; 42 mg L^{-1} daily max. - No visible sheen - WET testing	Previously conducted study of effects of discharges to hypoxic zone; subsequently removed COD and BOD limits in the latest permit
Region 6, Territorial Seas	No discharges to areas intermittently exposed, in parks or wildlife refuges, or within 1,300 ft of oyster/seagrass beds	- Toxicity testing similar to Region 6, OCS	Critical dilutions based on water depth, pipe diameter, and flow rate; CORMIX2 model
Region 9, California	None	- Oil and grease: 29 mg L^{-1} monthly avg.; 42 mg L^{-1} daily max. - No visible sheen - Limits on 9 metals, cyanide, and phenols - Monitoring for 26 chemicals - WET testing	- Annual discharge volume limits are set for each platform - Conduct study of on-line oil-and grease monitors - Companies must submit a study to the USEPA to determine the feasibility of disposal of produced water by means other than discharge
Region 10, Cook Inlet, Alaska, old permit	- To shallow water or other sensitive areas - Within certain distance of coastal marsh, river mouth, parks, wildlife areas	- Oil and grease: 29 mg L^{-1} monthly avg.; 42 mg L^{-1} daily max. - No visible sheen - Limits on various pollutants	NA
Region 10, Cook Inlet, Alaska, new permit (3/06)	- To shallow water or other sensitive areas - Within certain distance of coastal marsh, river mouth, parks, wildlife areas	- Oil and grease: 29 mg L^{-1} monthly avg.; 42 mg L^{-1} daily max. - Limits for each of the 9 platforms for 8 toxic pollutants - WET testing	- Collection of water column and sediment samples at 50-m intervals over a grid - Samples analyzed for total aromatic hydrocarbons, total aqueous hydrocarbons, copper, manganese, lead, nickel, zinc

Produced sand consists of slurried particles, which surface from hydraulic fracturing, and the accumulated formation sands and other particles including scale, which is generated during production (MMS 2007). This waste stream also includes sludges generated in the produced water treatment system, such as solids removed in filtration. Produced sand is transported to shore and disposed of as nonhazardous oil-field waste. Estimates of total produced sand generated from a production platform range from 0-35 bbl d^{-1} (USEPA 1993).

Three other types of fluids that may be used during exploitation activities are well treatment, workover, and completion fluids. Well treatment fluids, which consist of inhibited acids and petroleum base solvents that are pumped into the well to improve production (USEPA 1993), are not discharged into the sea. Workover fluids are used to maintain or improve existing well conditions and production rates on wells that have been in production. Completion fluids are brines that are used to displace the drilling fluid and protect formation permeability. Excess workover and completion fluids may be discharged to the sea. Principal contaminants can include oil and grease, metals, and various organic compounds (USEPA 1993). Fluids circulated through the wellbore are centrifuged to remove any residual hydrocarbons before discharging to the sea.

Decommissioning

Decommissioning is the process of dismantling production and transportation facilities and restoration of depleted producing areas in accordance with BOEMRE requirements and/or regulations. Various methodologies have been developed to remove offshore production facilities structures during decommissioning (MMS 2005). These methods are generally grouped and classified as either explosive or non-explosive, and they can be deployed and operated by divers, remotely operated vehicles (ROVs), or from the surface. Factors considered by operators in selecting a method include the target size and type, water depth, economics, environmental concerns, and weather conditions.

For offshore pipelines, the most common international practice is to abandon the pipeline in place (Scandpower Risk Management Inc. 2004). Prior to abandonment, pipelines are purged until the hydrocarbon levels are undetectable. In some cases, after the pipeline is purged, the pipe may be recovered as scrap.

D.3.2 Impact Factors

Eight impact factors were identified in association with development and production activities, including: 1) facility installation; 2) presence of structures; 3) drilling discharges; 4) operational discharges; 5) marine debris; 6) air pollutant emissions; 7) support activities; and 8) structure removal. **Table D-9** summarizes the environmental resources potentially affected by each impact factor.

Table D-9. Impact factors associated with development and production which potentially affect plankton and water quality resources.

Resource	Facility Installation	Presence of Structures	Drilling Discharges	Operational Discharges	Marine Debris	Air Pollutant Emissions	Support Activities	Structure Removal
Water quality	---	---	o	o	o	---	---	---
Plankton	---	---	o	---	---	---	---	---

X = potentially significant impact with mitigation recommended; o = minor or negligible impact, no additional mitigation recommended; -- = no impact.

D.3.3 Impacts

Effects of Facility Installation

Seafloor-disturbing activities during installation of production facilities will resuspend bottom sediments, crush benthic organisms, and produce turbidity. The total area of seafloor disturbed during a typical offshore platform installation is estimated to be 2 ha (MMS 2007). Spars and subsea facilities usually disturb smaller areas.

The detailed impacts of facility installation will depend on the type of facility selected for a particular project. Sources of impact for conventional, bottom-founded structures include:

- towing of components to the site;
- placement of structures on the seafloor, including foundation templates, platform jackets, manifolds, well trees, flowline sleds, umbilical termination units, and other equipment;
- driving of piles or anchor piles into the seafloor (e.g., with a hydraulic hammer);
- anchoring of barges during facility installation; and
- effluent discharges, air pollutant emissions, and noise from barges and tugs involved in the facility installation.

Pipeline installation for any particular project is likely to take several weeks to several months. For impact analysis, it is assumed that a pipelaying barge, assisted by an offshore marine supply vessel and crew/work boat, will install pipeline(s) on pre-determined “right of way” corridors. Typically, sections of pipeline are welded together and laid on the seafloor as the barge moves along the pipeline route, using anchors to hold position. If a dynamically positioned pipelaying barge is used for some portion of the work, then anchoring impacts are normally avoided along those corridors.

Pipeline installation will crush benthic organisms under the pipeline and anchors and introduce turbidity in the immediate vicinity of the pipelaying operations. Generally, it is estimated that 0.32 ha of seafloor are disturbed for each kilometer of pipeline installation (Cranswick 2001). Assuming a total corridor length of 25 km for a block relatively close to shore and 160 km for a block far from shore, the impact areas are 8 and 50 ha, respectively. The area actually affected by anchoring will depend on water depth, wind, currents, cable length, the size of the anchor and cable, distance between anchor movements, etc.

Most of the seafloor is expected to consist of soft-bottom benthic habitat. The main concern with regard to potential impacts is the placement of anchors in areas such as deepwater coral communities or chemosynthetic communities. These areas are associated with elevated densities of epifauna and fishes, and are considered relatively rare and ecologically important.

Effects of the Presence of Structures (including Noise and Lights)

In contrast to exploratory drilling rigs, production facilities typically remain in place for 20-30 y. During this time, the physical presence of the platform, as well as noise and lights from routine operations, may affect marine biota including plankton. Shading of the ocean surface is limited to the area immediately below a platform and/or within the shadow cast by the platform topsides.

Effects on Plankton

Zooplankton and ichthyoplankton may be attracted to lights associated with offshore structures; phytoplankton will remain unaffected by offshore structures. Light emissions from operations are likely to have negligible impacts on planktonic communities due to the small area of ocean affected.

Offshore platforms attract fishes, providing shelter and food in the form of attached fouling biota (Gallaway and Lewbel 1982; Wilson et al. 2003, 2005). Offshore structures typically attract epipelagic fishes such as tunas, dolphin, billfishes, and jacks (e.g., Holland et al. 1990; Higashi 1994). Stanley and Wilson (2000) reported finding 10,000-30,000 fishes associated with individual platforms; the lowest numbers were found at the largest and deepest structures. The density of fishes around platforms was 10 times greater than in open water. This “artificial reef effect” is generally considered a beneficial impact.

An additional potential benefit of fouling communities, including attached invertebrates, and fish attracted to the platform structure is the organic waste (e.g., pseudofeces, feces) generated and released into the water column.

Effects of Drilling Discharges

The fate and effects of drilling discharges during exploration have been discussed previously. Effects during development drilling are qualitatively similar. However, because numerous wells are typically drilled at each production location, the areal extent and severity of impacts are potentially greater than for exploratory drilling.

Continental Shelf Associates, Inc. (2006) studied drilling discharge impacts at several sites on the Gulf of Mexico continental slope in water depths of 1,033-1,125 m, with an emphasis on the benthic fate of muds and cuttings discharges. Two sites were sampled post-exploration and three sites were sampled post-development. Both WBFs and SBFs were used at these sites. Cuttings deposits covered a maximum area of 108 ha at one post-development site, compared with about 13 ha for a single exploratory well. At both post-exploration and post-development sites, areas of SBF cuttings deposition were associated with elevated organic carbon concentrations and anoxic conditions. Areas within about 500 m of drillsites had patchy zones of disturbed benthic communities, including microbial mats, areas lacking visible benthic macroinfauna, zones dominated by pioneering stage assemblages, and areas devoid of surface-dwelling species. Infaunal and meiofaunal densities generally were higher near drilling, although some faunal groups were less abundant near drillsites. Some stations near drilling had lower diversity, lower evenness, and lower richness indices compared with stations away from drilling. Some stations affected by drilling were dominated by high abundances of one or a few deposit-feeding species, including known pollution indicators. The severity of these impacts was greatest at two post-development sites that had the largest discharge volumes of SBF cuttings during drilling.

Results of simulation modeling, and their quantitative characteristics relative to water column impacts, are addressed in **Section D.4.3**.

Effects of Operational Discharges

Routine discharges during production include produced water, workover and completion fluids, treated sewage, and domestic wastes (including food waste); deck drainage; and miscellaneous discharges.

Produced water is likely to be the largest effluent discharge during production and has the potential to affect water quality near offshore production facilities by adding hydrocarbons, trace metals, and biochemical oxygen demand to the environment. Studies indicate that produced water has low intrinsic toxicity (International Association of Oil & Gas Producers 2005). Environmental effects have been evaluated in several studies. Studies have demonstrated accumulation of produced water contaminants in sediments around discharging facilities, but limited environmental effects (Neff 2002; International Association of Oil & Gas Producers 2005). The results of ecological and human health risk assessments indicate that constituents in produced water discharges present very little, if any, toxicological risk to the biota or to humans eating fish or shellfish from the area (Continental Shelf Associates, Inc. 1997).

Workover and completion fluids (brines) are expected to be diluted rapidly and have little or no impact on water quality. In the open ocean, these discharges will be diluted rapidly to ambient concentrations and conditions within tens of meters of the discharge point.

Sanitary and domestic waste from manned production facilities and support vessels may affect concentrations of suspended solids, nutrients, and chlorine, as well as generating BOD. It is assumed that one person generates 100 L d^{-1} of sanitary waste and 220 L d^{-1} of domestic waste. It is predicted that sanitary wastes have an associated BOD of 240 mg L^{-1}. These discharges are expected to be diluted rapidly in the open ocean (MMS 2007). Impacts are likely to be undetectable beyond tens of meters from the source.

As discussed previously, deck drainage consists of all waste resulting from rainfall, rig washing, deck washings, tank cleaning operations, and runoff from curbs and gutters, including drip pans and work areas. Offshore production facilities are designed to contain runoff and prevent oily drainage from being discharged. Because of the separation and treatment of water from oily areas prior to discharge, deck drainage is not expected to produce a visible sheen or any other detectable impacts on water quality. Assuming a typical surface area of about 10,000 m^2 for a production facility and a maximum monthly rainfall of about 100 mm, the monthly average deck drainage would be 1,000 m^3.

Additional miscellaneous discharges typically occur from numerous sources on an offshore platform. Examples include uncontaminated freshwater and seawater used for cooling water and ballast, desalination unit discharges, blowout preventer fluids, and boiler blowdown discharges (USEPA 1993). These discharges must meet MMS requirements and are expected to be diluted rapidly in the open ocean. Impacts on water quality are likely to be undetectable beyond tens of meters from the source.

Effects of Marine Debris

All solid waste generated during development and production will be transported to shore for disposal at approved facilities. In general, less solid waste is generated during production than during drilling activities. Monthly solid waste based on historical data for a typical drillship is expected to be about 40,000 kg, including general waste, galley waste, used waste oil and oil/fuel filters, absorbents, oily water, cardboard, plastic, paper, batteries, wood, etc. Most petroleum companies have implemented waste management programs that apply the principles of source reduction, reuse, and recycling to reduce the amount of waste generated.

Disposal of trash and debris in the ocean is prohibited under MMS regulations, and drilling rigs operate under a Garbage Management Plan to ensure adherence to these regulations. However, occasionally material from drilling rigs may accidentally fall overboard.

Pieces of debris that fall overboard, such as welding rods, buckets, and pieces of pipe, are eventually colonized by epibiota. They also attract fishes due to their physical structure on the otherwise flat seafloor, resulting in a minor, local impact on the benthic community (Shinn et al. 1993). The impact is limited to a few meters to tens of meters from the wellbore.

D.4 Accidents

Accidents may occur during any phase of offshore hydrocarbon activities (prospecting, exploration, or development and production). Potential sources considered in this analysis include 1) a crude oil spill from a blowout; 2) a diesel fuel spill; 3) a drilling fluid base oil spill; and 4) streamer cable fluid leak.

D.4.1 Crude Oil Spill from a Blowout

A crude oil spill is a rare event that could occur as a result of a blowout. A blowout is an uncontrolled flow of reservoir fluids into the wellbore, and sometimes catastrophically to the surface. A blowout may consist of saltwater, oil, gas, condensate, or a mixture of these. During drilling, all wells are equipped with a blowout preventer, a special assembly of high-pressure valves fitted to the top of a well to prevent high-pressure oil or gas from escaping.

Worldwide statistics from offshore drilling provide a reasonable basis for evaluating spill risk. Based on the earlier summary of spill risk prepared by Holand (1997), the average blowout frequency for exploration drilling in the U.S. Gulf of Mexico was 0.00593 blowouts per well drilled, or 1 blowout per 169 exploration wells drilled. Similarly, the MMS Safety and Environmental Management Program blowout incident rate for 1996 to 1999 was approximately 5 blowouts per 1000 well starts, or 1 per 200 (MMS 2001). For the North Sea, the estimated frequency is 0.00630 blowouts per well drilled, or 1 blowout per 159 exploration wells (Holand 1997).

Historically, most blowouts do not result in oil spills. For example, of the 151 well blowouts reported in the Gulf of Mexico from 1971 to 1995, only 18 (i.e., 12%) resulted in oil spills. The total volume released from all of these spills was 1,000 bbl of crude oil and condensate (MMS 2001). Between 1964 and 1999, almost all offshore spills (94%) from drilling- and production-related operations on the U.S. outer continental shelf were less than or equal to 1 bbl in size (Anderson and LaBelle 2000). The *Deepwater Horizon* spill of April 2010, however, is expected to affect the average size of historical oil spills in the Gulf of Mexico. As of January 2011, no new oil spill statistics have been developed that take into consideration the *Deepwater Horizon* spill. Generally, the historical data indicate that a blowout occurring and resulting in a large oil spill of any size is very unlikely.

The environmental and socioeconomic effects of a crude oil spill could vary substantially depending on the size of the spill, its chemical characteristics, the oceanographic and meteorological conditions at the time, and the effectiveness of spill response measures. At a minimum, the spill could affect water quality by producing an oil slick on the sea surface and increasing hydrocarbon concentrations due to dissolved components and small oil droplets. A subsurface blowout could also affect plankton in the water column through direct contact.

The impacts of crude oil exposure on phytoplankton have been investigated addressed through laboratory studies (i.e., mesocosms) and in the field following spills. Research efforts addressing oil exposure impacts to phytoplankton have variably addressed specific plankton species of interest, the effects of crude oil and dispersants on primary productivity, and the effects of specific oil components. Several representative results are outlined below.

Kusk (1981) conducted comparisons of aromatic hydrocarbon exposure among the marine diatom *Phaeodactylum tricornutum* and several species of marine and freshwater phytoplankton. Marine phytoplankton was found to be more sensitive to aromatic hydrocarbons than freshwater phytoplankton, while *P. tricornutum* was determined to be of intermediate sensitivity. Bate and Crafford (1985) documented the inhibition of phytoplankton photosynthesis from the water soluble fraction (WSF) of used lubricating oil. Riznyk et al. (1987) characterized the short-term effects of PAH exposure to the phytoneuston (i.e., microlayer at the sea surface), noting an initial inhibitory effect on phytoneuston populations contaminated with fluoranthene and production rates quickly returning to normal. Varela et al. (2006) assessed the impact of the *Prestige* oil spill on chlorophyll, primary production, zooplankton biomass, and species composition of phytoplankton and zooplankton. By comparing historical data to post-spill determinations, they found only minor changes in community structure evident, with no clear patterns noted. Observed differences were attributed to natural variability of the ecosystem, with no significant changes to plankton community structure evident.

Siron et al. (1991) determined that the diatom *Phaeodactylum tricornum* and the chlorophyte *Dunaliella tertiolecta* tolerated exposure to the WSF of Arabian light crude oil at levels up to 1.6% and 3.6%, respectively. Later in mesocosm studies, Siron et al. (1993) documented the fate and effects of dispersed crude oil under icy conditions. Kelly et al. (1999) evaluated the effects of phenanthrene exposure on phytoplankton primary productivity.

Hsiao et al. (1978) assessed the effect of crude oil and dispersants on the primary production of Arctic marine phytoplankton and seaweed. In mesocosm experiments, Harrison et al. (1986) evaluated the effects of crude oil and dispersant exposure on phytoplankton.

Pérez et al. (2010) evaluated fuel toxicity to a flagellate (*Isochrysis galbana*) and a coastal phytoplankton assemblage in their feasibility assessment of variable fluorescence. Jiang et al. (2010) summarized the toxic effects of the water accommodated fractions (WAF) of oil on marine plankton.

In general, the effects of crude oil exposure to phytoplankton appear to vary depending on the composition of the community studied, the location of the spill, the chemical composition and total volume of crude oil spilled, and the degree of weathering. Some research has indicated a toxic effect of hydrocarbon exposure, while other results indicate an enhancement of primary production. Effects of oil exposure on phytoplankton communities must also be gauged against natural variability, as well as the season during which the spill occurs (Varela et al. 2006). Losses of phytoplankton and/or diminution of water column primary productivity may be expected from an oil spill, with areal extent of such effects depending upon the size of the spill. The duration of such losses will be dependent upon the rate of weathering (e.g., rate of loss of toxic components via evaporation or dissolution), the rate of degradation by bacteria, the rate of sedimentation (e.g., via zooplankton pellets, adsorption to suspended material). While localized or relatively short term effects on phytoplankton may be expected, long term changes in phytoplankton community structure are not.

Deepwater Horizon Oil Spill

On 20 April 2010, an explosion and fire on BP's *Deepwater Horizon* offshore drilling rig killed 11 men. The rig, located on Mississippi Canyon Block 252 (MC252) in the U.S. Gulf of Mexico, sank and left the oil well leaking tens of thousands of barrels of oil per day into the Gulf. In what has become the worst oil spill in U.S. history, hundreds of species and their habitats along the coastal areas of Louisiana, Mississippi, Alabama, Texas, and Florida, as well as human uses of these resources, may have been affected.

The *Deepwater Horizon* well released oil and gas for 87 d until the well was successfully capped on 15 July. The National Incident Command Flow Rate Technical Group estimated that 4.93 MMbbl +10% were released from the well. Containment actions captured approximately 800,000 bbl of oil prior to the well being capped. Between 30 April and 15 July, approximately 771,000 gal. of chemical dispersant were added to the oil and gas flow at the wellhead.

Of the total oil spilled, approximately 1.2 MMbbl were estimated to be naturally or chemically dispersed, the majority of that at the wellhead. Throughout the spill, hydrocarbons and other associated fractions that escaped subsea collection systems at the wellhead, most likely as a mixture of oil, gas, and hydrate, resulted in some hydrocarbons reaching the surface and some remaining at depth either dissolved in the water column and or as small droplets.

The catastrophic release of oil and natural gas has provided an unprecedented opportunity to study the effects of a deepwater release of hydrocarbons on the marine environment. Thus far, only a few scientific peer-reviewed journal publications have been issued; those identified to date are summarized below. In addition, a series of government reports and preliminary findings have been published.

Camilli et al. (2010) presented results of hydrocarbon plume tracking, transport, and biodegradation associated with the *Deepwater Horizon* spill. Data acquired during a subsurface hydrocarbon survey conducted between 19 and 28 June 2010 were summarized. An autonomous underwater vehicle (AUV) and a ship-cabled sampler (i.e., sampling rosette with a Tethys *in-situ* membrane inlet mass spectrometer) were employed during the survey. Findings indicated the presence of a continuous plume over 35 km in length, at approximately 1,100-m depth that persisted for months without substantial biodegradation. Samples collected from within the plume revealed monoaromatic petroleum hydrocarbon concentrations in excess of 50 $\mu g\ L^{-1}$. These data indicate that monoaromatic input to this plume was at least 5,500 $kg\ d^{-1}$, which is more than double the total source rate of all natural seeps of the monoaromatic petroleum hydrocarbons in the northern Gulf of Mexico. Dissolved oxygen concentrations suggested that microbial respiration rates within the plume were not appreciably more than 1 $\mu M\ O_2\ d^{-1}$.

Valentine et al. (2010) characterized the microbial community at the *Deepwater Horizon* spill site. The *Deepwater Horizon* event resulted in suspension of oil in the Gulf of Mexico water column because the leakage occurred at great depth. The distribution and fate of other abundant hydrocarbon constituents (e.g., natural gases) are also important in determining the impact of the leakage but are not yet well understood. The survey was conducted between 11 and 21 June 2010. Investigators measured dissolved hydrocarbon gases at depth using chemical and isotopic surveys and on-site biodegradation studies. Propane and ethane were the primary drivers of microbial respiration, accounting for up to 70% of the observed oxygen depletion in fresh plumes. Propane and ethane trapped in deep water may therefore promote rapid hydrocarbon respiration by low-diversity bacterial blooms, priming bacterial populations for degradation of other hydrocarbons in the aging plume. Valentine et al. (2010) estimated that methane, ethane, and propane released from the *Deepwater Horizon* leak will exert a biological oxygen demand in the deep plume horizon of up to 8.3×10^{11} g O_2 for methane respiration, 1.3×10^{11} g O_2 for ethane, and 1.0×10^{11} g O_2 for propane. They compared these calculations to a 968,000-bbl oil spill at the surface and dispersed into the subsurface, with a maximum biological oxygen demand for oil of 4.4×10^{11} g O_2. The sum of these values, $\sim 1.5 \times 10^{12}$ g of O_2, provides an estimate of the maximum integrated deep water O_2 anomaly expected from this event, with roughly 15% of the oxygen loss occurring in fresh plumes from respiration of propane and ethane. From these estimates, Valentine et al. (2010) predicted that roughly two-thirds of the ultimate microbial productivity in deep plumes will arise from metabolism of natural gas. They also predicted 1) the occurrence of boom-and-bust cycles of bacterial succession beginning with propane, ethane, and butane consumers, followed by the consumers of various higher hydrocarbons and methane; and 2) a plume bacteria population responding to persistent mixing of bacteria, oxygen, and hydrocarbons within non-plume waters, which could presumably lead to attenuation in the aging plumes.

Hazen et al. (2010) reported that the dispersed hydrocarbon plume stimulated deep sea indigenous proteobacteria that are closely related to known petroleum-degraders. They detected a deep sea oil plume from 1,099-1,219 m at distances of up to 10 km from the wellhead. Due to its composition, the plume was likely dispersed MC252 oil, a conclusion also reached by Camilli et al. (2010). At most locations where the plume was detected there was a slight decrease in oxygen concentration indicative of microbial respiration and oxygen consumption as would be expected if the hydrocarbons were being catabolized. Oxygen saturation within the plume averaged 59% while outside the plume it was 67%. Extractable hydrocarbons (e.g., octadecane) ranged from non-detectable in the non-plume samples to 9.21 $\mu g\ L^{-1}$ in plume samples. Volatile aromatic hydrocarbons were significantly higher in the plume interval (mean: 139 $\mu g\ L^{-1}$) than in the non-plume samples from similar depths. The average temperature within the plume interval was 4.7°C and pressure was 1,136 dB. Soluble orthophosphate, total ammonia-N, and nitrate-N were detected at similar concentrations within and outside the plume interval. Hazen et al. (2010) determined that hydrocarbon-degrading genes coincided with the concentration of various oil contaminants. Changes in hydrocarbon composition with distance from the source and incubation experiments with environmental isolates demonstrated faster than expected hydrocarbon biodegradation rates at 5°C. Based on these results, the potential exists for intrinsic bioremediation of the oil plume in the deep water column without substantial oxygen drawdown.

A comprehensive summary of ongoing research associated with the *Deepwater Horizon* spill is beyond the scope of this analysis. However, NOAA has regulatory oversight over spill research related to natural resource damage assessment. Ongoing and completed study efforts can be found at http://www.noaa.gov/sciencemissions/bpoilspill.html.

D.4.2 Diesel Fuel Spill

A diesel fuel spill is an accident that could occur during any phase of offshore hydrocarbon activities. Potential sources include vessel collisions or groundings, tank ruptures, or a hose break during at-sea refueling operations. A large spill, such as one resulting from a diesel tank rupture, is considered to be an extremely rare event. The probability has not been estimated, but historical data for a highly active region (the Gulf of Mexico) include no such incidents between 1981 and 1999 (Anderson and LaBelle 2000; MMS 2007). Historical data indicates that most diesel spills are <1 bbl, and for spills greater than this, the median size is 5 bbl (MMS 2000).

The environmental effects of a diesel fuel spill will depend on the size of the spill, the oceanographic and meteorological conditions at the time, and the effectiveness of spill response measures. In general, a diesel fuel spill is subject to rapid dispersal, weathering, evaporative losses and dissipation throughout the water column. A diesel spill has the potential to affect local water quality by increasing hydrocarbon concentrations. Water column biota near the spill site, such as plankton, could be affected, because diesel fuel is highly toxic. While motile biota may actively avoid a large oil spill, planktonic forms are unable to avoid contact.

The effects of diesel fuel exposure to plankton are variable, with impacts mediated by the degree of weathering and the relative concentrations of toxic fractions, as well as the sensitivity of the species exposed. The toxic effects of oil exposure, including diesel fuel exposure, typically fall into two categories – those associated with coating of an organism and those due to uptake of hydrocarbons and the subsequent disruption of cellular metabolism (Lobban and Harrison 1997). Upon the initial release of diesel fuel, portions of the plankton community will die as a result of exposure to the most toxic fractions of spilled diesel fuel. Toxicological tests indicate that marine plankton are very sensitive to the WSF or water accommodated fractions (WAF) of oil, including the middle distillates which include diesel. The median effective/lethal concentrations of diesel fuel are typically in the $\mu g\ L^{-1}$ or $mg\ L^{-1}$ levels and vary depending upon the chemical composition of the fuel. Exposure impacts are species- and developmental stage-specific. In general, oil toxicity increases with increasing carbonic chain length and benzene ring number.

When spilled onto the ocean surface, diesel fuel that has a lower specific gravity than seawater will not sink, while heavier fuel oils may sink. Diesel fuel that remains on the ocean surface will undergo dispersion, dissolution, evaporation, and photooxidation (NOAA, 2006). Photooxidation has been shown to increase the relative toxicity of diesel. Diesel floating on the ocean surface will not pass through the water column unless adsorbed onto the surface of water column particulates. As diesel fuel is dispersed (e.g., by wave action), it may form droplets small enough be kept in suspension and moved by currents.

Only a limited number of studies have directly addressed and characterized the toxicity of diesel fuel to phytoplankton. Gordon and Prouse (1973) characterized exposure effects for three oils (i.e., Venezuelan crude, No. 2 fuel oil, and No. 6 fuel oil) on the photosynthesis of natural phytoplankton communities from Nova Scotia and the northwest Atlantic Ocean. They determined that all of the oils tested can inhibit photosynthesis, and the degree of inhibition depends upon oil type and concentration. No. 2 fuel oil was the most toxic. Under certain conditions, low concentrations of Venezuelan crude oil were also found to stimulate photosynthesis. Nayar et al. (2005) noted signs of acute toxicity to autotrophs (phytoplankton) and autotrophic bacteria in diesel fuel exposure experiments. As weathering and dissolution proceeded, a stimulatory effect was evident at lower concentrations. Bacterial heterotrophs responded positively to all concentrations of diesel fuel due to abundance of a carbon source, reduced grazing pressure, and reduced competition for nutrients from phytoplankton. Short term (i.e., 96-h) studies of the effect of diesel fuel WSF exposure on the growth of the marine microalgae *Chaetoceros calcitrans*, as conducted by Bhattacharjee and Fernando (2008), revealed drastic suppression of growth at 80% WSF concentrations; a diesel oil concentration of 36.56-38.02 mg L^{-1} was established as the 96-h EC_{50} value. Phatarpekar and Ansari (2000) evaluated the toxic effects of the WSF of four different fuel oils on the microalga *Tetraselmis gracilis*. Depending on different physico-chemical properties, the hydrocarbons showed different inhibitory effects on the growth of *T. gracilis*.

D.4.3 Drilling Fluid Base Oil Spill

SBFs contain a synthetic base oil that is mixed with other constituents to prepare the drilling fluid. In the Gulf of Mexico, an offshore region with frequent drilling activity, there were

53 SBF spills between 2001 and 2004 (MMS 2007). Most spills were less than 50 bbl, but three were greater than 1,000 bbl. Two of the three large spills were caused by an emergency disconnect of the marine riser, and the third by riser failure.

A drilling fluid base oil spill is expected to sink to the seafloor (Boland et al. 2004). Most of the impact is expected to occur on the seafloor, where the SBF accumulates. Per Neff et al. (2000), concentrations of base fluid in solution in the water column following a discharge of cuttings are unlikely to exceed about 1 mg L^{-1} at any time. Because of the low toxicity of synthetic base fluids (e.g., linear alpha olefins, internal olefins) to water column organisms, Neff et al. (2000) concluded that there is no risk of direct toxicity of the settling SBF cuttings to water column organisms.

Modeling Results for Accidental Release of Drilling Muds

A recent drilling mud discharge analysis evaluated the fate of an accidental release of a low toxicity, mineral oil based drilling fluid (LTOBM) into the marine environment at a water depth of approximately 1,000 m (CSA International, Inc. 2010). Modeling, using both CORMIX and MUDMAP models, was based on the release of 584 bbl of drilling fluid with a density (fluid weight) of 9.8 ppg. The drilling fluid had a bulk density of 1,198 kg m^{-3}. The grain size distribution for 75% of the particles in the fluid ranged from 8.6-17.9 µm, with the smallest particle size class of 3.7 µm. The final MUDMAP model runs used the actual drilling fluid particle size distribution from laser granulometry, which indicated smaller fine particles were dominant.

The model scenarios that were run were as follows:

- CORMIX (near field) model runs as an instantaneous discharge;
    - under low (0.9 kn), and
    - high (1.5 kn) current conditions; and
- MUDMAP (far-field) model runs with
    - 2-h discharge duration using literature-derived particle size distribution for “standard” drilling fluid, and
    - 4-h discharge duration using particle size distribution in drilling fluid sample as determined by laser granulometry.

The initial CORMIX modeling indicated that the plume of drilling fluid is rapidly dispersed to very low concentrations within a short distance from the discharge point. **Figure D-5** presents the CORMIX-predicted plumes of the discharged drilling fluid under mean (low) and maximum (high) current conditions. The plume sinks, since its density exceeds that of the ambient seawater. While the plume sinks, it also drifts in response to the ambient currents, eventually reaching the seabed several kilometers from the discharge site.

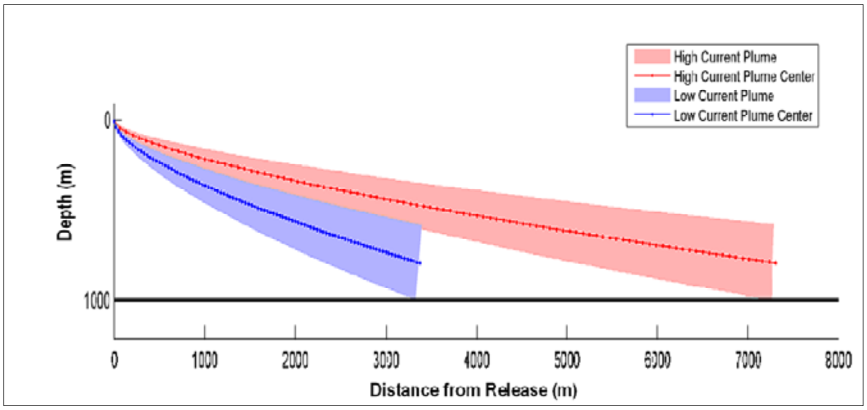

Figure D-5. Horizontal and vertical extent of drilling fluid plume predicted by CORMIX near-field model under low and high current speeds (From: CSA International, Inc. 2010).

Using the estimated mean current speeds (0.9 kn), the plume is predicted to reach the seabed 122 minutes after the release at a distance 3,300 m from the discharge site. Under maximum currents (1.5 kn), the plume reaches the seabed 161 minutes after the release at a distance of 7,250 m from the discharge site.

Figure D-6 shows the CORMIX-predicted dilution of the concentration along the plume centerline (where the concentration is highest). Dilution was rapid with the initial concentration diluted by a factor of 10,000 within a distance of 1 km from the discharge site, and by a factor of 100,000 by the time the plume reached the seabed. The curves of excess concentration ended when the plume hit the bottom at the assumed 1,000-m depth. For example, the base fluid concentration of 1,430 parts per million (ppm) was diluted to 0.143 ppm within 1 km of the discharge point and diluted to 0.0143 ppm by the time the plume reached the seabed.

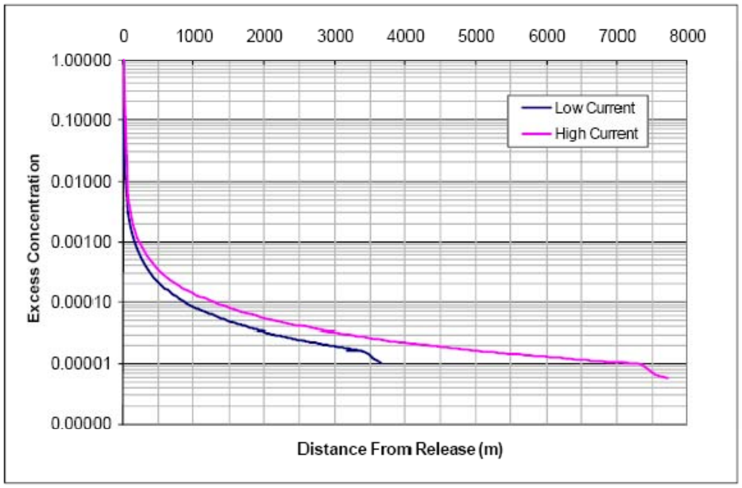

Figure D-6. Dilution of drilling fluid along the plume centerline predicted by the CORMIX near-field model under low (0.9 kn) and high (1.5 kn) current conditions (From: CSA International, Inc. 2010).

Fluid particles were carried both east and west of the release and modeling indicated that the fluid did not form a uniform layer over the seabed as it settled, but rather covered the area with a patchy distribution of particles, however, the depositional thickness was not measurable. The MUDMAP simulation also indicated ~50% of the fluid particles were still in suspension after 30 d following the release, however, the fluid components were not measurable or detectable (i.e., below background levels). The predicted water column concentrations of drilling fluid 30 d after the discharge were far below background levels of total suspended solids in open ocean waters (about 1 mg L^{-1} total suspended solids [TSS]).

Figures D-7 and **D-8** show the predicted concentrations in the drilling fluid plume at 4 and 24 h, respectively, after the release as it moved toward the northeast and dispersed. At 4 h after discharge, the area where the predicted concentration of 1 mg L^{-1} occurred is relatively small. At 24 h, only the 0.1 mg L^{-1} and lesser contours were depicted to the east of the discharge point (i.e., concentrations >0.1 mg L^{-1} no longer occurred).

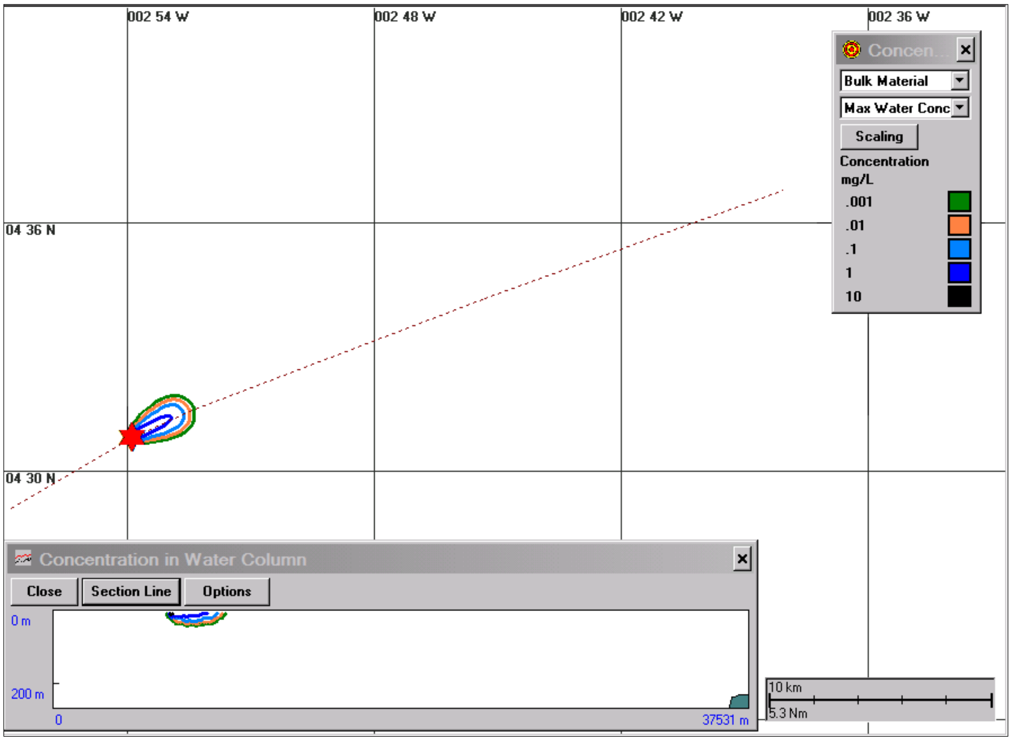

Figure D-7. Predicted water column concentrations of drilling fluid 4 h after discharge using the measured drilling fluid grain size distribution. The inset shows the vertical cross-section along the dotted line in the plan view (From: CSA International, Inc. 2010).

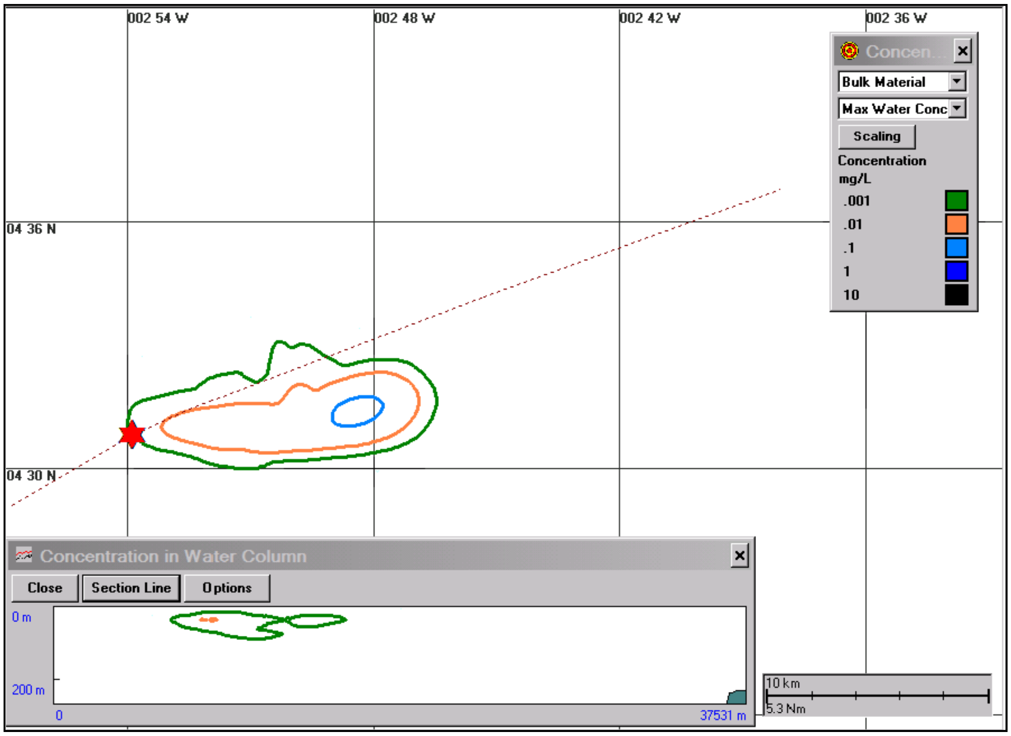

Figure D-8. Predicted water column concentrations of drilling fluid 24 h after discharge using the measured drilling fluid grain size distribution. The inset shows the vertical cross-section along the dotted line in the plan view (From: CSA International, Inc. 2010).

D.4.4 Streamer Cable Fluid Leak or Spill

Streamer cables towed by seismic survey vessels typically contain a light aliphatic hydrocarbon (similar to kerosene) for electrical insulation and neutral buoyancy. Breaks in the cable are rare and usually occur when currents drag the cables around a fixed structure (e.g., a platform). Fish bites from large fishes may also occasionally puncture towed streamer cables. If a streamer cable were damaged or began leaking, small volumes of the cable fluid could be released into the ocean. In most cases, the spill will be limited to the volume of one section of the streamer, which is roughly 100-200 L of fluid (Continental Shelf Associates, Inc. 2004).

The released fluid is expected to evaporate rapidly and be quickly diluted by seawater. The area that could be affected by a spill of cable fluid is expected to be within a few meters to tens of meters of the cable. The spill will have a brief, localized impact on water quality by producing a sheen on the sea surface. The impacts will be minor.

D.5 Cumulative Effects

Cumulative effects are those resulting from the incremental effects of a proposed action when added to other past, present, and reasonably foreseeable future actions, regardless of who undertakes them. Cumulative effects can result from individually minor, but collectively significant, actions taking place over time. **Table D-9** outlines expected cumulative impacts of OCS oil and gas operations on water quality and plankton.

Table D-9. Potential cumulative effects associated with OCS oil and gas activities.

Environmental Resource	Routine Effects (excluding Accidents)	Other Regional Activities Affecting the Resource	Significant Cumulative Effect Likely?
Water quality	• Turbidity from drilling discharges; elevated nutrients, suspended solids, and BOD from other effluents	• Effluents from existing ship traffic • Agricultural runoff and urban effluents • Spills from tankers and other ships	No
Plankton	• Minor, transient effects due to effluent discharges	• Effluents from existing ship traffic • Spills from tankers and other ships	No

D.6 References Cited

Anderson, C.M. and R.P. LaBelle. 2000. Update of comparative occurrence rates for offshore oil spills. Spill Science & Technology Bulletin 6:303-321.

Ayers, R.C., Jr., T.C. Sauer, Jr., D.O. Stuebner, and R.P. Meek. 1980a. An environmental study to assess the effect of drilling fluids on water quality parameters during high rate, high volume discharges to the ocean, pp. 351-381. In: Symposium, Research on Environmental Fate and Effects of Drilling Fluids and Cuttings. 21-24 January 1980, Lake Buena Vista, FL.

Ayers, R.C., Jr., T.C. Sauer, Jr., R.P. Meek, and G. Bowers. 1980b. An environmental study to assess the impact of drilling discharges in the mid-Atlantic. I. Quantity and fate of discharges, pp. 382-418. In: Symposium, Research on Environmental Fate and Effects of Drilling Fluids and Cuttings. 21-24 January 1980, Lake Buena Vista, FL.

Bate, G.C. and S.D. Crafford. 1985. Inhibition of phytoplankton photosynthesis by the WSF of used lubricating oil. Marine Pollution Bulletin 16:401-404.

Baud, R.D., R.H. Peterson, G.E. Richardson, L.S. French, J. Regg, T. Mongomery, T.S. Williams, C. Doyle, and M. Dorner. 2002. Deepwater Gulf of Mexico 2002: America's Expanding Frontier. U.S. Department of the Interior, Minerals Management Service, Gulf of Mexico OCS Region, New Orleans, LA. OCS Report MMS 2002-021. 148 pp.

Bennett, R.M. 2008. Slant-leg jack-up rig increases water depth. http://www.rigzone.com/news/insight/insight.asp?i_id=5

Bhattacharjee, D. and O.J. Fernando. 2008. Short term studies on effect of water soluble fractions of diesel on growth of *Chaetoceros calcitrans*, Paulsen. Research Journal of Environmental Toxicology 2(1):17-22.

Bureau of Energy, Minerals, and Resource Evaluation (BOEMRE). 2010. Oil and gas well drilling on Federal offshore leases since 1960. Accessed at: http://www.boemre.gov/stats/PDFs/Oil-GasDrillingWeb.pdf. Accessed: October 2010. Derived from Technical Information Management System, Regional Quarterly Report, through June 2007.

Boothe, P.N. and B.J. Presley. 1989. Trends in sediment trace element concentrations around six petroleum drilling platforms in the northwestern Gulf of Mexico, pp. 3-21. In: F.R. Engelhardt, J.P. Ray and A.H. Gillam (eds.), Drilling Wastes. Elsevier Applied Science, New York. 867 pp.

Camilli, R., C.M. Reddy, D.R. Yoerger, B.A.S. Van Mooy, M.V. Jakuba, J.C. Kinsey, C.P. McIntyre, S.P. Sylva, and J.V. Maloney. 2010. Tracking hydrocarbon plume transport and biodegradation at *Deepwater Horizon*. Science 330(6001): 201-204.

Canadian Association of Petroleum Producers (CAPP). 2005. Drilling an offshore well in Atlantic Canada. http://www.capp.ca.

Canadian Association of Petroleum Producers (CAPP). 2006. Offshore drilling rigs in Canada. http://www.capp.ca.

Continental Shelf Associates, Inc. 1997. Gulf of Mexico produced water bioaccumulation study, definitive component. Prepared for the Offshore Operators Committee, New Orleans, LA.

Continental Shelf Associates, Inc. 2004. Geological and geophysical exploration for mineral resources on the Gulf of Mexico outer continental shelf. Final programmatic environmental assessment. U.S. Department of the Interior, Minerals Management Service, Gulf of Mexico OCS Region, New Orleans, LA. OCS EIS/EA 2004-054. July 2004. https://www.gomr.mms.gov/PDFs/2004/2004-054.pdf.

Continental Shelf Associates, Inc. 2006. Effects of oil and gas exploration and development at selected continental slope sites in the Gulf of Mexico. Volume II: Technical Report. U.S. Department of the Interior, Minerals Management Service, Gulf of Mexico OCS Region, New Orleans, LA. OCS Study MMS 2006-045. 636 pp. http://www.gomr.mms.gov/PI/PDFImages/ESPIS/3/3875.pdf

CSA International, Inc. 2010. Fate and potential effects: Drilling fluid accidental release at the Mahogany Deep-2 wellsite, West Cape Three Points Block, Offshore Ghana. March 2010. Prepared for Kosmos Ghana, LLC, Dallas, TX.

Cranswick, D. 2001. Brief overview of Gulf of Mexico OCS oil and gas pipelines: Installation, potential impacts, and mitigation measures. U.S. Dept. of the Interior, Minerals Management Service, Gulf of Mexico OCS Region, New Orleans, LA. OCS Report MMS 2001-067. August 2001. http://www.mms.gov/itd/pubs/2001/2001-067.pdf

Gallaway, B.J. and G.S. Lewbel. 1982. The ecology of petroleum platforms in the northwestern Gulf of Mexico: A community profile. U.S. Fish and Wildlife Service, Office of Biological Services, Washington, DC. FWS/OBS-82/27. 92 pp.

Global Security. 2008. Offshore (systems). http://www.globalsecurity.org/military/systems/ship/offshore.htm. Accessed: June and July, 2008.

Gordon, D.C. and N.J. Prouse. 1973. The effects of three oils on marine phytoplankton photosynthesis. Marine Biology 22(4):329-333.

Guo, B., S. Song, J. Chacko, and A. Ghalambor. 2005. Offshore Pipelines: Design, Installation and Operations. Elsevier Inc., Oxford, UK. 289 pp.

Harrison, P.J., W.P. Cochlan, J.C. Acreman, T.R. Parsons, P.A. Thompson, H.M. Dovey, and C. Xiaolin. 1986. The effects of crude oil and Corexit 9527 on marine phytoplankton in an experimental enclosure. Marine Environmental Research 18:93-109.

Hazen, T.C., E.A. Dubinsky, T.Z. DeSantis, G.L. Andersen, Y.M. Piceno, N. Singh, J.K. Jansson, A. Probst, S.E. Borglin, J.L. Fortney, W.T. Stringfellow, M. Bill, M.S. Conrad, L.M. Tom, K.L. Chavarria, T.R. Alusi, R. Lamendella, D.C. Joyner, C. Spier, J. Baelum, M. Auer, M.L. Zemla, R. Chakraborty, E.L. Sonnenthal, P. D'haeseleer, H.-Y.N. Holman, S. Osman, Z. Lu, J.D. Van Nostrand, Y. Deng, J. Zhou, and O.U. Mason. 2010. Deep-sea oil plume enriches indigenous oil-degrading bacteria. Sciencexpress 24 August 2010.

Higashi, G.R. 1994. Ten years of fish aggregating device (FAD) design and development in Hawaii. Bull. Mar. Sci. 55(2-3):651-666.

Hinwood, J.B., A.E. Potts, L.R. Denis, J.M. Carey, H. Houridis, R.J. Bell, J.R. Thomson, P. Boudreau, and A.M. Ayling. 1994. Drilling activities, pp. 126-206. In: J.M. Swan, J.M. Neff, and P.C. Young (eds.), Environmental Implications of Offshore Oil and Gas Development in Australia. The Findings of an Independent Scientific Review. Australian Petroleum Exploration Association (APEA) and Energy Research and Development Corporation (ERDC). Christopher Beck Books, Queensland, Australia. ISBN 0 908277 17 2.

Holand, P. 1997. Offshore blowouts: Causes and control. Gulf Publishing Co., Houston, TX. 163 pp.

Holland, K.R., R.W. Brill, and R.K.C. Chang. 1990. Horizontal and vertical movements of yellowfin and bigeye tuna associated with fish aggregating devices. Fish. Bull. 88:493-507.

Hsiao, S.I.C., D.W. Kittle, and M.C. Foy. 1978. Effects of crude oils and the oil dispersant Corexit on primary production of Arctic marine phytoplankton and seaweed. Env. Poll, 15(3):209-221.

International Association of Oil & Gas Producers. 2003. Environmental aspects of the use and disposal of non-aqueous drilling fluids associated with offshore oil & gas operations. Report No. 342. May 2003. http://www.ogp.org.uk/pubs/342.pdf.

International Association of Oil & Gas Producers. 2005. Fate and effects of naturally occurring substances in produced water on the marine environment. Report No. 364. February 2005. http://www.ogp.org.uk/pubs/364.pdf.

International Association of Oil & Gas Producers. 2007. Environmental performance in the E&P industry: 2006 data. Report No. 399. October 2007. http://www.ogp.org.uk/pubs/399.pdf.

Jiang, Z., Y. Huanga, X Xua, Y. Liaoa, L. Shoua, J. Liua, Q. Chena, and J. Zeng. 2010. Advance in the toxic effects of petroleum water accommodated fraction on marine plankton. Acta Ecologica Sinica 30(1):8-15.

Kelly, L.D., L.R. McGuinness, J.E. Hughes, and S.C. Wainright. 1999. Effects of phenanthrene on primary production of phytoplankton in two New Jersey estuaries. Bull Environ. Contam. Toxicol. 63:646-653.

Kusk, K.O. 1981. Comparison of the effects of aromatic hydrocarbons on a laboratory alga and natural phytoplankton. Bot. Marina 24(11):611-613.

Lobban, C.S., and P.J. Harrison. 1997. Seaweed Ecology and Physiology. Cambridge University Press, Cambridge, New York. 366 pp.

Minerals Management Service (MMS). 2000. Gulf of Mexico Deepwater Operations and Activities: Environmental Assessment. U.S. Department of the Interior, Minerals Management Service, Gulf of Mexico OCS Region, New Orleans, LA. OCS EIS/EA MMS 2000-001.

Minerals Management Service (MMS). 2001. Gulf of Mexico OCS Oil and Gas Lease Sale 181, Eastern Planning Area. Final Environmental Impact Statement. U.S. Department of the Interior, Minerals Management Service, Gulf of Mexico OCS Region. OCS EIS/EA MMS 2001-051. June 2001.

Minerals Management Service (MMS). 2005. Structure removal operations on the Gulf of Mexico outer continental shelf: Programmatic environmental assessment. U.S. Dept. of the Interior, Minerals Management Service, Gulf of Mexico OCS Region, New Orleans, LA. OCS EIS/EA MMS 2005-013. https://www.gomr.mms.gov/PDFs/2005/2005-013.pdf.

Minerals Management Service (MMS). 2007. Gulf of Mexico OCS Oil and Gas Lease Sales: 2007-2012. Western Planning Area Sales 204, 207, 210, 215, and 218; Central Planning Area Sales 205, 206, 208, 213, 216, and 222. Final Environmental Impact Statement. U.S. Dept. of the Interior, Minerals Management Service, Gulf of Mexico OCS Region. OCS EIS/EA MMS 2007-018. April 2007.

Minerals Management Service (MMS). 2008. Mobile Offshore Drilling Unit. U.S. Department of the Interior, Minerals Management Service, Herndon, VA. http://www.mms.gov/ooc/Assets/KatrinaAndRita/BackgrounderMODU.pdf. Accessed: 25 June 2008.

National Research Council. 1983. Drilling Discharges in the Marine Environment. National Academy Press, Washington, DC. 180 pp.

Nayar, S., B.P. Goh, and L.M. Chou. 2005. Environmental impacts of diesel fuel on bacteria and phytoplankton in a tropical estuary assessed using in situ mesocosms. Ecotoxicology 14(3):397-412.

Neff, J.M. 1987. Biological effects of drilling fluids, drill cuttings and produced waters, pp. 469-538. In: D.F. Boesch and N.N. Rabalais (eds.), Long-Term Effects of Offshore Oil and Gas Development. Elsevier Applied Science Publishers, London.

Neff, J.M. 2002. Bioaccumulation in marine organisms. Effect of contaminants from oil well produced water. Elsevier, London.

Neff, J.M. 2005. Composition, environmental fates, and biological effects of water based drilling muds and cuttings discharged to the marine environment: a synthesis and annotated bibliography. Prepared for Petroleum Environmental Research Forum (PERF) and American Petroleum Institute by Jerry M. Neff, Battelle, Duxbury, MA. 83 pp.

Neff, J.M., S. McKelvie, and R.C. Ayers, Jr. 2000. Environmental impacts of synthetic based drilling fluids. Report prepared by Robert Ayers & Associates, Inc. U.S. Department of the Interior, Minerals Management Service, Gulf of Mexico OCS Region, New Orleans, LA. OCS Study MMS 2000-064. 118 pp.

National Oceanic and Atmospheric Administration (NOAA). 2006. Fact sheet: small diesel spills (500-5,000 gallons). NOAA, Hazardous Materials Response and Assessment Division, Seattle, WA.

Offshore. 2007. Fixed platforms remain important production facilities after more than 60 years. Offshore, September 01, 2007. Volume 67, Issue 9. http://www.offshore-mag.com/articles/article_display.cfm?ARTICLE_ID=307368&p=9.

Pérez, P., E. Fernández, and R. Beiras. 2010. Fuel toxicity on *Isochrysis galbana* and a coastal phytoplankton assemblage: growth rate vs. variable fluorescence. Ecotoxicol. Env. Safety 73(2):254-261, doi: 10:1016/j.ecoenv.2009.11.010.

Phatarpekar, P.V., and Z.A. Ansari. 2000. Comparative toxicity of water soluble fractions of four oils on the growth of a microalga. Bot, Marina 43(4):367-375, doi: 10.1515/BOT.2000.037.

Ray, J.P. and R.P. Meek. 1980. Water column characterization of drilling fluids dispersion from an offshore exploratory well on Tanner Bank, pp. 223-252. In: Symposium, Research on Environmental Fate and Effects of Drilling Fluids and Cuttings. 21-24 January 1980, Lake Buena Vista, FL.

Regg, J.B., S. Atkins, B. Hauser, J. Hennessey, B.J. Kruse, J. Lowenhaupt, B. Smith, and A. White 2000. Deepwater development: A reference document for the deepwater environmental assessment Gulf of Mexico OCS (1998 through 2007). OCS Report MMS 2000-015. U.S. Dept. of the Interior, Minerals Management Service, Gulf of Mexico OCS Region, New Orleans, LA. https://www.gomr.mms.gov/PDFs/2000/2000-015.pdf.

Riznyk, R.Z,, J.T. Hardy, W. Pearson, and L. Jabs. 1987. Short-term effects of polynuclear aromatic hydrocarbons on sea-surface microlayer phytoneuston. Bull. Environ. Contam. Toxicol. 18:1037-1043.

Scandpower Risk Management Inc. 2004. An Assessment of Safety, Risks and CostsAssociated with Subsea Pipeline Disposals. Report for the U.S. Dept. of the Interior, Minerals Management Service, Gulf of Mexico OCS Region, New Orleans, LA. Report No. 32.701.001/R1. September 2004.

Schlumberger. 2008a. Oilfield glossary. http://www.glossary.oilfield.slb.com/search.cfm.

Schlumberger. 2008b. EverGreen burner. http://www.slb.com/content/services/testing/surface/evergreen.asp.

Shinn, E.A., B.H. Lidz, and C.D. Reich. 1993. Habitat impacts of offshore drilling: Eastern Gulf of Mexico. U.S. Dept. of the Interior, Minerals Management Service, Gulf of Mexico OCS Region, New Orleans, LA. OCS Study MMS 93-0021. 73 pp.

Siron, R., G. Giusti, B. Berland, R. Morales-Loo, and E. Pelletier. 1991. Water-soluble petroleum compounds: chemical aspects and effects on the growth of microalgae. Sci. Total Environ. 104:211-227.

Siron, R,, E. Pelletier, D. Delille, and S. Roy. 1993. Fate and effects of dispersed crude oil under icy conditions simulated in mesocosms. Mar. Environ. Res. 35:273-302.

Stanley, D.R. and C.A. Wilson. 2000. Seasonal and spatial variation in the biomass and size frequency distribution of fish associated with oil and gas platforms in the northern Gulf of Mexico. Final report for the U.S. Department of the Interior, Minerals Management Service Gulf of Mexico OCS Region, New Orleans, LA. OCS Study MMS 2000-005.

U.S. Environmental Protection Agency (USEPA). 1993. Development Document for Effluent Limitation Guidelines and New Source Performance Standards for the Offshore Subcategory of the Oil and Gas Extraction Point Source Category. EPA 821-R-93-003. Office of Water, Washington, DC.

Valentine, D.L., J.D. Kessler, M.C. Redmond, S.D. Mendes, M.B. Heintz, C. Farwell, L. Hu, F.S. Kinnaman, S. Yvon-Lewis, M. Du, E.W. Chan, F.G. Tigreros, and C.J. Villanueva. 2010. Propane respiration jump-starts microbial response to a deep oil spill. Science 330:208-211.

Varela, M., A. Bode, J. Lorenzo, M.T. Álvarez-Ossorio, A. Miranda, T. Patrocinio, R. Anadón, L. Viesca, N. Rodríguez, L. Valdés, J. Cabal d, Á. Urrutia, C. García-Soto, M. Rodríguez, X.A. Álvarez-Salgado, and S. Groom. 2006. The effect of the ''Prestige'' oil spill on the plankton of the N–NW Spanish coast. Mar. Pollut. Bull. 53:272-286, doi:10.1016/j.marpolbul.2005.10.005.

Veil, J.A. 2006. Why are produced water discharge standards different throughout the world? Presentation at the 13th IPEC, San Antonio, TX. October 19, 2006. 56 pp.

Veil, J.A., M.G. Puder, D. Elcock, and R.J. Redweik, Jr. 2004. A white paper describing produced water from production of crude oil, natural gas, and coal bed methane. Argonne National Laboratory. January 2004. 87 pp.

Veil, J.A., T.A. Kimmell, and A.C. Rechner. 2005. Characteristics of produced water discharged to the Gulf of Mexico hypoxic zone. Report prepared by the Environmental Assessment Division, Argonne National Laboratory, Argonne, IL for the U.S. Department of Energy, National Energy Technology Laboratory. August 2005. ANL/EAD/05-3. 76 pp.

Wilson, C.A., A. Pierce, and M.W. Miller. 2003. Rigs and reefs: a comparison of the fish communities at two artificial reefs, a production platform, and a natural reef in the northern Gulf of Mexico. Prepared by the Coastal Fisheries Institute, School of the Coast and Environment, Louisiana State University. U.S. Dept. of the Interior, Minerals Management. Service, Gulf of Mexico OCS Region, New Orleans, LA. OCS Study MMS 2003-009. 105 pp.

Wilson, C.A., M.W. Miller, Y.C. Allen, K.M. Boswell, and D.L. Nieland. 2005. Effect of depth, location, and habitat type, on relative abundance and species composition of fishes associated with petroleum platforms and Sonnier bank in the northern Gulf of Mexico. Prepared by the Coastal Fisheries Institute, School of the Coast and Environment. Louisiana State University. U.S. Dept. of the Interior, Minerals Management Service, Gulf of Mexico OCS Region, New Orleans, LA. OCS Study MMS 2006-037. 97 pp.